INFORMATION TO USERS

This manuscript has been reproduced from the microfilm master. UMI films the text directly from the original or copy submitted. Thus, some thesis and dissertation copies are in typewriter face, while others may be from any type of computer printer.

The quality of this reproduction is dependent upon the quality of the copy submitted. Broken or indistinct print, colored or poor quality illustrations and photographs, print bleedthrough, substandard margins, and improper alignment can adversely affect reproduction.

In the unlikely event that the author did not send UMI a complete manuscript and there are missing pages, these will be noted. Also, if unauthorized copyright material had to be removed, a note will indicate the deletion.

Oversize materials (e.g., maps, drawings, charts) are reproduced by sectioning the original, beginning at the upper left-hand corner and continuing from left to right in equal sections with small overlaps. Each original is also photographed in one exposure and is included in reduced form at the back of the book.

Photographs included in the original manuscript have been reproduced xerographically in this copy. Higher quality 6" x 9" black and white photographic prints are available for any photographs or illustrations appearing in this copy for an additional charge. Contact UMI directly to order.

UMI

University Microfilms International
A Bell & Howell Information Company
300 North Zeeb Road, Ann Arbor, MI 48106-1346 USA
313/761-4700 800/521-0600

Order Number 9224853

Geology of missing strata: The post-Devonian of New York State

Sarwar, Golam, Ph.D.

City University of New York, 1992

U·M·I
300 N. Zeeb Rd.
Ann Arbor, MI 48106

GEOLOGY OF MISSING STRATA: THE POST-DEVONIAN OF NEW YORK STATE

by

GOLAM SARWAR

A dissertation submitted to the Graduate Faculty in Earth and Environmental Sciences in partial fulfillment of the requirements for the degree of Doctor of Philosophy, the City University of New York

1992

This manuscript has been read and accepted for the Graduate Faculty in Earth and Environmental Sciences in satisfaction of the dissertation requirement for the degree of Doctor of philosophy.

4/14/92
Date

GERALD M. FRIEDMAN
Chair of Examining Committee

4/14/92
Date

Executive Officer

Dr. Robert H. Fakundiny

Professor Somdev Bhattacharji

Professor Nicholas Coch

Supervisory Committee

The City University of New York

ABSTRACT

GEOLOGY OF MISSING STRATA: THE POST-DEVONIAN OF NEW YORK STATE

by

Golam Sarwar

ADVISOR: Professor Gerald M. Friedman

Paleotemperatures of samples from ten Paleozoic rock units of New York State have been assessed from fluid-homogenization temperatures, oxygen isotope ratios, organic maturation and clay-diagenesis data. All studied samples show paleotemperature signatures much higher than expected from their present position with respect to the surface. The observed pattern of lateral variation in paleotemperatures in the studied rocks and lack of past igneous activity that could significantly affect their paleotemperature signatures suggest that the high temperatures were attained from normal geothermal heat during deep burial. Fluid-inclusion and oxygen-isotope data of mineral cements indicate that most of the cements were precipitated from hot subsurface brines. However, no evidence suggests that the brine was expelled from deeper parts of the basin toward the basin margin, nor that fluid squeezed out of the eastern orogenic belt migrated across the northern Appalachian foreland basin toward the craton. The paleotemperature signatures of the studied rocks thus reflect the ambient geothermal temperature as a principal function of burial depth. Maximum burial depths of the studied samples were calculated from their maximum paleotemperature data and an inferred paleogeothermal gradient of 30°C/km and a mean annual surface temperature of 20°C. Subtracting the thicknesses of extant younger rocks (up to end-Devonian) in southern New York from the maximum burial depths of samples, the thicknesses of former post-Devonian strata at various study locations were estimated. Isopach maps of post-Devonian strata show that two NE-SW elongate belts of greater post-Devonian sediment accumation, one in southeastern New York and the other in central New York, each ranging from at least

3km to more than 6km in thickness were present. From the thickness of extant Carboniferous rocks in Pennsylvania and other geologic considerations, it is inferred that most of the post-Devonian strata in New York were in fact post-Carboniferous in age. Based on known preservation rates of molassic sediments elsewhere, it is estimated that sedimentation continued in New York up to Late Permian.

Upthrusted Alleghanian mountains in eastern and northeastern Pennsylvania, and possibly in southeastern New York, were probably the main source of sediments in the south and southeast, and newly uplifted landmass along the Findlay - Algonquin arch and the Bronson Hills anticlinorium in western New England were sources to the northwest and east respectively. Sedimentation took place in alluvial fans, braid plains, flood plains and isolated lakes or remnants of the older epicontinental seaway.

Exhumation of these rocks probably began in the Late Permian, around 255 Ma. Late Permian to Middle Triassic time witnessed very rapid exhumation followed by exponentially decreasing exhumation rates up to the Miocene epoch. After the Miocene, the exhumation rates again seem to have increased.

The "surface uplift" rates in New York State could not be quantified from this study, but it was shown that from late Permian to the Miocene, "rock uplift" rates dominated over "exhumation" rates leading to net uplift of the surface. Since the Miocene, exhumation rates are greater than rock-uplift rates resulting in decrease in average surface elevations everywhere with the possible exception of the Adirondack mountains. Geodetic releveling data and geomorphic characteristics indicate that surface uplift is presently taking place in the Adirondack mountains.

The three ages of uplift of the northern Appalachian basin - Late Carboniferous-Permian, Cretaceous, and Tertiary - frequently cited in geologic literature, do not strictly apply to New York State. Results of this study indicate that while the areas south of New York State were upthrusted and folded by Alleghanian compression in the Late Carboniferous - Early Permian interval, New York State remained or was transformed into an inland basin receiving sediments from Alleghanian uplifts. Uplift in New York lagged behind and probably did not begin until late Permian. The Cretaceous period, according to this study, did not mark an episodic uplift, but the waning stage of

the earlier, Late Permian-Middle Triassic, rapid uplift. The Tertiary uplift in New York is substantiated by data only from the Adirondack mountains.

Epeirogenic crustal movement seems to have been the dominant process in New York. The Late Permian-Middle Triassic rapid exhumation of rocks was probably due mainly to passage of eastern North America over hot spots/mantle plumes which caused doming, thinning and stretching of the lithosphere in the area leading ultimately to break up of the continents along the old suture. The continued uplift in New York State, although at a decelerating rate, up to at least the Miocene time and apparently at a very rapid rate at present in the Adirondack mountains also can not be explained by plate marginal processes. Many mechanisms of epeirogenic uplift have been proposed, but which of these apply to New York State is not known.

ACKNOWLEDGMENT

I am deeply thankful to Prof. Gerald M. Friedman for acting as my advisor. He suggested the topic and provided guidance and help in all aspects of this work. Thanks to my committee members, Dr. Robert H. Fakundiny, Prof. Somdev Bhattacharji, and Prof. Nicolas Coch for critically reviewing the manuscript and providing useful suggestions. Dr. Fakundiny also gave me free access to the core samples and pertinent information in the New York State Geological Survey depository. Dr. D.W. Fisher gave me directions to many good outcrops from his unique memory bank: his help is greatly appreciated. Thanks to Dr. William Kelley who helped me obtain core samples from the Geological Survey warehouse by operating the forklift and carrying heavy boxes, none of which I could have done alone. Prof. Hitoshi Homa has my gratitude for helping me with X-ray diffraction. I am grateful to Mrs. Sue Friedman for providing various logistic support for this work. Thanks to Prof. Cherukapalli Nehru, Chairperson of Department of Geology of Brooklyn College during much of this work, and Prof. Daniel Habib, Ph.D. Executive Officer of Department of Earth and Environmental Sciences of CUNY, for their support. I benefited a lot from discussions with my friend Ali Kaya. Faye Melas, Joachim Amthor, Lillian Hess, and Ramesh Challapalli provided fruitful company in Troy and Brooklyn at various times. I thank my wife, Milly, for keeping up with my odd hours during this work. This acknowledgment would be incomplete without paying tributes to my parents who always wanted their children to get a higher education.

This work was supported by a PSC-CUNY grant (#669198) to Prof. Gerald M. Friedman; the Northeastern Science Foundation, Troy, New York; a student Honorarium award from New York State Geological Survey; and a grant from Geochem Laboratories, Cambridge, Massachusetts. Much of the laboratory work was done in the Northeastern Science Foundation, Troy, New York.

TABLE OF CONTENTS

BURIAL DEPTHS OF CAMBRIAN AND ORDOVICIAN ROCKS

LIST OF TABLES

LIST OF FIGURES

CHAPTER 1: INTRODUCTION

The post-Devonian geologic history of the northern Appalachian basin has been a subject of controversy ever since it was proposed in 1970's (Epstein et al. 1977; Harris et al. 1978; Harris, 1979) that the surficial rocks in New York have been exhumed from great depths after removal of strata much of which might have been post- Devonian in age.

Except for the Cenozoic cover of Long Island and parts of Staten Island, and the Triassic rocks of the Newark Basin in the southeastern end of the state, the rocks exposed in New York range from Precambrian to Upper Devonian in age. Mainly on the basis of the absence of post-Devonian strata in New York, traditional leaning has been toward the opinion that since the end-Devonian, little sediment had accumulated in New York (see Meckel, 1970, for example) and the region has largely witnessed a continuous cycle of erosion.

However, many recent studies, using techniques as diverse as fluid inclusions, stable isotopes, clay diagenesis, organic maturation, fission tracks, and K-Ar dating, have found that the rocks currently exposed at the surface or at shallow depths had experienced high paleotemperatures (see chapter 4 for a comprehensive review). According to most of these studies, the high paleotemperatures measured in these rocks were attained during deep burial, and to account for the burial it became necessary to infer that much of the eroded strata was post-Devonian in age.

A great many implications arise from the results of these studies. If sedimentation indeed continued long after the Devonian in New York, as many of these studies suggest, this will require revision of much of the present concepts of post-Devonian geologic history of the area and a plethora of new problems. For example, how long after the Devonian did sedimentation continue?; what were the depsitional environments?; what was the paleogeography like?; where did the additional sediments come from?; what happened to these sediments? etc. Unfortunately, because of the limited scope (areally or temporally) of most of the previous studies, most of these questions remain

unanswered.

In the present broad-based study, samples from as many as ten rock units, collected from the unfolded Paleozoic section west of the Hudson Valley, have been analyzed for paleotemperature signatures by using four principal techniques, namely, fluid inclusions, organic maturation, clay diagenesis, and stable isotopes. Through analytical and interpretive methods described in chapter 4, ultimately the spatial variation in the amount of missing strata in New York has been estimated. Attempt has been made to reconstruct the possible depositional setting and paleogeography of post-Devonian New York. Exhumation rates of rocks of different areas have been determined from the results of this study and available fission-track ages. Finally, the cause and mechanism of vertical motion that brought the formerly deeply buried strata to the surface have been explored.

CHAPTER: 2

GEOLOGICAL SETTING

The Appalachian basin of eastern North America is a multi-stage foreland basin located between the Appalachian orogen to the east and the stable interior provinces to the west (figs. 2.1, 2.2). Its eastern and southeastern boundaries are marked by the crystalline core of the Appalachian (the Piedmont Province), and western and northwestern margins by the Cincinnati Arch and the Findlay-Algonquin Arch, respectively. These arches, which are basement-involved structural highs, separate the Appalachian basin from the intra-cratonic Illinois and Michigan basins (fig. 2.1). The Appalachian basin extends from Newfoundland in the north to Alabama in the south. North of New York State, the basin becomes greatly constricted, and in northwest Newfoundland it tapers off between the Laurentian Shield and the so called "Dunnage Terrane" (fig. 2.2). In Alabama, the folded Paleozoic rocks of the Appalachian basin plunge beneath the post-orogenic Mesozoic-Cenozoic strata in the Mississippi Embayment of the Gulf Coast Plain (Thomas, 1985).

The origin and evolution of the Appalachian basin can be linked with a series of tectonic events along the eastern margin of North America. The earliest, pre-Appalachian, "Grenville Orogenic Cycle", probably comprised a number of tectonic events between 1100 and 800 Ma (Stockwell, 1961; Rodgers, 1967). Granulite facies Grenvillian rocks make up the basement under much of the Appalachian basin and are exposed in several anticlinoriums and domal uplifts throughout the basin (Rodgers, 1967).

In New York State the Grenvillian basement is exposed in the Adirondack and Hudson Highlands (fig. 2.3) and outside New York, in the Laurentian Shield of Ontario, Canada, the Green Mountains of Vermont, certain gneissic domes of eastern Connecticut and the Reading Prong of New Jersey and northeastern Pennsylvania (Rodgers, 1967). In the Adirondacks a number of metasedimentary and metavolcanic stratigraphic units ranging between amphibolite and granulite facies and several phases of folding and

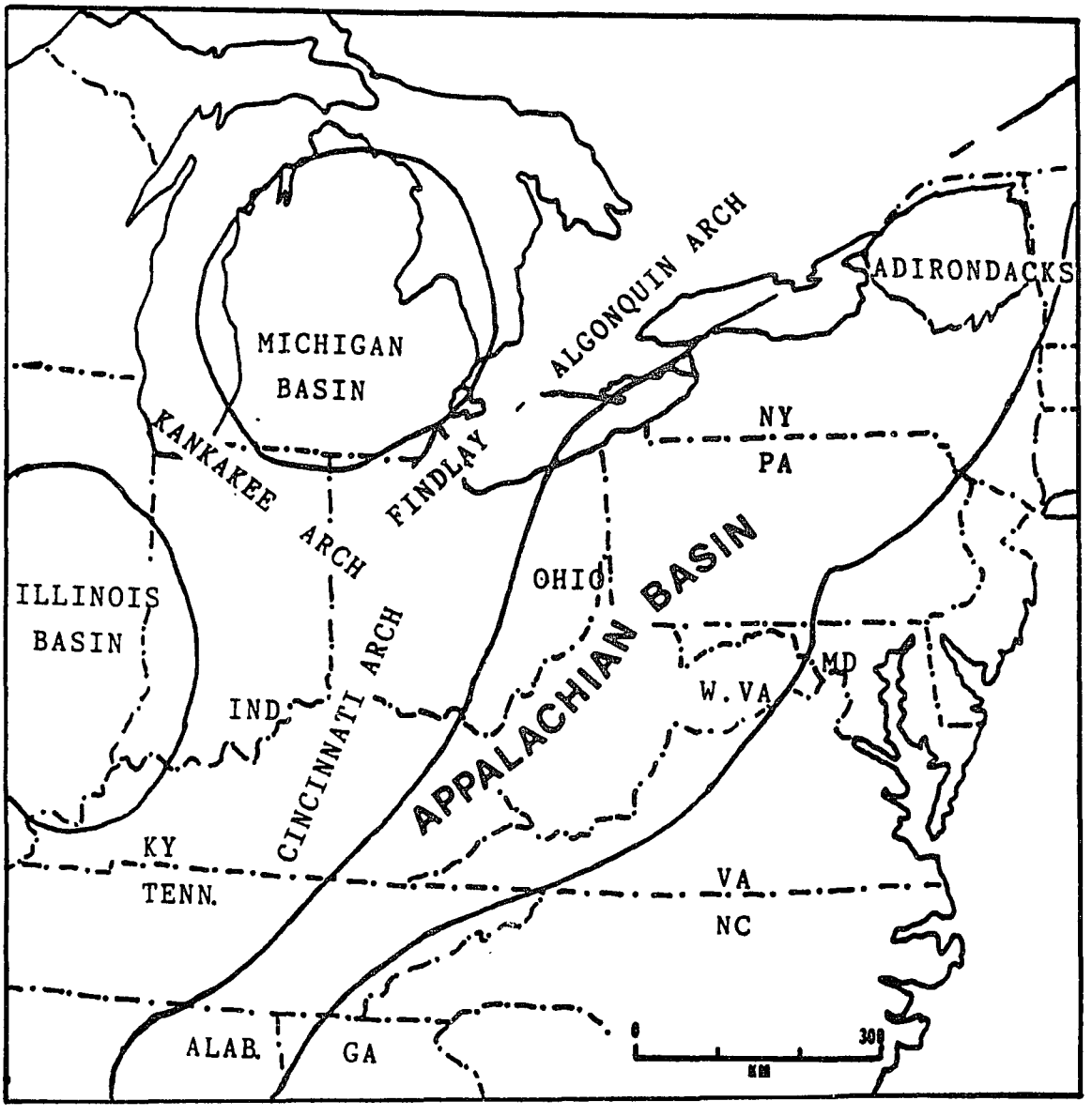

Figure 2.2: Map showing the location of the Appalachian foreland basin relative to the interior basins and arches of the eastern North America. (Modified from Tankard, 1986).

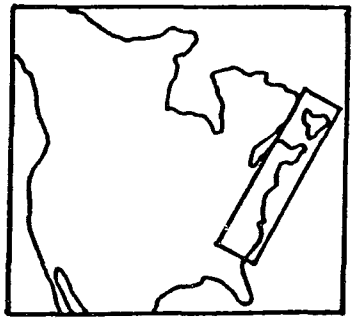

KEY

1 Hamburg Terrane
2 Taconic Terrane
3 St. Lawrence Terrane
4 Humber Arm Terrane
5 Hare Bay Terrane
6 Lake Erie
7 Lake Ontario
GP Gaspe Peninsula
NFL Newfoundland
ADR = Adirondacks

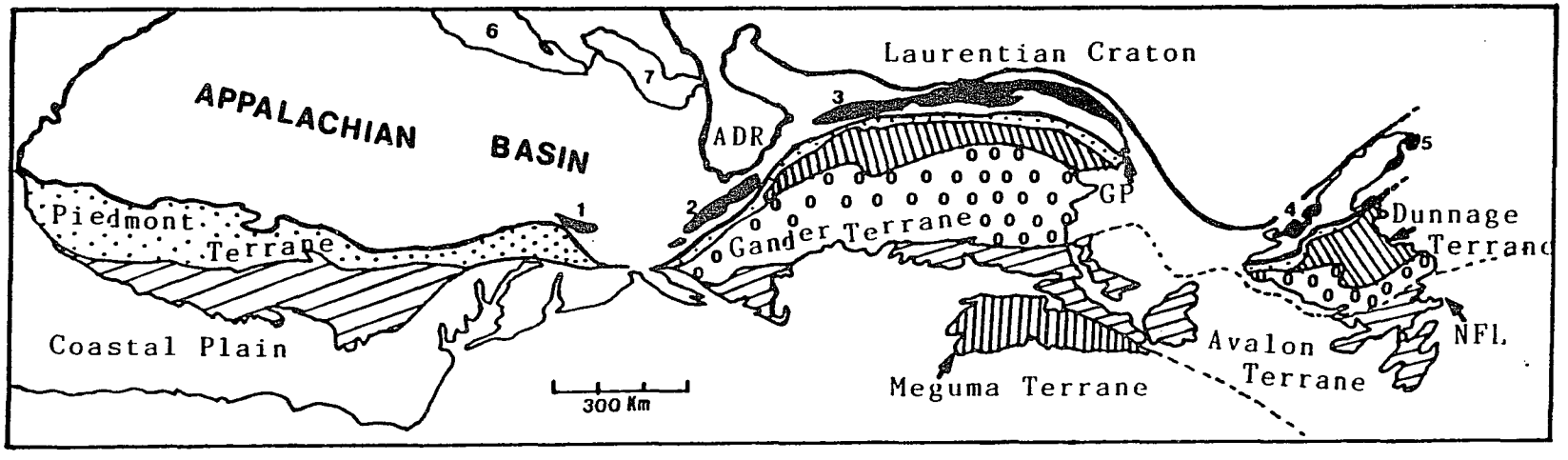

Figure 2.2: Map showing the position of the Appalachian foreland basin with respect to the "suspect terranes" of the Appalachian orogen. (Modified from William and Hatcher, 1982, and Faill, 1985).

Figure 2.3: Geologic map of New York. (Simplified from Geological Survey of New York State Museum map in Geogram, 1988 series. Approximate locations of the Mesozoic kimberlites are taken from Dennison, 1983 and Kay et al. 1983)

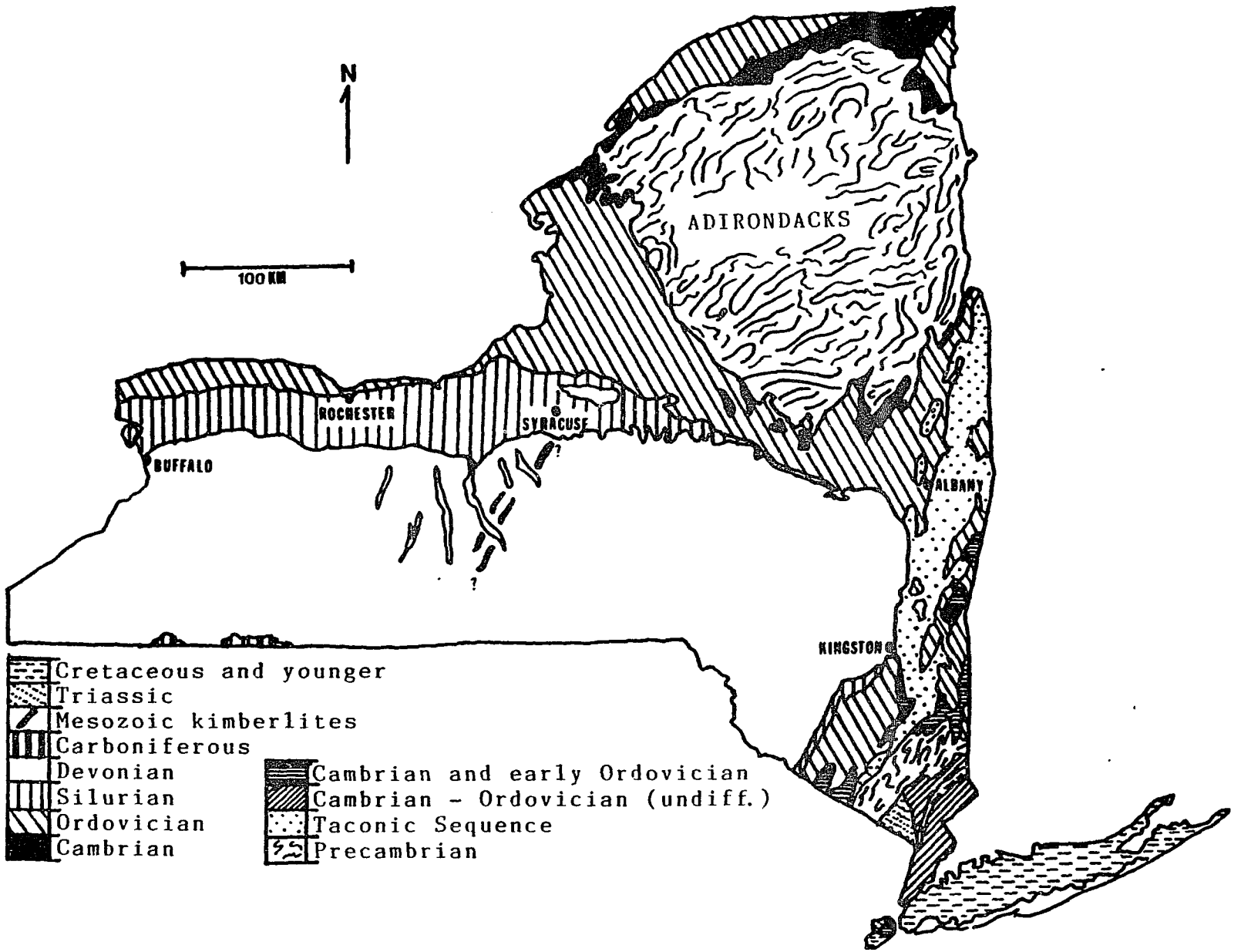
N
100 KM
ADIRONDACKS
ROCHESTER
SYRACUSE
BUFFALO
ALBANY
KINGSTON
Cretaceous and younger
Triassic
Mesozoic kimberlites
Carboniferous
Devonian
Silurian
Ordovician
Cambrian
Cambrian and early Ordovician
Cambrian - Ordovician (undiff.)
Taconic Sequence
Precambrian

associated magmatic intrusuions have been recognized (Weiner et al. 1984; Isachsen et al. 1991, ch.4). Radioactive ages of 1.02-1.33 Ga have been measured in tonalites, while the youngest pegmatite intrusion show an age of 930 Ma.

The birth of the Appalachian basin can be traced back to the late Precambrian when rifting of the Grenvillian basement on the eastern side of the North American craton created an Atlantic-type passive margin (Price and Hatcher, 1983; Tankard, 1984). Seismic and gravity data seem to indicate the presence of the attenuated geometry of this transition (Cook et al. 1979, 1981; Price and Hatcher, 1983; Ando et al. 1984). Price and Hatcher (1983, figs.7,9) draw the locus of the rifted margin along a line marking steep gradients in Bouger gravity anomaly that extends from northeastern Connecticut through southeastern Pennsylvania to southern Alabama. In New York state, this inferred rift margin passses through its southeastern corner, nearly parallel to the trends of the Hudson Highlands-Reading Prong.

On this late Precambrian passive margin, initially rift-clastics were deposited and are probably represented by the coarse clastics of the Ocoee Group ("Great Smoky Supergroup" in Price and Hatcher, 1983) in the Great Smoky Mountains of Tennessee and North Carolina and the Glenaram Group of Maryland and Pennsylvania (Rodgers, 1967). In New York area, Precambrian clastics are absent, suggesting that the rifting and opening of the Proto-Atlantic or Iapetus Sea took place later in the Northern Appalachian region.

By Late Cambrian the passive margin had stabilized into a carbonate shelf, which persisted into the early Ordovician. The sedimentary record of this earliest carbonate shelf is well preserved throughout the basin in the carbonate rocks of the Beekmantown Group (Cambro-Ordovician) in the northern and central Appalachians and of the Knox Group in the southern Appalachians. In New York, western Vermont and western New England region, the rocks of this interval show a distinct east-west facies transition. A shallow shelf environment existed over much of New York and as far east as the northern flanks of the Hudson Highlands and western flanks of the Green Mountains in Vermont and Berkshire Mountains in Massachusetts (Broughton et al. 1966; Isachsen et al. 1991, ch. 4). The basal shelf sequence consists of clean quartzite or sandstones everywhere - the

Early Cambrian Poughquag Formation (of the Wappinger Group, fig. 2.4) in southeastern New York and Potsdam Formation (of the Beekmantown Group, fig. 2.4) elsewhere in New York (Fisher, 1977). The marine facies of the Potsdam Formation is younger (Upper Cambrian) than Poughquag, indicating progressive westward spread of the sea through the early Cambrian - early Ordovician interval. Deposition of these basal clastics, which had their sources in the cratonic lowlands to the west, were followed by extensive carbonate sedimentation. In southeastern New York, the carbonates of the Wappinger Group (Cambro-Ordovician) were deposited while in central and western New York the carbonates of the Beekmantown Group were deposited.

While deposition of carbonates was going on throughout New York State, farther east, probably east of the present- day Green and Berkshire mountains, deposition of both coarse and fine grained detrital sediments was taking place in a slope-rise environment (Fakundiny et al. 1989). These sediments, spanning the early Cambrian to early Middle Ordovician interval, are now represented by muddy sandstones (Rensselaer, Bomosen), quartzite (Mud Pond, Diamond Rock), Taconic Allochthon (figs. 2.3, 2.4) east of the Hudson River. These older rocks of the slope-rise sequence are thicker and coarser grained to the west indicating a western provenance, probably the Laurentian lowlands (Fakundiny et al. 1989).

2.1: THE TACONIC OROGENY:

Passive margin deposition was terminated by the Taconic tectonic event which began in the early Middle Ordovician and lasted through the early Silurian. The Taconic event involved collision of the North American continental margin with a belt of oceanic island arcs above an east-southeast dipping subduction zone (Williams, 1979; Rowley and Kidd, 1981; Hiscott et al. 1986). Evidence of former existence of the subduction zone and volcanic island arcs are found in the ophiolites, tectonic melange and mafic volcanic rocks of the Dunnage tectonostratigraphic zone of Newfoundland (Kean and Strong, 1975; Williams and Hatcher, 1982; Price and Hatcher, 1983).

As the continental margin approached the subduction zone, the seaward part of the carbonate shelf floundered, probably due to "normal faulting caused by plate flexure

Figure 2.4: Major Palcozoic and Mesozoic stratigraphic units of New York and their general lithologic composition. (Adapted from Fakundiny et al. 1988).

AGE	ROCK UNIT	LITHOLOGY
Late Cretaceous 80 mya	Magothy (?) Formation Raritan Formation	sand, gravel
Late Triassic - Early Jurassic 215 mya	Newark Group	red shale, siltstone, diabase
Early Pennsylvanian 320 mya	Olean Formation	conglomerate
Early Mississippian 360 mya	Knapp Formation	shale, siltstone
Late Devonian 360-375 mya	Conewango Group Conneaut Group Canadaway Group West Falls Group Sonyea Group Genesee Group	siltstone, shale, sandstone siltstone, shale, sandstone siltstone, shale, sandstone siltstone, shale, sandstone siltstone, shale, sandstone siltstone, shale, sandstone
Middle Devonian 375-385 mya	Tully Formation Hamilton Group Onondaga Formation	limestone shale, sandstone limestone
Early Devonian 385-410 mya	Tristate Group Helderberg Group	siltstone, shale limestone
Late Silurian 410-420 mya	Rondout Formation Salina Group Lockport Group	dolostone, limestone dolostone, evaporite, shale dolostone, limestone
Early Silurian 420-440 mya	Clinton Group Medina Group	shale, sandstone, limestone sandstone
Late Ordovician 440-460 mya	Queenston Formation Lorraine Group Utica Formation	red shale, sandstone shale, siltstone, sandstone black shale
Middle Ordovician 460-480 mya	Trenton Group Martinsburg Formation Black River Group Normanskill Group Chazy Group	limestone, shale shale, sandstone limestone, dolostone shale, sandstone limestone
Early Ordovician and Cambrian 480-540 mya	Beekmantown Group Stockbridge Group Wappinger Group Taconic sequence	dolostone, sandstone, shale, sandstone

with downbending" (Hiscott et al. 1986). As convergence continued, stacked thrust-sheets presumably overrode the outer parts of the continental terrace and resulted in rapid flexural downwarping of the ancestral continental slope and rise (Price and Hatcher, 1983; Quinlan and Beaumont, 1984; Tankard, 1986). The downwarped continental margin bounded on the oceanic side by the rising Taconic orogenic belt created the elongate Appalachian foreland basin between Newfoundland and Alabama. Recent COCORP data suggest that the Taconic-age overthrust is up to 14km thick in the Southern Appalachians, but this may have been insufficient to establish much relief above sea level in the Taconic orogenic belt, because these sheets were probably emplaced on a continental margin at water depths of several kilometers (Cook, 1984; Quinlan and Beaumont, 1984; Stockmal et al. 1986).

In the deepest part of this young foreland basin, close to the orgogenic belt, argillaceous limestones with slide sheets were deposited first, followed by dark graptolitic shale and flysch derived from the orogenic belt (Hiscott et al. 1984). So, for the first time the source of clastic sediments had shifted from west to east.

In New York, east of the Hudson River, and western New England these deep-water flysch sediments are represented by the Middle Ordovician Normanskill Group of the Taconic allochthon. The rocks of the Normanskill Group show clear evidence of an eastern provenance. These rocks coarsen and thicken to the east and also contain volcanic ash, metamorphic rock fragments and "exotic sand-sized grains of chromite" indicating that the sediments were derived from volcanoes and upthrusted oceanic sediments of the accretionary prism to the east (Stevens, 1970; Fakundiny et al. 1989).

While the eastern part of the foreland basin, proximal to the orogenic belt, deepened under thrust-loads, the western, landward part probably became the locus of a shifting "peripheral bulge" (Quinlan and Beaumont, 1984; Tankard, 1986). Peripheral bulging or upwarping is believed to result from visco-elastic adjustment of the lithosphere to marginal thrust-loading. If the load remains in place for a long period of time, the proximal part of the basin subsides while the peripheral part of the basin upwarps and contracts toward the thrust-load (fig. 2.5).

Peripheral upwarping due to Taconic thrust-loading is believed to have caused

Figure 2.5: Foreland deformation model of Quinlan and Beaumont (1984). (**a**) Stages (1, 2, 3) of deformation of a viscoelastic plate under an applied load. As the load remains stationary for a long period of time, viscoelastic relaxation causes uplift of the forebulge and its migration toward the load. (**b**) Stages (1, 2, 3) of deformation in a foreland basin in response to thrust-loading at the basin margin. If the thrust load remains stationary for a long period of time, uplift of the forebulge on the platform side of the basin and it's migration toward the thrust-belt (stage-2) cause widespread erosion. (After Quinlan and Beaumont, 1984, and Tankard, 1986).

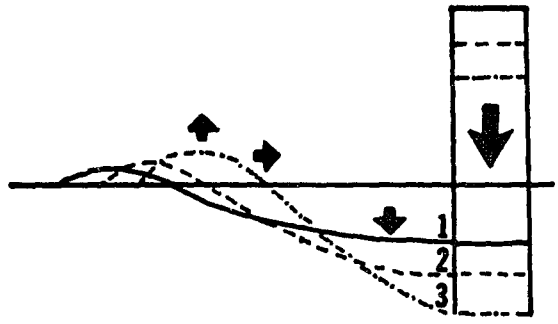

(a)

1. Overthrust loading - flexural deformation

2. Relaxation phase - viscoelastic response

3. Renewed overthrust loading - flexural deformation

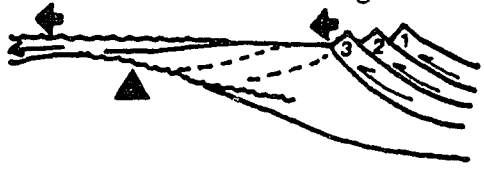

Active overthrusting

← Sediment dispersal

Overthrust-forebulge migration

▲ Reference point for forebulge behaviour

(b)

widespread erosion of the late Cambrian and early Ordovician carbonates of the ancestral passive margin and is represented by the Knox-Beekmantown unconformity throughout the Appalachian basin (Quinlan and Beaumont, 1984; Tankard, 1986). Jacobi (1981) had also hypothesized the origin of this unconformity with the aid of a "forebulge", but the mechanism of erosion proposed by him differs in detail from that of Quinlan and Beaumont (1984).

The Knox-Beekmantown unconformity corresponds to the sub-Tippecanoe unconformity, one of the six major unconfomities recognized by Sloss (1963) for the North American craton. Sloss (1963, 1972, 1978) related these unconformities to global, eustatic sea level drops, and showed that similar unconformities could be recognized in Russia and Europe. Although Sloss' unconformities and sequences bounded by them become obscured in the mobile belts of the Appalachian and the Cordillera, it is certain that sea-level changes of the inferred global scale affacted the later areas. Therefore, basin margin thrust-loading and "peripheral upwarping" (Quinlan and Beaumont, 1984) may not have been the only, or the primary, cause of erosion that resulted in the Knox-Beekmantown unconformity in the Appalachian basin. Perhaps, thrust-load induced upwarping and eustatic sea-level drop occurred simultaneously in response to major plate readjustments and this enhanced the rate of erosion.

Throughout New York, this early Middle Ordovician unconformity is well represented by the prominent hiatus above the Beekmantown Group (Rickard, 1973; Fisher, 1977). However, there are other unconformities, although more local in extent, within the Ordovician sequence of New York state. These include several unconformities within the Beekmantown Group, especially in the Mohawk and Champlain Valleys, and one above the Middle Ordovician Chazyan carbonates (Fisher, 1977). Moreover, the post-Chazyan unconformity, so prominent in New York, is not present over much of the Appalachians (COSUNA Correlation Chart, 1985). How these locally restricted unconformities relate to Quinlan and Beaumont's (1984) model (fig. 2.5) is not known. The role of eustatic sea-level changes and/or epeirogenic crustal movements in the northern Appalachian basin (see Friedman, 1987a, 1988) in creating these unconformities should also be considered.

The stratigraphic position and tectonic relationships of the Taconic allochthon have long been a source of controversy which is still not fully resolved (Friedman et al. 1982, p.35-46). The allochthon consists of Lower Cambrian to pre-Upper Ordovician clastic sequences that contain the slope-rise sediments of the pre-Taconic passive margin as well as the deep-water flysch deposits (Normanskill Group) of the foreland basin. The allochthon is believed to have been transported 150 to 200km from the east of the present Green and Berkshire mountains and thrust upon the largely coeval shelf carbonates and clastics to the west (Friedman et al. 1982; Stanley and Ratcliffe, 1985). There is considerable debate concerning the nature of the lower contact of the allochthon, which is rarely exposed. Some workers propose that the Taconic allochthon was thrust upon the synorogenic flysch sediments ("autochthonous", see below) rather than on shelf carbonates (Zen, 1967,1972; Bosworth et al. 1988).

The mechanism of emplacement of the Taconic allochthon has been explained in terms of large-scale, submarine gravity sliding westward from an Ordovician-age uplift along the present-day Green Mountain axis (Bird, 1969; Bird and Dewey, 1970) on to the carbonate shelf. This interpretation, however, suffers from lack of sufficient evidence of an Ordovician uplift of the Green Mountain axis (Friedman et al. 1982, p.37). According to Williams and Hatcher (1982), the Taconic "suspect terranes" (including the Taconic, St. Lawrence Terrane of Quebec and Humber Arm Terrane of Newfoundland, fig. 2.2) were emplaced by a westward transport of the allochthons to the eastern subduction zone and represent "an attempt to submerge the North American margin beneath an overriding oceanic plate ." If this is true, the Taconic allochthon must have come from farther east than previously thought.

The former extent of the Taconic allochthon to the west is not known. There are some indications that it was upthrusted on the eastern edge of the Adirondacks, and might have extended an undetermined distance to the west (Whitney and Davin, 1987).

In southeastern New York, the Taconic allochthon is succeeeded by a late Middle Ordovician (Mohawkian) "autochthonus" terrigenous sequence (Snake Hill shale and Quassaic sandstones and conglomerate). These rocks record the progressive basin filling and westward encroachment of the terrigenous detritus through time. Elsewhere in New

York, the shallow-marine carbonates of the Black River Group (fig. 2.4) were forming when terrigenous sedimentation began in southeastern New York. Marine transgression on the post- Chazyan erosional surface was as widespread as ever before (Broughton et al. 1966; Isachsen et al. 1991, ch. 7) and may be interpreted, in Quinlan and Beaumont's (1984) scheme, as having occurred due to subsidence in response to a renewed thrust-loading to the east. Eustatic sea-level rise has also been invoked (Tankard,1986). The Taconics-derived sediments steadily encroached upon the shelf carbonates (Black River and overlying Trenton Group) and finally buried them as far west as the shore of Lake Ontario in the form of the Utica Shale and sandstones and shales of the Lorraine Group (fig. 2.4; Fisher, 1977).

The end of the Ordovician in the northern and central Appalachian basin was marked by deltaic sedimentation. An enormous delta, known as the Queenston Delta, eventually spread west to the midcontinent and south into Virginia (Broughton et al. 1966; Isachsen et al. 1991, ch. 7). In western New York the Lorraine Group rocks are conformably overlain by the non-marine deltaic strata of the Queenston Formation (fig. 2.4).

In the eastern part of New York it was, however, a time of erosion and is represented by yet another prominent unconformity. The unconformity is most marked in the Shawangunk Mountains where flat-lying, Silurian Shawangunk Conglomerate rests on tilted, Middle Ordovician Snake Hill shales. About 800m of the Upper Ordovician section might have been lost from eastern New York (Fakundiny et al. 1989). The erosion and deformation of Ordovician rocks in the eastern part of New York suggest that toward the end of the Ordovician Taconic deformation progressed from the east into New York State. The deformation was accompanied by block faulting in eastern and southeastern Adirondacks as well as the lower Hudson Valley, and ultrabasic intrusions (Cortlandt Mafic Complex) and metamorphism (Bedford Gneiss) in the Manhattan Prong. The extensive Taconic deformations and magmatic events of New England and eastern Canadian seaboard have been summarized by Rodgers (1967, 1971). In Central and Southern Appalachian, Taconic deformation was relatively mild.

The late Ordovician disturbance in New York was probably related to the arrival of the "Gander microcontinent" that was accreted east of an earlier "Dunnage

microcontinent" along the northeastern margin of the orogen (Williams and Hatcher, 1982). The collision with the Gander microcontinent probably caused a major uplift of the Taconics and caused shedding of enormous detritus from which the Queenston delta formed.

The Silurian, although the shortest of the Paleozoic periods, was marked by the most diverse depositional environments in New York region. When the Silurian period began, probably the entire state of New York was dry land with much of the state covered by red mud-flats of the Queenston delta (Broughton et al. 1966; Isachsen et al. 1991, ch. 7). A brief incursion of the sea took place in western New York in the early Silurian, but was soon halted by another upsurge in the Taconics when another, smaller pulse of clastics spread across the state and is now preserved in the deltaic rocks of the Medina Group.

Following the deposition and reworking of the Medina strata, the Silurian shoreline gradually advanced eastward. The Silurian sea was relatively shallow, and fluctuated from well-oxygenated to anoxic conditions probably in response to frequent eustatic changes or epeirogenic earth movement. In this sea the faunally and lithologically diverse sediments (sandstones; black, green and red shales; limestones; conglomerates; ironstones) of the Clinton Group were deposited (Rickard, 1975; Isachsen et al. 1991, ch. 7).

During the deposition of the Clinton Group sediments in central and western New York, more than 300m of quartz sand and pebbles of the Shawangunk Formation were deposited in southeastern New York and Pennsylvania in alluvial fans and braided streams. The fluvial sediments of the Shawangunk Formation were the products of the rapidly eroding Taconic Mountains to the east where tectonism had stopped in the early Silurian (Epstein and Lyttle, 1987).

The Taconic Mountains served as the major sediment source until the end of the Clinton time when the Rochester Shale was deposited. The Rochester Shale represents the final stages of the erosional decay of the orogen. This faunally diverse marine shale was deposited over much of New York and Ontario. In the west and northwest, the crest of the Algonquin Arch served as a high-energy shoreline along which a carbonate platform,

dominated by crinoidal shoals, was maintained while deposition of mud (Rochester Shale) took place farther east (Tankard, 1986).

The Taconic Mountains in the northernmost part of the Appalachians probably survived longer than farther south. Sediments derived from these lands, principally the Green Mountain Anticlinorium, accumulated mainly as turbidites in deep troughs to the east in east-central New England from late Ordovician to early Devonian time (Faill, 1985; Osberg, 1988). Somehow the late Silurian - early Devonian clastics from this source failed to reach New York, and even western New England, despite the proximity. Farther north, from the Gaspe Peninsula, part of these sediments might have bypassed the low-lying Laurentian craton and deposited in the Michigan basin (Faill, 1985).

After Clinton, the carbonates of the Lockport Group were deposited in the western half of New York and in the Ontario Peninsula in a shallow, clear and warm sea. The earliest coral reefs of New Yok are found in the Lockport dolostones. In east-central New York the Lockport carbonates grade into shale, and in southeastern New York at this time the fluvial sandstones and conglomerates of the upper Shawangunk Formation were accumulating.

In late Silurian time the climate in New York region turned arid and the sea withdrew to the west of New York leaving behind hypersaline embayments and lagoons on a vast sabkha-type mud flat. In this depositional setting, gypsiferous shales and thick salt deposits of the Salina Group formed in central and western New York. In the southeast, the Bloomsburg and Poxono Island shales were deposited at this time, but no evaporites are known (Rickard, 1975). The lithologic change from conglomerate and sandstones of the Shawangunk Formation to shales of the Bloomsburg and Poxono Island formations probably reflects progressivly deeper erosion into older argillaceous source rocks in the Taconics.

As the Silurian drew to a close, the Taconic land barrier to the east finally disappeared to permit influx of fresh seawater from the east (Isachsen et al. 1991, ch. 7). During this time the carbonates of the Cobblskill, Glasco and Rondout formations were deposited.

Warm and clear epicontinental sea covered vast areas of the Appalachian basin in the

early part of the Devonian when two prominent carbonate units, the Helderberg Group and Onondaga Formation, were deposited. The Helderberg and equivalent carbonates extend into Tennessee to the south and central Ohio to the west (COSUNA, 1985). The younger Onondaga and equivalent carbonates occur as far south as Kentucky and as far west as Ohio. The Onondaga Formation is well known for its coral reefs in New York and Ontario. Deposition of these carbonates was, however, not uninterrupted. The sea had withdrawn temporarily from all but southeastern New York, northwestern Pennsylvania and parts of Ohio in between, resulting in widepread erosion of the Helderberg limestones. In New York the erosional truncation of the Helderberg limestones moves deeper to the west and is complete in the Finger Lake area (Isachsen et al. 1991, ch. 8). The sea returned for a short time after the erosion of the Helderberg carbonates when the mainly clastic sediments of the Tristate Group (fig. 2.4) were deposited. Most prominent of the Tristate Group is the thin, basal Oriskany Sandstone which formed over much of northern and central Appalachian Basin. Another short-lived marine regression allowed erosional truncation of the Tristate rocks. When the sea returned, deposition of the Onondaga Formation began under a vast stretch of epicontinental sea that rivaled the Helderberg sea in size.

2.2: THE ACADIAN OROGENY:

The begining of the tectonic disturbance known as the "Acadian orogeny" was signalled in the early Devonian by a widespread volcanic event when the Tioga ash fall, centered in Virginia, almost covered the entire basin (Faill, 1985). In New York the Tioga Metabentonite occurs within the Onondaga Limestones at the base of it's youngest member, the Seneca. Although, the Acadian plate-tectonic event was centered, like the Taconic event, on New England and the Canadian Maritime Provinces, only slightly more eastward, it was quite distinct from its precursor.

The Acadian orogeny is believed to have resulted from a complex continent - continent collision between Laurentia, Armoria (Hercynian Europe), and possibly Gondwana with a number of terranes, or microcontinents, caught in between. On the basis of paleomagnetic data, Kent (1985) proposes that the "Traveler Terrane" (central

New England and New Brunswick, Canada) rotated clockwise and was welded against Laurentia in the Devonian. This was followed by northward translation of the successively outboard terranes, Avalon and Meguma, and a counter-clockwise rotation of the Meguma, which may have been associated with the early phase of the Alleghenian orogeny. According to William and Hatcher (1982) and Ettensohn (1985a), however, the Acadian orogeny best coincides with the accretion of the Avalon Terrane. In New Brunswick and Nova Scotia, evidence of deformation in the Upper Devonian and Carboniferous strata (Rodgers, 1967) suggests that there may not have been a significant break between the Acadian and succeeding Alleghenian orogeny in those areas.

Thus, unlike the Taconic event, which was marked by head-on collision of a continent and island arcs, the Acadian event was characterized by oblique convergence and transcurrent movement between continental blocks. Because of this, large-scale overthursts, so typical of the Taconic orogeny, are unknown for the Acadian. Instead, the Acadian orogeny was marked by widespread magmatic intrusion, metamorphism, faulting and folding, mainly in New England and the Canadian Maritime Provinces (Rodgers, 1967, 1970; Price and Hatcher, 1983; Faill, 1985; Osberg, 1988). The Merrimack Trough, trending NNE-SSW across Connecticut, Massachusetts and New Hampshire probably marked the axis of the Acadian Orogeny (Rodgers, 1970)

Although the brunt of the Acadian orogeny was on the northeastern margin of the Appalachian basin, it affected the entire length of the basin. The evidence in support of Acadian disturbance in the south is mainly isotopic and indicates Acadian-age metamorphism of various parts of the crystalline southern Appalachians (Faill, 1985). Several faults in the southern Appalachian were also active at this time, and the overriding of the North American craton by the Inner Piedmont - Blue Ridge thrust sheet that began during the Taconic orogeny continued in the Acadian (Hatcher, 1978; Hatcher and Zietz, 1980). In New York, the best evidence for the Acadian orogeny is found in the deformation and metamorphism of the Precambrian rocks of the Hudson Highlands (Fakundiny et al. 1989).

Within the basin-proper, and even at its margin, evidence of the Acadian orogeny is scanty and, at best, subtle. Arguments have been made for an Acadian age of the

folded and faulted Silurian and Lower Devonian rocks of the Helderberg Escarpment in eastern New York (see Marshak, 1986). These post-Taconian structures, however, have also been suspected to be of Alleghanian origin (Zadins, 1984; Faill, 1985; Marshak, 1986). In general, it has been difficult to separate the subtle Acadian structures from the superimposed, stronger Alleghanian structures.

Within the basin, the strongest manifestation of the Acadian Orogeny is neither structural nor magmatic, but sedimentological. An enormous volume of clastic sediments, stripped from the Acadian Mountains, prograded over the northern and central Appalachians from northeastern source terrains during the middle and late Devonian and far exceeded the amount of sediment involved in the Taconic clastic wedge. The Acadian clastic wedge, popularly known as the 'Catskill Delta,' was a composite wedge and consisted of many pulses of subaerial alluvial fan-delta progradation (Isachsen et al. 1991, fig. 8.16).

In New York, the entire Middle and Upper Devonian sequence can be divided into five time-transgressive, west- ward prograding facies (fig. 2.6) interspersed with thin calcareous units that represent short breaks in terrigenous sedimentation and episodes of marine transgressions. The 'Portage-A facies' consists of relatively unfossiferous, black or greenish-gray shales and is inferred to have formed in a relatively deep, dysaerobic basin (Fakundiny et al. 1989; Isachsen et al. 1991, ch. 8). The 'Portage-B facies' consists of black and dark gray shales with thin turbidites and represent deposition on the basin-floor, slope and open shelf below the wave base. The 'Chemung facies' originated in shallow-water, peritidal to subtidal shelf environments. The 'Chattaraugus facies', found only in the Upper Devonian, represents interbedded marine and non-marine sedimentation in a peritidal zone. The 'Catskill facies' represents the subaerial delta and exhibits fining-upward cycles of channel deposits of cross-bedded sandstones and overbank deposits of red, green and gray shales. The 'Pocono facies', consisting of thick-bedded, quartz-pebble conglomerate and sandstones, represent braided-stream deposits on a piedmont.

In the Middle Devonian Hamilton Group, the occurrence of several thin limestone units (Cherry Valley, Stafford, Centerfield, Tichenor, Menteth and Portland Point

Figure 2.6: Generalized stratigraphic cross-section of the Devonian in New York showing various facies of the Catskill fan-delta complex. (Modified from Rickard, 1981).

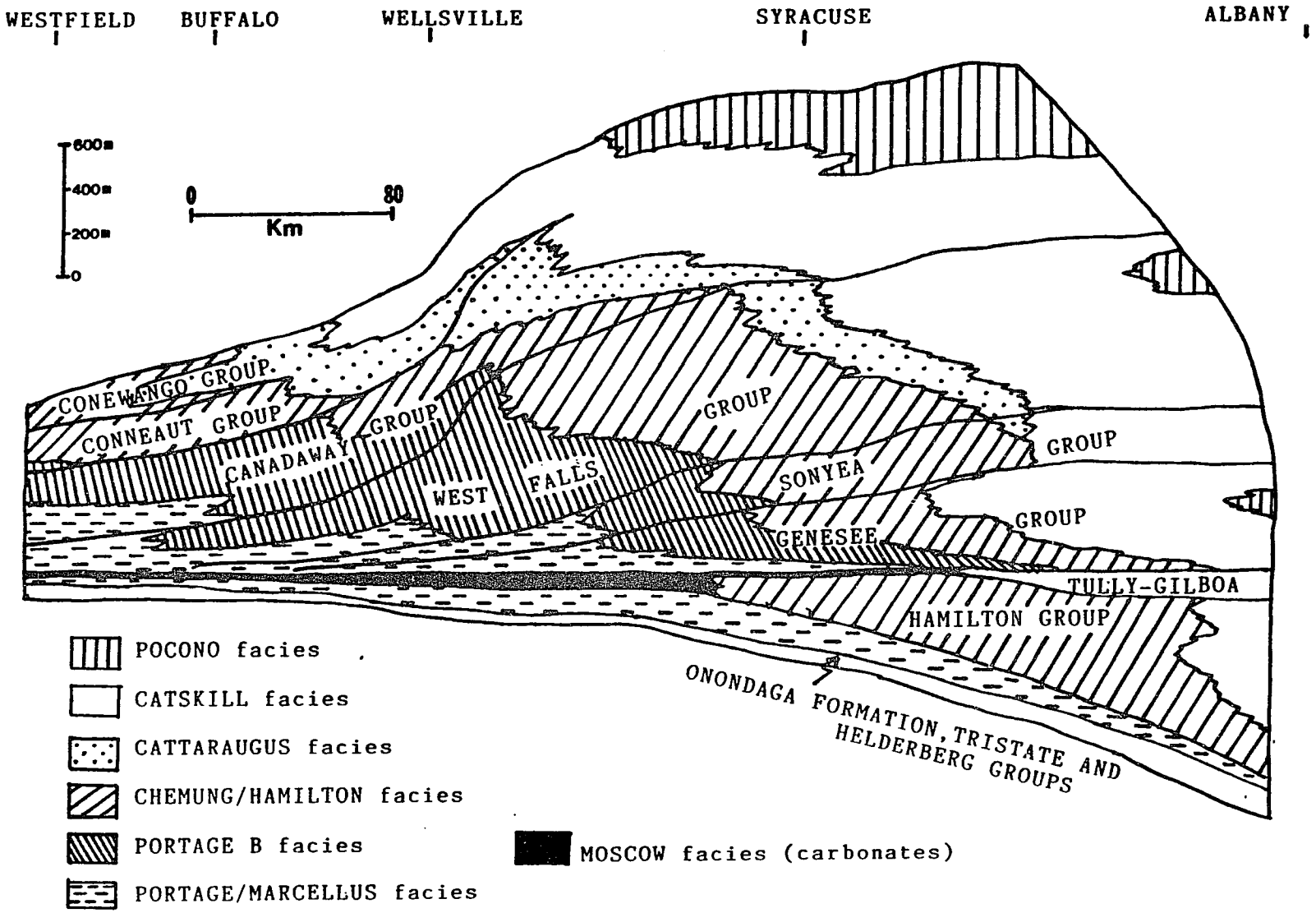
WESTFIELD
BUFFALO
WELLSVILLE
SYRACUSE
ALBANY
600
400
200
0
0
80
Km
CONEWANGO GROUP
CONNEAUT GROUP
CANADAWAY GROUP
WEST FALLS GROUP
SONYEA GROUP
GENESEE GROUP
TULLY-GILBOA
HAMILTON GROUP
ONONDAGA FORMATION, TRISTATE AND HELDERBERG GROUPS
POCONO facies
CATSKILL facies
CATTARAUGUS facies
CHEMUNG/HAMILTON facies
PORTAGE B facies
PORTAGE/MARCELLUS facies
MOSCOW facies (carbonates)

members) in western and central New York probably indicates periods of interruption in supply of terrigenous sediments from the newly rising Acadian Mountains. Probably, the most significant break in the development of the Catskill deltaic sedimentation took place at the end of the Middle Devonian when the limestones of the Tully Formation were deposited over much of New York with the exception of the eastern part (Heckel, 1973; Rickard, 1975).

The building of the "Catskill delta" resumed in full force from the begining of the Upper Devonian and the landward facies prograded steadily over the seaward facies to the west throughout the Upper Devonian. This indicates that the subsidence of the basin was more than matched by sediment supply from the Acadian Mountains during this interval. In fact, progradation of the subaerial part of the delta toward western New York was so rapid that the Catskill delta has been called a "tectonic fan-delta complex" (Johnson and Friedman, 1969; Friedman and Sanders, 1978). No limestone units are known in the Upper Devonian of New York, and brief periods of relatively rapid deepening of the basin are probably indicated by tongues of several black shales confined to the western half of the state (Rickard, 1975). These black shales too are missing from the latest Devonian Conneaut and Conewango groups indicating that toward the end of the Devonian the subaerial Catskill fan-delta complex had reached the western margin of New York State.

The sedimentologic record of the late Paleozoic is missing from most part of New York. Scattered patches of the Lower Mississippian Knapp Formation and the Lower Pennsylvanian Olean Formation are found only along the southern border of New York (fig. 2.3). These are the northerly extensions of the post-Devonian clastic wedge (Pocono) of Pennsylvania. It is possible that these rocks once covered more extensive areas in New York but were subsequently removed by erosion (Friedman and Sanders, 1982; Johnsson, 1986; Gerlach, 1987).

The Catskill deltaic deposition is believed to have shifted southward through the Devonian-Mississippian time in response to successive collisions of the St. Lawrence, New York and Virginia promontories with the obliquely converging Avalon microcontinent (Ettensohn, 1985a,b). The Lower Mississippian clastics of the Pocono

Wedge in south-central Pennsylvania and southwestern Virginia and the equivalent shales (Chattanooga) of Tennessee and Alabama probably represent the dying stage of the Catskill deltaic sedimentation and the Middle Mississippian carbonates overlying these rocks mark the end of the Acadian Orogeny (Ettensohn, 1985a).

2.3: THE ALLEGHANIAN OROGENY:

The late Paleozoic (Carboniferous - Permian) Alleghanian orogeny reorganized much of the Appalachian basin into its present structural configuration. The Alleghanian orogeny is distinct in that its most spectacular deformation, the folding of the Valley and Ridge Province, was within the basin, whereas the Acadian and Taconic deformations were confined to the eastern orogenic belt. Secondly, the effects of the Alleghanian orogeny were felt most strongly in the southern and central Appalachian, whereas the Acadian and Taconic orogenies were centered in the northeastern edge of the basin. Also, unlike the previous two orogenies, the Alleghanian orogeny was marked by little magmatism.

A number of similarities, however, exist between the Alleghanian and the Taconic orogenies. Like the Taconic, the Alleghanian was a compressive tectonic event, this time associated with convergence and collision between Laurasia and Gondwanaland (Hatcher, 1978). Both were also marked by extensive thrusting. But, while Taconic thrusting was confined to the eastern basin margin, the Alleghanian thrusting was in the form of decollement in which the Paleozoic cover in the southern and central Appalachians moved northwestward along subhorizontal faults (decollements) above the basement into the basinal part (Gwinn, 1964; Perry, 1978; Hatcher and Zietz, 1980; Price and Hatcher, 1983; Faill, 1985). The net northwestward displacement of the detached rocks is estimated at 200km in Alabama, Tennessee and Kentucky and about 100km in Pennsylvania (Gwinn, 1964; Cook et al. 1979; Ando et al. 1983). Fault splays from the master decollement zone created folds, step faults and listric thrust faults in the Valley and Ridge and the Plateau provinces (Gwinn, 1964; Faill, 1985). These rootless structures gradually become diminutive from southeast to northwest into the Applachian Plateau where only broad and open folds are found.

In New York, deformation that may be attributed to the Alleghanian orogeny includes (1) the broad and open folds in the plateau in south-central New York, north of the Pennsylvania border, (2) tight folds and thrust faults in a "miniature valley and ridge province" along the Hudson Valley (Marshak, 1986), and (3) mesoscopic and microscopic structures like joints, mechanical twins, solution cleavage, crenulation cleavage, pencils and deformed fossils (Engelder and Engelder, 1977; Engelder and Geiser, 1979, 1980; Geiser and Engelder, 1983).

The open folds along the southern border of New York have limbs that dip at angles of only 1-2° and trend about ENE-SWS (Tillman and Barnes, 1982). These folds may have resulted from decollement tectonism located in the subsurface Salina rocks (Gwinn, 1964; Jacoby and Dellwig, 1974) and mark the northern termination of large-scale Allleghanian structures in the Appalachian Plateau.

The fold-thrust belt of the Hudson Valley has much smaller-scale structures than those in the Valley and Ridge province with which it is apparently continuous. The trend of the structures in the Hudson Valley is also different, NNE-SSW, as opposed to the NE-SW trend in the the Valley and Ridge. There is considerable disagreement as to the age of these structures in the Hudson Valley: both Acadian and Alleghanian have been proposed (see Marshak, 1986 for discussion).

The meso- and microscopic structures found in the Paleozoic rocks, primarily Devonian, of New York are believed to represent "layer-parallel shortening fabrics" resulting from the Alleghanian orogeny (Engelder and Geiser, 1979, 1980; Geiser and Engelder, 1983). These authors recognize two non-coaxial phases of Alleghanian deformation from these fabrics. The effects of the early or "Lackawanna Phase" deformation are found mainly in the Hudson Valley and are interpreted as a possible product of strike-slip motion between the Avalon microcontinent and North America. The shortening fabrics that occur throughout the Plateau as well as the Valley and Ridge Province, and are parallel to the trend of major structures, have been attributed to the "Main Phase" of the Alleghanian orogeny which has been correlated with the final convergence of Africa against North America and the accreted terranes.

It has proved difficult to firmly establish the timing of the Alleghanian orogeny.

Structural evidence from the southern Maritime Province suggests a nearly continuous or spasmodic orogenic movement from Middle Devonian to early Permian with no clear boundary separating the Acadian from the Alleghanian events (Rodgers, 1967). In the Appalachian Plateau and Valley and Ridge Province, the Alleghanian movement seems to have begun in the post-Lower Permian (Rodgers, 1967; Van der Voo, 1979), while in the southern Appalachian the movement may have begun as early as the Mississippian (Rodgers, 1967). According to Geiser and Engelder (1983) the "Lackawanna Phase" of Alleghanian deformation in New York was probably initiated in the Pennsylvanian whereas the "Main Phase" began in the early Permian.

2.4: POST-ALLEGHANIAN PERIOD:

There is no direct sedimentological record of the end Devonian - Late Triassic interval in New York, although much has been written about the missing post-Devonian strata (chapter 3). Triassic - Jurassic rocks of the Newark Supergroup are preserved only in the Rockland County of southeastern New York (Sanders, 1963, 1974). These rocks represent the northeastern extremity of the Newark- Gettysburg Basin, the largest of the onshore Triassic basins of eastern North America.

These basins began forming in the Late Triassic as the late Paleozoic supercontinent drifted north, probably over a hotspot (Morgan, 1980) or across a tensional stress field (Bedard, 1985). The crust was pulled apart along old fractures, sutures and transforms, legacy of the three preceding plate tectonic events, and rifting of the crust and the definitive opening of the Atlantic Ocean began. The extension along the proto-Atlantic axis led to the formation of at least 30 clastic and evaporitic 'synrift' basins in North American and African plates (Manspeizer and Cousminer, 1988). Onshore in eastern North America, these basins are now part of the Piedmont Province. Recurrent subsidence due to downwarping of the ductile crust followed by faulting in the brittle crust allowed accumulation of huge quantities of terrestrial sediments in these small basins amounting to 7-9km in the Newark-Gettysburg Basin alone (Sanders, 1963; Olsen et al. 1982).

The Triassic basins were closed basins with internal drainage and are characterized by fluvial sandstones and conglomerates that thicken toward the axis of the basins where

they interfinger with deep water lake deposits (Manspeizer and Cousminer, 1988).

In New York, the rocks of the Newark Supergroup (Stockton and Brunswick formations) were intruded by the Palisade diabase sills about 195 Ma in the early Jurassic time (Fakundiny et al. 1989). Similar sills and flood basalts of early Jurassic time occur in nearly all the Triassic basins of eastern North America (Boer et al. 1988).

Another Mesozoic magmatic event in New York, unrelated to the Triassic basins, is represented by kimberlite dike swarms of the eastern Finger Lake district between southwest of Syracuse and Ithaca. Most of these kimberlites crop out as vertical dikes in prominent N-S joint sets (Kay et al. 1983). Radiometric dates (~140 Ma) suggest a Late Jurssic to Early Cretaceous age for some of these dikes (Basu et al. 1984). These intrusions, along with other kimberlites, occur along a trend extending from Tennessee to New York coinciding with the "Keel Line", or the deepest part of the Appalachian Basin (Dennison, 1983; Kay et al. 1990). According to Dennison (1983), the dikes were intruded along fractures that developed along the Keel Line as a result of stretching due to post-Alleghanian isostatic rebound. Mantle fragments in some kimberlites around Ithaca suggest that the magma was derived from the mantle at depths of 150km or more (Kay, 1990).

Evidence for mixed Mesozoic-age uplift in New York come from Tillman and Barnes' (1983) work with fluid inclusions in mineralized faults of west-central New York and fission-track data of Miller and Duddy (1986), Duddy et al. (1987), and Miller (1990).

The post-Cretaceous was a time of extensive erosion when the modern landscapes of New York and much of the Appalachians were sculpted (Rodgers, 1967). Much of the eroded sediments have found their way into the encroaching Atlantic Ocean; some of it has been deposited in the Coastal Plain Province. In New York, Cretaceous and younger deposits (Raritan and Magothy formations) of the Coastal Plain are confined to parts of Long Island and Staten Island. Evidence of continuing uplift in the Adirondacks has been cited by Isachsen (1985).

The lack of sedimentological record requires that the entire post-Devonian geological reconstruction of New York be based on several lines of indirect evidence, which will be

discussed in the following chapters. Surely, erosion dominated the post-Devonian geologic histroy of New York, but how much erosion took place and when it began remain to be resolved.

CHAPTER: 3

PREVIOUS STUDIES

Prior to the 1980s, it was generally believed that since the end of Devonian time little sediment had accumulated in the Northern Appalachian Basin of New York and the Alleghanian Orogeny had failed to have much impact on sedimentation in this area (Meckel, 1970). This interpretation was primarily based on the absence of post-Devonian strata from much of New York and apparent thinning or pinch-out of many post-Catskill units to the northeast (Wood et al. 1969; Edmunds, 1979).

However, a look at the distribution of Paleozoic rocks in the Northern Appalachian suggests that this interpretation may have been premature. As seen in figure 3.1, the Devonian Isopach map shows a northwestward thinning from a maximum preserved thickness in eastern Pennsylvania. A south-to-north thinning is not observed and the edge of Devonian outcrops is marked abruptly by erosional retreat (to the south) of the Helderberg and Onondaga escarpments across New York State.

The Conodont Color Alteration Index (CAI) isograds of the Ordovician and Silurian through Middle Devonian carbonates of the northern Appalachian also have a NNE-SSW trend with the isograd values increasing to the east (fig. 3.2). The Upper Devonian - Mississippian CAI isograd map (fig. 3.3) also shows a projected northeast-ward increase in CAI values in New York state. If the CAI values were acquired from burial heating (Harris et al. 1978; Harris, 1979), it can be inferred from figures 3.2 and 3.3 that the Devonian and possibly younger overburden once extended over the Adirondacks.

The thickness of extant Carboniferous strata in northeastern Pennsylvania is 1.5km (Levine, 1986). Provenance studies by Pelletier (1958) and Edmunds (1979) indicate a predominant southeastern source and a secondary northeastern source. The northeastern source may not necessarily have been New York, but farther northeast, probably the northern New England and the Canadian Maritime Provinces, where tectonism was apparently continuous from the Acadian to the Alleghanian (Rodgers, 1967).

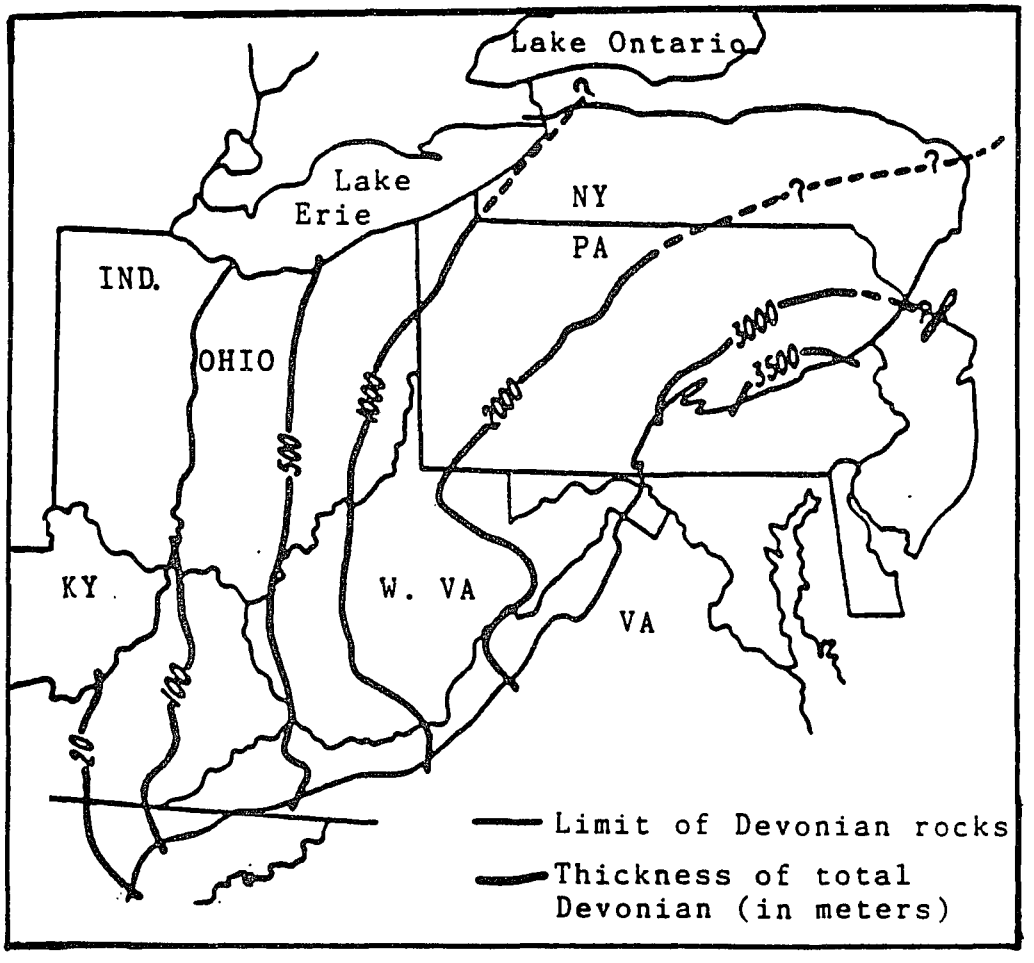

Figure 3.1: Isopach map of the total Devonian in central and northern Appalachians. Isopleths are dashed where only part of the Devonian remains. (After Faill, 1985).

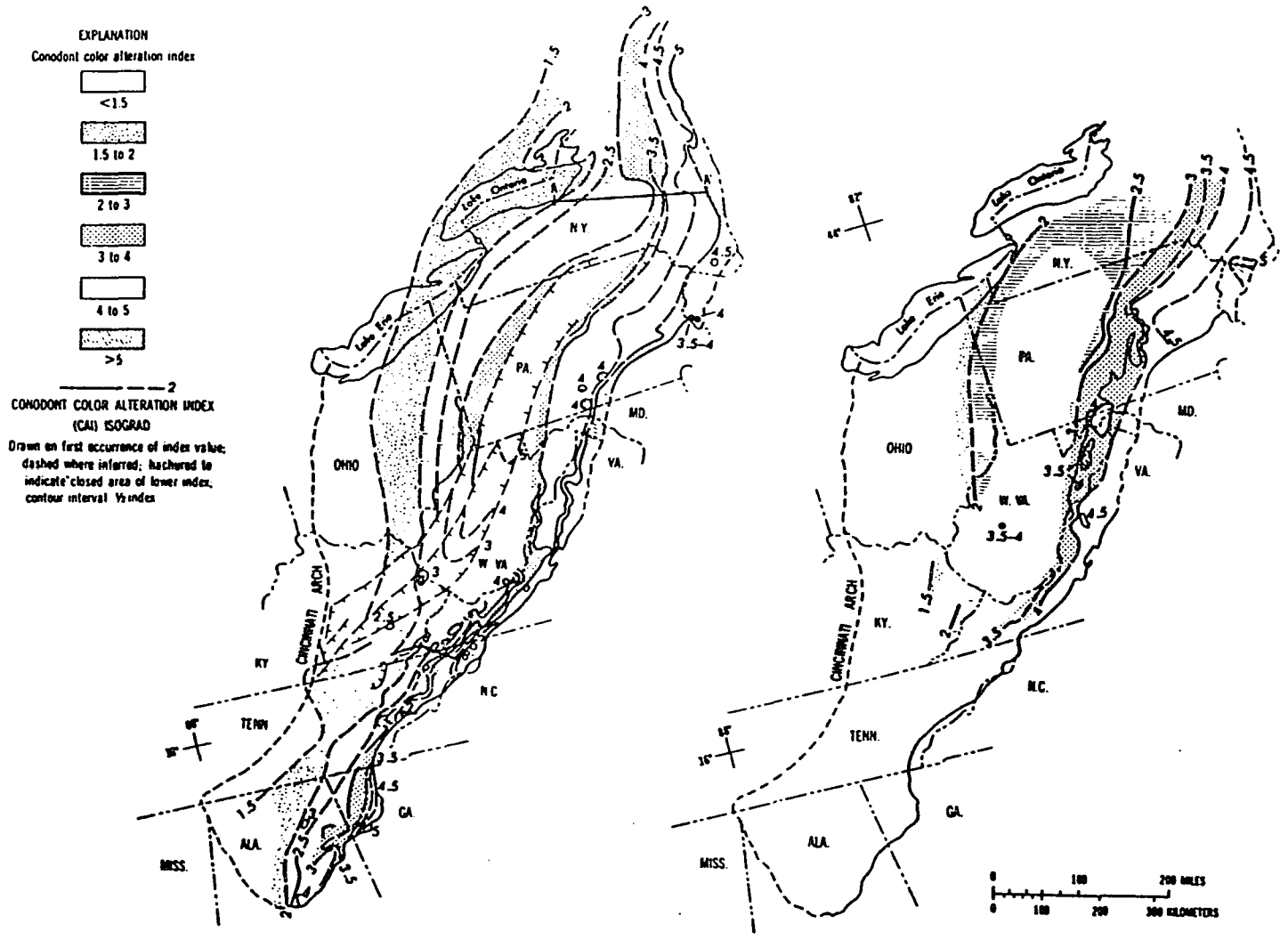

Figure 3.2: Conodont color alteration index (CAI) isograd map for (A) Ordovician carbonate rocks and (B) Silurian through Middle Devonian limestones in the Appalachian basin. (From Harris, 1979).

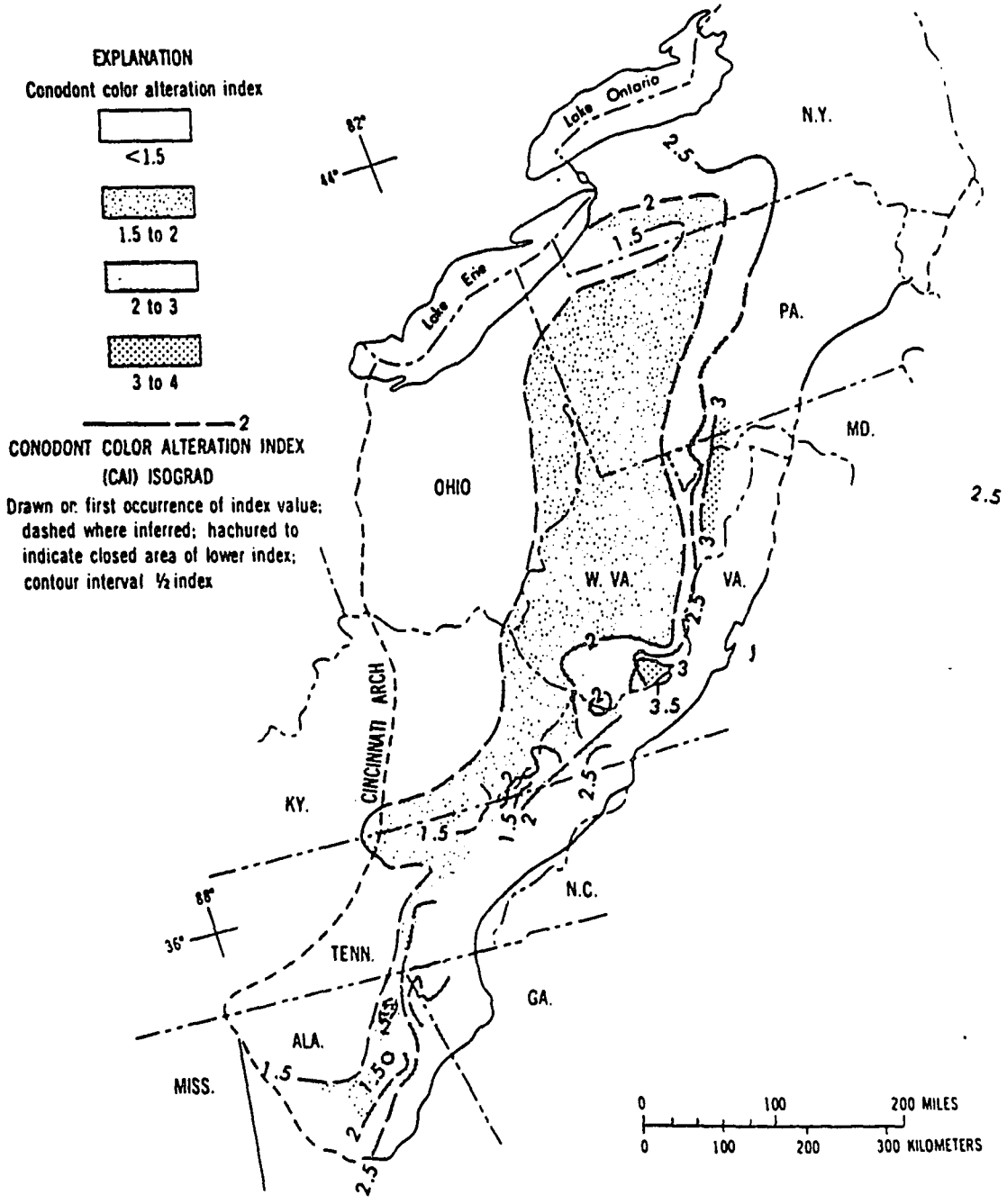

Figure 3.3: Conondont color alteration index (CAI) isograd map for the Upper Devonian through Mississippian carbonate rocks in the Appalachian basin. (From Harris, 1979).

Consequently, the New York region may still have been receiving sediments in the Carboniferous time. Sedimentation may have been largely in the form of subaerial deltaic deposits much like those in the Late Devonian, or the Carboniferous in Pennsylvania and farther south. As in the example of the Devonian outcrops, the northern extent of the Carboniferous rocks along the southern border of New York is also marked by an erosional boundary. The question is: how much of these younger rocks were once present in New York, and when and how they were removed?

In the last decade a significant number of publications have challenged the former notion of little or no post- Devonian sedimentation in New York. Most of these studies, discussed below, are based on various paleotemperature signatures of the surficial or shallow subsurface rocks in New York and adjoining areas. The inferred paleotemperatures are rather high and have generally been interpreted as having been acquired during deep burial. Deep burial of these rocks requires the former presence of post-Devonian strata much thicker than previously thought.

The earliest works that allude to former deep burial of the surface-exposed strata in New York are perhaps those by Epstein et al. (1977), Harris et al. (1978), and Harris (1979). As seen in figure 3.2, the CAI values for Silurian- through-Middle Devonian carbonates range from 2.5 to 4.5 west to east along the northern erosional edge of these rocks south of the Mohawk Valley. In the Ordovician carbonates, CAI of 3 is found in outliers within the Adirondack itself and CAI of up to 5 is found along the Adirondack's eastern margin. If the Middle Devonian carbonates of New York (approximately 380 m.y old) started being uplifted in the late Pennsylvanian, coinciding with the onset of the Alleghanian orogeny, then the maximum time of burial and heating was about 100 m.y (see Harris, 1979). Using Harris' (1979, fig. 2) method of calculating the lowest possible "maximum paleotemperature" from CAI and burial time, a temperature range of 110 - 250° C is obtained for the CAI range of 2 - 4.5. If uplift began in the Middle Triassic, coinciding with the rifting of the eastern North America, a maximum burial time of 180 m.y can be assumed (Harris, 1979), and paleotemperatures of 100 - 240° C are obtained for the same CAI range. If a paleogeothermal gradient of 30°C/km and a mean annual surface temperature of 20°C (sect. 4.7.2) are used, these temperatures translate into about

2.5km post-Middle Devonian overburden near the southwestern margin of the Adirondacks and a staggering 7.6km along the Hudson Valley, southeast of the Adirondacks.

On the basis of conodont data from Epstein et al. (1977), the presence of Paleozoic outliers in the Canadian Shield, and lack of unequivocal evidence from isopach maps of former absence of late Paleozoic rocks in the Northern Appalachian, Crough (1981) concluded that southeastern Canada and New England were elevated and eroded at least 4km relative to the Central Appalachian. According to Crough (1981), the uplift took place in the Cretaceous - Early Tertiary time when the northeastern part of North America moved over a hotspot.

Friedman and Sanders (1982), on the basis of vitrinite reflectance of anthracite-grade plant debris, alteration index of associated carbonized kerogen, conodont alteration index, and authigenic mineralogy in the uppermost Middle Devonian Gilboa Formation of the eastern Catskill Mountains, concluded that the Catskill Mountains were once buried to a depth of about 6.5km. They used Hood et al.'s (1975) method (sec. 4.4) to calculate the maximum paleotemperature (190° C) from a vitrinite reflectance of 2.5% and an assumed heating time of 200 m.y. Then using a paleogeothermal gradient of 26°C/km and a mean annual surface temperature of 20°C, they calculated a burial depth of 6.5km for the Gilboa samples.

Friedman and Sanders' (1982) study came under attack from Levine (1983), who questioned the various assumptions and measurement errors inherent in Hood et al.'s (1975) diagram, the choice of a long heating time and a low geothermal gradient and the use of vitrinite reflectance data from a single sampling site. Friedman and Sanders (1983) responded that while the use of higher geothermal gradients makes a considerable difference in their estimate of burial depths, a much lower heating time (35 m.y) increases the burial depths by only about 1km for any geothermal gradient used. Friedman and Sanders (1982), however, show that a vitrinite reflectance gradient of 1.4%/km measured in boreholes of the Southern Anthracite Field, Pennsylvania by Levine (1983) was too high for the Catskills. For a vitrinite reflectance of 2.5% in the Gilboa samples, this gradient means a burial depth of only 1.79km, but a paleo-

geothermal gradient of 91-105° C/km. No evidence exists for such a high paleogeothermal gradient in the Catskill region. The basal Paleozoic rocks in the area, 4.5 km below Gilboa, show no evidence of metamorphism which would be expected if such a high geothermal gradient existed (Friedman and Sanders, 1982).

A different source of evidence, perhaps overlooked by both Friedman and Sanders (1982, 1983) and Levine (1983), and one that makes Friedman and Sander's estimate of burial depth not too surprising, is stratigraphic. At least 2.4 km of post-Gilboa, Upper Devonian strata are preserved in western New York (Rickard, 1975) and depositional thickness increased to the east (Catskill region) towars the Acadian sediment source. Projecting this thickness over the Catskill site, it requires about 4km (not 6.5km) post-Devonian cover to explain the vitrinite reflectance of 2.5% using Friedman and Sander's (1982) method. If one uses a higher geothermal gradient (for example 30° C/km, approximately the present average geothermal gradient of New York, Hodge et al. 1982) and the mean vitrinite reflectance (not the maximum), the estimated thickness of post-Devonian strata in this area decreases to less than 3km.

Tillman and Barnes (1983), on the basis of fluid- inclusion study of mineralized faults and fractures in the Upper Ordovician Oswego sandstones of northwestern New York, inferred that fracturing and mineralization represented two episodes of post-Alleghanian deformation. The first period of deformation was associated with a cooling (176°C to 120°C) event and took place when these rocks were at depths of 3 to 3.5 km. A second episode of deformation, in the form of normal faulting, was associated with another cooling (112°C to 76°C) event and resulted from 1 to 2km uplift and erosion during the Cretaceous. A paleogeothermal gradient of 25°C/Km would require a burial depth of 5-6km for these rocks to attain the above temperatures, but Tillman and Barnes (1983), without elaborating, rejected these as "too high a figure based on other geologic lines of evidence". They inferred that the geothermal gradient was locally elevated as a result of migration of warm basinal fluid orignating from clay dehydration at a deeper level.

Lakatos and Miller (1983), in their fission-track study of apatite and zircon particles, concluded that the lowermost Upper Devonian strata in the Catskill area were buried to

about 4km in the last 125 m.y and between 4 and 7km prior to that under younger deposits. The conclusions of this study are in line with those of Friedman and Sanders (1982).

Gale and Siever (1986) studied the diagenesis of Catskill facies sandstones in southeastern New York. They concluded that these rocks suffered deep burial during the late Paleozoic and uplift and erosion after the Allegheny Orogeny".

On the basis of fission-track and clay-diagenesis study of the lower Middle Devonian Tioga Bentonite across New York State (fig. 3.4), Johnsson (1986) suggested that this geologically isochronous unit might have been buried to about 7km in eastern New York. Projecting the thickness of the post-Tioga Devonian section of New York onto the outcrop belt of the Tioga Bentonite, he inferred that nearly 4km of post-Devonian sedimentary rocks, now eroded, once covered the area. This estimate is about the same as that implied in Friedman and Sanders' (1982) study.

Karig (1987) questioned Johnsson's (1986) interpretation of deep burial of the Tioga Bentonite bed on the ground that the low uniform paleogeothermal gradient of 20 - 25°C/km used by Johnsson to calculate the burial depths may have been inappropriate. For example, the abrupt increase in inferred paleotemperature (i.e, low fission- track age and high illite concentration south of Syracuse in fig. 3.4), could have resulted from a thermal anomaly associated with the kimberlite dike swarms of the eastern Finger Lake area (fig. 2.3; Karig, 1987). Johnsson (1987) replied that the occurrence of these dikes also coincides with the axis of greatest sediment accumulation, or the "keel line", in the Appalachian Basin (Dennison, 1983), so that it was difficult to separate out the paleotemperature signatures of rocks of central New York originating from deep burial from those imprinted by the dikes. In section 4.7.2, the possible role of the Finger Lake dikes in the paleotemperature history of New York is discussed.

Urschel and Friedman (1984), on the basis of fluid inclusion, oxygen isotope, and vitrinite reflectance studies of the Lower Ordovician Beekmantown carbonates of the upper Hudson and Champlain valleys concluded that these rocks may have been buried to as much as 7km. If one assumes that the Middle Ordovician to Upper Devonian section elsewhere in New York (5km, Rickard, 1975; Fisher, 1977) once extended to

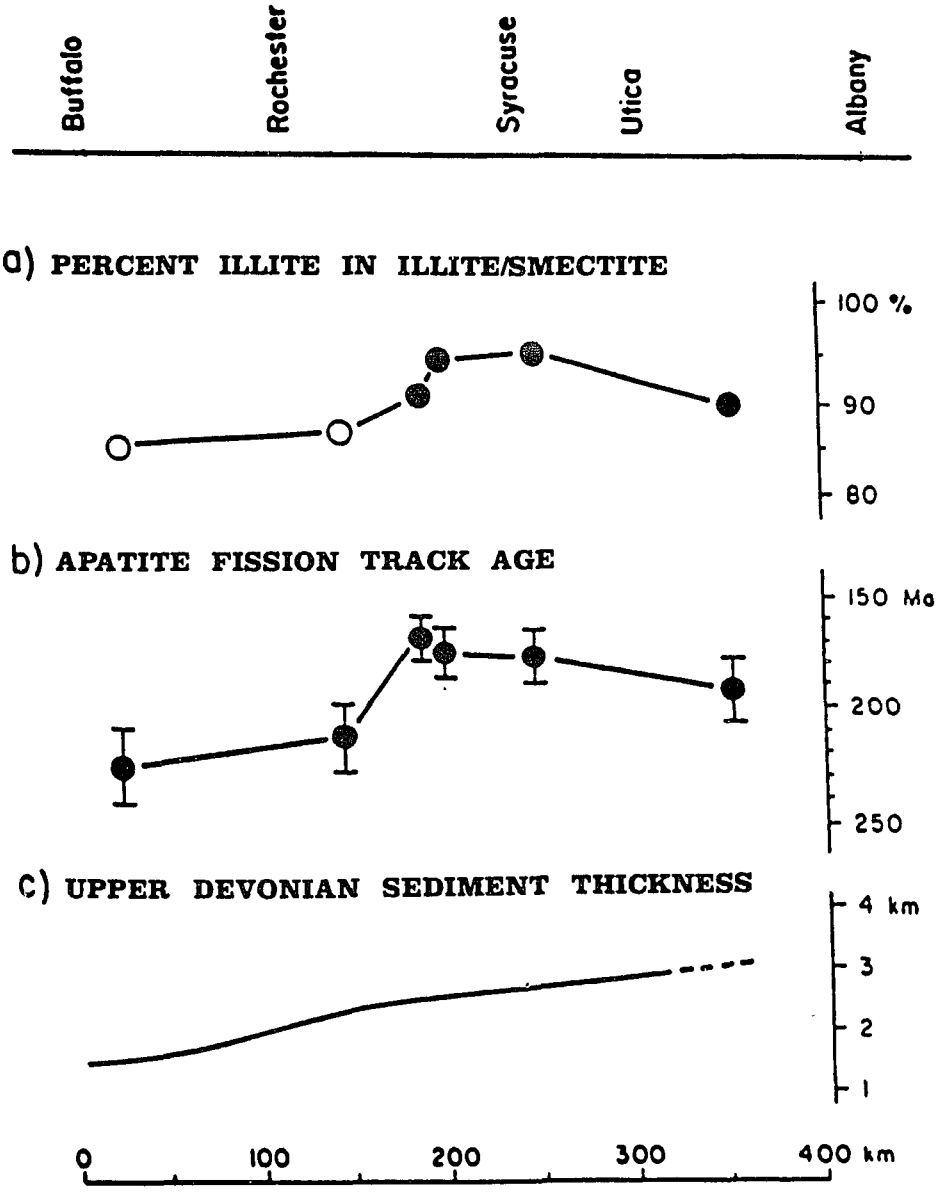

Figure 3.4: West to east profiles of (a) percentage of illite and (b) apatite fission track ages of the Middle Devonian Tioga metabentonite across New York State, and (c) estimated thickness of the overlying Upper Devonian sediments projected on the profiles from southern New York. (From Johnsson, 1986).

this area, a 2km post-Devonian overburden is necessary to account for the 7km burial.

In a similar study on the Middle Ordovician Chazy Group carbonates of the Champlain Valley, Brockerhoff and Friedman (1987) inferred a former burial depth of about 5km for these rocks. Since no stratigraphic section separates the Chazy rocks from the underlying Beekmantown, the inconsistency in the estimated burial depths of these two units (Urschel and Friedman, 1984; Brockerhoff and Friedman, 1987) probably is due to a low number of fluid-inclusion data on which the paleotemperature and burial estimates were mainly based in both studies.

On the basis of vitrinite reflectance, sediment compaction and fluid-homogenization temperature study in the anthracite district of northeastern Pennsylvania, Levine (1986) inferred a former burial depth of 6-9km for the extant Carboniferous strata. However, according the Levine, the paleomagnetic ages for the folding and paleobotanical ages of the youngest rocks in the area delimit the maximum time of burial and deformation to a relatively short interval (290 - 270Ma). The high sedimentation rate required for the proposed burial of these rocks in such a short time would be geologically unrealistic. He proposed rapid tectonic burial under Alleghanian overthrusts as a possible burial mechanism. Although structural evidence for a large overthrust in the area is lacking, Levine (1986) contends that thrusting could be in the form of smaller imbricate slices and could at least serve as proximal source for very rapid sedimentation. One could argue that similar mechanism of burial could have operated in southeastern New York, not far from the northeastern anthracite region and cause the deep burial of the Devonian strata (Friedman and Sanders, 1982; Lakatos and Miller, 1983) there. Levine's (1986) study thus shows a significant departure from his earlier contention (Levine, 1983) that the Catskill area could not have been buried under thick Carboniferous overburden.

In Cherry Valley, east-central New York, Gurney and Friedman (1987) studied fluid inclusions, oxygen isotopes and vitrinite reflectance of the Lower Devonian Helderberg and lower Middle Devonian Onondaga limestones. They inferred a former burial depth of about 5km for these rocks. Projection of the 2.5km thick post-Tioga Devonian section of southern New York onto Cherry Valley indicates a former presence of about 2.5km

post-Devonian strata. This estimate is consistent with the result of Johnsson's (1986) work, which included Tioga samples from the same Cherry Valley outcrops, but were based on entirely different techniques. As described before, the Tioga Bentonite bed occurs within the Onondaga Formation.

Similarly, fluid-inclusion studies of the Middle Silurian Lockport dolostones of western New York suggest a former burial depth of 5km (Friedman, 1987a, 1987b). A lower estimate of 4km is given by Gross and Engelder (1989), who studied the fracture system and fluid-homogenization temperatures of the fracture-filling calcite in the same rocks. A former presence of 2.5 to 3km post-Devonian strata can be inferred for the area between Buffalo and Rochester, if the thickness of the post-Lockport rocks between southwestern and southcentral New York is projected onto the Buffalo-Rochester transect.

Gerlach's (1987) Lopatin modeling, based on regional vitrinite reflectance trend in the Upper Devonian Rhinestreet Formation (black shale) in south-central New York, shows that a northward extension of the Carboniferous strata from Pennsylvania is necessary to account for the high thermal maturities observed in the studied rocks. His estimate of the "minimum" thickness of the Carboniferous rocks in the study area ranges between 1.20 and 3.37km.

Beaumont et al. (1987) used a mathematical- geodynamic model to simulate the possible effects of the Alleghanian orogeny on the Late Paleozoic evolution of the sedimentary basin of the eastern interior of North America. They reconstructed the maximum sediment thickness distribution in some undisturbed parts of the Appalachian basin at the height of the Alleghanian orogeny by using moisture-content data from near-surface coals. The model that agrees with these data predicts that the Alleghanian overthrusts had thickened the crust by as much as 20km in the Appalachian and Ouachita orogens. The predicted erosion required to bring the coals to the surface exceeds 15km in some areas. In New York, according to their model, post- Alleghanian erosion ranged from about 3km in western New York to about 9Km in southeastern New York (fig. 3.5). It is interesting to note the similarity of this predicted value for southeastern New York with the 6-9km burial of the Carboniferous strata in northeastern Pennsylvania

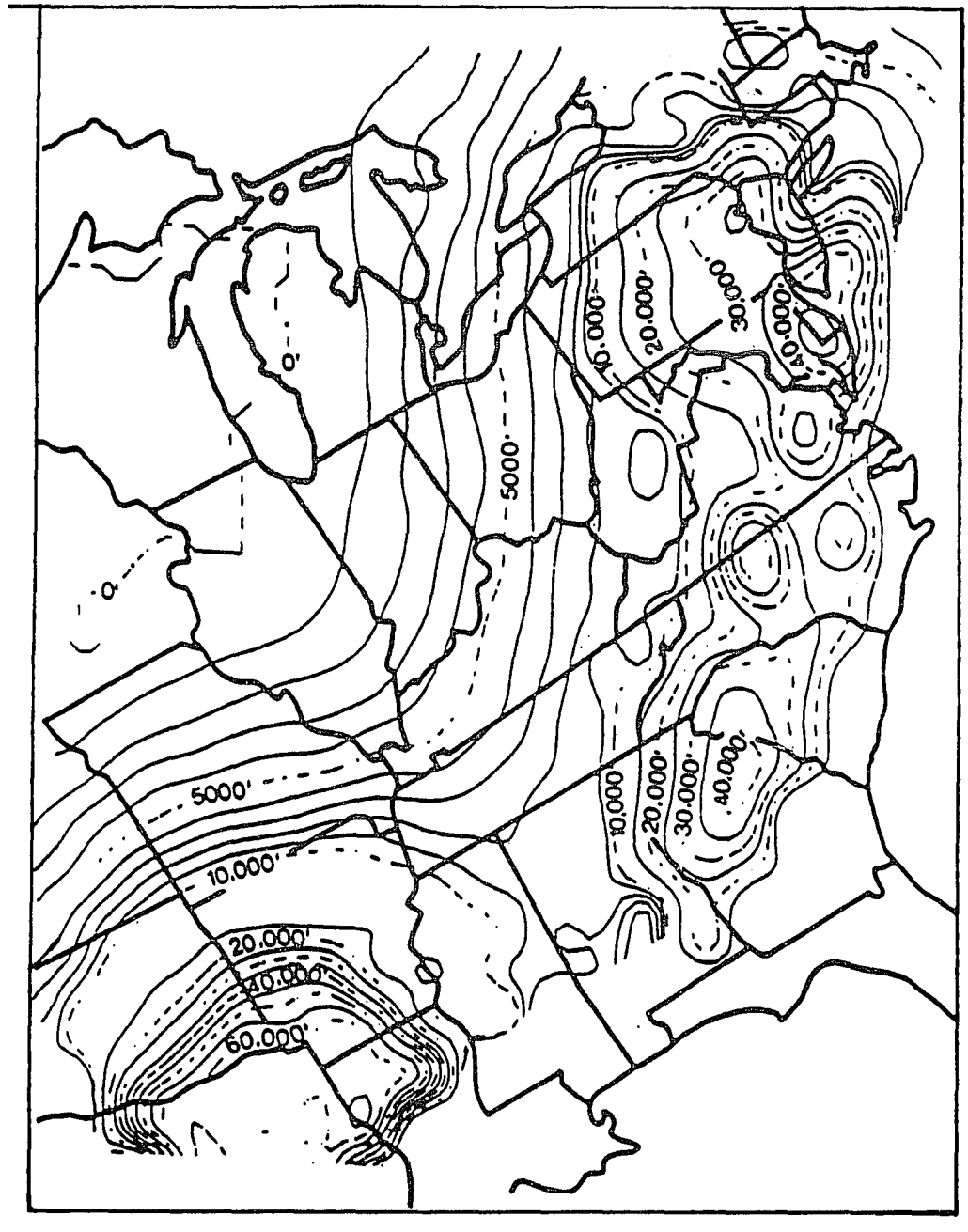

Figure 3.5: Isopachs (in feet) of predicted missing strata from the Appalachian basin due to post-Alleghanian erosion, based on mathematical geodynamic model of Beaumont et al. (1987). See text for details.

inferred by Levine (1986).

Jackson et al. (1988) studied the authigenic magnetite content in the Helderberg (Lower Devonian) and Onondaga (lower Middle Devonian) carbonates along the east-west outcrop belt extending from Albany, New York to southeastern Ontario, Canada (fig. 3.6). Like the fission-track age and illite-content profiles (fig. 3.4) of Johnsson (1986), the magnetite-content profile shows a sharp peak near Syracuse, New York. Previous paleomagnetic studies indicate that the authigenic magnetites had formed no later than late Paleozoic. Jackson et al. (1988) attributed the correlation between the high magnetite and illite content to temperature-dependent diagenesis triggered by orogenic fluid derived from the east: the maximum burial temperatures and hence the strongest diagenetic effects occurred in the vicinity of Syracuse.

Miller and Duddy (1989) studied apatite fission-track ages of surficial Middle to Upper Devonian sandstones across New York State and obtianed results similar to those of Lakatos and Miller (1983) and Johnsson (1986). Although their interpretation of uplift history of the Devonian rocks differ in details from Johnsson's (1986) interpretation, they also came to the conclusion that substantial thickness of post-Devonian strata - ~2-3km in western New York and 'greater than 3-4km' in the Catskill region - have been lost.

Most of the studies discussed above deal with small areas and single rock units. With the exception of the studies by Johnsson (1986), Jackson et al. (1988) and Miller and Duddy (1989), spatial variation in paleotemperature and burial estimates are not shown even in studies that cover relatively large areas. To reconstruct a comprehensive scenario of the burial history of the Paleozoic rocks in New York, the spatial variations in the various paleotemperature signatures of selected rock units have to be determined.

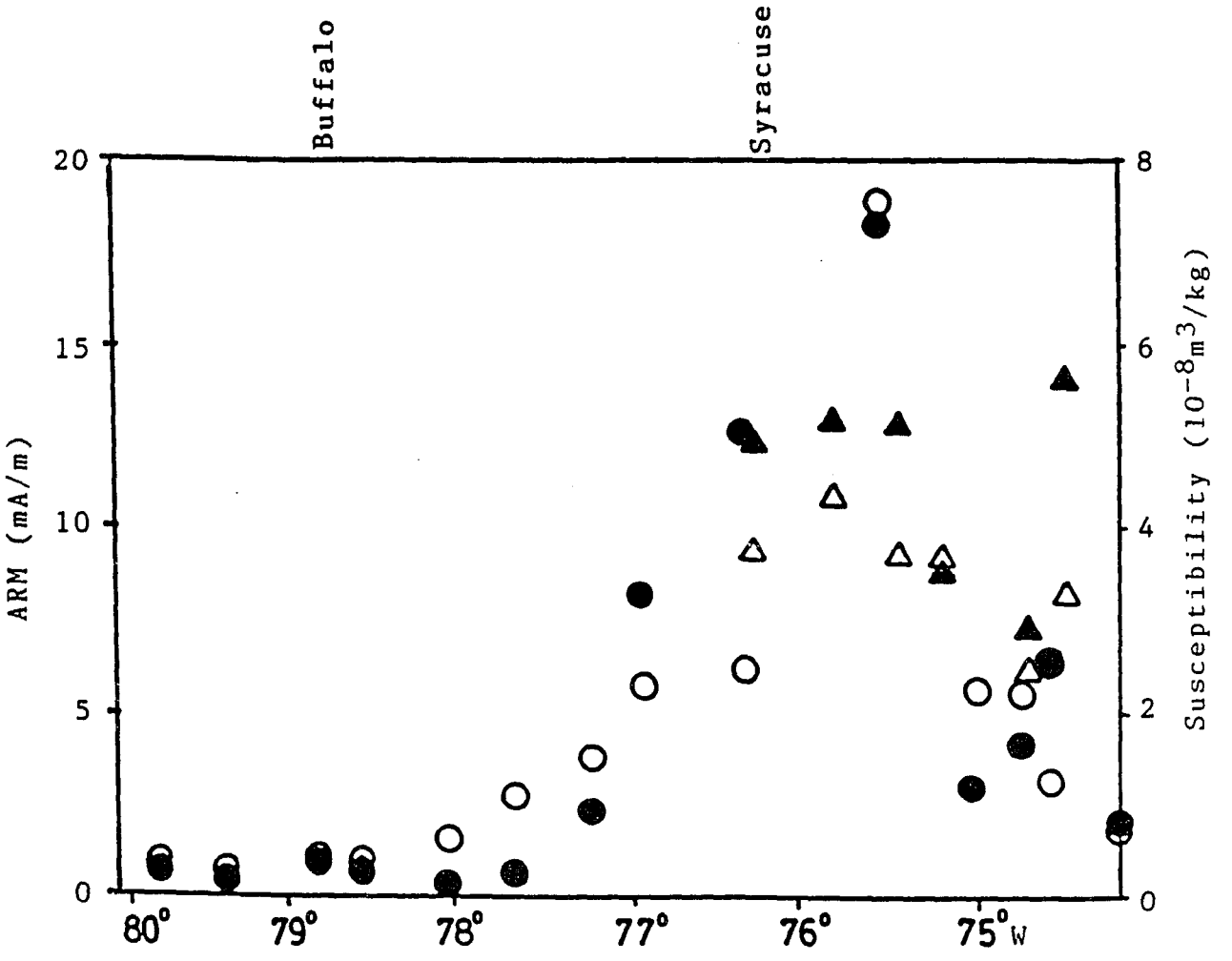

Figure 3.6: Magnetite-content profiles of Jackson et al. (1988), showing spatial variation in ARM (anhysteretic remanent magnetization) intensity (solid symbols) and low-field susceptibility (open symbols) of the Onondaga (circles) and Helderberg (triangles) carbonates. Notice the sharp peak near Syracuse and compare it with figure 3.4.

CHAPTER: 4

RESEARCH METHOD

4.1: SAMPLING:

Sampling for the proposed study has to meet two important requirements: (1) it has to be representative of the Paleozoic sequence over the study area as much as possible, and (2) the samples must be suitable for laboratory analyses aimed at determining paleotemperatures.

Carbonates with grain-rich fabric (grainstones and packstones) provide the best cements for fluid inclusion and isotope analyses. However, cement-filled vugs and fractures in any rock type serve equally well. For organic maturation analysis, black shales are most suitable, but dark, organic- rich carbonates may also be used. Any type of shale may be studied for clay diagenesis, but when black shales are studied, the results supplement organic maturation data and become more useful. Considering these points, the following units have been sampled and studied.

Middle Devonian:	Onondaga Formation (limestone) Marcellus Formation (black shale)
Lower Devonian:	Helderberg Group (limestone)
Upper Silurian:	Salina Group (carbonates, evaporites, and shale)
Middle Silurian:	Lockport Group (carbonates)
Lower Silurian:	Clinton Group (carbonate components only)
Upper Ordovician:	Utica Formation (black shales), Trenton Group (carbonates), Black River Group (carbonates)
Upper Cambrian- Lower Ordovician:	Beekmantown Group (carbonates)

In addition to these rock units, samples from whatever unit were available in cores were collected, provided these were suitable for laboratory analysis.

Samples have been collected from ninety locations of New York state and two

locations of the Ontario Province of Canada. Sample-location maps for individual rock units are shown in chapters 6 through 12. Thirty two of these are core sample locations. The core samples were provided by New York State Geological Survey, and include samples drilled by the Department of Transportation (DOT) of New York, the Supercollider Study Project, the Eastern Gas Shale Project (EGSP), and various other companies. The rest of the samples have been collected from outcrops.

4.2: PETROGRAPHY:

Standard thin sections of carbonate samples have been examined in order to identify types of cements and establish a paragenetic sequence among the various diagenetic components.

Late-stage cements post-date early cements and most compaction features, and may post-date stylolites and fractures. Such cements often include clear, poikilotopic calcite (Moore, 1984), "xenotopic" (Friedman, 1965) dolomite crystals (Gregg and Sibley, 1984), and saddle dolomite (Radke and Mathis, 1980). Identification of late-stage cements is important, because they generally form in the burial environment, and fluid inclusion and isotope data from these cements may reveal the paleotemperatures and extent of burial experienced by the host rocks. Staining techniques (Friedman, 1958) have also been used for quick identification of calcite and dolomite.

4.3: FLUID INCLUSION STUDY:

Fluid inclusions are small, usually microscopic, samples of fluid trapped within a mineral crystal. They may be trapped in various growth irregularities or 'defects' in the crystal during its growth from the same fluid yielding "primary" fluid inclusions, and in microfractures that were healed during crystal growth or at a later time yielding "pseudo-secondary" and "secondary" fluid inclusions, respectively.

Fluid inclusions provide an important tool for determining paleotemperatures and compositions of the fluid at the time of trapping and have been widely used in the studies of ore deposits (Roedder, 1971, 1976, 1979a, 1984; Leach et al. 1975; Mangos and Arribos, 1988; Poty and Pagel, 1988; Roedder and Howard, 1988), igneous and

metamorphic petrogenesis (Roedder and Coombs, 1967; Weisbroad and Poty, 1975; Touret, 1977; Roedder, 1979b; Swanenberg, 1980; Crawford, 1981), sediment diagenesis (Aulstread and Spencer, 1985; Doborek, 1987; Goldstein, 1988; Lee and Friedman, 1987; Nahnybida et al. 1988; McLimans and Videtich, 1989), and thermal history of sedimentary basins (Pollastro and Barker, 1986; Videtich et al. 1988; McLimans and Videtich; 1989; Tilley et al. 1989).

Fluid-inclusion geothermometry is based on five major assumptions (Roedder and Bodnar, 1980). These are:

(1) the inclusion originally traps a one-phase fluid,

(2) the volume of the inclusion does not change after trapping,

(3) nothing is added to or lost from the inclusion after trapping,

(4) the effects of pressure are known, and

(5) the origin of inclusions is known.

Assumption 1:

In some examples, although an inclusion can simultaneously trap 2 phases (such as, two immiscible fluids, or a liquid and a vapor phase), it is usually rare. Therefore, assumption 1 is generally considered valid (Roedder and Bodnar, 1980; Burrus, 1986).

The one-phase fluid trapped in an inclusion may subsequently change into two or more phases. Most common, however, is the change into a liquid and a vapor phase. According to Sorby (1858) this happens due to differential shrinkage of the fluid and the enclosing crystal possibly in response to subsequent cooling of the host rock. The fluid shrinks more than the crystal resulting in a vacuum which is occupied by the vapor phase. In such two-phase inclusions the vapor phase generally takes the form of a circular bubble (fig. 4.1a).

In the laboratory, the two phases in an inclusion change back to one phase when the crystal is heated in a Fluid-Inclusion Heating-Freezing Stage. Upon heating, the liquid in the inclusion expands at the expense of the vapor bubble and ultimately the vapor bubble disappears (fig. 4.1b). The opposite happens when the vapor/liquid volume ratio is very large. The temperature at which one of the phases disappears, that is, one

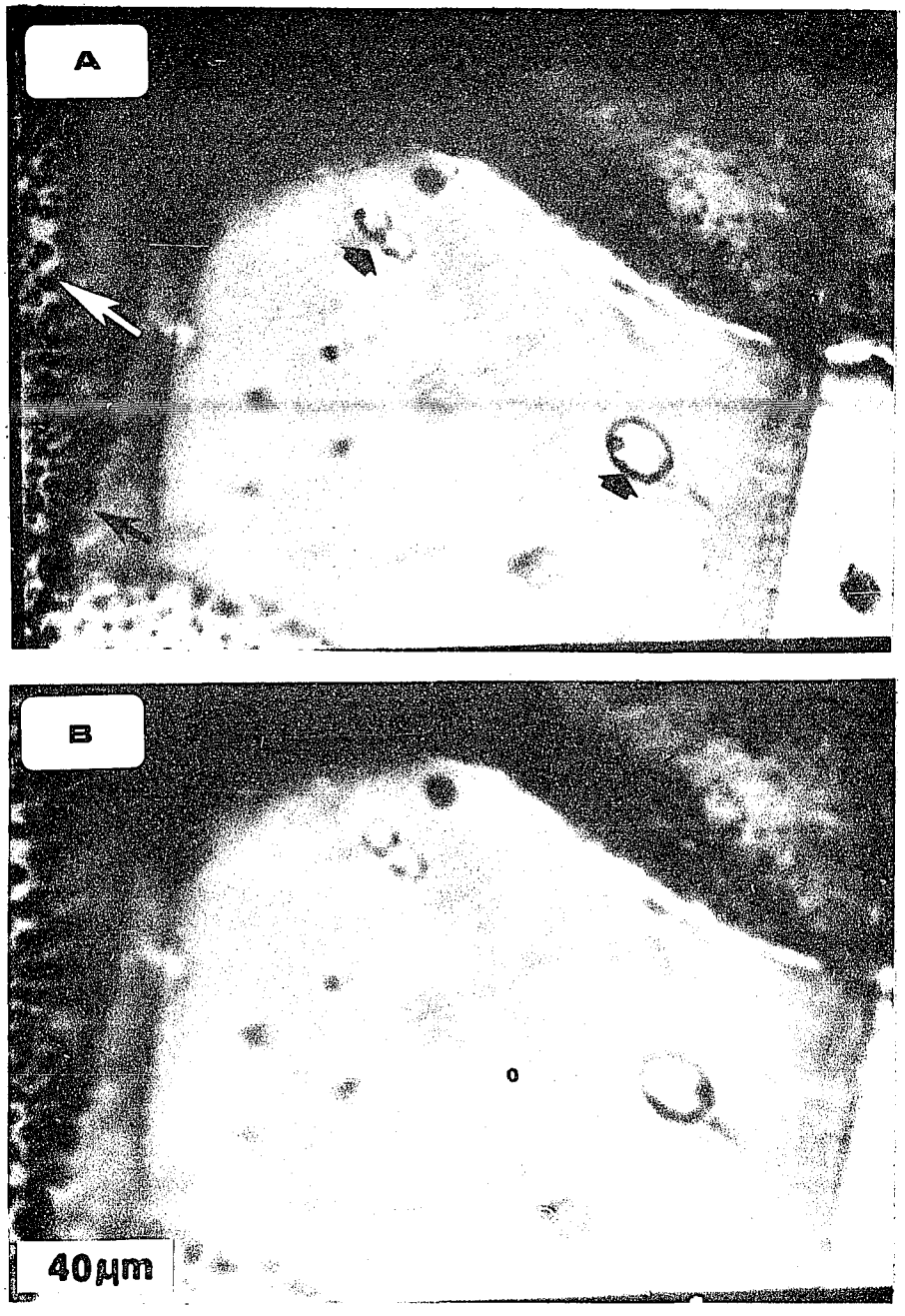

Figure 4.1: Photomicrographs showing two phase (liquid + vapor) primary inclusions (smaller arrows) in fluorite (A) before heating, and (B) after homogenization into the liquid phase. Lines of secondary inclusions (thick arrows) cut across crystal boundaries. (sample from the Helderberg Group, location - 9).

homogeneous phase appears, is called the "homogenization temperature" (Th). Homogenization temperatures generally provide a minimum estimate of the trapping temperature of the inclusion, but with 'pressure correction' the trapping temperature can be approximately determined (see below).

Assumption 2:

Assumption 2 is perhaps most critical for geothermometric study. If post-entrapment volume change occurs, it can alter the homogenization temperature (Th) of an inclusion significantly. Burrus (1986) shows how an initial Th of 135° C may change to 179° C due to only 5% increase in inclusion volume. Post-entrapment change in inclusion volume commonly takes place when the host rock is subjected to elevated temperatures, and may be a serious problem in soft minerals. Expansion of inclusions due to releaze of pressure as the rock is brought to the surface is believed to be very small and the resulting error in Th measurements can be ignored (Roedder and Bodnar,1980).

Figure 4.2 shows how the Th of an inclusion may change or 're-equilibrate' under geologic conditions. If the host mineral is subjected to elevated temperature as a result of subsidence, as shown in this example, the pressure inside the inclusion may increase dramatically over the external pore-fluid pressure on the mineral. Depending on the mechanical strength of the host mineral, the overpressure inside the inclusion may cause either brittle fracture of the inclusion wall (decrepitation) resulting in leakage of the inclusion-fluid, or permanent, plastic deformation (stretching) of the wall without leakage of the fluid. When stretching occurs to the extent that the internal pressure equals the external pore pressure, the inclusion is 're-equilibrated' to the new pressure and temperature conditions (defined by the point B in fig. 4.2) and follows a different isochore (line of constant volume in a P-T diagram).

Stretching behavior of inclusions in fluorite and sphalerite has been studied in the laboratory by Bodnar and Bethke (1984), and Prezbindowski and Larese (1987) have studied the same for calcite. That the homogenization temperatures are reset in discrete jumps, as new isochore paths are followed by a stretching inclusion, is amply verified in Prezbindowski and Larese's (1987) experiment. Bodnar and Bethke (1984) and Rowan (1985) show that for inclusions of same composition, greater overheating is necessary

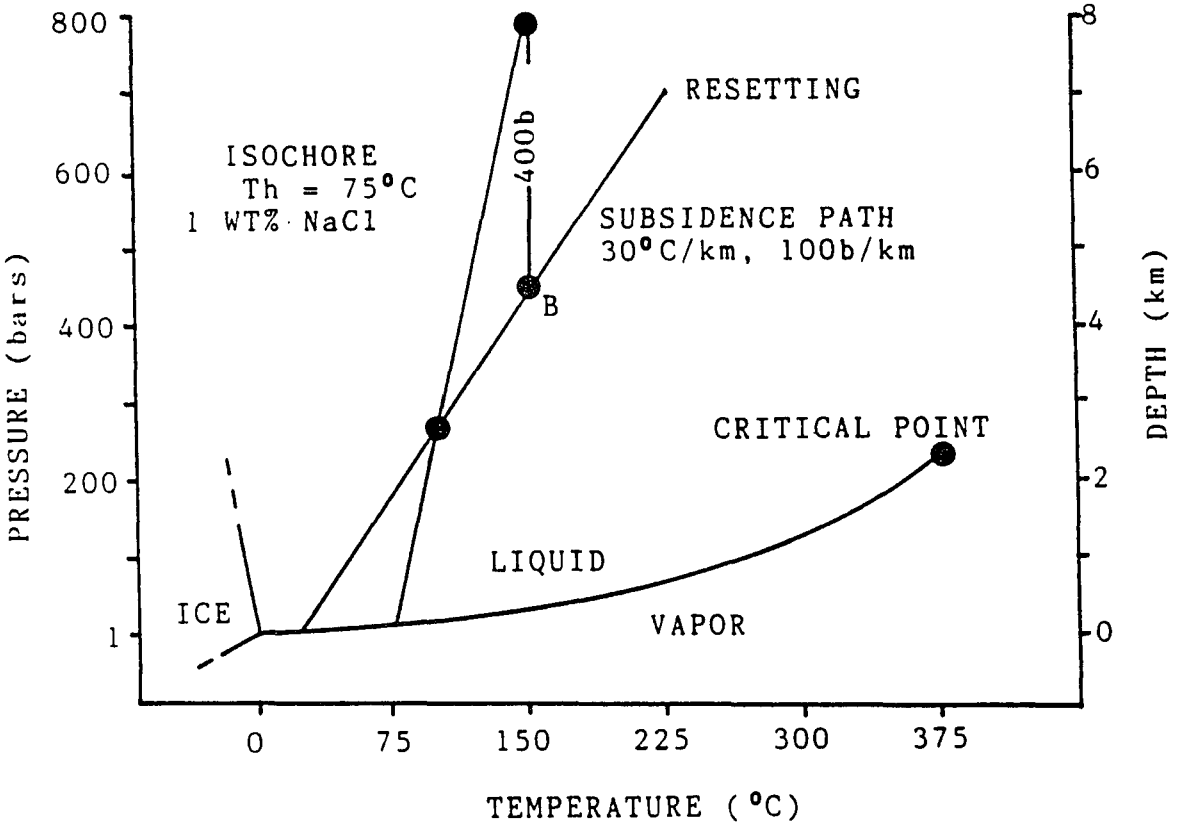

Figure 4.2: Hypothetical example of natural resetting of fluid-homogenization temperature (Th) of an inclusion as a result of subsidence. The inclusion develops an internal pressure greater than a hydrostatic pore fluid pressure if the host rock continues to subside along the PT path shown. After burial to point A, the excess internal pressure is about 400 bars. This differential stress may cause the inclusion to either "stretch" or "decrepitate", and the reset inclusion (point B) follows a new isochore. (From Burrus, 1987).

to initiate stretching of smaller inclusions and, for a given amount of overheating, regularly shaped (especially, rounded) inclusions stretch less than irregularly shaped inclusions.

The main problem in identifying stretching is that there is seldom any physical sign that the observer can use to determine if an inclusion has been stretched. Even in experiemental studies (Bodnar and Bethke,1984; Prezbindowski and Larese, 1987), volume changes of inclusions due to overheating are so small that these cannot be measured directly, and that stretching has occurred is inferred only from measured increase in Th of the inclusions.

Assumption 3:

The third assumption has similar implications to assumption 2 and some additional ones. If fluid is lost from an inclusion, it has the same effect as that of an increase in volume of the inclusion - both will cause an artificial increase in Th. Furthermore, post-entrapment exchange between fluids in the inclusion and the formation may change the composition of the fluid inclusion and may lead to geologic misinterpretations.

If leakage of an inclusion occurs due to overheating and manifests in decrepitation, it may be easily recognized. "Hydrofracturing" and "intersection of twin lamellae and fractures with fluid inclusions" have been cited as other possible mechanisms of leakage (Goldstein, 1986). Twin lamellae and fractures may be identifiable, but, according to Goldstein (1986), healed hydrofractures may defy microscopic identification. It is not certain whether hydrofracture-related leakage is a common problem in geological studies. Roedder and Skinner (1968) have experimentally demonstrated that fluid inclusions usually "do not leak" under overheating, until the point of decrepitation is reached.

Assumption 4:

Homogenization temperature usually gives a minimum estimate of the trapping temperature (Tt) of an inclusion, and to derive the Tt a "pressure correction" is necessary. Roedder and Bodnar (1980), Burrus (1987) and Shepherd et al. (1985) have discussed the various methods and difficulties of pressure correction. In most cases, an independent estimate of paleopressure at the time of trapping of the inclusion is required.

If the pressure is known, then the T_t can be obtained by using a combination of published P-V-T-X phase diagrams (Haas, 1976; Potter and Brown, 1975, 1976). Potter (1977) provides simplified P-T diagrams for aqueous solutions of various salinities from which the "pressure correction" can be read directly. The salinities in Potter's (1977) diagrams can be determined from the final melting temperatures (Tm) of fluid inclusions in the same heating-freezing stage (see below).

An independent estimate of paleopressure is, however, seldom available, especially when missing overburden is involved. Even when the thickness of the missing overburden can be estimated, the problem of choosing between hydrostatic and lithostatic pressure remains (Roedder and Bodnar, 1980).

A convenient method of determining paleopressure (therefore, trapping temperature) involves using two sets of coeval inclusions in the same mineral crystal containing fluids of different compositions, which were present as immiscible fluid at the time of trapping (Roedder and Bodnar, 1980). The two immiscible fluids commonly found in sedimentary rocks are oil and water. If inclusions separately containing oil and water with their respective vapor phases can be proved to have been coeval, then their isochores will intersect at the pressure and temperature of trapping (Burrus,1987; Videtich et al. 1988).

Assumption 5:

Primary inclusions in a given crystal may have been trapped at different stages of the crystal's growth, from fluids of varying chemical compositions. Often, "secondary" inclusions form in fractures that open and heal after the formation of the host-crystal. For studies aimed at determining the sequence of rock-fluid interaction, it becomes essential to establish the origin of fluid inclusions as well as identify different inclusion populations with distinct compositional and thermal signatures.

Hollister (1981) and Roedder (1984) have reviewed the various criteria for distinguishing between "primary" and "secondary" inclusions. Relatively large and isolated inclusions, or clusters of such inclusions are generally considered primary (figs. 4.1, 4.3). However, clusters of small inclusions may result from decrepitation of a large primary inclusion, hence their origin is a late phenomenon. When inclusions outline the

growth zones of a crystal, their primary origin is readily proved. Because "secondary' inclusions form in healed fractures, they are generally found disposed in a linear fashion (figs. 4.1, 4.3). By slightly varying the plane of focus in a microscope, these inclusions are seen lying along a plane. When a line or trail of inclusions crosses a crystal boundary and extends into an adjacent crystal, a secondary origin becomes unquestionable. In general, secondary inclusions are also quite small.

4.3.1: Determination of fluid composition:

Fluid inclusions are also used to determine the composition of the fluid from which the crystals have precipitated, although the smallness of inclusions pose severe technical problems. Assumption 3, above, is the most critical assumption for compositional study.

The various techniques available for compositional study include freezing-temperature determination, crushing- stage method, bulk-extraction technique, gas chromatography, atomic emission spectroscopy, fluorescence microscopy, neutron activation analysis, laser and ion-microprobe, Ramon Spectroscopy etc. Roedder (1972), Hollister (1981), and Shepherd et al. (1985) have published critical reviews of these techniques. Most of these methods are destructive, i.e., the samples have to be crushed, and rely on the availability of relatively large volumes of fluids from the inclusions. This condition is not easily met in sedimentary rocks. Laser excited Ramon Spectroscopy, although a non- destructive method, is limited to determining the amounts of polynuclear species only and the typical small size (<15 μm) of inclusions in sedimentary rocks poses a serious problem. Fluorescence microscopy, another nondestructive method, is limited to identifying some, not all, organic liquids (Roedder, 1972).

The simplest of all the techniques for detrmining fluid composition is the study of the freezing behavior of the inclusions. In this method, a given inclusion is frozen in a standard Heating-Freezing Stage by passing depressurized cold nitrogen gas over the sample. Because of the small size of inclusions, generally considerable supercooling (sometimes exceeding 100° C) is necessary to freeze the fluid into ice crystals (fig. 4.3a). In very small inclusions, even the ice crystals are generally not observed, and when the vapor bubble suddenly shrinks or disappears, freezing is supposed to have occured. This

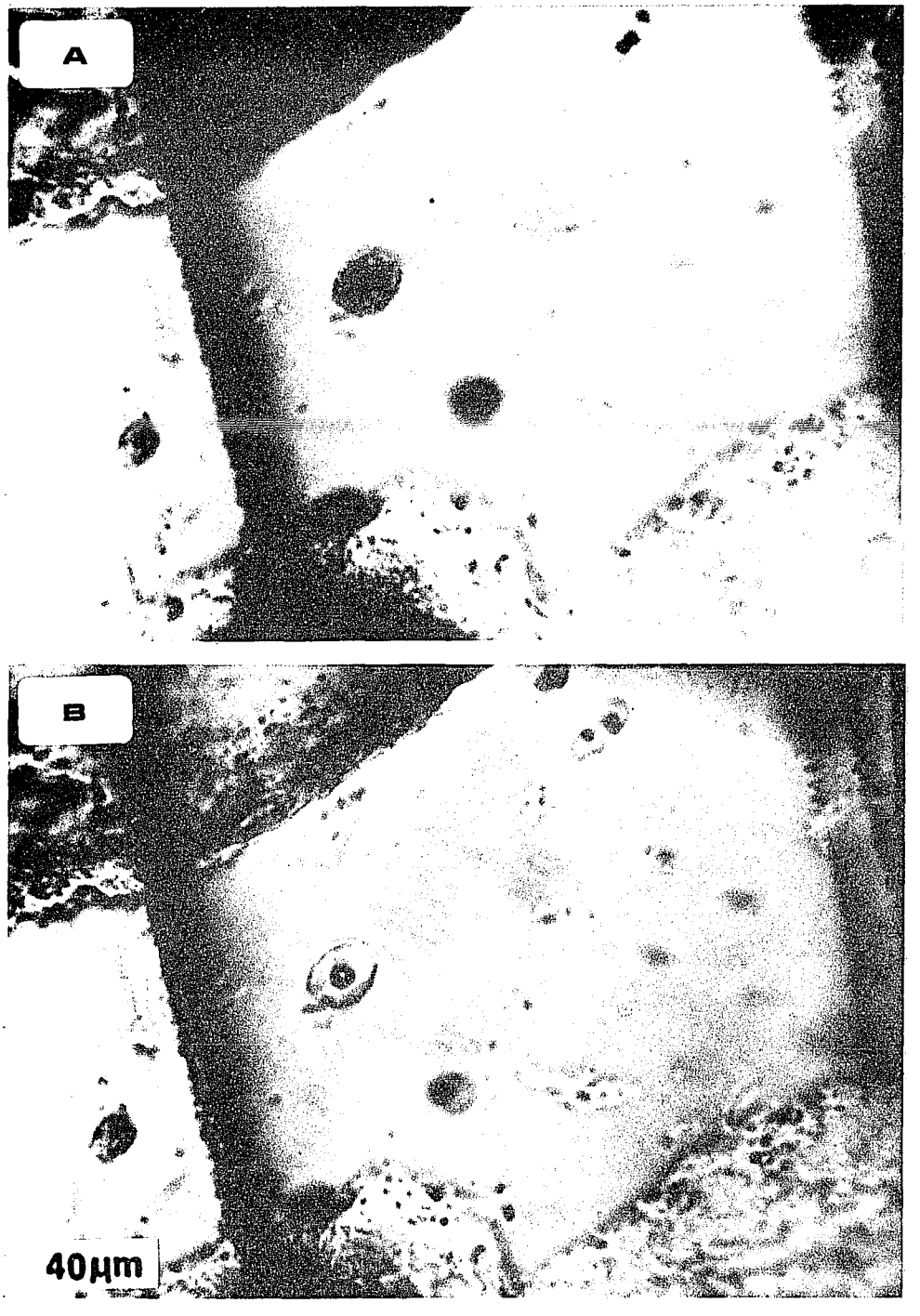

Figure 4.3: Photomicrographs of the same inclusions of figure 4.1 showing (A) their frozen state attained through supercooling, and (B) the return of the vapor bubbles after the last ice crystals have melted as a result of slow heating. The temperature at which the last ice crystal of a frozen inclusion melts is the freezing temperature (Tm) of the inclusion fluid.

freezing temperature is, however, not the freezing temperature of the inclusion fluid. To determine true freezing temperature, the frozen inclusion is gradually reheated and the temperature at which the last ice crystal melts (fig. 4.3b) is considered the true freezing temperature (also called 'melting temperature', or 'Tm'). In very small inclusions Tm is measured at the point when the vapor bubble suddenly reappears, or makes a final sweeping movement toward its pre-freezing position in the inclusion.

Use of "Tm" as composition indicator is based on the assumption that the inclusion contains a simple $NaCl-H_2O$ solution. From experimental studies, the dependance of freezing point depression of water on salinity (wt. % NaCl) is well-known. The salinity of inclusion fluids can be determined from the following relationship (Potter et al. 1978):

$$Ws = 1.76958O - 4.2384 \times 10^{-2}O^2 + 5.2778 \times 10^{-4}O^3 \pm 0.028,$$

where Ws = the weight percent NaCl in solution and

O = freezing point depression in °C.

Inclusion fluids may, of course, contain other salts, but it is generally agreed that for mixed Ca-Na-K-Mg chloride solutions, the error in estimating salinity (NaCl-equivalent) using the 'freezing-point depression' method is less than 5% (Clynne and Potter, 1977).

Another method of qualitatively determining the presence of the dominant salt is from the 'temperature of first melting (Tfm)' of the ice crystals. The **Tfm** is believed to represent the eutectic temperature. Where there is no solid-solution between the solid phases, eutectics are invariant points and, therefore, the first melting occurs at a temperature determined solely by the composition of the end-member components. For example the eutectic temperature of $NaCl-H_2O$ system is -20.8° C, $CaCl_2-H_2O$ is -49.5°C, $KCl-H_2O$ is -10.6°C and $CaCl_2-NaCl-H_2O$ is -52°C (Shepherd et al. 1985). This potentially important method is, however, seriously constrained by the difficulty of identifying the first melting of ice, especially in small inclusions.

4.3.2: Sample preparation and examination:

In this study, the fluid-inclusion samples were prepared first by cutting chips from hand samples with a low speed hand saw. Doubly polished thin sections, about 200

microns thick, were made from the chips. The thin sections were made selectively from grainstones and from cement veins and vugs of any rock type. From the adjacent part of a sectioned chip standard thin sections were made for petrographic examination. Three to seven samples from each location were prepared in this way. The fluid-inclusion thin sections were broken into several small pieces and studied in a USGS Heating-Freezing Stage (University of Arizona) equipped with a Nikon binocular microscope. Details of this instrument are given in Hollister et al. (1981).

Rate of heating during homogenization runs were initially maintained at about 2°C/minute, but later reduced to 0.5°C/minute when the homogenization temperatures were approached. The same rate was maintained during freezing runs. Homogenization temperature of each inclusion was measured 2 to 3 times, but the results did not vary by more than 0.3° C. Freezing measurements were taken only in relatively large and clear inclusions, and immediately after homogenization measurements. Two freezing runs per inclusion were carried out at times. The results occasionally varied, but not by more than 0.5°C.

4.3.3: Data presentation and interpretation:

Whether the inclusions are primary or secondary was determined using criteria discussed under assupmtion 5. Histograms of Th were made from all the Th measured in one location. Only a few Tm measurements could be taken from samples of one location. The raw data are presented in Appendix- B through J.

On the basis of observations made in this study, it is difficult to determine if some fluid inclusions have reequilibrated (assumptions 2,3). Inclusions with unusually large bubbles or 'necked' shapes have not been measured in order to minimize collection of data from potentially leaked inclusions. However, if artificial increase in Th has occurred due to post-entrapment reheating without leakage and exhcgae of fluid/vapor with the environment, the reset Th only approaches the highest post-entrapment temperature, not exceed it. This is experimentally shown by Prezbindowski and Larese (1987). Barker and Goldstein (1990), based on their study of fluid inclusions in subsurface calcite cements in 46 diverse geologic systems that are presently at or near their maximum burial temperatures, also found excellent correlation between present

formational temperatures and Th_{mode} (i.e., mean of Th in the highest modal class) as well as Th_{mean}. Therefore, reset Th serves as 'maximum recording geothermometers' (Burrus, 1987; Barker and Goldstein, 1990). Since one of the major goals of this study is to determine the maximum paleotemperatures experienced by the studied rock units, resetting of Th, if it had occurred, does not pose a serious problem to this study.

In this study, in order to assess the maximum Th at a location and to compare them between locations, the average of all the Th readings in the highest 20°C interval of the Th histograms of individual locations has been used. The highest 20°C interval has been chosen because at least five Th readings are available in this interval at every location. This average, named "Th_{max}" in this study, is similar to Th_{mode} of Barker and Goldstein (1990), but would be a little higher in most cases.

Attempts have been made to derive true trapping temperatures of fluid inclusions by pressure correction (see section 16.1, for example). But these attepmts largely failed due to lack of necessary data. In this study, **Th** therefore represents the lower limit of the true trapping temperature of an inclusion. Consequently, the Th_{max} also represents a lower limit of the maximum temperatures experienced by the rocks containing the inclusions.

4.4: ORGANIC MATURATION ANALYSIS:

Organic materials undergo various physical and chemical changes after burial. These changes are influenced by temperature, pressure and geologic time, but the relative importance of these factors is a subject of controversy. 'Maturity' is a measure of post-depositional alteration of organic matters. There are numerous methods of assessing maturity of organic matters in sediments (Heroux et al. 1979; Crelling and Dutcher, 1980), but 'vitrinite reflectance' (Ro) is most widely used. It is the primary standard by which coal is ranked (Stach et al. 1982) and is routinely used to evaluate hydrocarbon source rocks.

Vitrinite is the principal maceral type in coal and makes up 50 - 90% of most North American coals (Crelling and Dutcher, 1980). It is generally the most abundant constituent of sedimentary kerogen (Dow and Connors, 1982). Most vitrinite macerals are derived from the cell-wall materials or woody tissue of plants. Vitrinite is formed in

the diagenetic environment by humification of these materials.

With increasing maturity, the aromatic lamellae of vitrinite become more ordered resulting in a systematic increase in optical reflectivity (Dow and Connors, 1982). This reflectivity (vitrinite reflectance) is measured as the percentage of light (ranges between 0.3 and 5%) vertically incident on a polished vitrinite surface, that is reflected back vertically to the viewer.

Although vitrinite reflectance measuring procedures were first developed for coal petrology, these have been widely used in the study of disseminated organic matter, or kerogen, in rocks that do not contain coal (Castano and Sparks, 1975; Cardott and Lombard, 1985; Houseknecht and Mattews, 1985; Guthrie et al. 1986; Clayton, 1989; Connolly, 1989, and many others). Separation and measuring techniques of vitrinites of kerogen are discussed by Dow and Connors (1982) and Stach et al. (1982).

As many Ro measurements as possible are taken from a rock sample - usually 50 are recommended (Castano and Sparks, 1975). A high number of Ro readings is necessary in order to separate out 'primary' and 'recycled' vitrinites. Although it is not always possible to separate them, vitrinites recycled from erosion of older rock units generally tend to show higher Ro. Also, vitrinites in highly weathered or oxidized samples show higher Ro. In core samples, another source of non-indigenous vitrinite is from caving. Vitrinites from this source usually show lower reflectance values. Only the primary or indigenous vitrinites can be used for maturity analysis. Despite all precaution, it is often difficult to identify the primary vitrinite population from Ro histograms when several populations are present. To overcome this problem, it has become a common practice to use mean Ro to represent organic maturity.

How vitrinite reflectance data can be best used to estimate paleotemperatures experienced by a given rock has remained unresolved. It is generally agreed that temperature is the dominant factor influencing vitrinite reflectance, and that the effect of pressure is negligible in most cases (Crelling and Dutcher, 1980; Barker, 1983). The source of contention is the role of geologic time. There are various models that relate time, temperature, and organic maturity. These may be broadly divided into (A) those that propose geologic time as an important factor (Lopatin, 1971; Hood et al. 1975;

Tissot and Welte, 1978; Waples, 1980), and (B) those that propose geologic time as having only a limited importance (Barker, 1983,1988; Price, 1983; Barker and Pawlewicz, 1986).

In Hood et al.'s (1975) model, the role of time is important. Fundamental to this model is the tenet that chemical reaction in organic materials follow a first-order kinetics (i.e., obey Arrhenius Equation), and the reaction rate doubles with every 10° C increase in reaction temperature (Lopatin, 1971). Based on data from various deep wells with reasonably well-understood geologic histories, Hood et al. (1975) related 'maximum burial temperature' (Tmax) and 'effective heating time' (Teff) with LOM (Level of Organic Metamorphism) of rocks (fig. 4.4). **Teff** is the time interval during which a specific rock has been within 15°C of the Tmax. LOM is a scale ranging from 1 to 20 (20 representing the anthracite-metanthracite boundary) with which many maturity indicators, including Ro, can be correlated (Hood et al. 1975, fig.2). As seen in figure 4.4, the maximum burial temperature of a given rock can be estimated from its vitrinite reflectance values (via LOM) only if the Teff is known. Frequently, this information is not available.

Lopatin's (1971) and modified-Lopatin's (Waples, 1980) models are most widely used to represent the thermal maturation history of sediments. However, these models can not be directly used in the present study. In these models, it is necessary to know a priori the burial history of a given rock unit.

Barker (1983) and Price (1983) questioned the validity of time-dependent models of organic maturation on both theoretical and empirical grounds. According to them, there is no evidence from the natural system that petroleum generation - maturation reactions have first-order reaction kinetics; on the contrary, laboratory experiments show that these reactions follow multiple-order kinetics. Price (1983) also shows that mean vitrinite reflectance data from deep wells of several sedimentary basins of the world have a strong correlation with ambient temperatures but not with burial times for any temperature interval. Full organic maturation at a given temperature is believed to be achieved within 1 M.Y (and as short as 1000 - 10,000 years in hot geothermal systems) after which reaction time has no effect. That the geologically older sediments often show

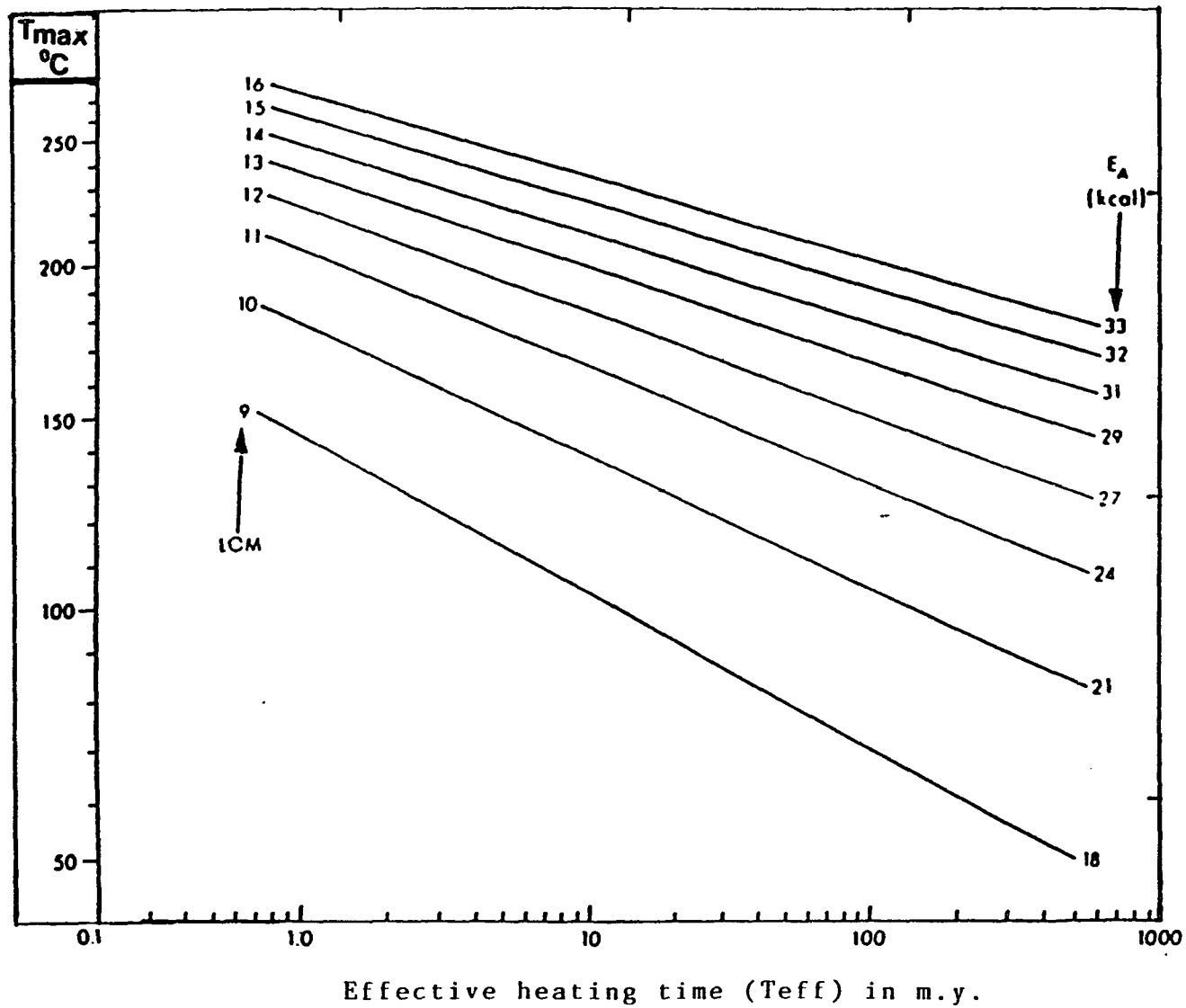

Figure 4.4: Relationship of Level of Metamorphism (LOM) to maximum temperature and effective heating time (Teff). See text for explanation. (After Hood et al. 1975).

higher organic maturity than younger sediments at the same burial temperatures can be explained, according to Price (1983), by the greater chance the older rocks have of being affected by major thermal events. Based on their findings, Barker (1983), Price (1983), and Barker and Pawlewicz (1986) propose that vitrinite reflectance can be used directly as an absolute geothermometer. The following linear regression equation of Barker and Pawlewicz (1986), based on data from 35 geologic systems, show the relationship between maximum burial temperature (Tmb) and mean vitrinite reflectance (Rm).

$$\ln (Rm) = .0078Tmb - 1.2$$

In a later publication, Barker (1988), however, shows that although the time-dependent and time-independent models use different approaches, they show comparable fit with data from natural systems. This is because, he explains, the time-dependent models such as that of Lopatin (1971) are heavily weighted toward reaction occurring near the maximum burial temperature, because these models rely on the reaction rate doubling with every 10°C temperature increase. Similarly, Hood et al.'s (1975) model only considers the reaction time within 15°C of the maximum burial temperature.

Since land plants first appeared only in the latest Silurian time, vitrinites are generally absent in pre- Devonian rocks. Bulk of the organic matters in these rocks are exinites (spores, pollens, cutinites) and amorphous sapropelic substances (Staplin, 1975). It was observed by Teichmuller (1952) that in rocks containing both coal and exinite it was possible to roughly estimate the rank of coal on the basis of color and reflection changes in exinite. That is, exinite changes color from yellow through brown to black in response to increasing temperature. Later, a numerical scale called Thermal Alteration Index (TAI) was introduced (Staplin, 1969, 1975) to represent color alterations of exinite and for the purpose of correlation with other maturation indicators. Direct relationship between TAI and temperature has not been established probably because TAI is based largely on a qualitative property, color. However, temperatures can be estimated from TAI via its equivalent Ro (table 4.1) following methods described above.

Table 4.1: Interconversion of thermal alteration index (TAI) and vitrinite reflectance values (Ro). (From Geochem Laboratories, Houston, 1988).

Thermal alteration index (TAI)	Descriptive maturity terminology	Vitrinite reflectance (%Ro)
1.00	Immature	
1.10	--	
1.20	--	
1.30	--	0.30
1.40	--	0.33
1.50	--	0.37
1.60	--	0.40
1.70	--	0.43
1.80	Moderately immature	0.45
1.90	--	0.48
2.00	--	0.50
2.10	--	0.55
2.20	Moderately mature	0.60
2.30	--	0.70
2.40	--	0.75
2.50	--	0.80
2.60	Mature	0.90
2.70	--	0.93
2.80	--	0.95
2.90	--	0.98
3.00	--	1.00
3.10	--	1.13
3.20	--	1.25
3.30	--	1.38
3.40	--	1.40
3.50	--	1.63
3.60	Very mature	1.75
3.70	--	1.88
3.80	--	2.00
3.90	--	2.13
4.00	--	2.25
4.10	--	2.38
4.20	Severely altered	2.50
4.30	--	2.75
4.40	--	3.00
4.50	--	3.50

(Table 4.2 continued)

4.60	--	4.00
4.70	--	
4.80	--	
4.90	--	
5.00	Metamorphosed	4.50

Tissot et al. (1980) discussed several problems of TAI measurements and usefulness. These are (1) the subjective nature of color determination and calibration problems between laboratories, (2) dependence of color on the original nature of plants involved and thickness of particles inspected, (3) color alteration by early diagenetic processes, such as oxidation, and (4) hydrogen- poor particles with a high aromacity are darker than hydrogen-rich partciles with a low aromacity, even if they have the same thermal history.

4.4.1: Sample examination and interpretation:

In the present study, all Ro and TAI measurements were done by Geochem Lab of Houston. In Devonian shale samples both Ro and TAI were measured whereas in Devonian carbonates only TAI was measured. In pre-Devonian shales, because of reasons mentioned above, only TAI was measured. No TAI measurements were made on pre-Devonian carbonates when it was found that the TAI data from Devonian carbonates were quite inconsistent with other data. The Ro histograms and TAI data are presented in relevant chapters.

From mean Ro (and Ro-equivalents of TAI) data of samples of individual locations the maximum burial temperatures were calculated using Barker and Pawlewicz's (1986) equation, because, unlike Hood et al.'s (1975) method, no assumption about the the heating duration has to be made in this method.

4.5: CLAY DIAGENESIS:

Burial diagenesis of clay minerals provides a useful tool for determining thermal maturity of sediments (Weaver, 1960; Burst, 1969). A number of diagenetic changes in clay minerals are observed with increasing burial. The most important mineralogical

change involves the transformation of smectite to illite through a series of mixed-layer illite-smectite (I/S) intermediaries (Dunoyer de Segonzac, 1970; Perry and Hower, 1970; Weaver and Beck, 1971; Eslinger and Pevear, 1988; Moore and Reynolds, 1989).

Smectite, which typically comprises 20-50% of most young shales, becomes increasingly scarce in older and/or deeply buried rocks (Eslinger and Pevear, 1988). A similar decrease in the abundance of mixed-layer clays and kaolinite is observed in these rocks. At the same time, the percentages of illite and chlorite increase.

Studies of several basins around the world show that I/S are typically randomly stratified to a depth of approximately 10,000 ft where, in some wells, an abrupt increase from about 40% to 70-80% illite is observed (Hower, 1981; Eslinger and Pevear, 1988). At these depths, the shale also assumes an ordered structure of alternating illite and smectite layers with extra illite randomly distributed. In other wells the transition from random to ordered inter- stratification is more gradual and in some wells, especially in rapidly buried sequences, the transition occurs at greater depths. In wells where information is available to depths greater than 20,000 ft, the percentage of illite is generally found to be 90 or more (Eslinger and Pevear, 1988)

The nature of chemical reaction involved in smectite- illite transition in mixed layer I/S is not clear, or perhaps not unique, and several models have been proposed (see Moore and Reynolds, 1989, p. 144-157). The problem of clear understanding of the transformation mechanism perhaps emanates from a lack of concensus on the nature of illite and smectite (for example, whether these should be treated as discrete minerals, particles of mixed composition, or solid solutions).

The chemistry of the transformation, however, requires that K an Al are incorporated into the newly formed illite. According to Hower et al. (1976), the original smectite layers remain intact and K and Al, derived from dissolution of K-feldspars, are substituted into the smectite structure to create illite. Silica, Mg and Fe released from smectite, if retained in the system, form chlorite and quartz. According to Boles and Franks (1979), Al is derived from dissolution and removal of part of the silica from the original smectite so that part of the smectite is "cannibalized" and the total amount of clay is reduced. Nadeau et al. (1985) and Inoue et al. (1987) also proposed a stepwise

dissolution and recrystallization reaction. The transformation process also causes expulsion of interlayer water from smectite, probably due to contraction of the layers resulting from an increase in charge as Al substitutes for Si (Eslinger and Pevear, 1988).

The primary controls on the smectite-illite transformation reaction are believed to be temperature, time and rock and fluid chemistry. Of these, temperature has the most well-documented effect. High burial temperature apparently releases K necessary for illitization from coarse K-feldspar and mica (Perry and Hower, 1970; Weaver and Wampler, 1970; Weaver and Beck, 1971; Hower, 1981; Smart and Clayton, 1985). Pressure is probably not that important because it has been shown that pressures found in deep- burial environments are not high enough to dehydrate the interlayer water from smectite (Colten-Bradley, 1985; Eslinger and Pevear, 1988, p. 5-16).

The effect of time on smectite-to-illite reaction is controversial. In some experimental and field studies, reaction kinetics has been shown to be important (Eberl, 1978; Pevear et al. 1980; Ramsayer and Boles, 1986). However, Weaver's (1978) compilation of data, extending over an age range of 325 million years, shows temperature, not time, as the major control on illitization. It appears that kinetic factors are important in the lower temperature portion of the diagenetic sequence, particularly in younger (Tertiary) rocks (Eslinger and Pevear, 1988, p. 5-21). In older rocks, temperature is probably the most important factor.

Fluid and rock compositions are the other factors that play an important role in the smectite-to-illite reaction (Robertson and Lahan, 1981). However, little information is available on the composition of pore fluids in shale. It is at least certain that the shale must have sufficient K to satisfy the requirements of the smectite-illite reaction.

Smectite-illite transition has been used for measuring thermal maturity of sediments in two ways. The first one uses the percentage of illite in I/S clays to infer a range of temperature in which these percentages are observed in oil wells (Hoffman and Hower, 1979; Johnsson, 1986; Pollastro and Barker, 1986). For example, less than 50% illite in randomly stratified I/S indicates temperatures below 100° C; 60-80% illite layers indicate temperatures of 100-175° C, roughly coinciding with the "oil window"; and 85-95%, ordered illite layers indicate temperatures near or above 200° C (Hoffman and

Hower, 1979; Eslinger and Pevear, 1988). According to Weaver et al. (1984), 5% illite in I/S was found at about 210° C. The reaction rarely goes to 100% illite probably because K-feldspar, the main source of K, is exhausted before this stage is reached.

Another widely used geothermometer is "illite crystallinity index (I.C)" (Kubler, 1968; Stalder, 1979; Kisch, 1980; Duba and William-Jones, 1983; Guthrie et al. 1986). It is expressed as the width of the basal, 001, diffraction peak of illite at half its height. As ordering increases in I/S, variability of d-spacing decreases because the illite layers become more alike. In other words, the structure becomes more homogeneous and crystalline. This is reflected in the narrowing or sharpening of the 001 peak at 10Å. The peak can therfore be compared to a histogram, the smaller width of which represent greater homogeneity or crystallinity of the mineral (Duba and William-Jones, 1983).

A firmly established relationship between I.C and temperature is yet to be known. However, I.C has been used to mark boundaries between metamorphic zones in pelitic rocks. For example, I.C of 0.42° 2θ is considered the boundary between "diagenetic zone" and "anchimetamorphic zone" or "anchizone", and I.C of 0.25° 2θ the boundary between "anchizone" and "epizone" (Kubler, 1968; Weaver and Boekstra, 1984). Various attempts have been made to assign temperature ranges to these zones. On the basis of fluid-inclusion data from vein quartz in shale, Frey et al. (1980) found a minimum temperature of 200° C for the beginning of anchizone (i.e, I.C equal to or less than 0.42° 2θ) and 270°C for the advanced stages of anchizone. Weaver et al. (1984) placed the beginning of anchizone at 280°C and the beginning of epizone at 360°C based on isotopic and bottom-hole temperatures of the Cambrian Conasauga shale of the southern Applachians (fig. 4.5).

4.5.1: Sample preparation, examination and interpretation:

In this study, the shale samples were prepared for x- ray diffraction using methods described by Jackson (1979) and Moore and Reynolds (1989). The samples were washed, dried and, in case of outcrop samples, the surface layers were discarded by scrpping. The samples were then crushed to mm-sized particles using an iron mortar and a pestle. The crushed samples were passed through a 0.2mm sieve to collect the -0.2mm powder. The powder was then treated successively with .1N HCl and 6% H_2O_2 solutions to remove

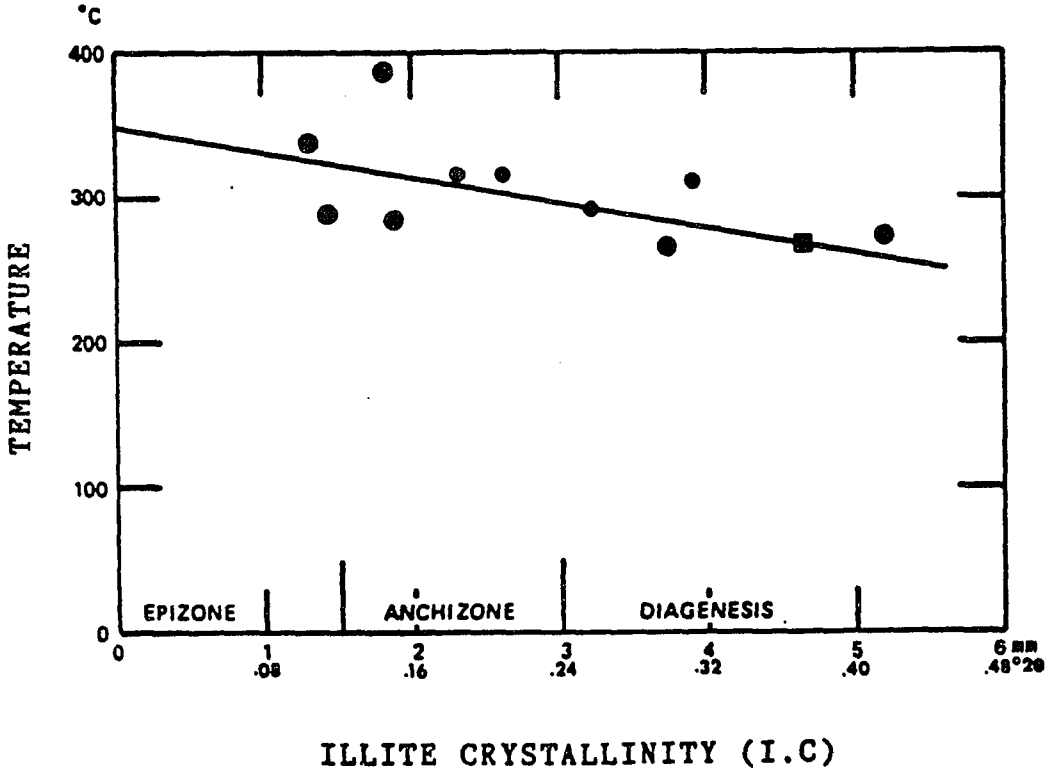

Figure 4.5: Temperature - Illite Crystallinity (I.C) relationship diagram of Weaver et al. (1984) based on their study of the Cambrian Canasauga shale of the southern Appalachians.

carbonates and organic matters respectively. Subsequently they were dispersed in distilled water in graduated beakers and the - 20μm, -6μm, and -2μm size fractions were separated by gravity sedimentation and decantation using settling times for different grain sizes calculated by Jackson (1979). Water containing the -6μm and -2μm fractions were centrifuged to concentrate the clay. The concentrated water-clay mixture was sedimented on glass slides by an eye-dropper. Two slides were made with the -2μm fraction for every shale sample. Only a few slides with -6μm fraction were made. The slides were placed on ceramic tiles in an oven and exposed to low temperatures (~50°C) where they dried in about two hours.

The above procedure provided roughly oriented clay samples required to measure the basal reflections by x-ray. The -2μm samples were used for x-ray analysis to avoid measuring the detrital illites which are generally of larger size (Eslinger and Pevear, 1988). Both slides with -2μm fraction were x-rayed to see if intra-sample variation existed. One of the slides was then solvated with ethylene glycol by dripping from an eye-dropper and drying for a brief period. The solvated sample was then x-rayed again. Glycol-solvation is necessary for identification of certain clay minerals, such as the smectite, which expands upon glycol treatment to its specific basal spacing (Eslinger and Pevear, 1988, A-22).

The clay samples were analyzed by a RIGAKU X-ray diffractometer, DMAX IIB with CuKa radiation of 2KW maximum intensity. For each sample, scanning was done between 4° and 30° at a goniometer speed of 1°/minute and voltage of 40KV. A 'peak finding program' automatically calculated the peak positions, peak intensities, and the widths of the peaks at half of their heights. Width of the 10Å peak found this way provided the I.C (in °2θ) for each sample. The percentages of illite were calculated by using the positions of the 001/002 and 002/003 I/S peaks (table 4.2) after Moore and Reynolds (1989).

Percentage of illite in I/S and I.C. of the shale samples of a study location were used to estimate the paleotemperatures experienced by the samples at that location. Whereas the percentage of illite in I/S gave an estimate of the temperature range, each I.C. value could be used to obtain a certain temperature from figure 4.5.

Table 4.2: The positions of 001/002 and 002/003 reflections of mixed-layer illite/smectite in glycolated clay samples for estimating percentage of illite. (From Moore and Reynolds, 1989).

	001/002		002/003		
% Illite	d(Å)	°2θ	d(Å)	°2θ	°Δ2θ
10	8.58	10.31	5.61	15.80	5.49
20	8.67	10.20	5.58	15.88	5.68
30	8.77	10.09	5.53	16.03	5.94
40	8.89	9.95	5.50	16.11	6.16
50	9.05	9.77	5.44	16.29	6.52
60	9.22	9.59	5.34	16.60	7.01
70	9.40	9.41	5.28	16.79	7.38
80	9.64	9.17	5.20	17.05	7.88
90	9.82	9.01	5.10	17.39	8.38

4.6: STABLE ISOTOPE ANALYSIS:

Measurements of oxygen and carbon isotopic composition of various components of carbonate rocks have become a common practice in modern diagenetic studies (see Zenger et al. 1980; Arthur et al. 1983; Schneiderman and Harris, 1985; and Shukla and Baker, 1988 for references). There are two principal uses of stable isotope studies: (1) to determine the nature (marine, meteoric, hypersaline, hydrothermal etc.) of the diagenetic fluids, and (2) to determine the formational temperatures of the minerals in which they are measured.

The usefulness of isotopes for the above purposes rely on "isotopic fractionation" or partial separation of isotopes (owing to their different weights) which can occur during physical and chemical reactions. The fractionation factor for the $CaCO_3$-H_2O system in which the CO_3^{2-} ions in calcite are in equilibrium with the oxygen and carbon in water is given by

$$\alpha = \frac{(^{18}O/^{16}O)\ CO_3^{2-}}{(^{18}O/^{16}O)\ H_2O} \quad \ldots\ldots (1)$$

where $(^{18}O/^{16}O)CO_3^{2-}$ is the ratio of ^{18}O to ^{16}O in the carbonate ions and $(^{18}O/^{16}O)H_2O$ is their ratio in water. If the oxygen isotopes behave identically chemically, would equal 1. The same type of relationship also applies for carbon (^{13}C, ^{12}C) isotopes.

The value of "α" varies with temperature which makes possible the use of oxygen-isotope data for paleotemperature determination. Also, for a given temperature, the $^{18}O/^{16}O$ of carbonate should vary directly with the same of water. This makes it possible to infer the nature of the carbonate- precipitating fluid by analogy with isotopic compositions of modern meteoric, marine and hypersaline waters.

In oxygen and carbon isotopic analysis of a sample, it is customary to present the data in terms of difference in $^{18}O/^{16}O$ or $^{13}C/^{12}C$ (expressed as $\partial^{18}O$ or $\partial^{13}C$) between the sample and a common standard rather than the absolute isotopic ratios. The ∂O^{18} is mathematically expressed as

$$\delta^{18}O = \frac{(^{18}O/^{16}O_{sample} - {}^{18}O/^{16}O_{standard})}{(^{18}O/^{16}O_{standard})} 1000 \ldots\ldots (2)$$

The standards used are generally either PDB (belemnite of Pedee Formation) or SMOW (Standard Mean Ocean Water).

The temperature dependence of oxygen-isotope fractionation between water and some $CaCO_3$ phases are shown in fig. 4.6. The calcite-water fractionation determined from

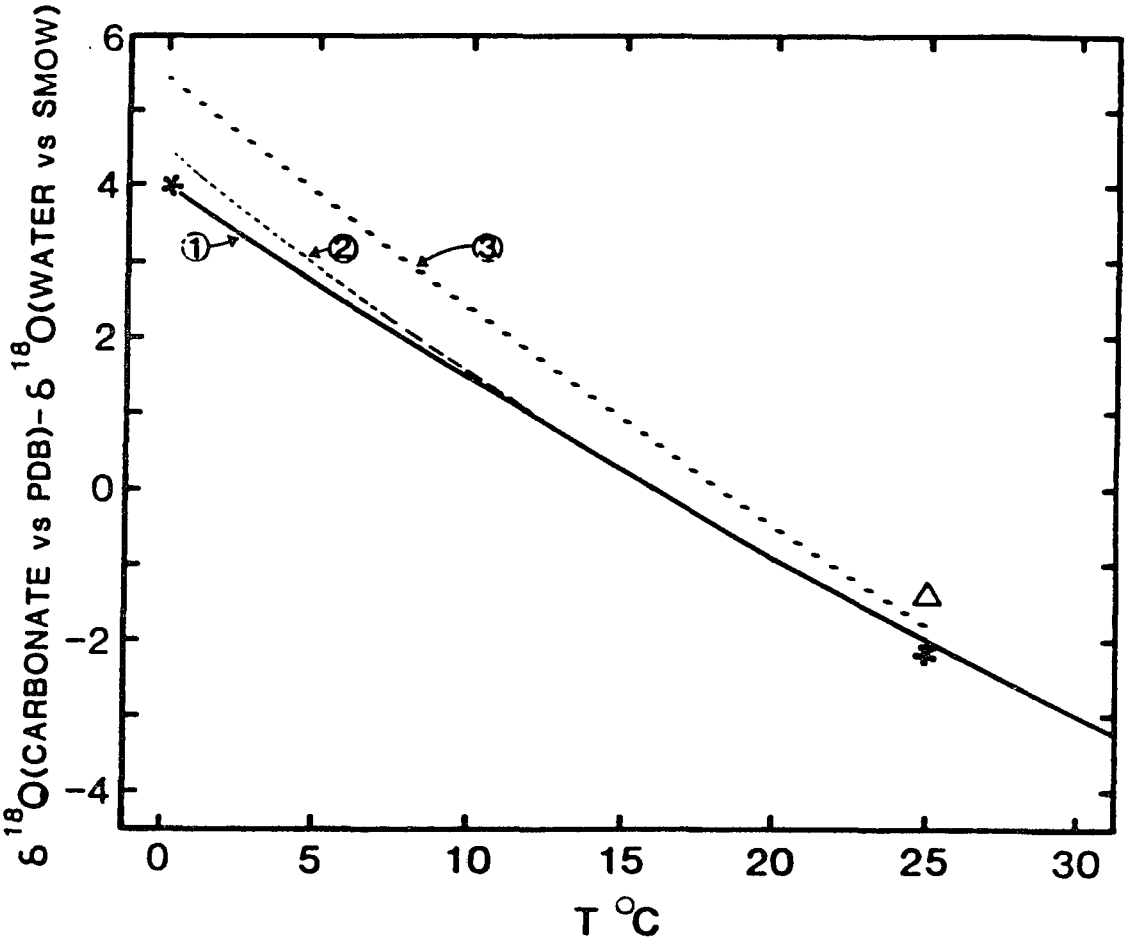

1 Calcite - water (Friedman and O'Neil, 1977)

2 Biogenic calcite - water (Epstein et al, 1953; Craig, 1965)

3 Aragonite - water (Grossman and Ku, 1981)

* Theoretical calcite - water (Bottinga, 1968)

△ Inorganically precipitated aragonite at 25°C (Tarutani et al, 1969)

Figure 4.6: Oxygen isotopic fractionation between different phases of calcium carbonate and water at low temperatures. (From Anderson and Arthur, 1983).

experimental biogenic and inorganic reactions as well as theoretical calculations agree quite well at all temperatures except below 10°C (Anderson and Arthur, 1983, p.1-26).

The equation for Craig's (1965) curve in fig. 4.6 is

$$T°C = 16.9 - 4.2\,(\delta_c - \delta_w) + 0.13\,(\delta_c - \delta_w)^2 \quad \ldots\ldots (3)$$

where $\delta_c = \delta^{18}O$ of calcite, and

$\delta_w = \delta^{18}O$ of water

Although, theoretically $^{13}C/^{12}C$ ratio of calcite samples could be used to determine temperature of precipitation, the fractionation of carbon isotopes between calcite and water has been found to be rather insensitive to temperature changes (Anderson and Arthur, 1983, p.1-80). This is probably because (1) the amount of fractionation between ^{13}C and ^{12}C is less than that between ^{18}O and ^{16}O, and (2) the mass of dissolved carbon in natural water is much less than that of oxygen and, as a result, carbon isotopes are more affected by local chemical processes (Dott and Stanton, 1981, p. 164). Relative contribution from dissolved organic matter may also change the local carbon content of water enormously (Anderson and Arthur, 1983).

The isotopic geochemistry of dolomite is not well understood (Land, 1980; Anderson and Arthur, 1983; Machel and Mountjoy, 1986). The problem stems from the fact that well-ordered dolomite has not been synthesized at low temperatures typical of sedimentary and diagenetic environments. Extrapolation of results of high temperature experiments show that dolomite concentrates ^{18}O by approximately 6% relative to coprecipitated calcite (Northrop and Clayton, 1966; O'neil and Epstein, 1966). A 2- 6% relative concentration has been reported for some Holocene dolomites (Land, 1980; 1983). Fritz and Smith (1970) synthesized poorly-ordered "protodolomite" at temperatures as low as 25°C and suggested that the small fractionation commonly observed between calcite and dolomite results from initial deposition of dolomite as metastable "protodolomite". The temperature of precipitation of "protodolomite" is given by the following relationship (Fritz and Smith, 1970):

$$T°C = 31.9 - 5.55\ (\delta_d - \delta_w) + 0.17\ (\delta_d - \delta_w)^2 \quad \ldots\ (4)$$

where $\delta_d = \delta^{18}O$ of dolomite, and

$\delta_w = \delta^{18}O$ of water.

In both equation 3 and 4, δ_w is unknown, and a suitable value has to be assumed in order to calculate the paleo- temperature of precipitation. This is a major weakness of the isotopic method of paleotemperature determination, and the problem is compounded by diagenetic reactions. In the diagenetic environment, the pore fluids may undergo isotopic exchange with the host rock and change progressively (Clayton et al. 1966; Hitchon and Friedman, 1969; Dickson and Coleman, 1980). One can use a known range of δ_w values of modern formation waters in carbonate rocks to obtain at best a rough estimate of paleotemperatures. In this method, however, the local variations in pore-water isotopic composition across an ancient sedimentary basin can not be reasonably accounted for.

However, fluid-inclusion data, if available from the same sample, can provide some constraints on the isotopic composition of the diagenetic fluid. As previously discussed (chapter 4.3.1), the temperature of melting (Tm) of fluid inclusions can be used to estimate the salinity (%NaCl) of the trapped fluid. For water of a known salinity, a range of $\delta^{18}O$ values, from modern analogues, can be used to calculate temperatures. For example, Friedman (1987a) uses δw values of 2 - 8‰ SMOW for inferred saline to hypersaline waters. However, Tm can be measured with reasonable accuracy only in relatively large inclusions, and in sedimentary carbonate minerals inclusions are rarely of large size, which constrains wide application of this method.

Another major problem encountered in isotope studies is with sampling. Several generations of cements with different isotopic signatures may fill the same interstice in a sedimentary rock (Scholle and Halley, 1985; Kaufman et al. 1990). These cement zones are commonly few tens of microns or less in thickness and the conventional methods of drilling cements out of a sample by using a dental drill or needle is too coarse. Thus, the cement specimen used in isotope analysis usually represents a bulk sample and the data obtained is an average for different generations of cements. This also creates a problem in using Tm data from fluid inclusions since Tm data applies only

to specific fluids trapped in specific inclusions and do not represent an average condition.

4.6.1: Sample preparation and interpretation:

Considering the above limitations and the fact that the oxygen-isotope paleotemperatures calculated in this study for any rock unit vary widely, often in the same sampling location, and do not generally match the paleotemperature trend derived from other methods, isotope analysis was restricted to 50 samples from the Devonian and Silurian carbonates. The Ordovician and Cambrian carbonates, which were sampled in a later field season, were not analyzed for isotopes.

The samples for this study were analyzed by Geochron Laboratories, Cambridge, Massachusetts. The analytical techniques involved in mass spectrometry are discussed in Faure (1977) and other textbooks on isotopes. The cement samples were obtained mainly by using a dental drill on polished slabs or chips. The slabs or chips were cut opposite to fluid-inclusion thin sections. Sometimes, samples were obtained by breaking cements from a thin section with a needle under a microscope after fluid- inclusion work has been done on the thin section.

Temperatures of formation for calcite were calculated using Craig's (1965) equation, and those for dolomite by using Fritz and Smith's (1970) equation (section 4.6). A range of $\delta^{18}O_{water}$, 2 - 8‰ (SMOW), were used following Friedman (1987a) and several other reports of similar range in deep basinal brines (Land and Prezbindowski, 1981; Moore and Druckman, 1981; Roedder, 1984, p.318; Halley, cited in Barker and Halley, 1986).

4.7: DATA INTERPRETATION:

4.7.1: Comparison and refinement of paleotemperature data:

Paleotemperatures experienced by the studied samples were assessed on the basis of fluid inclusion, oxygen isotope, organic maturation and clay diagenesis data. Although each of the above methods has various limitations (see sections 4.3 - 4.6), application of more than one method to each sample, as has been attempted in this study, reduced uncertainties and placed better constraints on paleotemperatures.

Spatial changes in paleotemperatures of individual rock were determined. Since

systematic sampling was primarily limited to outcrops, spatial changes were examined along certain transects in New York state - transects along which most of the outcrops are located. Comparison of paleotemperature profiles of stratigraphically adjacent rock units along a transect allowed further refinement of paleotemperature data and profiles. In these refinements (chaters 8, 11, and 16), it was assumed that when the maximum temperature wass reached in a rock unit, the units immediately above and below that unit in a given location also attained their maximum temperatures. If paleotemperature data was not available in one of these rock units, the temperature is inferred on the basis of an assumed paleo-geothermal gradient (section 4.7.2) and the unit's stratigraphic distance from the adjacent rock unit in which such data was available. The procedure resulted in refined paleotemperature profile of adjacent rock units along a given transect and introduced an additional stratigraphic constraint on paleotemperature data.

4.7.2: Choosing a paleo-geothermal gradient:

Reconstruction of ancient geothermal gradient is critical for any burial study. Such a reconstruction is possible from measured changes in inferred paleotemperature through a given stratigraphic interval of an area (Levine, 1986; Stern and Reesman, 1986). In absence of such information, one has to rely on the tectonic history of the basin, and use data from modern analogs.

In most modern sedimentary basins temperature gradients range from 20 to 45°C/km, but in recent rift basins gradients as high as 80°C/km have been measured (Hanor, 1987). Geothermal gradients measured today in eastern and mid-continent North America ranges from 20° C/km to 40°C/km (Jones and Wallace, 1974; Hodge et al. 1982, 1984; Harrison et al. 1983; Dutton and Land, 1988). In New York, the present day geothermal gradients, calculated from bottom-hole temperatures of relatively deep boreholes by Hodge (1982, 1984) show some spatial variation (fig. 4.7). High temperature gradient of about 40° C/km occurs in a pocket southwest of Syracuse, and in the rest of western New York it ranges between 20°C/km and 36°C/km (fig. 4.7). In eastern New York, no information on the present-day geothermal gradients is available, probably because of paucity of deep boreholes. However, relatively low heat-flow measurements from the Adirondacks and other areas of eastern New York are comparable to those in western

Figure 4.7: (a) Map of New York State showing surface heat-flow measurements. (b) Map of the western half of the state showing the present-day geothermal gradients (°C/km) based on corrected bottom-hole temperatures. (From Hodge, 1984).

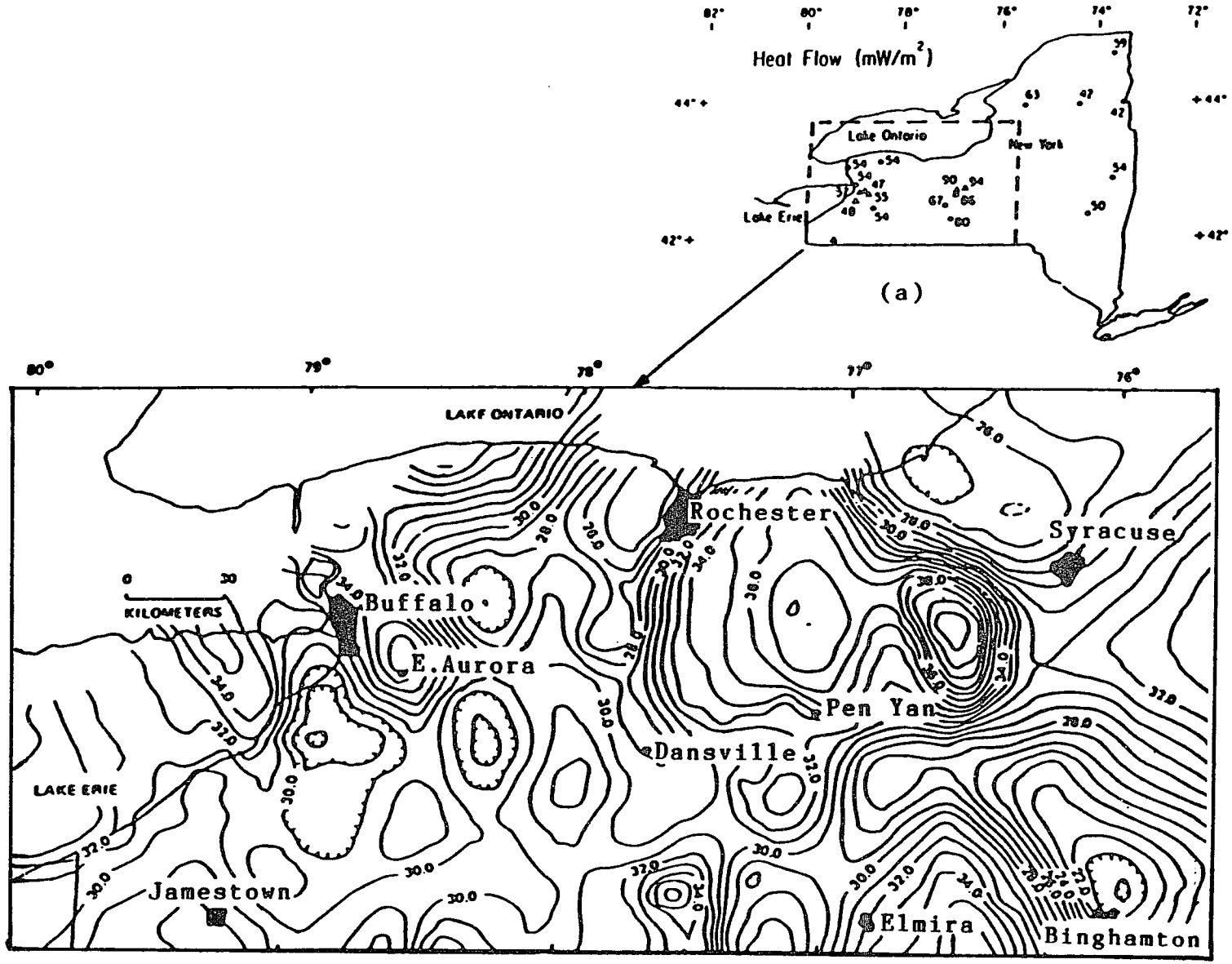
Heat Flow (mW/m²)
Lake Ontario
New York
Lake Erie
(a)
LAKE ONTARIO
Rochester
Syracuse
Buffalo
E.Aurora
Pen Yan
Dansville
LAKE ERIE
Jamestown
Elmira
Binghamton
KILOMETERS
(b)

New York (fig. 4.7), and an average geothermal gradient of about 30°C/km is probably a reasonable estimate for the eastern half of the state.

Findings in New York and other areas of similar geologic setting suggest that, the paleo-geothermal gradients of New York might have been within the range shown by the present gradients. On the basis of fission-track dates of the Middle Devonian Tioga bentonite and the bentonite bed within the Upper Ordovician Black River Group, Johnsson (1985) had calculated a paleotemperature gradient of 20° C/km for northcentral New York. From vertical vitrinite reflectance profiles of two boreholes, Levine (1986) calculated a paleotemperature gradient of 33°C/km for the southern Anthracite District of Pennsylvania. In the Alberta Basin of Canada, estimated paleotemperature gradients range from 27° C/km to 40° C/km in which the gradients are believed to have increased from the Rocky Mountains in the west to the plains in the east (Hitchon, 1984; Kalkreuth and McMechan, 1984; Connolly, 1989; Tilley et al. 1989).

Thus, acceptance of the average present-day geothermal gradient of 30° C/km for the eastern and western parts of New York State as the paleo-geothermal gradients during maximum burial, sometime in the late Paleozoic time, may be a reasonable approximation. However, the relatively high heat flow and geothermal gradient seen southwest of Syracuse (fig. 4.7) need special scrutiny; objections have been raised against Johnsson's (1986) use of a gradient of 26°C/km in this area (Karig, 1987).

According to Hodge (1984), this thermal anomaly may be due to convective upwelling along fractures that may extend into the basement rock. However, it is unlikely that this anomaly existed in the late Paleozoic time - fracturing in rocks of this region has been atrributed to post-Alleghanian uplift and stretching (Barnes and Tillman, 1983; Dennison, 1983). That is, the high heat flow and geothermal gradient in central New York is a later development and must have occurred after much of the younger rocks have been eroded. Even if this later geothermal gradient was 40° C/km or higher, a rock unit in this area might already have experienced high temperatures earlier when the gradient was lower but burial was deeper. Therefore, the newly established higher geothermal gradient most probably did not increase the thermal maturity of any rock in the area.

Karig suggested that heat flow associated with the late Jurassic dikes of the eastern Finger Lake district (fig. 2.3) could have overheated the rocks of that area and given a false impression of deep burial (see chapter 3). However, published information on heat flow from dikes indicate otherwise. Dikes, especially the thin ones, act as geologically instantaneous heat pulses that can heat up the host rock only around their immediate contacts (Delaney, 1987). McCelland-Brown (1981) shows that for a 1.25m thick dike in Scotland, temperature decreased exponentially in the host rock, already having an ambient temperature of 150°C, from 760°C at the contact to 375°C only at a distance of 1.2m from the contact. Buchan and Schwarz (1987), in their study of remanent magnetization in the host rock around a 38m thick dike of the Northwestern Territories, found that at a distance of 37m from the contact the remanent magnetization remained undisturbed, indicating that heat, even from such a thick dike, had failed to significantly raise the temperature (and reset the remanent magnetization) of rocks only at a distance of 37m.

Among the 82 dikes reported from a NW-SE trending narrow zone - 25km by 45km - running parallel to Lake Cayuga between Syracuse and Ithaca, the thickest one is only 3.5m thick (Kay et al. 1983; Kay and Foster, 1986). Another dike reaches a thickness of 1m, and the rest are between a few cm and 0.75m thick. Heat generated from these thin dikes could not have possibly travelled very far. Moreover, the dike swarm was emplaced over an interval of 145 ± 7 to 120 Ma (Kay et al. 1983), implying that there was no possibility of a combined heat effect. Evidence, such as sharp contacts of these dikes with the host rock, lack of metamorphism in the adjacent rocks, texture, and vertical extent of very thin dikes that are believed to have originated in the upper mantle have led workers to believe that these dikes were not emplaced by magmatic flows, but by "fluidization mechanism", in which fragmented materials were transported in a fast-moving gas stream (Foster, 1970; Reitan et al. 1970; Kay et al. 1983; Kay and Foster, 1986). If this interpretation is correct, the possibilities of overheating the surrounding rocks and establishing a sustained, elevated geothermal gradient seem even more remote, because a gaseous flow must have had a much lower heat capacity than a magmatic flow. Moreover, because most dikes cool very quickly, hydrothermal circulation, which

is known to be an important process during cooling of large igneous bodies, fail to become established (Delaney, 1987).

Considering the above evidence and arguments, it is believed that the present higher geothermal gradient southwest of Syracuse was not existent at the time of deepest burial of the rocks of central New York, and the late Jurassic dikes had played little or no role in overprinting the paleotemperature signatures of rocks of central New York, except possibly at their contacts. Moreover, none of the samples in this study was collected from the vicinity of these dikes. There is also no evidence of any other igneous activity that could have affected the rocks under the present study. Therefore, in this study an average paleo-geothermal gradient of 30° C/km was used for the entire sampling area in New York State. Previous studies in New York that used a gradient of 25-30° C/km include those of Friedman and Sanders (1982), Lakatos and Miller (1983), Johnsson (1985, 1986), Friedman (1987a) and Gerlach (1987). McKenzie (1981) and Issler (1984) recommend the use of present-day geothermal gradient in predicting and interpreting thermal maturation data in thermally old (more than 150 m.y.) basins.

4.7.3: Calculation of maximum burial depths and thickness of eroded strata:

The maximum burial depth of a rock unit at a study location was calculated from its refined maximum paleotemperature (section 4.7.1) by first subtracting a mean annual surface temperature of 20° C and dividing the remainder by the paleogeothermal gradient of 30° C/km (section 4.7.2). The mean annual surface temperature of New York is now about 12° C (Hodge, 1984), but considering a more equitorial position of the study area during the Paleozoic - Mesozoic time, use of 20°C appears to be a reasonable approximation (see Friedman and Sanders, 1982, Lakatos and Miller, 1983).

The thickness of eroded strata at a study location was determined by subtracting the projected thickness of younger rocks preserved elsewhere in New York State. Thickness data from Rickard (1973, 1975) and Fisher (1977) were used for this purpose. Justification for such projections is given in relevant chapters.

CHAPTER 5: THE BEEKMANTOWN GROUP

5.1: STRATIGRAPHY AND DEPOSITIONAL HISTORY:

The Cambro-Ordovician (Croixian-Canadian) Beekmantown Group of the northern and central Appalachians and the equivalent Knox Group of the southern Appalachian and Ohio represent the first extensive carbonate shelf deposits of the Appalachian foreland basin (chapt. 3).

In New York, the Beekmantown rocks are exposed in a roughly circular, although discontinuous, belt along the margin of the Adirondack Highlands (fig. 5.1). The greatest thickness of the Beekmantown Group in New York occurs in the Champlain Valley and in the subsurface of southcentral and eastcentral New York (Rickard, 1973; Fisher, 1977). Including the upper Cambrian Potsdam Sandstone, the total thickness in these areas exceed 700m. The Beekmantown rocks thin toward northwestern New York and disappear beneath Lake Ontario. Across Lake Ontario, in Canada, the upper Ordovician Black River and Trenton carbonates rest directly on the Precambrian basement (Rickard, 1973, pls. 12, 13 and 14). The northwest-ward thinning of the Beekmantown Group is probably due to post-Beekmantown erosion and does not reflect a depositional pinch-out in that direction. More than 300m of Beekmantown rocks escaped erosion and are preserved in the Ottawa-Bonechere Graben northwest of New York across the St. Lawrence River (Rickard, 1973, pl. 19).

In New York, the Beekmantown Group consists of several formations; all except the basal Potsdam Sandstone are limestones or dolostones (fig. 5.1). There appears to be some uncertainty in the status of the Potsdam Sandstone with respect to the Beekmantown Group. Rickard (1973) excludes the Potsdam Formation from the Beekmantown Group, whereas Fisher (1977) includes its upper part within Beekmantown. The COSUNA chart (1985) includes the entire Potsdam Formation within the Beekmantown Group.

In the Mohawk Valley, the Potsdam Formation has very limited exposure, not exceeding 30m in thickness (Fisher, 1977). The overlying Galway Formation in the

Figure 5.1: The outcrop belt (darkened) and stratigraphic relationships of the Beekmantown Group. (Adapted from Fisher, 1977).

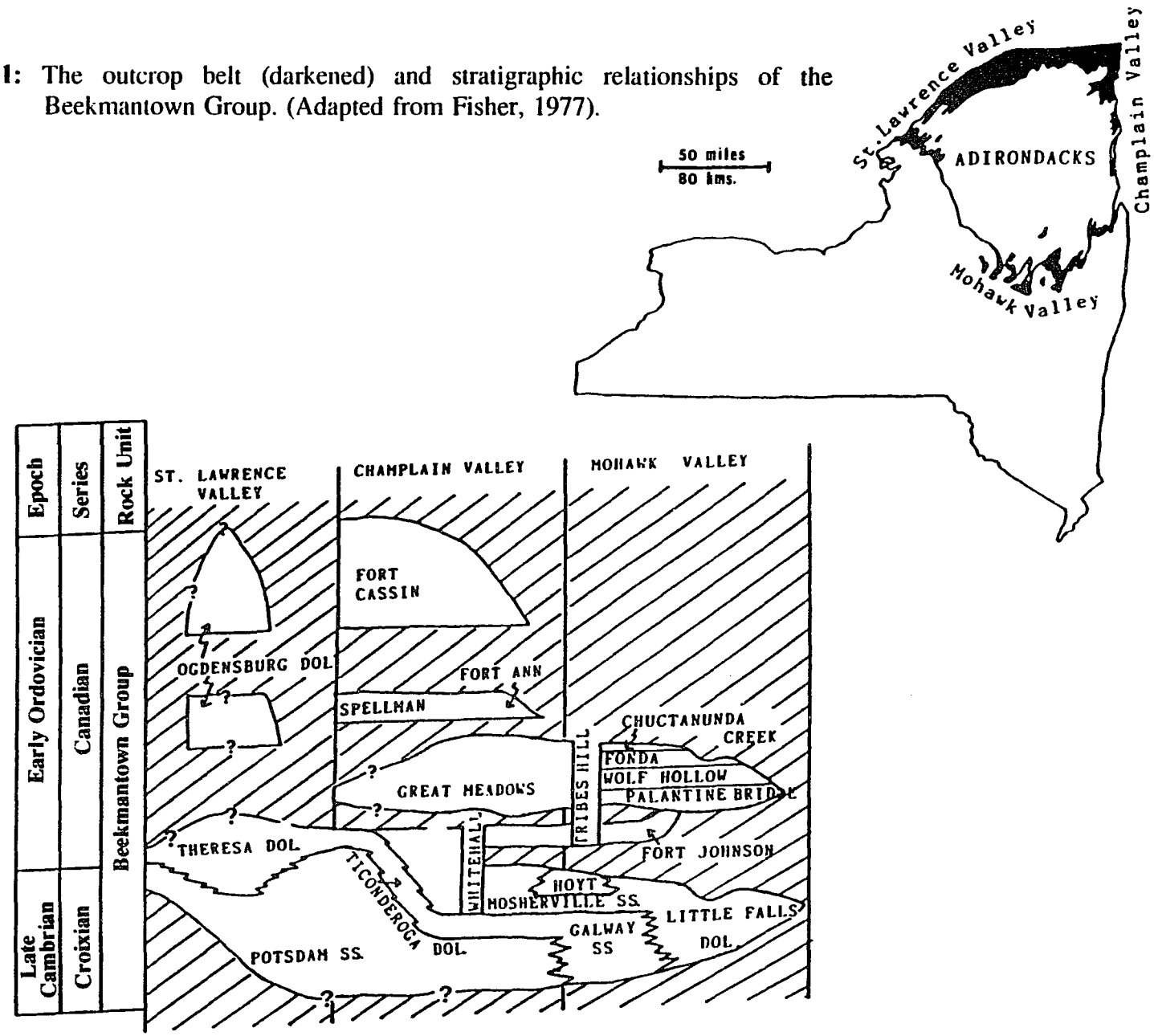

Mohawk Valley consists of sandstones, dolostones and sandy dolostones. It is equivalent to the Theresa Formation of the St. Lawrence Valley which is a more pure dolostone but still contains a considerable amount of quartz sand. The Theresa-Galway rocks are believed to have formed in a supratidal to intertidal environment (Fisher, 1977). The Galway Formation is succeeded by and partly equivalent to the Little Falls Dolostone in the western part of the Mohawk Valley (fig. 5.1). An intertidal to shallow subtidal (above the wave base) environment of deposition has been inferred for this formation (Fisher, 1977).

In the eastern part of the Mohawk Valley, the upper part of the Little Falls Formation grades into the Mosherville Sandstone and Hoyt Limestone (fig. 5.1). The Mosherville Sandstone shows bidirectional cross-bedding with foresets as thick as 30cm. These structures indicate the former presence of dunes or megaripples in a subtidal environment dominated by ebb- and flood-tides. The Hoyt Limestone is well known for its algal domes and is believed to have formed in an intertidal to shallow subtidal environment (Owen and Friedman, 1984). These units are succeeded by the limestones and dolostones of the Tribes Hill Formation in the Mohawk Valley. The Tribes Hill Formation is inferred to have been deposited in a supratidal to shallow subtidal environment dominated by intertidal shoals (Friedman and Braun, 1975).

In The St. Lawrence Valley, the Theresa Formation is unconformably overlain by the Ogdensburg Dolostone (Canadian) which is stratigraphically younger than the Tribes Hill Formation of the Mohawk Valley (fig. 5.1). The Beekmantown Group of the Champlain Valley consists of a greater number of rock units than in the Mohawk and St. Lawrence Valleys, but these rocks were not included in this study and are, therefore, not discussed here. Urschel (1984) and Urschel and Friedman (1984) have studied the paleotemperatures of the Beekmantown rocks of the Champlain and eastern Mohawk valleys (see tables 5.2).

5.2: SAMPLING LOCATIONS:

The sampling locations for the Beekmantown Group are shown in figure 5.2. Most of the samples were collected from the southeastern margin of the Adirondacks where excellent

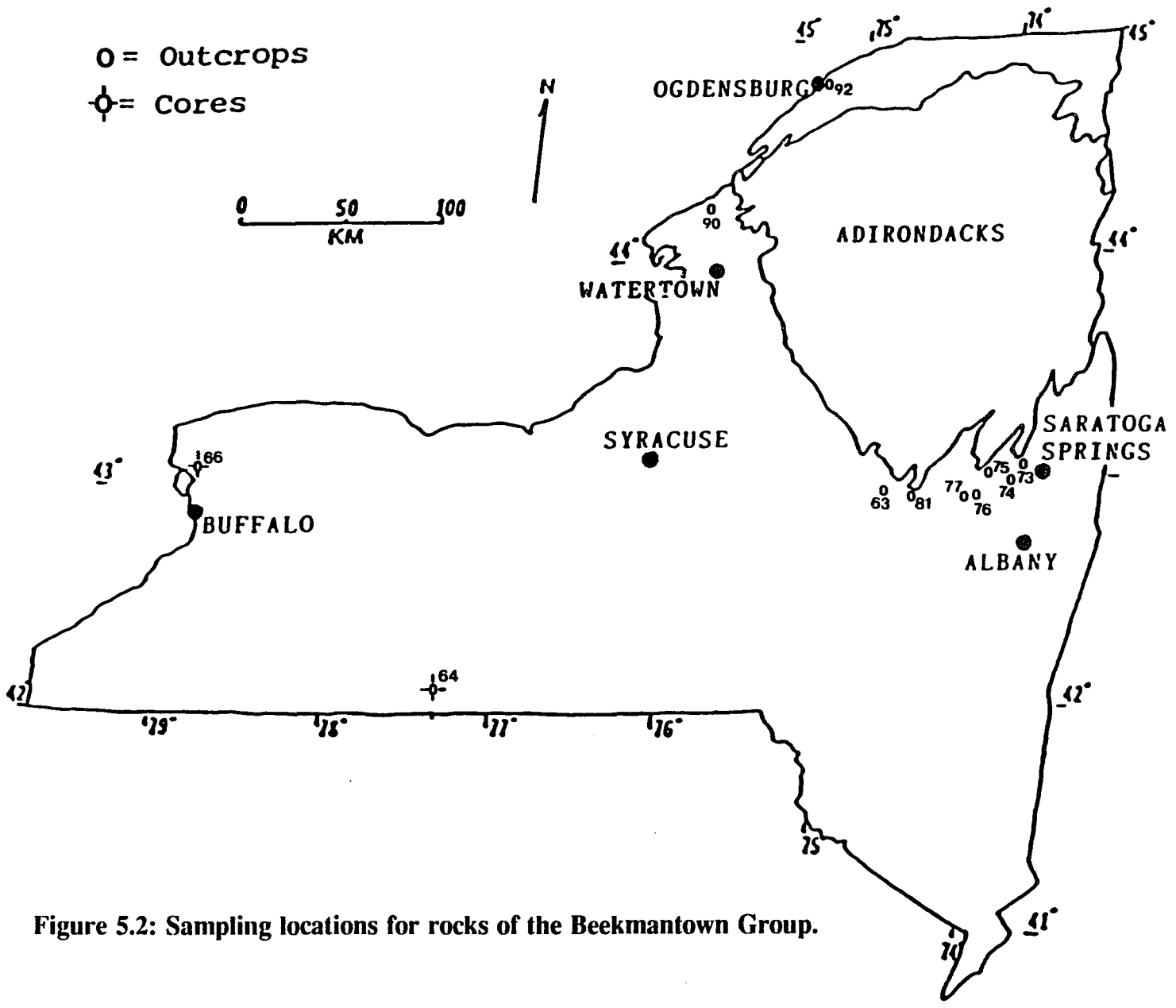

Figure 5.2: Sampling locations for rocks of the Beekmantown Group.

exposures are found. Samples were also collected from the St. Lawrence Valley, but most of these samples were not suitable for this study. Only in locations 90 and 92 (fig. 5.2) fluid-inclusion measurements could be taken. Core samples were collected from two locations (66 and 68).

5.3: GENERAL PETROGRAPHY OF THE SAMPLES:

Most of the Beekmantown samples collected for this study were from coarse, sandy dolostones as this lithology is the predominant one in the Theresa, Galway, Little Falls and Tribes Hill formations. The Beekmantown rocks in the eastern Mohawk Valley region consist of abundant cement- filled vugs and fractures (fig. 5.3). The vugs are as large as 8cm in diameter and roughly circular to irregular in shape (fig. 5.3a). Healed fractures are not very common and generally less than a few cm in width but in location - 76, fractures as wide as 25cm (fig. 5.3b) have been observed. Rocks containing these vugs and fractures were preferentially sampled.

The healed fractures in the eastern Mohawk Valley contain only sparry calcite, whereas the vugs contain any combination of calcite, dolomite and quartz except that quartz does not occur independently in any vug. Where quartz is found, it occurs as euhedral crystals lining the cavity wall and is usually followed by saddle dolomite (fig. 5.4a). In a few samples, where dolomite and sparry calcite coexist, the calcite grows on dolomite (fig. 5.4b).

Vugs and fractures filled with secondary minerals become sparse in the Beekmantown rocks along the western margin of the Adirondacks. The Theresa dolostones in this region are generally bio-mottled and contain lenses of clean, quartz sandstone. The dolomite appears to be of replacive origin, stylolitization is severe, and late cements are rare. The Potsdam Sandstone in location - 90 shows some quartz overgrowths. In location - 92, however, the Ogdensburg Dolostone contains abundant vugs and short, bedding-parallel veins filled with sparry calcite.

The core samples of the Theresa Dolostone of location - 66 consist of dark-gray, hemispheroidal stromatolites with small calcite-filled vugs (fig. 5.5). In the other core samples of location-68, the Theresa Dolostone is coarse and sandy and contains fine fractures healed with dolomite that ranges in texture from saddle dolomite to dolomite

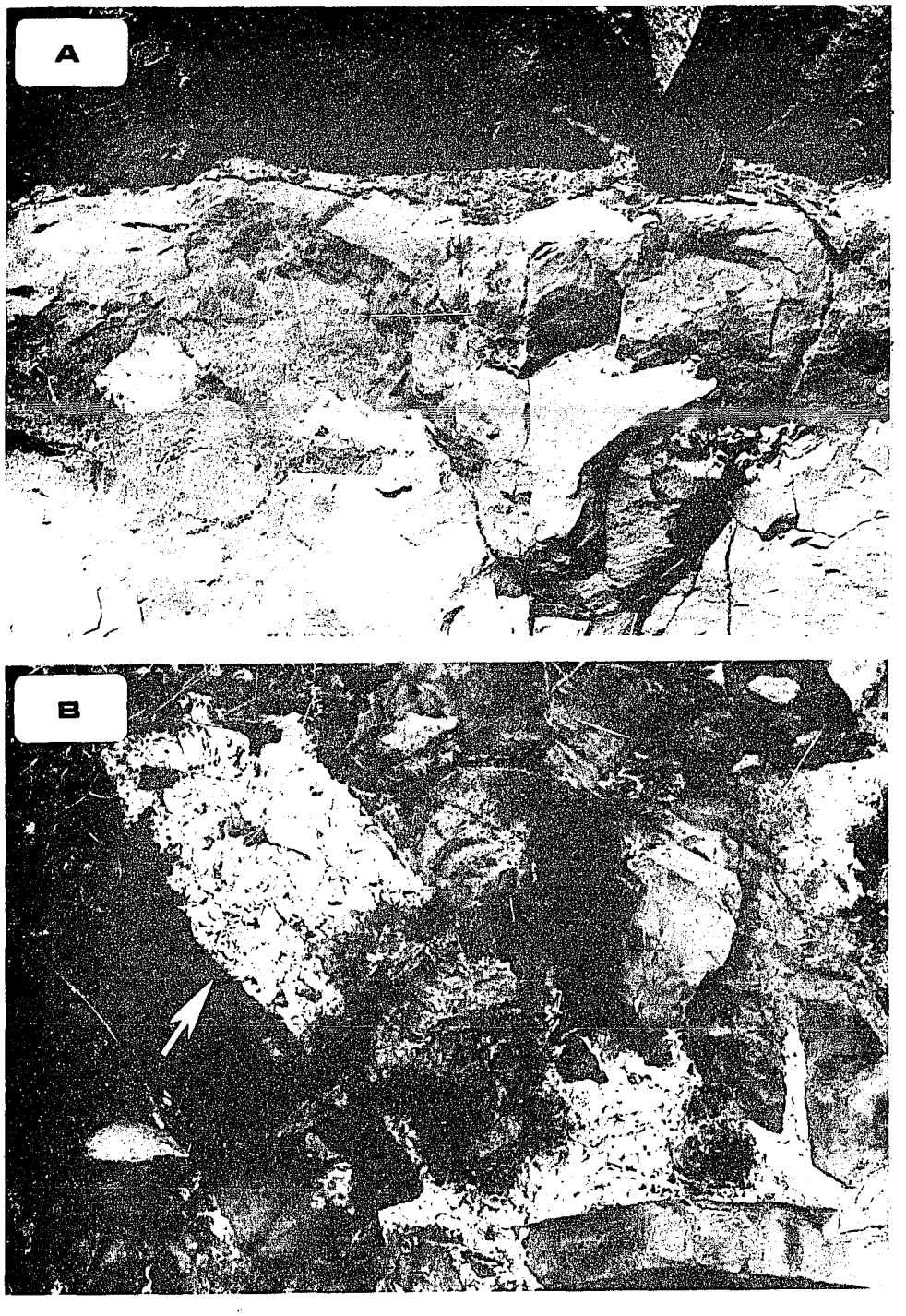

Figure 5.3: Outcrop photographs showing (A) semicircular to elongate calcite-filled vugs (marked by arrows) in the dolostones of the Tribes Hill Formation, location - 77, and (B) unusually wide calcite-filled fracture (marked by arrow) in the Tribes Hill Formation of location - 76. Lens cap is 6cm. in diameter.

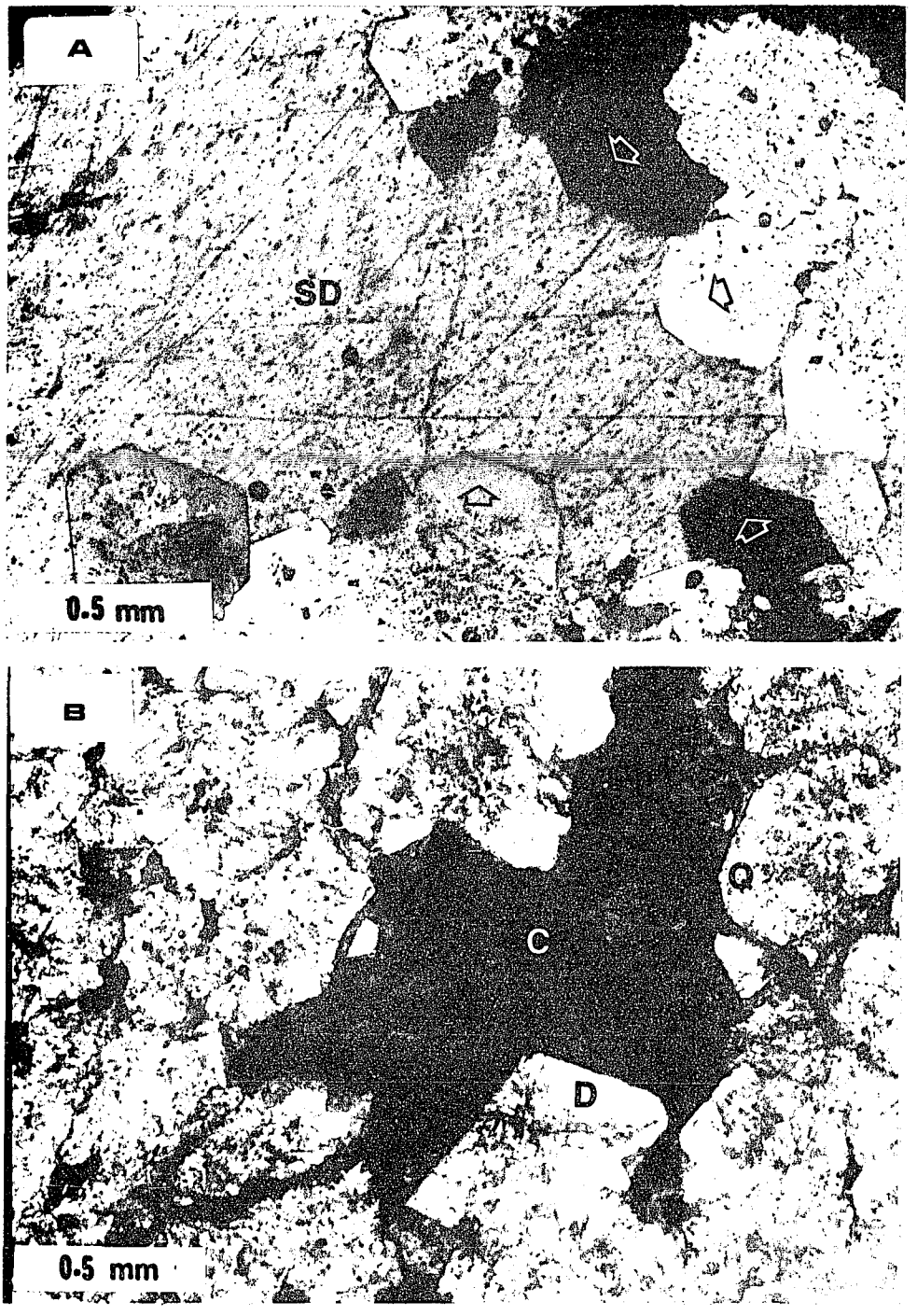

Figure 5.4: Photomicrographs showing (A) part of a vug from the Tribes Hill Formation of location-63 in which euhedral quartz crystals (shown by arrows) line the wall of the vug and are followed by saddle dolomite (SD), and (B) coexisting quartz (Q), sparry calcite (C) and dolomite (D) in a vug from the Tribes Hill Formation of the same location. Calcite has precipitated last in these vugs.

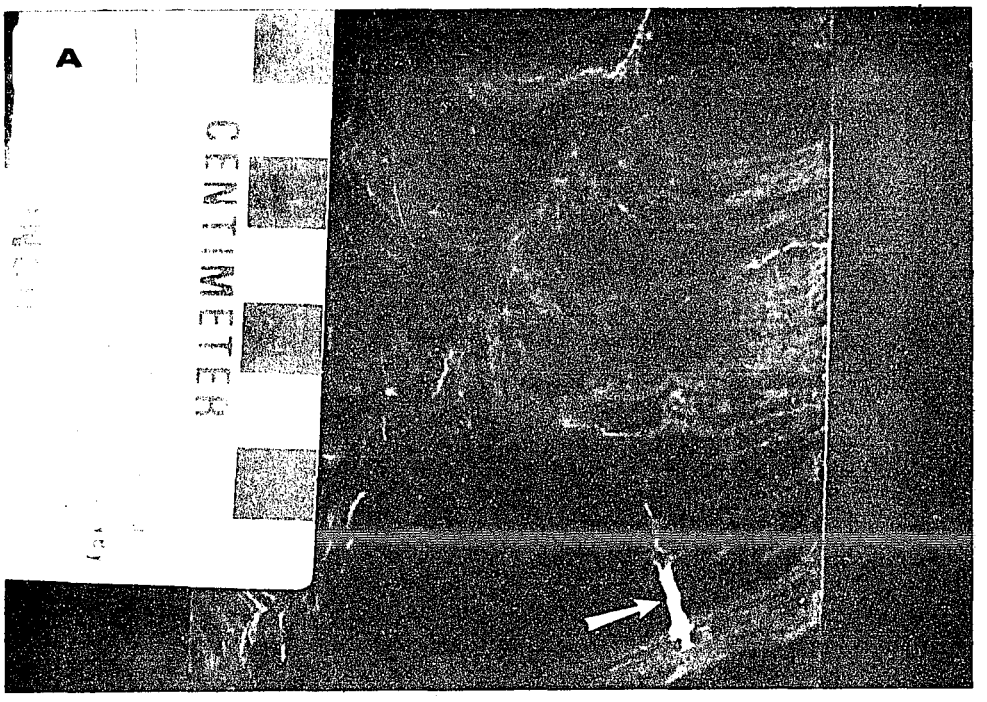

Figure 5.5: Core-sample section of Theresa Formation showing small calcite-filled vug (marked by arrow) in stromatolitic dolostone. From Location-66.

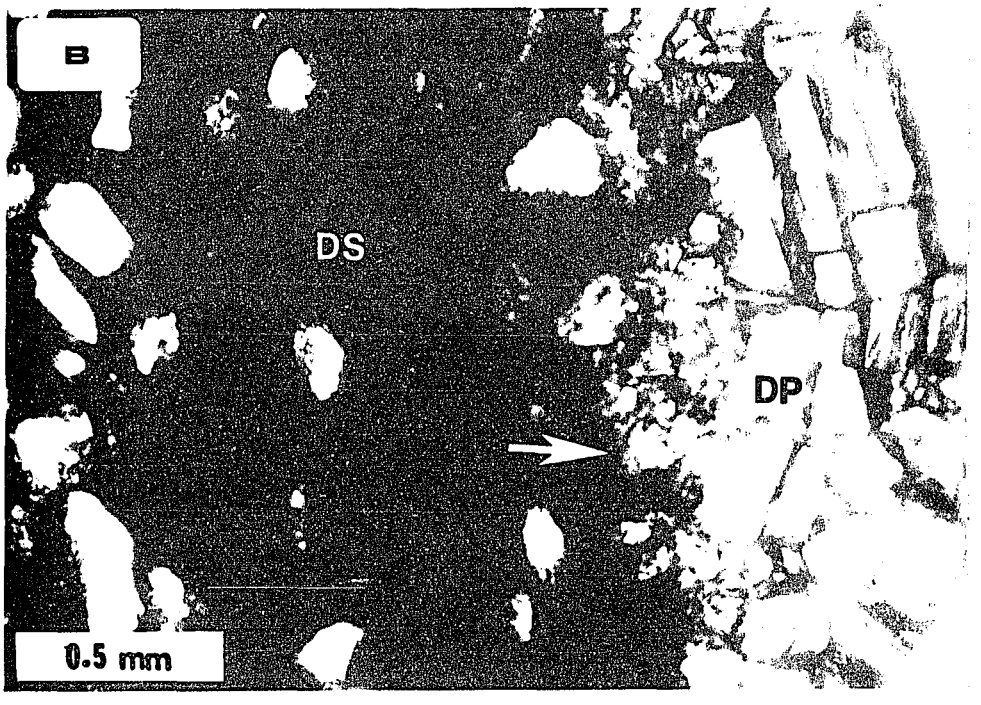

Figure 5.6: Photomicrograph of sandy dolostone (DS) of the Theresa Formation of location - 68 showing part of a fine fracture filled with saddle dolomite (SD) and dolomite with planar boundaries (DP). Arrow marks the margin of the fracture.

with planar boundaries (fig. 5.6), resembling idiotopic - C dolomites of Gregg and Sibley (1984).

5.4: FIUID-INCLUSION DATA:

Vug- and fracture-filling sparry calcite, saddle dolomite and quartz of the Beekmantown Group generally contain abundant two-phase aqueous fluid inclusions (fig. 5.7). Histograms of fluid-homogenization temperatures (Th) of the Beekmantown samples from various locations are shown in figure 5.8. Maximum homogenization temperatures (Th_{max}) are also shown. Table 5.1 shows the 'Tm's and corresponding 'Th's for various locations. Figure 5.9 plots Th_{max} against study locations along the margin of the Adirondacks. All the measurements except those in location-90 were taken from vug- and fracture-filling calcite, saddle dolomite and quartz. In location-90, the inclusions were measured in quartz overgrowths in the Potsdam Sandstone. Detailed inclusion data are presented in Appendix - B.

Urschel (1984) and Urschel and Friedman (1984) have studied fluid-inclusion temperatures of Beekmantown samples from the Champlain, upper Hudson and eastern Mohawk Valley, and the results are shown in table 5.2. Some of their sampling locations in the Mohawk Valley overlap with those in this study. It is however, not possible to construct Th- histograms or calculate Th_{max} for individual location from their data, because only the ranges of Th, not individual readings, for any location were reported in their study. The implications of their inclusion data are discussed in section 5.6.3.

5.5: STABLE ISOTOPE DATA:

Stable isotope ratios of the Beekmantown samples were not measured in this study. Urschel (1984) and Urschel and Friedman (1984) measured oxygen and carbon isotopes of eight Beekmantown samples from the Champlain, upper Hudson and eastern Mohawk Valley region. Their isotope data is presented in table 5.2 and discussed in section 5.6.3.

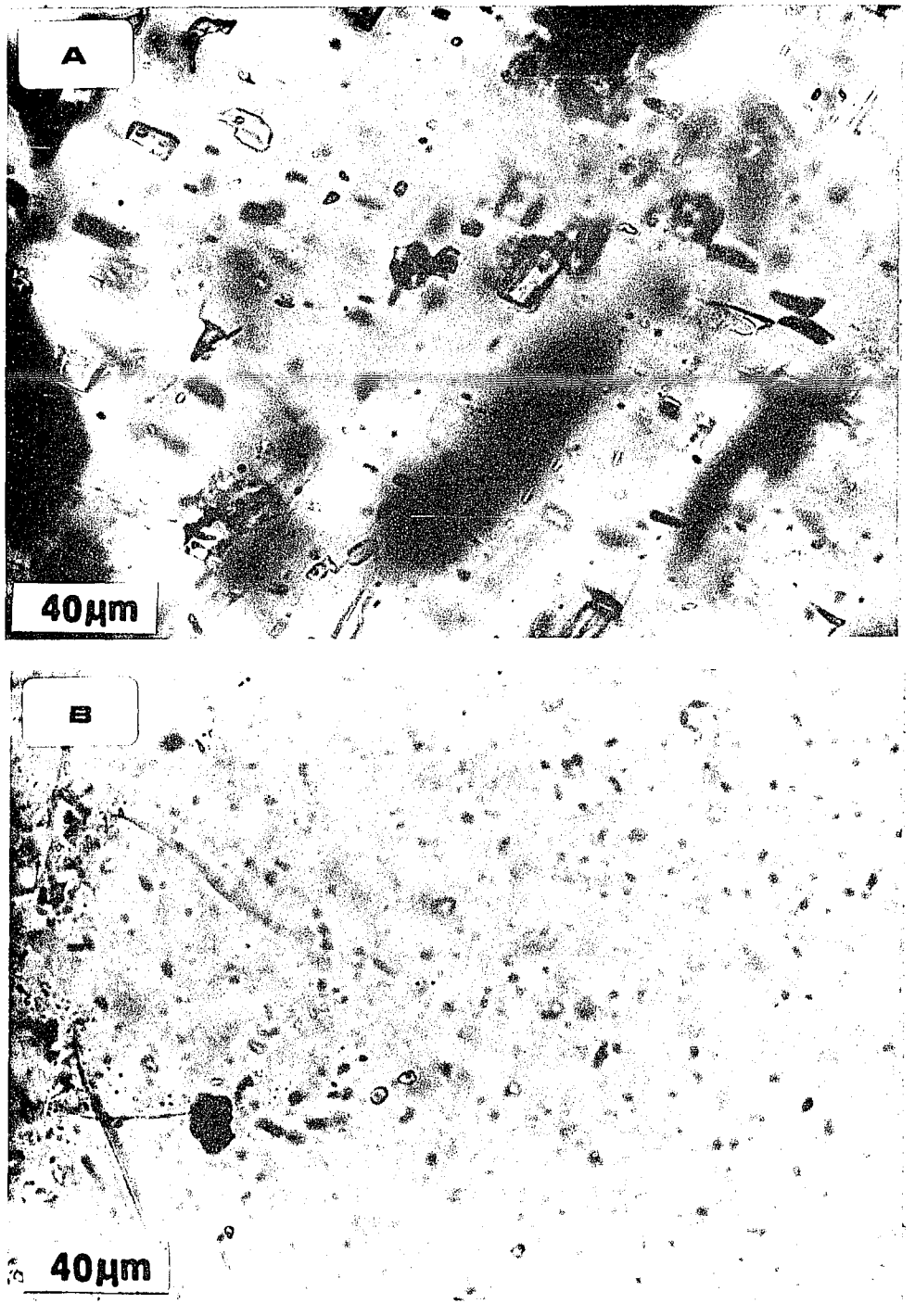

Figure 5.7: Photomicrographs showing (A) primary, two-phase aqueous inclusions in the vug-filling calcite of figure -24, and (B) primary, two-phase aqueous inclusions in vug-filling quartz of the Theresa Formation of location - 73.

Figure 5.8: Fluid-homogenization temperature (Th) histograms of Beekmantown samples from various study locations (of fig. 5.2). Calculated maximum homogenization temperatures (Th_{max}) are also shown.

LOCATION: 73

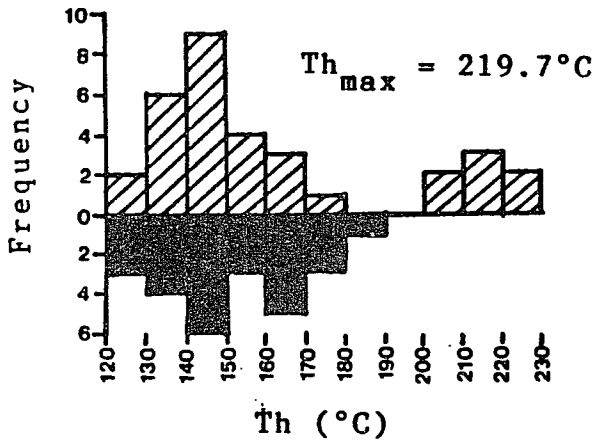

LOCATION: 74

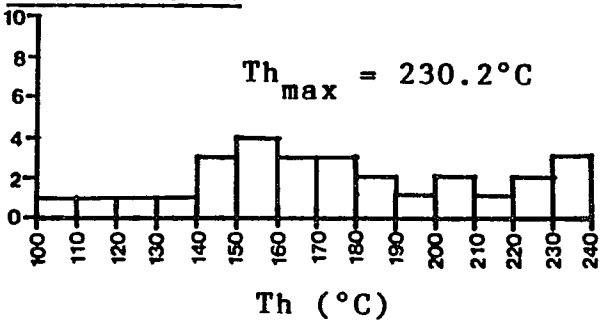

LOCATION: 75

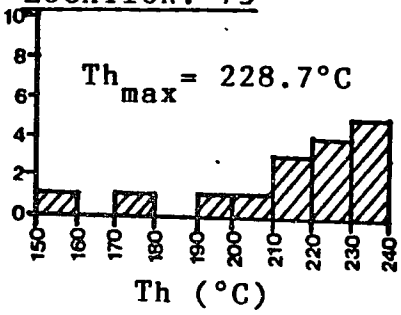

LOCATION: 76

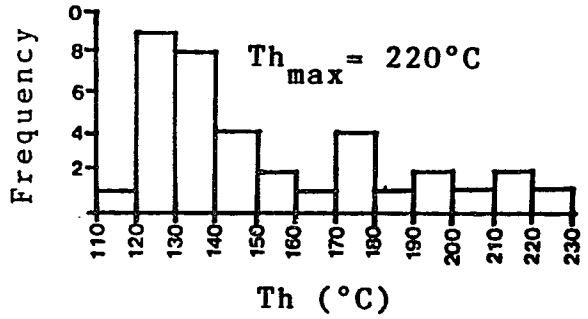

LOCATION: 77

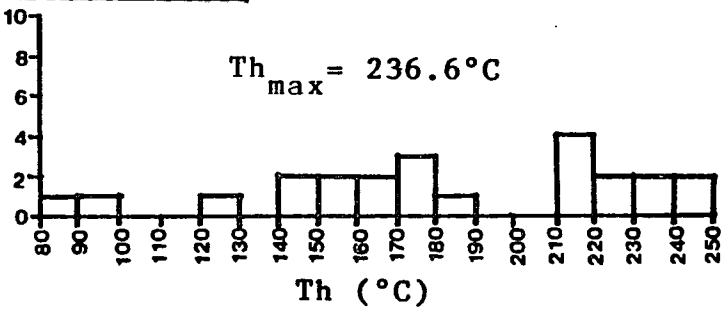

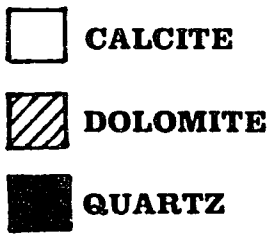

LOCATION: 81

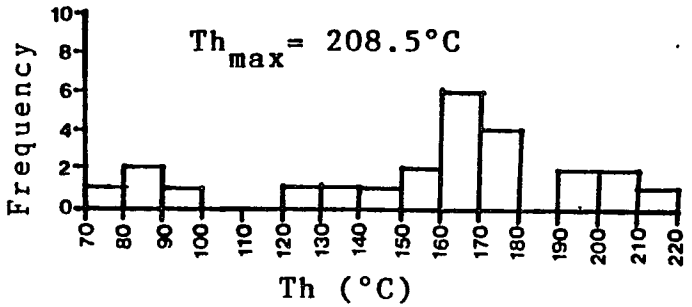

LOCATION: 63

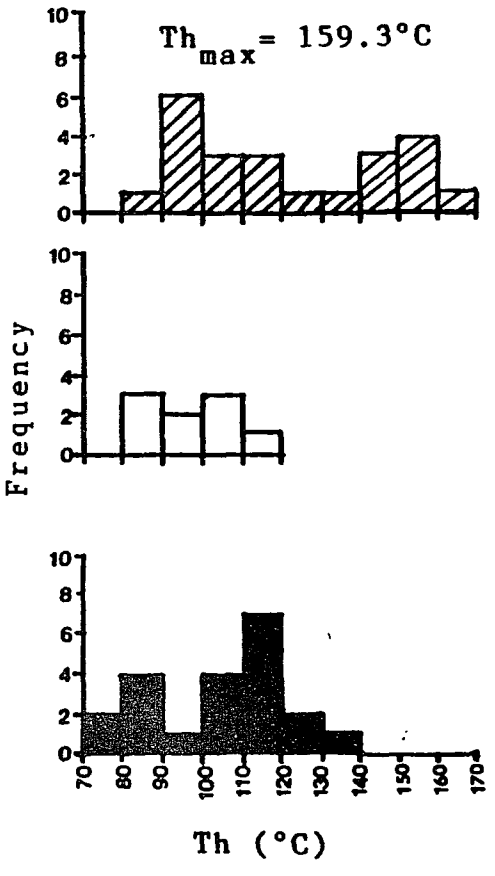

LOCATION: 66

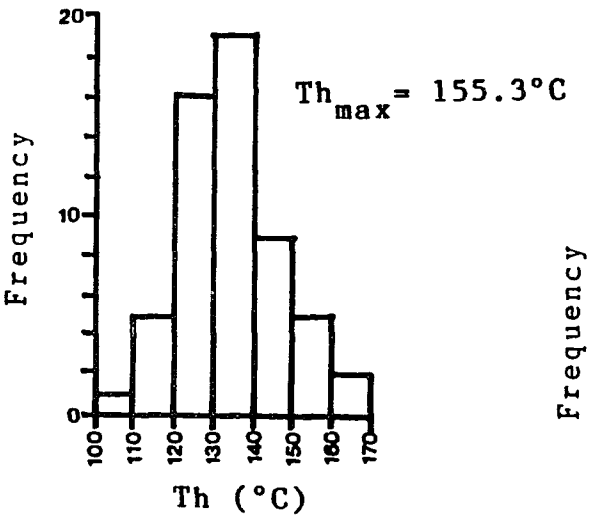

LOCATION: 68

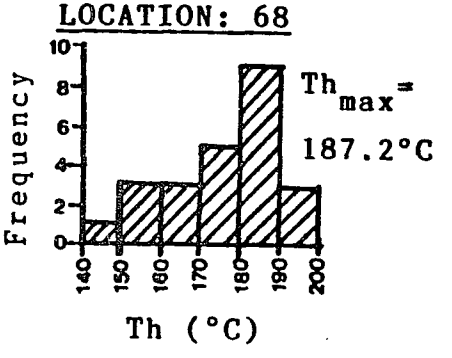

LOCATION: 92

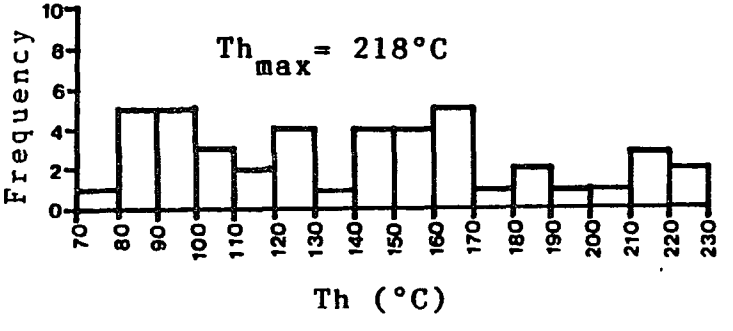

LOCATION: 90

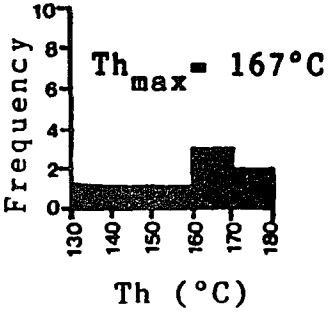

Table 5.1: Melting temperatures (Tm), corresponding homogenization temperatures (Th), and calculated salinity (wt% NaCl) of fluid inclusions in the late-stage cements of the Beekmantown Group.

Location	Type of cement	Tm (°C)	*Salinity (wt% NaCl)	Th (°C)
74	Sparry calcite	+1.2	---	186
	Sparry calcite	+0.7	---	165.4
	Sparry calcite	0.0	---	206
75	Saddle dolomite	-20.6	23.08	206
76	Sparry calcite	-10.0	13.98	130.6
	Sparry calcite	-10.4	14.40	139
	Sparry calcite	-15.0	18.78	120
77	Sparry calcite	-22.0	24.04	228.3
	Sparry calcite	-12.0	16.04	145
	Sparry calcite	-2.9	4.78	218
81	Sparry calcite	+1.1	---	125
63	Mega-quartz	-18.0	21.20	113.4
	Mega-quartz	+1.0	---	100.6
92	Sparry calcite	+2.5	---	190
	Sparry calcite	+2.5	---	217.6
	Sparry calcite	-15.0	18.78	130
66	Sparry calcite	-26.0	26.60	135
	Sparry calcite	-20.6	23.08	124
	Sparry calcite	-21.0	23.35	124.7
	Sparry calcite	-22.0	24.04	148
	Sparry calcite	-21.7	23.83	153
68	Saddle dolomite	-22.0	24.04	185.5

* Salinity was calculated according to Potter et al's (1978) method (see section 5.3.1)

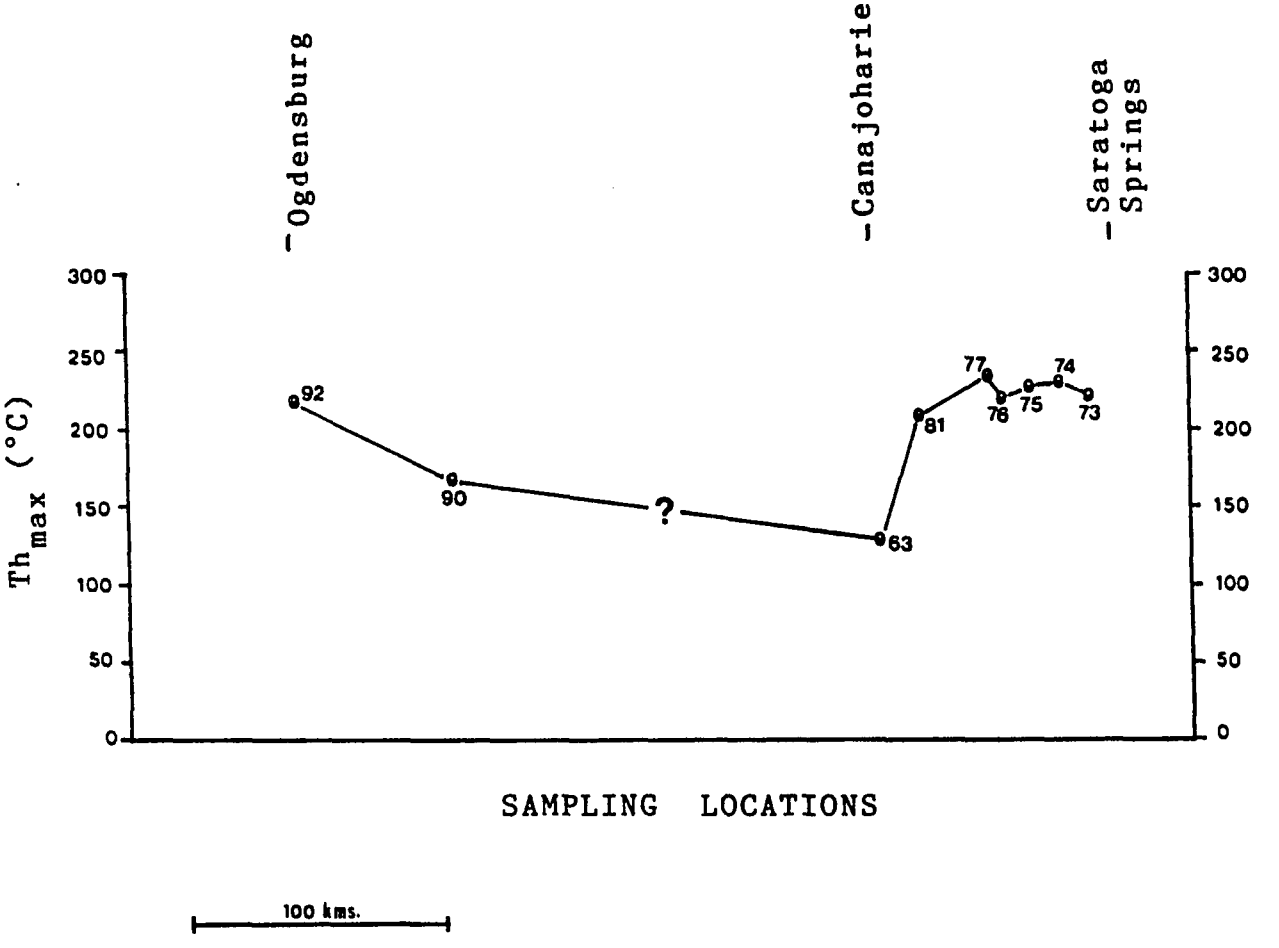

Figure 5.9: Plots of Th_{max} against sample locations along Saratoga Springs - Ogdensburg transect.

Table: 5.2: Fluid-homogenization (Th) and melting temperatures (Tm) and stable isotope ratios of Beekmantown samples from the Champlain (CV), upper Hudson (HV) and eastern Mohawk (MV) valleys. Taken from Urschel and Friedman (1984).

Sample location	Sample type	No. of inclu-sions	Range of Th (°C)	Range of Tm (°C)	$\delta^{18}O$ ------ $\delta^{13}C$ (‰ PDB)
Core (MV)	Saddle dol.	10	59 - 150	-12 to -39	-13.01 -1.5
Core (MV)	Dol. vein	8	102 - 121	-12 to -17 -3.2	-11.17
Tribes Hill (MV)	Dol. vein	5	109 - 130	-7 to -15	-9.91 -2.4
Tribes Hill (MV)	Calcite cement	7	116 - 303	N.A	N.A
Fort Ann (HV)	Dol. vein	15	117 - 190	-5.0	-12.62 -1.8
Baldwin Corners(HV)	Dolost.	4	123 - 160	-8 to -12	-6.8 -1.4
Smith Basin (HV)	Calcite	N.A	N.A	N.A	-10.10 +2.9
Ticon-deroga(CV)	Dol. vein	9	123 - 160	-12 to -15	-13.98 -2.9
Ticon-deroga(CV)	Dolost.	2	140 - 145	N.A	-7.38 -0.9
Plattsburg	Dol. vein	9	68 - 153	-33.4	N.A

5.6: INTERPRETATION:

5.6.1: Paragenetic sequence of cements:

The vugs and fractures postdate lithification and replacive dolomitization in the Beekmantown rocks. The mineral phases found in vugs and fractures, therefore, precipitated from diagenetic fluids as late-stage cements. Although no direct inference on the temperature of precipitation can be made from petrography, saddle dolomite found in some of these vugs and fractures is believed to form in the burial environment from relatively high temperature fluids (Radke and Mathis, 1980; Lee and Friedman, 1987; Machel, 1987)

Along the margin of the Adirondacks, fractures in the Beekmantown rocks contain only sparry calcite (section 5.3). No direct cross-cutting relationship between vugs and healed fractures was observed. But, from the observation that the last stage mineral in vugs containing co-existing mineral phases is also sparry calcite (fig. 5.4b), it is possible that the two sparry calcites were roughly contemporaneous. If so, the fractures are younger than the vugs, but developed before many of the vugs were completely filled. The timing of precipitation of vug-filling calcites of location-66 and fracture-filling dolomite of location - 68 (figs. 5.2, 5.5, 5.6) relative to the late cements of the Beekmantown Group along the margin of the Adirondacks, discussed above, could not be determined in this study.

The paragenetic position of the syntaxial quartz overgrowths in the Potsdam Sandstone of location 90 relative to the vugs and fractures in rest of the Beekmantown rocks could not be established because no vug or healed fracture was found in location-90. However, it is more likely that the vug- and fracture-filling cements are younger than the quartz overgrowths.

5.6.2: Fluid-inclusion data:

Fluid-homogenization temperatures (Th) measured in the Beekmantown rocks generally show a wide range in every sample location (fig. 5.8). For example, the range in measured Th in location 77 is 80 to 250° C. Thus, it appears that the vug- and fracture-filling cements in which all measurements, except those in location 90, were

taken, precipitated from fluids of a large temperature range, probably over a long period of time.

Figures 5.8 and 5.9 show that the upper limit of Th (Th_{max}) reached by the vug- and fracture-filling cements was more than 200° C everywhere except in location 63, 66, 68 and 90. Because of geographical proximity of the study locations between 73 and 81 (fig. 5.2), similarities in general Th and Th_{max} values in these locations are expected and observed (figs. 5.8, 5.9). However, the Th_{max} of 159.3° C at location #63 seems anomalously low. Whether this low Th_{max} is real may be determined from comparison of paleotemperature signatures of other rock units in the same and nearby locations (see chapter 8).

The Th histograms from most of the study locations do not show distinct populations (fig. 5.8). In some locations, there is apparent unimodality (locations 66 and 68) and bimodality (location 73) of Th. These modes probably represent temperature regimes in which most of the vug- and fracture-filling cements precipitated and most of the inclusions were trapped. However, additional Th measurements may change these histograms. Also, no clear separation can be made in the Th of different mineral cements. Sparry calcite and saddle dolomite, whether from the same location (for example, location 63) or different locations, show a similar range of Th. Only quartz (locations 73, 63 and 90), in general, seems to have formed in relatively lower temperatures. The relatively low Th of quartz is consistent with petrographic evidence of an early precipitation (lower temperature?) of quartz in the vugs of locations 73 and 63 and as overgrowths at location - 90 (section 5.6.1).

The Th measured by Urschel (1984) and Urschel and Friedman (1984) from the Champlain, upper Hudson and eastern Mohawk valleys (table 5.2) show some agreement with the data presented here, but, as mentioned earlier, lack of sufficient readings in their study makes any conclusion or comparison difficult. However, high temperature inclusions (Th of 190°, 206° and 303° C) do occur in some of their study areas (table 5.2).

Like Th, fluid melting temperatures (Tm) of the late stage cements of the Beekmantown Group vary widely, often within the same study location (for example, 77

and 92, table 5.1). The majority of the 'Tm's, however, are between -10° C and - 26° C corresponding to salinities of 14 and 26.6 wt% NaCl (Potter et al. 1978). The high 'Tm's (0 to +2.5, table - 3) probably represent the incongruent melting temperatures of hydorhalite ($NaCl.2H_2O$) from solutions of high initial salinity of 23 to 26 wt% NaCl (Roedder, 1962; Shepherd et al. 1985). When a frozen inclusion of 26% salinity is heated, the ice may melt abruptly at -21.1° C. leaving hydrohalite and the fluid. Upon further heating, the final hydrohalite crystal melts at +0.1° C (Roedder, 1962). The few high 'Tm's of the Beekmantown samples seem abberant and were most probably the melting temperatures of the last hydrohalite crystals. Due to similar birefringence of ice and hydrohalite, it is often difficult to distinguish them from one another. It is, thus, argued here that the fluids in these inclusions actually contain 23 to 26 wt% NaCl.

The 'Tm's measured by Urschel (1984) and Urschel and Friedman (1984) between the eastern Mohawk and Champlain valleys (table 5.2) are broadly similar to those measured in this study, although they obtained only large negative Tm values, some of which are as high as -39° C.

No systematic variation between "Th" and corresponding "Tm" (that is, salinity) is observed in the Beekmantown rocks of any location (table 5.1) probably indicating that the salinity of the diagenetic fluids changed through time, like fluid temperature, at different locations, but was independent of temperature changes.

5.6.3: Stable isotope data:

In the eastern Mohawk, upper Hudson and Champlain Valley areas, $\delta^{18}O$ values of mainly vein-filling calcite and dolomite reported by Urschel and Friedman (1984) range from -9.91 to -13.98‰ PDB (table 5.2). Corresponding $\delta^{13}C$ values are between -3.2 and +2.9‰ PDB, although all except one carbon value are negative.

The difficulty of interpreting isotope values from bulk cement samples has been discussed in chapter 4.6. However, carbonate cements depleted in $\delta^{18}O$ (PDB) are generally interpreted as (1) a product of mixing of diagenetic fluids with isotopically light meteoric water, or (2) a product of precipitation from hot fluids (Friedman, 1987a).

Since Th measured in the same samples are high (table 5.2), it is believed that the

depleted $\delta^{18}O$ (PDB) values reflect high temperature fluids, not mixing with meteoric water. The inferred high salinity (from low Tm) of the inclusion fluids also suggest that these were deep, subsurface brines. Very light $\delta^{18}O$ (PDB) values of deep- burial carbonate cements have been reported in many publications (Mates and Mountjoy, 1980; Zenger, 1983; Prezbindowski, 1985; Wornick and Land, 1985; Lee and Friedman, 1987; Saigal and Bjorlykke, 1987; Zenger and Dunham, 1987; Kaufman et al. 1990). According to Urschel and Friedman's (1984) calculations, based on various hypothetical values of δ_w, the oxygen isotope values represent formational temperatures of 74° to 205° C.

Light $\delta^{13}C$ values (table 5.2) could represent the influx of light meteoric water as well as influx of ^{13}C-depleted CO_2 derived from bacterial or inorganic degradation of organic matters (Faure, 1977).

CHAPTER: 6: THE BLACK RIVER AND TRENTON GROUPS

6.1: STRATIGRAPHY AND DEPOSITIONAL HISTORY:

The late Middle Ordovician (Mohawkian) limestones of the Black River and Trenton groups in New York are exposed around the Adirondack Highlands in the Mohawk Valley, the Tug Hill Plateau, Black River Valley, and in a few areas of the Champlain Valley (fig. 6.1). In the subsurface, these units occur in the western two-thirds of the state (Kreidler et al. 1972; Rickard, 1973). Within the Appalachian Basin, these and equivalent carbonates also occur in Pennsylvania, eastern Ohio, West Virginia, Kentucky and parts of Maryland, Virginia, Tennessee, Georgia and Alabama (COSUNA Chart, 1985) and southern Quebec (Mehrtens, 1988). West of the basin proper, they occur in the subsurface of western Ohio, Indiana, and the Michigan and Illinois basins (see Keith, 1988). The Black River and Trenton carbonates, especially the Trenton, are important hydrocarbon reservoirs in Ohio, Michigan, Indiana and Kentucky and have been targets of exploration throughout the eastern North America (Keith, 1988).

The maximum thickness (~400m) of the combined Black River and Trenton rocks in New York occurs in the subsurface of central New York (Rickard, 1973, pls. 7, 8). The thickness decreases toward east, west and north. In the Adirondack borderland areas (fig. 6.1), their combined thickness increases from zero in the eastern Mohawk Valley to about 200m in the Tug Hill Plateau, and in the Champlain Valley a maximum thickness of 12m of Black River and 61m of Trenton are found (Fisher, 1977, pl. 2).

In New York, the Black River and Trenton groups are divided into several formations (fig. 6.1). In the type area of the Black River Valley, the Black River Group consists of, in ascending order, the Pamelia, Lowville, House Creek and Watertown ("Amsterdam" in eastern Mohawk Valley) formations. The Trenton Group consists of the Selby, Napanee, Kings Falls (Larrabee in the Mohawk and Champlain valleys), Sugar River (Glens Falls in the Champlain Valley), Denley (equivalent to the Dolgeville in westernmost Mohawk Valley), and Hiller formations. The Trenton Group carbonates of the Tug Hill Plateau and Black River Valley are equivalent to the Utica Shale of much of the Mohawk Valley and the Snake Hill Shale of the Hudson and Champlain valleys. The carbonate-shale boundary moved westward with time, and in the Tug Hill Plateau the Utica Shale overlies the Trenton (fig. 6.1) reflecting the gradual westward encroachment of clastic sediments over a carbonate shelf as a result of the Taconic Orogeny in the east (section 2.1).

Figure 6.1: Stratigraphic relationships of the Black River and Trenton Group carbonates in the Mohawk Valley, Tug Hill Plateau and Black River Valley, New York. (Adapted from Fisher, 1977).

LATE MIDDLE ORDOVICIAN
LATE ORDOVICIAN
EPOCH
MOHAWKIAN
CINCINNATIAN
SERIES
BLACK RIVER
TRENTON
LORRAINE
GROUPS
TUG HILL PLATEAU
BLACK RIV. VALLEY
MOHAWK VALLEY
PAMELIA FM.
LOWVILLE FM.
WATERTOWN FM.
SELBY FM.
HAPAREE FM.
KINGS FALLS FM.
SUGAR RIVER FM.
POLAND LST.
DENLEY FM.
RUSSIA LST.
RUST LST.
STEUBEN LST.
HILLER FM.
UTICA SHALE
WHETSTONE GULF FM.
PULASKI FM.
OSWEGO FM.
FRANKFORT
HOUSE CREEK LST.
DOLGE-VILLE FM.
UTICA SHALE
SCHENECTADY FM.
AMSTERDAM LST.
LOWVILLE FM.
LARRABEE LST.
SHARK HILL SHALE
TUG HILL PLATEAU
ADIRONDACKS
BLACK RIVER VALLEY
MOHAWK VALLEY
CHAMPLAIN VALLEY

The rocks of the Black River Group were deposited in a supratidal to shallow subtidal environment (Walker, 1973; Fisher, 1977). From the basal Pamelia to the House Creek Formation the rocks were deposited in a gradually deepening shelf in supratidal to high-energy subtidal environments. The sediments of the Watertown Formation are believed to have formed in a low-energy, subtidal environment, probably in protected lagoons.

There was probably a temporary withdrawl of the sea from much of New York toward the end of the Black River interval, marked by a hiatus between the Black River and Trenton Groups in the Mohawk and Black River valleys and part of the Tug Hill Plateau (fig. 6.1). Deposition of the Trenton limestones resumed as a result of the "Early Trentonian Transgression" which began with the "Vermontian Phase" of the Taconic Orogeny (Titus, 1988).

The lowest units of the Trenton Group, the Selby and Napanee formations, were probably deposited in nearshore, protected lagoons (Titus and Camerron, 1976), much like the underlying Watertown carbonates. According to Titus (1988), the lower part of the overlying Kings Falls was deposited in offshore barrier shoals and the upper part of the Kings Falls and the Sugar River carbonates were deposited in shallow and deeper subtidal environments respectively, indicating progressive deepening of the shelf.

Subsidence continued into the lower Denley interval when bioclastic turbidites ("shelf-to-basin facies") were deposited in the Mohawk Valley (Mehrtens, 1988; Titus, 1988). The occurrence of turbidites in the Denley Formation decreases to the northwest and passes into lagoonal and shoal facies in Ontario (Brookfield, 1982). In the deeper basin to the southeast, the Utica and equivalent Snake Hill shales were deposited. The Dolgeville limestones and shales (fig. 6.1) represent the carbonate-shale transition on a gentle slope (Titus, 1988).

The middle and upper Denley limestones, however, show evidence of renewed shoaling and an eastward migration of shallow-water facies with time (Titus, 1988). The gentle slope of the lower Trentonian time was transformed into a steep bank margin, where the basinal shale and the platform carbonate converged.

The shoaling of the platform culminated with the deposition of the Steuben Limestone. Following this, a new phase of uplift ("the Hudson Valley Phase") of the Taconic landmass took place in the east resulting in rapid subsidence of the Trentonian platform (Titus, 1988). The upper part of the Steuben Limestone and the Hiller Limestone were deposited in deepening water to be finally buried by the Utica Shale. The unconformity between the Hiller Limestone and the overlying Utica Shale in the Tug Hill Plateau and Black River Valley (fig. 6.1) was probably the

result of a rapid and short-lived epeirogenic uplift which was associated with local, mild folding of the Trentonian rocks (Titus, 1988).

6.2: SAMPLING LOCATIONS:

Figure 6.2 shows the sampling locations of the Black River and Trenton groups. All samples, except those of location-64, were collected from the Upper Ordovician outcrops fringing the Adirondacks in the Mohawk Valley, Tug Hill Plateau and Black River Valley. The only core samples were collected from location 64 and 65. No sample was collected from the Champlain Valley.

6.3: GENERAL PETROGRAPHY OF THE SAMPLES:

The samples from the Black River and Trenton groups are mainly limestones, and locally dolostones. In the south- eastern end of the studied outcrop belt, at location 61 (fig. 6.2), coarse grained dolostones with semi-circular to irregular vugs (0.5 to 6cm wide) are found. The vugs are filled with sparry calcite (fig. 6.3a). The host dolostone contains rhombic dolomite with floating relics of micrite.

Between location 61 and 89, all the samples were collected from limestones which vary widely in depositional fabric. Samples of the Black River Group from location 83 consist of finely laminated, peloidal mudstone with fenestral structures and abundant, wiggly sheet cracks (fig. 6.3b). The fenestrae and the sheet cracks are filled with sparry calcite cement. Samples of the Trenton Group from location-84 are skeletal grainstones with abundant intergranular, coarse, sparry calcite. Calcite-filled skeletal molds, especially of ostracodes, are common.

At location 65, the samples of the Black River Group (Pamelia and Lowville formations) consist primarily of micrites and wackestones. In the Lowville samples, thin isolated veins, skeletal molds, and small vugs filled with sparry calcite were found.

The Black River samples of locations-85, 87 and 88 are skeletal-oolitic-intraclastic grainstones. Sparry calcite occurs mainly as intergranular, poikilotopic and shelter cements in these samples (fig. 6.4). Skeletal molds filled with sparry calcite are also common. The sparry calcite generally grows on a fine drusy calcite fringe on skeletal particles (fig. 6.4a). At location-89, samples from the Black River Group consist of coarse grained dolostones with calcite-filled vugs.

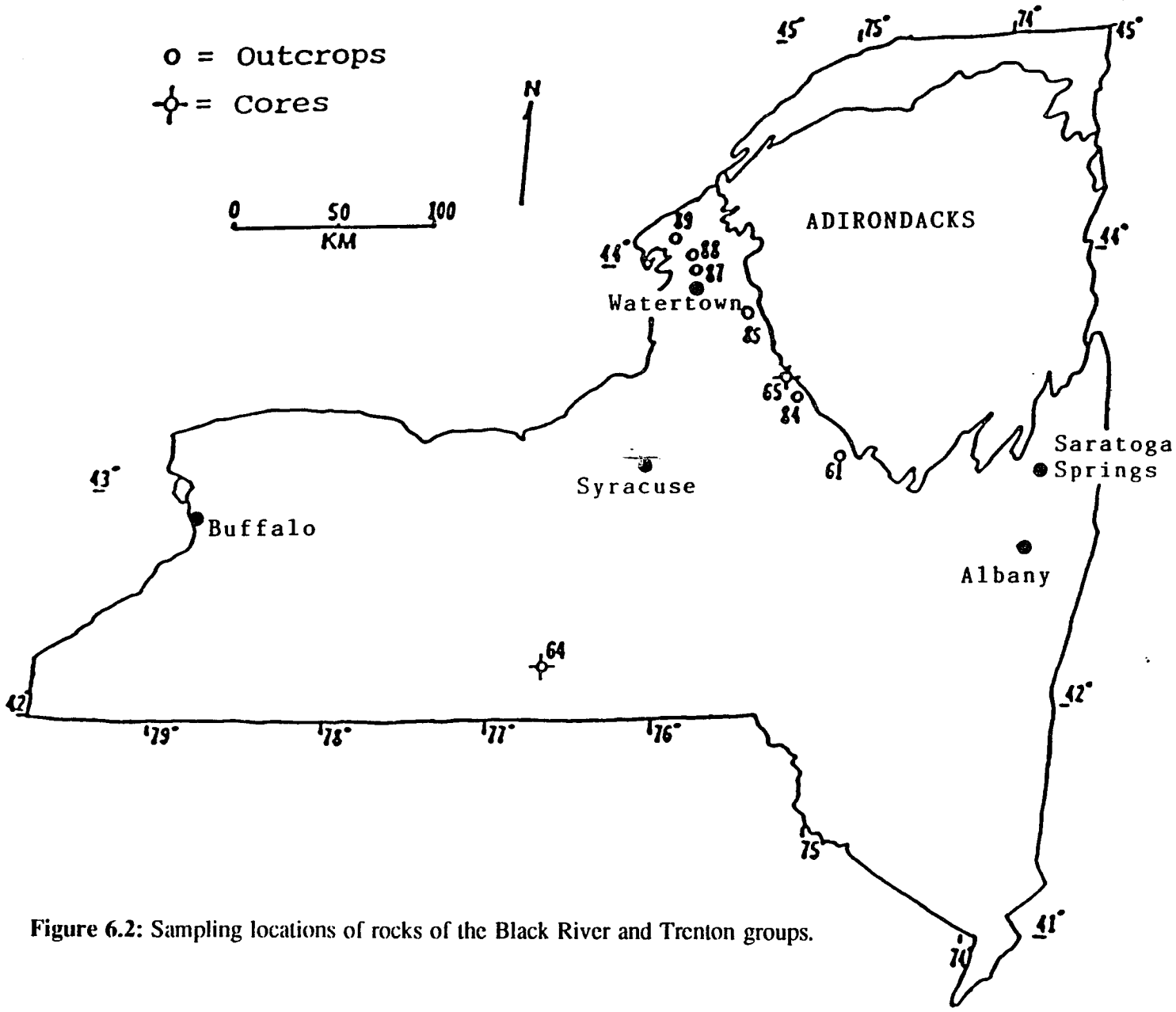

Figure 6.2: Sampling locations of rocks of the Black River and Trenton groups.

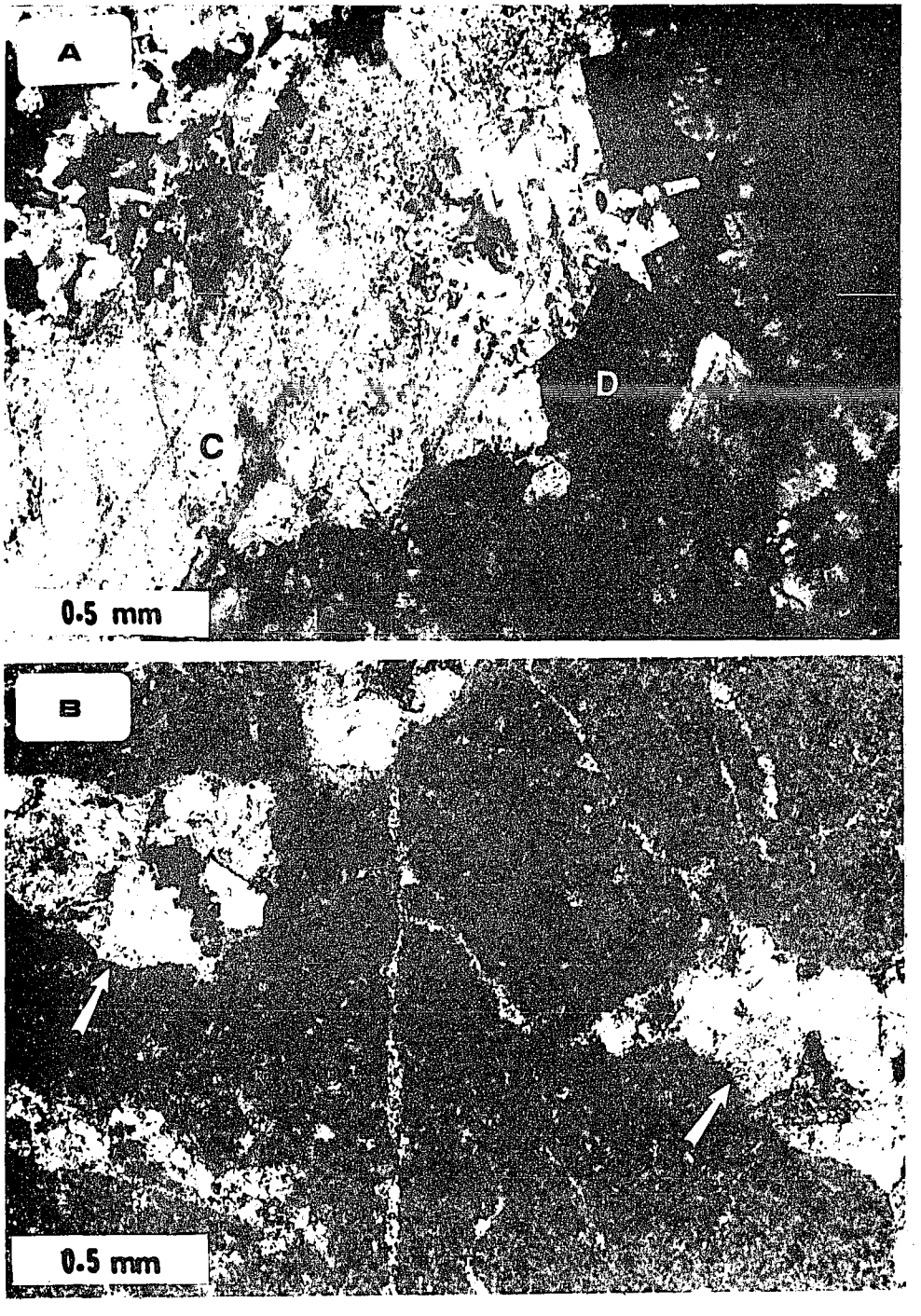

Figure 6.3: Photomicrographs showing (A) part of a calcite (C)-filled vug in the dolostone (D) of the Trenton Group, location - 61, and (B) calcite-filled fenestral cavities (marked by arrows) connected by sheet cracks in the micrite of the Black River Group, location-83.

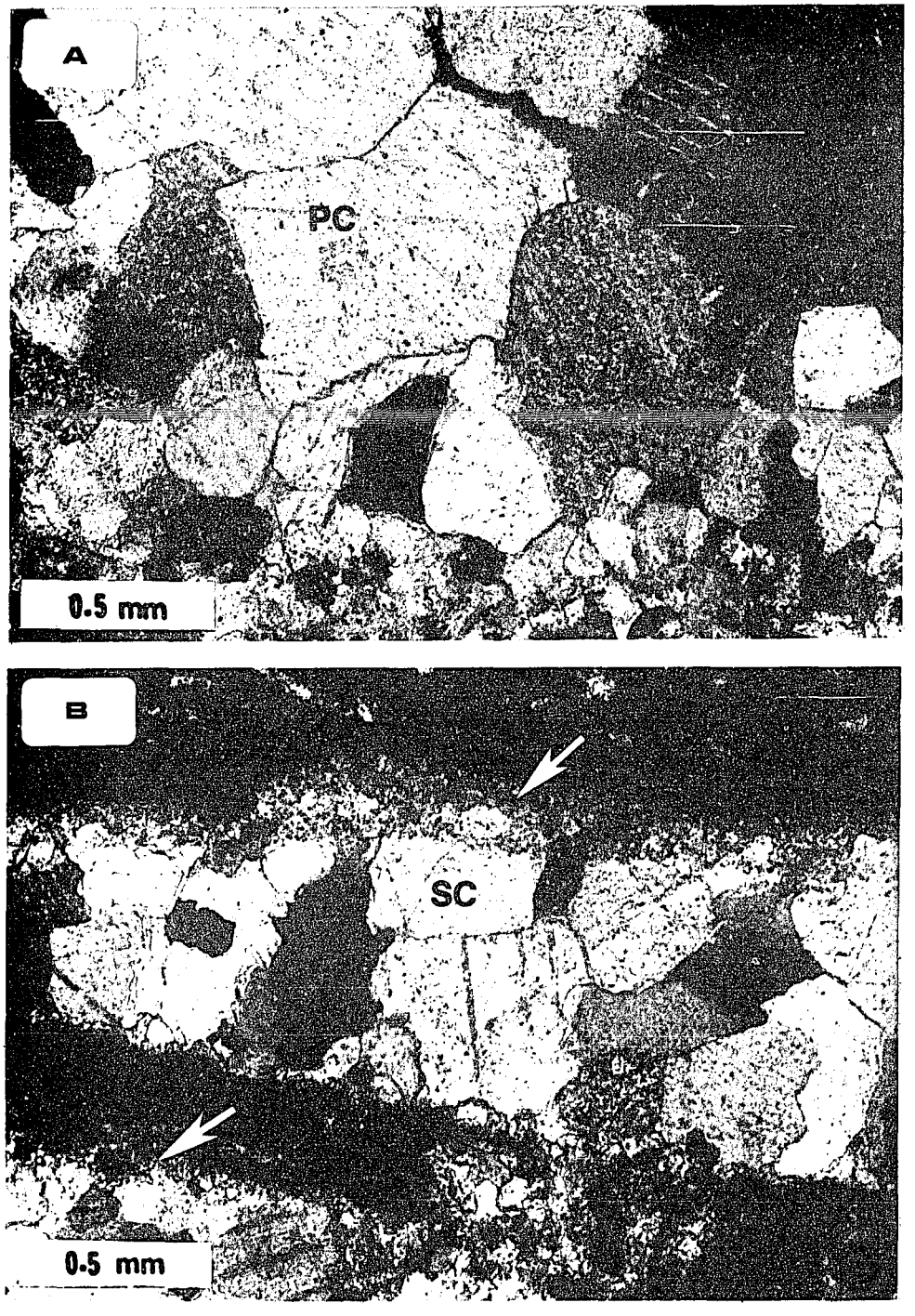

Figure 6.4: Photomicrographs showing (A) poikilotopic calcite cement (PC) in the grainstones of the Trenton Group, location-84, and (B) shelter cement (SC) in skeletal grainstones of the Black River Group of location-88. Note the fine drusy calcite lining (marked by arrows) on skeletal particles.

At location 64, samples from both the Black River Group and Trenton Group consist of dark gray, finely laminated micritic limestone with vugs and prominent vertical and inclined veins filled with sparry calcite and saddle dolomite (fig. 6.5). The veins are as wide as 1.5cm. Sparry calcite alone fills most of the vugs and veins (fig. 6.5a), but in a few veins it coexists with saddle dolomite. In fractures with coexisting mineral cements, the fracture walls are generally lined by sparry calcite, and dolomite mainly occurs in central portions of the veins (fig. 6.5b). However, some dolomite grows directly on fracture walls and, rarely, in spaces surrounded by calcite.

6.4: FLUID-INCLUSION DATA:

Two-phase primary inclusions (fig. 6.6) are common in calcite and dolomite cements described above. Figure 6.7 shows the fluid-homogenization temperature (Th) histograms of the Black River and Trenton samples from various locations. Histogram for location 83 is not shown because only three Th readings were available in samples of this location (see Appendix - C). The maximum homogenization temperatures (Th_{max}) are also shown. In table 6.1, the few measured 'Tm's, corresponding 'Th's and the calculated salinities (equivalent wt% NaCl) are listed against study locations. Figure 6.8 shows the Th_{max} values plotted against sample locations. Detailed inclusion data are presented in Appendix - C.

6.5: INTERPRETATION

6.5.1: Paragenetic sequence of cements:

A generalized paragenetic sequence can not be established for the entire Black River - Trenton carbonates because of insufficient data. However, limited interpreta- tions can be made.

The calcite and dolomite cements in healed fractures of location-64 are probably the latest cements in the Black River and Trenton carbonates. Since calcite crystals generally line the fracture walls (fig. 6.5b), most of the calcite must have formed earlier than saddle dolomite. Fluid-inclusion data also support this interpretation (section 6.5.2). Saddle dolomite has been interpreted as a product of precipitation from relatively high temperature fluids (Radke and Matthis, 1980; Lee and Friedman, 1987).

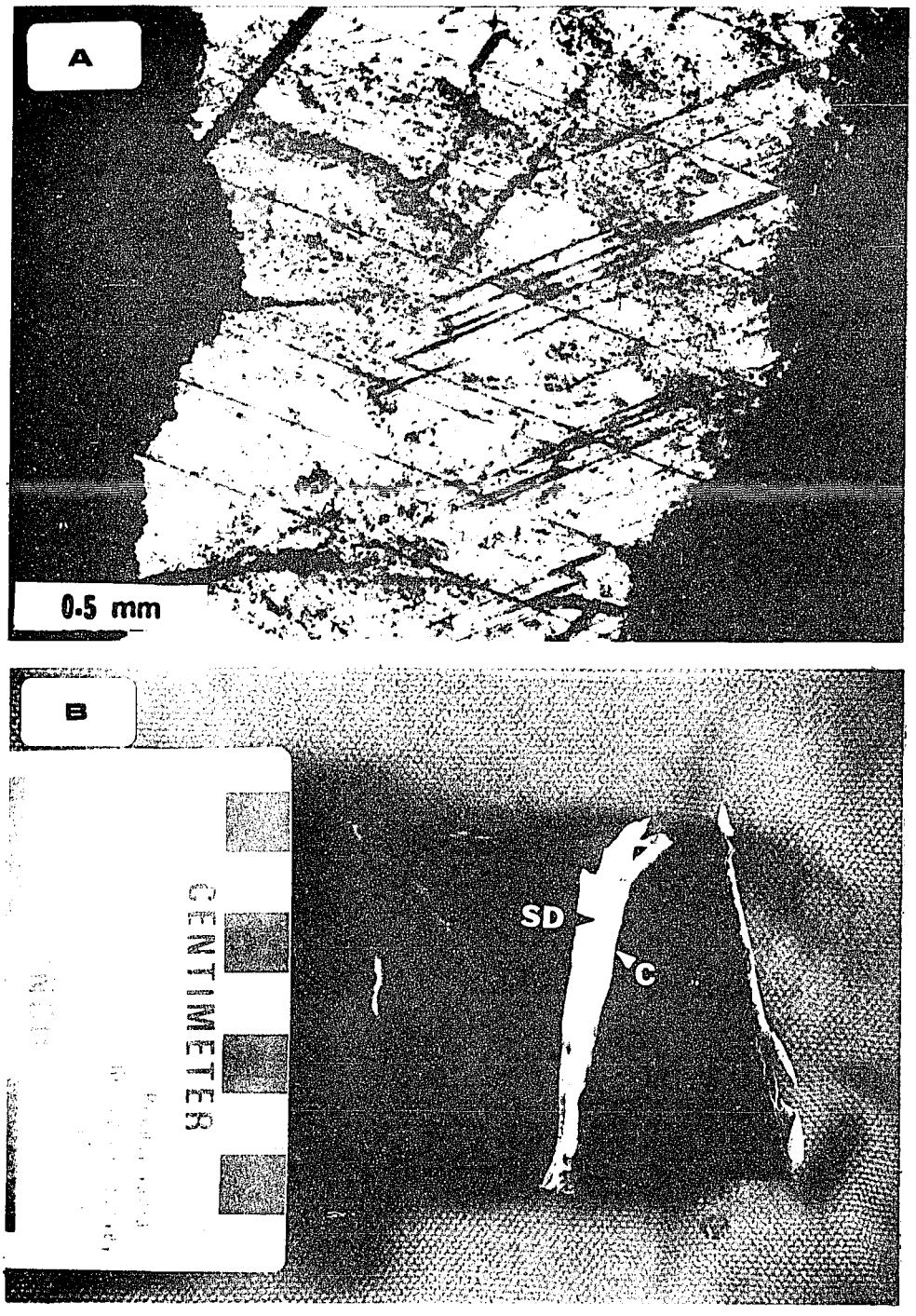

Figure 6.5: (A) Photomicrograph of dark, micritic limestone of the Black River Group of location - 64 showing a thin, vertical fracture filled with calcite, and (B) core-sample section of micritic limestone of the Black River Group of the same location showing a wider vertical fractures filled with calcite (C) and saddle dolomite (SD). Calcite (appears darker because of staining with alizarin red solution) lines the fracture walls and saddle dolomite occurs in the central portion of the fracture.

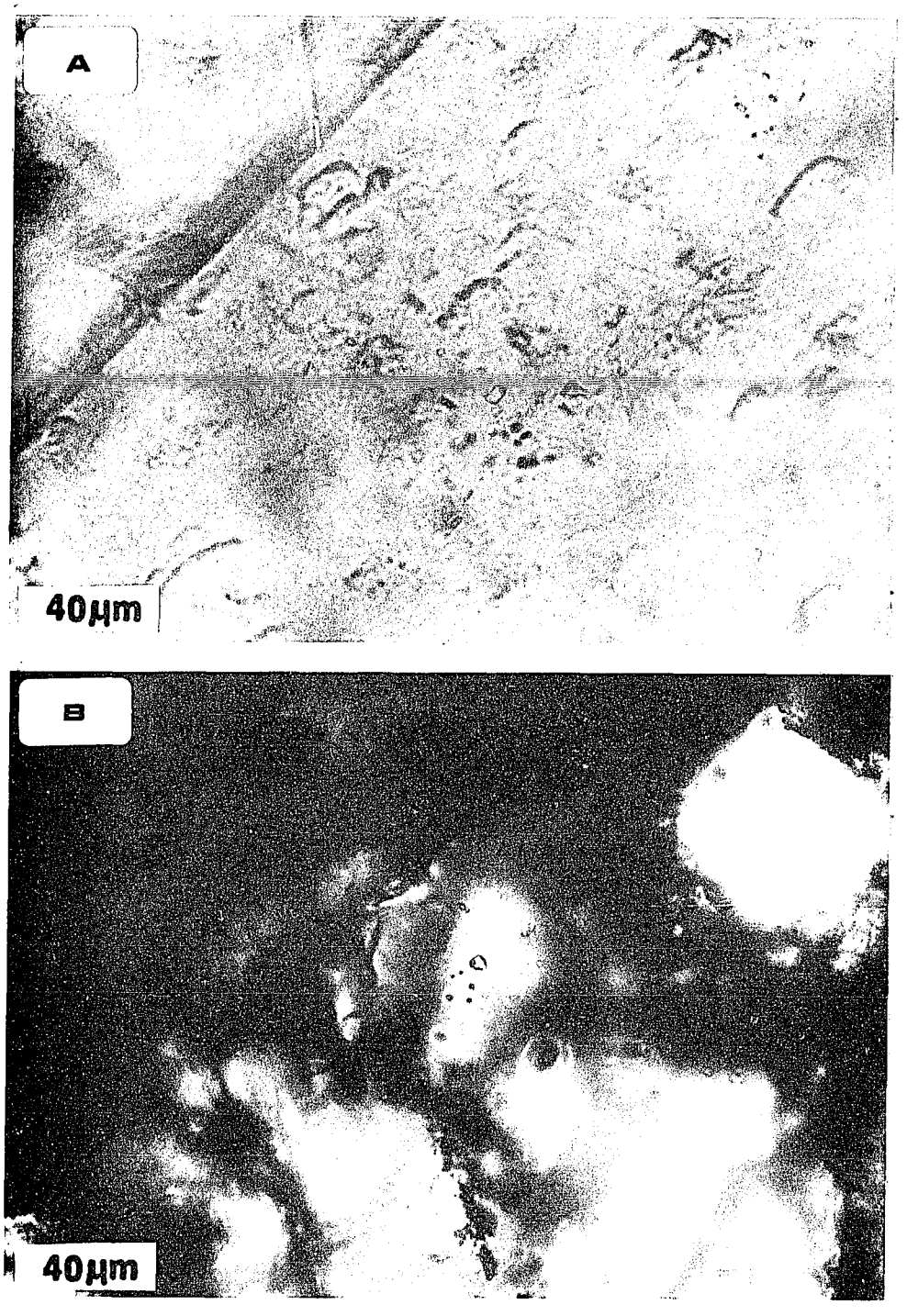

Figure 6.6: Photomicrographs showing primary two-phase fluid inclusions in (A) calcite of skeletal mold from Black River Group of location-65, and (B) fracture-filling saddle dolomite in the Black River Group of location- 64.

Figure 6.7: Fluid-homogenization temperature (Th) histograms of Black River and Trenton Group samples from various locations. The maximum homogenization temperatures (Th_{max}) are also shown.

LOCATION: 61

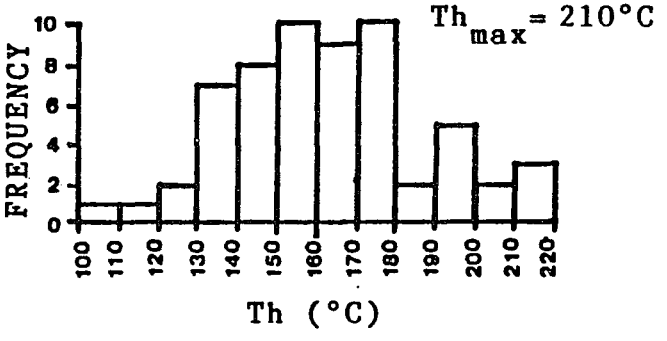

LOCATION: 65

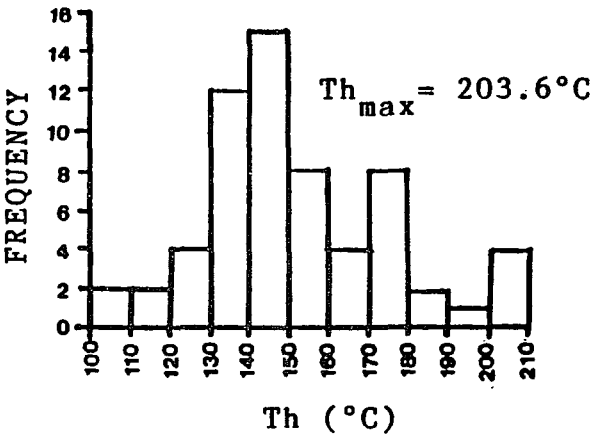

LOCATION: 84

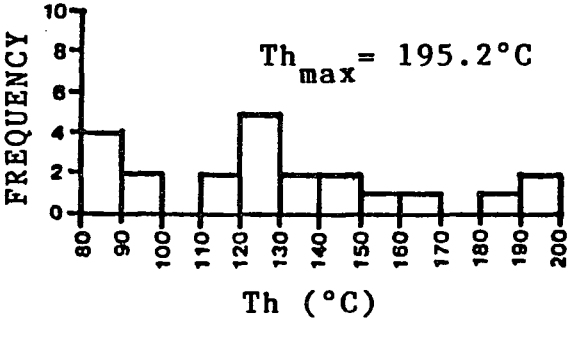

LOCATION: 85

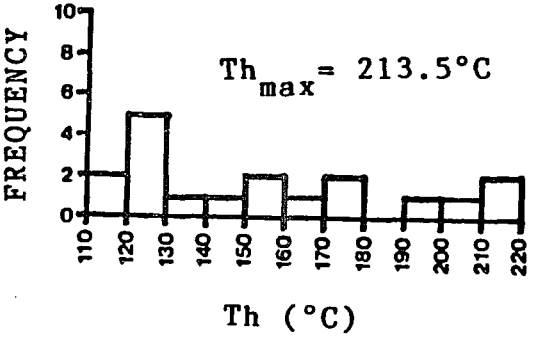

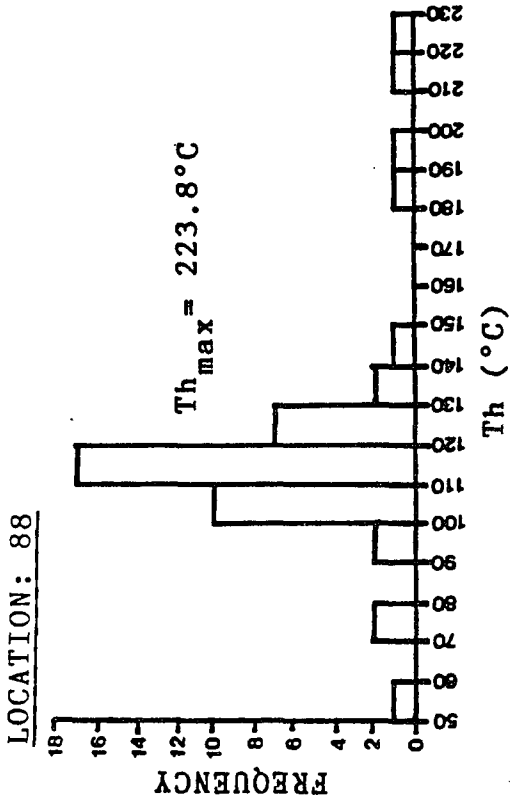
LOCATION: 88
Th_{max} = 223.8°C
FREQUENCY
Th (°C)

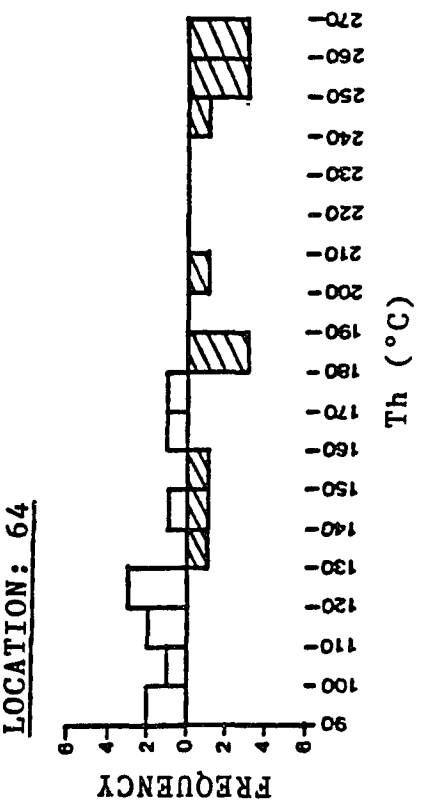
LOCATION: 64
FREQUENCY
Th (°C)

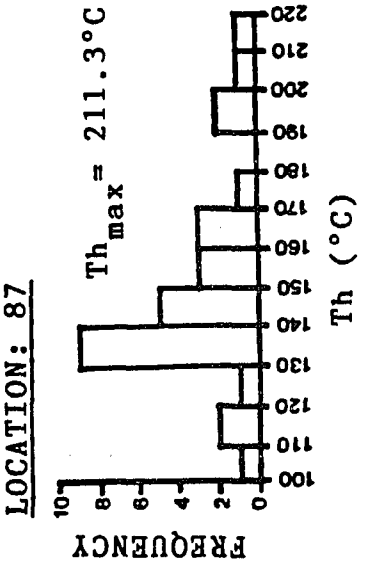
LOCATION: 87
Th_{max} = 211.3°C
FREQUENCY
Th (°C)

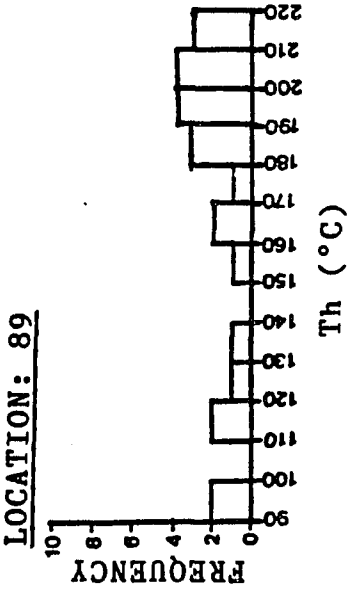
LOCATION: 89
FREQUENCY
Th (°C)

Table 6.1: Fluid-melting temperatures (Tm), corresponding homogenization temperatures (Th), and calculated salinity (wt% NaCl) of inclusions in cements of the Black River and Trenton Group carbonates.

Location	Type of cement	Tm (° C)	*Salinity (wt% NaCl)	Th (° C)
61	Vug-filling sparry calcite	-22.7	24.5	130
		-23.5	25.03	132
		-24.7	25.8	140.4
		-23.3	24.9	166
84	Sparry calcite in skeletal mold	-11.8	15.8	130
65	Vug-filling sparry calcite	-2.5	4.1	145
		+1.5	---	148
		-5.8	8.9	150
		-2.4	4.0	147
85	Intergranular sparry calcite	+1.6	---	120.6
87	Intergranular sparry calcite	-18.0	21.2	160
88	Intergranular sparry calcite	-20.0	22.6	114
64	Fracture-filling saddle dolomite	-11.3	15.3	180
		-15.0	18.78	265

* Salinity was calculated according to Potter et al's (1978) method (see section 5.3.2).

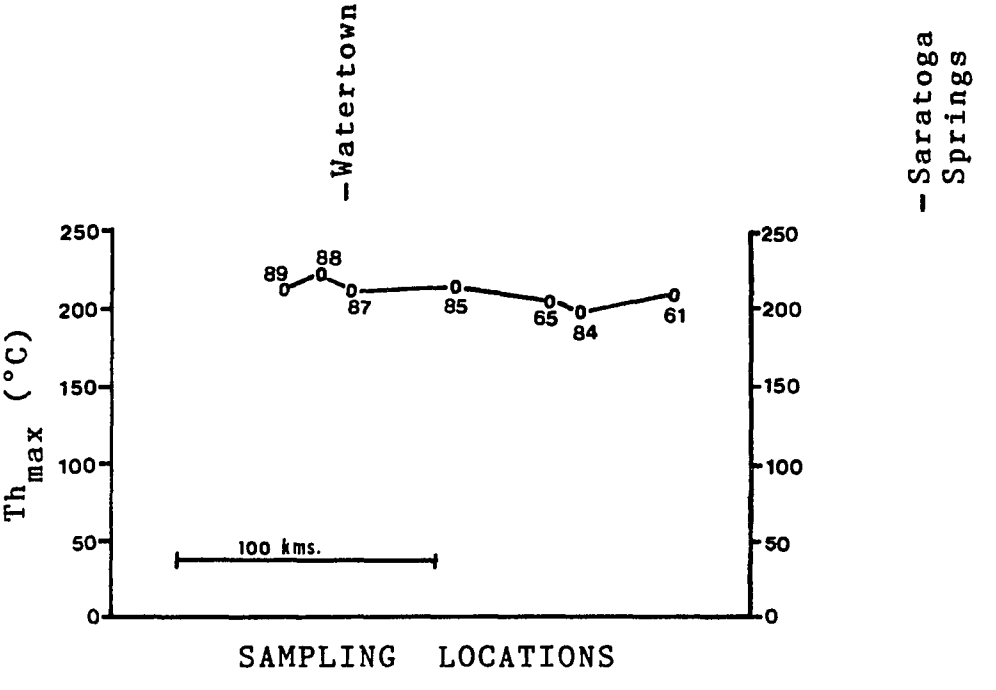

Figure 6.8: Maximum homogenization temperatures (Th_{max}) of the Black River and Trenton samples plotted against sampling locations along the margin of the Adirondacks.

The poikilotopic and shelter cements (sparry calcite) in locations 84, 85, 87 and 88 formed later than the fine, drusy calcite that grew on sediment particles (fig. 6.4b). Calcite in skeletal molds of location 84 are probably of the same generation as the poikilotopic cements because, like the latter, it also grows on fine drusy calcite, lining inner skeletal walls. Poikilotopic calcite crystals and clear sparry-calcite mosaic filling shelters and cavities (figs. 6.3, 6.4) have been considered products of deep burial diagenesis (Moore, 1985).

The calcite-filled vugs in location 61 formed after replacement dolomitization of the host rock was complete. Similarly, the calcite-filled vugs in location 89 post-date the dolostones in which they occur. In both locations the vugs probably formed through leaching of unstable carbonate components.

6.5.2: Fluid-inclusion data:

Fluid-homogenization temperatures (Th) of the Black River - Trenton carbonates show a wide range in every sample location (fig. 6.7). Particularly large are ranges in locations 88 (50 - 230° C) and 64 (90 - 280° C). Such large range of Th persists in cements whether they are intergranular (locations 84, 85, 87, 88), fracture-filling (locations 64), or vug-filling (locations 61, 65, 89) cements, indicating that all these cement types formed from fluids of progressively changing temperatures.

Although the ranges of Th are similar in the above types of cements, most of the Th in intergranular cements of locations 84, 85, 87 and 88 are clustered around 120-130° C, while most of the Th in vug-filling cements of locations 61, 65 and 89 are clustered around 140 - 160° C (fig. 6.7). The Th in fracture-filling cements of location 64 are widely distributed, and Th in saddle dolomite are generally higher (130° to 270° C) than that in calcite (90 to 180° C). However, a relatively large number of Th in saddle dolomite are between 250° and 280° C. This probably means that the most active precipitation of cements took place at the highest temperatures in the fractures, at an intermediate temperature in the vugs and at the lowest temperatures in intergranular spaces.

A comparison of Th_{max} shows that except for the very high Th_{max} (269° C) of core samples from location 64, the Th_{max} of all locations along the south and southwestern margin of the Adirondacks are close to or slightly higher than 200° C (fig. 6.7, 6.8). These temperatures are consistent with range of temperatures interpreted from conodont color alteration index (CAI) values of Ordovician carbonates in the study are (chapter 3), but do not reflect the westward decreasing trend in CAI isograds along the southern margin of the Adirondacks (fig. 3.2).

The majority of the fluid-melting temperatures (Tm) in the late-stage cements of the Black River and Trenton Group carbonates are very low signifying high salinity of the inclusion fluids (table 6.1). Only in locations 65 and 85, 'Tm's with higher values (-5.8 to +1.6° C) were found. Following interpretation of high 'Tm's in the Beekmantown rocks (section 5.6.2), it is believed that some of the high 'Tm's of locations 65 and 85 actually represent the incongruent melting temperatures of hydrohalite in inclusions fluids of high initial salinity.

There is no correlation between 'Tm's and 'Th's in location-65 or anywhere else within the small data set (table 6.1). Lack of such correlation is also evident in the Beekmantown rocks (table 5.1), and the possible reason has been discussed in section 5.6.2.

CHAPTER 7: THE UTICA SHALE

7.1: STRATIGRAPHY AND DEPOSITIONAL HISTORY:

The Utica Shale (Mohawkian - Cincinnatian) is a prominent black shale unit in New York and is exposed along the southern and southwestern fringes of the Adirondacks (fig. 6.1, chapter 6). In the subsurface, it occurs in the western two-thirds of the state (Rickard, 1973). In the easternmost Mohawk Valley, Hudson Valley and Champlain Valley (fig. 6.1), the Utica Shale grades into the Snake Hill and Bushkill (of the Martinsburg Group) black shales. The maximum thickness (~2300m) of these shales occurs in southeastern New York from where the thickness decreases northward and eastward to about 760m in the Champlain Valley and 50m near Lake Ontario (Fisher, 1977, pl.4). In the Appalachian Basin, equivalent shales occur in New Jersey, Pennsylvania, eastern Ohio, northwestern Maryland, Virginia, West Virginia, eastern Kentucky, Tennessee (COSUNA Chart, 1985) and Quebec (Mehrtens, 1988).

The Utica Shale consists of dark gray to black, fissile and thinly laminated shale. Fine pyrite nodules and laminae and thin calcareous interbeds are locally common. To the east, the equivalent Snake Hill Shale shows subtle changes in lithology. It comprises dark gray to black, bluish- and greenish-gray silty shale interbedded with thin, cross-laminated siltstones and fine-grained sandstones.

These shales represent deposition in a basin-to-slope environment of the Taconic foreland basin (Hay and Cisne, 1988). The Snake Hill Shale was deposited in the deeper basin to the east, while the Utica Shale was deposited in the shallower part of the basin and on the slope in the west, interfingering with the Trentonian carbonate platform (section 6.1). Sedimentation was mainly in the form of hemipelagic settling of argillaceous particles derived from the eastern Taconic mountains and transported westward by surface currents (Ross, 1976; Hay and Cisne, 1988). Due to proximity of the sediment source, the sedimentation rate was higher in the Snake Hill Shale than the Utica Shale and, in Hay and Cisne's (1988) estimate, the rates were 200-250m/m.y and 50-100m/m.y, respectively.

Study of the faunal abundance and diversity, lithology, organic- and carbonate-carbon

content led Hay and Cisne (1988) to infer that the Utica and Snake Hill shales were deposited in an oxygen-deficient basin. However, contending earlier interpretation by Rudemann (1935) that these black shales formed within barred basins and separate troughs of limited circulation, Hay and Cisne (1988) infer that the oxygen deficiency resulted from strong density stratification probably "established by local humid climate in the area and by stagnant conditions in the world ocean".

Toward the end of the Mohawkian interval, the basin and the western carbonate platform subsided rapidly, probably as a direct consequence of the "Hudson Valley Phase" of the Taconic orogeny (Titus, 1988). The Utica Shale, which had maintained a fairly narrow zone of interfingering with the carbonate platform in northcentral New York (represented by Dolgeville Formation, fig. 6.1) throughout the Champlainian time, spread westward relatively rapidly, and by early Cincinnatian time buried the platform as far west as the Ontario Province, Canada (fig. 6.1).

7.2: SAMPLING LOCATIONS:

Figure 7.1 shows the sampling locations of the Utica Shale. All samples except those of location-64 were collected from its outcrops belt in the Mohawk Valley and the Tug Hill Plateau (see figs. 6.1, 7.1). Core samples were collected from location-64.

7.3: ORGANIC MATURATION DATA:

Since pre-Devonian rocks contain little or no vitrinites, the Utica samples were analyzed for thermal alteration index (TAI) only. The organic matters in the Utica samples include herbaceous spore-pollen (most of which are degraded), amorphous-sapropel, inertinite and some woody-structured (?) materials. The Geochem Laboratory's data sheet shows no relationship between the TAI of a sample and the percentage of the above types of organic matter. Table 7.1 shows the TAI and equivalent Ro for various sampling locations.

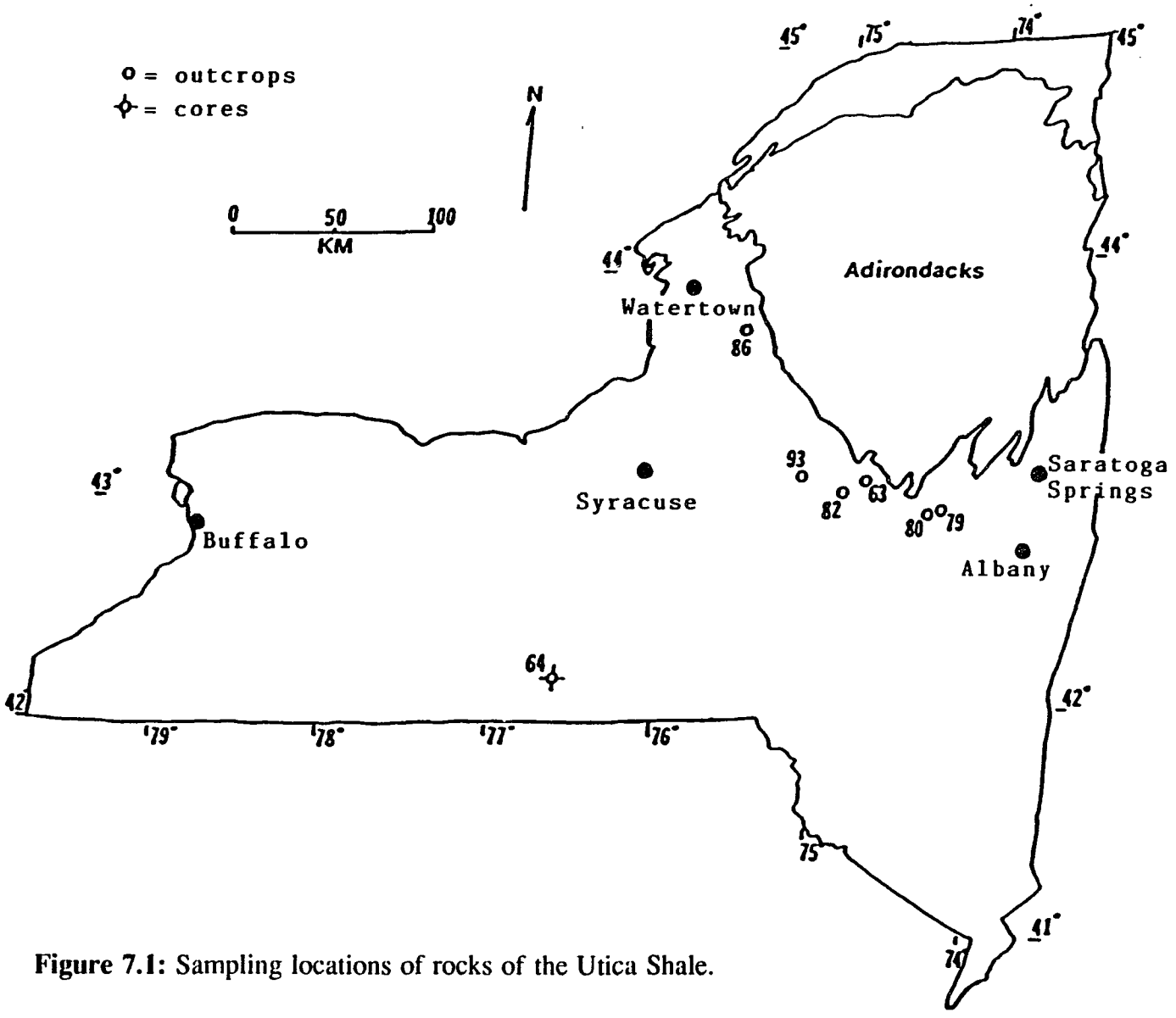

Figure 7.1: Sampling locations of rocks of the Utica Shale.

Table: 7.1: TAI and equivalent Ro values (from table 4.1, ch. 4) of Utica Shale samples from various locations, and calculated paleotemperatures.

Sample location	Sample number	TAI	Ro (%)	* Maximum burial temperature (° C)
79	UT-1A	3.5	1.63	216
80	UT-2A	3.0	1.0	154
63	UT-3A	2.8	0.95	147
82	UT-4A	2.6	0.90	140
93	UT-5A	2.4	0.75	117
	UT-5B	2.4	0.75	117
86	UT-6A	2.7	0.70	145
64	JM-1	3.8	2.0	242

* Temperatures were calculated from Ro values according to Barker and Pawlewicz's (1986) method. See section 5.4.

7.4: CLAY DIAGENESIS DATA:

X-ray diffractograms of both air-dried and glycolated samples from various locations are shown in figure 7.2. Peaks of different mineral phases are labelled, and Illite crystallinity indices are also shown. The peaks at 12.5° 2θ (7.05 A) and 25.2° 2θ (3.53 Å) at locations 93 and 64 have been labelled Chlorite (CH) 002/Kaolinite (K) 001 and CH(004)/K(002), respectively, because the closeness of peaks of pure chlorite and pure kaolinte at these positions makes it very difficult to determine if these two peaks represent single mineral phases or an admixture of chlorite and

Figure 7.2: X-ray diffractograms of (a) untreated and (b) glycolated Utica samples from sample locations of figure 7.1. Illite crystallinity (I.C) values are also shown.

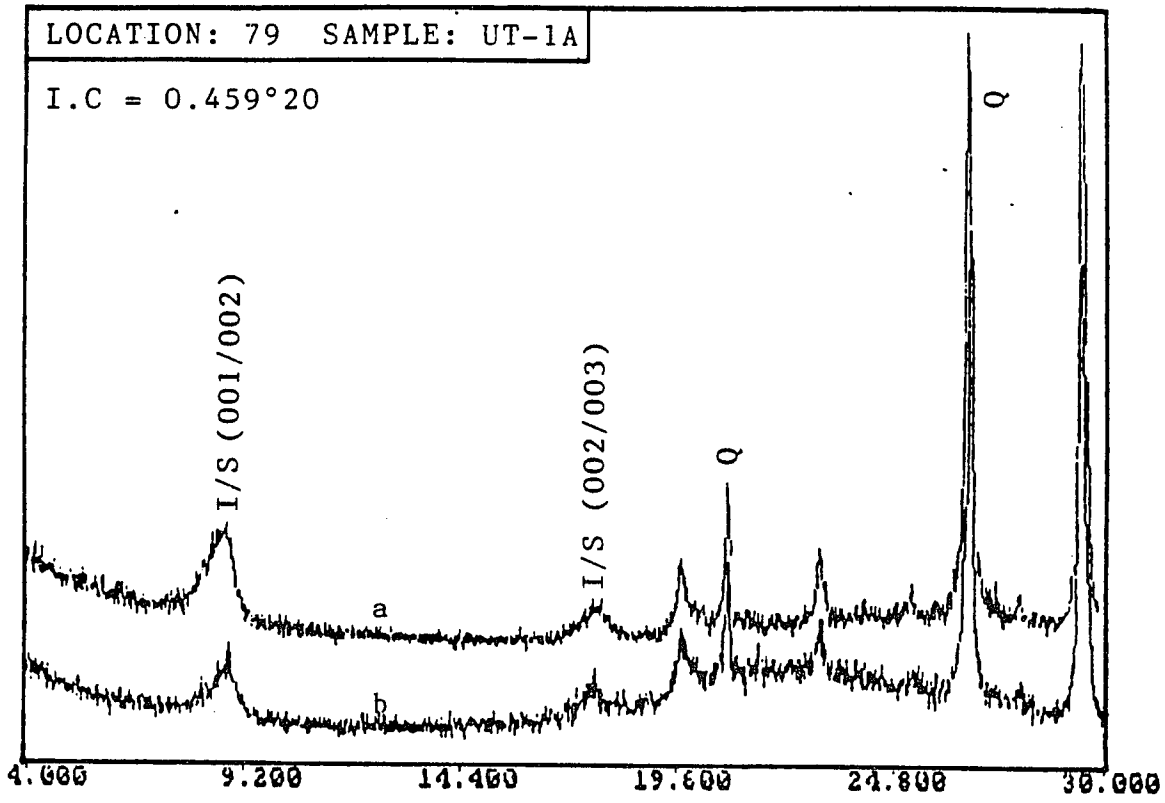
LOCATION: 79 SAMPLE: UT-1A
I.C = 0.459°2θ
I/S (001/002)
I/S (002/003)
Q
Q
a
b
4.000
9.200
14.400
19.600
24.800
30.000
°2θ

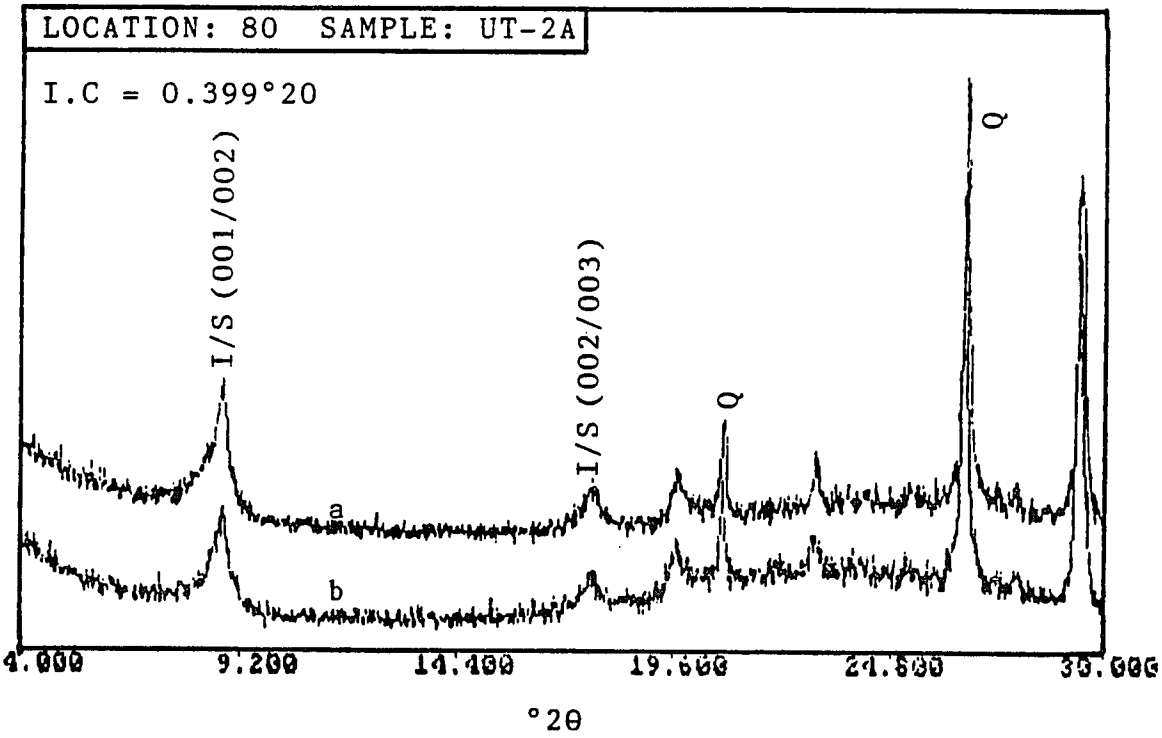
LOCATION: 80 SAMPLE: UT-2A
I.C = 0.399°2θ
I/S (001/002)
I/S (002/003)
Q
Q
a
b
4.000
9.200
14.400
19.600
24.800
30.000
°2θ

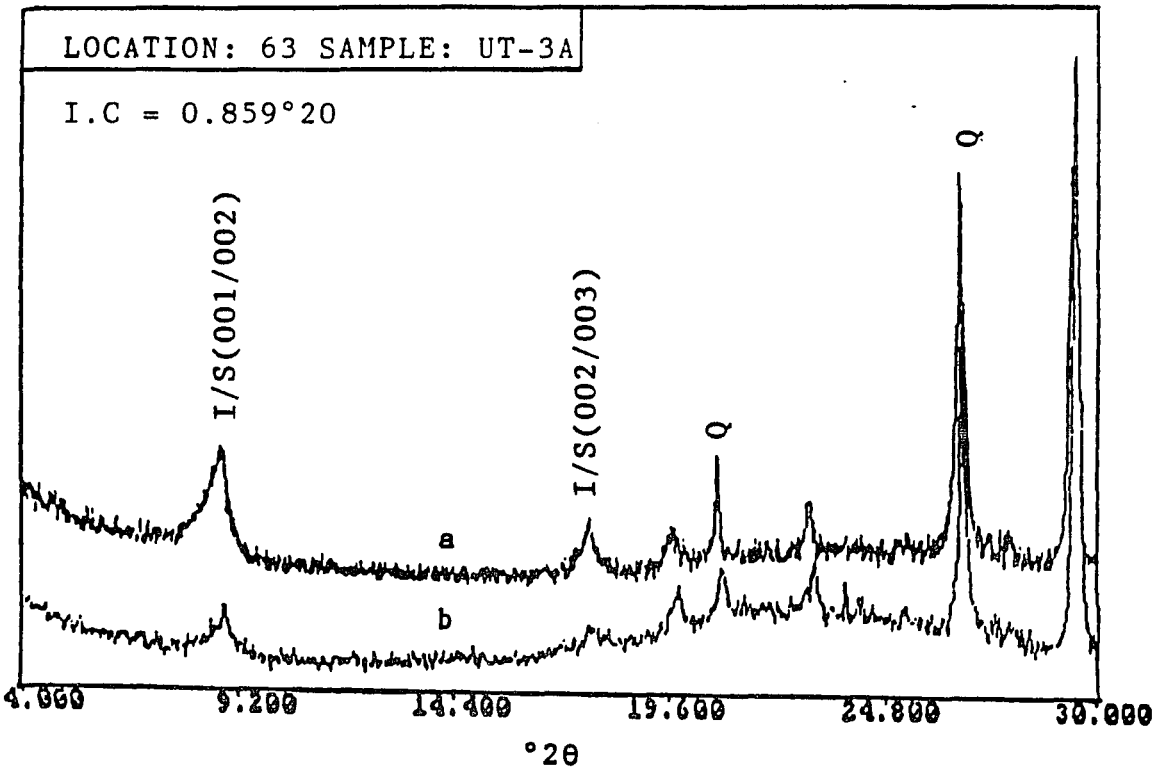
LOCATION: 63 SAMPLE: UT-3A
I.C = 0.859°20
I/S(001/002)
I/S(002/003)
Q
Q
a
b
4.000
9.200
14.400
19.600
24.800
30.000
°2θ

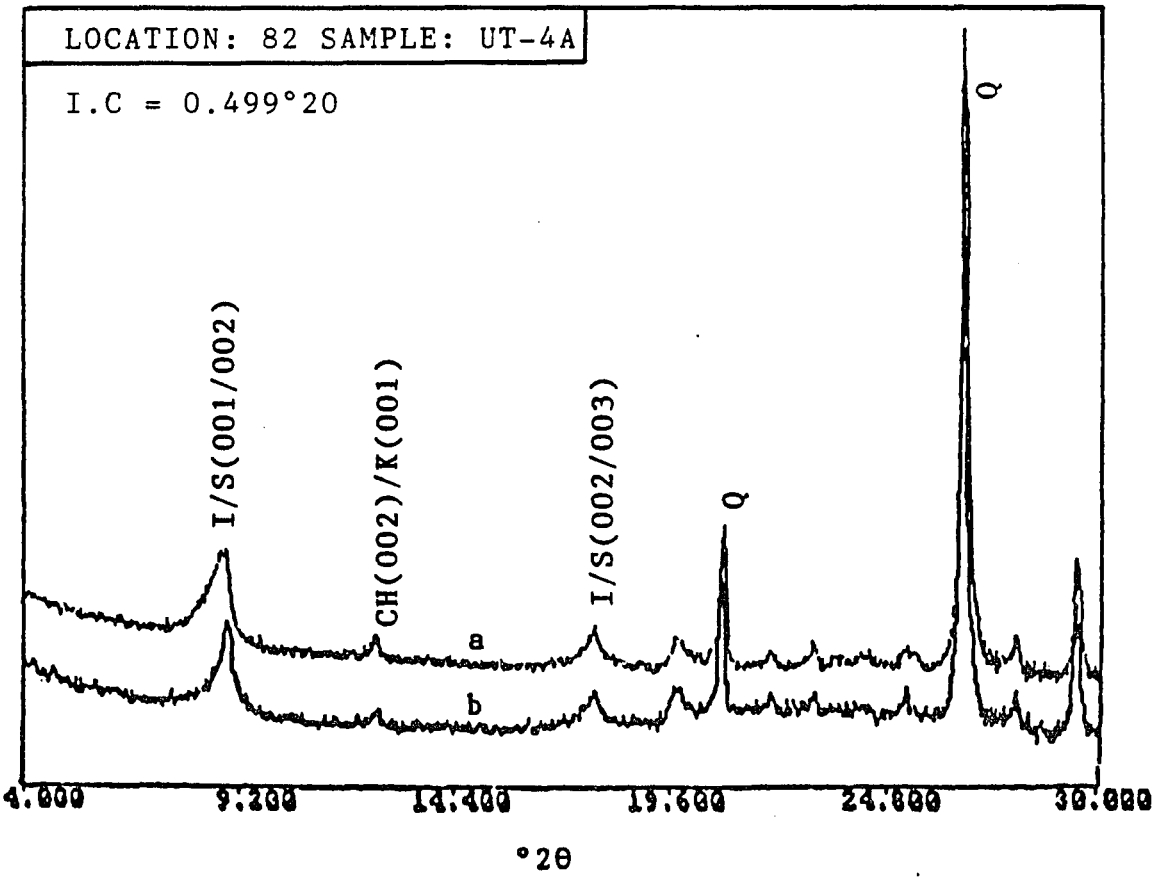
LOCATION: 82 SAMPLE: UT-4A
I.C = 0.499°20
I/S(001/002)
CH(002)/K(001)
I/S(002/003)
Q
Q
a
b
4.000
9.200
14.400
19.600
24.800
30.000
°2θ

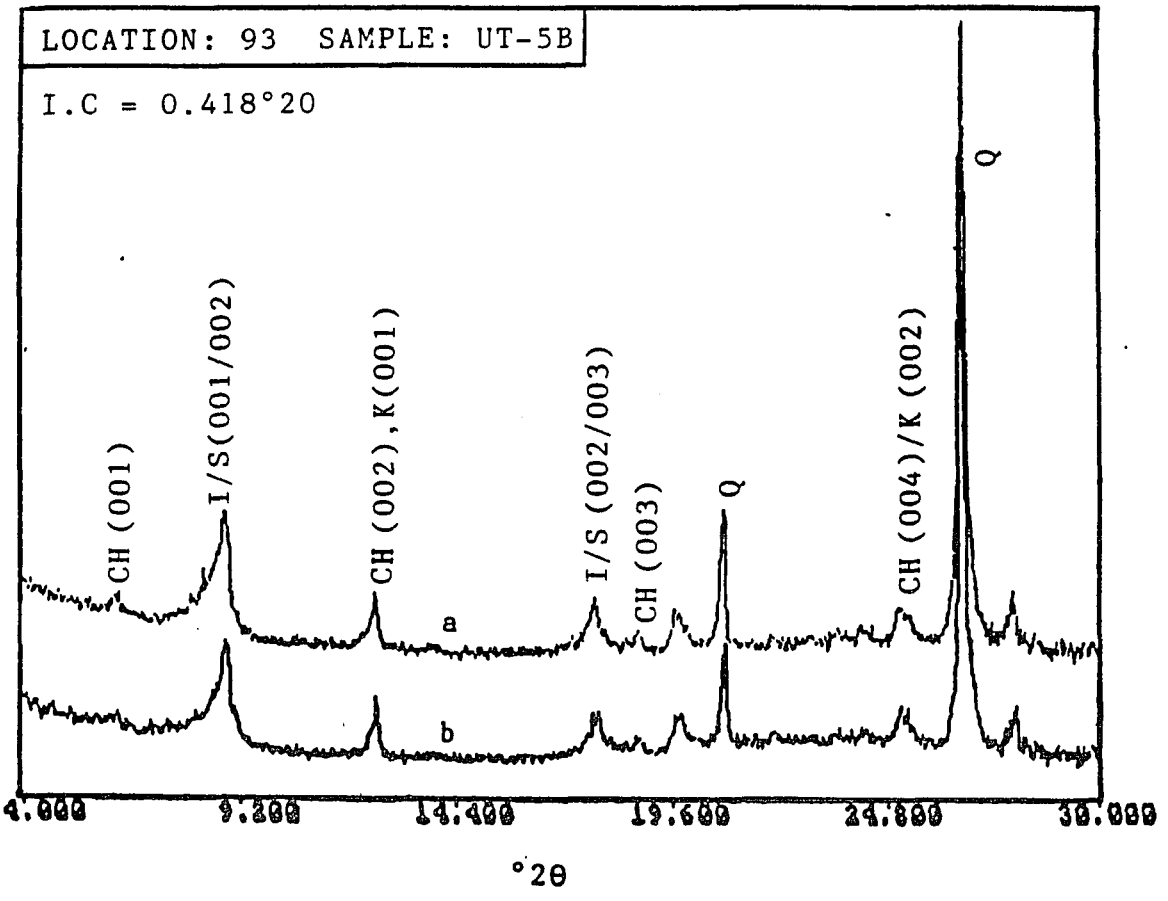
LOCATION: 93 SAMPLE: UT-5B
I.C = 0.418°2θ
CH (001)
I/S(001/002)
CH (002),K(001)
I/S (002/003)
CH (003)
Q
CH (004)/K (002)
Q
a
b
4.000
9.200
14.400
19.600
24.800
30.000
°2θ

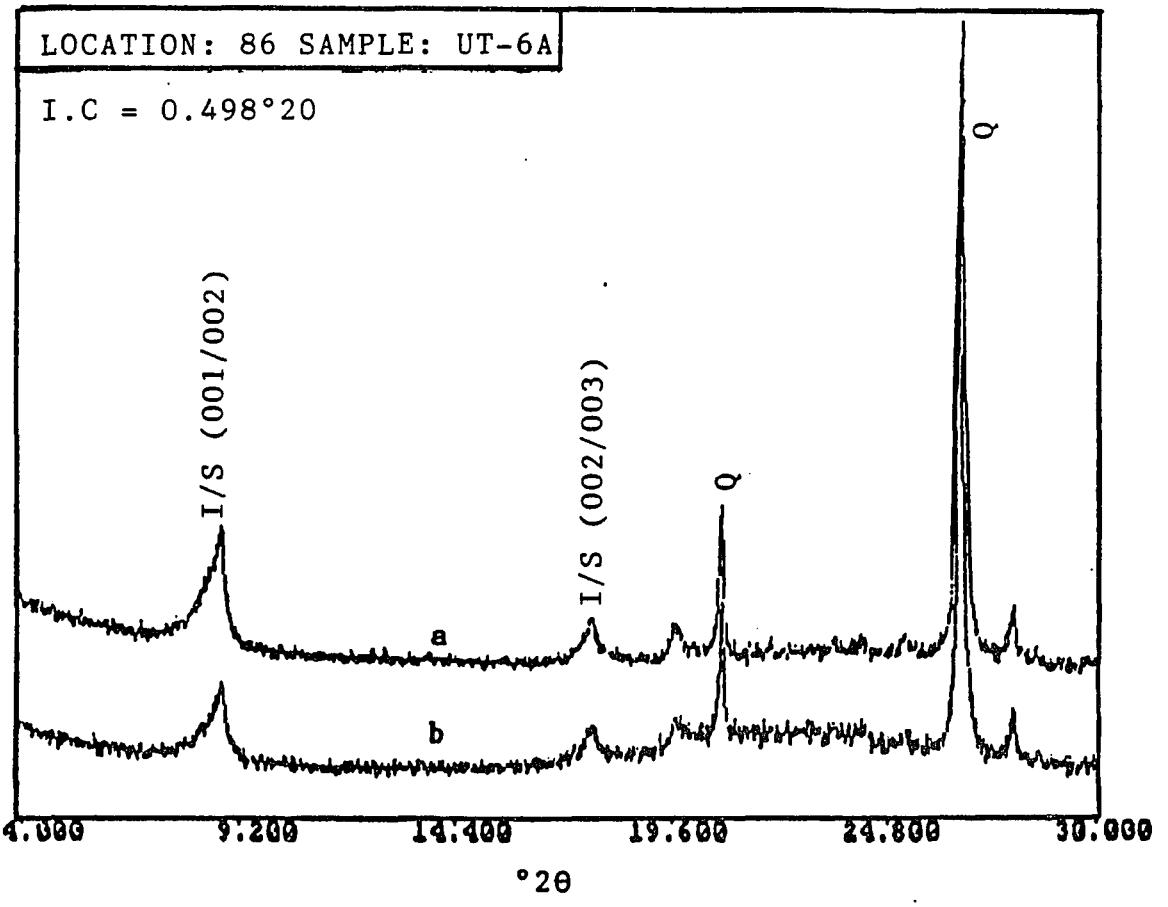
LOCATION: 86 SAMPLE: UT-6A
I.C = 0.498°2θ
I/S (001/002)
I/S (002/003)
Q
Q
a
b
4.000
9.200
14.400
19.600
24.800
30.000
°2θ

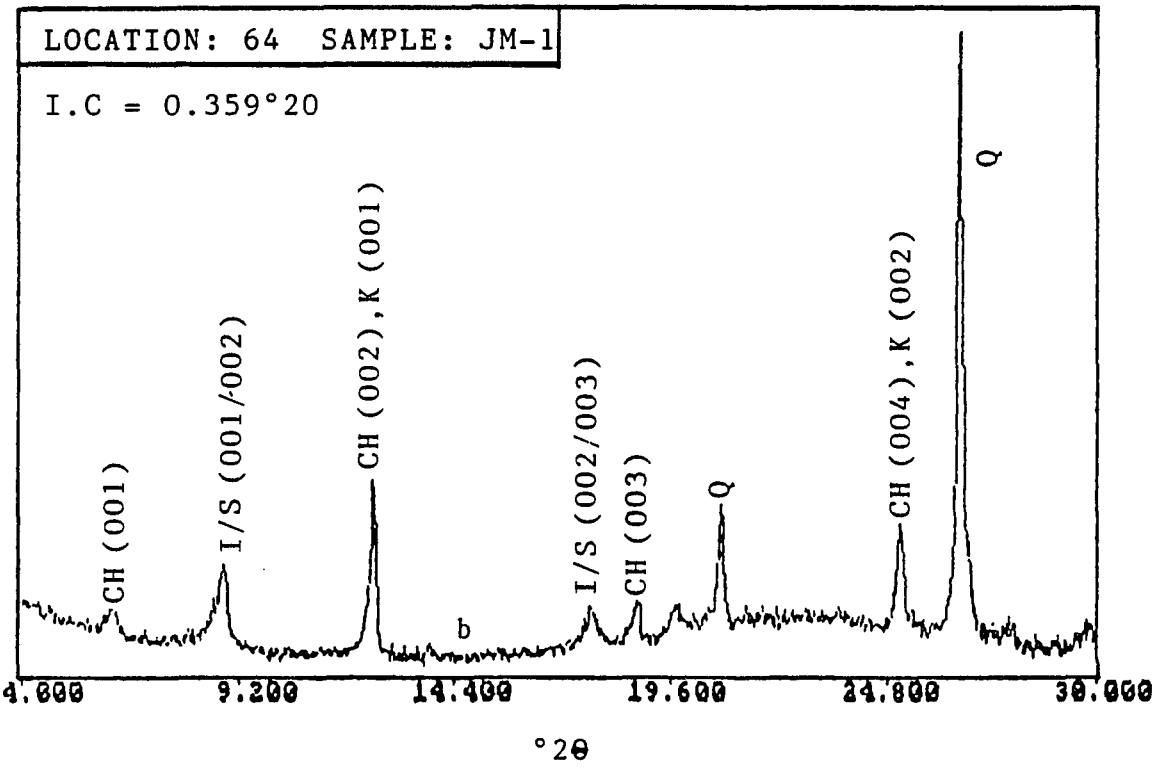
LOCATION: 64 SAMPLE: JM-1
I.C = 0.359°20
CH (001)
I/S (001/002)
CH (002),K (001)
b
I/S (002/003)
CH (003)
Q
CH (004),K (002)
Q
4.000
9.200
14.400
19.600
24.800
30.000
°2θ

kaolinite (Moore and Reynolds, 1989, p.210). However, the presence of chlorite is evident from occurrence of its 001 peak at 6.2° 2θ (14.1 A) and 003 peak at 18.8° 2θ (4.7 Å), which are not interfered by kaolinite. Whether kaolinite is present can be definitively determined only by rigorous experimental procedures (Moore and Reynolds, 1989, p.210-211): these were not undertaken in this study.

Table 7.2 below shows the calculations involved in determining the percentage of illite in the studied samples. The complete x-ray data are presented in Appendix-D.

Table: 7.2: Calculated percentage of illite (%illite) in the Utica samples based on the difference (in °2θ) between peak positions of 001/002 and 002/003 illite-smectite (I/S).

Location no.	Sample no. I/S peak (° 2θ)	Position of 001/002 I/S peak (° 2θ)	Position of 002/003	Δ(°2θ)	*Illite (%)
79	UT-1A	8.84	17.76	8.92	90-100
80	UT-2A	8.84	17.76	8.92	90-100
63	UT-3A	8.86	17.76	8.90	90-100
82	UT-4A	8.86	17.76	8.90	90-100
93	UT-5A	8.88	17.76	8.88	90-100
86	UT-6A	8.84	17.76	8.92	90-100
64	JM-1	8.88	17.76	8.88	90-100

* Calculations are based on Moore and Reynolds (1989) method (see section 4.5.1, table 4.2). Peak positions are shown in figure 7.2 and presented in Appendix-D.

7.5: INTERPRETATION

7.5.1: Organic maturation data:

The thermal alteration index (TAI) of the Utica samples range between 2.4 and 3.8, which correspond to vitrinite reflectance (Ro%) of 0.75 and 2.0 respectively (table 7.1). Following Barker and Pawlewicz's (1986) method of estimating maximum burial temperature (section 4.4), the Ro values can be used to estimate maximum burial temperatures of the Utica samples. The calculated paleotemperatures range between 116°C for location 93 to 242° C for location 64 (table 7.1). In figure 7.3, the paleotemperatures are plotted against sampling locations.

Paleotemperatures estimated from TAI (via equivalent Ro) of the Utica samples are considerably lower than those indicated by clay diagenesis in all but location-79 (fig. 7.3) and 64 (not included in fig. 7.3, but see table 7.1 and the following section). The reason for this inconsistency may be twofold: firstly, all the Utica samples, except those of location - 64, are outcrop samples. Although the samples were carefully scrapped and washed to rid them of weathered and oxidized surfaces, the procedure may not have been fully satisfactory. Thus, the measured TAI may reflect values variably altered by weathering. Secondaly, as Tissot et al. (1987) point out, a visual coloration index, such as TAI, is generally an average measurement of optical reflections of various types of organic matter which may respond differently to the same amount of heating. Average TAI measurements, therefore, may not accurately reflect thermal maturity. Moreover, the abundance of degraded and amorphous organic matter in the Utica samples probably pose additional problems in TAI measurements. It is therefore believed that the low 'TAI's obtained from locations 80, 63, 82, 93 and 86 (table 7.1, fig. 7.3) under-represent the true maturity of the samples.

7.5.2: Clay diagenesis data:

Figure 7.2 shows that there is no or very little difference in the peak positions between the XRD patterns of untreated and glycolated samples of any location. This observation suggests that swelling-type clays, particularly smectite, are absent, or present in very low proportions in these samples (Eslinger and Pevear, 1988, p. A-22; Moore and Reynolds, 1989, p.250). Absence of a peak near 5.2° 2θ in all the samples also indicate the absence of randomly inter- stratified illite/smectite clays and the presence of illite as the dominant component (Moore and Reynolds, 1989, p.250).

Samples of the Utica Shale from all sample locations contain illite in the mixed-layer illite/smectite (I/S) in excess of 90% (table 7.2). Such high percentage of illite suggests that paleotemperatures of 200° C or more were probably reached in all the sample locations (section 4.5). In figure 7.3, the paleotemperature line parallel to 200°C marks the limit set by percentage of illite in mixed-layer I/S. Presence of chlorite and apparent absence, or presence in very low quantity, of kaolinite also indicates high burial temperatures (Eslinger and Pevear, 1988, p.210-211).

Illite crystallinity index (I.C) of the studied samples of Utica Shale varies between 0.359° 2θ and 0.499° 2θ in six sample locations; only in location - 63, the I.C. is a relatively high 0.859° 2θ (fig. 7.2). Using Weaver et al.'s (1984) temperature - I.C. diagram (fig. 4.5), a temperature range of 240°C to 265°C is obtained for the Utica samples (table 7.3). In figure 7.3, the I.C. - temperature profile of the Utica Shale along the margin of the Adirondacks is also shown.

Comparison of the three profiles in figure 7.3 shows that the I.C. temperatures are even higher than the limiting temperature values (~200°C), indicated by percentage of illite in I/S, in all but location #63 where an I.C. temperature of about 170° C is obtained. The fact that I.C. temperatures are in general higher than 200° C, indicated by the percentage of illite in I/S, is not surprising. The percentage of illite in I/S, as discussed in section 4.5, only gives an approximate temperature range, but for more than 90% illite, the upper limit is more or less open until the metamorphic stage (illite to mica) is reached. So, the 200° C limit set by percentage of illite does not invalidate the I.C. temperatures.

At location #63, the downward trend in the I.C.- temperature profile mimics the TAI-temperature profile. Moreover, the Th_{max} of the Beekmantown rocks at location #63 is also anomalously low (section 5.6.2). Thus, paleo- temperatures calculated from three different methods show relatively low temperatures at this location. In chapter 8, this matter is considered in more details.

ble 7.3 : Paleotemperatures of the Utica Shale calculated from I.C. using Weaver et al.'s (1984) temperature-I.C. relationship diagram (see fig. 4.5).

Location no.	Sample no.	I.C. 2θ (mm)	Temperature (° C)
79	UT-1A	0.459 (5.8)	246
80	UT-2A	0.399 (5.05)	260
63	UT-3A	0.859 (10.9)	170
82	UT-4A	0.499 (6.3)	240
93	UT-5B	0.418 (5.3)	250
86	UT-6A	0.498 (6.3)	240
64	JM-1	0.359 (4.5)	275

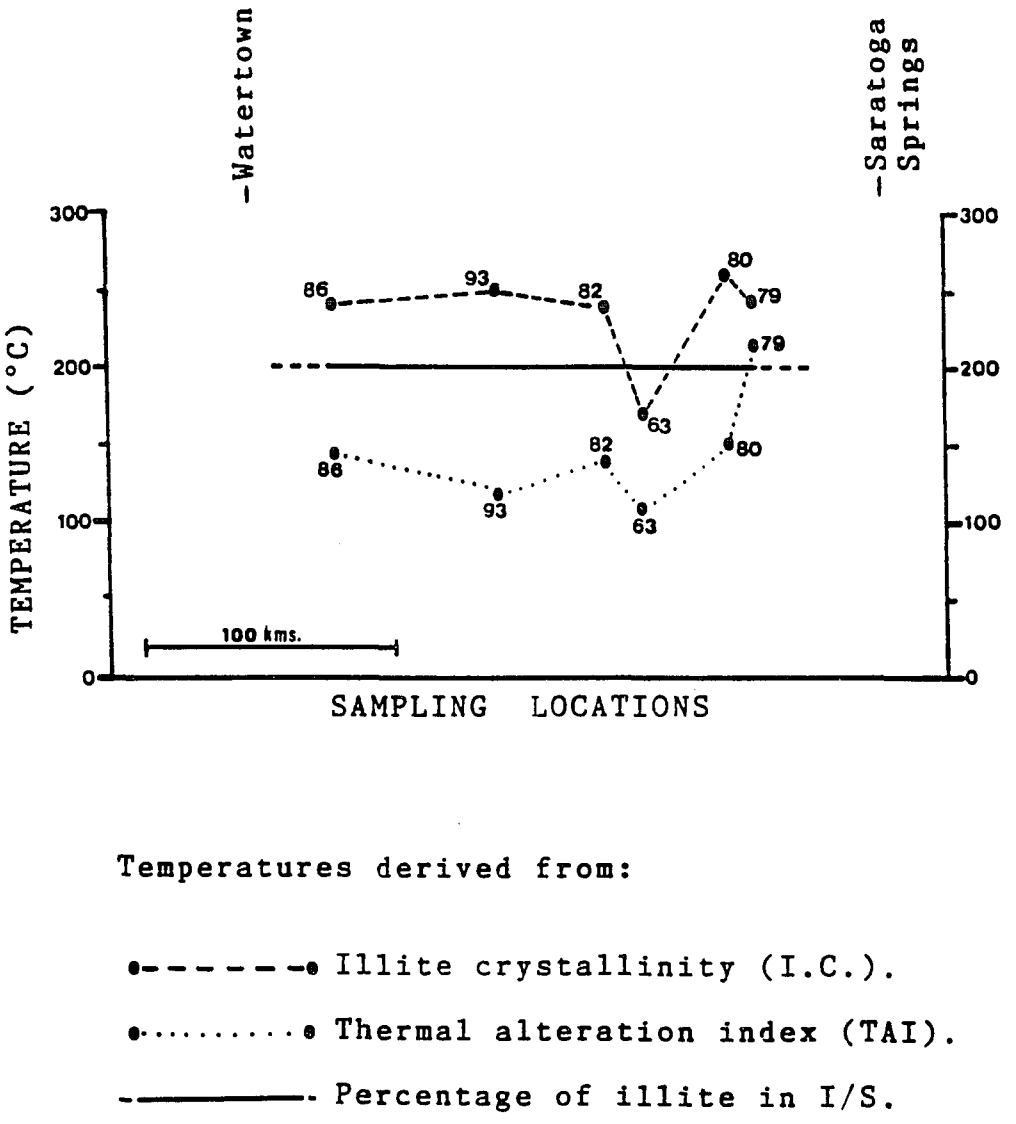

Figure 7.3: Paleotemperature profiles of the Utica Shale through sample locations along the southern margin of the Adirondacks.

CHAPTER 8

REFINED PALEOTEMPERATURES AND BURIAL DEPTHS OF CAMBRIAN AND ORDOVICIAN ROCKS

8.1: PALEOTEMPERATURE PROFILES ALONG THE SOUTHERN AND SOUTHWESTERN MARGIN OF THE ADIRONDACKS:

Because the Cambro-Ordovician Beekmantown carbonates, and the Late Ordovician Black River-Trenton carbonates and Utica Shale crop out in a roughly matching belt along the southern and southwestern margins of the Adirondack Highlands (chapters 5, 6, 7), their paleotemperatures can be compared in order to obtain refined paleotemperature profiles (section 4.7.1).

In figure 8.1, the paleotemperature profiles of the Beekmantown Group (from fig. 5.9), Black River - Trenton groups (from fig. 6.8) and Utica Shale (from fig. 7.3) between Saratoga Springs and Ogdensburg have been put together for comparison. As discussed in section 7.5.1, the TAI-temperature profile of the Utica Shale has little meaning, except at locations #79 and #63 where the TAI temperatures show compatible or meaningful relationship with the other profiles. Between location #73 and #89, the Th_{max} of Beekmantown and Black River - Trenton rocks are higher or very close to 200°C at every location except location 63. This is consistent with the general temperature limit of about 200° C set by the percentage of illite in I/S of the Utica Shale (represented by the straight line in fig. 8.1). However, the Th_{max} values of the Beekmantown rocks at locations #63 and #90 are anomalously low and require re-examination.

The Th_{max} of vug- and vein-filling cements of the Beekmantown rocks at location #63 is only 159.3° C (fig. 5.8), much lower than those in Beekmantown rocks to the east and Black River - Trenton rocks to the northwest, along the margin of the Adirondacks. At location #63, the Black River - Trenton carbonates are missing, and the Utica Shale directly overlies the Tribes Hill Formation of the Beekmantown Group. Illite crystallinity

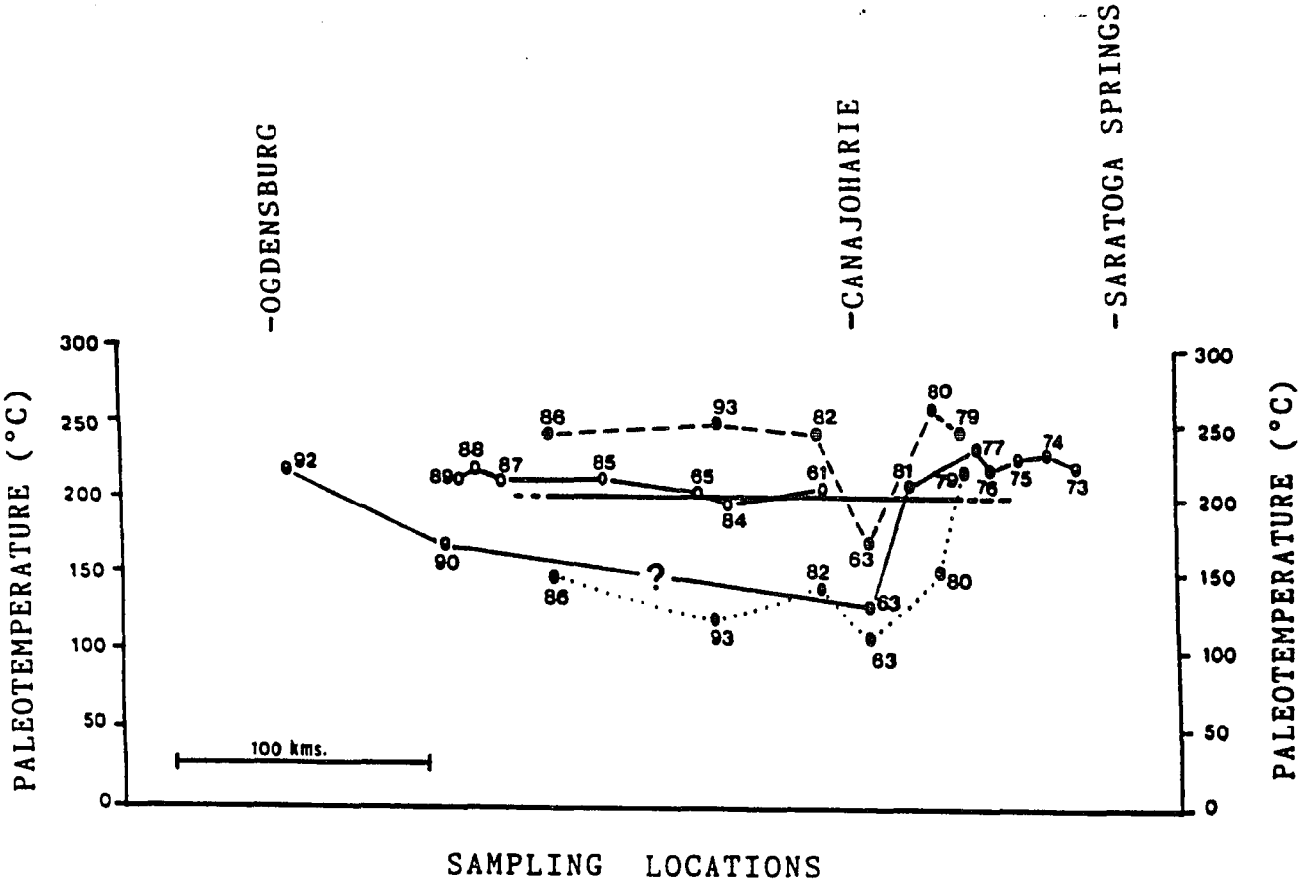

Figure 8.1: Paleotemperature profiles based on Th_{max} of the Beekmantown and Black River - Trenton carbonates, and on TAI, I.C and percentage of Illite in I/S of the Utica Shale.

index (I.C.) of Utica samples at this location indicates temperatures of about 170° C. Two Utica samples of location #63 both show TAI of 2.3 (equivalent Ro of 0.7) indicating a temperature of only 108° C (table 7.1). Although the usefulness of TAI data in quantitative paleotemperature assessment has been questioned before, the fact that Th_{max} and I.C. also indicate relatively low temperatures probably lends some credence to the drop in TAI values at these locations, if not to the TAI values themselves. The only data that indicates high paleotemperature at location 63 is the presence of more than 90% illite in I/S of the Utica samples. However, it should be noted that the Th_{max} of 159.3° C was based on pressure-uncorrected Th, and therefore represents a lower limit of the maximum paleotemperature reached. The I.C.-temperature of 170° C of the Utica Shale was obtained by extrapolating Weaver et al.'s (1984) diagram, and therefore may not be very reliable. The true maximum paleotemperature at this location might indeed have been 200° C or more - consistent with the presence of more than 90% illite in I/S of the Utica Shale.

Stratigraphic evidence also seems to support evidence of lower paleotemperature at location #63. During the deposition of the Black River and Trenton carbonates, the area of Canajoharie (location #63) is believed to have remained emergent as a local topographic high, which is indicated by pinching out of these carbonates toward this area (Fisher, 1977; Fisher, pers. comm., 1989). Perhaps this area had remained a local, structural high in the later periods of subsidence. Thus, the Beekmantown and Utica rocks of location #63 were probably never buried as deep (and subjected to temperatures as high) as the same rocks on either side along the transect of figure 8.1.

The relatively low Th_{max} of Beekmantown samples of location #90 may be misleading. At this location, the 'Th's were measured in quartz overgrowths of the Potsdam Sandstones (Beekmantown Group), not in vugs or fractures. The quartz overgrowths are believed to have formed earlier and in shallower depths than vug- and fracture-filling cements elsewhere in the Beekmantown Group (section 5.6.2) and probably do not contain fluid inclusions that would show the higher (uncorrected) Th. Moreover, location #90 is within 15km of location #89 where the Th_{max} of Black River-Trenton samples is 212° C. It is unlikely that the maximum paleotemperature

would drop so drastically in locations #90. Unlike location #63, there is no evidence for the former presence of a topographic high at this location. Therefore, it seems that the Th_{max} of location #90 can not be used in the refined paleotemperature profiles.

The refined paleotemperature profiles are shown in figure 8.2. For Beekmantown and Black River - Trenton groups, the profiles are their Th_{max} profiles, and therefore represents a lower limit of the maximum paleotemperatures reached by these units along the transect. The temperature profile of the Utica Shale, however, is based on I.C. temperatures, and represents the upper limit of maximum temperatures reached by this unit.

One of the two major modifications in the refined paleotemperature profiles of figure 8.2 was made around location #90. Based on arguments presented above, the Th_{max} of this location is raised only a little (about 6° C for a stratigraphic separation of ~200m between the samples of locations #89 and 90) above the end of the Black River - Trenton profile. Between location #87 and location #61, the Beekmantown rocks have been lost due to post-Beekmantown erosion, and the Black River Group now directly overlies the Grenvillean rocks (Fisher, 1977, pl.3). The Beekmantown profile, therefore, pinches out against the Black River - Trenton profile as shown in figure 8.2. East of location #63, the Amsterdam limestone is correlative of the Black River Group (fig. 6.1), but no sample was collected from these rocks. The Black River - Trenton profile pinches out against the Beekmantown profile west of location #63 following, as discussed above, the real pinch-out of the Black River and Trenton carbonates near this location. The other major modification was made in the I.C. temperature profile of the Utica Shale at location-63. The upper limit of maximum paleotemperature at this location is accepted as 200° C, based on the presence of more than 90% illite in I/S. At location #63, therefore, both the lower limit (i.e., Th_{max}) and upper limit of maximum temperature (i.e., I.C. temperarture) show a sharp drop (fig. 8.2).

It is believed that with accurate pressure correction, the Th_{max} profiles of the Beekmantown and Black River - Trenton groups would have closely matched the I.C.-temperature profile of the Utica Shale: they would have been only a little higher on

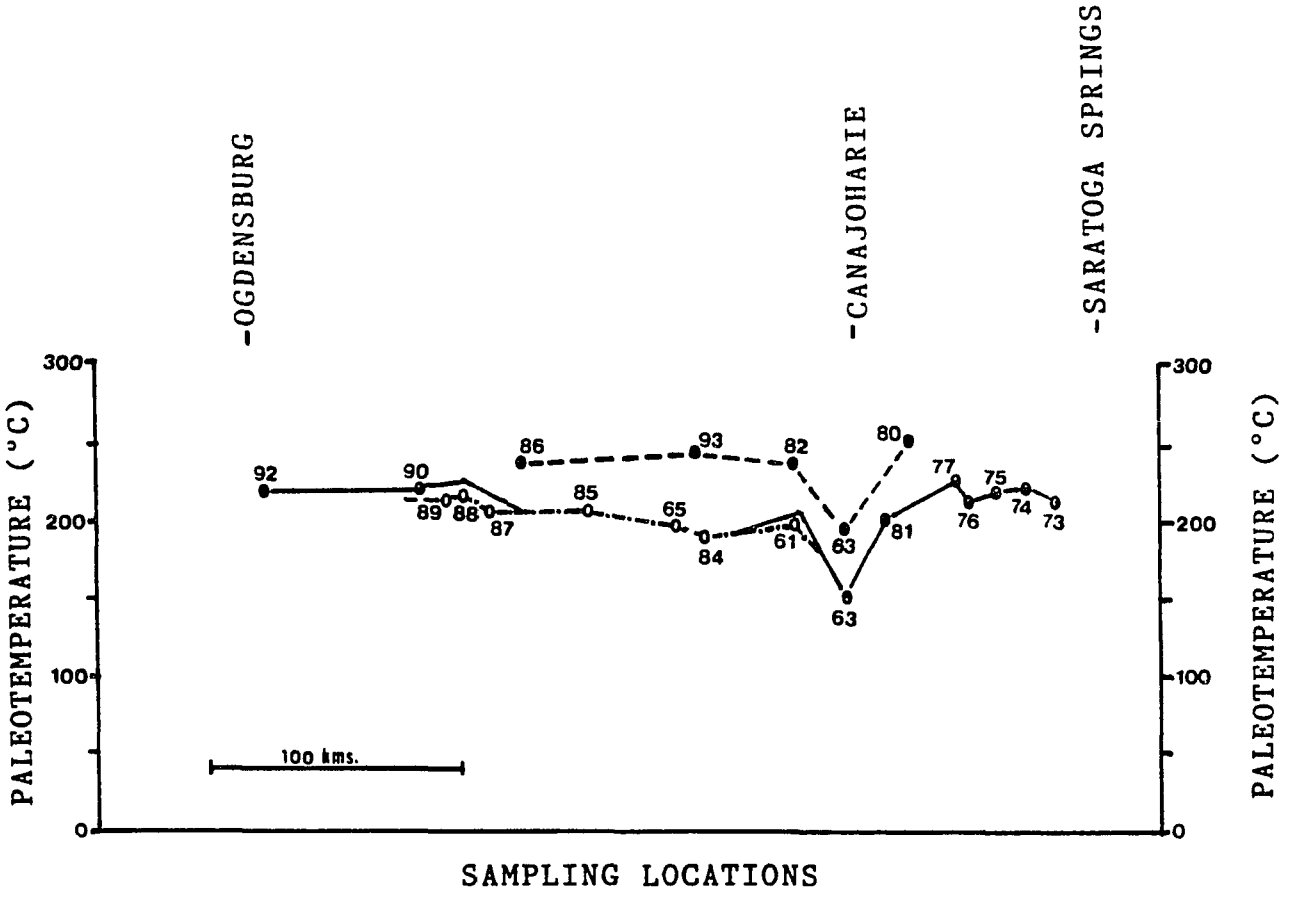

Figure 8.2: Refined paleotemperature profiles for the Beekmantown and Black River-Trenton groups and Utica Shale. See text for explanation.

account of their lower stratigraphic position. Pressure correction of Th is difficult, especially when missing overburden is involved. The reader is referred to section 16.1, where an attempt has been made at pressure correction.

8.2: PALEOTEMPERATURES OF THE CAMBRIAN AND ORDOVICIAN CORE SAMPLES FROM SOUTHCENTRAL AND WESTERN NEW YORK:

The three core sample locations of southcentral and western New York, namely, 64, 66 and 68 (see location maps of figs. 5.2, 6.2), are well outside the Saratoga Springs - Ogdensburg transect and, therefore, refinement of paleotemperatures at these locations has to be done on the basis of data from the cores alone.

At location #64, the Th_{max} of fracture-filling calcite and dolomite cements of Trenton carbonate samples (present depth: 3207m) is 269.3° C (fig. 6.7). In the overlying Utica Shale samples of the same core (present depth: 3040m), an I.C. of 0.359° 2θ has been measured (fig. 7.2). According to Weaver et al.'s (1984) I.C. - temperature relationship diagram, this I.C. values corresponds to a temperature of about 275° C (table 7.3). Therefore, the Th_{max} of 269.3° C is taken for the lower limit of the maximum paleotemperature of the Trenton samples, and the I.C. temperature of 275° C is taken for the upper limit of the maximum paleotemperature of the Utica Shale samples.

At location #68, core samples of only the Theresa Formation (Beekmantown Group) were available for study. Samples from a depth of 4088m show a Th_{max} of 187.2 C (fig. 5.8). This temperature is taken for the lower limit of maximum paleotemperature of these samples.

Similarly, at location #66 in western New York, dolostone samples of only the Theresa Formation were available for study. Samples from a depth of 980m showed a Th_{max} of 155.3° C (fig. 5.8), which is accepted as the lower limit of the maximum paleotemperature of the Beekmantown samples at this depth. However, paleotemperature data of the Silurian and Devonian rocks are also available from this area, and are discussed in context with the Beekmantown paleotemperature in chapter 16.

8.3: SOURCE OF HEAT:

The source of heat that caused high Th_{max} in fluid inclusions of the Beekmantown and Black River-Trenton carbonates and high I.C. and more than 90% illite in mixed-layer I/S of the Utica Shale needs to be investigated.

There is no evidence of Phanerozoic igneous activity in the vicinity of the Saratoga-Ogdensburg transect (fig. 5.2) or in western New York. The youngest igneous intrusions in the Adirondack massif are about 930 million years old (Weiner et al. 1984), and can not be regarded as a cause of thermal anomaly in the Paleozoic time. The Mesozoic ultramafic dike intrusions in the Finger Lakes region are probably too far from the Adirondacks to have any influence on the paleotemperature profiles of figure 8.2. It is also unlikely that the rocks at locations #64 and 68 were affected by this thermal event (see section 4.7.2).

Mineral phases showing high Th but lacking direct evidence of former deep burial have often been interpreted as having precipitated from warm, deep basinal fluids that migrated to shallow depths, especially toward the basin margin. This assumption underlies most current models of MVT-mineralization, although the models lack consensus on almost every other detail (see Noble, 1963; Jackson and Beales, 1967; Sharp, 1978; Anderson and Macqueen, 1982; Cathles and Smith, 1983, Graven and Freeze, 1984; Bethke, 1986; Gregg and Shelton, 1989). An important implication of these theoretical models is that the minerals forming from such fluids do not reflect the normal geothermal temperature of an area and, therefore, Th data obtained from them may not be directly used to estimate former depths of burial on the basis of a presumed 'normal' paleogeothermal gradient.

A number of arguments, however, point against possible entrapment of the high Th inclusions of the Beekmantown and Black River - Trenton groups from hot fluids at shallow depths. Perhaps the strongest evidence against shallow depth of entrapment comes from the high paleotemperatures of the overlying Utica Shale, as indicated by its I.C. and illite content. It is improbable that the general thermal maturity of an impermeable shale unit like Utica was caused by interaction with hot fluids. Anderson and Macqueen (1982), describing characteristics of MVT mineral deposits, state that

"geothermal gradients of 25-30° C/km are typical of these environments, yielding average host rock temperatures that are significantly less than 100-150° C" (typical range of Th in MVT minerals). The Utica Shale is not even the host rock of the studied cements in this case; it is the overlying rock unit. It should show much lower paleotemperatures if the measured Th in the underlying rocks were acquired from hot fluids at shallow depths. Clearly, the data indicates otherwise.

The same argument can be made for the anthracite rank coal samples in the Middle Devonian Gilboa Formation of the Catskills Mountains (Friedman and Sanders, 1982; see chapter 3) and the high paleotemperatures indicated by the Middle Devonian Marcellus Shale in eastern and central New York (chapter 13). To the knowledge of this researcher, interaction with hot fluid has not been proposed as a mechanism for increasing thermal maturity of either clay minerals or coal.

Also, no significant difference in Th has been found between inclusions of inter particle cements in the host rock and fracture- or vug-filling cements of the Beekmantown and Black River-Trenton groups. If the fracture- and vug- filling cements had precipitated from hot fluids emerging from below (fractures are believed to be the most common pathways for these fluids), the Th measured in these cements should have been consistently higher than those measured in interparticle cements.

Moreover, the presence of healed fractures does not necessarily mean that they were conduits for upward migrating fluids. The healed fractures in the Beekmantown and Black River-Trenton rocks, which are not very abundant in any case, may have formed as "hydraulic fractures" under the influence of abnormal fluid pressure developed during deep burial (Engelder, 1985; Oertel and Engelder, 1985). The presence of Utica Shale as a caprock on top of the Trenton Group may have caused the "abnormal fluid pressure", and fluids expelled from the Utica Shale as a result of mechanical compaction and smectite-to-illite trasformation may have circulated into the fractures below (and probably above) and precipitated cements in them. If so, the paleotemperature signatures of these rocks reflect ambient, formational temperatures, not a thermal anomaly caused by large-scale intrusion of hot extra-formational brine.

Another external source of fluid, perhaps more plausible than the above in the present example, could have been the Taconic thrust belt along the Champlain and Hudson valleys (see Oliver, 1986; Whitney and Davin, 1987). However, at the height of the Taconic thrusting event the Beekmantown, Black River - Trenton and Utica Shale were buried to shallow depths - so the rock units themselves were yet to be subjected to high burial temperatures. Moreover, the fluid driven westward by the thrusts, supposing it happened, did not have to be hot as Oliver (1986) postulates. In fact, much of this fluid may have been low-temperature, meteoric water driven by the hydraulic head established by the Taconic thrust-created topography (or even the later Acadian and Alleghenian topography). According to Graven and Freeze (1984), such meteoric waters actually lower the geothermal gradient near the orogenic belt and raise it in areas far from the orogenic belt. So, even if fluid from the orogenic belt moved into the Champlain, Hudson and Mohawk valleys, it may not have increased the temperature in the rocks of these areas. Moreover, the high Th_{max} in the St. Lawrence Valley (location 92) and the low Th_{max}, I.C. and TAI of location 63 are difficult to explain by fluid flow from the orogenic belt east and southeast of the Adirondacks. The relatively low Th_{max} of 155.3° C at location #66 in western New York (also see chapter 16 for evidence of low temperature in other rock units in western New York), while supporting Oliver's (1986) contention of decreasing cratonward temperatures of orogenic fluids, runs contrary to the model of Graven and Freeze (1984). In short, none of the proposed mechanisms of large-scale basinal or orogenic fluid flow explains the observed paleotemperature patterns of the studied Cambrian and Ordovician rocks.

Considering the above arguments, it is inferred that paleotemperatures indicated by Th_{max} of the Beekmantown and Black River-Trenton rocks and percentage of illite and I.C of the Utica Shale reflect formational temperatures acquired from normal geothermal heat caused by burial. The combination of high Th and low Tm in these rocks (sections 5.6.2, 6.5.2) and depleted $\delta^{18}O$ values in the Beekmantown samples (section 5.6.3) suggest that the fluids trapped in the inclusions were hot formational brines.

8.4: MAXIMUM BURIAL DEPTHS:

Two separate computations of "maximum burial depths" are possible from the refined paleotemperature data (sections 8.2): one representing a lower estimate of burial depths based on pressure-uncorrected Th_{max} of the Beekmantown and Black River - Trenton groups, and the other representing a higher estimate of burial depths based on I.C. - temperatures of the Utica Shale. Both computations are necessary because the I.C. - temperature data are few and do not cover many sampling locations, whereas Th_{max} data are available from many more locations.

Figure 8.3 shows the maximum burial-depth (lower limit) profiles of the Beekmantown and Black River - Trenton groups calculated from the refined Th_{max} profile of figure 8.2 and plotted against sampling locations. The burial depth profiles of the younger rocks in figure 8.3 have been constructed from their stratigraphic thicknesses in the area or from their projected thicknesses from the south : the procedure is discussed below.

Following procedure discussed in section 4.7.3, burial depths at each location of the Beekmantown and Black River - Trenton units along the Saratoga Springs - Ogdensburg transect were calculated by subtracting an assumed mean annual surface temperature of 20° C from the Th_{max} and then dividing the remainder by an average paleo-geothermal gradient of 30° C/km.

East of location #63, a very thin (less than 20m thick) unit of Amsterdam limestones, equivalent to the Black River carbonates of the west and northwest, is present. It is not shown separately in the burial depth profiles because of the small scale involved - it is, however, included within the overlying Ordovician units. Around location #90, the stratigraphic separation between the tops of Beekmantown and Trenton is about 250m (Fisher, 1977, pl. 3). In Ogdensburg area (location #92), Black River and Trenton carbonates have been eroded, but in the Ottawa region of the Quebec Basin a combined thickness of 770m of Black River - Trenton carbonates are preserved (Douglas, 1970, chart II). This thickness is projected on to location #92 and connected with the top of Black River - Trenton at location #90.

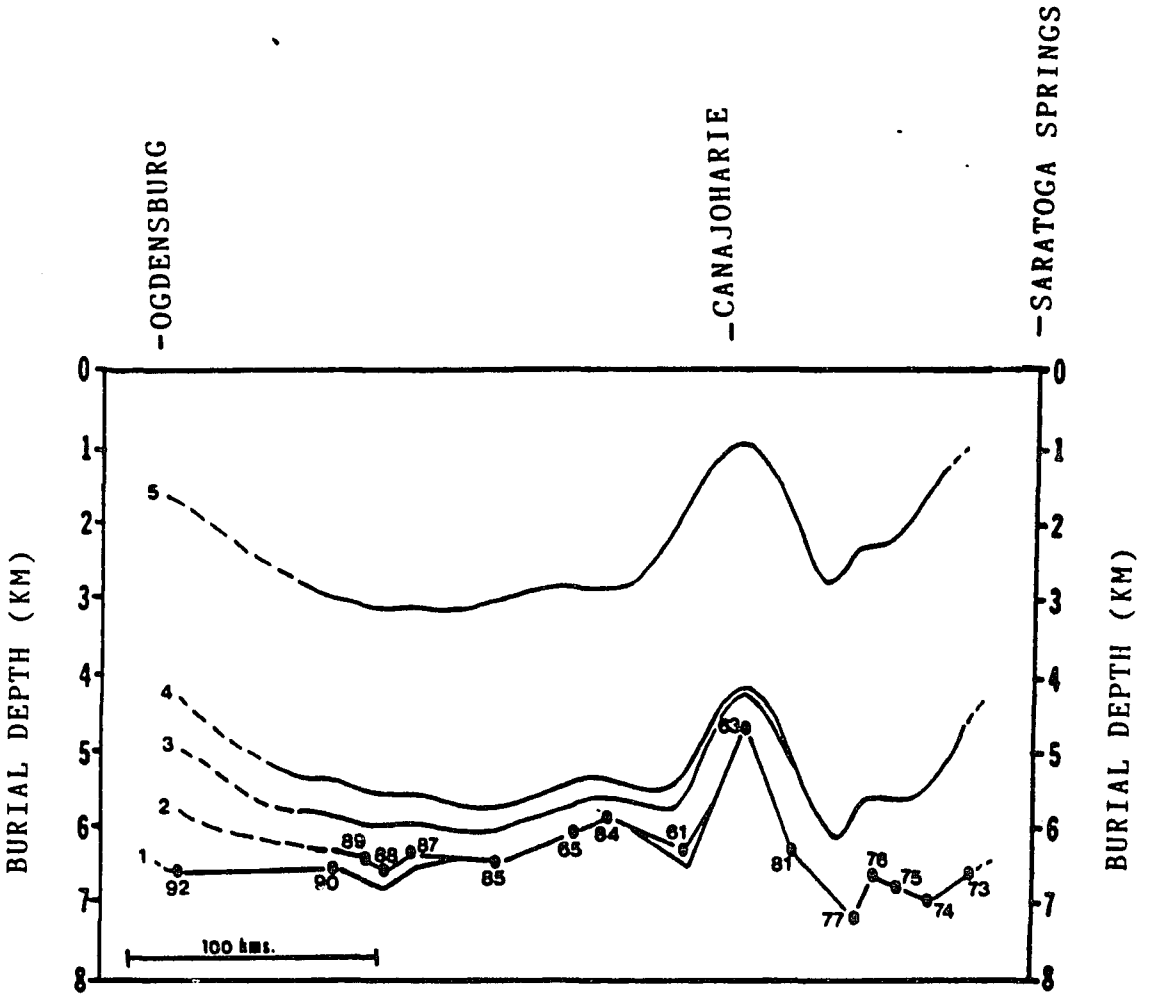

EXPLANATION:

1 Top of Beekmantown Group

2 Top of Black River - Trenton groups

3 Top of Ordovician

4 Top of Silurian

5 Top of Devonian

Figure 8.3: Maximum burial depth (lower limit) profiles of different rock units along the Saratoga Springs - Ogdensburg transect, based on refined Th_{max} profiles of the Beekmantown and Black River - Trenton groups. See text for explanation.

The Ordovician rocks overlying the above carbonates include the Utica - Frankfort - Schenectady shales in the east and attain a thickness of 1.8km in the Schenectady - Saratoga Springs area (Fisher, 1977, pl.3). These shale units thin rapidly to the west, and in Canajoharie (location #63), the total thickness is only about 400m. West and northwest from Canajoharie, the Utica Shale thins steadily, and the combined thickness of the post-Trenton Ordovician is only 300m around locations #65 and 84. In the Pulaski - Watertown area (locations 88 - 90), although the Utica Shale thins even more, the overlying Frankfort Shale passes and thickens into equivalent Oswego - Pulaski sandstones and shales and is overlain by the Queenston Shale, totalling a thickness of 0.5km. The total thickness of the post-Trenton Ordovician section in the Ottawa region is about 870m thick (Douglas, 1970, chart II), this thickness is projected on to location #92 to mark the top of the Ordovician.

The Silurian section in New York is relatively thin and the northern erosional edge of the Silurian rocks is tens of kilometers removed from the Saratoga Springs - Ogdensburg transect, except in the east near location #63 where the two come within 15km of one another (see geologic map in fig. 2.3). The thickness of the Silurian section, therefore, has to be projected on to the entire transect from the south. The implication behind such projection is that the Silurian rocks did not change significantly in thickness from south to north in New York. Thickness measurements indeed show that within the area in which the Silurian rocks are preserved, the rocks change in thickness in an east - west direction, not north - south (Rickard, 1973, pl.2). The same is largely true for the Ordovician and Devonian sections of New York (Rickard, 1973, pl.4; Fisher, 1977, pl.3; Crough, 1981). In Syracuse area, the thickness of the entire Silurian section is about 460m. The thickness decreases rapidly eastward along the Silurian outcrop belt to zero, due south of the transect between locations #81 and 77 in figure 8.3. From here, swinging southest to south through the Helderberg Mountains and along much of the Hudson Valley, the Lower Devonian Helderberg Group carbonates rest directly on Upper Ordovician rocks. In figure 8.3, therefore, the top of the Silurian section pinches out east of location #81. The thickness of 460m in the Syracuse area, when projected northward, falls on locations 87 to probably 90. Location #92 is slightly northeast of

location #90; so the same thickness of 460m for the Silurian section is projected on to this location. There is no Silurian rock preserved in the Quebec Basin (Douglas, 1970, chart II); therefore projecting the thickness from the Syracuse area was the only available alternative.

In a similar method, the thicknesses of the total Devonian section of southern New York from Rickard (1973, pl. 4) is projected on to the transect. The thickness of the total Devonian section varies from 2.5km due south of locations 87 through 92 along the southern border of New York to about 3.4km due south of location #73 in south- eastern New York. The top of Devonian in figure 8.3 is drawn on the basis of changing thickness of the total Devonian in an east - west direction along the southern border of New York (Rickard, 1973, pl. 4).

8.5: THICKNESS OF POST-DEVONIAN STRATA

As shown in figure 8.3, the minimum thickness of post- Devonian strata removed from the Saratoga Springs - Ogdensburg transect is represented by the separation between the projected top of the Devonian and the surface of zero burial. The minimum thicknesses of former post-Devonian strata at different locations, taken from figure 8.3, are listed in table 8.1. In addition, table 8.1, shows the estimated thicknesses of post-Devonian strata at the three core sample locations discussed in section 8.2.

Estimates of the maximum thickness (upper limit) of post-Devonian strata that might have been present can be made only in those locations where the Utica Shale was sampled (figs. 7.1, 8.1, 8.2). Temperatures estimated from I.C. values yield the maximum temperatures in the Utica Shale, except in location #63, where the percentage of illite in I/S provide the maximum temperature (section 8.1). Table 8.2 below presents the maximum thicknesses of former post-Devonian strata at different locations calculated from these temperatures. The same procedure, discussed above, of projecting the thicknesses of younger (than Utica) units from the south has been followed.

Table 8.1: Estimated minimum thicknesses of post-Devonian strata removed from various study locations of Cambrian and Ordovician rocks. See text for explanation.

Location no.	Rock unit	Th_{max} (°C)	Burial depth (km)	Projected thickness of overlying rocks (km)	Thickness of former post-Devonian rocks (km)
73	Beekmantown	219.7	6.65	5.55	1.1
74	--	230.2	7.0	5.6	1.4
75	--	228.7	6.95	5.5	1.45
76	--	220.0	6.66	5.4	1.26
77	--	236.6	7.22	5.4	1.8
81	--	208.5	6.28	4.68	1.6
63	--	159.3	4.65	3.85	0.8
61	Trenton	210.0	6.33	3.86	2.47
65	Black River	203.6	6.12	3.78	2.34
85	--	213.5	6.45	3.57	2.88
87	--	218.3	6.6	3.5	3.1
88	--	223.8	6.79	3.5	3.29
89	--	216.0	6.53	3.5	3.03
90	Beekmantown	220.0	6.66	3.5	3.16
92	--	218.0	6.6	3.88	2.72
66	--	155.3	4.51	2.1	2.41
68	--	187.2	5.57	4.64	0.93
64	Trenton	269.3	8.3	3.86	4.44

Table 8.2: Estimated maximum thicknesses of post-Devonian strata removed from various study locations of the Utica Shale. See text for explanation.

Location no.	Rock Unit	Temp. (° C)	Burial depth (km)	Projected thickness of overlying rocks (km)	Thickness of former post-Devonian rocks (km)
79	Utica Shale	246	7.5	4.3	3.2
80	--	260	8.0	4.3	3.7
63	--	200	6.3	3.85	2.45
82	--	240	7.26	3.7	3.56
93	--	250	7.66	3.5	4.16
86	--	240	7.26	3.4	3.86
64	--	275	8.5	3.7	4.8

CHAPTER: 9: THE CLINTON GROUP

9.1: STRATIGRAPHY AND DEPOSITIONAL HISTORY:

The early Middle Silurian (Niagaran) Clinton Group of New York is exposed along the Silurian outcrop belt between Niagara Falls in the west and Utica in the east (fig. 9.1). It is only about 36m thick in the Niagara Falls area from where it thickens eastward to about 100m, southeast of Syracuse, and then thins again to about 45m in the Utica area (Rickard, 1975). East of Utica, it is erosionally truncated by the Late Ordovician - Late Silurian unconformity. In the subsurface of New York, the Clinton Group occurs as far east as the Delaware county (Kreidler et al. 1972). In southeastern New York, the sandstones and conglomerates of the Shawangunk Formation are equivalent to the Clinton Group rocks of western and central New York. Elsewhere in the Appalachian Basin, the Clinton Group occurs in eastcentral and western Pennsylvania, eastern Ohio, and parts of West Virginia and Tennessee (COSUNA Chart, 1985).

The Clinton Group of New York consists of a very diverse group of rock units with many lithologies and many hiatuses (fig. 9.1). Most of the lower units are thin with limited lateral extent. Well known among these are the so called "Clinton Ironstones" (Furnaceville, Sterling Station and Wolcott Furnace in fig. 9.1) consisting of oolitic hematite. Sandstones, shales, limestones and conglomerates are the other lithologies found in the lower Clinton.

A considerable stratigraphic break exists between the lower and upper Clinton Group rocks in the area between Niagara Falls and Sodus Bay whereas farther east, deposition was more continuous (fig. 9.1). The stratigraphy of the upper Clinton Group is also more complex in the east. Two more hematitic ironstone units (Westmoreland and Kirkland) occur above the Sauquoit-Otsquago formations. The Kirkland Formation is unconformably overlain by the Herkimer and Jordanville sandstones. The latter two are equivalent to the Rochester Shale in the west. The Rochester Shale is capped by the Decew and Gates dolostones between Niagara Falls and Sodus Bay. Farther east, the

Figure 9.1: The outcrop belt (in black) and stratigraphic relationships of the Clinton Group in New York. (Adapted from Rickard, 1975).

MIDDLE SILURIAN
NIAGARAN
CLINTON GROUP
EPOCH
SERIES
ROCK UNIT
- Niagara Falls
- Rochester
- Sodus Bay
- Syracuse
- Utica
THOROLD SS.
NEAHGA SH.
HICKORY CORNER LS.
REYNALES LS.
APPLEWOOD SH.
MEDINA GROUP
ROCHAY DOL.
IRONDEQUOIT LS.
ROCHESTER SHALE
DECEW DOL.
GATES DOL.
LOCKPORT GROUP
WILLIAMSON SH.
IRONDEQUOIT LS.+SH.
ROCHESTER SHALE
RODAC SS.
WALLINGTON LS.
BEAR CREEK SH.
STERLING STATION
FURNACEVILLE MEM.
SODUS SH.
WOLCOTT LS.
ONEIDA CONGL.
WOLCOTT FURNACE MEM.
SAUQUOIT SH. +SS.
OTSQUAGO SS.
WILLOWVILLE SH.
WESTMORELAND MEM.
DAVES DOL.
HERKIMER SS.
CLERELAND MEM.
JORDANVILLE SS.
NIAGARA FALLS
ROCHESTER
SYRACUSE
UTICA
80 kms.
Adirondacks

Lockport Group overlies the Rochester Shale and the Herkimer-Jordanville sandstones (fig. 9.1).

Following the deposition and reworking of the deltaic sediments of the early Silurian Medina Group, the Silurian shoreline gradually advanced as far east as Oneida County (Broughton et al. 1966). The Silurian sea was relatively shallow and fluctuated from well-oxygenated to anoxic conditions probably because of frequent changes in sea level. In this sea, the faunally and lithologically diverse sediments of the lower Clinton Group were deposited (Fakundiny et al. 1989; Isachsen et al. 1991).

The Irondequoit Limestone, with its algal and bryozoan patch reefs, trilobites and a large variety of brachiopods indicate a return to "normal" open marine conditions following the restricted, anaerobic conditions in which the underlying Willimson black shales had formed (Broughton et al. 1966). The sea deepened and spread eastward during the deposition of the Rochester Formation, a shale interbedded with limestones and calcareous shales. The open marine depositional environment of the Rochester Shale is attested by the presence of more than 200 species of fossils (Broughton et al. 1966). The northwestern shore of the Rochester sea probably coincided with the trend of the Algonquin Arch in Ontario (fig. 2.1) where the crinoidal bank - biohermal facies of the Rochester Formation was dominant (Brett, 1982; Tankard, 1986). The carbonate platform gently sloped southeastward and the depositional facies changed successively into bryozoan patch reefs, argillaceous limestones, and calcisiltite-rich shale (Brett, 1982). The southeastern shoreline of the Rochester sea is represented by the beach deposits of the Herkimer Sandstones (fig. 9.1). The sea during the Clinton interval, thus, appears to have been a narrow, northeast-southwest trending seaway. The maximum depth of the seaway was probably only about 50m (Brett, 1982).

9.2: SAMPLING LOCATIONS:

The Clinton samples were collected only from two locations (fig. 9.2). These are core samples obtained from the drilling operation of the Supercollider study project.

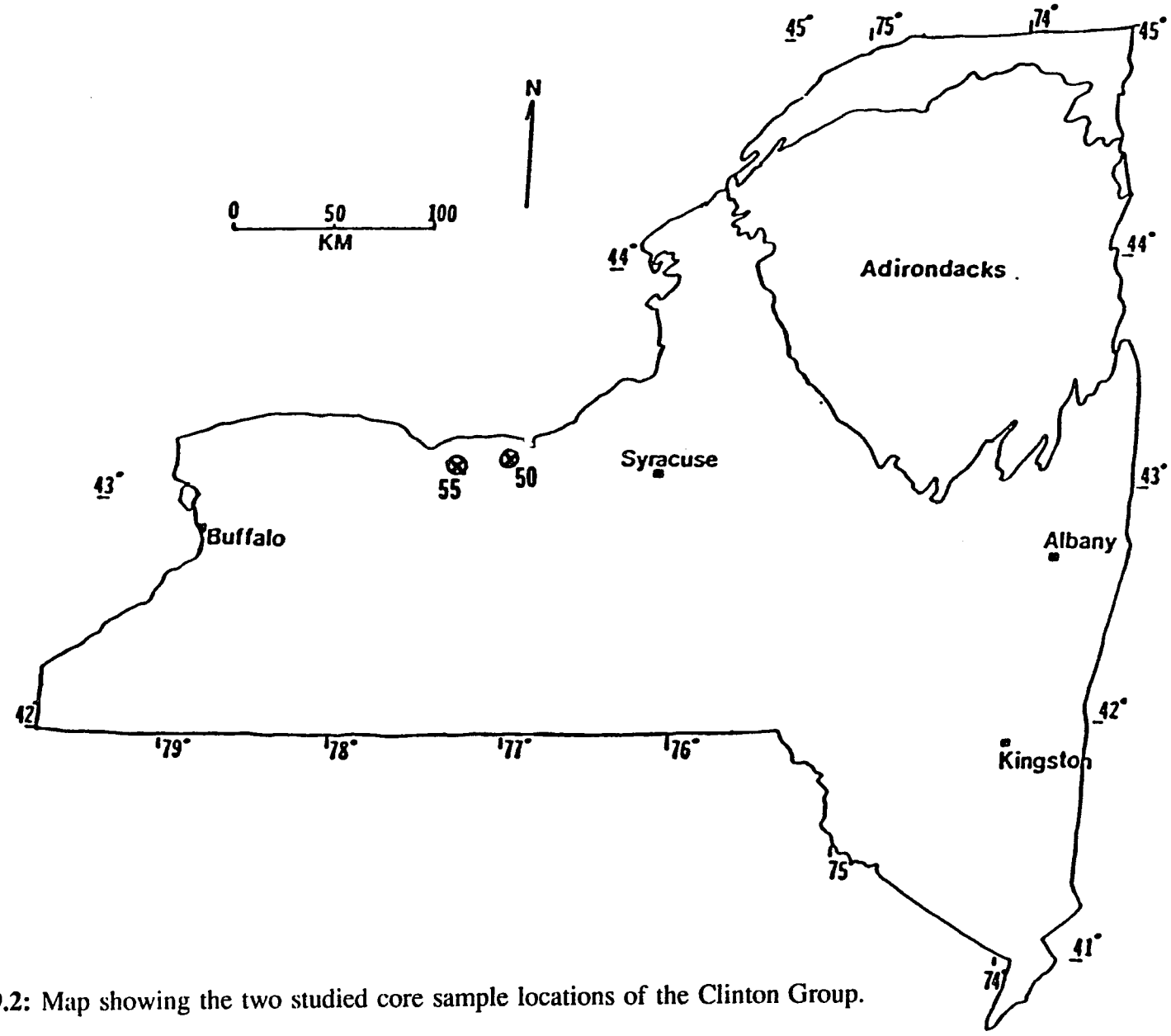

Figure 9.2: Map showing the two studied core sample locations of the Clinton Group.

9.3: GENERAL PETROGRAPHY OF THE SAMPLES:

Samples of location 50 are from the Rochester Shale and they range from skeletal wackestone to grainstone in depositional fabric. Many coral chambers and bryozoan zooecia are filled or partially filled by granular quartz. The chamber walls are generally lined with relatively small "dogtooth" calcite spar which are followed by fibrous chalcedony or clear megaquartz (fig. 9.3a). In many coral chambers, coarse spary calcite succeeds quartz and fills the innermost space (fig. 9.3b). Interparticle cements are sparry calcites, part of which has grown as syntaxial overgrowths on echinoderm fragments (fig. 9.4a).

At location #55, the samples are from the Renayles Formation (fig. 9.1) and consist of dolostones with a packstone-grainstone depositional fabric. The fine grained skeletal matrix has been replaced by fine, rhombic dolomite while the large skeletal particles, such as bivalve and brachiopod shells, have often been partially replaced by quartz along with large rhombic dolomite (fig. 9.4b).

9.4: FLUID-INCLUSION DATA:

Fluid-homogenization (Th) histograms and Th_{max} for samples of locations #50 and #55 are shown in figure 9.5. At location #50, the inclusions were measured in both granular megaquartz inside coral cavities and in intra- and inter-particle calcite spars. No measureable two-phase inclusion was found in the "dogtooth" calcite spar that line the coral cavities (fig. 9.3). At location #55, the inclusions were measured in megaquartz replacing brachiopod and bivalve shells (fig. 9.4b).

Only one melting temperature (Tm) could be measured from samples of the Clinton Group. The Tm, measured in quartz cement of location #55, is -17.4° C.

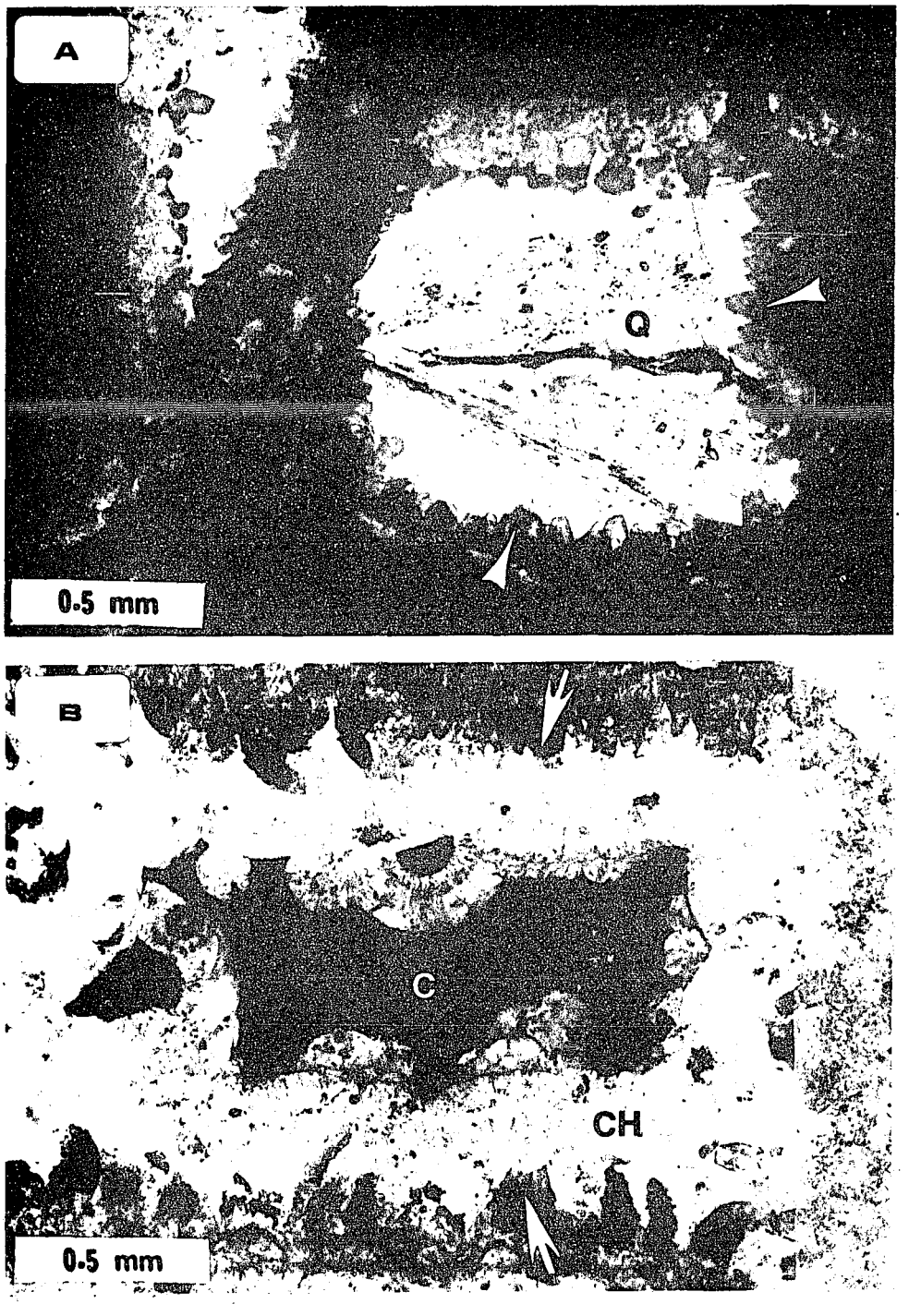

Figure: 9.3: Photomicrographs showing (A) coral cavities lined with "dogtooth" calcite spar (marked by arrows) and filled with megaquartz (Q), and (B) a coral cavity lined with dogtooth spar (marked by arrows), followed by fibrous chalcedony (CH) and finally by coarse sparry calcite (SC). The calcite appears dark because of staining. Both samples are from location #50.

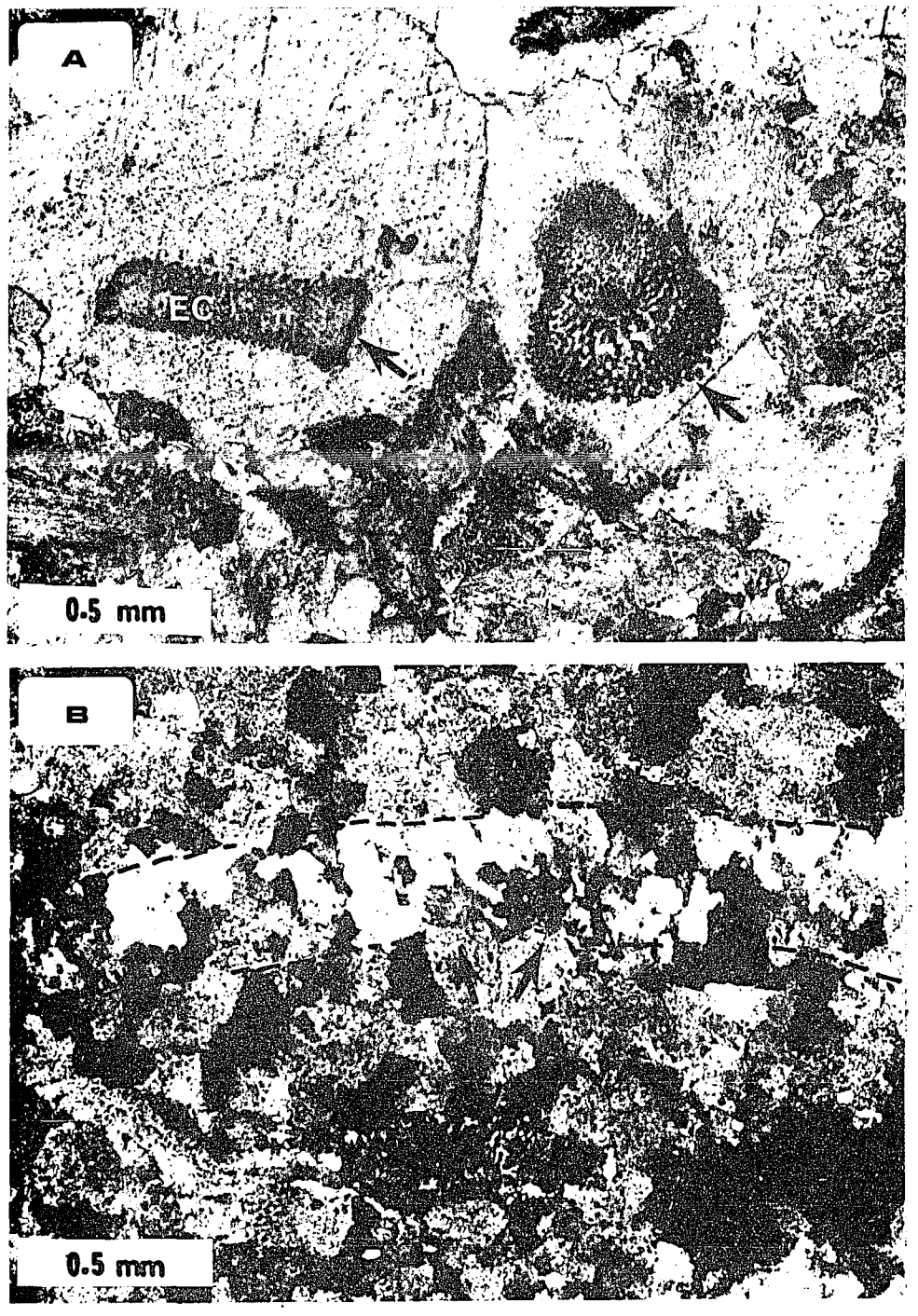

Figure 9.4: Photomicrographs showing (A) interparticle sparry calcite cement including syntaxial overgrowths on echinoderm fragments (marked by arrows) in a sample of location #50, and (B) silicified bivalve shell (within dashed lines) in the dolostone of location #55. Note the two dolomite rhombs of the matrix rock (marked by arrows) penetrating the shell. See text for explanation.

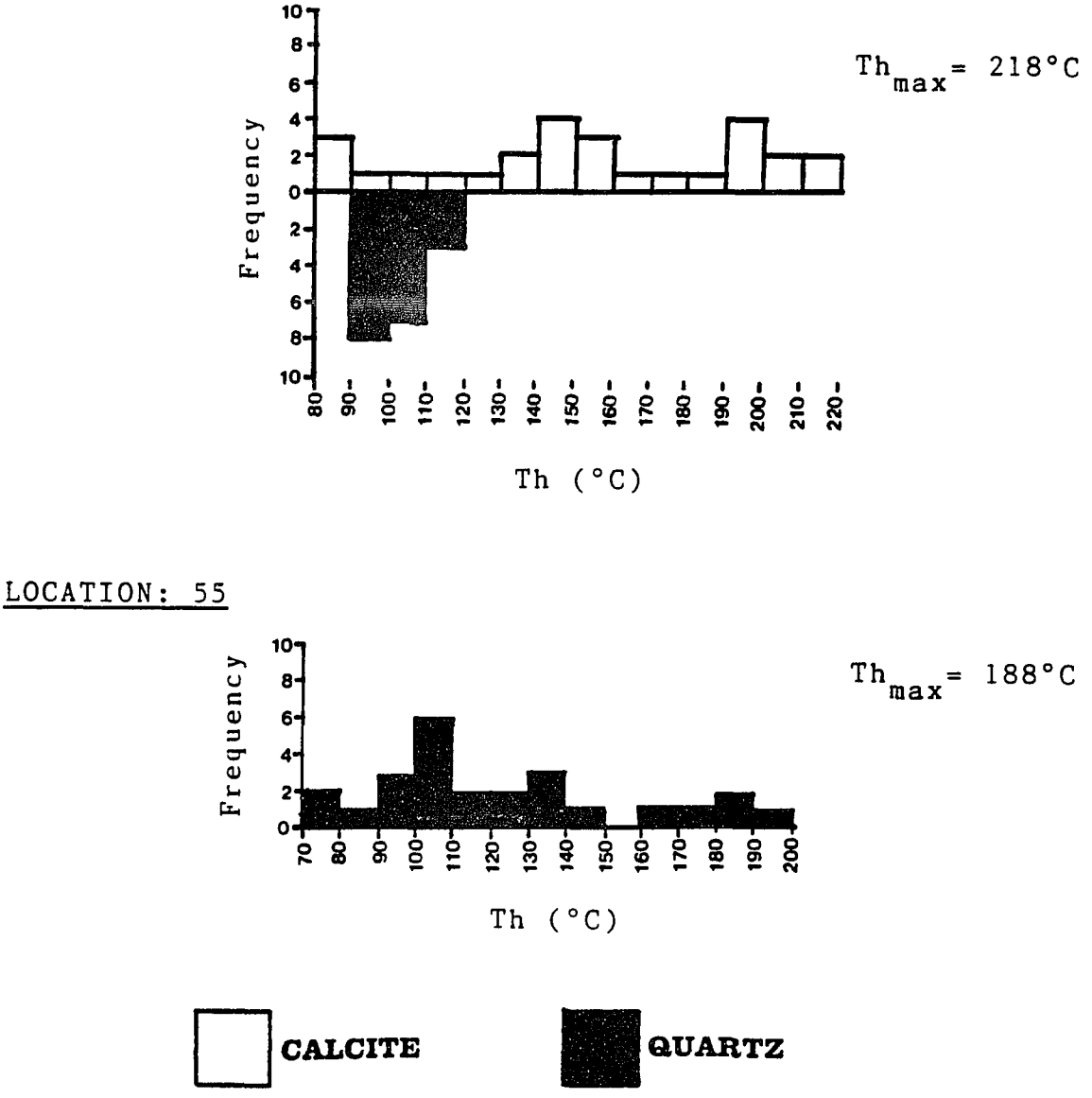

Figure 9.5: Fluid-homogenization (Th) histograms of samples from the two locations of the Clinton Group. The maximum homogenization temperatures (TH_{max}) are also shown.

9.5: INTERPRETATION:

9.5.1: Paragenetic sequence of cements:

Petrographic relationships suggest that in location #50, precipitation of the small "dogtooth" calcite spar along cavity walls of corals was followed by precipitation of quartz and finally by coarse sparry calcite. The inter-granular calcite cement, much of which are syntaxial overgrowths on echinoderm fragments, probably began to precipitate at about the same time as or even earlier than quartz and continued to precipitate alongside the latest calcite spar inside coral cavities. Although petrographic relationships are not clear enough to draw this conclusion, this is suggested by Th data (section 9.5.2).

At location #55, silicification occurred selectively in skeletal components, especially in calcitic bivalve shells. According to Maliva and Siever (1988), silicifica- tion of calcitic fossils occurs along thin solution films in which calcite dissolves and silica precipitates. The studied samples of location #55 are now completely dolomitized except for the silicified fossil fragments. It is difficult to determine when dolomitization had begun relative to silicification in these rocks, but from the observation that the silicified shells have been penetrated by dolomite rhombs of the matrix rock (fig. 9.4b), it can be inferred that dolomitization had continued after silicification.

9.5.2: Fluid-inclusion data:

At location #50, Th in quartz that precipitated inside coral chambers has a narrow range, between 90° C and 120° C (fig. 9.5). On the other hand, calcite cement shows a much wider spread of Th, between 80° C and 220° C. This large range probably represents different types and generations of calcite cements in location #50. Most of the high Th values measured in samples of this location are from the latest calcite inside coral chambers while most of the low Th values are from interparticle, echinoderm-syntaxial calcite. However, the latest calcite of coral chambers do contain few inclusions with low Th, and the intergranular calcite contains few inclusions with high Th. This observation suggests that both types consist of different generations of cements that precipitated under different temperature regimes, but while much of the cementation

in intergranular spaces took place at a relatively lower temperature, that in coral chambers took place at higher temperatures.

At location #55, the Th in quartz replacing bivalve shells range between 70° C and 200° C, suggesting that replacement of calcite by quartz took place over a large temperature interval. This range is considerably different from the narrow range of Th in quartz of location #50, but similar to that of calcite (fig. 9.5). One measured Tm of -17.4° C in quartz of location #50 indicates a salinity of 18.5 wt% NaCl of the inclusion fluid.

In chapter 16, the Th_{max} of the Clinton Group at locations 50 and 55 are compared with paleotemperatures of other Silurian and Devonian rock units.

CHAPTER 10: THE LOCKPORT GROUP

10.1: STRATIGRAPHY AND DEPOSITIONAL HISTORY:

The Middle Silurian (late Niagaran) Lockport Group dolostones are exposed along the Silurian outcrop belt in the western half of New York (fig. 10.1). These rocks represent the eastern extension of thicker Niagaran carbonates of the cratonic interior basins of Illinois and Indiana (Zenger, 1965). The Lockport Group is about 60m thick in the Niagara Falls area from where it gradually thins eastward and pinches out near Ilion in east central New York (fig. 10.1). In the subsurface of west central and western New York its thickness pattern matches that of the surface exposures. Within the Appalachian Basin, the Lockport and equivalent carbonates occur in the western half of Pennsylvania, eastern parts of Ohio, West Virginia and eastern Kentucky (COSUNA Chart, 1985).

The Lockport Group in New York generally consists of dolostones and minor limestones with intraclasts, ooids, peloids and skeletal components comprising corals, echinoderms, mollusks, brachiopods, stromatolites, stromatoporoids, bryozoans and trilobites (Zenger, 1965; Shukla and Friedman, 1983). Secondary minerals, such as saddle dolomite, fluorite, sphalerite and galena are locally common in vugs and fractures (Kinsland, 1977; Friedman, 1987a,b, 1989). Stylolites and pressure solutions are especially abundant in the west (Gross and Engelder, 1989).

In the Niagara Falls area, the Lockport Group is subdivided into four formations (fig. 10.1). These are, in ascending order, the Gasport, Goat Island, Eramosa and Oak Orchard formations. In older publications (for example, Zenger, 1965), the basal Decew dolostone is considered a unit of the "Lockport Formation", but Fisher (1977) includes it within the underlying Clinton Group.

The Gasport Formation is a coarse-grained dolostone and, locally, a limestone with coral-crinoidal structures that have been interpreted as bioherms and biostromes (Zenger, 1965; Crowley, 1973; Mesolella, 1978). The Goat Island, Eramosa and Oak Orchard formations are finer grained dolostones containing crinoids, stromatolites, and stromatoporoids; but no bioherms (Zenger, 1965). To the west the, the three lower

Figure 10.1: The outcrop belt (inset) and stratigraphic subdivisions of the Lockport Group in New York. The numbers represent geologic quadrangles. (Adapted from Zenger, 1965 and Fisher, 1977).

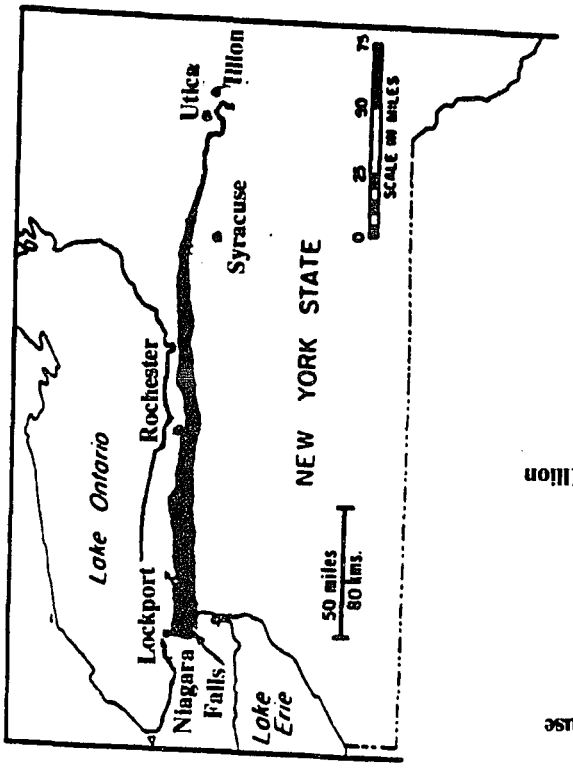
Utica
Tilton
Syracuse
Rochester
Lake Ontario
NEW YORK STATE
Lockport
Niagara Falls
Lake Erie
50 miles
80 kms.
0
25
50
75
SCALE IN MILES

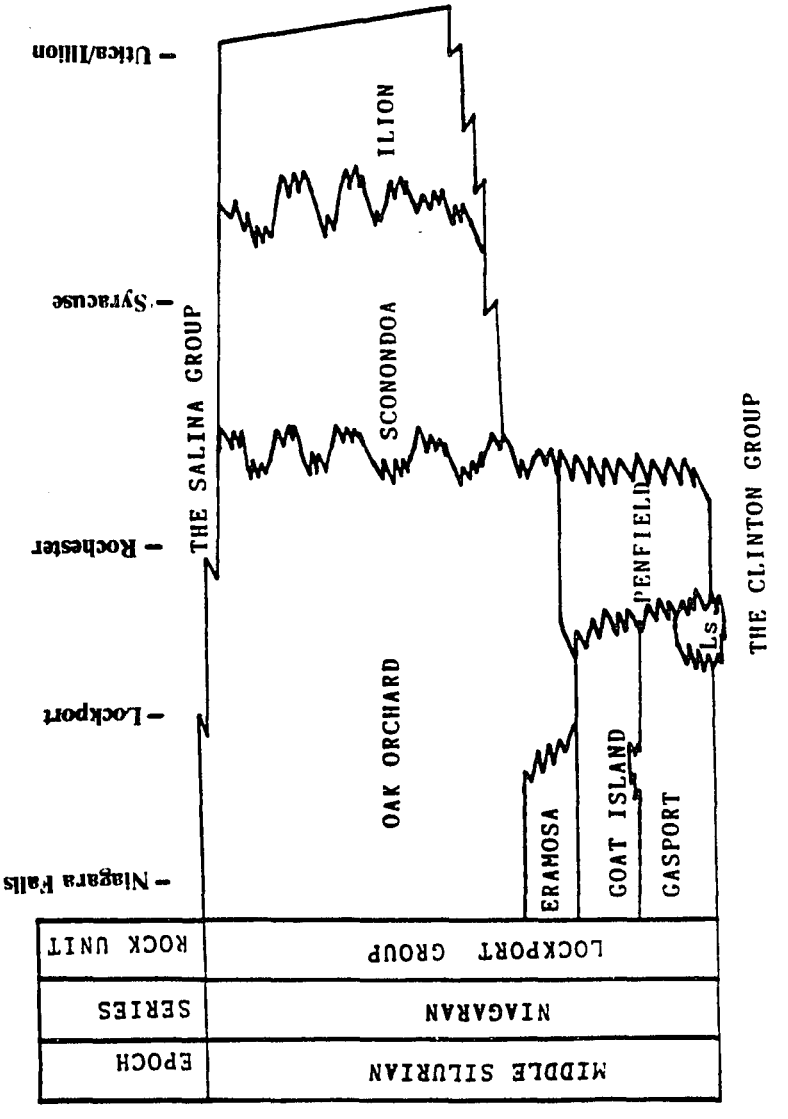
Utica/Tilton
Syracuse
Rochester
Lockport
Niagara Falls
THE SALINA GROUP
ILION
SCONONDOA
OAK ORCHARD
ERAMOSA
GOAT ISLAND
GASPORT
PENFIELD
Ls
THE CLINTON GROUP
LOCKPORT GROUP
NIAGARAN
MIDDLE SILURIAN
ROCK UNIT
SERIES
EPOCH

formations of Lockport grade into the quartz-rich carbonates of the Penfield Formation (fig. 10.1). The Lockport Group between Clyde and Oneida is undifferentiated and is called the Sconondoa Formation. It is sparsely fossiliferous and consists of fine grained limestones and dolostones. In the easternmost exposures, the Lockport Group is represented by the Ilion Formation (fig. 10.1) consisting of shale, dolomitic shale and stromatolitic dolostones. Farther east, it is probably represented by the Herkimer (Clinton Group) - Salina Group disconformity (Zenger, 1965).

The Lockport Group carbonates were deposited in a shallow subtidal to supratidal environment in a warm and shallow sea, probably under evaporitic conditions (Zenger, 1965; Friedman and Shukla, 1980; Shukla and Friedman, 1981, 1983). In the western half of the outcrop belt (fig. 10.1), the Lockport Group represents a shallowing-upwards cycle begining with the coral-crinoidal rocks and bioherms/ biostromes of the Gasport Formation and culminating in the stromatolite-bearing rocks of the upper Oak Orchard Formation (Shukla and Friedman, 1983). The facies change toward the east into stromatolitic dolomicrite and gypsiferous and dolomitic shale with sparse or no fossils and increasing quartz content (Zenger, 1965, Challapalli, 1989) probably indicate the presence of a sabkha-type environment in the east. However, shoreline deposits of this age have not been positively recognized in New York (Fakundiny et al. 1989). The presence of an abundant and diverse marine fauna, coarse-grained fabric, and bioherms in the lower Lockport Group of western New York and thickening of this facies toward the continental interior (Zenger, 1965) probably indicate the presence of more open marine conditions and deeper waters to the west and northwest. However, the presence of supratidal-facies rocks at the top of the Lockport Group in the western outcrops (Zenger, 1965; Shukla and Friedman, 1983) and the upward transition of the Lockport into the Salina Group suggest that between the Niagaran and Cayugan time the sea gradually withdrew from this area and moved farther west.

10.2: SAMPLING LOCATIONS:

Figure 10.2 shows the sampling locations of the Lockport Group. Samples from locations 51, 52 and 54 are samples cored by the Supercollider study project. Samples

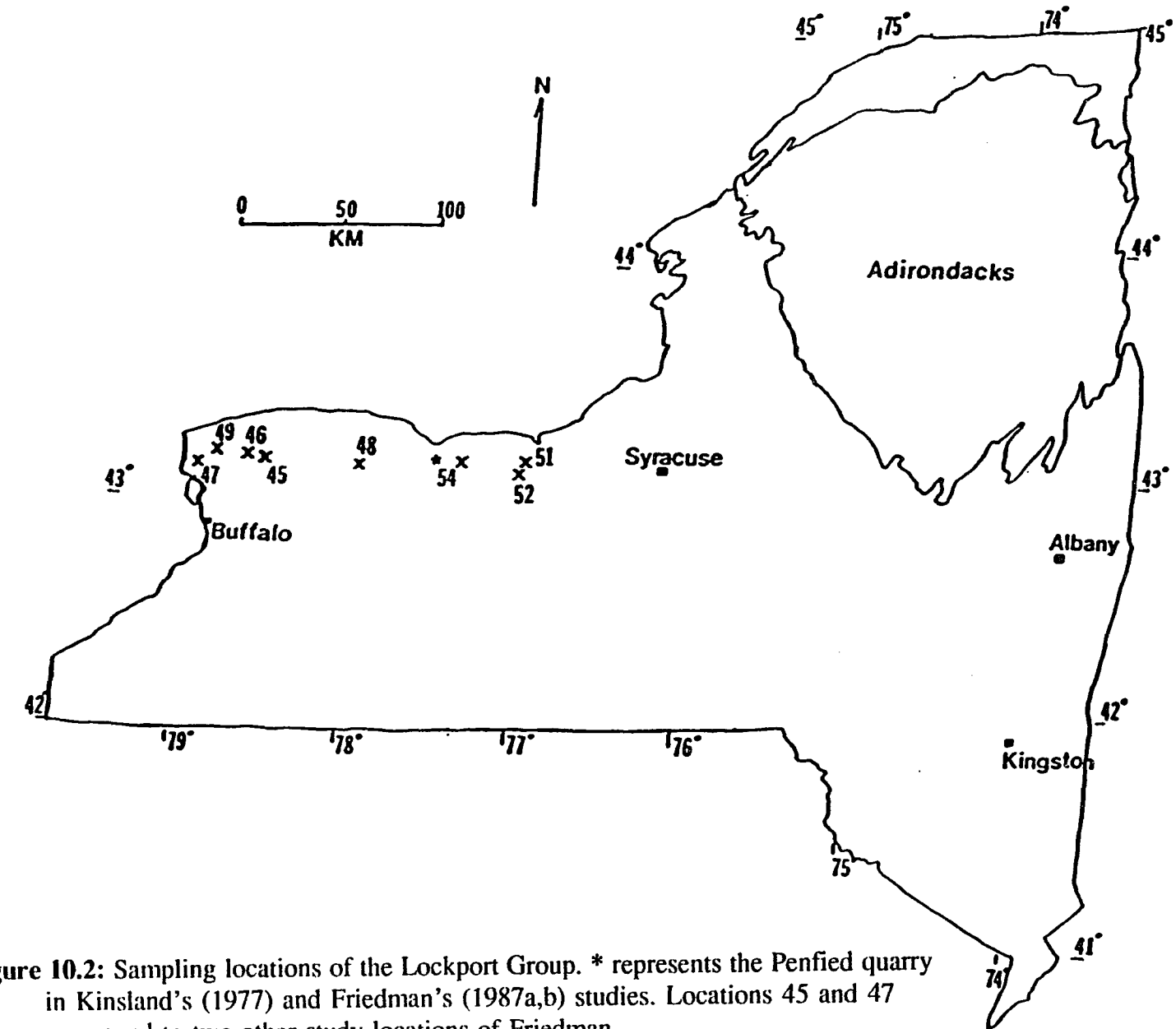

Figure 10.2: Sampling locations of the Lockport Group. * represents the Penfied quarry in Kinsland's (1977) and Friedman's (1987a,b) studies. Locations 45 and 47 corrspond to two other study locations of Friedman.

from location-49 are also core samples, but these were obtained from shallow drilling operation by the Department of Transportation, New York. The rest of the Lockport samples in this study were collected from outcrops.

10.3: GENERAL PETROGRAPHY OF THE SAMPLES:

Most of the Lockport samples collected for this study are dolostones with grainstone to packstone depositional fabric and vugs and veins filled with secondary minerals. A number of core samples of a different lithology were collected from locations - 51, 52 and 54. These samples are from the Sconondoa Formation and consist of laminated and algal-laminated dolomicrites with partings and vugs filled with gypsum. Rarely, very thin fractures filled with calcite were found.

All the samples between location 48 and 47 (fig. 10.2) are from the Gasport Formation. Most of these samples are medium-grained dolostones with grainstone or packstone fabrics. Where the original sediments were micrites, as indicated by the presence of relic textures, the dolomite is present in the form of fine rhombs. In small vugs and patches without obvious boundaries, an inward gradation from relatively large rhombs to dolomite with non-planar boundaries, finally to saddle dolomite is frequently observed (fig. 10.3a). This change in dolomite crystal form is commonly accompanied by an increase in crystal size. In some samples, dolomitization is incomplete and calcitic skeletal components and interpartcile as well as intraparticle and crinoid-syntaxial sparry calcite cements are locally preserved (fig. 10.3b). At location 48, coral cavities partially or completely filled with micro- and megaquartz are observed. In some coral chambers quartz coexists with saddle dolomite. The saddle dolomite generally occupies a central position in these chambers (fig. 10.4a).

Most characteristic of the Lockport samples, especially of those from between locations 45 and 47 (fig. 10.2), is the occurrence of vug- and vein-filling saddle dolomite. The veins are as wide as 8cm while the vugs range from a few mm to 7cm in diameter (fig. 10.4b). In veins and completely filled vugs, the saddle dolomite is generally sparkling white and coarse sucrosic. In incompletely filled vugs, the saddle dolomite crystals that line the vug walls are milky white to yellowish white and generally

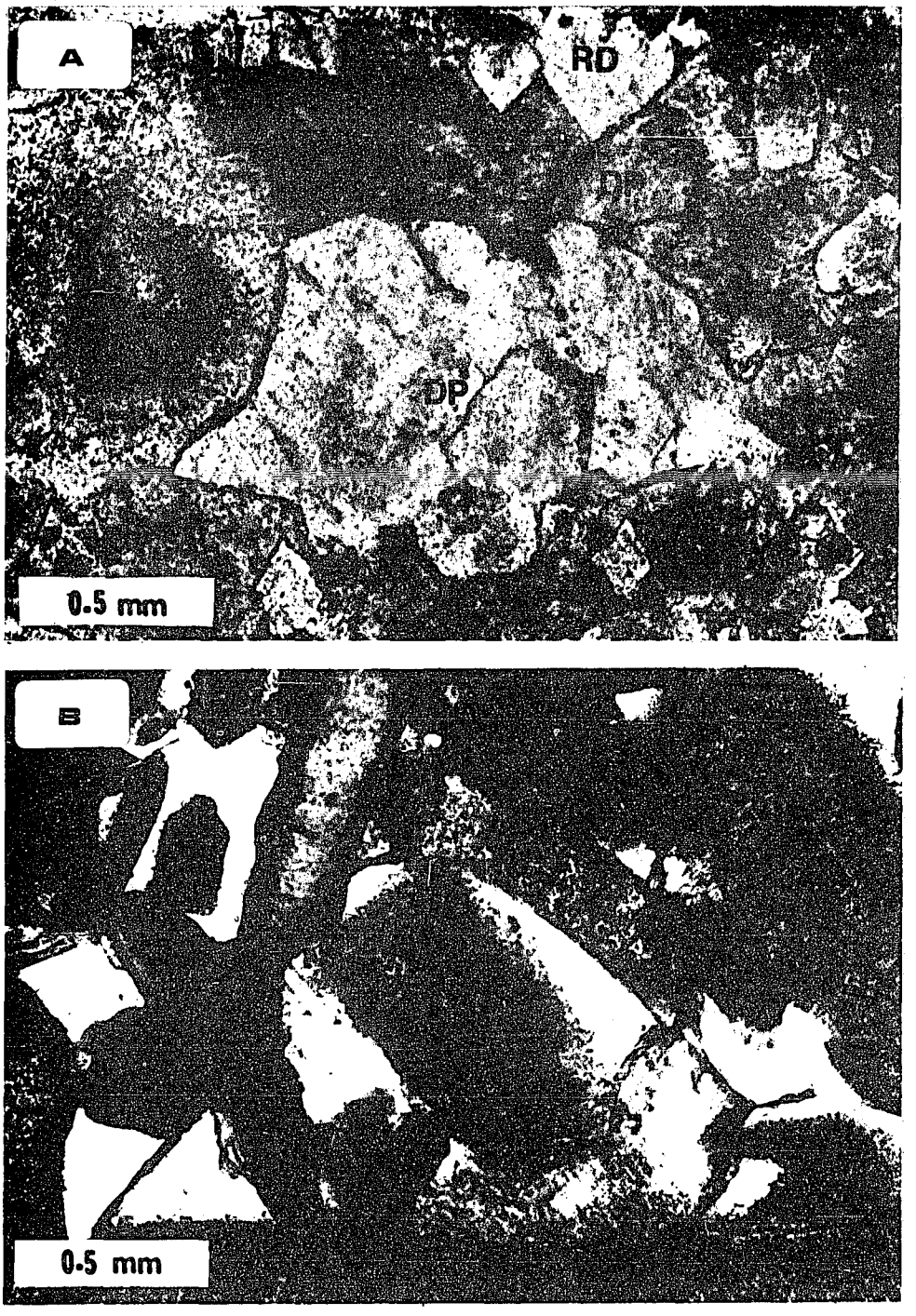

Figure 10.3: Photomicrographs of samples from the Lockport Group: (A) A vug in dolostone lined with rhombic dolomite (RD), which is followed by dolomite with planar boundaries (DP) and finally by dolomite with non-planar boundaries (DN) toward the center of the vug. From location - 45. (B) Crinoidal grainstone with original calcitic componenets (crinoidal particles and syntaxial cement) preserved in the dolostone of location - 46.

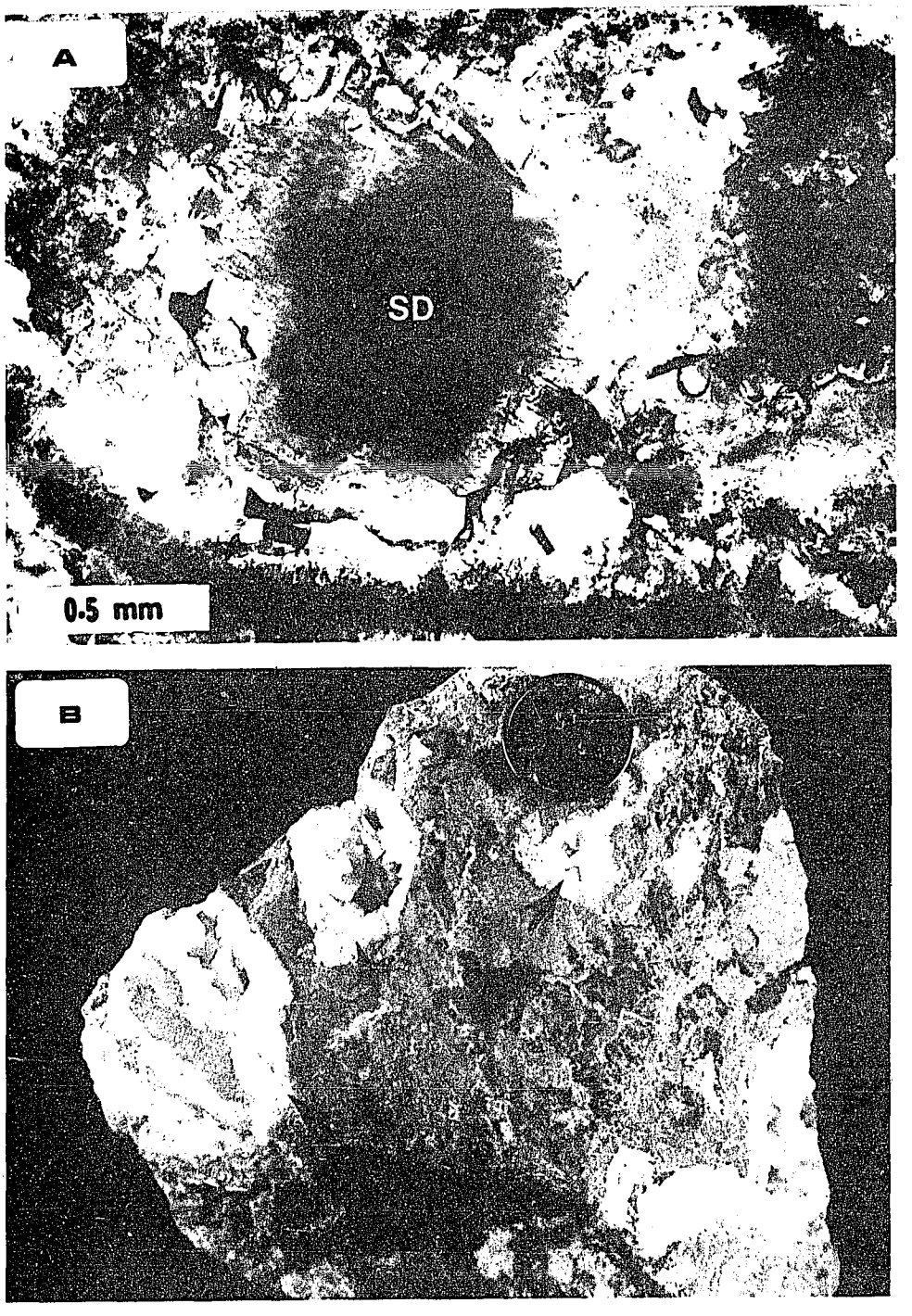

Figure 10.4: Samples of the Lockport Group. (A) Photomicrograph showing a coral chamber lined with fibrous chalcedony, followed by saddle dolomite (SD) toward the center of the chamber. The dissolution boundary between quartz and saddle dolomite is marked by arrows. From location - 48. (B) Hand sample from location -45 showing vugs (marked by arrows) partially or completely filled with milky white saddle dolomite crystals. Penny for scale.

much coarser than those in the sucrosic variety. In thin sections, saddle dolomite crystals show characteristic curved faces and sweeping extinctions (fig. 10.5).

Occurrence of sphalerite, fluorite and galena in vugs and fractures of the Lockport Group was first described by Robinson (1825). Recent studies describing them include those by Kinsland (1977), Shukla and Friedman (1983), and Friedman (1987a,b, 1989). These minerals were, however, not found in the samples collected for this study.

10.4: FLUID-INCLUSION DATA:

Figure 10.6 shows the fluid-homogenization (Th) histograms of the Lockport samples from various locations. The maximum homogenization temperatures (Th_{max}) are also shown. In samples from locations 51, 52 and 54, unfortunately, measureable inclusions were not found. The gypsum in vugs and partings in these samples contains few two-phase inclusions, but when gypsum chips were heated to about 100-120°C, numerous dense microfractures developed and propagated in all directions, and the chips turned yellowish-brown and opaque. Microfracturing of gypsum in these samples was probably due to thermal expansion of water in the gypsum structure. Homogenization of none of the two- phase inclusions was observed through the above amount of heating, suggesting that the Th of the inclusions was greater than 100°C. However, inclusions in soft minerals like gypsum are easily susceptible to stretching and leaking and Th data obtained from gypsym may not be very reliable (Roedder, 1979). At location 48, although quartz cement occurs in some coral chambers, they are devoid of measureable two-phase inclusions. Therefore, inclusions were measured in saddle dolomite except at location 46, where they were measured in calcite cement.

Six 'Tm's measured in the Lockport samples range between -5°C and -32°C, corresponding to a salinity range of 7.8 to 31.2 wt% equivalent NaCl (table-10.1).

Fluid-inclusion temperatures of the Lockport Group carbonates have been measured by other workers (Kinsland, 1977; Friedman, 1987a,b). Kinsland (1977) measured Th of fluorite crystals from the Penfield quarry, just east of Rochester (* in fig. 46), and found a Th range of 132 -142° C. Friedman (1987a,b) measured Th and Tm of saddle dolomite, calcite, fluorite and sphalerite from three locations which corrspond to the location

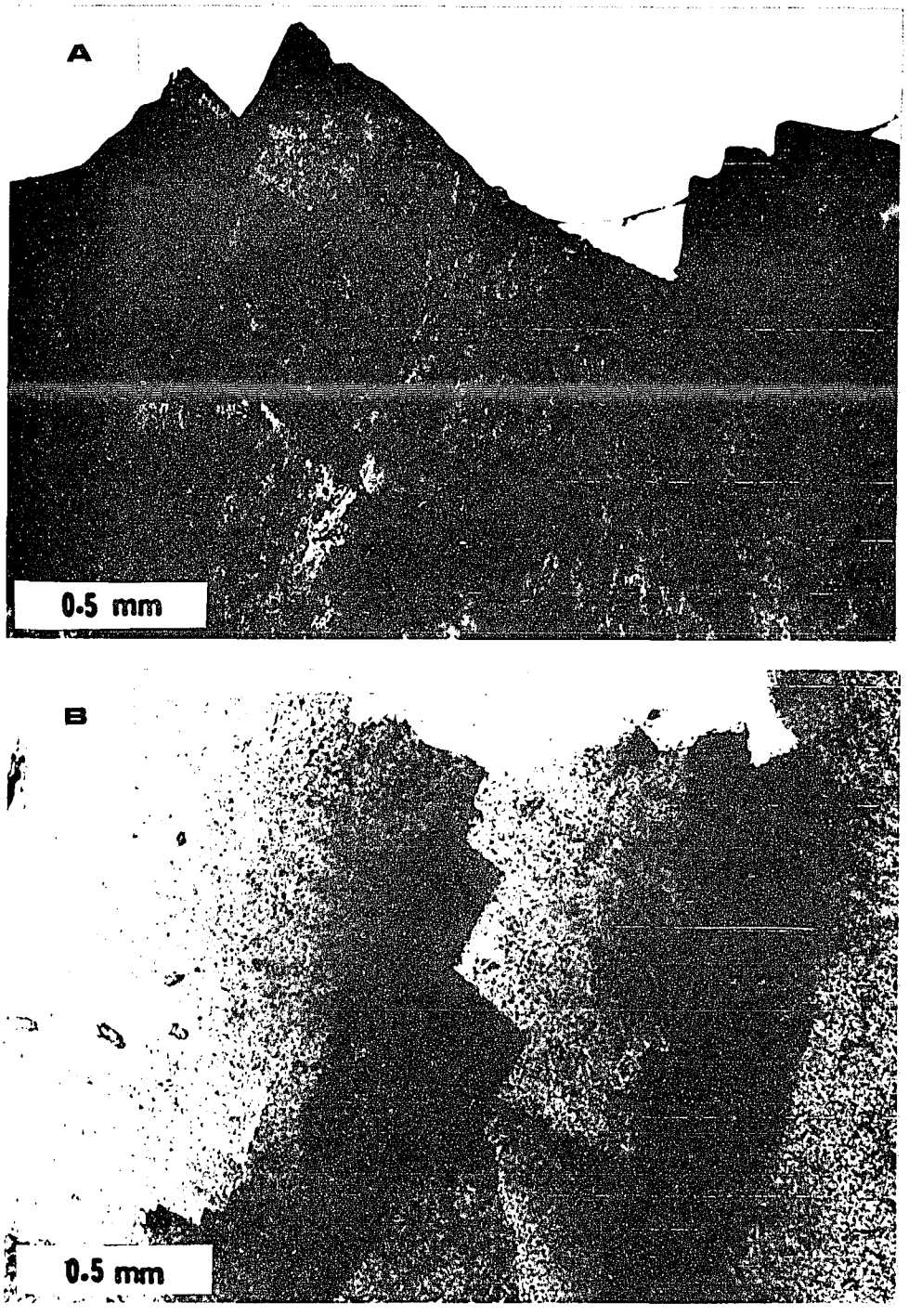

Figure 10.5: Photomicrographs of saddle dolomite from the Lockport Group of location 47 showing (A) curved crystal faces, and (B) sweeping extinction that characterize saddle dolomites.

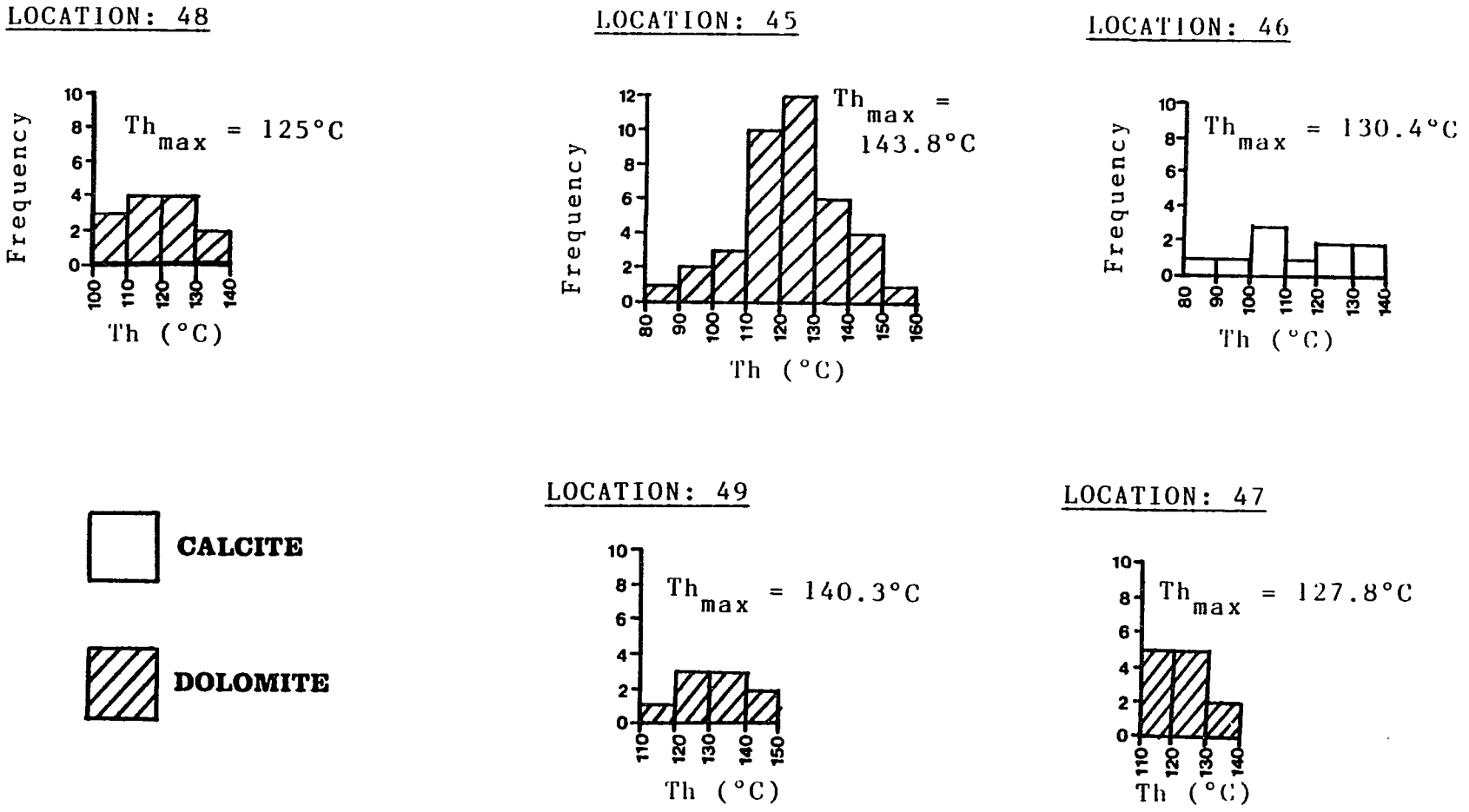

Figure 10.6: Fluid-homogenization temperature (Th) histograms for the Lockport samples from various study locations. The maximum homogenization temperatures (Th_{max}) are also shown.

Table 10.1: Melting temperatures (Tm), corresponding homogenization temperatures (Th), and calculated salinity (wt% equivalent NaCl) of fluid inclusions in cements of the Lockport Group.

Location no.	Type of cement	Tm (°C)	*Salinity (wt% NaCl)	Th (°C)
45	Saddle dolomite	-26.5	26.9	121
	Saddle dolomite	-32.0	30.5	130.4
	Saddle dolomite	-33.0	31.2	83
46	Calcite	-5.4	8.4	117
	Calcite	-20.6	23.0	94
49	Saddle dolomite	-32.0	30.5	143.2

*Salinity was calculated according to Potter et al.'s (1978) method (section 4.3.2).

45, 47 and * of figure- 6. He found a mean Th of ~150° C for saddle dolomite, a range of 80 - 179°C with a cluster at 130 - 140° C for sphalerite, a range of 167 - 177° C for fluorite, and a range of 137 - 139°C for calcite. The Tm in these minerals ranged from -4 to -21°C (6 to 23 wt% equivalent NaCl). The variations in Th and Tm among the three locations, however, were not specified.

10.5: STABLE ISOTOPE DATA:

Three saddle dolomite samples, one each from locations 45, 47 and 48, were analyzed for oxygen and carbon isotope ratios. The isotope data and calculated temperatures of formation are presented in table 10.2. Friedman (1987a) measured O-isotopes of ten saddle dolomite samples of the Lockport from locations 45, 47 and * (fig. 10.2), but isotope data from individual locations were not presented separately. He found a $\delta^{18}O$ range of -9.07 to -11.11‰ PDB (+21.5 to +19.4‰ SMOW) and a calculated temperature range of 101 to 193° C.

Table 10.2: Oxygen and carbon isotope values of three saddle dolomite samples from the Lockport Group and the calculated temperatures of formation.

Location no.	Sample no.	$\delta^{18}O$ (‰ PDB)	$\delta^{13}C$ (‰ PDB)	*Calculated temp. (°C) for $\delta^{18}O_{water}$ = 2-8‰ SMOW
45	LP-1	-7.3	+4.3	98 - 156
47	LP-3	-7.92	+4.5	104 - 163
48	LP-4	-6.85	+4.2	94 - 151

10.6: INTERPRETATION:

10.7.1: Paragenetic sequence of cements:

From petrographic relationships in the studied samples (figs. 47a, 48a), it is clear that the vug- and vein-filling saddle dolomites are the latest cements in the studied samples of the Lockport Group. Even in many incompletely filled vugs, saddle dolomite is the last mineral to precipitate indicating that following precipitation of saddle dolomite no major mineralizing fluid(s) passed through the studied sampling locations. However, in some examples calcite and fluorite have been shown to postdate saddle dolomite (Friedman, 1987a).

In some vugs an inward grading from rhombic dolomite to dolomite with nonplanar boundaries is observed (fig. 10.3a). According to Gregg and Sibley (1984), dolomite with non-planar boundaries (such as these and saddle dolomite) form above a 'critical roughening temperature' (CRT) of at least 50° C. The sequence of dolomite crystal morphology in the above mentioned vugs, thus, probably represent an increase in fluid temperature through the interval of time during which the vugs were filled.

The interparticle sparry calcite cements (fig. 10.3b) probably formed before replacement dolomitization of the host rock and precipitation of saddle dolomite. Calcitic particles and cements are found only in small pockets within samples which are

otherwise completely dolomitized.

10.6.2: Fluid-inclusion data:

Fluid-homogenization temperature (Th) of the saddle dolomite in the studied samples of the Lockport Group ranges beltween 80° and 160° C (fig. 10.6) indicating precipitation of saddle dolomite over a considerable temperature interval. A similar range of precipitation temperature is indicated by calcite cement of location 46 (fig. 10.6).

The 'Th' data of this study is consistent with that of Kinsland (1977), who measured a Th range of 132-142° C in fluorite of the Lockport Group from the Penfield quarry (location * of fig. 46). The data is also within the range of Th reported from calcite, saddle dolomite and sphalerite of locations - 45, 47 and * reported by Friedman (1987a,b). However, Friedman (1987a, b) reports a Th range of 167-177° C in fluorite of these locations, which is considerably higher than the Th measured in fluorite by Kinsland (1977) and in saddle dolomite in this study.

The inclusion fluids of both saddle dolomite and calcite have very high salinities (table 10.1). This data, along with Th, suggests that hot, subsurface brine was involved in the precipitation of these mineral cements.

10.6.3: Stable isotope data:

The paleotemperature range obtained from oxygen-isotope data (table 10.2) assuming a $\delta^{18}O_{water}$ of 2 to 8‰ (SMOW) is consistent with the range of Th obtained from the same locations (fig. 10.6). For example, at location-45 the inferred isotopic paleotemperature range is 98-156° C while the range of Th is 80-160° C; at location-47, isotopic paleotemperatures of 104-163° C correspond to Th range of 104-140° C, and at location-48 these are 94-151° C and 100-140° C, respectively.

In chapter 16, the paleotemperatures of the Lockport Group are discussed in context with those of other Silurian and Devonian rock units.

CHAPTER: 11: THE SALINA GROUP

11.1: STRATIGRAPHY AND DEPOSITIONAL HISTORY:

The Late Silurian (Cayugan) Salina Group in New York is exposed along the Silurian outcrop belt between the Niagara Falls in the west and Schoharie County in the east (fig. 11.1). Eastward from the Niagara Falls area, where it is about 115m thick, the Salina Group thickens to about 300m in the Syracuse area and then thins and pinches out in the Schoharie County (Rickard, 1975). In southeastern New York, the Salina Group is correlative with the shales and sandstones of the uppermost Bloomsburg Formation and the overlying Poxono Island Formation. In the subsurface of New York, the Salina rocks are encountered as far east as the Otsego and Delaware counties (Kreidler et al. 1972). Elsewhere in the Appalachian Basin, the Salina Group occurs in north-central and northwestern Pennsylvania, eastern and central Ohio, parts of West Virginia and in eastern Kentucky (COSUNA Chart, 1985).

In New York, the Salina Group is divided into four formations. These are, in ascending order, the Vernon, Syracuse, Camillus and Bertie (fig. 11.1). The Bertie Formation in further subdivided into three units, namely, the Fiddlers Green, Scajaquada and Williamsville. At the eastern end of the outcrop belt, the Camillus and Bertie formations are undifferentiated and are known as the Brayman Formation (fig. 11.1).

The Vernon Formation consists of red and green shales and dolomitic and gypsiferous shales. The Syracuse Formation comprises gray and green shales, dolomicrite, dolomitic and gypsiferous shales, collapse breccia, and is well known for thick salt accumulation in central New York. The Camillus shale is a varicolored, finely laminated shale containing abundant dolomicrite and argillaceous dolostones (Treesh, 1972). The Bertie Formation consists primarily of dolomicrite with local limestone beds and lenses, and dolomitic shales, argillaceous dolostones and gypsiferous dolostones (Hamell and Ciurca, 1986). The Bertie Group is especially well known for its Eurypterid fauna. The Brayman Formation in the east is a dark, pyritic shale.

The arid conditions that began toward the end of the Lockport deposition in New

Figure 11.1: Outcrop belt (in black) and stratigraphic relationships of the Salina Group in New York. (Adapted from Rickard, 1975).

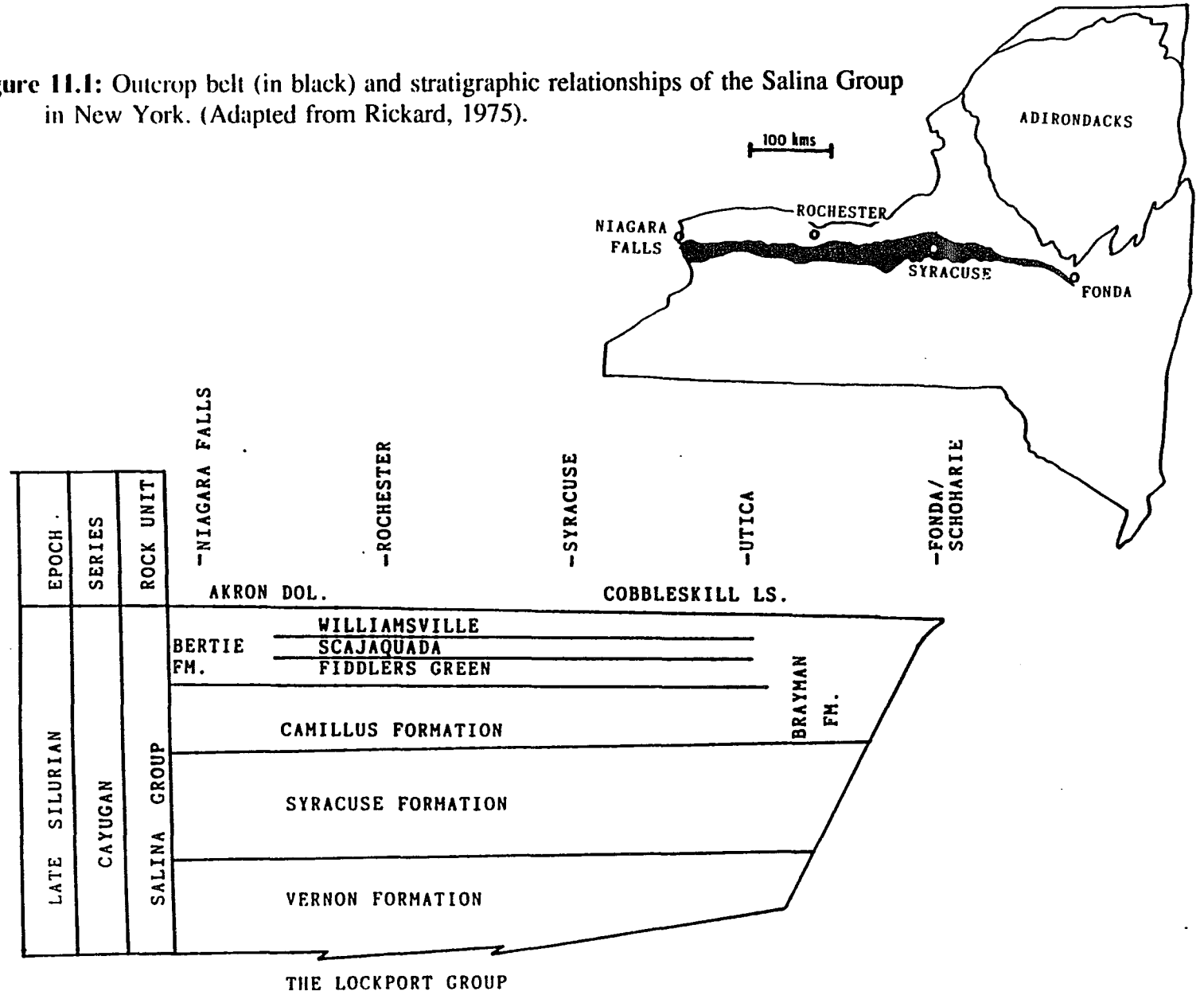

York became pervasive during Cayugan time, resulting in the deposition of the Salina Group. Much of New York and the central Appalachian was probably a vast sabkha-type coastal plain dotted with highly saline embayments and lagoons, many of which periodically became completely landlocked (Broughton et al. 1966). Deposition in each formation took place in a variety of sub-environments including sabkha, hypersaline lakes, intertidal, restricted and non-restricted subtidal, semi-restricted lagoons and estuary etc. (Treesh and Friedman, 1974; Hamell and Ciurca, 1986). Whenever evaporation exceeded inflow of water, thick evaporite deposits, such as the halite salts of the Syracuse Formation and the gypsum beds of the Bertie Formation, formed in hypersaline lakes and lagoons. Fossils in the Salina Group are rare, except for stromatolites, and consist mainly of high salinity- tolerant eurypterids and ostracodes. Presence of these non-algal fossils and absence of the ubiquitous mudcracks characterize the limited open subtidal-to-intertidal environments of deposition within the Salina Group.

11.2: SAMPLING LOCATIONS:

Figure 11.2 shows the sampling locations of the Salina Group. Samples from locations 51, 52 and 53 are core samples drilled by the Supercollider study project. Core samples from locations 56 and 57 were drilled by the Department of Transportation, New York. The only outcrop samples are from locations 58 and 59.

11.3: GENERAL PETROGRAPHY OF THE SAMPLES:

Most of the samples collected from the Salina Group are dolomicrites and dolomitic shales with gypsum-, dolomite- and quartz-filled vugs. At location 59 (fig.11.2), samples from the Camillus Formation contain white saddle dolomite and gypsum. Samples collected from locations 56, 57 and 58 are from the Vernon, Syracuse and Bertie formations, respectively. They contain spherical to irregular vugs filled or partially filled by gypsum, saddle dolomite and quartz, but vugs filled with more than one of the above, if they exist, were not found in the samples collected. The gypsum was either of the clear, selenite variety or of the more common, yellowish white type consisting of

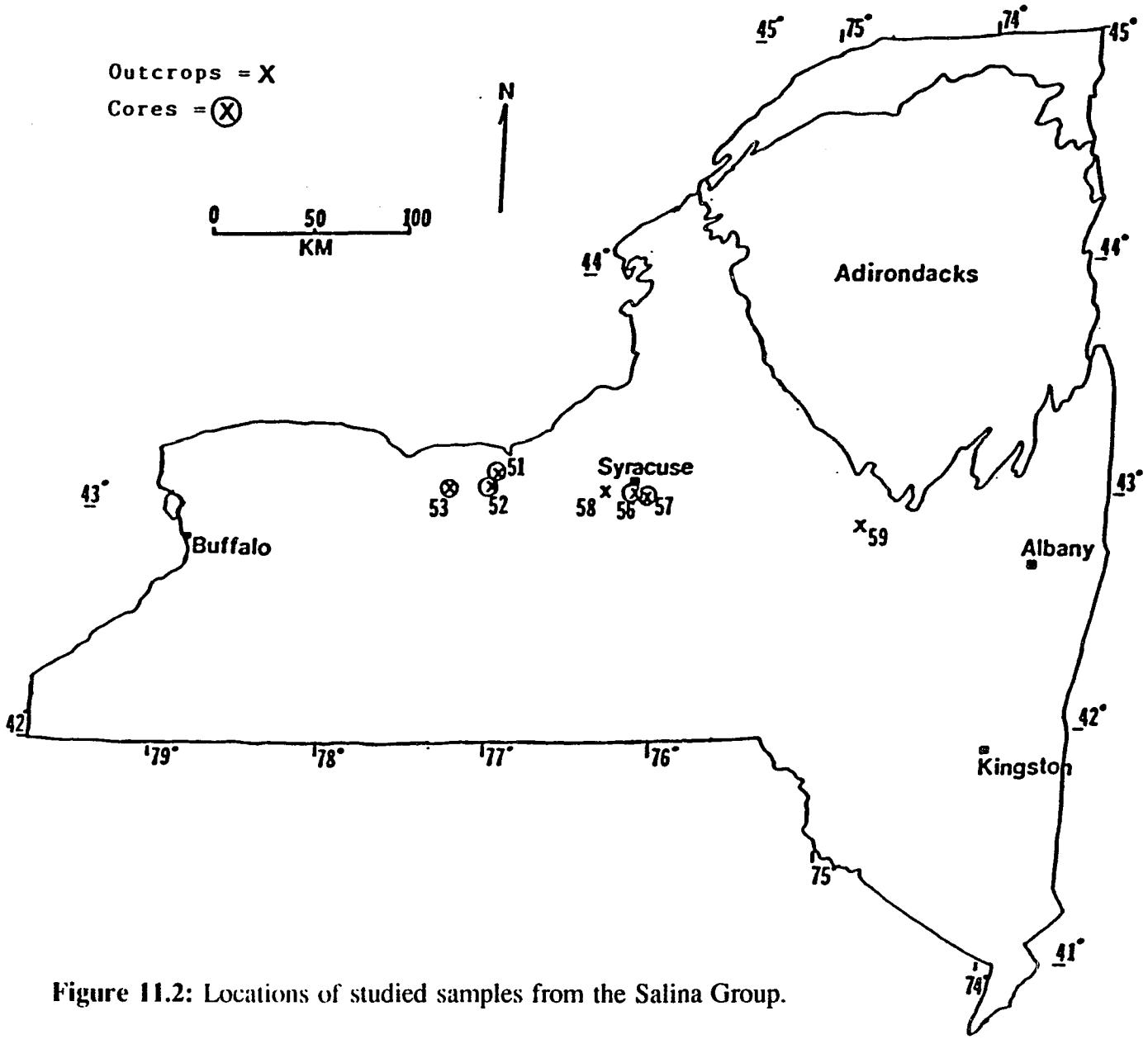

Figure 11.2: Locations of studied samples from the Salina Group.

smaller lath-shaped crystals. Quartz-filled vugs were few and found only in samples from location 57 (fig. 11.3a). The quartz crystals in completely filled vugs are anhedral and subhedral micro- to megaquartz, whereas in some incompletely filled vugs, prismatic quartz crystals with euhedral terminations are found. In locations 51, 52 and 53, the dolomicrite samples were collected from the Vernon Formation, and they contain thin gypsum partings as well as gypsum-filled vugs (fig. 11.3b).

11.4: FLUID-INCLUSION DATA:

Although the Salina Group samples were collected from a number of locations (fig. 11.2), reliable two-phase inclusions were found in samples of only two locations, 57 and 58. In location 56, clear selenite crystals contained a large number of one-phase (fig. 11.4a) and a few two-phase aqueous inclusions. But, when selenite chips were heated to about 120° C, they quickly turned powdery white and opaque making it impossible to study the homogenization temperatures of the two-phase inclusions. Also, between 120° and 130° C, massive leakage of fluids along cleavage planes was observed. The numerous one-phase inclusions were probably the main source of the leaked fluid. Few two-phase inclusions homogenized between 90° and 120° C, but others could not be measured because the chips turned opaque. The same is true for the gypsum samples of locations 51, 52 and 53; not a single inclusion could be measured in samples from these locations.

At location 59, although the samples contained saddle dolomite, the saddle dolomite only showed numerous very small (less than 2 micron in diameter) inclusions, too small to study. The saddle dolomite in samples of location 58 and the authigenic quartz in samples of location 57 yielded sufficient two-phase inclusions for homogenization measurements. Th-histograms for these two locations are shown in figure 11.5. The detailed fluid-inclusion data are presented in Appendix -G.

11.5: ORGANIC MATURATION DATA:

One sample of dark, dolomitic shale from location 58 was analyzed for organic maturation. The vitrinite reflectance (Ro) histogram is shown in figure 11.6. The sample has a mean Ro (%) of 0.97.

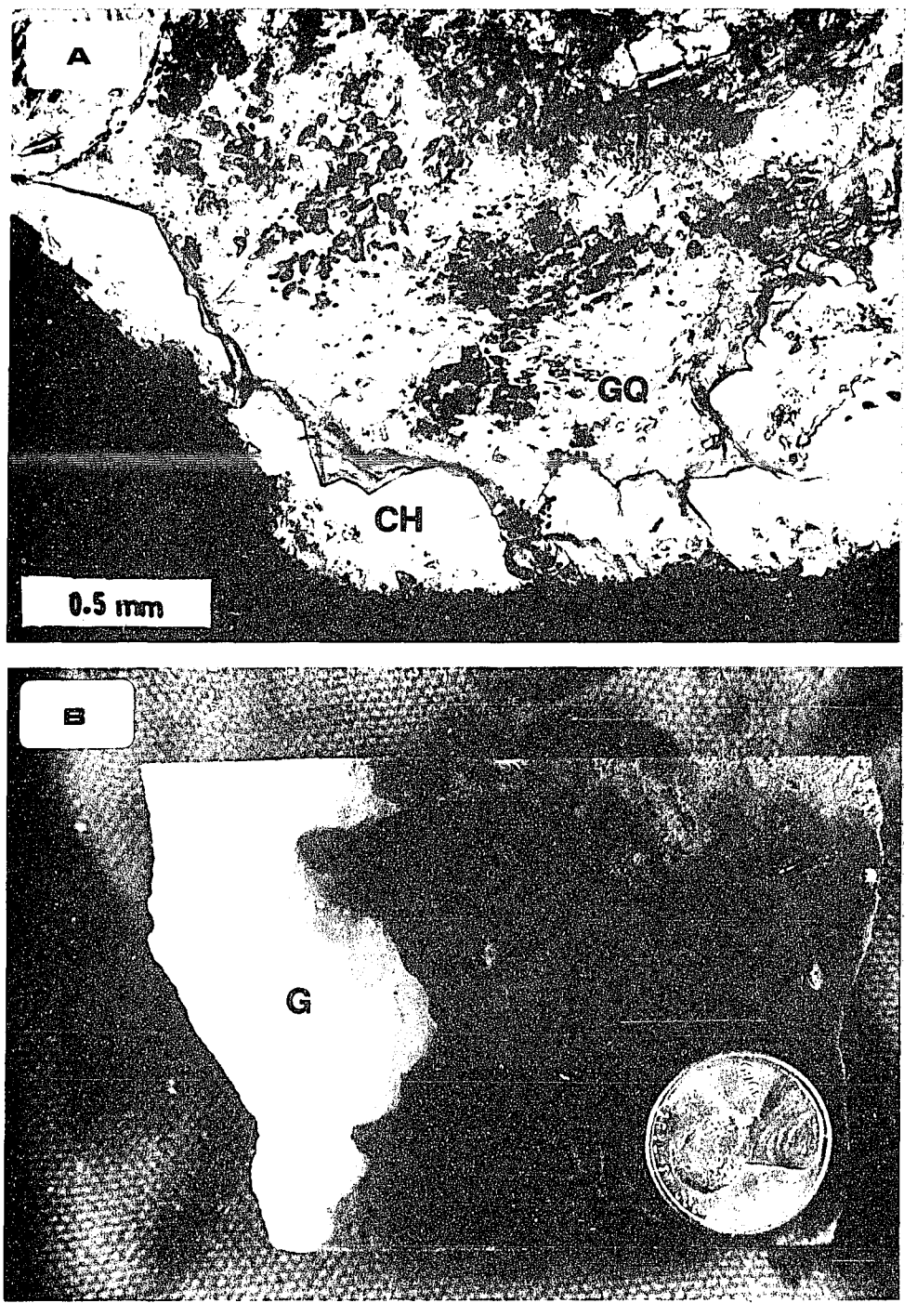

Figure 11.3: (A) Photomicrograph of sample from the Syracuse Formation of location #57 showing part of a quartz-filled vug in dark dolomicrite. Fibrous chalcedony (CH) lines the vug, and is followed by granular quartz (GQ) containing abundant fluid inclusions. Plane polarized light. (B) Core sample of Vernon shale of location #51, showing part of a gypsum(G)-filled vug in dark dolomicrite. Penny for scale.

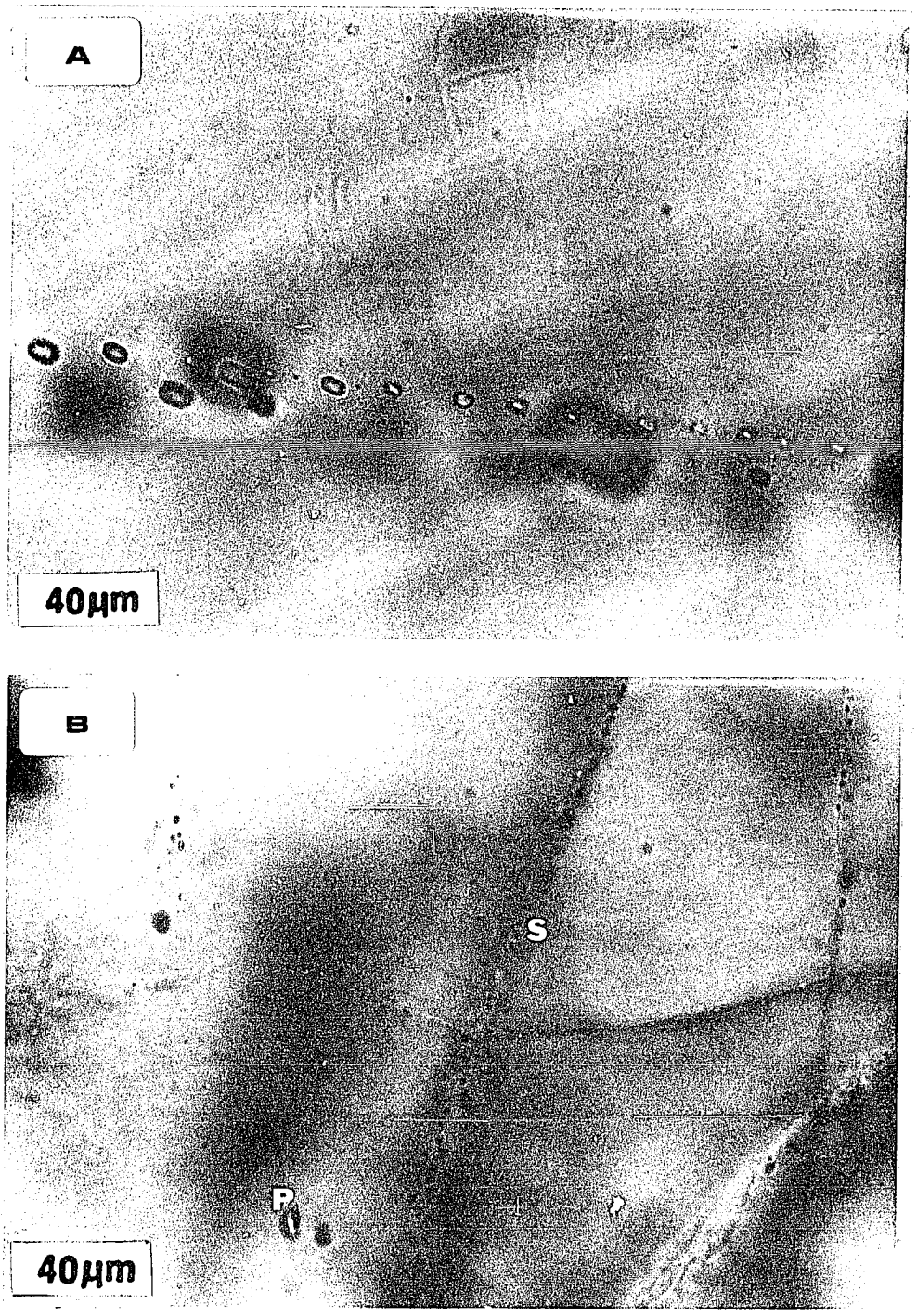

Figure 11.4: Photomicrographs showing (A) a line of secondary, one-phase fluid inclusions in gypsum of the Vernon Shale of location - 51, and (B) a relatively large, isolated, primary two-phase inclusion (thin arrow) next to a line of very small secondary inclusions in vug-filling quartz shown in figure 11.3A.

LOCATION: 57

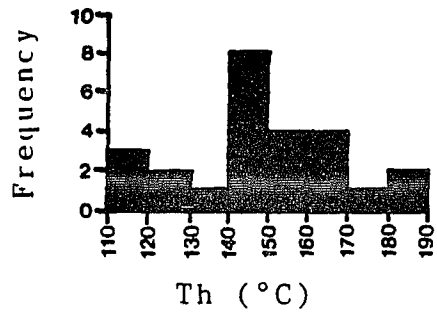

Th_{max} = 182.6°C

Tm = -15° to -20°C
(3 readings)

LOCATION: 58

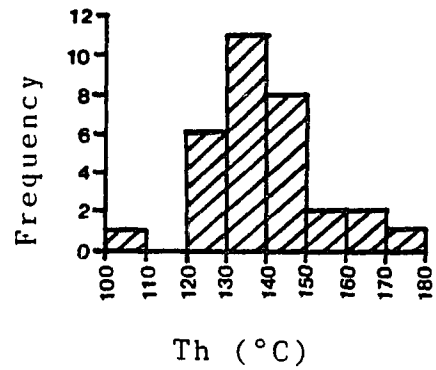

Th_{max} = 166.8°C

Tm = -21°C
-23°C

QUARTZ DOLOMITE

Figure 11.5: Fluid-homogenization temperature (Th) histograms for the studied Salina samples of two locations. The maximum homogenization temperatures (Th_{max}) and melting temperatures (Tm) are also shown.

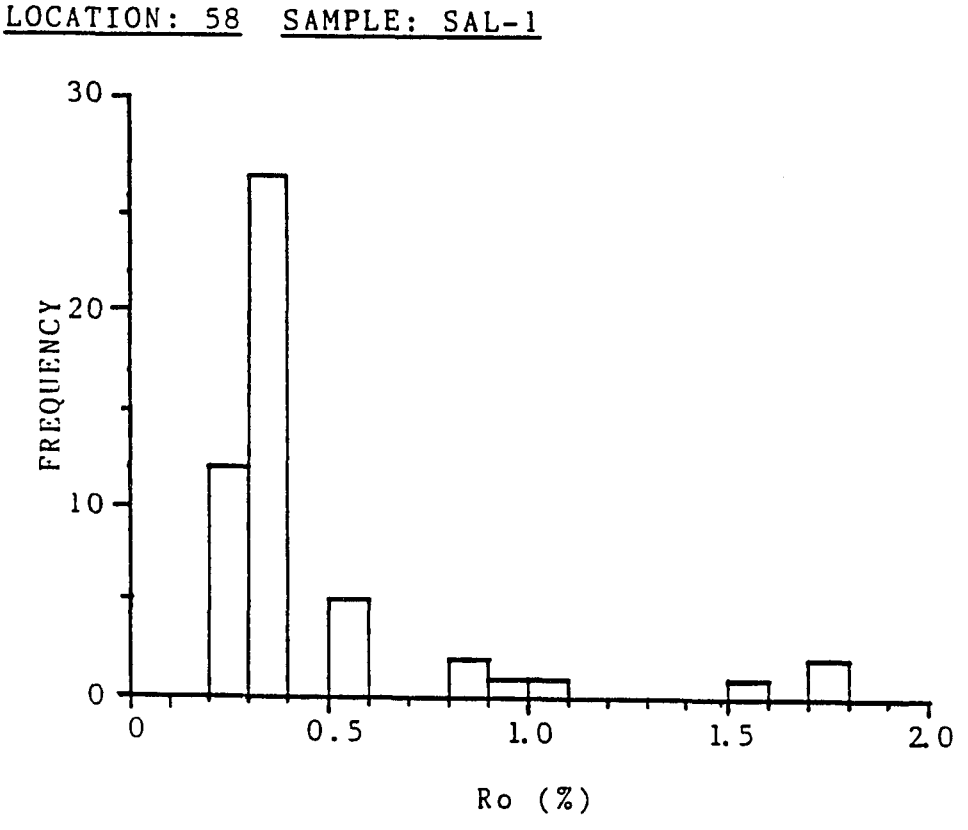

Figure 11.6: Vitrinite reflectance (Ro) histogram of a shale sample from location - 58.

11.6: STABLE ISOTOPE DATA:

One saddle dolomite sample from location 58 was measured for stable isotopes. The sample shows a $\delta^{18}O$ value of -8.02‰ PDB and a $\delta^{13}C$ value of -25.9‰ PDB.

11.7: CLAY DIAGENESIS DATA:

XRD patterns of two samples of the Vernon Shale from locations 51 and 52 are shown in figure 11.7. Since the x-ray analysis of the glycolated and untreated clay samples of the late Ordovician Utica Shale and the Middle Devonian Marcellus Shale failed to show any significant difference, only glycolated samples of the Vernon Shale were analyzed. Samples from other locations of the Salina Group (fig. 11.2) consist primarily of dolomicrite, and these were not x- rayed. Table 11.1 shows the calculations involved in determining the percentage of illite in the Vernon samples. The peak positions are labeled in figure 11.7 and detailed x-ray data are presented in Appendix- G.

Table 11.1: Calculated percentage of illite (%illite) in the Vernon Shale samples based on the difference (in °2θ) between the peak positions of 001/002 and 002/003 illite/smectite (I/S).

Location no.	Sample no.	Position of 001/002 I/S peak (°2θ)	Position of 002/003 I/S peak (°2θ)	Δ °2θ	%illite*
51	VR-1	8.92	17.80	8.88	90-100
52	VR-2	8.90	17.70	8.80	90-100

* Calculations are based on Moore and Reynold's (1989) method.

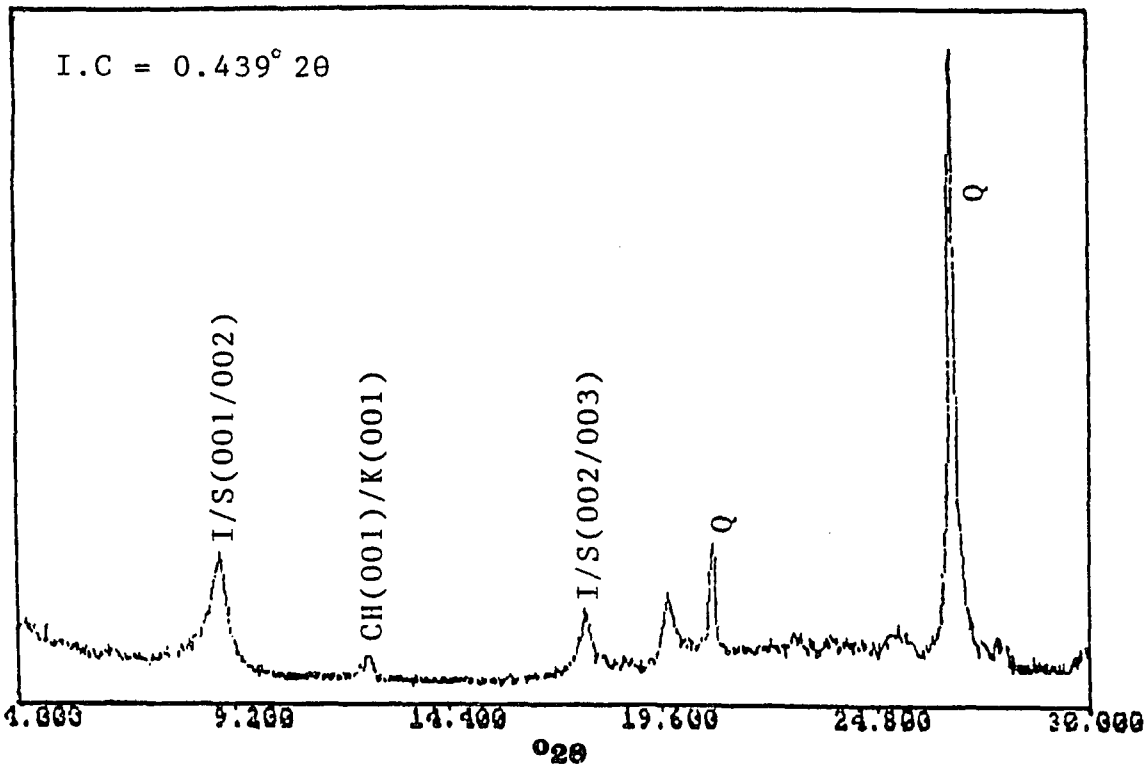

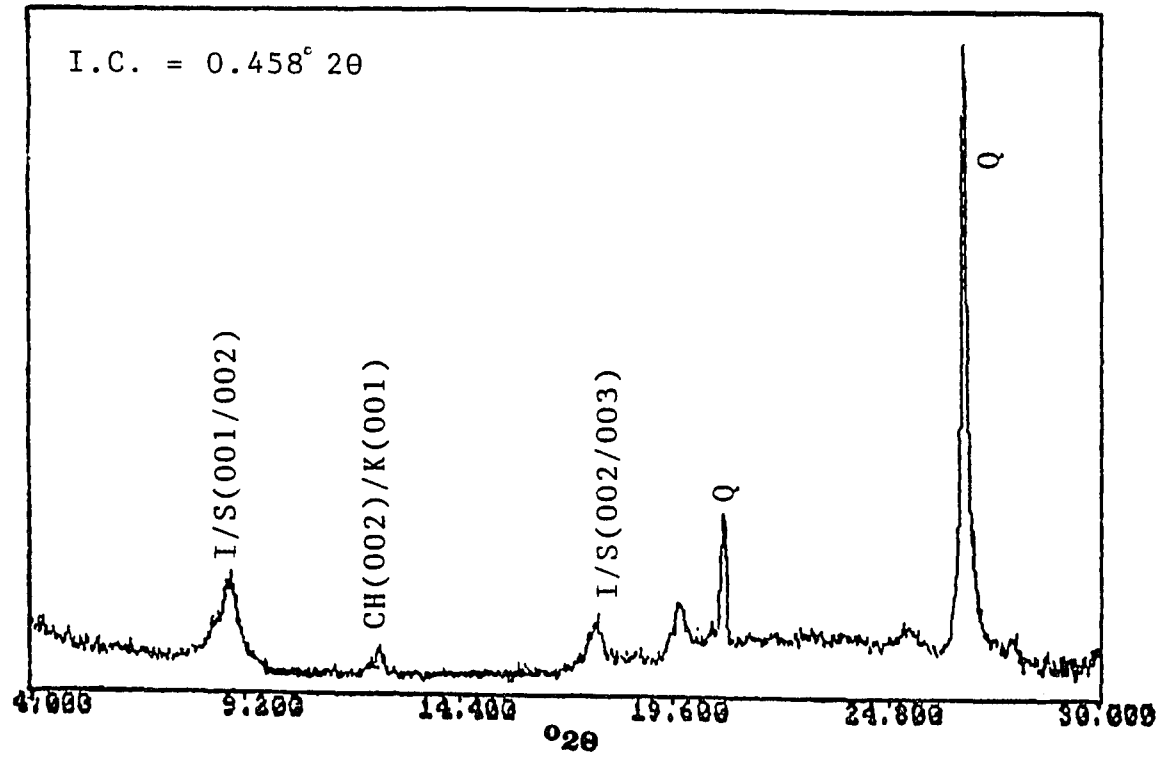

Figure 11.7: X-ray diffractograms of glycolated clay samples from the Vernon Shale oflocations 51 and 52. I.C = Illite Crystallinity index.

11.8: INTERPRETATION:

1.8.1: The paragenetic sequence of cements:

Vugs in the Salina Group probably formed through leaching of anhydrite nodules by fresh water, perhaps early in the diagenetic history. Similar formational mechanism has been proposed for the vugs of the Lockport Group (Friedman, 1987a, 1989). Some of the leached vugs in the Salina Group have subsequently been filled by saddle dolomite and quartz. Gypsum found in some vugs were probably originally nodular anhydrite that somehow survived early dissolution and later hydrated to gypsum as the rocks were brought to the surface. It is also possible that anhydrite reprecipitated in leached vugs and cavities as a late-stage mineral directly from hot brines in the burial environment (Murray, 1964).

Although a paragenetic sequence between the vug-filling minerals could not be established from the limited study, it is believed that all vug-filling minerals - saddle dolomite, quartz and anhydrite (? now gypsum) - formed late in deep- burial environment from relatively high-temperature fluids (see section 11.8.2).

11.8.2: Fluid-inclusion data:

In the Salina Group samples of locations 57 and 58, although the inclusions were studied in two different minerals - saddle dolomite and quartz - the measured ranges of Th are similar, 110-190° C and 100-180° C respectively (fig. 11.5). Similarly, Tm ranges between -15° C (equivalent wt% NaCl of 18.8) and -20° C (equivalent wt% NaCl of 22.6) in quartz cement of location-57, and between -21° C (equivalent wt% NaCl of 23.3) and -23° C (equivalent wt% NaCl of 24.7) in saddle dolomite of location-58. Fluids trapped in both mineral cements, therefore, represent hot brines. The same is true for gypsum (originally anhydrite) in which some inclusions homogenized between 90° and 120° C before the gypsum chips became opaque in the heating-freezing stage rendering further measurements impossible (section 11.4). Inclusions that did not homogenize between 90° and 120° C obviously had higher Th, probably similar to the high Th values found in saddle dolomite and quartz.

11.8.3: Organic maturation data:

The mean Ro(%) of a dolomitic shale sample of location- 58 is 0.97, indicating a

maximum burial temperature of 150° C (Barker and Pawlewicz, 1986). This is about 17°C less than the Th_{max} (166.8° C) of the same location. It is possible that the inconsistency is due to the sample being a dolomitic shale in which carbonate diagenesis may have somehow altered the reflectance of the vitrinite macerals.

11.8.4: Stable isotope data:

The $\delta^{18}O$ value of one saddle dolomite sample of location-58 is -8.5‰ PDB which reflects a formational temperature of 104-164°C using a $\delta^{18}O_{water}$ value of 2-8‰ SMOW in Fritz and Smith's (1970) equation. This temperature is within the range of Th of location 58.

11.8.5: Clay diagenesis data:

Two Vernon Shale samples, one each from locations-51 and 52, have more that 90% illite in their mixed-layer I/S (table 11.1) indicating temperatures in the vicinity of 200°C (section 4.5). Illite crystallinity index (I.C) of these two samples - 0.439° 2θ and 0.458° 2θ (fig. 11.7). According to Weaver et al.'s (1984) diagram (fig. 4.5), these I.C. values correspond to temperatures of approximately 255° C and 245° C, respectively.

In chapter 16, the significance of these temperatures of the Salina Group are treated in context with paleotemperature signatures of other Silurian and Devonian units.

CHAPTER 12: THE HELDERBERG GROUP

12.1: STRATIGRAPHY AND DEPOSITIONAL HISTORY:

The Lower Devonian (Ulsterian) Helderberg Group is a prominent limestone unit in the Northern and Central Appalachian Basin. South of New York, it extends into northeastern New Jersey, Pennsylvania, eastern Ohio, Maryland, Virginia, West Virginia, eastern Kentucky and northeastern Tennessee (COSUNA chart, 1985). In southeastern New York, the Helderberg carbonates are about 140m thick and are conformably overlain by the rocks of the Tristate Group. However, to the west, the Helderberg Group is erosionally truncated to deeper and deeper levels until it is completely beveled in central New York (fig. 12.1). In southeastern New York, where its complete section is preserved, the Helderberg Group is divided into seven formations. These are, in ascending order, the Manlius, Coeymans, Kalkberg, New Scotland, Becraft, Alsen and Port Ewen (fig. 12.1).

The Helderberg carbonates have been interpreted by Laporte (1967, 1969) on the basis of a theoretical model of epeiric, warm and clear-water sedimentation pattern proposed by Irwin (1965). According to this interpretation (also see Fakundiny et al. 1989; Isachsen, et al. 1991, Chapt. 8), the lower part of the Manlius Limestone with its oncoids, scour-and-fills, birdseye structures and mud cracks was deposited in a supratidal to intertidal environment. The upper part of the Manlius with its low-diversity marine fauna, wave-ripple marks, cross-strata and occasional stromatoporoid biostromes, is believed to have formed in a low- to moderate-energy subtidal environment behind a protective barrier. Thus, the Manlius Formation as a whole formed in the Zone-Z of Irwin (1965).

The Coeymans Formation, consisting of clean, medium to coarse-grained, often cross-stratified limestones, few coral bioherms and a benthic fauna dominated by pelmatozoans was probably deposited in a high-energy subtidal environment located above the fairweather wave base (Zone - Y of Irwin). The Kalkberg and New Scotland formations, based on their lithology, sedimentary structures and faunal assemblage, are believed to have formed at successively deeper water below the fairweather wave base,

Figure 12.1: The outcrop belt and stratigraphic subdivisions of the Helderberg Group in New York. (Adapted from Rickard, 1975).

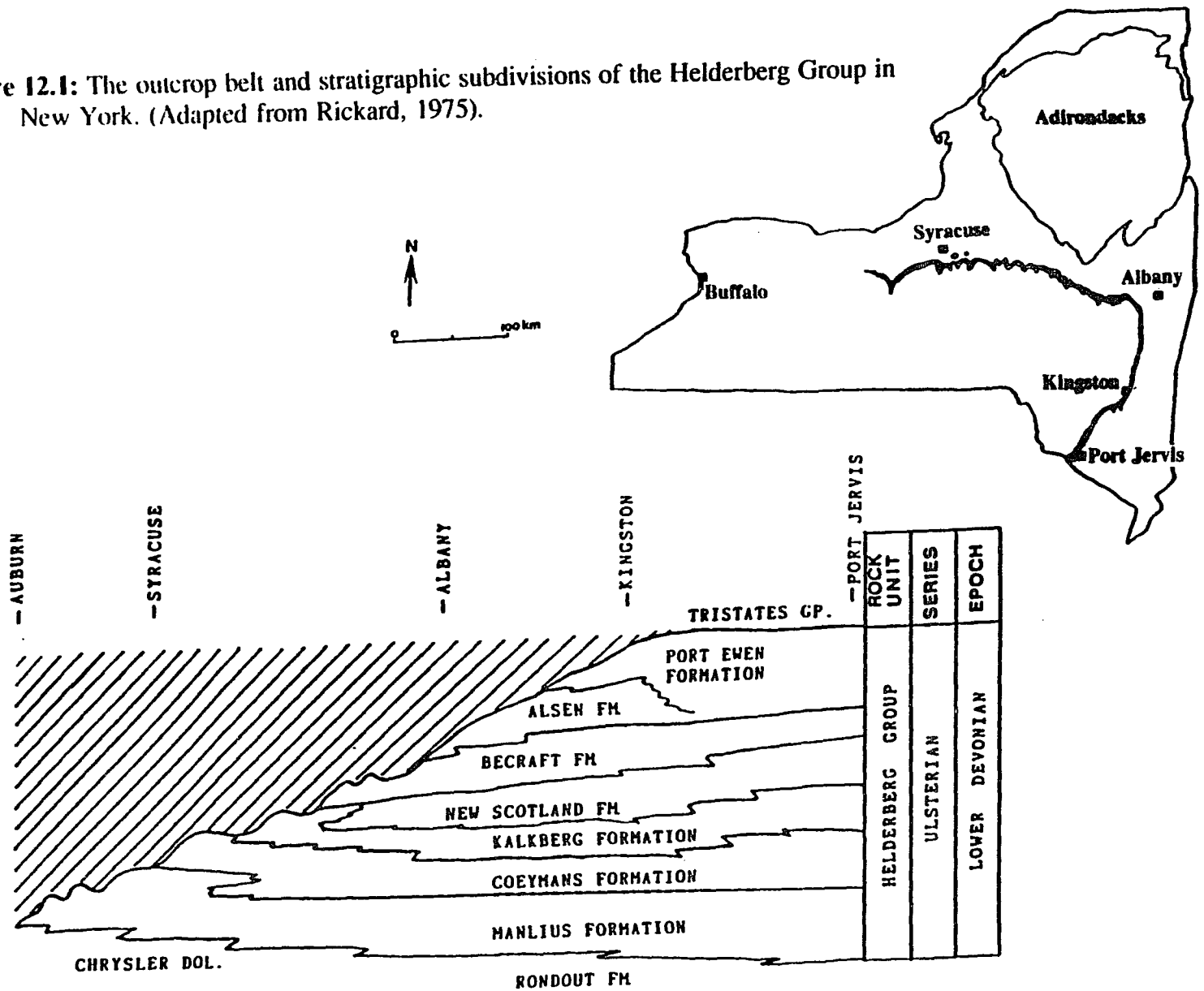

which correspond to Zone - X of Irwin (1965).

These units laterally grade into one another and they are time-transgressive (Laporte, 1967, 1969; Fakundiny et al. 1989; Isachsen et al. 1991, Chapt. 8). The pattern of lateral grading as well as vertical stacking of the various epeiric carbonate facies is partly repeated in the upper Helderberg Group. The Becraft Limestone is similar to the Coeymans, while the Alsen and Port Ewen correspond to the Kalkberg and New Scotland formations, respectively.

12.2: SAMPLING LOCATIONS:

The sampling locations of the Helderberg carbonates are shown in figure 12.2. The Helderberg samples include both outcrop and core samples. Some additional core samples were obtained but were found unsuitable for fluid-inclusion study, because of their micritic composition and lack of vug- or vein-filling cements. These sampling locations are not shown in figure 12.2.

12.3: GENERAL PETROGRAPHY OF THE SAMPLES:

Most of the Helderberg samples are coarse skeletal grainstones and packstones, because sampling was biased toward coarse-textured rocks. At locations 26 and 27 of eastern New York, the samples were collected from the Becraft Formation of the upper Helderberg Group. These are slightly pinkish, coarse crinoidal grainstones with subordinate amount of bivalve and brachiopod shells. Fractures healed with sparry calcite are common. These are up to 3cm wide and oriented both vertical and parallel to subparallel to the bedding (fig. 12.3). Coarse, sparry calcite and crinoid-syntaxial calcite commonly fill the grain interstices (fig. 12.4). Petrography of the Becraft Formation from these locations have been described in details by Simensen and Friedman (1991).

In central New York (locations 7, 28, 8, 29 and 9) all the samples are skeletal grainstones and packstones with relatively few crinoids. Corals and stromatoporoids are more common than in southeastern New York, and probably reflects a sampling bias toward the upper part of the Manlius Formation and the Coeymans Formation. Rocks of the upper Helderberg Group (Becraft, Alsen and Port Ewen formations) are missing from central New York (fig. 12.3). In addition to inter-particle calcite, samples from these

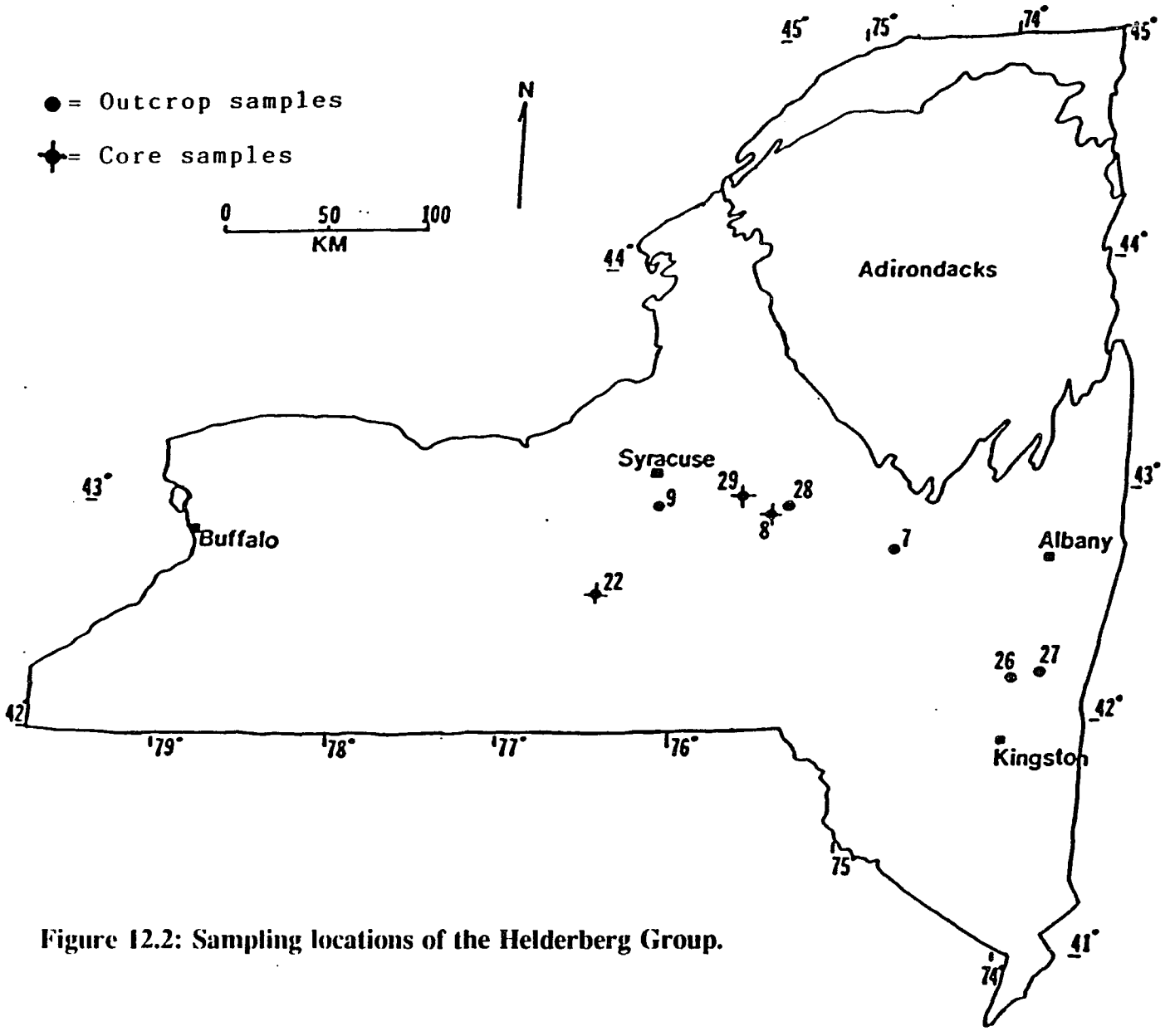

Figure 12.2: Sampling locations of the Helderberg Group.

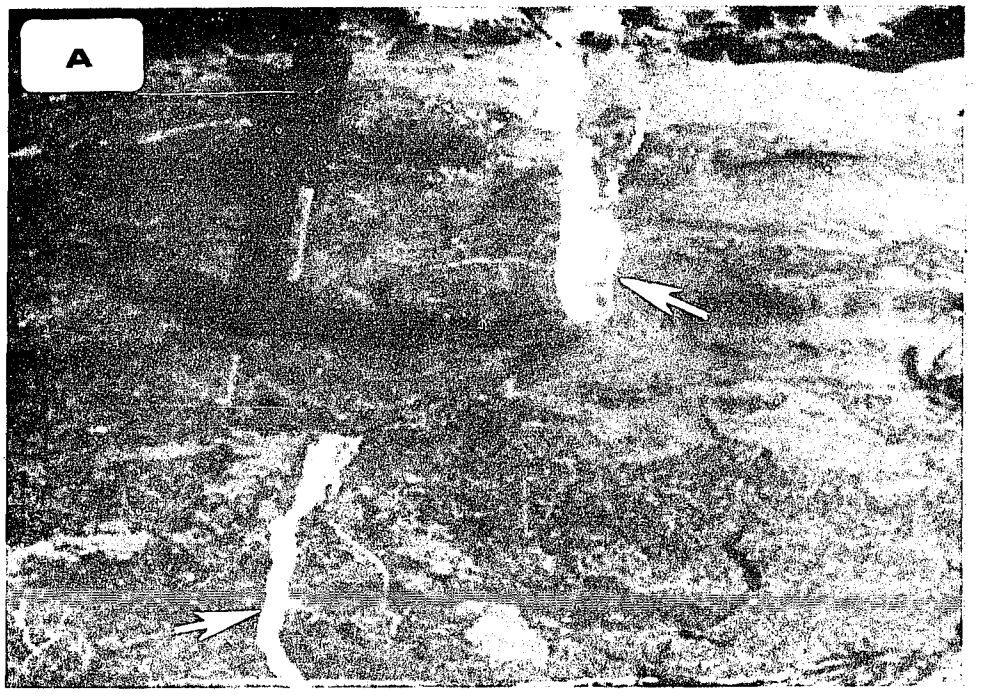

Figure 12.3: Outcrop photo showing calcite-healed fractures (marked by arrow) in coarse, crinoidal grainstones of Becraft Formation of location-26. Hammer is 35cm. in height.

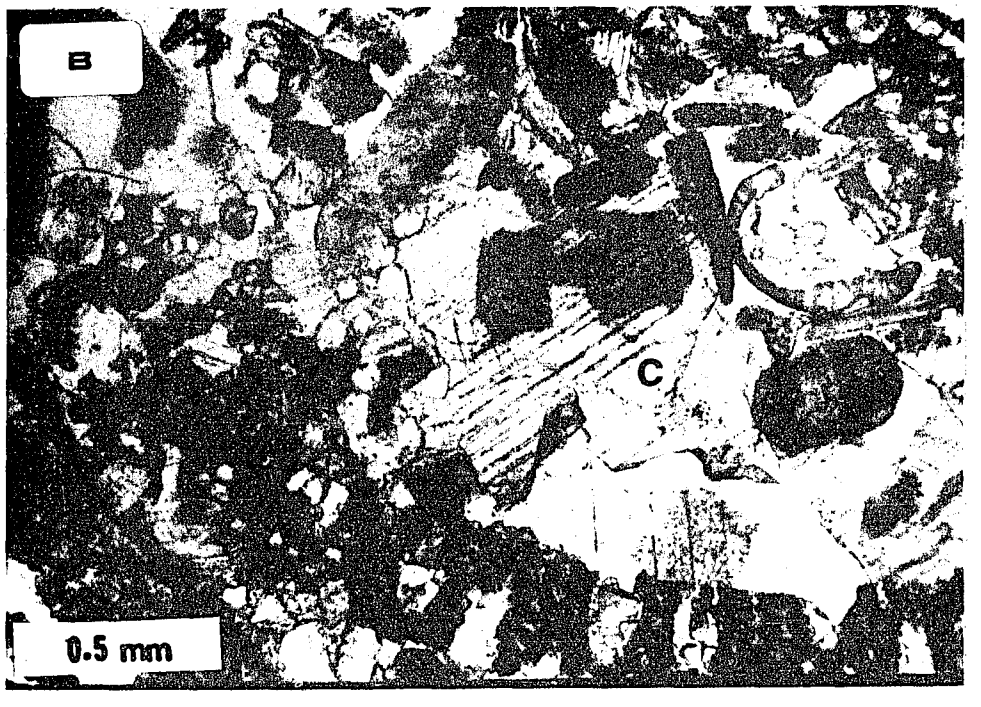

Figure 12.4: Photomicrograph showing coarse sparry calcite cement filling particle interstices and as syntaxial overgrowths on echinoderm particles. Sample from Becraft Formation of location - 27.

locations commonly contain sparry calcite in coral chambers (fig. 12.5a). Partial replacement of crinoid ossicles and bivalve shells by fibrous chalcedony is observed in samples from the Kalkberg Formation at location 8 and Coeymans Formation at location 29. At location 9, saddle dolomite and fluorite occur in vugs and veins in the Manlius Formation (fig. 12.5b).

In the core samples of the Manlius Formation from south-central New York (location 22), coral chambers are filled with sparry calcite.

12.4: FLUID-INCLUSION DATA:

Figure 12.6 shows the Th histograms along with Th_{max} for samples from various locations of the Helderberg Group. Individual readings are presented in Appendix- H. In table 13.1, the few measured "Tm"s, corresponding "Th"s and calculated salinities of the inclusion fluids are presented. In figure 12.7, Th_{max} values are plotted against sampling locations.

The inclusions were measured in calcite cement in all but location 9, where a large number of inclusions was found in vug-filling fluorite and some in saddle dolomite (fig. 4.1). The calcite cement in which the inclusions were measured were from healed fractures at locations 26 and 27, from calcite in recrystallized molluskan shells and coral cavities at locations 8 and 28, from calcite of skeletal mold at location 28, from vug-filling saddle dolomite and fluorite of location 9 and from calcite of coral chambers of location 22. Inclusion data from location 7 is taken from Gurney and Friedman (1987), who measured them in inter-particle calcite cements. For the 5 Th readings between 135° and 155° C, an approximate average of 140° C is taken as the Th_{max} for location 7. Individual Th readings were not provided by Gurney (1986) or Gurney and Friedman (1987). The one Th reading between 190° and 195° C in Gurney's (1986) original histogram is considered non-representative and is not included here (fig. 12.7). It is much above the general Th population, and is probably a result of stretching.

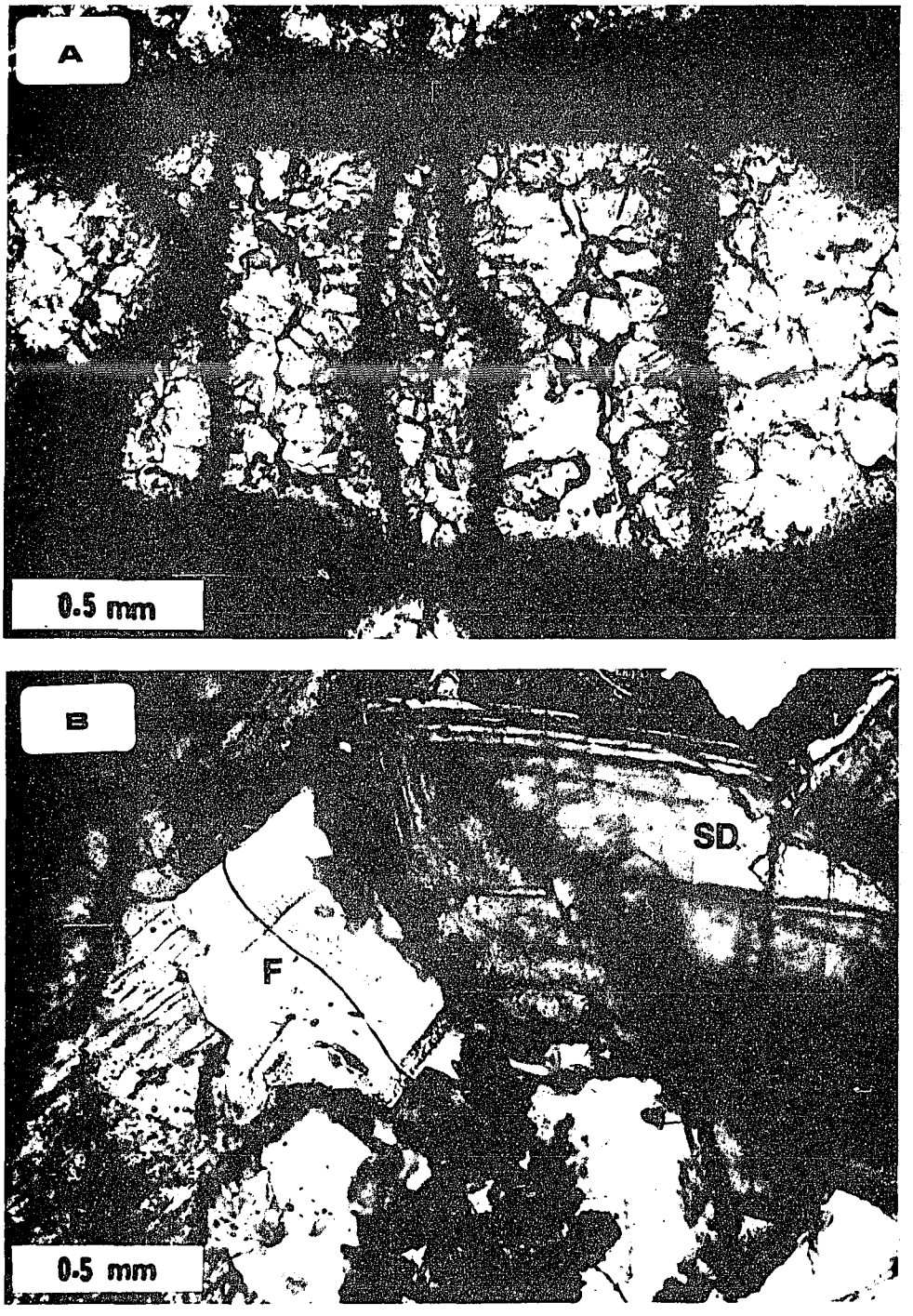

Figure 12.5: Photomicrographs showing (A) coral chambers filled with sparry calcite cement. Sample from skeletal grainstone of location - 29, and (B) vug-filling saddle dolomite (SD) and fluorite (F) of location - 9.

Figure 12.6: Fluid-homogenization temperature (Th) histograms for samples of the Helderberg Group. Calculated maximum homogenization temperatures (Th_{max}) for each study location are also shown.

LOCATION - 26

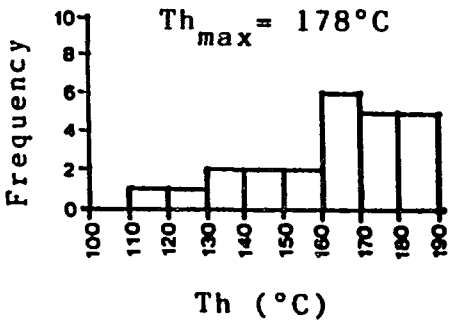

LOCATION - 27

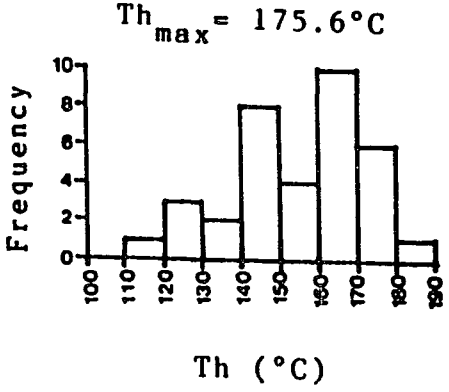

LOCATION - 7

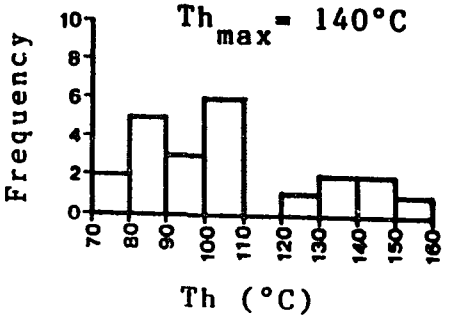

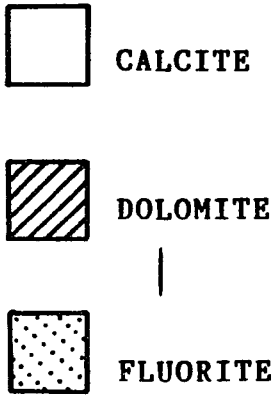

LOCATION - 28

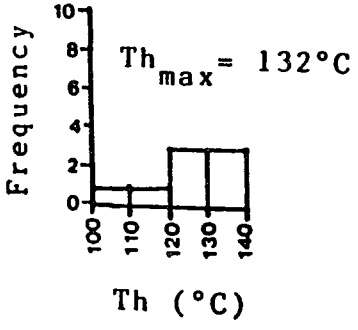

LOCATION - 8

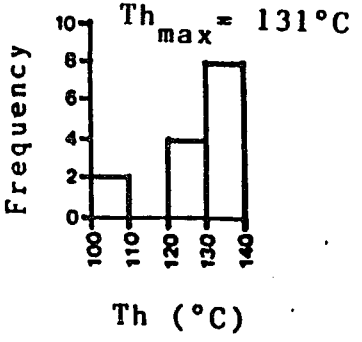

LOCATION - 9

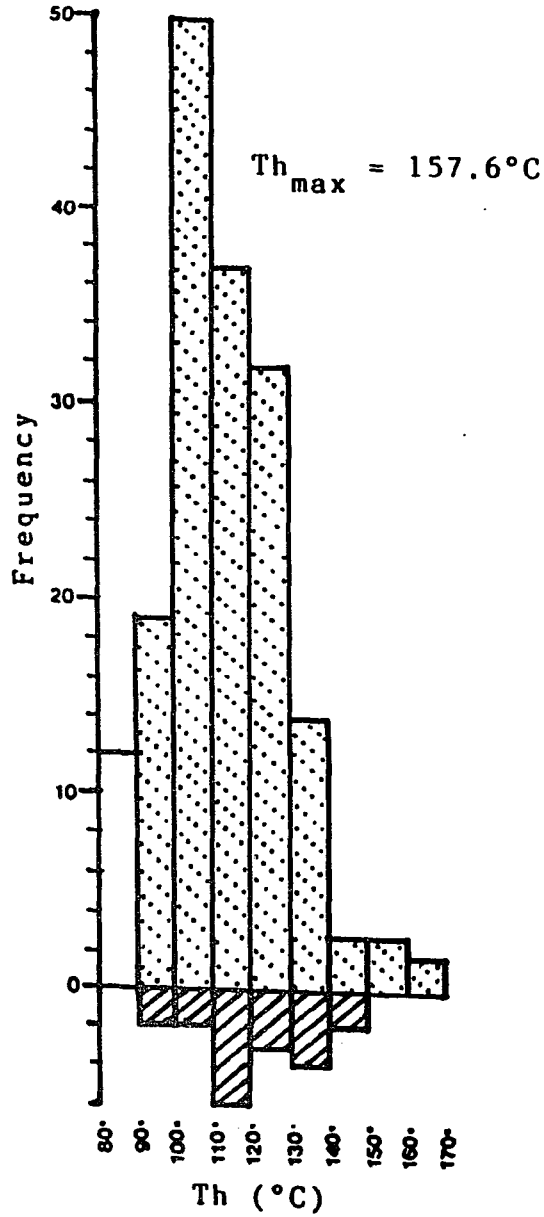

LOCATION - 29

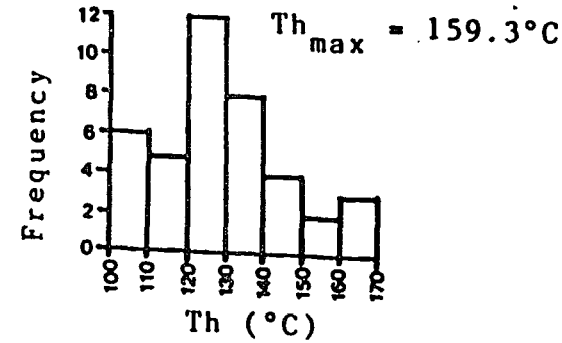

LOCATION - 22

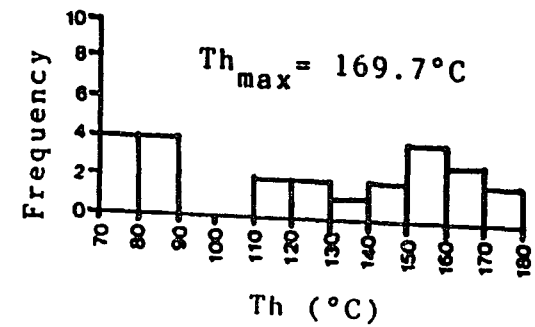

Table 12.1: Melting temperatures (Tm), corresponding homogenization temperatures (Th), and calculated salinity (equivalent wt% NaCl) of fluid inclusions in cements of the Helderberg Group.

Location	Type of cement	Tm (°C)	*Salinity (wt% NaCl)	Th (°C)
26	Fracture-filling calcite	+3.2	---	138
		+0.2	---	165.3
27	Fracture-filling calcite	-3.1	5.1	170.5
		-12.0	16.0	187
8	Calcite in recrystallized bivalve shell	-12.5	16.5	126
29	Calcite in recrystallized bivalve shells	-7.4	10.9	137.5
		-7.9	11.6	128
		-9.7	13.6	134
		-13.7	17.7	149.9
9	Vug-filling fluorite	-24.0	25.3	152.7
22	Calcite in coral chamber	-24.0	25.3	151
#7	Calcite (unspecified)	-7 to -15	10.4-18.8	

* Salinity was calculated according to Potter et al.'s (1978) method (section 4.3.2)

data from Gurney and Friedman (1987).

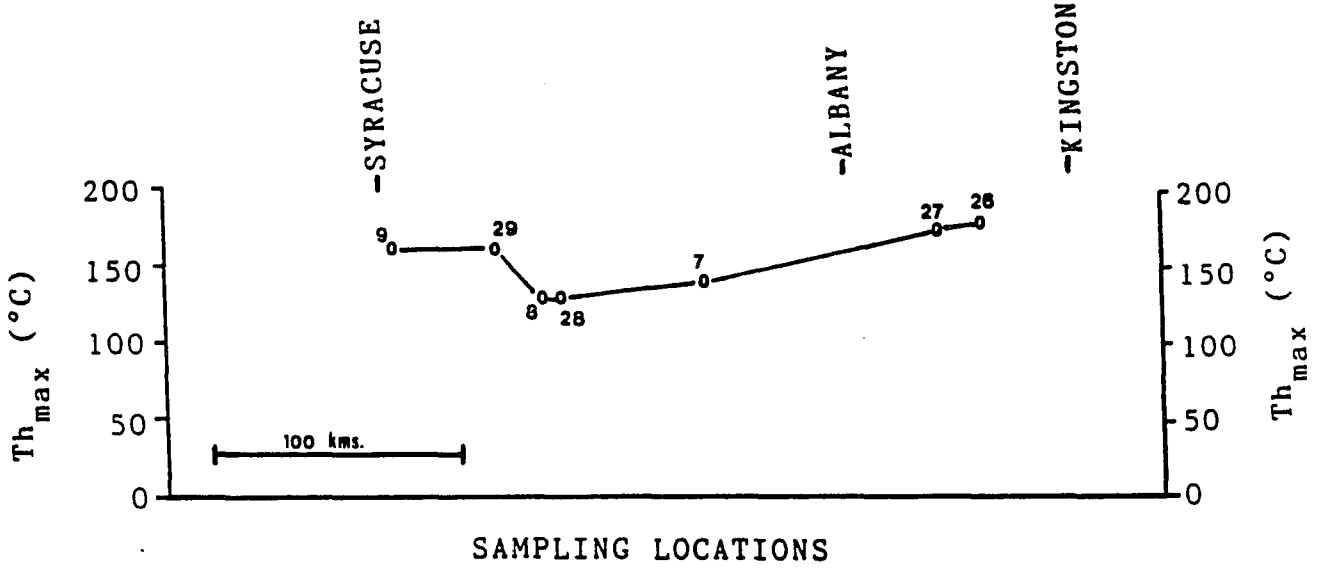

Figure 12.7: Th_{max} of the Helderberg Group carbonates plotted against study locations.

12.5: STABLE ISOTOPE DATA:

Oxygen and carbon isotopic ratios were measured in vein- and vug-filling calcite and dolomite in seven locations of the Helderberg Group. Isotope data for location 7 were taken from Gurney and Friedman (1986). Table 12.2 presents the ^{18}O and ^{13}C values and the calculated paleotemperatures.

12.6: INTERPRETATION

12.6.1: Paragenetic sequence of cements:

Fractures in the Helderberg carbonates of southeast New York (locations 26 and 27, fig. 12.3) post-date lithification and stylolitization. The calcite cement that healed these fractures, therefore, of late origin. Inter- and intra-particle (especially in coral chambers) sparry calcite cement of southeast New York, and probably of elsewhere, formed earlier than the fracture-filling calcite. The vug-filling saddle dolomite and fluorite of central New York (location 9) probably formed later than most of the inter- and intra-particle cements, because the vugs must have formed after the host-rock was well-consolidated (cemented).

The boundaries of vugs are always sharp and marked by dissolution of the host rock. The presence of saddle dolomite in these vugs also indicate mineral precipitation at relatively high temperature in the burial environment (Radke and Mathis, 1980).

12.6.2: Fluid-inclusion data:

Fluid-inclusion homogenization temperatures (Th) of the Helderberg Group carbonates show a wide range (fig. 12.6) in most of the study locations suggesting that the inclusions were trapped from fluids of various temperatures, probably over a long period of time. However, at locations 28 and 8, the ranges of measured Th are relatively small - between 100° and 140°C - at both locations (fig. 12.6). The inclusions from these two locations were found in calcite of skeletal molds and recrystallized bivalve fragments. Although it is possible that cements of these specific types precipitated within a narrow range of temperature, examination of the Th histogram of the nearby

Table 12.2: Oxygen and carbon isotope data from the Helderberg carbonates and calculated paleotemperatures. All measurements were made in calcite except in location - 9 where measurements were made in dolomite.

Location no.	Sample no.	$\delta^{18}O$ (‰ PDB)	$\delta^{13}C$ (‰ PDB)	*Temperatures (° C)
26	B-5	-6.18	+0.1	60 - 102
	B-6	-8.4	+0.5	74 - 121
27	B-3A	-6.37	-0.9	61 - 104
**7	___	-5.8	+0.7	57 - 100
	___	-8.3	+1.6	73 - 120
	___	-8.4	+2.1	74 - 121
28	HLB-1	-9.18	+2.2	80 - 129
8	OTK-1	-3.36	+3.3	43 - 82
29	OC-1	-3.07	+3.1	41 - 80
	OM-1	-4.3	+2.0	48 - 90
9	HLB-4 (dol.)	-5.2	+2.9	80 - 135
22	CGH-1	-6.66	+1.7	62 - 107

* Temperature of formation calculated by using Craig's (1965) equation for calcite and Fritz and Smith's (1970) equation for dolomite, and assuming a $\delta^{18}O_{water}$ value of 2 to 8‰ SMOW.

** Data from Gurney and Friedman (1987).

locations 29 (fig. 12.6), where the inclusions were also measured in recrystallized bivalve fragments, suggests that this was not the case. Additional Th measurements at locations 8 and 28 may reveal the presence of a wider range than those measured in this study, or these small ranges may truly represent the local temperature regimes at the time of cement precipitation. Comparison with paleotemperature signatures of the overlying Onondaga and Marcellus formations will help to determine whether the Th and Th_{max}

data of the Helderberg Group carbonates represent true values or are artifacts of number of inclusions measured (see chapter 15).

It is apparent from figures 12.6 and 12.7, that the maximum Th_{max} of the Helderberg Group occurs in southeast New York (locations 26, 27) and in the subsurface of south-central New York (location - 22). The Th_{max} profile (fig. 12.7) along the outcrop belt of the Helderberg also shows a high (although lower than the Th_{max} of locations 26, 27 and 22) south-southeast of Syracuse in central New York.

The salinities of inclusion fluids in the Helderberg carbonates, calculated from 'Tm's, are generally high, ranging between 10 and 26 equivalent wt% NaCl, except at location 27, where one measured salinity is 5.1% (table 12.1). The positive 'Tm's of location 26 most probably represent incongruent melting temperatures of hydrohalite (see section 4.3.1) and thus do not represent true salinity of the inclusion fluids. The data (table 12.1) suggests that the inclusion fluids of the Helderberg carbonates were mostly hypersaline brines. All of these inclusions were trapped at temperatures above 125° C. There is, however, no correlation between Th and Tm (table 12.1), similar to that observed in other rock units.

12.6.3: Stable-isotope data:

The $\delta^{18}O$ values of calcite and dolomite cements of the Helderberg Group range between -3.36 and -9.18‰ PDB (table 12.2). Light $\delta^{18}O$ values such as these have been reported in carbonate cements of known deep burial origin by many authors (Mattes and Mountjoy, 1980; Zenger, 1983; Prezbindowski, 1985; Woronick and Land, 1985; Lee and Friedman, 1987; Saigol and Bjorlykke, 1987, Zenger and Dunham, 1987; Kaufman et al. 1990). Similar isotopic values have been measured in carbonate cements of the Helderberg and other Paleozoic rocks of central and eastern New York state (Urschel and Friedman, 1984; Broeckerhoff and Friedman, 1987; Gurney and Friedman, 1987; Friedman, 1987a,b; Simensen and Friedman, 1991).

The paleotemperatures calculated from the $\delta^{18}O$ values (table 12.2), are generally well below the range of Th measured in the same sample locations. Although there are some overlaps between the two temperature ranges in some locations and none in others

(locations 8 and 29), the most inconsistent relationship is between Th_{max} of individual locations with the maximum isotopic paleotemperature of the same locations. The reason for this may be that (1) the range of $\delta^{18}O_{water}$ (2-8‰ SMOW) used in calculating isotopic paleotemperature may be incorrect, or (2) the maximum paleotemperatures at which only part of the cement was precipitated can never be derived from the average $\delta^{18}O$ values of the bulk cement samples that were used for isotopic measurements in this study.

CHAPTER 13: THE ONONDAGA FORMATION

13.1: STRATIGRAPHY AND DEPOSITIONAL HISTORY

The Middle Devonian (Erian) Onondaga Formation is one of the most extensively exposed rock units in New York State. It outcrops from Buffalo eastward to Albany, then southward to Port Jervis (fig 13.1). Outside New York, it is exposed in the Ontario Province of Canada, in New Jersey and Pennsylvania. The limestones of the Onondaga Formation have been widely studied, especially by paleontologists (see references in Oliver, 1976 and Friedman, 1985). It is particularly well known for coral-crinoidal bioherms that occur throughout its exposures from Albany to the Niagara Peninsula, Ontario as well as in the subsurface of western and central New York and northwestern Pennsylvania (Oliver, 1954, 1956, 1976; Turner, 1977; Mesolella, 1978; Kissling and Coughlin, 1979; Lindemann, 1979; Williams, 1980; Friedman, 1985; Wolosz and Paquette, 1989).

In its type locality in Onondaga County, central New York, the Onondaga Formation is 21.5m thick, whereas in the eastern and western parts of the state it reaches up to 49m (Friedman, 1985). The four members of the Onondaga Formation are, from oldest to youngest, Edgecliff, Nedrow, Moorehouse and Seneca (fig. 13.1).

The Edgecliff Member consists primarily of skeletal calcarenites, dominated by brachiopods and crinoids in the lower part and by rugose and tabulate corals in the upper part (Oliver, 1954). The well known bioherms of Onondaga is mainly restricted to the Edgecliff Member. South of the Helderbergs, Edgecliff becomes finer grained and less fossiliferous (Lindemann, 1979).

The Nedrow Member consists of thinly bedded, fine- grained argillaceous limestones comprising brachiopods, gastropods and few corals. The Moorehouse Member is thick-bedded, cherty and micritic with shaly partings comprising a fauna of brachiopods, gastropods, cephalopods, trilobites which is restricted mainly to central New York (Oliver, 1954). The uppermost, Seneca Member is also a cherty micrite but differs from

Figure 13.1: The outcrop belt and stratigraphic subdivisions of the Onondaga Formation in New York and southeastern Ontario Province. (From Rickard, 1975).

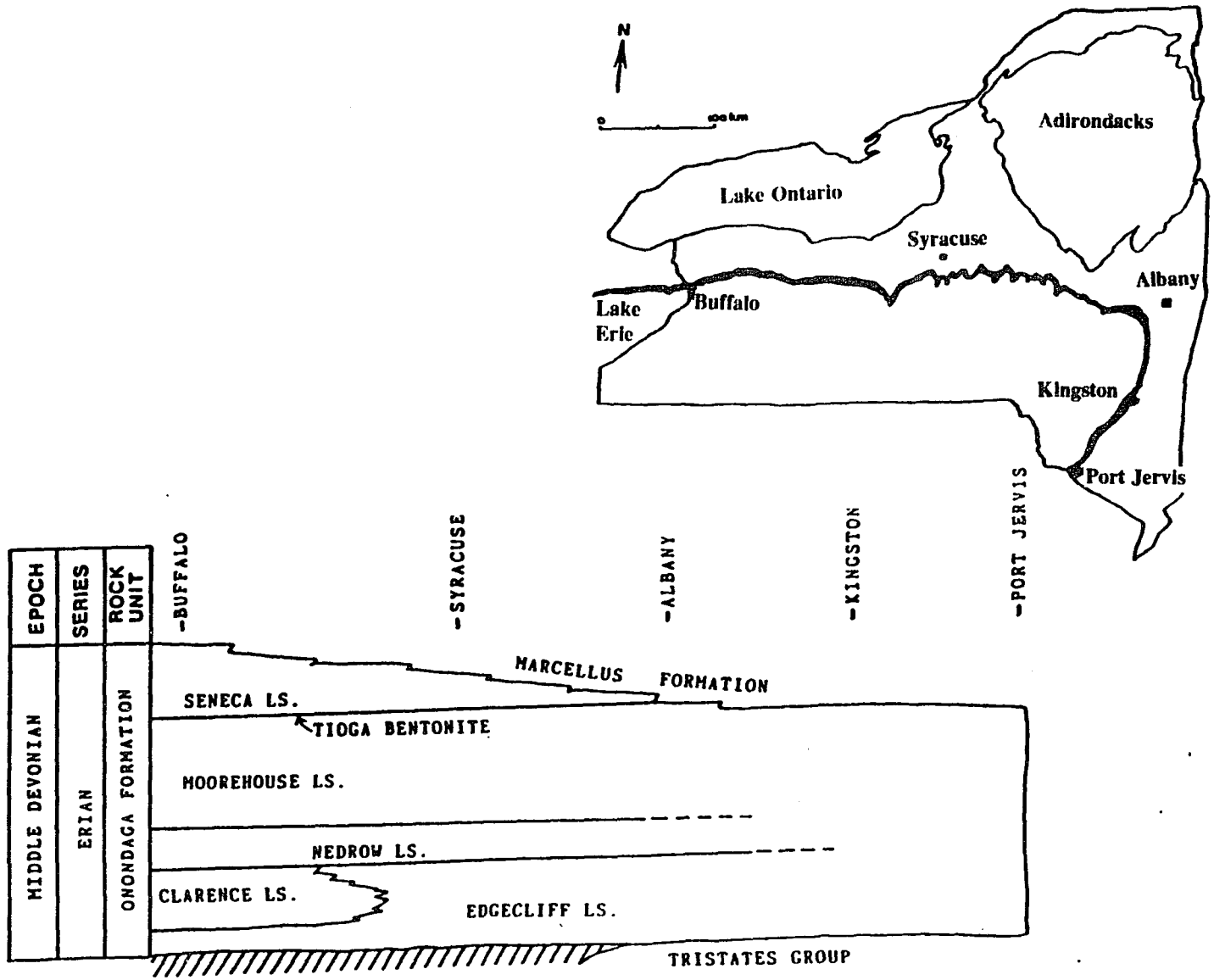
N
Adirondacks
Lake Ontario
Syracuse
Albany
Lake Erie
Buffalo
Kingston
Port Jervis
EPOCH
SERIES
ROCK UNIT
MIDDLE DEVONIAN
ERIAN
ONONDAGA FORMATION
-BUFFALO
-SYRACUSE
-ALBANY
-KINGSTON
-PORT JERVIS
MARCELLUS FORMATION
SENECA LS.
TIOGA BENTONITE
MOOREHOUSE LS.
NEDROW LS.
CLARENCE LS.
EDGECLIFF LS.
TRISTATES GROUP

Moorehouse in faunal assemblage. The Seneca Member has a more restricted occurrence than the other three members, and does not persist east of Cherry Valley, central New York (fig. 13.1). At the base of the Seneca Member is a remarkably uniform, 15 to 20cm thick bentonite clay layer, the Tioga Metabentonite, which is also recognized in the subsurface throughout Pennsylvania and adjacent areas of West Virginia, Ohio and southwestern New York.

The carbonates of the Onondaga Formation were deposited in a westward-transgressing, shallow, northeast-trending epicontinental sea with a major connection to the open ocean to the southwest and a minor connection to the east (Lindemann and Feldman, 1987). In the early Eifelian, the skeletal sediments of the Edgecliff Member, including the coral-crinoidal bioherms were deposited in the sea between Albany and the Niagara Peninsula in shallow water. However, the sparsity of bioherms in central New York (Oliver,1976, fig.5) and isopachous maps of the Onondaga Formation (Mesolella,1978, figs. 17,18) suggest that water was deeper in central New York than in eastern and western parts of the state where reefs flourished and thicker accumulation of Onondaga sediments took place. Thus, the paleogeography along an east-west transect consisted of a symmetric shelf- basin-shelf pattern. The lithofacies in the Nedrow, Moorhouse and Seneca members in central New York represent deepening water and relatively carbonate-starved conditions (Lindemann and Feldman, 1987).

In southeastern New York, between Albany and Port Jervis (fig. 13.1), the carbonates of Onondaga were deposited in a "structural basin", as opposed to the "topographic basin" of central New York (Mesolella, 1978; Lindeman and Feldman, 1987). In this basin, coarse grained and argillaceous sediments were deposited in the shallow carbonate shelf in the north, south of Albany, a thicker accumulation of bryozoan bafflestones took place in the shelf-margin farther south and an even thicker accumulation of biocalcisiltites took place on the slope in Port Jervis area (Lindemann and Feldman, 1987).

13.2: SAMPLING LOCATIONS:

Figure 13.2 shows the sampling locations of the Onondaga Formation. Most of the samples were collected from its outcrop belt along the edge of the Devonian exposures

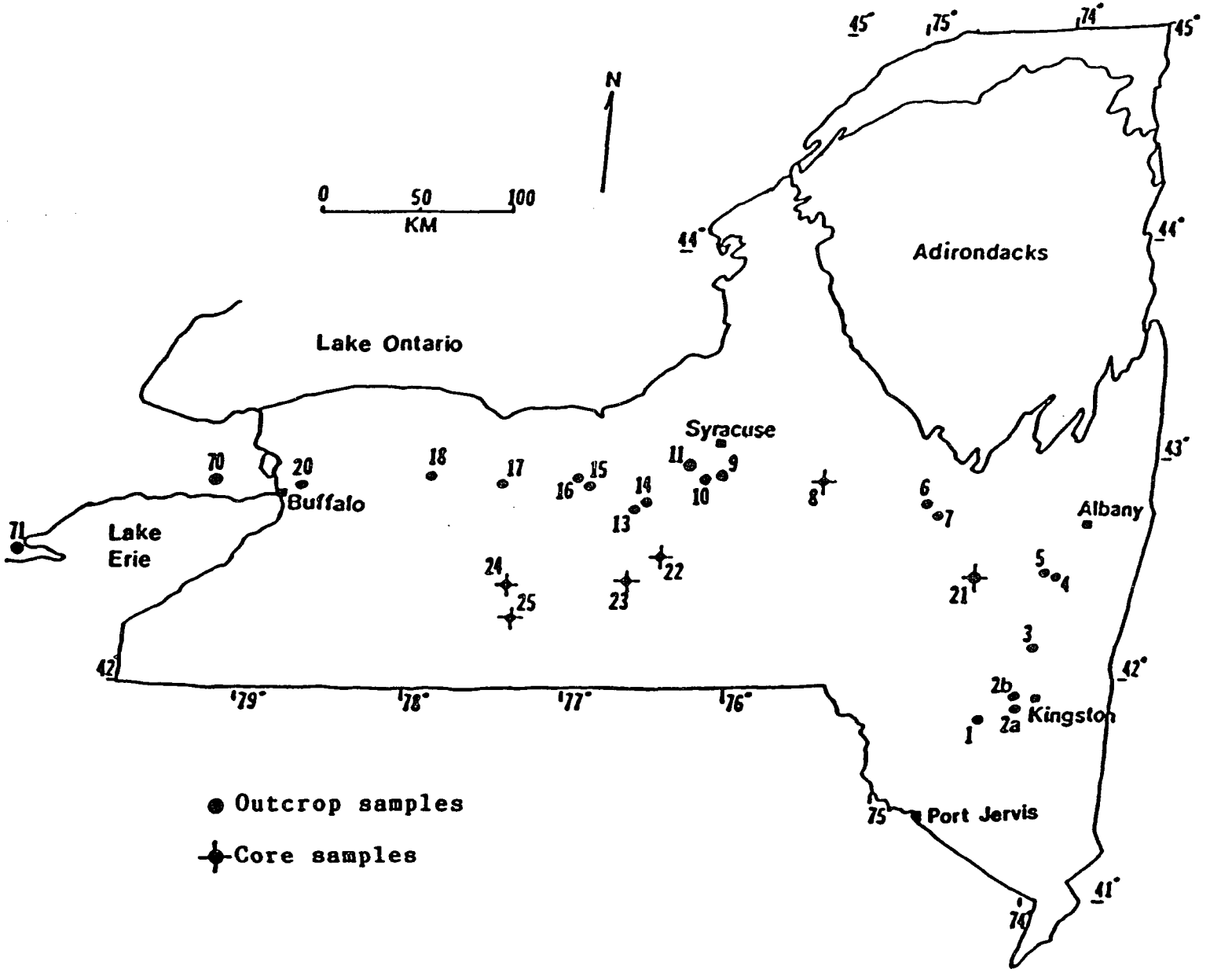

Figure 13.2: Sampling locations of the Onondaga Formation.

in New York. Two sampling locations are from the Ontario Province. The samples from southcentral New York (fig. 13.2) are core samples.

13.3: GENERAL PETROGRAPHY OF THE SAMPLES:

The petrographic characters of the Onondaga samples vary considerably across the region and often from sample to sample within the same locality. In general, the samples south of the Helderberg Mountains (locations 1, 2 and 3, fig. 13.2) are micrites or skeletal-peloidal wackestones. The Onondaga rocks in these locations are cut by thin calcite-healed fractures which are primarily vertical to bedding and secondarily, parallel and subparallel to bedding. The fractures are generally less than 1cm in width and many are thinner than 1mm (fig. 13.3a). The calcite spar in these fractures is generally twinned.

Samples from the Albright, Robert's Hill and Mount Tom bioherms (locations 4, 5 and 6; see Oliver, 1976) are coral-crinoidal grainstones and packstones. Many of the coral chambers have been filled by calcite cement that generally range from microspar along the septal wall to coarse spar in the center of the chambers (fig. 13.3b). Sparry calcite is also found in interskeletal vugs and shelters around coral particles. Rarely, microquartz is found to partially replace crinoid ossicles. Cement-healed fractures have not been observed or sampled in these locations.

From Cherry Valley (location 7) all the way to southeastern Ontario (locations 70 and 71), partial silicification of the Onondaga carbonates, especially of the skeletal components, becomes a common feature (fig. 13.4). Quartz-replacement occurs in the form of fibrous and locally spherulitic chalcedony, granular microquartz, and megaquartz. Bivalve shells and crinoid ossicles are more prone to replacement by chalcedony (fig. 13.4a) whereas the coral chambers are generally filled by micro- and megaquartz (fig. 13.4b). Where calcite and quartz coexist in the same coral chamber, quartz appears to have precipitated early, either growing directly on the septal wall or on an earlier, fine drusy calcite lining the wall. The quartz is then followed by subhedral sparry calcite which generally fills the remaining space (fig. 13.4b).

Cement-healed fractures are again observed in samples from locations 8, 10 and 13. The cement includes sparry calcite and, at locations 10 and 13, both calcite and saddle

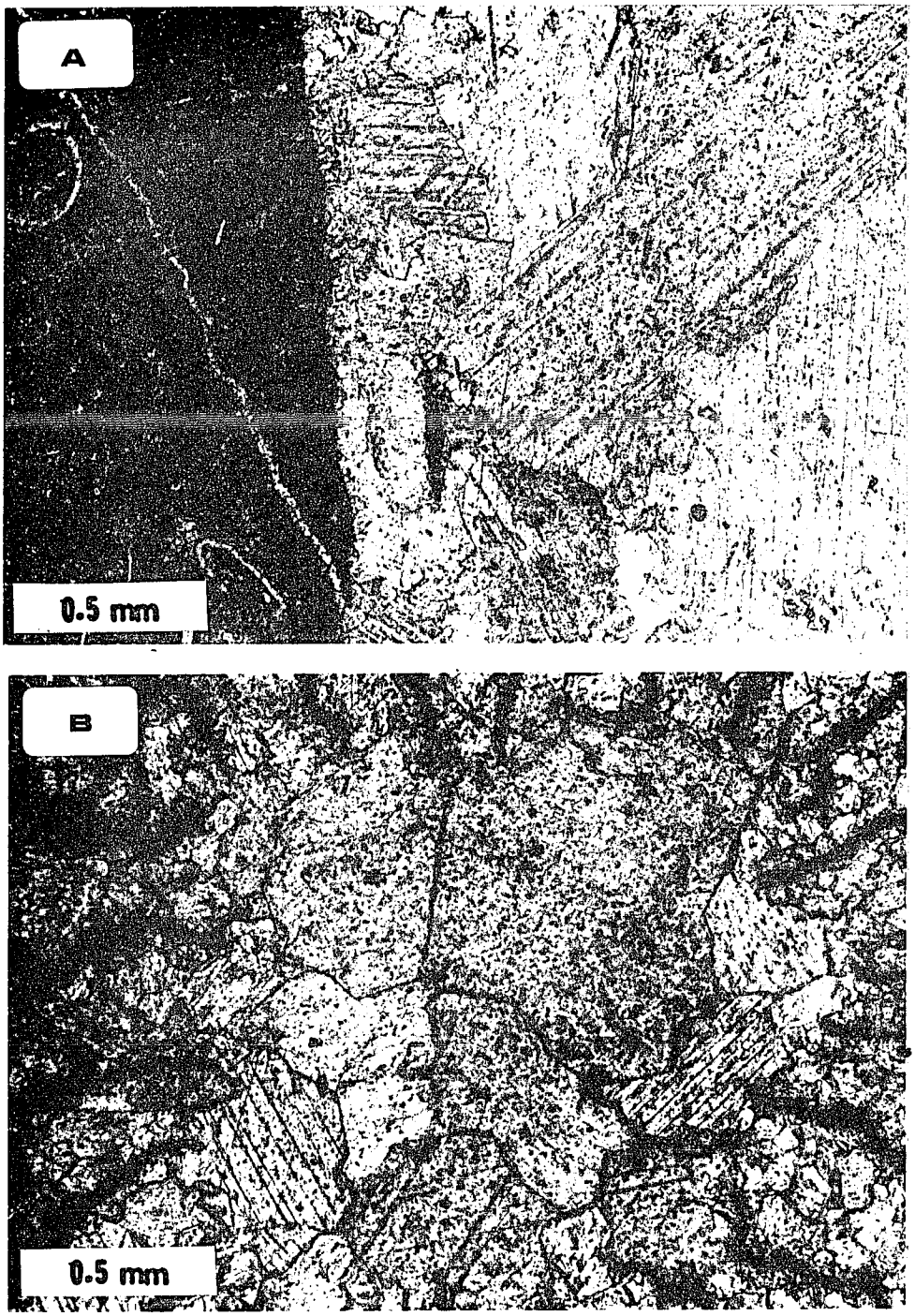

Figure 13.3: Photomicrographs of Onondaga samples. (A) Part of a thin vertical fracture in dark micritic limestone filled with twinned sparry calcite. Location- 1. (B) Horizontal section through a solitary rugose coral showing coarse sparry calcite in the central cavity and finer calcite cement in the surrounding chambers. Location 5.

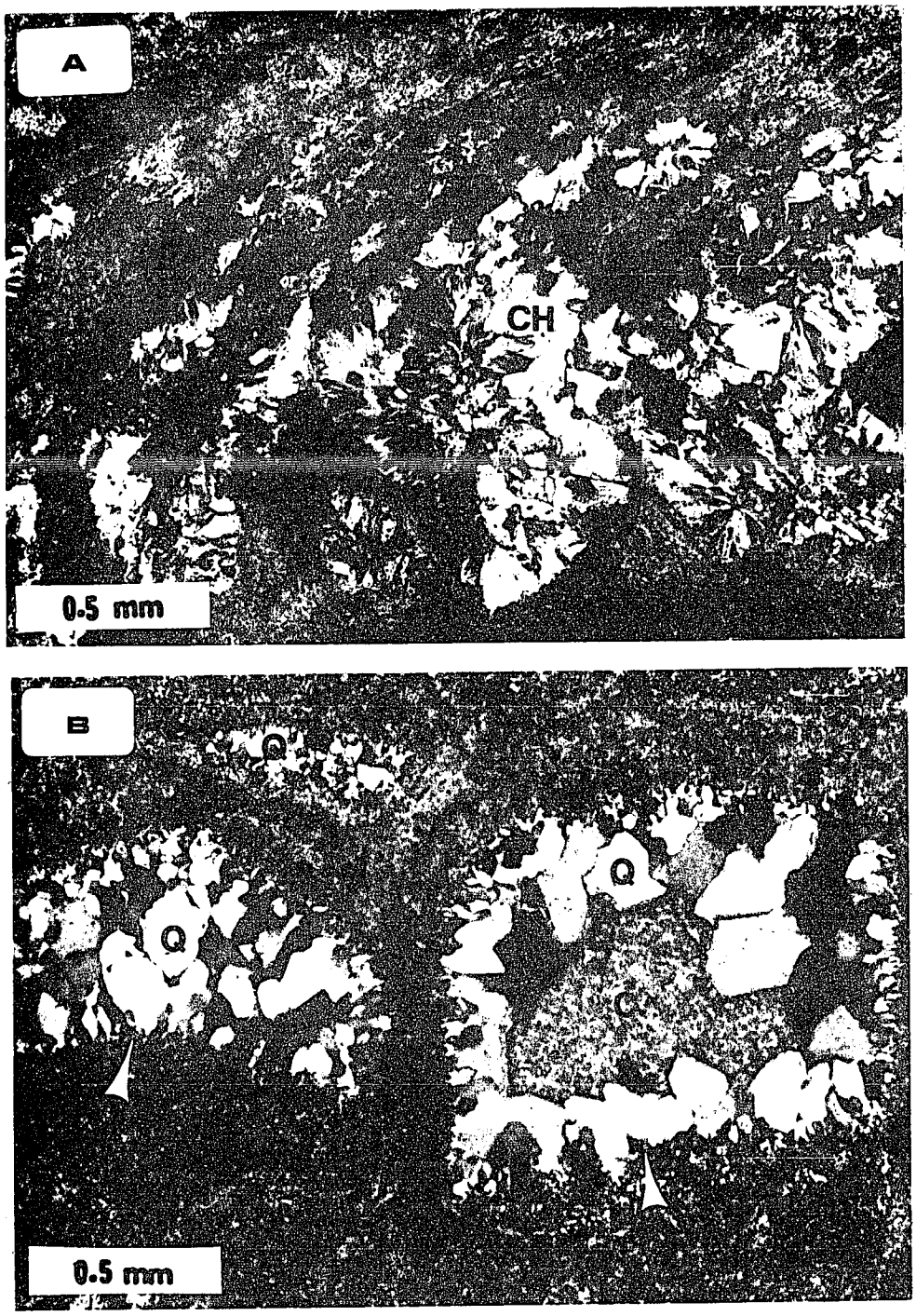

Figure 13.4: Photomicrographs of Onondaga samples. (A) A bivalve shell partially replaced by spherulitic chalcedony. Location - 8. (B) Three coral chambers lined by an early rim of small, bladed calcite (arrows) which is followed by granular quartz (Q). Quartz completely fills the two coral chambers on the left, but is followed by coarse sparry calcite (C) in the chamber at right. Location - 7.

dolomite (fig. 13.5a). The saddle dolomite in these fractures always grow directly on the fracture walls and calcite either coats the saddle dolomite or grows on the wall not occupied by saddle dolomite (fig. 13.5a). West of location 10, healed fractures were not observed or sampled.

Between locations 11 and 16 (fig. 13.2), the Onondaga rocks are mainly micrites and skeletal-peloidal wackestones. Only in location 13, skeletal grainstone-packstone fabric was observed. West of location 16, all the samples are from coral-crinoidal grainstones and packstones. These samples are from various bioherms in western New York and southeastern Ontario (Oliver, 1976).

The core samples from locations 22, 23, and 25 in southcentral New York (fig. 13.2) are micrites and skeletal wackestones. Samples from locations 22 and 25 show vertical calcite-healed microfractures. In addition, sparry calcite occurs in skeletal molds (fig. 13.5b). Core samples from location 24 represent a prominent subsurface bioherm (Turner, 1977). The samples are coral-crinoidal grainstones which show considerable vuggy and intra-skeletal porosity.

13.4: FLUID-INCLUSION DATA:

The fluid-homogenization (Th) and melting (Tm) temperatures of the Onondaga Formation have been measured primarily in calcite and secondarily in quartz and dolomite cements. Figure 13.6 shows the Th histograms for every location of the Onondaga Formation. The calculated maximum homogenization temperatures (Th_{max}) are also shown for each locality. The cements in which the Th and Tm were measured are from healed fractures and veins at locations 1, 2, 3, 8, 10, 13 and 22, and from inter- and intraparticle spaces at other locations. Table 13.1 shows the measured 'Tm's, corresponding 'Th's and calculated salinities. In figure 13.7 the Th_{max} values are plotted against sample locations. The raw Th data is presented in Appendix I.

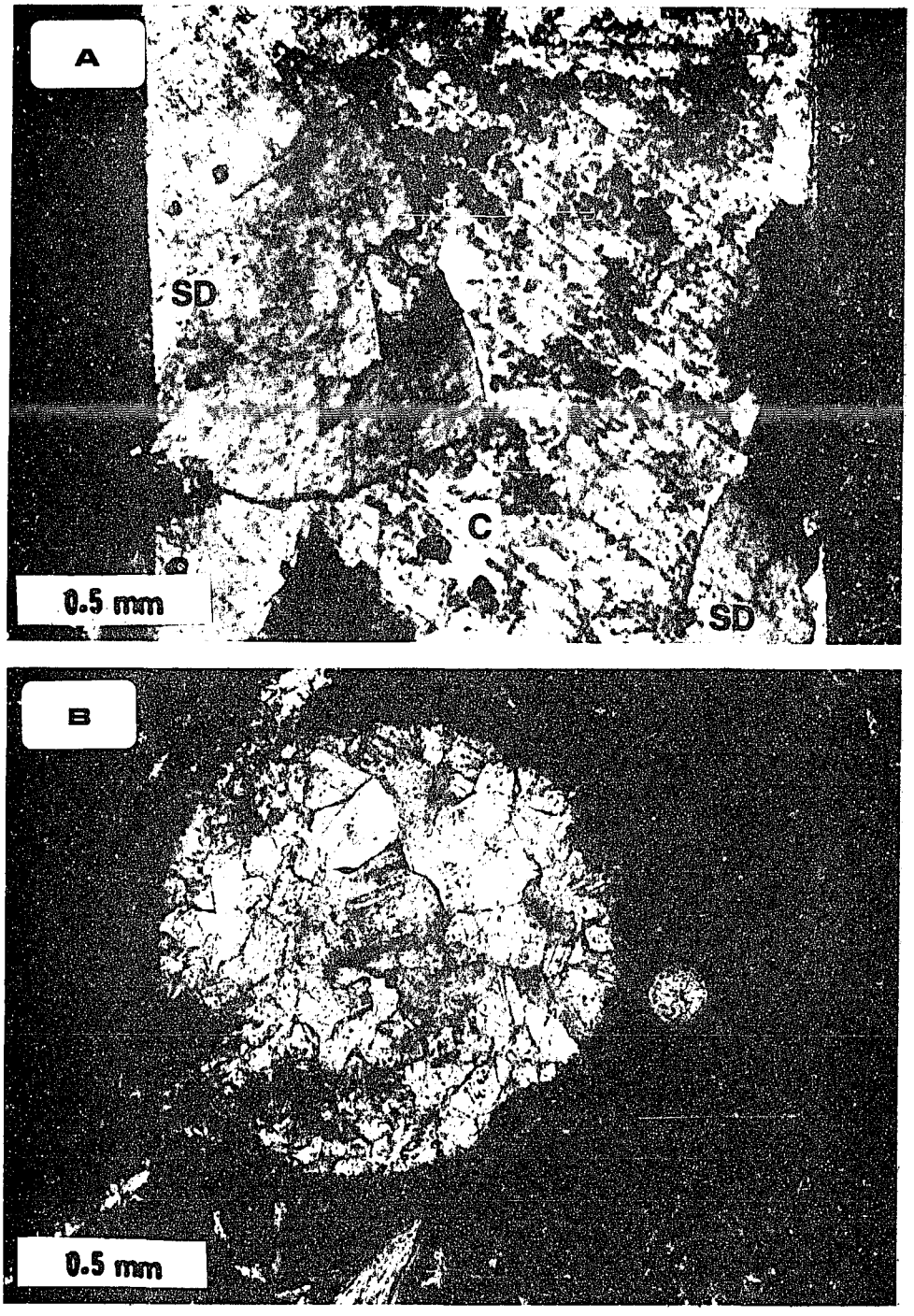

Figure 13.5: Photomicrographs of Onondaga samples. (A) A vertical fracture in micritic limestone filled with saddle dolomite (SD) that precipitated directly on the fracture wall and calcite which grows on saddle dolomite or on the wall not occupied by saddle dolomite. Location - 10. (B) Skeletal mold in wackestone filled with sparry calcite. Location - 22.

Figure 13.6: Fluid-homogenization temperature (Th) histograms for the Onondaga samples from various study locations. The maximum homogenization temperatures (Th_{max}) are also shown.

LOCATION - 1

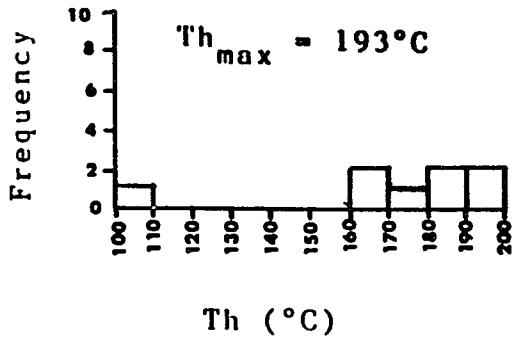

LOCATION - 2

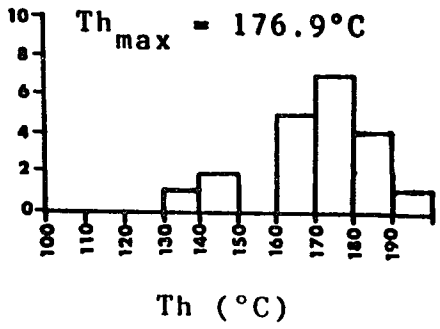

LOCATION - 3

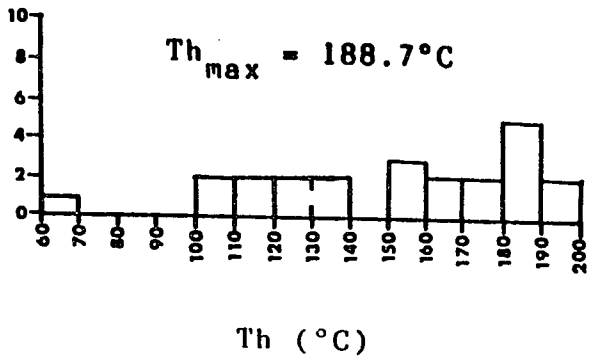

LOCATION - 4

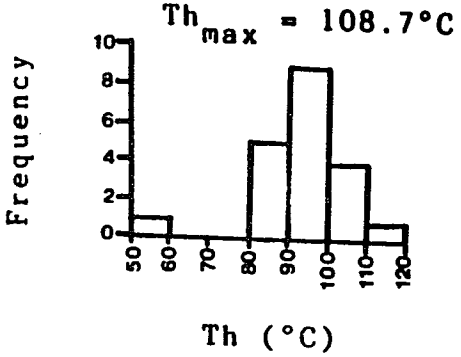

LOCATION - 5

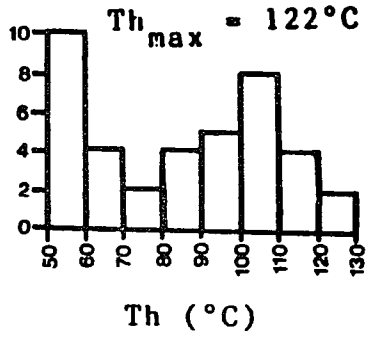

LOCATION - 6

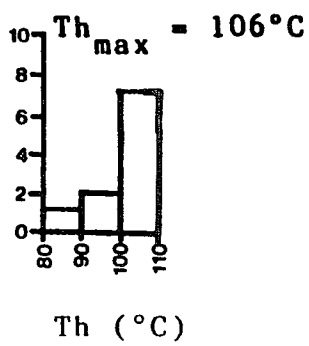

LOCATION - 7

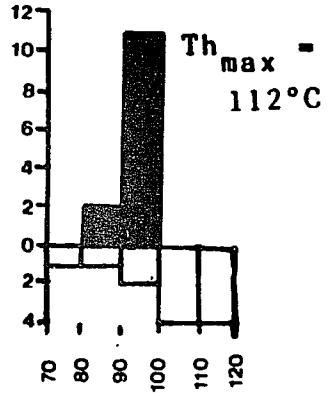

CALCITE QUARTZ DOLOMITE

LOCATION - 8

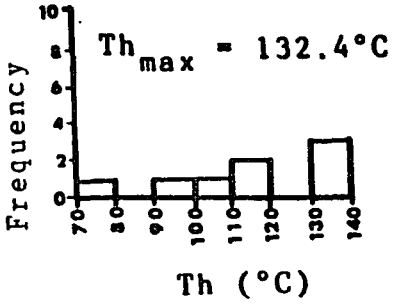

LOCATION- 9

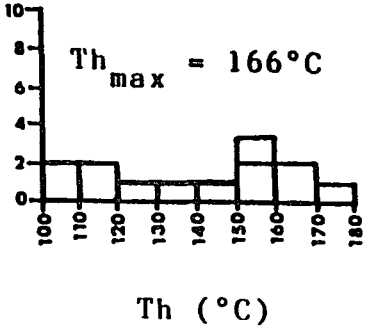

LOCATION- 10

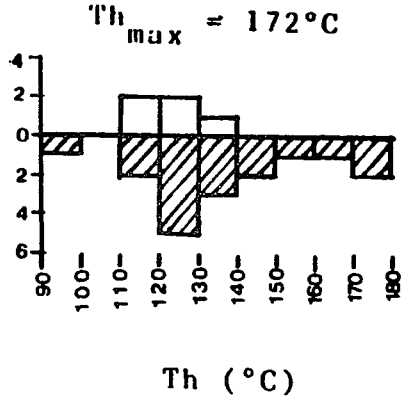

LOCATION-13

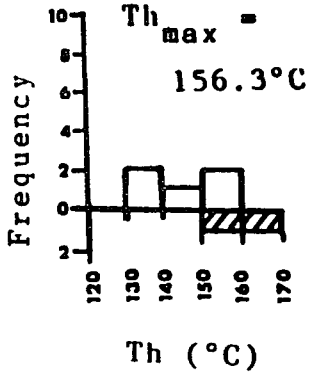

LOCATION-17

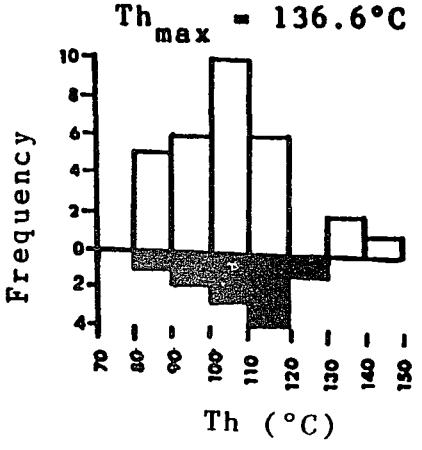

LOCATION-18

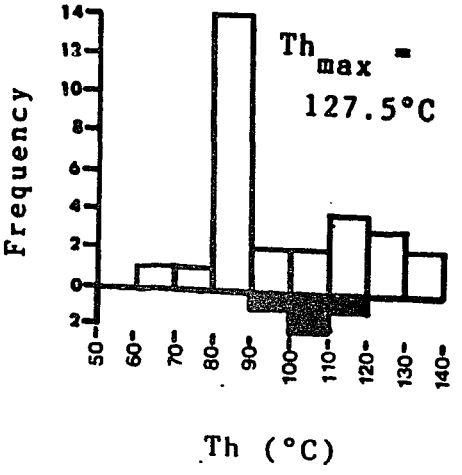

LOCATION-20

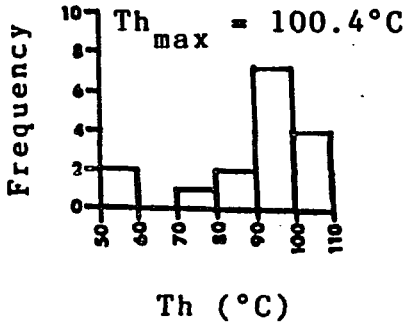

LOCATION-70

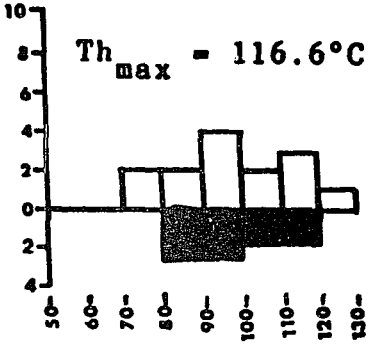

LOCATION-71

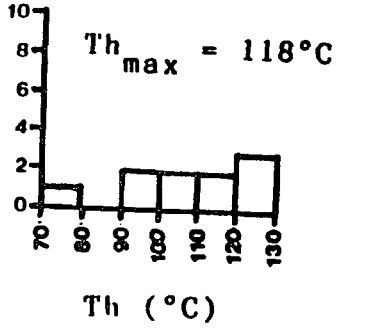

LOCATION-22

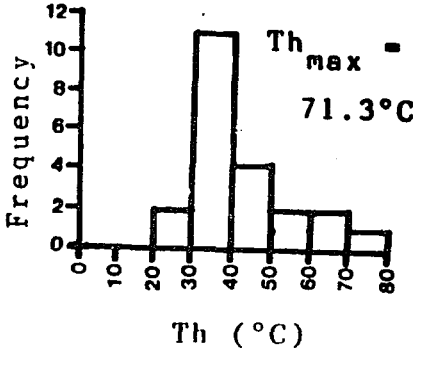

LOCATION-24

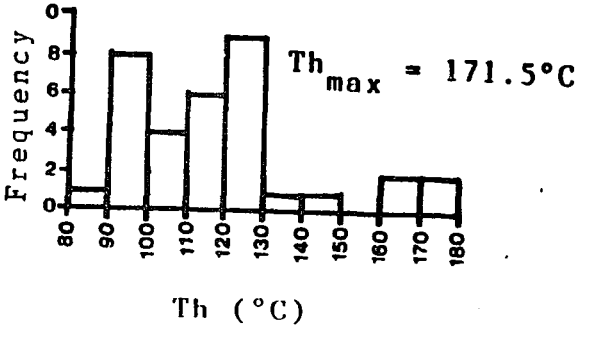

Table 13.1: Melting temperatures (Tm), corresponding homogenization temperatures (Th) and calculated salinity (equivalent wt% NaCl) of fluid inclusions in the Onondaga Formation.

Location	Type of cement	Tm (C)	*Salinity (wt% NaCl)	Th (°C)
1	Fracture-filling calcite	-16.3	19.8	190
2	Fracture-filling calcite	-11.4	15.4	180.3
		-15.0	18.8	176.3
3	Fracture-filling calcite	-0.3	0.5	182.5
		-1.2	2.0	199
		-4.2	6.7	155
		-3.2	5.3	123.9
5	Calcite in coral chambers	-4.6	7.3	115.6
6	Calcite in coral chambers	-16.0	19.6	101
		-14.0	17.9	101.5
7	Megaquartz in coral chambers	-9.8	13.7	94.1
8	Fracture-filling calcite	-13.0	17.0	133.4
10	Fracture-filling dolomite	-15.6	19.3	144
		-14.7	18.5	165.8
13	Fracture-filling dolomite	-15.9	19.5	152.3
17	Calcite in coral chambers	-9.0	13.5	133
18	Calcite in coral chambers	-10.3	14.3	92
72	Vug-filling calcite	-15.0	18.8	155
		-17.9	21.1	130.2
24	Calcite in coral chambers	-17.7	20.9	126

* Salinity was calculated according to Potter et al.'s (1978) method (section 4.3.1)

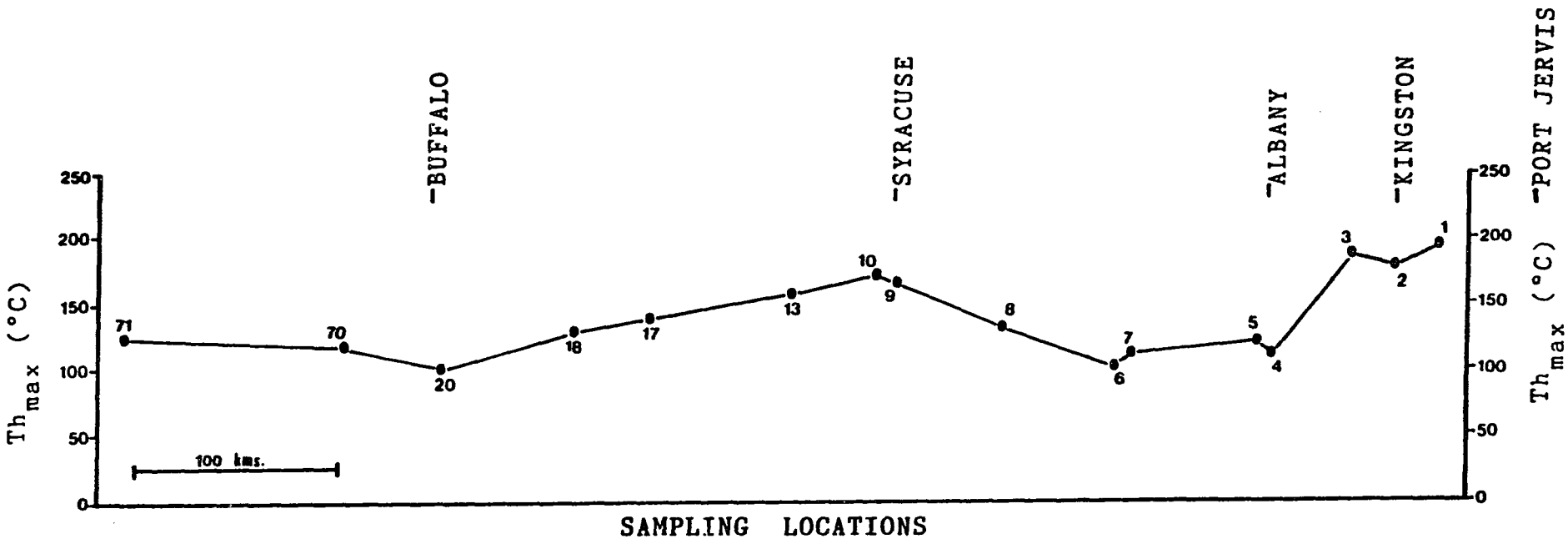

Figure 13.7: Th_{max} of the Onondaga carbonates plotted against sample locations.

13.5: STABLE ISOTOPE DATA:

Oxygen and carbon isotopes were measured in vein- and vug-filling cements of 13 samples of the Onondaga Formation. Table 13.2 presents the measured $\delta^{18}O$ and $\delta^{13}C$ values and the paleotemperatures calculated from them.

Table 13.2: Oxygen- and carbon-isotope data measured in cements of the Onondaga Formation, and calculated paleotemperatures.

Location no.	Cement type	$\delta^{18}O$ ‰PDB	$\delta^{13}C$ ‰PDB	#Calculated paleotemperature in (°C) for $\delta^{18}0$ = 2-8‰ SMOW
1	Calcite (fracture)	-5.98	+0.8	58 - 101
2	Calcite (fracture)	-4.78	+0.7	51 - 92
3	Calcite (fracture)	-8.9	-0.7	78 - 125
5	Calcite	-5.98	+2.8	58 - 101
	(coral cham.)	-4.0	+3.4	46 - 86
6	Calcite (coral cham.)	-3.75	+3.0	45 - 85
*7	Calcite	-6.6	+2.1	62 - 115
	(inter-particle)	-7.2	+2.0	66 - 110
8	Calcite (fracture)	-7.3	+1.2	67 - 112
9	Calcite (skeletal mold)	-2.78	+2.1	40 - 78
10	Dolomite (vug)	-8.5	+2.4	108 - 170
17	Calcite (coral cham.)	-10.25	+0.6	87 - 137
18	Calcite (coral cham.)	-7.92	+1.1	71 - 117
20	Calcite (coral cham.)	-7.44	+1.1	68 - 113
22	Calcite	-8.5	+1.6	75 - 122
	(fracture)	-7.8	+3.4	70 - 116

(Table 13.2 continued)

23	Calcite (fracture)	-8.9	-3.3	78 - 125
24	Calcite (inter-particle)	-2.97	+1.7	40 - 79

Calculation based on Craig's (1965) equation for calcite and Fritz and Smith's (1970) equation for dolomite (see section 4.6). * Data from Gurney (1986).

13.6: ORGANIC MATURATION DATA:

The Onondaga limestones contain an abundance of kerogen organic matter. Thermal alteration index (TAI) of which was measured in samples of fifteen locations (table 13.3). The kerogen in these samples are dominated by degraded herbaceous and relic amorphous-sapropelic material; inertinite is generally third in abundance and a few samples show sparse woody-structured materials. There appears to be no correlation between the amount of different types of organic matter present in a sample with its TAI.

13.7: INTERPRETATION

13.7.1: Paragenetic sequence of cements:

Sparry calcite cement in the healed fractures of southeast New York (locations 1, 2 and 3) post-date lithification and most compaction features. Although these cements exhibit twinnning, which may have resulted from subsequent tectonic stress, they are not cut across by bedding parallel stylolites which is commonplace in the host rock. This observation indicates that the fractures were healed after compaction and stylolitization, probably under the overburden load, had ended.

Sparry calcite cement found in coral cavities and inter-particle spaces in the Albright, Roberts Hill and Mount Tom bioherms (locations 4, 5 and 6 respectively) are believed to have formed earlier than the fracture-filling cements of southeastern New York. It is unlikely that while the Onondaga rocks of southeastern New York were well cemented by the time the fractures formed, those at locations 4, 5 and 6 (fig. 13.2) were still very much porous.

Table 13.3: Thermal alteration index (TAI), equivalent vitrinite reflectance (Ro) and calculated maximum burial temperatures of some carbonate samples of the Onondaga Formation.

Location no.	Sample no.	TAI	% Ro	*Calculated maximum burial temp. (° C)
2	OX-2	2.3	0.7	108
3	OX-3A	3.2	1.25	182
4	AB-58	3.0	1.0	154
5	R-74	2.7	0.93	145
7*	___	___	1.48	204
8	OTO-1	2.5	0.8	126
10	OG-7	2.8	0.95	148
11	OG-8	2.9	0.98	152
14	OG-10	2.3	0.7	108
16	OG-12	2.2	0.6	89
	OG-12A	2.3	0.7	108
17	OG-13	2.8	0.95	148
18	L-11A	3.3	1.38	195
20	OG-15	2.3	0.7	108
21	OG-23	3.6	1.75	225
22	CGO-2	2.3	0.7	108
24	SYO-3	2.7	0.93	145

Maximum burial temperature calculated according to Barker and Pawlewicz's (1986) method (section 4.4).
* Data from Gurney and Friedman (1987). No TAI value available.

In the Onondaga rocks between eastcentral New York (location 7) and Ontario (location 71), quartz precipitation within coral chambers followed an early rim of small, bladed calcite crystals (fig. 13.4b). Rim cements of such morphology are commonly of phreatic freshwater origin (Longman, 1980; Scoffin, 1987). Granular quartz grows directly on this rim cement, or is separated from it by a sharp, dissolution boundary. Since coarse sparry calcite, when found, fills the last remaining space in the coral chambers (fig. 13.4b), a paragenetic sequence of bladed, calcite rim cement to quartz to sparry calcite is inferred in the coral chambers. The sequential position of inter- particle sparry calcite cement (no interparticle quartz cement is found) in the same rocks with

respect to the cements of coral chambers is not clear. However, inter- particle calcite cement also grows on the early rim cement that envelopes most particles. Therefore, it is, like the quartz of the coral chambers, younger than the rim cement. Fluid-inclusion data (section 13.7.2) sheds more light on the possible paragenetic sequence of inter-particle cements.

Fracture-filling saddle dolomite and calcite of central New York (locations 8, 10 and 13) are believed to be of later origin than the inter-particle cements discussed above, because the fractures, like those in southeastern New York, have cut through well lithified rocks (fig. 13.5a). The saddle dolomite in fractures of locations 10 and 13 must also have formed earlier than calcite of the same fractures (fig. 13.5a). From their geographical proximity (fig. 13.2), it can be assumed that fractures at location 8 and subsurface location 22 were probably cogenetic with those of locations 10 and 13, although they contain no dolomite. Whether these fractures and the cements in them were contemporaneous with the same of southeastern New York can not be established from petrographic study.

13.7.2: Fluid-inclusion data:

The Onondaga carbonates, like the other units in this study, exhibit a wide range of Th at every location (fig. 12.6), suggesting that these 'Th's recorded a relatively long history of trapping (and cementation) of fluids of various temperatures. Even, the Th range in fracture-filling cements (of locations 1, 3 and 10, for example) are large indicating that the fractures remained, probably intermittently, open for long enough to allow cement precipitation from fluids of widely varying temperatures.

The high Th_{max}s in the Onondaga Formation were, in most cases, measured in fracture-filling cements (for example, at locations 1, 2, 3, 10 and 13, figs. 13.6, 13.7). This probably implies that the cement in these fractures continued to form at the deepest burial (highest temperature) environment. The relatively low Th_{max} at locations 4, 5, 6, and 7 between Albany and Syracuse, and between location 17 and 71 were calculated from Th measured in inter- and intra-particle calcite cements. The general Th range in these cements and their lower Th_{max} are consistent with petrographic interpretation

(section 13.7.1) that these cements formed earlier (probably at a shallower depth and lower temperature) than the fracture-filling cements. The megaquartz cement in the coral chambers of locations 7, 17, 18, 70 and 71 in general also shows lower Th than the latest calcite of the coral chambers (fig. 13.6): the overlap between Th of calcite and quartz in the histograms of these locations is due to the fact that Th of interparticle calcite of these locations are also included in the histograms. Interparticle calcite and quartz in coral chambers in samples of these locations thus appears to have formed over a similar temperature/time interval. This is also consistent with the inferred paragenetic sequence of cements (section 13.7.1).

However, exceptions are noted at locations 9 and 24 where a high Th_{max} occurs in calcite of skeletal molds, and at locations 8 and 22 where low Th_{max} occurs in fracture-filling calcite. Two possibilities exist for the data at location 9 and 24: either the calcite in the studied skeletal molds formed in a similar temperature/time interval as that of fracture-filling cements of the nearby locations 10 and 13, or formed earlier at a lower temperature, but the inclusions have later re-equilibrated to a higher temperature. The fracture-filling cements of locations 8 and 22 either formed in fractures of a different generation (that formed at lower burial temperatures) or in fractures of the same generation, but reflect the maximum temperatures reached at those locations. These problems will be resolved in chapter 15 where paleotemperature signatures of different rocks units in the same or nearby locations are compared.

Salinity of the measured inclusion fluids of the Onondaga Formation, calculated from their 'Tm's, range between 0.5 and 22 equivalent wt% NaCl (table 13.1). Most of these (75%) calculated salinities are greater than 10%, representing hypersaline brines. Some relatively high 'Tm's (low salinities), especially in the fracture-filling calcite of location 3 (table 13.1), are probably incongruent melting temperatures of hydrohalite and therefore, not true representatives of fluid salinity (Roedder, 1962).

Again, there appears to be no systematic relationship between Th and corresponding Tm of the measured two-phase inclusions of the Onondaga Formation. It probably means that the salinity and temperature of the diagenetic fluids varied locally independent of one another.

13.7.3: Stable-isotope data:

The $\delta^{18}O$ values of calcite and dolomite cements of the Onondaga Formation range between -2.78 and -10.25‰ PDB (table 13.2). Light oxygen isotope values of this range is common in carbonate cements of deep burial origin (Mattes and Mountjoy, 1980; Zenger, 1983; Prezbindowski, 1985; Woronick and Land, 1985; Friedman, 1987a,b; Lee and Friedman, 1987; Saigol and Bjorlykke, 1987; Zenger and Dunham, 1987; Kaufman et al. 1990). The slightly positive $\delta^{13}C$ values of the Onondaga samples are also consistent with carbon isotope values of deep-burial cements reported in the above publications.

As seen in other units in this study, the maximum paleotemperatures calculated on the basis of oxygen isotope values are also generally much lower than Th_{max} in the same locations of the Onondaga (compare fig. 13.6 and table 13.2). Only at locations 5, 6, 7, 17, 18 and 20 the Th_{max} and maximum isotopic paleotemperatures are similar. The possible reasons for this inconsistency between the two data sets have been discussed before (sections 4.6, 12.6.3).

13.7.4: Organic maturation data:

Paleotemperatures calculated from the TAI values of the Onondaga Formation vary widely and independently of Th_{max} and inferred highest isotopic paleotemperatures of the same sample locations (compare fig. 12.6 and table 13.2 and 13.3). In a few locations (3, 8, 17, 20), the TAI temperatures and Th_{max} are very similar, but in others there is no match. Similarly, the TAI temperatures are within the range of inferred isotopic temperatures only in locations 10, 20 and 22.

Problems in application of TAI data have been discussed previously (section 4.4). Since much of the organic matter of the Onondaga samples are of relic or degraded varieties, it can be assumed that much of these TAI data under-represent the true maturity of the samples.

CHAPTER 14: THE MARCELLUS FORMATION

14.1: STRATIGRAPHY AND DEPOSITIONAL HISTORY:

The Middle Devonian (Erian) Marcellus Formation is the basal unit of the Hamilton Group and it conformably overlies the Onondaga Limestone (fig. 14.1). Its thickness ranges from nearly 250m in southeastern New York to less than 10m in the westernmost New York (Rickard, 1975; COSUNA Project, 1985). The Marcellus Formation occurs throughout northern and central Appalachians in northeastern New Jersey, Pennsylvania, Maryland, Virginia, and West Virginia, thinning from southeastern New York toward southern West Virginia, where it finally disappears (COSUNA chart, 1985).

In New York, the Marcellus Formation consists of very thinly bedded to massive, black and dark gray shale with minor argillaceous limestones and abundant pyrite and calcareous nodules (Van Tyne, 1982; Fakundiny et al. 1989). It is relatively unfossiliferous and consists mainly of pelagic ammonoids and conodonts and epipelagic brachiopods. Lithology, presence of pyrite and sparsity of benthic fauna suggest that the Marcellus shale was deposited in a dysaerobic basin (Fakundiny et al. 1989). It represents the basal Portage-A facies (distal basin) of the Catskill Deltaic complex (fig. 2.6) and marks the onset of the Acadian Orogeny in this region.

The Marcellus Formation in New York has been divided into several members (fig. 14.1). The oldest, Bakoven Shale is confined to eastern New York. The lower part of the Bakoven Shale is correlative with the youngest member, the Seneca, of the Onondaga Formation in western New York (Rickard, 1975). The Upper Part of the Bakoven Shale is known as the Union Springs Shale in central New York (fig. 14.1). It is a sooty black shale that intertongues with and finally overlies the Seneca Member of the Onondaga Formation. The base of the Marcellus Formation is therefore time-trangressive to the west and reflects the gradual westward encroachment of siliciclastic sediments on a retreating carbonate shelf as the Acadian Mountains began rising in the east (see section 2).

In central and westcentral New York, a thin argillaceous limestone unit, the Cherry Valley Limestone, overlies the Union Springs (fig. 14.1). The Cherry Valley Limestone grades into sandstone in eastern New York. This thin limestone unit and similar younger units within the terrigenous deposits of the Hamilton Group probably represent brief pauses in clastic sediment

Figure 14.1: The outcrop belt (in black) and stratigraphic subdivisions of the Marcellus Formation in New York State. (Adapted from Rickard, 1975).

N
0
100 km
Adirondacks
Syracuse
Albany
Buffalo
Kingston
Port Jervis
EPOCH
SERIES
ROCK UNIT
MIDDLE DEVONIAN
ERIAN
MARCELLUS FORMATION
Buffalo
Syracuse
Albany
Port Jervis
SKANEATELES FM.
CARDIFF SHALE
BRIDGEWATER SHALE
OATKA CREEK SHALE
CHITTENANGO SH.
CHERRY VALLEY LS.
UNION SPRINGS SH.
BAKOVEN SHALE
ONONDAGA FM.

influx from the east as a result of shifts in Acadian tectonism. Overlying the Cherry Valley Limestone are the Chittenango and Cardiff shales in central New York and the Oatka Creek Shale in western New York (fig. 14.1).

14.2: SAMPLING LOCATIONS:

Figure 14.2 shows the sampling locations of the Marcellus Formation. Most of the samples were collected from its outcrop belt. Core samples were obtained from four locations (22, 25, 32 and 36).

14.3: ORGANIC MATURATION DATA:

Figure 14.3 shows the vitrinite reflectance histograms for Marcellus samples of various locations. TAI was also measured in the same and some additional samples (table 14.1). The lack of correlation between mean Ro and TAI is obvious from table 14.1. Moreover, the TAI values of samples from the same locations (for example, locations 36 and 33) are very different.

Unfortunately, all samples did not yield vitrinites or enough vitrinites for useful interpretation. For example, at location 94 the yield of kerogen was very low and no vitrinite could be identified. In samples from location 95, the kerogen found was of degraded herbaceous - amorphous type and it was impossible to differentiate between exinite and vitrinite and to get reliable reflectance reading from either (Geochem Lab, Houston, pers. comm.). Also, the mean Ro values for location 36 and 25 may not be very meaningful because of the low number (10 and 29, respectively) of available readings. In sample MC-1 of location 33 and MR-3 of location 34, the "severely altered" vitrinites (Appendix-J) have been omitted from mean Ro calculation.

14.4: CLAY DIAGENESIS DATA:

X-ray diffractograms of untreated and glycolated clay samples from various locations are shown in fig. 14.4 along with their illite crystallinity index. The peaks of important clay minerals and quartz are labelled in the diffractograms.

Table 14.2 shows the calculations involved in determining the percentage of illite in the studied samples. Complete XRD data is presented in Appendix - J.

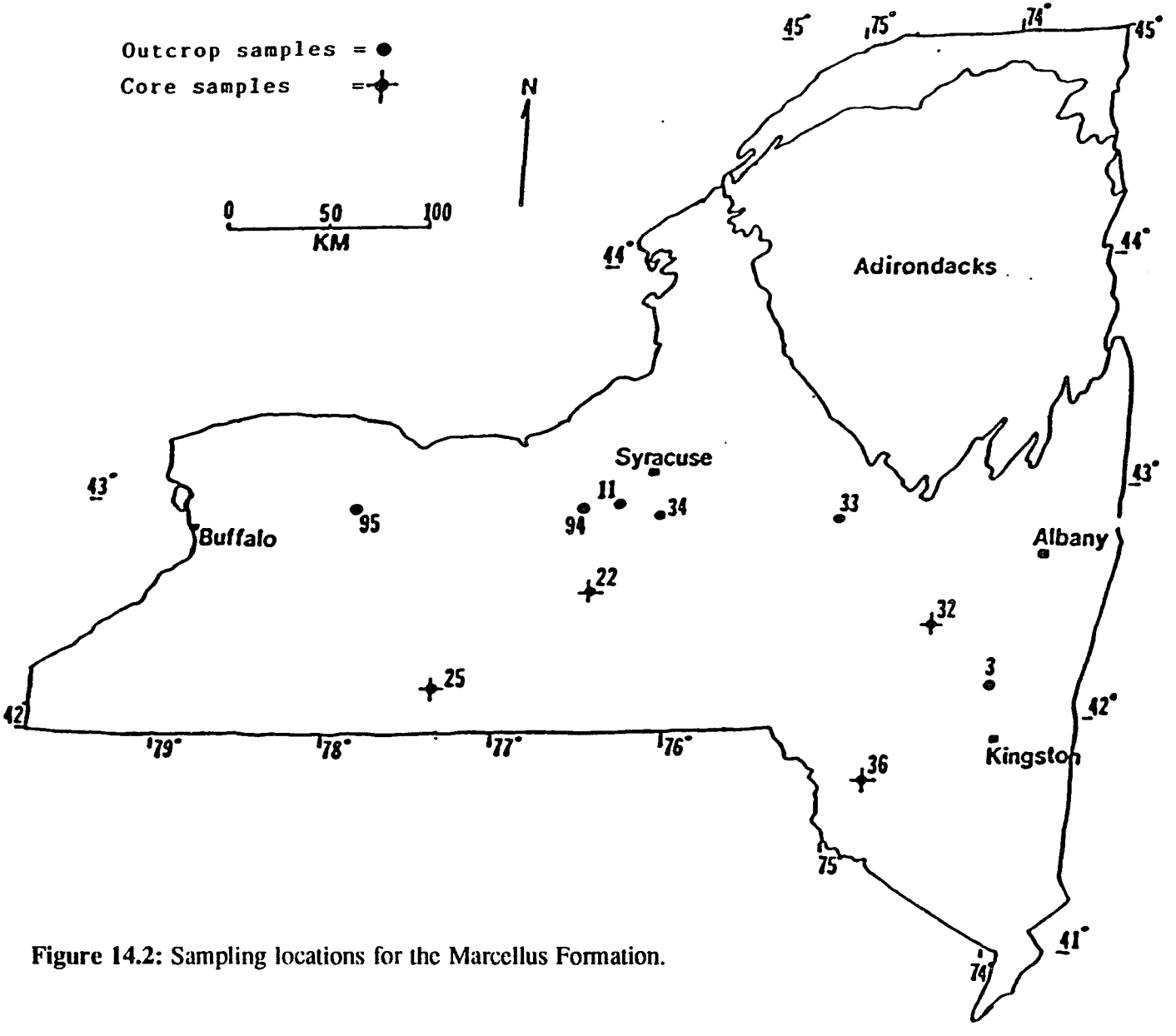

Figure 14.2: Sampling locations for the Marcellus Formation.

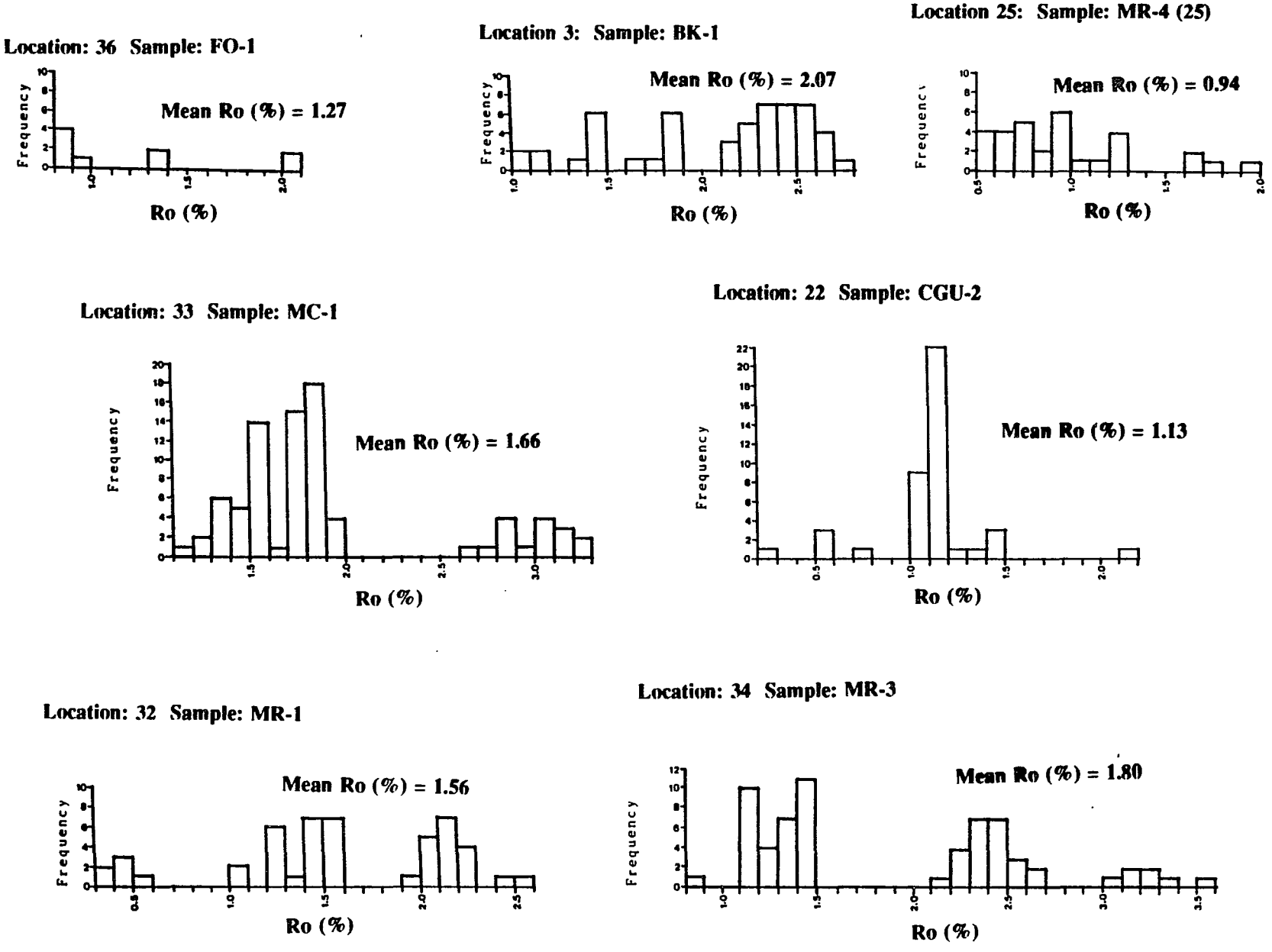

Figure 14.3: Vitrinite reflectance (Ro) histograms and mean Ro (%) of Marcellus samples from various locations.

Table 14.1: Table showing mean Ro and corresponding TAI of the Marcellus samples.

Sample loc.	Sample no.	Mean Ro(%)	TAI
36	FO-1	1.25	3.9
	FO-1A	____	2.4
3	BK-1	2.07	3.3
	BK-1A	____	3.4
32	MR-1	1.56	2.2
33	MC-1	1.66	2.4
	MR-2	____	3.2
34	MR-3	1.71	3.2
94	MR-5	____	2.8
95	MR-6	____	2.8
	MR-6A	____	2.6
22	CGU-2	1.13	3.3
25	MR-4(25)	0.94	2.5

14.5: FLUID-INCLUSION DATA:

At location-22, the Marcellus shale contains vertical and inclined fractures healed with sparry calcite. Fluid-homogenization temperatures (Th) are presented in the histogram of fig. 14.5 along with Th_{max}.

14.6: STABLE ISOTOPE DATA:

One vein-calcite sample from the Marcellus shale of location - 22 was analyzed for stable isotope ratios. The sample shows a $\delta^{18}O$ of -7.8‰ PDB and a $\delta^{13}C$ of +3.4‰ PDB. Using Craig's (1965) equation and a $\delta^{18}O_{water}$ of 2-8‰ SMOW, a temperature range of 70-116°C is obtained.

Figure 14.4: X-ray diffractograms of untreated (**a**) and glycolated (**b**) clay samples from the Marcellus Formation of various locations. Illite crystallinity index (I.C) are also shown.

LOCATION: 36 SAMPLE: FO-1

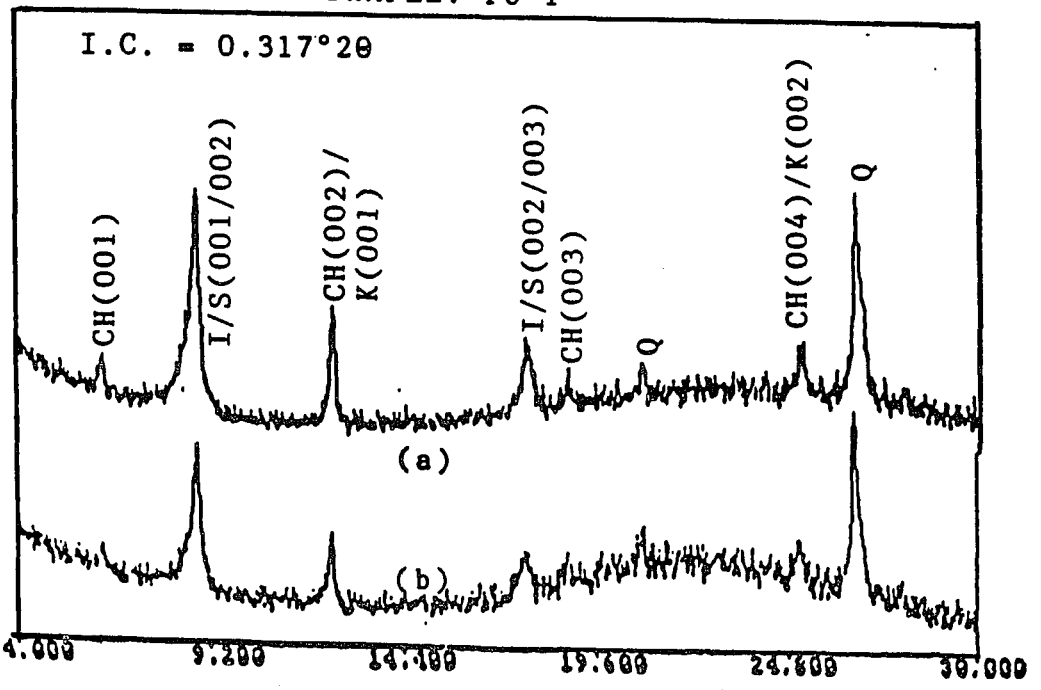

LOCATION: 3 SAMPLE: BK-1

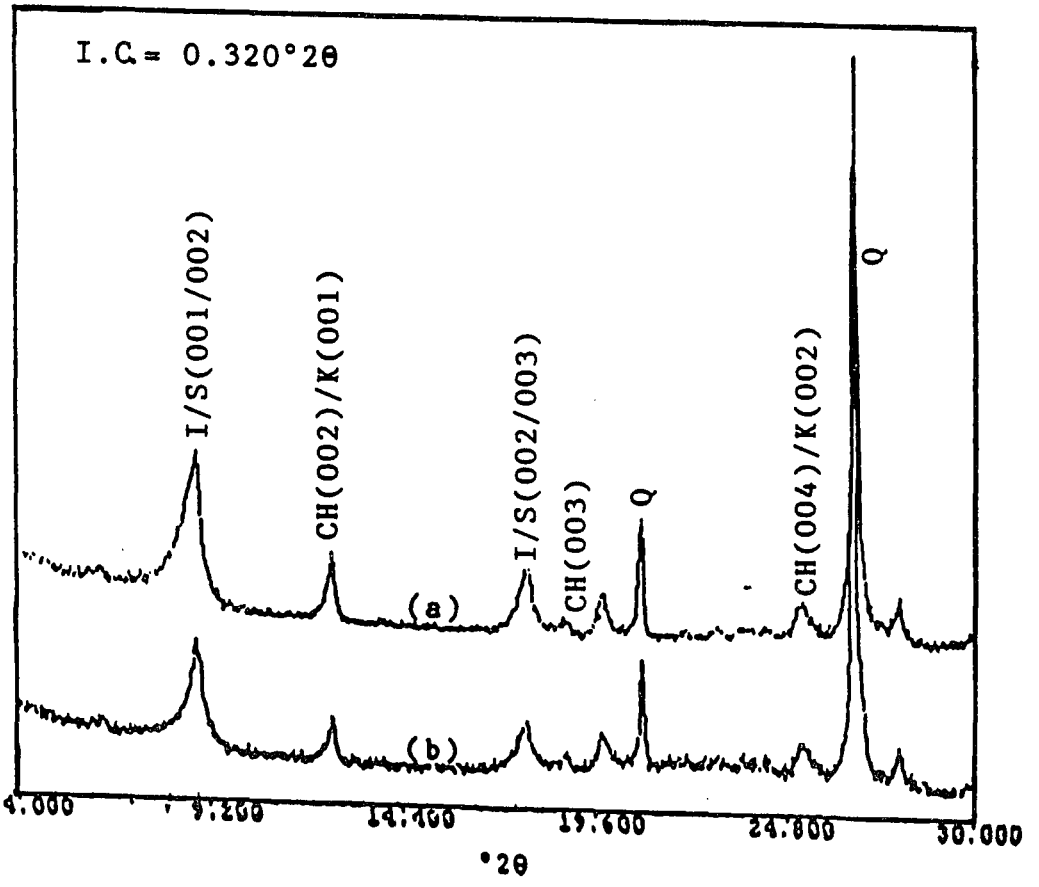

LOCATION: 32 SAMPLE: MR-1

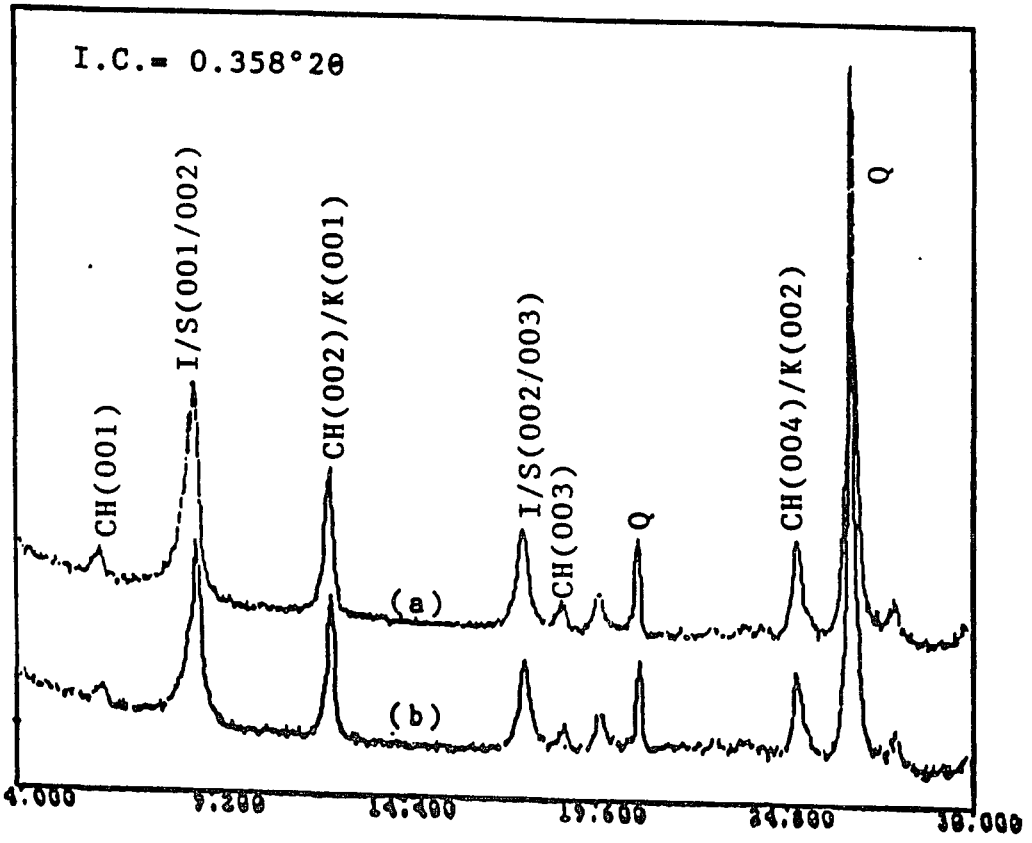

LOCATION: 33 SAMPLE: MR-2

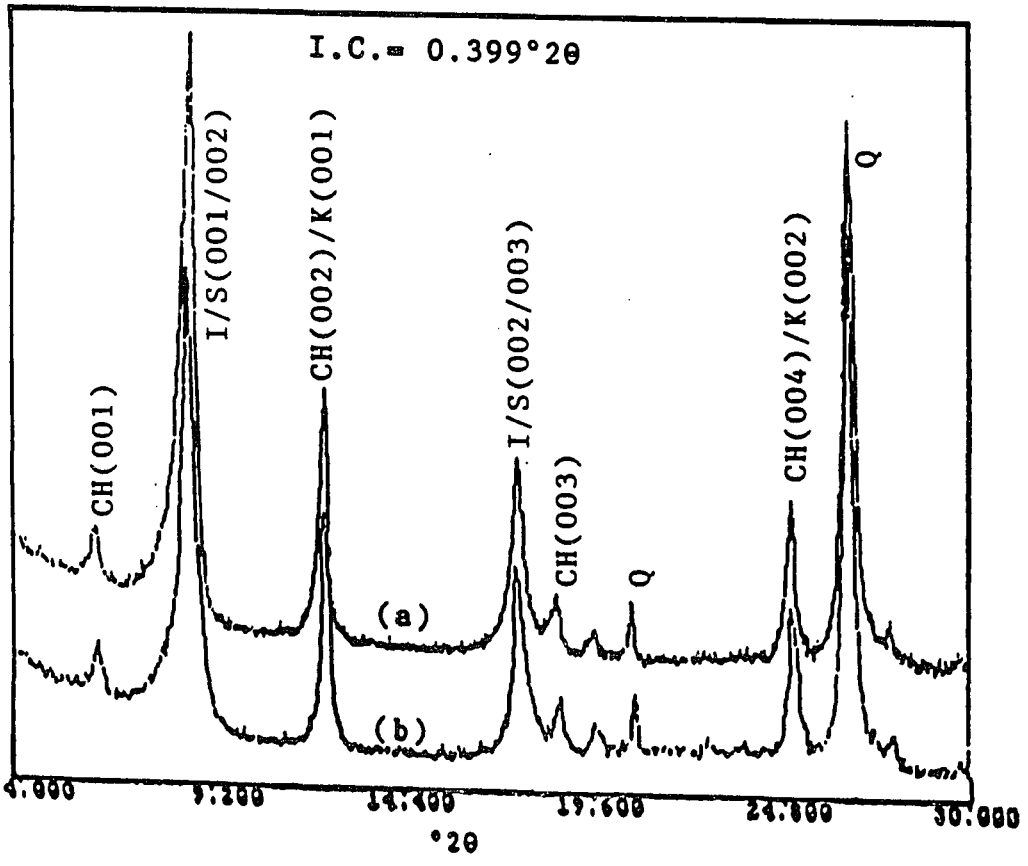

LOCATION: 11 SAMPLE: MC-5/6

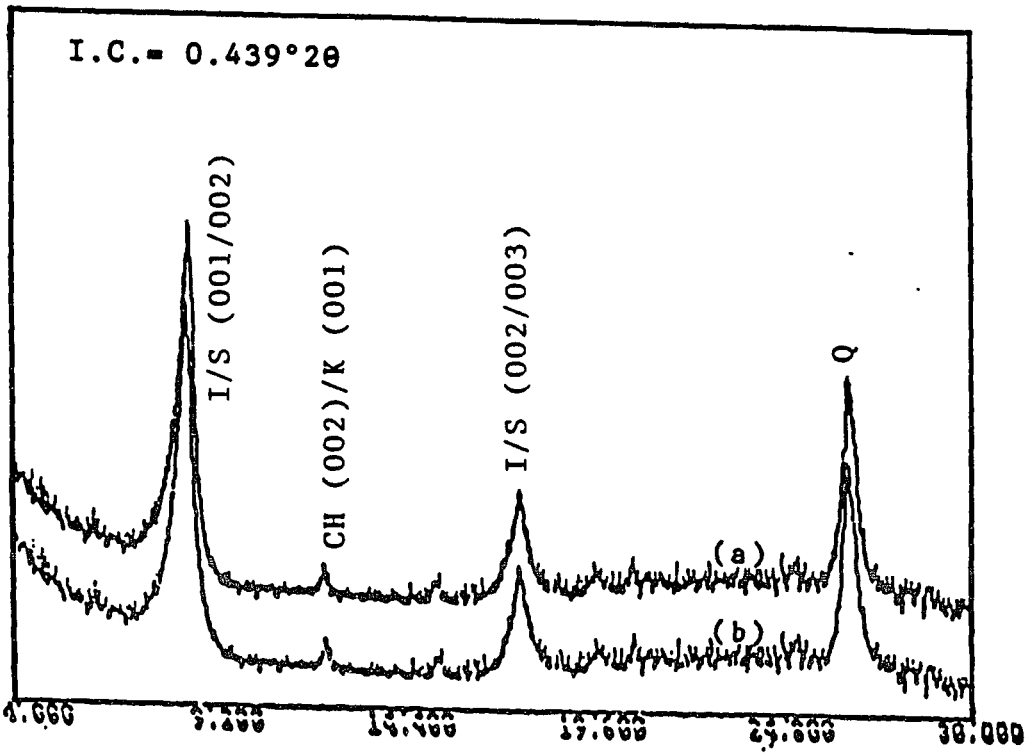

LOCATION: 22 SAMPLE: MR-4

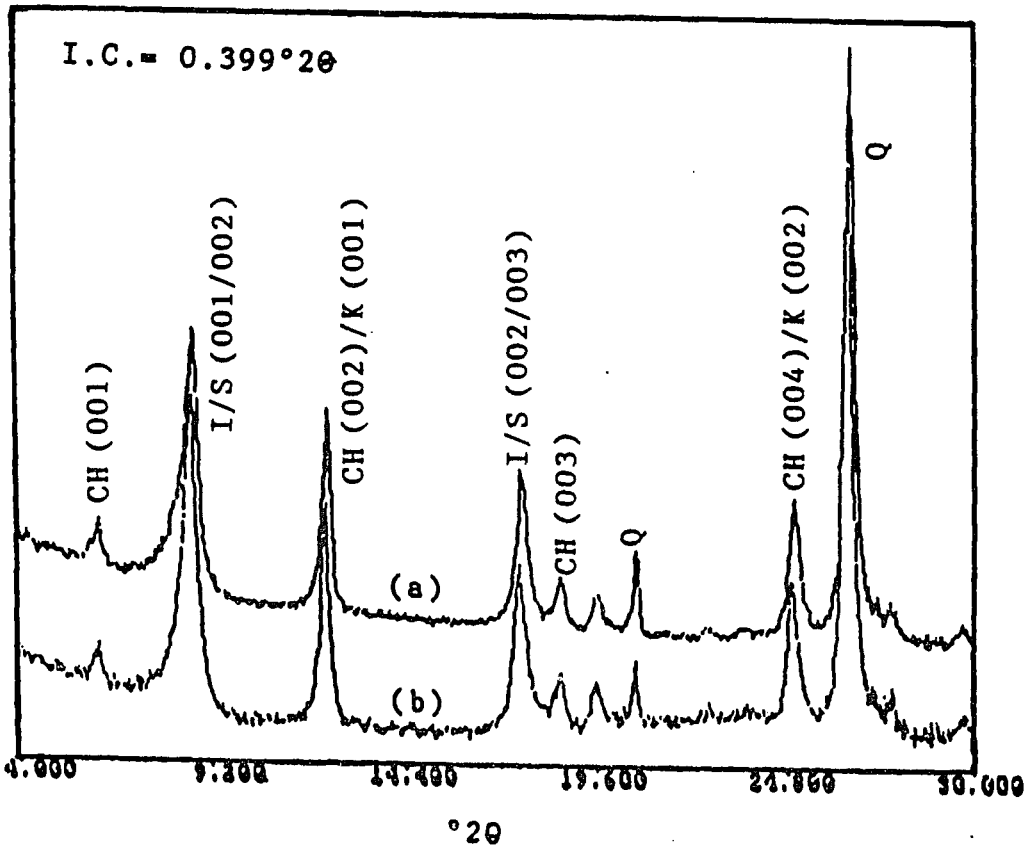

Table 14.2: Calculated percentage of illite (%illite) in the Marcellus samples based on the difference in peak position ($\Delta°2\theta$) of 001/002 and 002/003 illite/smectite (I/S).

Location no.	Sample no.	Position of 001/002 I/S peak (°2θ)	Position of 002/003 I/S peak (°2θ)	Δ2θ	*%illite
36	FO-1	8.86	17.3	8.44	90-100
3	BK-1	8.74	17.76	9.02	90-100
32	MR-1	8.86	17.78	8.92	90-100
33	MR-2	8.86	17.74	8.88	90-100
11	MC-5/6	8.78	17.78	9.00	90-100
22	CGU-2	8.84	17.78	8.94	90-100
	MR-4(22)	8.70	17.66	8.96	90-100
25	MR-4(25)	8.84	17.78	8.94	90-100

*Calculation of %illite is based on Moore and Reynold's (1989) method (see table 4.2). Peak positions are shown in XRD patterns in fig. 14.4 and presented in Appendix J.

14.7: INTERPRETATION

14.7.1: Organic maturation

Mean vitrinite reflectance (Ro%) of the measured Marcellus samples range from 0.93 to 2.07, corresponding to a maximum burial temperature range of 145° to 247° C (table 14.3). The mean Ro of locations 36, 22 and 25 are relatively low (1.25, 1.13 and 0.94) and give maximum burial temperatures of 182°, 170° and 146° C, respectively. However, there are several questions about these Ro values.

At location 36, the same sample in which vitrinite measurements were taken shows a I.C. index of 3.17°2θ, the lowest (therefore, probably the highest paleotemperature) of all the Marcellus samples in this study. The same sample also shows a TAI of 3.9 (equivalent Ro of 2.07). Moreover, the mean Ro of 1.25 was based on only 10 readings, much less than 50 normally recommended (Castano and Sparks, 1974). Therefore, it is likely that Marcellus rocks at location 36 have a higher mean Ro (higher maximum burial temperature) than 1.25 calculated

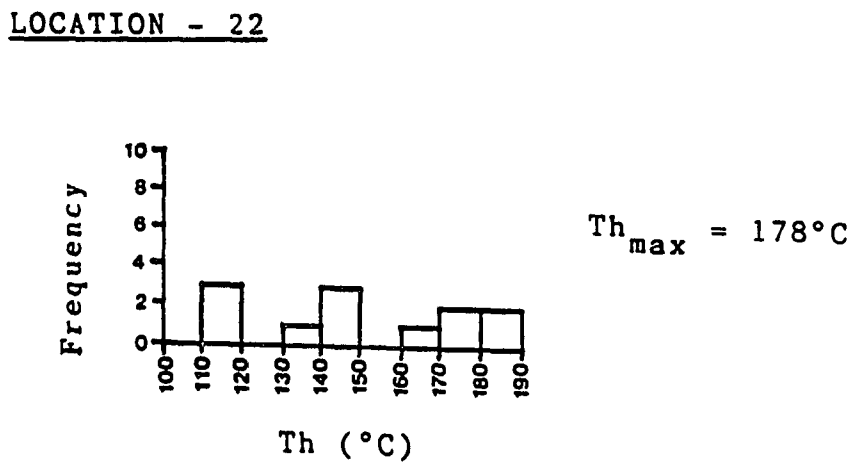

Figure 14.5: Fluid-homogenization temperature (Th) histogram for vein-calcite in the Marcellus Formation of location- 22. Maximum homogenization temperature (Th_{max}) is also shown.

Similarly, at location 25, the mean Ro of 0.94 has been calculated from relatively few (29) readings and may not be a reliable measure of true thermal maturity of the rocks. The same sample at location 25 has an I.C. of 0.398° 2θ which is similar to those at locations 33 and 32 where the corresponding mean Ro are considerably higher (table -14.3). At location 22, 46 vitrinite measurements were taken, and the mean Ro of 1.13 should be more reliable than those of locations 36 and 25. However, the Th_{max} of fracture-filling calcite in the Marcellus shale of location 22 is 178° C, (fig. 14.5), slightly higher than the mean Ro-derived maximum (?) burial temperature. Since Th_{max} in this study represents a lower limit of maximum burial/trapping temperature (section: 4.3.3), the mean Ro of 1.13 could not possibly represent the true thermal maturity of the Marcellus samples at location 22. An I.C. of 0.399° 2θ of the same sample (table 14.3) also indicates higher thermal maturity than that indicated by mean Ro. Probably more Ro measurements are necessary to determine a more appropriate mean Ro.

As mentioned in section 14.3, the samples at location 94 and 95 did not yield measurable vitrinites. In table 14.3, the mean Ro for samples of these locations were obtained from their TAI values using the conversion table 4.1. Since TAI values obtained in this study are generally inconsistent with other measures of paleotemperatures and often within themselves in a study location, the reliability of these converted Ro values are open to question.

In figure 14.6, paleotemperatures calculated from mean Ro (table 14.3) have been plotted against sample locations along the Marcellus outcrop belt in New York. Except for the relatively low temperature at location #36, which was most probably a function of low number of Ro readings available at this location, the trend of decreasing temperatures to the west is broadly similar to that exhibited by the I.C.-temperature profile.

14.7.2: Clay diagenesis data:

Figure 14.4 shows that there is no or very little difference in the peak positions between the XRD patterns of untreated and glycolated samples indicating that the swelling type clays, particularly smectite, is absent or present in very low proportions (Eslinger and Pevear, 1988, p. A-22; Moore and Reynolds, 1989, p.250). Absence of a peak near 5.2° 2θ in all the samples also indicates the absence of randomly inter-stratified illite/smectite clays and the presence of illite as the dominant component (Moore and Reynolds, 1989, p.250).

All the Marcellus samples in this study have more than 90% illite in their mixed-layer I/S (table 14.2), suggesting temperatures of 200° C or higher (Eslinger and Pevear, 1988). The I.C.

Table 14.3: Comparison of mean Ro and I.C. data and of calculated temperatures from them for the Marcellus samples.

Location no.	Sample no.	Mean Ro (Max. Ro) --- I.C.(°2θ(mm))	*Calculated temperature (° C)
36	FO-1	1.25 (2.1) 0.317 (4.0)	182 (249) 280
3	BK-1	2.07 (2.7) 0.320 (4.05)	247 (281) 280
32	MR-1	1.56 (2.5) 0.358 (4.53)	210 (271) 275
33	MC-1 MR-2	1.66 (2.0) 0.399 (5.05)	219 (243) 260
34	MR-3	1.71 (2.6)	222 (276)
11	MC-5/6	0.439 (5.55)	255
22	CGU-2 MR-4	1.13 (2.1) 0.399 (5.05)	170 (249) 260
25	MR-4(25)	0.94 (1.97) 0.398 (5.04)	146 (240) 260
94	MR-5	0.93	145
95	MR-6A	0.93	145

* Ro - temperatures were calculated from Barker and Pawlewicz' (1986) equation I.C.-temperatures were calculated from Weaver et al.'s (1984) diagram (see figure 4.5). The temperatures in brackets have been calculated from the maximum unaltered Ro (column 3) of the samples.

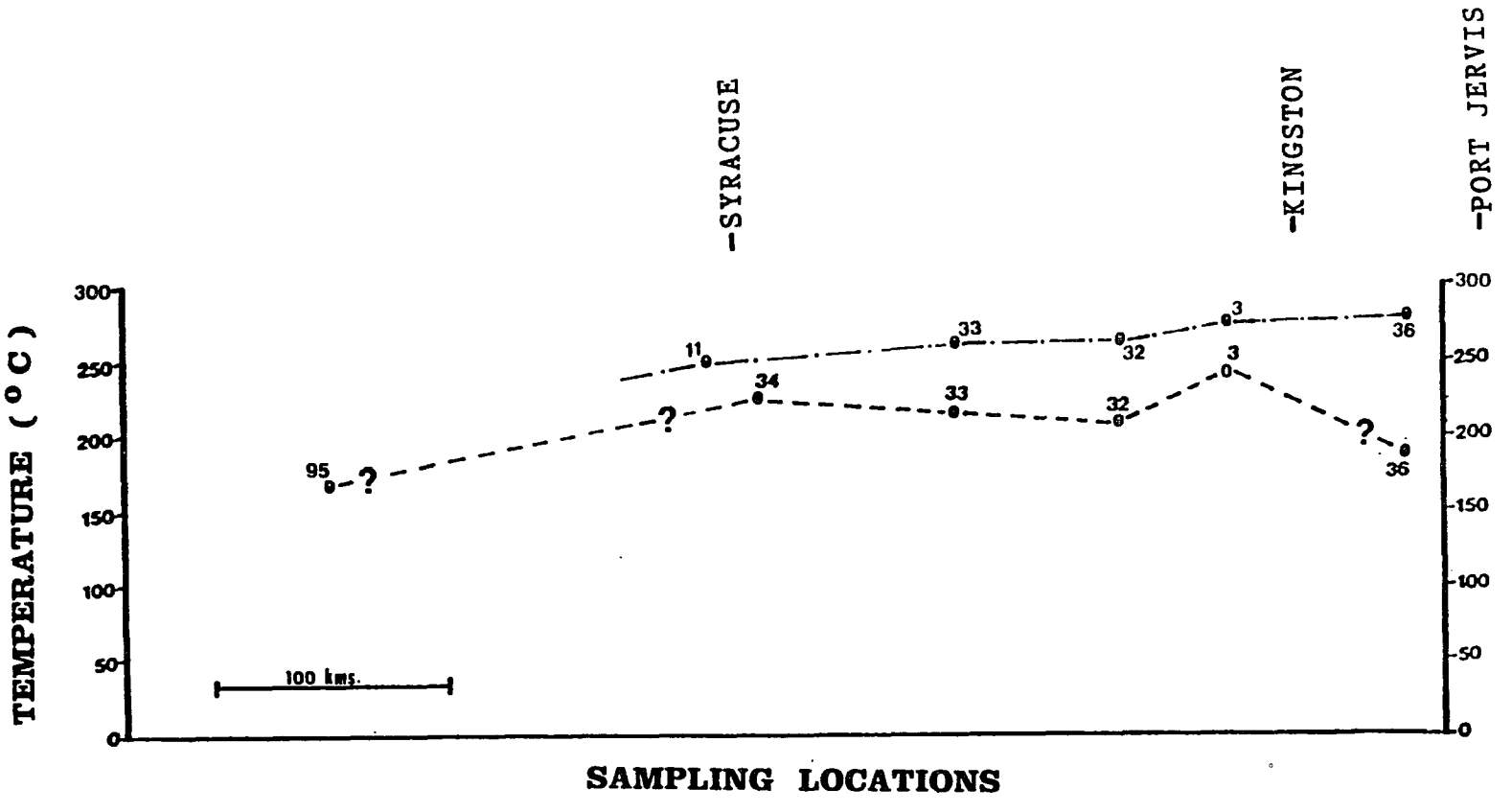

Figure: 14.6: Palcotemperature profiles of the Marcellus Formation along its outcrop belt based on temperatures calculated from mean Ro and I.C.

ranges from 0.317° 2θ at location 36 to 0.439° 2θ at location 11: all the I.C. indices are within the "anchizone" of Kubler (1967, 1968), except the 0.439° 2θ at location 11 which falls within the "diagenetic zone". Using Weaver et al.'s (1984) I.C.- temperature diagram (fig. 4.4), a temperature range of 255° to 280° C is obtained for the studied Marcellus samples (table 14.3).

Comparison of temperatures calculated from mean Ro and I.C. data of the same or nearby sampling locations show that I.C.-derived temperatures are consistently higher than temperatures calculated from mean Ro (table 14.3, fig. 14.6). The observed difference probably brings into question the universal applicability of Weaver et al.'s (1984) I.C -temperature and Barker and Pawlewicz's (1986) mean Ro -temperature relationships. Although Barker and Pawlewicz's (1986) work was based on data from 46 diverse geologic systems, as opposed to one of Weaver et al. (1984), and commands greater reliability, it has been found in this work that the number of Ro readings at a sampling location greatly affect the mean Ro and, therefore, the calculated paleotemperatures. However, if the temperatures are calculated from the "unaltered" (see Appendix J) maximum Ro reading of the sample, it is seen that these temperatures match the I.C.-temperatures rather well, despite the uncertainties (table 14.3). Possibly, the higher unaltered 'Ro's (Appendix J) represent the indigenous, not recycled, vitrinites. Since land plants were not very common in pre-Devonian time, the chances of getting older, more mature vitrinites in the Middle Devonian Marcellus samples are also low. Thus, although the data is sparse, it appears that similar maximum paleotemperatures are obtained from maximum Ro and I.C. of a sample.

Considering these points, it is assumed in this study that the I.C. - derived temperatures represent the probable maximum paleotemperatures the studied Marcellus samples might have experienced. It is also more convenient to use I.C. data for the purpose of comparison with paleo-temperatures obtained from older shale units (such as the Utica Shale) in which Ro readings are not available.

14.7.3: Fluid inclusion and Stable isotope data:

The fracture-filling calcite in the subsurface Marcellus rocks of locations 22 shows a Th_{max} of 178°C (fig. 14.5), which represents a lower limit of the maximum fluid trapping temperature in the Marcellus Formation at this location. Stable isotope data from the bulk cement of the same fracture are consistent with stable isotopic signatures of inferred deep burial cements (Mattes and Mountjoy, 1980, Zenger, 1983; Brockerhoff and Friedman, 1987; Gurney and

Friedman, 1987; Friedman, 1987a,b; Lee and Friedman, 1987; Kaufman et al. 1990 and many others). The calculated isotopic temperature range of 70° - 116° C, however, is much lower than the Th range. The cause of such relationship between Th and isotopic temperatures, which has been found more or less consistent in all the studied units, has been discussed previously (sections 4.6, 12.6.3).

CHAPTER: 15

REFINED PALEOTEMPERATURES AND BURIAL DEPTHS OF SILURIAN AND DEVONIAN ROCKS

15.1: PALEOTEMPERATURE PROFILES ALONG THE SILURO-DEVONIAN OUTCROP BELT:

Between Port Jervis in southeastern New York and southeastern Ontario, Canada, the Middle Devonian Onondaga and Marcellus formations are exposed, or lie in the shallow subsurface (figs. 13.1, 14.1). The Lower Devonian Helderberg Group carbonates are exposed between Port Jervis and west of Syracuse (fig. 12.1). Therefore, in the eastern half of the Port Jervis - southeastern Ontario transect, the paleotemperature profiles of these three formations can be compared to obtain refined temperatures. In the western half of the transect, the paleotemperatures of the Silurian rocks (chapters 9, 10, 11) can be used along with the profile of the Onondaga Formation to get similar results.

In figure 15.1, the paleotemperature profiles of the Devonian Helderberg Group, Onondaga Formation, Marcellus Formation, and Silurian Clinton, Lockport and Salina groups have been plotted against their sampling locations. The profiles for the Helderberg and Onondaga are their Th_{max} profiles taken from figures 12.7 and 13.7. The two (Ro and I.C -) temperature profiles of the Marcellus Formation are taken from figure 14.6. The short profiles of the Silurian units have been drawn on the basis of their Th_{max} data (chapters 9, 10 and 11).

A good match between Th_{max} of the Helderberg and Onondaga rocks of the same or adjacent locations is seen in figure 15.1. Only at location 7, the Helderberg Th_{max} is about 30°C higher than the Onondaga Th_{max}. Since at this location both units are quite thin (Helderberg, 64m; Onondaga, 37m) with only 15m of Tristate Group in between, it is unlikely that their temperatures at any given time would differ by as much as 30 C. It is believed that the higher Th were simply not found in the studied samples of the Onondaga Formation. In the refined profiles (see section 4.7.1 for refinement techniques) of figure 15.2, the Th_{max} of Onondaga at location 7 is raised close to that of the

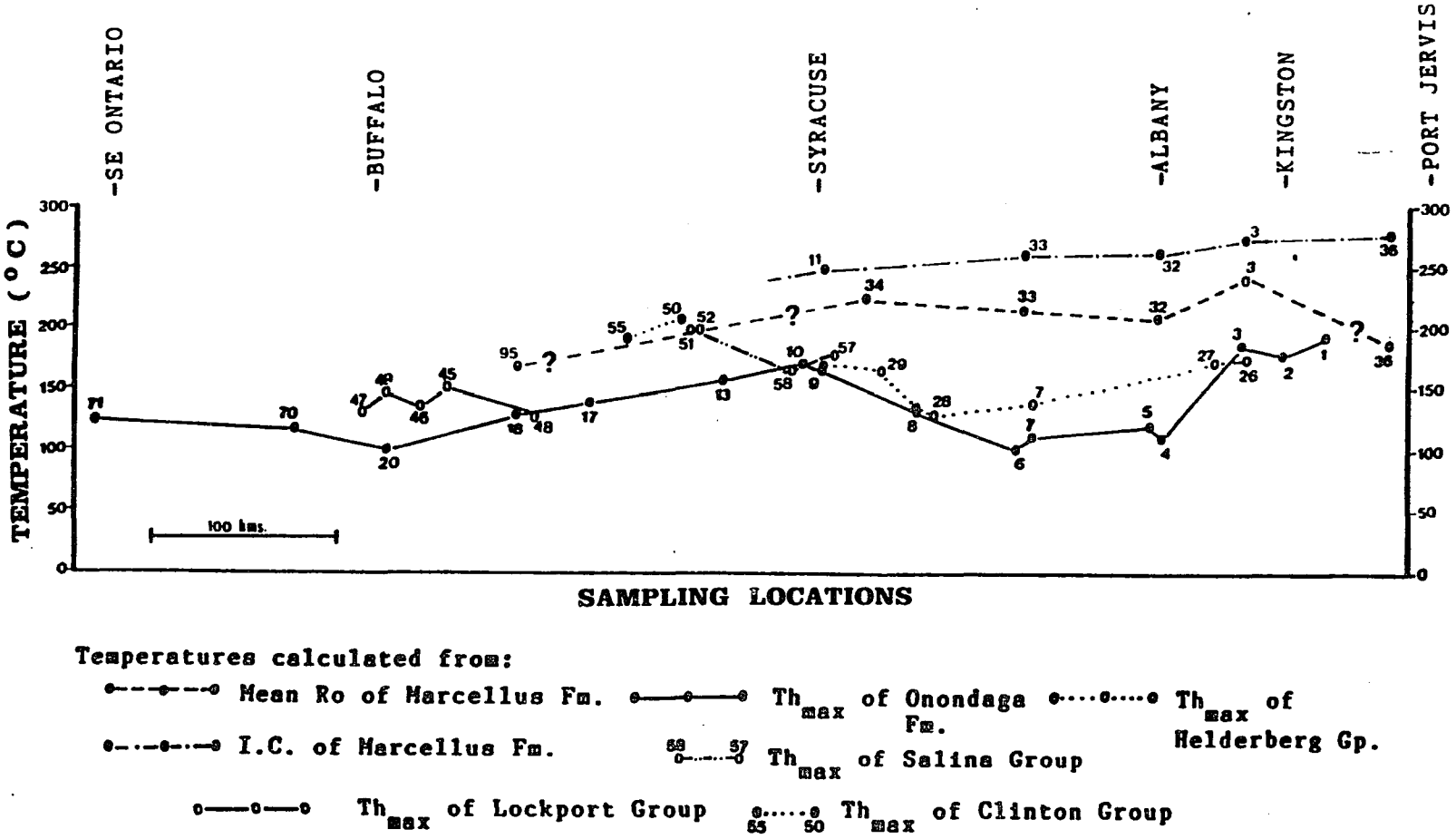

Figure: 15.1: Comparison of the paleotemperature profiles of the Lower Devonian Helderberg Group, Middle Devonian Onondaga and Marcellus formations, early Middle Silurian Clinton Group, Middle Silurian Lockport Group and the Upper Silurian Salina groups along their outcrop belt in New York State.

Helderberg Group. Then, since no Helderberg sample was studied between locations 7 and 27, the Helderberg profile between these two locations is lowered close to the Onondaga profile. Similar small adjustment are made between the two Th_{max} profiles near location 29 and between locations 3 and 26 (fig. 15.2).

The paleotemperature profiles of the Marcellus Formation are considerably higher than the Th_{max} profiles of the underlying Helderberg and Onondaga carbonates along the outcrop belt. This is because the Th_{max} profiles, being based on pressure-uncorrected Th, only represent a lower limit of the maximum paleotemperature profiles of the Helderberg and Onondaga rocks, whereas the I.C.-temperature profile of the Marcellus Formation probably represents the probable upper limit of the maximum temperatures experienced by the Marcellus rocks; the Ro-temperature profile occupies an intermediate position. With pressure correction, the Th_{max} profiles may have closely matched the temperature profiles of the Marcellus Formation.

However, **pressure correction** is a difficult task especially where missing overburden is involved (section 4.3). An example here will further prove this point. At location #3, for example, a probable maximum temperature of 280° C is indicated by the I.C. value of the Marcellus samples (see table 14.3). If one assumes a paleogeothermal gradient of 30° C/km and a mean annual surface temperature of 20° C (section 4.7.3), the calculation gives a burial depth of 8.6km. At such depth, the pressure on the inclusions of the underlying Onondaga Formation is most likely to be lithostatic. Considering an average lithostatic pressure gradient of 22.5MPa/km for sedimentary basins (Hanor, 1987, p.123), the pressure at a depth of 8.6km amounts to approximately 194MPa. Using this pressure and a salinity of 2 wt% NaCl for the inclusion fluid (for location #3, from table 13.1), a correction of 160° C (175° C for a salinity of 20 wt% NaCl) is obtained for the Onondaga Th_{max} of 189° C (Potter, 1977, fig. 1). The corrected Th_{max} then becomes about 349° C, which is 69° C higher than the I.C.-derived temperature of the overlying Marcellus samples at the same location!

Perhaps, the pressure estimated in the above calculation was not correct. To make up the difference between I.C.-temperature and Th_{max} (i.e., 91° C), a pressure of about 115MPa is required (Potter, 1977, fig. 1). Assuming a fully lithostatic pressure gradient,

a burial depth of about 5km is required. For the Marcellus samples to attain a paleotemperature of 280° C at 5km would require a geothermal gradient of 52° C/Km (after subtracting 20° C surface temperature). Such high geothermal gradient is unlikely to be found in foreland basins and is inconsistent with other estimates (20° - 40° C/Km) of present and past geothermal gradient in New York State and northern Pennsylvania (Friedman and Sanders, 1982; Hodge et al. 1982; Hodge, 1984; Johnsson, 1985, 1986; Levine, 1986).

It may be argued that the pressure was probably not fully lithostatic, but intermediate between lithostatic and hydrostatic (average hydrostatic gradient being 9 MPa/Km), and therefore the pressure of 115MPa could have been attained at a greater depth having required a more reasonable geothermal gradient. If one assumes an arbitrary intermediate pressure gradient of 15 MPa/Km, a burial depth of 7.6km and a paleogeothermal gradient of 34° C/Km are obtained, none of which are significantly different from the gradient of 30° C/Km assumed in this study and the burial depth of 8.6km calculated for the Marcellus sample of location #3.

Assumption of an intermediate pressure is partly justified for location #3, because the inclusions were measured in fracture-filling calcite cement. But unless the fractures were vertical and long relative to the overburden thickness, the pressure would still weigh heavily toward lithostatic (Roedder and Bodner, 1980, fig. 1). The fractures in the Onondaga Formation of location #3 are short and discontinuous, bedding parallel to gently inclined, and none of these fractures, at least their mineralized part, seemed to have extended into the overlying Marcellus (Bakoven member) shale. These observations suggest that the pressure was fully or nearly lithostatic. So, the problem of abnormally high geothermal gradient probably remains, if a pressure of 115 MPa is accepted in order to make I.C.- derived temperature and Th_{max} data compatible. Although, the use of an intermediate pressure gradient, such as 15 MPa/km, gives better results, the choice of such gradients can at best be very arbitrary and will not be considered here.

In short, the pressure correction can not be done with a reasonable degree of confidence from the existing data. Probably the best way of treating the I.C.-temperatures and Th_{max} is to accept them as limiting values: Th_{max} being the lower and I.C.-derived

temperatures being the upper limit of "maximum paleotemperature" experienced by the rock units in which these temperatures were estimated (see chapter 8).

In the refined paleotemperature profiles (see section 4.7.1) of figure 15.2, the profiles of Marcellus are not shown since all the other profiles are based on Th_{max}. However, I.C.-temperature data from the Marcellus Formation will be used in section 15.4 to constrain burial depths. In the western half of the profiles (west of Syracuse) in figure 15.2, adjustments have been made between the profile of the Onondaga Formation and those of the Silurian rocks. The vertical separation between the Th_{max} profiles of adjacent rock units shown in figure 15.2 take into account the stratigraphic distance between their tops: the method is described in section 4.7.1 and chapter 8. A comparison of figures 15.1 and 15.2 shows that a major adjustment was required between locations 9/10 and 18 where the profile of the Onondaga Formation had to be raised in order to match the higher Th_{max} profiles of the underlying Silurian rocks: the Onondaga rests directly on the Salina Group in western New York. Some adjustments have also been made around location #20, where the Onondaga rocks show a Th_{max} of only 100.4° C (figs. 13.6, 15.1) but the Lockport rocks at location #49, straight north of location #20 and stratigraphically separated from the Onondaga by only about 135m (Rickard, 1975, pl.3,4), have a Th_{max} of 140.3° C: so the Onondaga profile at location #20 had to be raised to about 137° C on the basis of a 30° C/Km paleogeothermal gradient. This adjustment receives support from Th_{max} of 155.3° C of the Beekmantown (Theresa Fm.) rocks at core location #66 (fig. 5.8). The closest sampling location of the Lockport Formation to location #66 is location #47 where a Th_{max} of 127.8° C has been measured (fig. 10.6). The Beekmantown samples were obtained from 881m below the Lockport samples of location #47, i.e., a difference of 27.5° C for a depth of 881m. This translates into a paleogeothermal gradient of 31° C/Km, which is remarkably similar to the 30°C/Km gradient used in this study.

West of Buffalo, at locations 70 and 71 of the Ontario Peninsula, Th data from only the Onondaga Formation were available: therefore, this part of the profile could not be compared with paleotemperature data from other units.

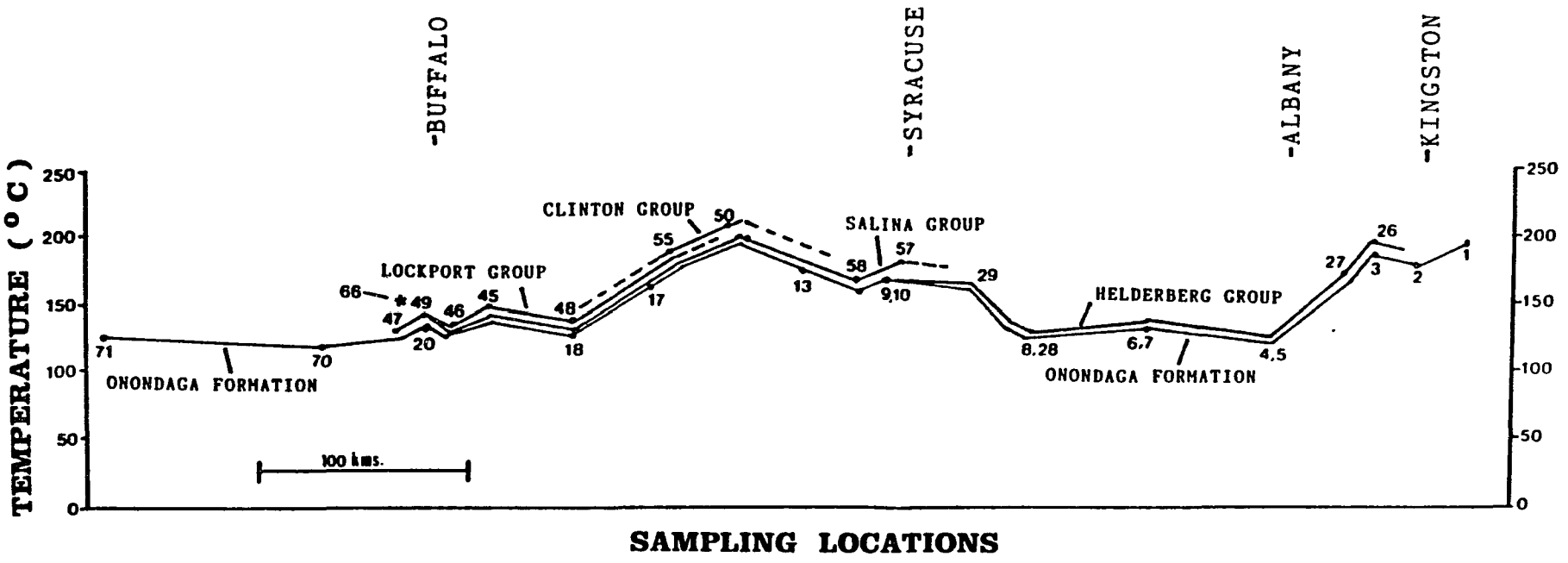

Figure: 15.2: Refined Th_{max} profiles of the Helderberg Group (Lower Devonian), Onondaga Formation (Middle Devonian), Clinton Group (early Middle Silurian), Lockport Group (Middle Silurian) and the Salina Group (Upper Silurian) along their outcrop belt in New York. The star (*) mark shows the Th_{max} of Beekmantown (Cambro-Ordovician) rocks at location #66. See text for explanation.

Figure 15.2 shows two highs in the Paleotemperature profiles; one in southeastern New York, roughly between Kingston and Port Jervis, and the other in central New York southwest of Syracuse.

15.2: PALEOTEMPERATURES OF DEVONIAN CORE SAMPLES FROM SOUTH-CENTRAL NEW YORK:

Devonian core samples were studied from four locations of southcentral New York. Three of these locations, #22, 24 and 25, are shown in figures 12.1, 13.1, and 14.1. One other location, #42, where only upper Devonian shales were cored, is plotted in figure 16.2 of chapter 16.

At location #22, paleotemperature data were available from four different rock formations (table 15.1). Except the clay diagenesis data from the Geneseo shale, paleo-temperature data from the other formations have been presented before (chapters 12, 13, and 14). In table 15.1 below these data are presented together for comparison.

Table 15.1: Paleotemperature data from core samples of location #22.

Rock unit	Sample no.	Sample depth(m)	*I.C. (°2‰(mm))	I.C.-temp. (°C)	**Th_{max} (°C)
Geneseo	GN-1	79.9	0.439(5.5)	255	---
Marcellus	MR-4	361.9	0.399(5.05)	260	---
	CGU-2	430.8	0.398(5.05)	260	178
Onondaga	CGO-1,2	442-444	---	---	71
Helderberg	CGH-1	476	---	---	169.7

* Illite crystallinity index. ** Maximum fluid-homogenization temperature.

Table 15.1 shows that the maximum Th_{max} of 178° C was measured in the Marcellus shale (in fracture-filling calcite, fig. 14.5). The Th_{max} in the fracture-filling cement of the underlying Onondaga Formation is an anomalously low 71° C. It is believed that the studied fracture-fillings cements of the Onondaga Formation were of a different generation from those of the Marcellus Formation or the underlying Helderberg. Following the method of paleotemperature refinement (section 4.7.1), the Th_{max} of the Onondaga Formation should be considered slightly more than 178° C and that of the Helderberg Group higher than Onondaga's. However, for the purpose of determining burial depths from Th_{max} it will suffice to consider the Th_{max} of Marcellus Formation alone (section 15.4). The upper limit of maximum paleotemperature reached at this location is 260° C (from I.C.) by the Marcellus formation.

At location #24, samples of only the Onondaga Formation were available for study. Samples collected from depths of 1085 - 1126m showed a Th_{max} of 171.5° C (fig. 13.6). This will be taken for the lower limit of the maximum paleotemperature reached by the Onondaga rocks at this location.

At location #25, Marcellus samples from a depth of 1158m show an I.C. of 0.398°2‰ which indicates a temperature of approximately 260° C (table 14.3). This temperature is taken for the upper limit of the maximum paleotemperature reached by the Marcellus rocks of this location.

At location #42, core samples of the Upper Devonian Rhinestreet Formation of the West Falls Group from a depth of 376.8m were studied. The samples contain more than 90% illite in I/S and have an I.C. of 0.599° 2‰. The temperature of 225° C, indicated by I.C. (fig. 4.5), is taken for the upper limit of the maximum temperature experienced by these samples of the Rhinestreet Formation.

15.3: SOURCE OF HEAT:

Except the narrow, NE-SW trending belt of Jurassic ultramafic dike intrusions of central New York (fig. 2.3) and small Devonian and younger (?) plutons and ultramafic dikes between the Reading Prong and Manhattan Prong of southeastern New York (Mose et al. 1976; Miller and Kent, 1989), igneous activity could not have affected the

paleotemperature signatures of the studied Silurian and Devonian rock units. Although locations 9, 10, 11, 22, 24, 25, 34, 57 and 58 are in the general area of the dikes, none of the samples was collected from within several kilometers of the dikes. As discussed in section 4.7.2, it is very unlikely that these dikes heated up the surrounding rocks more than a few meters from their contacts. Therefore, the possible thermal effects of the dikes may be ignored. Moreover, the highest Th_{max} in central New York occurs at location 50 (fig. 15.2), which is far from the dikes, suggesting that the dikes had little to do with the maximum paleotemperatures in the area.

The igneous intrusions of the Reading Prong - Manhattan Prong area are 35km or farther from the nearest sampling locations (3, 26, 27) of this study. It is unlikely that heat from the small plutons, which have been emplaced along fault zones (Mose et al. 1976), and the ultramafic dikes significantly raised the paleotemperatures of the Lower and Middle Devonian rocks 35km away. At best, these rocks were at relatively shallow depths by the end of the Devonian when the largest of the plutons - the Peekskill pluton - was emplaced (ca. 360 ma, Miller and Kent, 1989), and were, therefore, very mildly overheated. Deep burial heating of ~200° C or more, indicated by Th of the Helderberg and Onondaga carbonates, and Ro and I.C. of the Marcellus shale must have masked a possible earlier overheating caused by the intrusions.

Much of the arguement against upward and outward migration of hot basinal fluids in the northern Appalachian presented in chapter 8 apply here. The paleotemperature profiles show a high in southeastern New York in each studied rock unit (figs. 15.1, 15.2) and another high in central New York in all the rock units, except for the I.C.-temperature profile of Marcellus (fig. 15.1). High paleotemperatures were also measured in core samples of locations 22, 24 and 25 of south-central New York (section 15.2). In westernmost New York and the Ontario Peninsula the paleotemperatures are relatively low (fig. 15.2). Thus, high paleotemperatures are not confined to rocks at basin edges as implied by most of the "MVT deposit" models (see section 8.2).

The fracture-filling cements in the Helderberg and Onondaga carbonates of southeastern New York (locations 2, 3, 26 and 27) may have precipitated from fluids expelled from the proposed Alleghanian thrust sheets in the vicinity (Levine, 1986).

Th_{max} obtained from these cements are high (fig. 15.2). However, these fluids did not attain high temperature directly from frictional heat generated by thrusting, because thrust-generated heat at relatively shallow depths is not high enough (S. Bhattacharji, 1991, pers. comm.). Moreover, Alleghanian thrusting was not associated with significant igneous activity that could serve as a source of heat. It is more reasonable to infer that tectonic loading by the thrust sheets themselves, or burial by sediments shed rapidly from subaerially exposed parts of the thrust sheets (by as much as 9km in northeastern Pennsylvania; Levine, 1986) raised the temperature of the rocks in southeastern New York, and the high Th_{max} as well as high Ro and I.C. found in these rocks reflect the ambient paleotemperatures. The high paleotemperatures in central New York and low temperatures in western New York can not be explained by the existing simple models of cratonward fluid flow from marginal orogenic belts (Hitchon, 1984; Majorowicz et al. 1985; Oliver, 1986). It is therefore concluded that the variations in paleotemperatures as seen in the profiles of figure 15.2, reflect the temperatures of the rocks as a main function of burial depths.

15.4: BURIAL DEPTHS:

Figure 15.3 shows the plots of burial depths of five Silurian and Devonian rock units against their sampling locations along the Port Jervis - southeastern Ontario transect, based on the refined Th_{max} data taken from figure 15.2. Burial depths were calculated by subtracting a 20° C mean annual surface temperature from the Th_{max} of individual locations and then dividing the remainder by a paleo- geothermal gradient of 30° C/Km (section 4.7.3). Being based on Th_{max}, these burial depth profiles represent the lower limits of maximum burial depths reached by the rock units.

In the same figure, the preserved maximum thickness of the post-Onondaga Devonian strata from the southern border of New York State with Pennsylvania (Rickard, 1975, pl.4) has been projected on the transect. The thickness of post-Onondaga Devonian strata along the border due south of Buffalo area is 1.08km (Rickard, 1975, pl.4). The thickness increases eastward along the border to about 2.5km south of Syracuse. Eastward from this

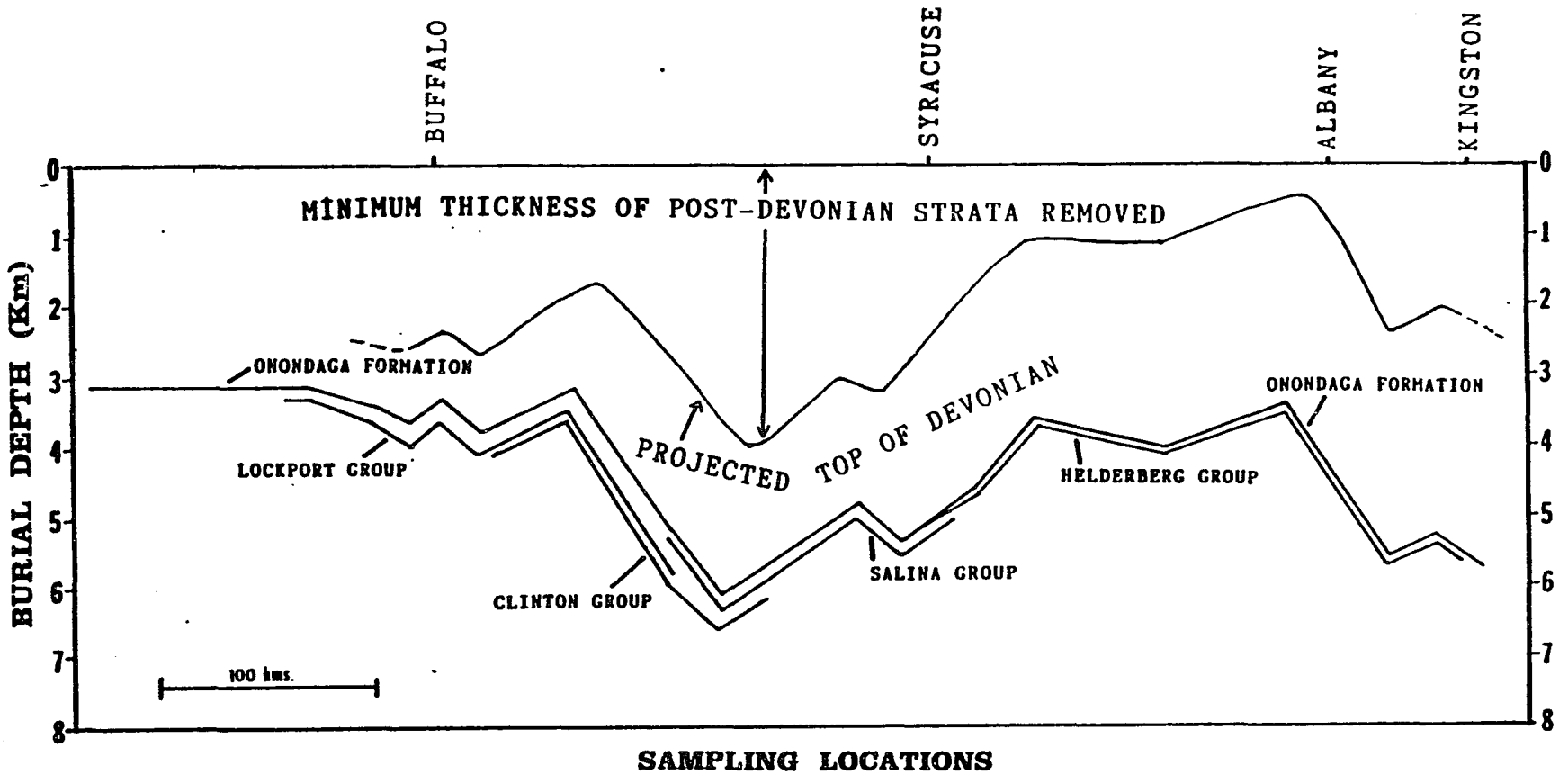

Figure 15.3: Burial depth profiles of the Helderberg Group (Lower Devonian), Onondaga Formation (Middle Devonian), Clinton Group (early Middle Silurian), Lockport Group (Middle Silurian), and the Salina Group (Upper Silurian) based on refined Th_{max} data. See text for explanation.

area, the Upper Devonian has been progressively (first the Conewango and Conneaut groups, then the Canadaway and West Falls groups) removed by erosion. In the projected thicknesses, it is assumed that the Upper Devonian rock units once extended to the eastern margin of New York State, and their maximum preserved thicknesses in the west are added to the preserved thicknesses of the older rocks in eastern half of New York and then projected on to the transect. Thus, at location #1, the post-Onondaga cover amounts to 3.63km (table 15.2). Subtracting the above thicknesses from the burial depth profile (based on the refined paleotemperature profile) of the Onondaga Formation, the minimum thicknesses of former post-Devonian strata at different locations along the transect are obtained (fig. 15.3, table 15.2). In table 15.2, the calculated minimum thicknesses of former post-Devonian strata at various locations, including those of south-central New York (section 15.2) not in the profiles, are shown.

Estimates of the maximum thickness of post-Devonian cover that might have been present can be made from the I.C. data of the Marcellus shale and the shales of the Salina Group (locations #51, 52). Table 15.3 below presents the maximum possible thickness of the post-Devonian strata at the relevant study locations based on I.C. - derived paleotemperatures.

A separate burial depth profile like figure 15.3 has not been constructed from the above data mainly because the data are so sparse. However, in chapter 16, data from table 15.3 as well as table 15.2 are used for constructing isopach maps of post Devonian strata.

Table 15.2: Estimated minimum thicknesses of post-Devonian strata removed from various study locations.

Location no.	Rock unit	*Th_{max} (° C)	Burial depth (km)	**Projected thickness of overlying rocks (km)	Thickness of former post-Devonian rocks (km)
1	Onondaga	193	5.76	3.63	2.13
2	---	176.9	5.23	3.45	1.78
3	---	188.7	5.62	3.55	2.07
4,5	---	122	3.4	3.2	0.2
6,7	Onondaga/ Helderberg	140	4.0	3.1	0.9
8,28	---	132.4	3.74	2.88	0.86
9,10	---	172	5.06	2.54	2.52
29	Helderberg	159.3	4.6	2.78	1.82
57	Salina	182.6	5.4	2.85	2.55
58	---	166.8	4.8	2.57	2.23
13	Onondaga	180	5.3	2.44	2.86
51	Salina	210	6.3	2.28	4.02
50	Clinton	218	6.6	2.5	4.1
55	---	188	5.6	2.37	3.23
17	Onondaga	178	5.2	2.07	3.13
18	---	120	3.3	1.4	1.9
48	Lockport	125	3.5	1.6	1.9
45	---	143.8	4.12	1.37	2.75
46	---	130.4	3.68	1.34	2.34
49	---	140.3	4.0	1.17	2.73
47	---	127.8	3.5	1.27	2.23
20	Onondaga	137	3.9	1.10	2.8
70	---	116	3.2	0.95	2.25
71	---	118	3.26	0.95	2.3
24	---	171.5	5.05	2.05	3.0
22	Marcellus	178	5.26	2.38	2.88

* Th_{max} = maximum homogenization temperature

** Distance between the studied samples and the projected tops of the Devonian on to the study locations (see section 15.4).

Table 15.3: Estimated maximum thicknesses of former post-Devonian strata at various locations.

Location no.	Rock unit	*I.C.-temp. (° C)	Burial depth (km)	**Projected thickness of overlying rocks (km)	Thickness of former post-Devonian rocks (km)
36	Marcellus	280	8.67	3.0	5.67
3	---	280	8.67	3.36	5.31
32	---	275	8.5	3.08	5.42
33	---	260	8.0	3.0	5.0
11	---	255	7.83	2.5	5.33
22	---	260	8.0	2.36	5.62
25	---	262	8.06	2.03	6.03
51	Salina	255	7.83	2.2	5.63
52	---	245	7.5	2.2	5.3
42	Rhinestreet	225	6.8	1.67	5.13

* I.C. = Illite crystallinity index.

** Distance between the studied samples and the projected tops of the Devonian on to the study locations (see section 15.4)

CHAPTER: 16:
POST-DEVONIAN ROCKS IN NEW YORK

16.1: ISOPACH MAPS OF POST-DEVONIAN ROCKS:

From the conclusions of chapters 8 and 15, it is possible to illustrate the spatial variation in the inferred thickness of former post-Devonian strata in New York State.

Two isopachous maps of post-Devonian strata have been constructed. The map in figure 16.1 is based on the minimum post-Devonian thickness data presented in tables 8.1 and 15.2, whereas the map in figure 16.2 is based on the maximum post-Devonian thickness data presented in tables 8.2 and 15.3. Like the tables themselves, these maps should be treated as limiting representations: figure 16.1 represents the minimum thicknesses of post-Devonian strata that, according to this study, were present as shown; figure 16.2 represents the maximum thicknesses of the same that might have been present.

In figure 16.1, although the trends of the isopachs are extrapolated in many areas, an interesting pattern is observed. The axis of the thickest post-Devonian strata (greater than 4Km) runs almost N-S parallel to 77°W longitude and then turns northeast toward the Adirondacks. The thickness decreases both eastward and westward from this axis only to increase again in westernmost and southeastern New York. The thickness of inferred post-Devonian strata increases to almost 3km north of Buffalo, but at locations #70 and 71 it decreases to 2.3km, suggesting that there might have been a local post-Devonian depocenter in the Buffalo-Niagara area. In eastern New York, the thickness drops to less than 1km before increasing to more than 2km in southeastern New York. Only two data points, locations #4/5 and #68 do not fit the isopachs. Probably the Th_{max} of both of these points under-represented the maximum Th, because the higher Th were not present in the samples studied.

Extension of the isopachs into the present Adirondacks region, as seen in figure 16.1, are based on the trends of the isopachs in the south, and admittedly stylized. However, from the post-Devonian thickness data at locations #87 - 90, so close to the Adirondacks, it is certain that at least 3km of post-Devonian strata occupied part of the southwestern

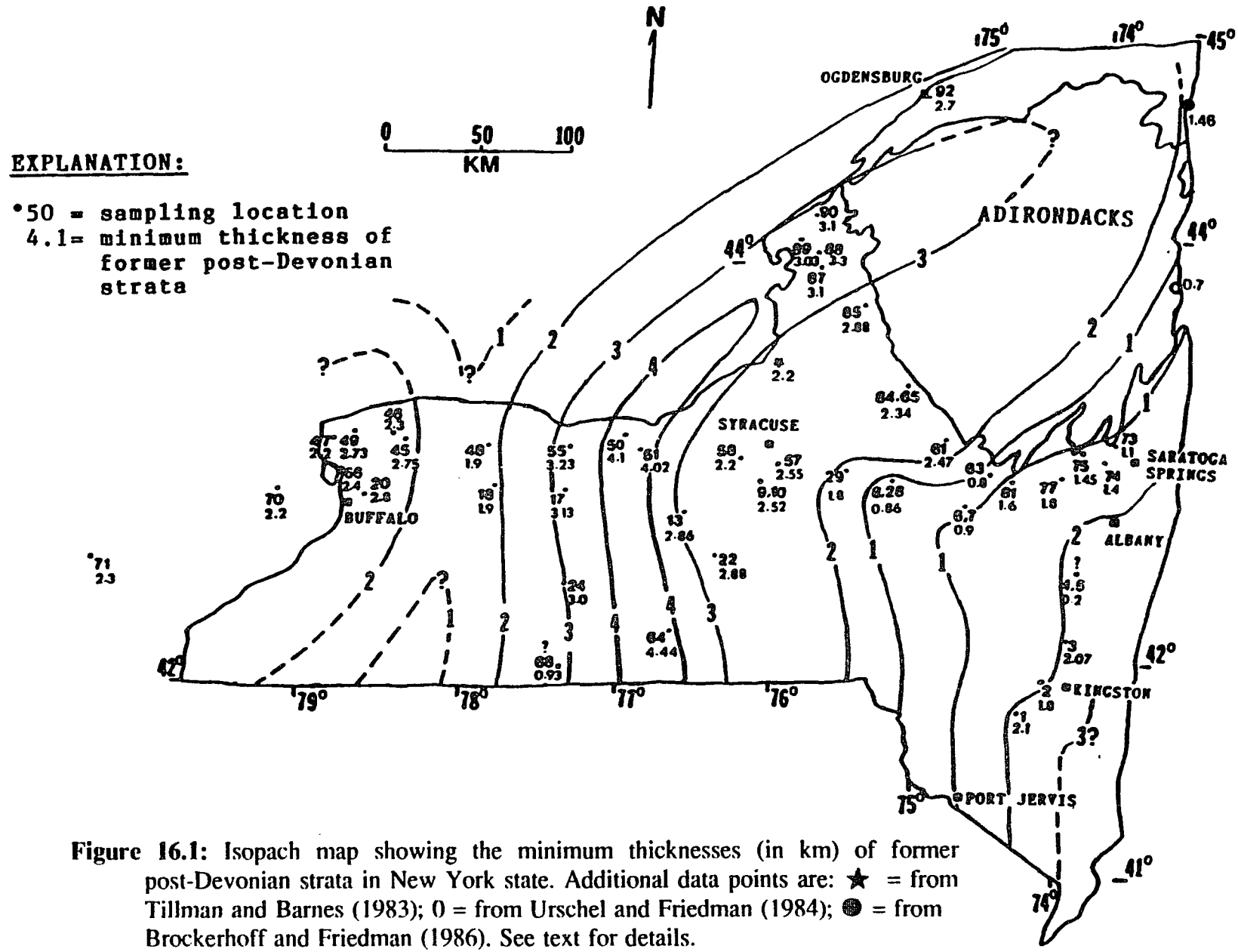

Figure 16.1: Isopach map showing the minimum thicknesses (in km) of former post-Devonian strata in New York state. Additional data points are: ★ = from Tillman and Barnes (1983); 0 = from Urschel and Friedman (1984); ● = from Brockerhoff and Friedman (1986). See text for details.

Adirondacks at one time. The map also suggests that the post-Devonian cover over the Adirondacks region thinned to less than 1km to the east. In the eastern portion of the Adirondacks, two additional data points of other workers (fig. 16.1) fit the isopach trends well (see section 16.2).

The isopach map of figure 16.2, representing the maximum possible thicknesses of former post-Devonian strata, is based on few data points, but despite the paucity of data points, some broad similarities between the two maps can be demonstrated. The axis of the maximum post-Devonian thickness in figure 16.2 is located approximately in the same area as in figure 16.1, only slightly broader and trending more eastward. The thickness also decreases toward east, and perhaps west (fig. 16.2). Also, an area of thinner post-Devonian rocks, aligned NE-SW, in eastern New York is similar to that in figure 16.1. Over the Adirondack region the two maps show little difference, except that in figure 16.2 a broader area in the southwest is covered by more than 3km thick post-Devonian strata.

16.2: COMPARISON WITH RESULTS OF PREVIOUS STUDIES:

A number of previous studies have addressed or alluded to the issue of post-Devonian rocks in the northern Appalachians (chapter 3), although none of these studies match the present study in scope. A comparison between the results of the present and previous studies show many general agreements.

Friedman and Sanders (1982) inferred that the Upper Devonian Gilboa rocks of the Catskill Mountains, eastern New York, were once buried under ~6.5Km of younger rocks (chapter 3). Their calculations were based on time-dependent organic maturation, following Hood et al. (1975), in which they inferred a temperature of 190°C for a vitrinite reflectance (Ro%) of 2.5. However, if the role of time is considered unimportant, as done by Barker and Pawlewicz (1986) and others (see section 4.4), an Ro (%) of 2.5 indicates a maximum temperature of 271°C. Subtracting 20°C as the mean annual surface temperature and dividing the remainder by 30°C/km geothermal gradient (section 4.7.1), a burial depth of 8.36km is obtained for the studied samples. The projected thickness of the total post-Gilboa Devonian section in New York onto the Catskills is 2.5km (Rickard, 1975, pl.4), which indicates a missing post-Devonian section

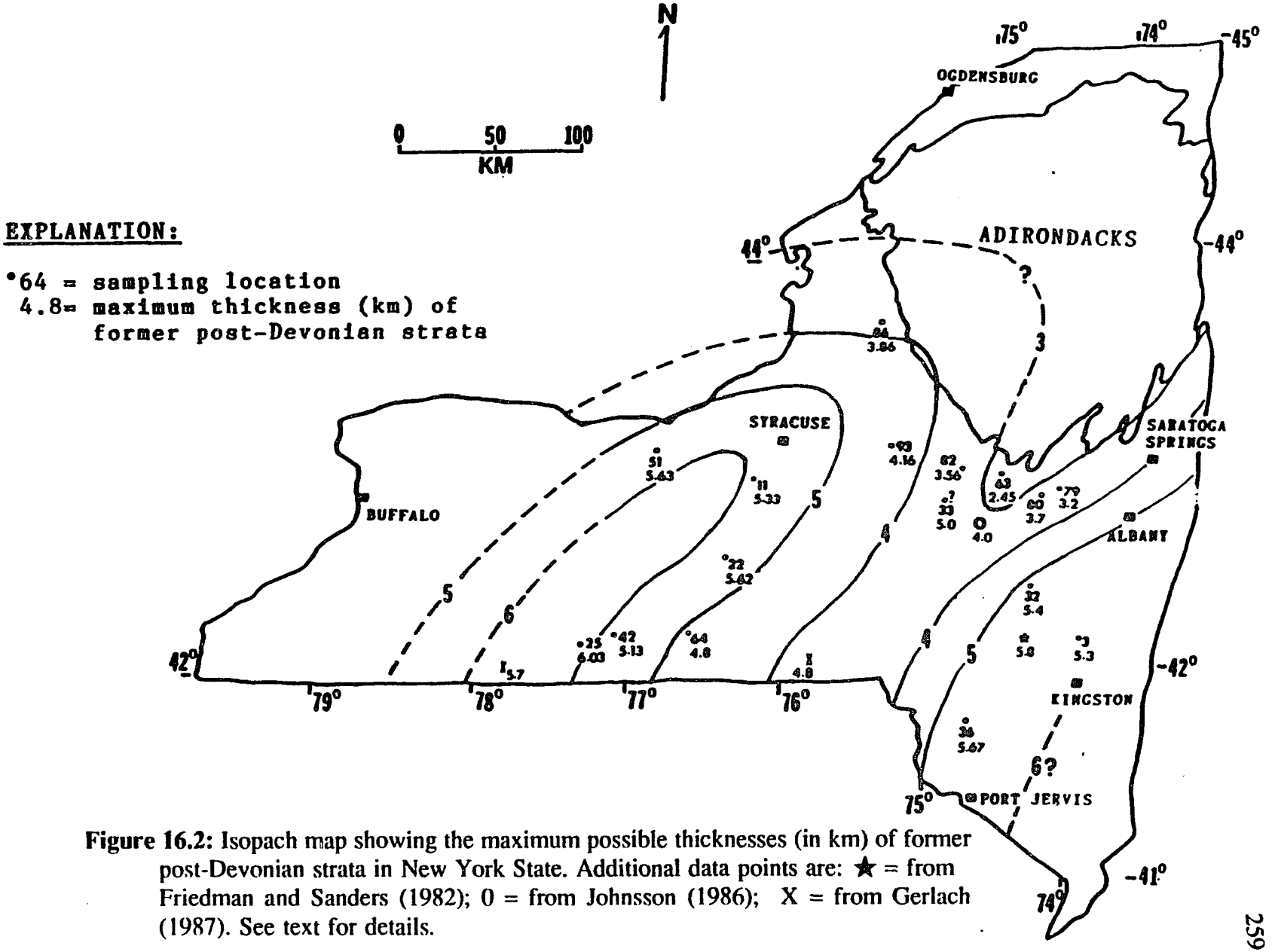

Figure 16.2: Isopach map showing the maximum possible thicknesses (in km) of former post-Devonian strata in New York State. Additional data points are: ★ = from Friedman and Sanders (1982); 0 = from Johnsson (1986); X = from Gerlach (1987). See text for details.

of 5.8km. This is consistent with the post-Devonian isopachs of figure 16.2.

In their fission-track study, Lakatos and Miller (1983) inferred that the sandstones of the earliest Late Devonian age (i.e., Gilboa Formation) in the Catskill Mountains experienced temperatures as high as 200° C in the past. According to calculations made in this study, this temperature was attained at a depth of 6km. Subtracting 2.5km younger Devonian strata, a post-Devonian thickness of 3.5km is obtained. Although this estimate is considerably less than 5.8km, estimated by Friedman and Sanders (1982) from farther north, it is well within the limit set by the two isopach maps of figures 16.1 and 16.2 for the Catskill region.

Miller and Duddy (1989), on the basis of fission-track analysis of apatite grains in Devonian sandstones, concluded that uplift and erosion removed ~2-3km thick younger strata from western New York and "greater than 3-4km" from the Catskill region. Their estimates are also consistent with the results of this study.

Tillman and Barnes (1983) measured Th of up to 176°C in the fracture-filling calcite of the Oswego Sandstone (Late Ordovician) from near Oswego (fig. 16.1). Subtracting a projected post-Oswego thickness of 3km (Rickard, 1975; Fisher, 1977) from a calculated burial of 5.2km, a post- Devonian thickness of 2.2km is obtained for the sampling area, which is in agreement with the isopachs of figure 16.1. It should be noted that Tillman and Barnes' (1983) Th were also pressure-uncorrected and therefore agreement with figure 16.1, based on similar Th, is expected.

Levine (1986) inferred a former burial depth of 6-9km for the extant Carboniferous rocks of northeastern Pennsylvania on the basis of vitrinite reflectance, sediment compaction and fluid inclusion data. This estimate is consistent with the inferred thickness of more than 6km post-Devonian rocks in southeastern New York (fig. 15.2). Friedman and Sanders (1982) had earlier proposed that the Carboniferous strata in Pennsylvania formerly extended across New York.

Two estimates of former thickness of post-Devonian rocks from the Champlain Valley, based on Th - one from the Plattsburg area (Brockerhoff and Friedman, 1986), the other from Ticonderoga area (Urschel and Friedman, 1984) - also fit the isopachs of figure 16.1. Near Plattsburg, Brockerhoff and Friedman (1986) measured a maximum

Th of 211°C in the Middle Ordovician Chazyan carbonates. If the projected thickness of 4.9km post-Chazyan rocks on Plattsburg area (Rickard, 1975; Fisher, 1977) is subtracted from the calculated burial depth of 6.36km, a post-Devonian thickness of 1.46km, consistent with the isopachs of figure 16.1, is obtained. In the Ticonderoga area, Urschel and Friedman (1984) measured a maximum Th of 206°C in the Beekmantown rocks. Subtracting a projected post-Beekmantown thickness of 5.5km from calculated burial depth of 6.2km, a post-Devonian thickness of 0.7km is obtained. This estimate also corresponds well with the isopachs of figure 16.1.

Johnsson (1986), on the basis of clay diagenesis and fission-track ages, inferred that in eastern New York nearly 4km post-Devonian strata was formerly present. In figure 16.2, Johnsson's easternmost study location falls between the two 4km isopachs, i.e., corresponds to thickness slightly less than 4Km.

Gerlach (1987), in his study of the Upper Devonian Rhinestreet shale along its outcrop belt in south-central New York (between two 'X' marks in figure 16.2), found that the mean Ro (%) values increases from 1.6 in the east to 1.8 in the west. Gerlach (1987) used a time-dependent Lopatin model to conclude that a minimum thickness of 1.2 - 3.7km of post-Devonian rocks extended from Pennsylvania into south-central New York. If these Ro values are converted to maximum paleotemperatures following Barker and Pawlewicz (1986), temperatures of 229°C and 214°C are obtained for the Rhinestreet samples from the western and the eastern end of Gerlach's (1987) transect, respectively. From the western end, if post-Rhinestreet Devonian section of 1.2Km (Rickard, 1975, pl.4) is subtracted from the calculated burial depth of 6.96km, a post-Devonian rock thickness of 5.7km is obtained. Similarly, subtracting 1.6km from the calculated burial depth of 6.46 km from the eastern end of the transect, a post-Devonian thickness of 4.8km (fig. 16.2) is obtained. Both of these estimates are fairly close to the isopach values of figure 16.2.

According to Beaumont et al.'s (1987) model, post-Alleghanian erosion has removed 2-3km rocks from southwestern New York, 3-6km from central New York and up to 9Km from southeastern New York (see fig. 3.5). In southwestern New York, the Uppermost Devonian is preserved (Rickard and Fisher, 1970). Therefore, 2-3km erosion

in southwestern New York (Beaumont et al. 1987) would mostly include post-Devonian rocks - consistent with isopachs of figure 16.1. If the projected thickness of 2km and 3.5km of upper Devonian rocks are subtracted respectively from south-central and southeastern New York, maximum thicknesses of 4km and 5.5km of post-Devonian sections are obtained for these areas. These estimates are also within the limits shown by figure 16.1 and 16.2.

The burial estimates of this study also compare well with those of Roden et al. (1990) and Roden (1991) from southern Appalachians. On the basis of fission-track ages of apatite grains in upper Devonian Hampshire and Chemung formations and middle Devonian Tioga Ash Bed, these findings suggests that erosional unroofing of ~3.1km post-Devonian strata took place in northwestern Cumberland Plateau (similar to western New York), and progressively deeper (not quantified by the authors) unroofing occurred to the east through the Valley and Ridge Province of northern West Virginia, Virginia and Maryland. These studies, however, do not indicate the former presence of a thicker post-Devonian section in a central position, as seen in New York (figs. 16.1, 16.2).

In summary, none of the estimates of former thicknesses of post-Devonian sections from various parts of New York or in contiguous states to the south, as indicated by previous studies, seriously contradicts the estimates made in this study (figs. 16.1, 16.2). It is seen that those studies in which paleotemperatures were determined from Th, give estimates of former post-Devonian thickness similar to those in figure 16.1, which is also based on Th measured in this study. The studies that were based on vitrinite reflectance yield results similar to figure 16.2. This is because temperature estimated from Ro and I.C. in this study were generally close, and figure 16.2 is based on I.C. temperatures.

CHAPTER: 17: DISCUSSION

The post-Devonian isopachs in New York (figs. 16.1, 16.2) show a NE-SW trend that is broadly similar to the trend of the total Devonian isopachs (see fig. 3.1). But, making a significant departure from the Devonian, a basin with two elongate troughs - one in central New York and the other in southeastern New York - appears to have developed in the post-Devonian time. Because southeastern New York was the site of greater sediment accumulation throughout the Devonian time, the only major change that took place in post-Devonian time was the development of a second trough in central New York. The trend of the isopachs suggest that the same feature was present at least in northern Pennsylvania.

17.1: POST-DEVONIAN SEDIMENTATION: DURATION AND SOURCE

Because the post-Devonian sedimentary record is missing from New York, much of the following discussion on possible source of the inferred post-Devonian sediments and timespan of sedimentation is based on indirect evidence, and part of it is conjectural.

A significant amount of Carboniferous sediments is preserved in Pennsylvania. The Carboniferous sedimentation pattern in Pennsylvania does not show any marked shift from the Devonian. Like the Devonian "Catskill", another clastic wedge, the 'Mauch Chunk - Pottsville clastic wedge' (Visean - Stephanian Series), spread over much of Pennsylvania from a southeastern source in response to the Alleghanian orogeny (Thomas and Schenk, 1988). Paleocurrent data, pebble-size distribution, sand-to-shale ratio and thickness distribution indicate a WNW- to NNW-directed sediment dispersal pattern through this time (Pelletier, 1958; Meckel, 1970). Some of these sediments must have reached New York, as evident from the preserved rocks of the earliest Mississippian Knapp Formation and Middle Pennsylvanian Olean Conglomerate in western and west central New York, north of the New York -Pennsylvania border (Rickard and Fisher, 1970; COSUNA Chart, 1985). However, the amount of inferred post-Devonian sediments in New York (figs. 16.1, 16.2) can not possibly be accounted for by Carboniferous sediments alone, at least by those coming from the southeastern source.

Although in eastern Pennsylvania the combined thickness of the Carboniferous rocks is about 3.4km (COSUNA Chart, 1985) - and the actual pre-erosional thickness may have been greater - the thickness decreases in practically all directions from eastern Pennsylvania. Moreover, except in eastern and southeastern Pennsylvania, a hiatus separates the Mississippian Mauch Chunk Formation from the Pennsylvanian Pottsville Formation indicating that after the deposition of the Mauch Chunk Formation a period of sub- aerial exposure and erosion followed over much of Pennsylvania including its northern and northeastern parts, contiguous to New York. This erosion is also evident from whatever is left of the Carboniferous in New York: the Olean conglomerate (maximum thickness of 28m), which is equivalent to the upper Pottsville, rests uncomformably on the latest Devonian Conewango Group in west central New York (COSUNA CHART, 1985). In southeastern New York, although no Carboniferous rocks are preserved, it can be assumed that sedimentation (from the southeastern source) and erosional history caused similar results as in northeastern Pennsylvania; i.e., much of the older Carboniferous sediments were eroded before the deposition of the Pottsville Formation. A generous estimate of at best 1km thick Pottsville and younger Carboniferous (Llewellyn Formation) sediments of the southeastern provenance can be made for the southern portions of New York state on the basis of their preserved thicknesses in Pennsylvania (see COSUNA Chart, 1985). This leaves one with two other choices to explain the post-Devonian sediment thicknesses in New York: (1) much of the sediment was post-Pennsylvanian in age, or (2) part of the sediments came from a different source or sources.

It has been proposed by Levine (1986) that the extant Carboniferous rocks of the anthracite region of eastern and northeastern Pennsylvania were buried to depths of 6-9Km before the Alleghanian folding took place in the region (see chapter 3). Accepting a limiting age of 290-270 Ma for the folding, from a paleomagnetic study by Van der Voo (1979), Levine (1986) inferred that only 10-15 million years were available for this 6-9km thick sediments to be accumulated. Since this would require an extraordinarily high sedimentation rate, Levine proposed rapid, tectonically emplaced load as the means of burial.

Supposing that the Alleghanian thrust blocks indeed overrode the anthracite district of Pennsylvania, as Levine (1986) proposes, it is very likely that sediments eroded from these blocks found their way into New York. These geologically instantaneous thrusted blocks were obviously susceptible to very rapid erosion, and sediments may have been carried to at least the southern parts of New York by young, high-gradient rivers. Supposing that about 1km of Pennsylvanian rocks (Olean Conglomerate represents remnants of these rocks in southern New York), equivalent to the Pottsville and Llewellyn formations of Pennsylvania, was already present in the southern portions of New York before the proposed thrust sheets (Levine, 1986) were emplaced, approximately 5km of younger strata (fig. 16.2) might have received their sediments from the thrust blocks. If one considers the maximum average preservation rate of about 400m/m.y. in the Alpine mollase (Van Houten, 1974), the estimated maximum thickness of 5km of post-Pennsylvanian strata in central and southeastern New York would require about 13 m.y. to accumulate. If the youngest age of the proposed emplacement of the tectonic load, i.e., 270 m.y., is accepted, it would take until 257 m.a., or the middle Permian for all the post-Devonian strata in the above-mentioned areas of New York to accumulate. But the tectonic source could have been established earlier - as early as 290 Ma (Levine, 1986) - and the required post-Devonian deposition in New York could have been completed by 277 Ma., or the early Permian. Other factors, however, could change these age estimates. The preservation rate might have been lower than 400m/m.y., or New York might have received sediments simultaneously from other sources: these two factors would have worked in opposite directions in defining the duration of post-Devonian sedimentation.

Other sources of post-Devonian sediments in New York can be speculated on. It is believed that in the Mississippian-Pennsylvanian interval, the Cincinnati Arch (fig. 2.1) was uplifted in response to thrusting in the Ouachitas and the southern Appalachians, and clastic sediments eroded from the arch entered the western side of the Appalachian basin in Ohio and Pennsylvania while deltas with southeastern provenance filled the eastern side (Donaldson and Schumaker, 1981; Beaumont et al. 1987). In fact, deltas are thought to have built southward into southern Illinois and Indiana in the Middle Pennsylvanian

time from sediments derived from the arch (Donaldson and Schumaker, 1981).

It can be argued that the northeastern end of the Cincinnati Arch, or the Findlay-Algonquin Arch (fig. 2.1) likewise served as a source of clastic sediments for New York at a later (Pennsylvanian - Permian) time. It is known that during the later part of the Carboniferous, Alleghanian thrusting migrated north to central and northern Appalachians (Rodgers, 1967; Dean and Skinner, 1988; Miller and Kent, 1988; Thomas and Schenk, 1988). Levine's (1986) tectonic loading probably represents this thrusting event. Geiser and Englander (1983) infer that the "main phase" of Alleghanian deformation in the northern Appalachians began in the early Permian. So it is possible that the advance of the thrusting toward New York sometime in the Pennsylvanian - Permian interval, bulged the Findlay - Algonquin Arch upward and a trough developed in central New York which received sediments eroded from the arch, following Beaumont et al.'s (1987) model (see fig. 2.5).

Another indirect evidence of a western provenance comes from the fault-bounded basins of the Canadian Maritime Province. Paleocurrent data suggests that for the late Pennsylvanian - early Permian siliciclastic sediments in these basins, the most important source was far to the west (Thomas and Schenk, 1988). Could this source be connected to the western source proposed for New York? This will probably never be known for sure, but the possibility can not be rejected.

The possibility of an eastern source also needs consideration. Several recent studies present evidence - mainly geochemical - of a strong late Paleozoic tectonism in New England, as far west as western Connecticut (see Gromet, 1989 for references). Widespread radiometric Permian ages in metamorphic minerals of this area has been interpreted by Gromet (1989) as a result of Permian metamorphism of relatively deep-seated rocks followed by rapid uplift and cooling. Biotite age ($^{40}Ar/^{39}Ar$) of 245 m.y. in the Bronson Hill Anticlinorium, running N-S across Connecticut, Massachusetts and Vermont, has been explained by Harrison and Spear (1987) as a consequence of "hinged uplift" of the region following Acadian thickening, the longest-lived uplift having occurred along the Bronson Hill Anticlinorium. What happened to the rocks that had to be removed in order for the deeper rocks, with Permian metamorphic signatures,

to be exhumed? Part of the sediments that originated from here may have reached New York.

In summary, the following speculations can be made with regard to the source(s) of post-Devonian sediments in New York: much of the sediment was probably derived from sub- aerially exposed Alleghanian thrust blocks in the vicinity of southeastern New York. However, sediments from a western or northwestern source may have partly contributed the sediments in central and western portions of New York. It is also possible that the site of the present Bronson Hill Anticlinorium in central New England had served as an eastern source. Sedimentation in New York probably continued into the middle Permian, but perhaps no later than the Permian.

17.2: POSSIBLE POST-DEVONIAN PALEOGEOGRAPHY AND DEPOSITIONAL MODEL:

From the preceding discussion, it is possible to speculate on the post-Devonian paleogeography of New York and adjacent areas, and on the general depositional model.

In this speculative model (fig. 17.1), the Alleghanian mountains stood in the vicinity of southeastern New York, principally in the present eastern and northeastern Pennsylvania (section 19.1), or even within southeastern New York. Beaumont et al. (1987, fig. 16c) show the northern extent of possible Alleghanian basement thrust along an arcuate boundary in southeastern New York. These mountains probably formed sometime in the Pennsylvanian - Permian interval, perhaps during the "main phase" (Geiser and Englander, 1983) of Alleghanian orogeny, in response to west and northwest-directed thrusting and, possibly, to associated "thin skin" folding of the superficial rocks in accord with the Alleghanian tectonic style (section 2.3). Being mainly thrust-generated, the mountains rose rapidly and were subjected to vigorous erosion. Clastic debris shed from these mountains were carried north, northwest and possibly west by young rivers and were deposited as alluvial fans and braided river deposits of gravel and coarse sand over a large part of southeastern New York (fig. 17.1). If the Late Pennsylvanian - Permian climate in the region became relatively dry, as Phillips and Peppers (1984) interpret, the consequent decrease in vegetation was

fig. 17.1: Speculative model showing post-Devonian paleogeography and depositional environments in New York. See text for discussion.

HIGHLANDS ALONG THE FINDLAY-ALGONQUIN ARCH
FLOOD PLAINS
LAKES
FLOOD PLAINS
HIGHLANDS ALONG THE BRONSON HILLS ANTICLINORIUM
ALLUVIAL FANS-BRAID PLAIN
ALLEGHANIAN MOUNTAINS
MAJOR SEDIMENT TRANSPORT PATHS
SECONDARY SEDIMENT TRANSPORT PATHS

probably especially favorable for development of alluvial fans. The model is similar to the present depositional system in the foreland of the Tien Shan range which was uplifted due to an early Tertiary compressional event between India and Asia, and extreme erosion in a very dry climate that followed led to the formation of large alluvial fans and braid plains (Allen et al. 1991).

North and west of the "alluvial fan - braided river" depositional environment, the rivers, devoid of much of their coarse sediment load, probably took on a sinuous or meandering pattern, and relatively smaller amount of sediments was deposited in this "flood plain" environment (fig. 17.1). It is also possible that the relatively steep gradient of these rivers, now carrying mainly finer grained sediments, aided the sediments to largely bypass this area and be deposited mainly in the narrow trough farther northwest. If the inferred highlands were indeed present along the present site of the Bronson Hill Anticlinorium (fig. 17.1), part of the flood-plain deposits may have been contributed by rivers coming down these highlands.

As previously discussed, the "trough" in central New York could have formed by downsagging in response to the "relaxation phase" following emplacement of the basin-margin thrusts (fig. 2.5). The trough could also have occupied the axial position of the pre-existent epicontinental seaway. However, it is unlikely that during the Pennsylvanian - Permian interval sea was still present in central New York. First, the preserved Pennsylvanian rocks of Pennsylvania are fluvial in origin; no marine facies are known. Second, in the Pennsylvanian - Permian interval the region south of New York witnessed folding, overthrusting and uplift - a very unfavorable time for the sea to return to central New York. Most probably, the inferred trough in central New York was an inland basin, covered or dotted with lakes or isolated remnants of the older Appalachian seaway. These may be compared to the ephemeral lakes in the foreland basin north of the Tien Shan range, China (Allen et al. 1991).

The trough, which extended into the southwestern Adirondack region, probably received sediments from the rivers flowing down the "Alleghanian mountains" in the southeast as well as the newly emergent "Findlay Algonquin Arch" in the northwest, and perhaps from the highlands in central New England. The arch probably did not attain

high relief, but was sufficiently high to serve as a second source of river-borne sediment to the trough in central New York. Sediments from these multiple sources probably also contributed to the greater thickness of post-Devonian sediments in central New York. Whether large deltas could have formed in this inland basin is difficult to ascertain. The inferred nearness of the Alleghanian mountains and rapid sedimentation rates make it more likely that the whole depositional system was similar to the Catskill "tectonic fan-delta complex" (Johnson and Friedman, 1969; Friedman and Sanders, 1978) of the Devonian in which subaerial deposits dominated the system.

What was the post-Devonian paleogeography north of New York like? It is possible that the same Findlay-Algonquin Arch extended in areas north and northwest of New York as newly uplifted landmass, but possibly lower in elevation than its southeastern parts. Moderate amounts of clastic sediments probably entered the basin through its north- eastern end, over the present Adirondack region. This may even have been a site of evaporite formation, because the climate was probably dry (Phillips and Peppers, 1984) and little siliciclastic sediments found passage through this area.

17.3: TIMING, RATES AND CAUSES OF UPLIFT:

When did subsidence and preservation of rocks in New York end and uplift begin? Before indulging in this discussion, it is important that the meaning of the word "uplift" is clearly defined.

"Uplift" is a much abused word in geology, and in the past "exhumation" (of rocks due to erosion) has frequently been mistaken for "surface uplift" (England and Molnar, 1990).

"Surface uplift" can only be determined with a reasonable accuracy when the positions of a surface (a topographic surface, a marker bed etc.) in the past and present, with respect to the "geoid" (a commonly used, valid substitute is the "mean sea level", provided its eustatic changes over the studied time interval are known), are known. This is near to impossible when one is dealing with ancient rocks with a complex geologic history in which much of the younger rocks have been eroded, as in the case of the northern Appalachian basin.

However, "exhumation" rates can be determined if the burial depths of a rock unit at present and at a specific time in the past are known. If fission-track dates of the rock unit are available, then it may even be possible to determine the changes in rates of exhumation through the given time interval (Doherty and Lyons, 1980; Miller and Lakatos, 1983; England and Molnar, 1990). As demonstrated below, the results of this study and available fission-track ages of various rock units in New York (Lakatos and Miller, 1983; Miller and Lakatos, 1983; Johnsson, 1986) can be used to determine the same.

In the present study, it has been shown that sedimentation in New York continued to approximately 257 Ma (section 17.1). It has been inferred by several authors that uplift of rocks in the central and northern Appalachian basin took place in late Pennsylvanian - Permian time coinciding with the Alleghanian orogeny (Friedman and Sanders, 1982; Hearns and Sutter, 1985; Levine, 1986; Elliot and Aronson, 1987; Beaumont et al. 1987): however, the subject loses perspective because little consensus exists on precisely when the Alleghanian orogeny came to an end (see section 2.3). The Alleghanian orogeny undoubtedly caused folding (ca. 290-270 Ma. in southern Pennsylvania, Van der Voo, 1979) and uplift of much of the Appalachian basin, but whether the entire basin was uplifted and subjected to exhumation during Pennsylvanian - Permian interval has not been proven. The notion that New York was also uplifted during the Alleghanian orogeny is not supported by the results of this study. It appears that while areas south of New York were uplifted, much of New York not only remained a depositional basin, but had received sediments eroded from the aforementioned Alleghanian uplift. Exhumation of the rocks could have begun perhaps around 255 Ma at the earliest.

According to the apatite fission-track study of Johnsson (1986; fig. 3.4, this study), the Tioga metabentonite (lower Middle Devonian) bed ascended through the 100° C 'closure temperature' at 236$\pm$17 Ma near Buffalo in western New York, at 183$\pm$13 Ma near Syracuse in central New York, and at 193$\pm$15 Ma at Cherry Valley in eastern New York. If the standard deviations are taken into account, exhumation of the Tioga metabentonite up through the 100°C isotherm could have occurred between late Permian

and late Triassic in western New York, early and middle Jurassic in central New York, and in early Jurassic in eastern New York. The fission-track dates of 125±4 m.y. for the lowermost Upper Devonian Gilboa strata in the Catskill Mountains (Lakatos and Miller, 1983) suggest that in eastern New York the same was taking place in the early Cretaceous. Miller and Duddy (1989) also measured an early Cretaceous (120-140 Ma) fission-track age for several Devonian samples in the Catskill region. The Tioga samples studied by them show an age of 245±8 near Buffalo, similar to the age range measured by Johnsson (see above), which would indicate a late Permian - early Triassic uplift in that area. However, according to Miller and Duddy (1989), all the many pre-Cretaceous ages they measured from western and central New York represented mixed ages that resulted from the inability of the surficial Devonian rocks to ever reach the closure temperature of apatite (110°C, according to them) so that the older fission tracks were not completely erased. The paleotemperature data obtained in this study and by many previous works, however, show that temperatures much in excess of 110° C were reached by the Devonian rocks across New York state. Therefore, Miller and Duddy's (1989) interpretation of a general early Cretaceous uplift across the state appears invalid, and differential uplift history indicated by other fission-track studies is accepted. Another fission-track study by Miller and Lakatos (1983) in the anorthosites of eastern Adirondacks shows that exhumation (although Miller and Lakatos call it "uplift") in this area has occurred at a slower rate between 147 and 86 m.y. (late Jurrasic - middle Cretaceous) and at a faster rate since then.

The above review of published literature shows that it is difficult to find a period when "uplift" was not taking place somewhere in New York state, and according to Isachsen (1985), it is taking place now in the Adirondacks at a very fast rate. Therefore, the three inferred ages of uplift in the northern Appalachian basin - late Pennsylvanian to Permian, Cretaceous and Tertiary - in works of various authors (see Friedman, 1990), apparently reflecting a stop-and-go process may not be strictly applicable to New York. Alternate interpretation, as discussed below, is possible.

In the Buffalo region, extrapolation of isopachs of figure 16.2 suggests that as much as 3.5km of post-Devonian rocks may have been present at the time of deepest burial

(ca. 255 Ma). The projected thickness of post-Tioga Devonian on the Buffalo region is 1.1km (Rickard, 1975): a total of 4.6km post-Tioga rocks. According to Johnssson's (1986) apatite fission-track study, the Tioga bentonite bed moved up through the 100°C isotherm at 236±17 m.y. This isotherm was probably at a depth of 2.66km (based on 30°C/km geothermal gradient and 20°C surface temperature). The Tioga bentonite had to be exhumed from a depth of 4.6km to 2.66km - a distance of 1.94km - in only about (255-236) 19 m.y. So, prior to 236 m.y. (middle Triassic), the uplift rate of rocks in the Buffalo area was about 102m/m.y. However, since 236 Ma, the average exhumation rate, with respect to the surface exposure of Tioga, has been only (2.66km/236m.y.) 12m/m.y. - a change of extraordinary magnitude. Similar sharp changes are apparent in other areas of New York (see table 17.1).

However, the time boundary of the extreme changes in exhumation rates seen in table 17.1 may be deceptive. For example, the exhumation rates in eastern New York could have been initially (Late Permian - Triassic) very rapid, as rapid or even faster than 102m/m.y. of the Buffalo area, followed by a sharp decline. Indeed, one line of evidence from the Triassic faulted basins of northeastern United States suggests that in southeastern New York the rate of exhumation was extremely high in the early and middle Triassic.

In the Newark - Gettysburg basin, the closest of the Triassic fault basins to southeastern New York, late Triassic non-marine strata rest unconformably on lower Paleozoic metamorphic rocks and locally on Precambrian basement (Sanders, 1963; Faill, 1973; Friedman et al. 1981). Results of this study (fig. 16.2) and others (Levine, 1986, for example), indicate that at about 255 Ma the site of the present Newark - Gettysburg basin must also have been buried under substantial thickness of late Paleozoic sediment load, most probably tectonically emplaced. The entire load had to be eroded before the development of the fault basin in the middle Triassic (approximately 230 Ma). The thickness of the section overlying the metamorphic rocks at the site of this basin was perhaps less than 6-9km, inferred for the thrust load in eastern Pennsylvania by Levine (1986), because by 255 Ma, part of it was eroded and probably ended up as sediments in New York (sections 17.1, 17.2). Accepting a maximum thickness of 5km, eroded in

TABLE 17.1: Calculated exhumation rates of the Paleozoic rocks at various locations in New York. See text for details.

Area	*Burial depth at ~255 Ma (in km) (rock unit)	+Age of uplif to a depth of 2.66km	Exhumation rate before arriving at 2.66km depth (m/m.y.)	Exhumation rate from 2.66km to the present surface (m/m.y.)
Buffalo	4.6 (Tioga)	236 (M. Triassic)	102	12
Syracuse	7.9 (Tioga)	183 (M.Jurassic)	73	14.5
Cherry Valley	7.1 (Tioga)	193 (E.Jurassic)	72	23.5
Catskills	8.7 (Gilboa)	124 (E.Cretaceous)	46	21.5
Eastern Adiron-dacks	8.5+ (Precambrian)	147 (L.Jurassic)	54+	18

* Taken from figure 16.2 and projected thickness of Devonian and older Paleozoic rocks at these locations. At the Adirondack location, the burial depth of the studied anorthosite samples below the basal Paleozoic Potsdam Formation is not known.

+ The first three data are from Johnsson (1986); Catskill data from Lakatos and Miller (1983); Adirondack data from Miller and Lakatos (1983). Miller and Duddy's (1989) data are similar to those of Johnsson (1986) for Buffalo area and of Lakatos and Miller (1983) for the Catskills.

25 m.y. (255-230), an exhumation rate of 200m/m.y. is obtained. The rate over this time interval probably could not have been much lower in the present Catskill region - the northeastern end of the the Newark-Gettysburg basin is only 80km from Lakatos and Miller's (1983) study location. Sometime after 230 Ma, the exhumation rate in the

Catskill region could have fallen off exponentially with time, so that the transition through 100°C isotherm did not have to be as drastic as seen in table 17.1. Similarly, one could argue that in other locations only the first few tens of million years (probably only the first few million years in case of the Buffalo area) witnessed extremely rapid rate of uplift followed by exponentially decreasing rates (fig. 17.2), thus maintaining the average rate of exhumation indicated by fission track data, but avoiding the sharp transitions.

The inferred late Permian - Middle Triassic rapid uplift and erosion can be related to the pre-rifting doming of eastern North America as it migrated over hot spots or mantle plumes (Burke et al. 1973; De Boer and Snider, 1979; Morgan, 1981). The observation that rapid exhumation began earlier in western New York (Buffalo region in table 17.1) and later in eastern New York (Catskills and eastern Adirondacks in table 17.1) probably reflects earlier passage (and doming and erosion) of western New York over the hot spot/mantle plume as the continent migrated northwestward. Doming apparently caused deep erosion and attenuation of the crust, and subsequent thermal subsidence, contraction, stretching and listric faulting resulted in the formation of the Triassic grabens and half grabens onshore and offshore eastern North America (Manspeizer and Cousminer, 1988 and sources therein). In the suggested exhumation paths of figure 17.2, the period between 255 Ma (probable begining of exhumation) and 230 Ma (age of basal Triassic strata in the Newark-Gettysburg basin), is shown as the time of rapid exhumation throughout the New York State that resulted from the aforementioned doming. Toward the end of this interval and in the aftermath, the exhumation rate dropped exponentially everywhere with the possible exception of south-eastern New York where the drop was probably more gradual. The arguments for a different rate in southeastern New York is as follows.

About 9km thick late Triassic (Carnian) - early Jurassic (Toarcian) fluvial and lacustrine sediments accumulated in the Newark-Gettysburg basin (Sanders, 1963; Olsen et al. 1982). Where did these sediments come from? Much of them, especially in the younger units of the Newark Supergroup came from the north and northwest (Faill, 1973; Manspeizer, 1985) indicating that at least the southeastern part of New York was probably being eroded at a relatively fast rate through at least the early Jurassic and

Figure 17.2: Graphs showing (1) changes in exhumation rates at five locations of New York State since the Late Permian, based on fission-track data presented in table 17.1, and (2) the suggested exhumation pathways based on arguments presented in the text.

BUFFALO REGION:

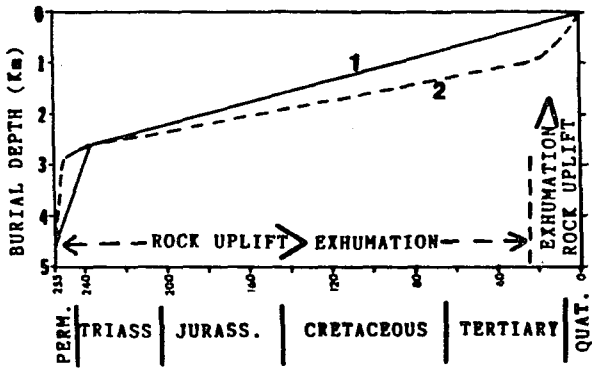

SYRACYSE REGION:

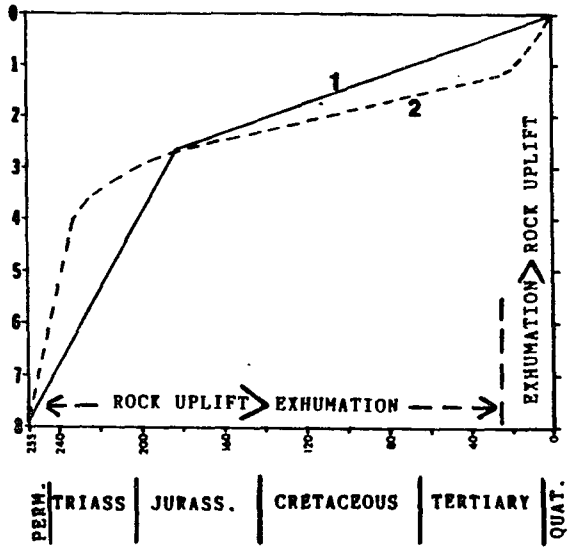

CHERRY VALLEY:

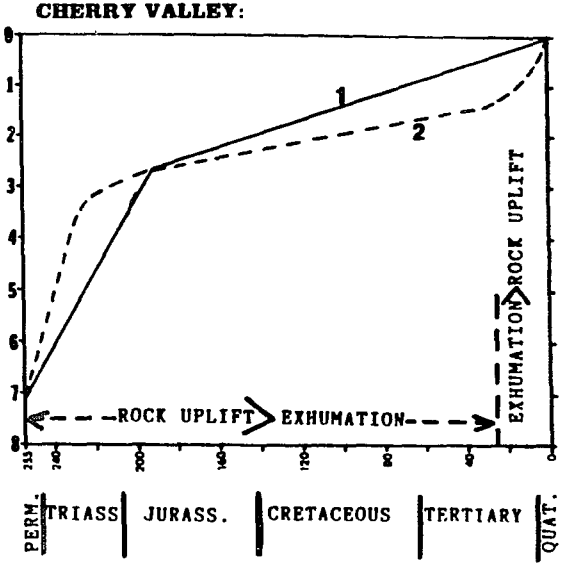

EASTERN ADIRONDACKS:

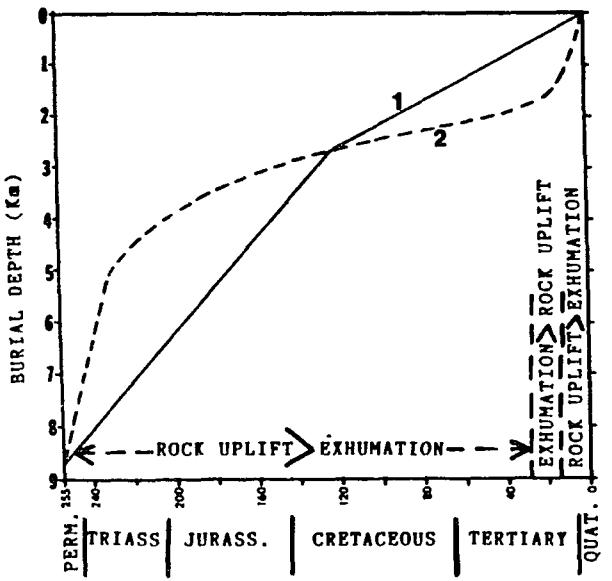

CATSKILLS:

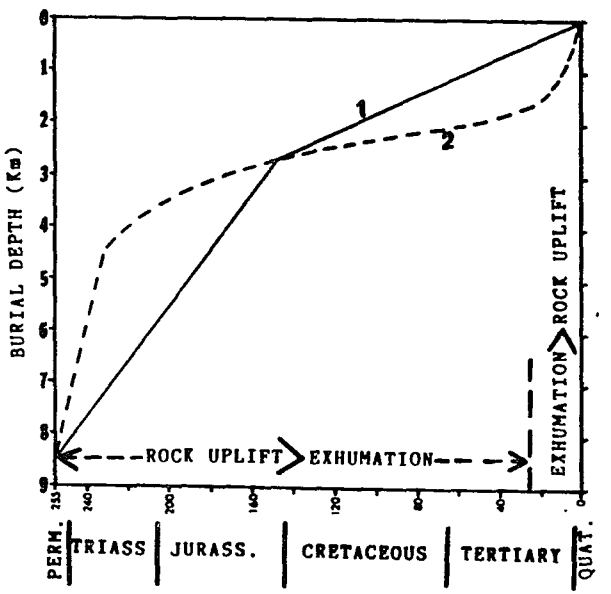

probably longer (fig. 17.2).

On the basis of volume calculation of Cenozoic sediments on the floors of the western Atlantic Ocean, Mathews (1975) estimated that an average of 2km of denudation of rocks between the "Fall Line" and the watershed coinciding with the Frontenac Axis that passes north-south through western New York must have occurred "since the begining of the Cenozoic (Ca. 65 Ma). This gives an exhumation rate of approximately 31m/m.y., which is faster than the average rates followed since the early Cretaceous in southeastern New York, late Jurassic in eastern Adirondacks, middle Triassic in the Buffalo area, and early and middle Jurassic in Cherry Valley and Syracuse area, respectively (table 17.1). Evidence suggests that an accelerated rate of erosion began in New Jersey and Pennsylvania in the Neogene - as early as the Miocene - when dissection of the the uplands of the Schooley and Kittitanny Mountains started (Mathews, 1975). Mathews also cites various evidence of a Neogene age for the begining of upland incision in the Atlantic province of Canada. Rodgers (1967) is of the opinion that the present elevations of much of the Appalachians were attained by the Eocene time, implying that since then erosion has been the dominant process. Continental glaciation in the north may also have contributed to a high rate of erosion in the Pleistocene time (White, 1973; Gurrieri and Musiker, 1990). Thus, it may be assumed that since at least the Miocene time, exhumation rates in New York have been relatively higher than the Paleogene. In figure 17.2, the upturn in the proposed exhumation paths since the Miocene time reflects this increase.

Although at the beginning of this section the difficulty of assessing the rate of "surface uplift" had been emphasized, it is nevertheless possible to reflect on the relative role of surface uplift in New York through the last 255 m.y. No doubt exists that surface uplift has taken place. The exposed middle and lower Paleozoic rocks of New York, which were buried to depths of many kilometers (and well below the Permian sea level) are now exposed at various elevations above the present sea level: the Precambrian basement is at an altitude of more than 1.5km in Mt. Marcy and Mt. Algonquin in The Adirondacks; the middle Devonian Hamilton Group rocks are at elevations of 1280m in the Slide Mountain of the Catskills (Broughton et al. 1966) and the Upper Devonian

clastics are at elevations of over 600m in the dissected plateau surface of southwestern New York (Rickard and Fisher, 1970). If the present elevations were indeed reached in the Eocene time (Rodgers, 1967), it can be inferred that "surface uplift" took place over most of New York between the Middle-Late Permian and Eocene time. During this interval, rate of "rock uplift" was greater than rate of "exhumation" (fig. 17.2) resulting in net "surface uplift" (see England and Molnar, 1990). Subsequent to the Eocene time, perhaps between Miocene and now, exhumation rate has been faster than "rock uplift" rate, resulting in average decrease in surface elevation.

However, the exhumation history of the Adirondack Highlands in the recent times probably followed a somewhat different path from the rest of New York. It has been inferred that the mineral assemblage of the surficial rocks of the Adirondacks were formed at PT conditions equivalent to those at depths of 25km (Fisher et al. 1979; Isachsen et al. 1991). Much, if not all, of this 25km of rocks must have been stripped prior to deposition of the Cambro- Ordovician carbonates, perhaps in an earlier episode of uplift.

Results of this study suggest that more than 8km Paleozoic rocks once covered the Adirondacks. This plus an additional but unknown thickness of Precambrian rocks have been lost during the last 255m.y. (table 17.1). Before the rocks studied by Miller and Lakatos (1983) crossed the 100°C isotherm, the exhumation rate was at least 54m/m.y. (table 17.1). But following the same arguments as before, it is believed that the exhumation rates were very high in the Triassic period followed by a sharp decline (fig. 17.2). Fission-track data of Miller and Lakatos (1983) suggests that since 147 Ma the exhumation rate in the Marcy Massif area of eastern Adirondacks dropped to 18m/m.y. (table 17.1). However, samples taken from the eastern boundary of the Adirondacks, about 40Km from the samples of the Marcy Massif, show a fission-track age of 86 m.y. meaning that the rate of exhumation at this location has been about (2.66km/86m.y.) 31m/m.y. since the middle of Cretaceous. From various neotectonic and geomorphic evidence, Isachsen (1985) suggests that the Adirondack Highlands is a Neogene domical uplift, which is currently experiencing an extraordinary uplift rate of 3.7mm/yr at the center of the dome. Although some questions remain about geodetic releveling

techniques (Isachsen, 1985) on which the above rate has been calculated, such high rates are probably indicative of geologically instantaneous velocities and may not be representative of long-term tectonic motion (Heinz et al. 1980). However, if Isachsen's (1985) calculations are correct, "surface uplift" is taking place in the Adirondacks at present (fig. 17.2). However, surface uplift rates represent average values that have to be computed over a large area (England and Molnar, 1990), and the presence of large relief within the Adirondacks and inferred local variation in exhumation rates (Miller and Lakatos, 1983) indicate that the average surface uplift rate in the Adirondack region is perhaps much smaller than 3.7mm/yr. Whether similar surface uplift is currently taking place elsewhere in New York is not known.

The proposed exhumation paths for rocks of different locations in New York, shown in figure 17.2, have to be treated as semi-quantitative trends at best. These pathways represent the interplay between rock uplift and erosion, and as previously discussed, the change in relative dominance of the two opposing processes seems to have taken place at about the Miocene time. These exhumation paths do not, for example, mean that rock uplift has stopped since the Miocene time or even slowed relative to the pre-Miocene time, but that erosion has had an upper hand over rock uplift. Accelerated erosion during the post-Miocene interval may have been related to Pleistocene glaciation, post-glacial crustal rebound and stream rejuvenation, or to other climatic factors. In the Adirondacks region, however, rock uplift seems to be dominating erosion at least for now. The proposed exhumation pathways also do not directly negate the proposed timings of uplift, i.e, Carboniferous-Permian, Jurassic-Cretaceous and Neogene in the Appalachian basin, but show that the initial uplift started later (Permo-Triassic) in New York and was most rapid in the early Triassic time. An episodic, rapid uplift in the Jurassic-Cretaceous period is not necessary to interpret the loss of Paleozoic strata from various areas of New York. Even in the Neogene time, the only evidence of rapid, episodic uplift comes from the Adirondacks.

What force has caused rock uplift in New York that seems to have continued since the late Permian?

As discussed earlier, the late Permian - middle Triassic rapid exhumation of rocks

may have been due to the thermal event that caused doming of the eastern North America and led to rifting of the continents. It is also possible that in the early part of this time interval, some component of the Alleghanian uplift affected New York State: the only difference is that it did so later in New York state than areas in the south. However, neither the possible delayed impact of the Alleghanian orogeny nor the pre- or synrift thermal event could possibly have sustained the rock uplift up to the Miocene time. Hot spots and mantle plumes thermally expand and uplift of rocks for a maximum duration of about 50 m.y (S. Bhattacharji, 1991, pers. comm.). Synrift uplift is usually confined to a narrow zone, commonly 10 - 20km, across the rift (Neugebauer, 1987; King and Ellis, 1990). New York State was initially farther than this from the rift, and has since steadily moved away from the rift (the present mid-Atlantic ridge). Nevertheless, within 50 my of these thermal events (i.e., by Early Jurassic), New York State should have stopped moving up; instead, it should have subsided in response to cooling of the lithosphere. But evidence suggests that this has not happened and "rock uplift" has continued to at least the Miocene time, and is taking place now in the Adirondacks area.

Therefore, post-Early Jurassic rock uplift in New York State probably can not be directly attributed to plate marginal processes. (The reader should also note that the pre-rifting doming was also not a plate marginal process, but an independent event that led to break up along an old suture). The crustal movement in New York State at least since the Early Jurassic and to a large extent since the late Permian, therefore, can be termed "epeiorogenic" (see Friedman, 1988a for discussion on present controversies on the subject).

Many possible mechanisms have been proposed for such uplift (see for example, McGetchin et al. 1980; Hinze et al. 1980). These include the much-discussed thermal expansion of the lithosphere due to a deep mantle plume or hot spot, thermal expansion due to shear heating because of relative motion along the lithosphere-asthenosphere interface, volumetric expansion accompanying partial melting, metamorphic reactions (basalt-eclogite) in the lower crust, hydration reactions (such as serpentinization) within the mantle, crustal thickening due to horizontal mass transfer, "trapping" of hot light

material released periodically from the core-mantle boundary by moving plates in areas where the lithosphere is thin, among others.

It is beyond the scope of this study to determine which mechanism(s) is/are responsible for the epeirogenic uplift in New York. Crough (1981) suggested that in the Cretaceous - early Tertiary time, southeastern Canada and New England area migrated over a hot spot, which resulted in 4km uplift of this region relative to the central Appalachians. New York State, at the periphery of this region, may have been uplifted to a lesser extent by this hot-spot swelling. However, available data from New York do not indicate rapid exhumation in the Cretaceous - Early Tertiary interval (table 17.1; fig. 17.2; also see Miller and Lakatos, 1983). Isachsen (1985) inferred the presence of a deep-seated heat source under the Adirondack region; the thermal front of this heat source has still not manifested itself at the surface.

In short, the cause of epeirogenic movement in New York State is not known, but some sort of subcrustal thermal anomaly is suspected.

CHAPTER 18: SUMMARY AND CONCLUSIONS

(1) Paleotemperatures of outcrop and core samples of ten Paleozoic rock units in New York State were assessed from fluid-homogenization temperatures (Th), oxygen isotope ratios, thermal alteration index (TAI), vitrinite reflectance (Ro), percentage of smectite in mixed-layer illite/smectite and illite crystallinity (I.C). Oxygen isotopes and TAI were found least useful for paleotemperature determination probably because of the difficulty of microsampling and uncertain assumptions ofisotopic composition of paleo-fluid in the case of oxyge nisotopes, and subjective attributes of laboratory measurements and inter-sample variation in organic composition and degree of degradation in the case of TAI.

(2) All studied samples show paleotemperature signatures much higher than what is expected from their position with respect to the surface. Since evidence of Paleozoic or younger thermal anomalies that could have affected the studied samples are lacking, it is believed that the paleotemperature signatures were attained during deep burial.

(3) High Th, very low fluid-melting temperatures (Tm), and light $\delta^{18}O$ (‰PDB) values of mineral cements indicate that most of the cements precipitated from hot subsurface brines. The spatial variation in Th of the studied rock units, however, is inconsistent with known models of expulsion of deep basinal brines toward shallow basin margins, or cratonward migration of fluids from the eastern orogenic belt: the paleotemperature signatures of the studied rock units thus reflect ambient geothermal temperatures as a principal function of burial depths.

(4) Comparison of maximum paleotemperatures obtained from different techniques shows that for shale samples, temperatures derived from I.C. and maximum Ro match reasonable well, and I.C.-derived temperatures were used to establish the maximum paleotemperatures experienced by all shale samples, because in the studied Ordovician shales Ro data was not available. For carbonate rocks, however, only a lower limit of maximum paleotemperature could be ascertained from Th_{max} (average of Th in the highest 20°C interval) data because the Th were

not pressure-corrected. Pressure correction could not be accomplished because of many uncertain assumptions involved. Th_{max} data was, however, farther refined by comparing data from different rock units of the same or nearby locations.

(5) On the basis of the average present-day geothermal gradient in New York State and studies of paleo-geothermal gradients in the northern Appalachians and other foreland basins, a geothermal gradient of 30°C/km at the time of maximum burial of the present rock units in New York appears to be an appropriate assumption. Similarly, a mean annual surface temperature of 20°C was assumed.

(6) The maximum burial depth for a rock unit at a given location was calculated from the maximum paleotemperature data at that location, a paleo-geothermal gradient of 30°C/km, and a mean annual surface temperature of 20°C. Two sets of maximum burial depth data were obtained: one from I.C.- derived temperatures of shales, the other from Th_{max} of carbonates. The latter only represented a lower limit of maximum burial.

(7) By projecting the thicknesses of the extant younger rocks (up to the end of the Devonian) in southern New York State on the studied rock units of all study locations and subtracting these thicknesses from the maximum burial data, the thicknesses of former post-Devonian strata at each study location in New York were estimated. Two sets of data emerged: one via Th_{max} showing the minimum thicknesses of post-Devonian strata that must have been present, and the other from I.C.-derived estimates of maximum burial showing the maximum possible thicknesses of post-Devonian strata that might have been present.

(8) Two isopach maps made from the two data sets show that two NE-SW elongate belts of greater post-Devonian sediment accumulation were present in New York: one in southeastern New York and the other in central New York. The isopach maps also show that the southwestern part of the present Adirondack mountains were covered under at least 3km of post-Devonian strata. All previous estimates and implications of former post-Devonian strata in New York are consistent with the results of this study.

(9) From the thickness of extant Carboniferous strata in Pennsylvania, it is inferred that most of the post-Devonian rocks in New York were in fact post-Carboniferous in age. Based on known preservation rates of molassic sediments elsewhere, it is estimated that sedimentation in New York continued up to Late Permian (ca. 255 Ma).

(10) Upthrusted Alleghanian mountains in eastern Pennsylvania were the main source of post-Devonian sediments, at least for southern New York. Sediments were rapidly eroded from these young mountains by steep-gradient rivers and deposited in a northwestward succession of alluvial fan-braid plains, flood plains, and lacustrine environments. Additional sediments probably came from an uplifted land mass along the Findlay-Algonquin Arch northwest of New York and high areas in western New England, perhaps along the axis of the present Bronson Hill anticlinorium. Central New York was probably the deepest part of an inland basin dotted with lakes or the isolated remnants of an older epicontinental seaway, which received sediments from these additional sources, brought down by rivers, leading to a second trough (besides southeastern New York) of greater post-Devonian sediment accumulation.

(11) The end of sedimentation and the beginning of exhumation in New York could have started as early as 255 Ma. Previously published fission-track ages of various rock units in different areas of New York imply that an early period of rapid exhumation of rocks was followed by a later period of much slower exhumation. Re-evaluation of the fission-track ages in the light of this study shows that the very rapid exhumation was probably characteristic of the Late Permian-Middle Triassic interval followed by an exponentially decreasing rate of exhumation until about the Miocene Epoch. Following the Miocene, the exhumation rates have again increased. Glacial and post-glacial rapid erosion may have contributed to this increase.

(12) The rate of "surface uplift" in New York State can not be quantified from the available information. However, published geologic information suggest that the present highest elevations in different areas of the northern Appalachians were

attained by the Miocene time. Thus, it can be assumed that "rock uplift" rates dominated over "exhumation" rates between 255 Ma and the Miocene time leading to net surface uplift. Since the Miocene, exhumation rates have dominated over rock uplift rates resulting in average decrease in surface elevation everywhere in New York with the possible exception of the Adirondack mountains, where surface uplift is currently taking place.

(13) The three ages of uplift of the northern Appalachians - late Carboniferous-Permian, Cretaceous and Tertiary - inferred by several authors do not strictly apply to New York State. This study shows that while the areas south of New York were uplifted during the late Carboniferous, New York State remained, or probably transformed into an inland depositional basin and received sediments shed from the mountains and landmasses uplifted by the Alleghanian event. Uplift in New York lagged behind, and did not probably begin until the Late Permian. Also, evidence of an episodic Cretaceous uplift is not definite; the Cretaceous period, according to this study, was at the waning end of very rapid uplift that characterized the Late Permian - Middle Triassic interval. Similarly, episodic Tertiary surface uplift is not seen as a general phenomenon in New York State, but as a local event in the Adirondack mountains.

(14) The most important driving mechanism for the initial rapid surface uplift in New York State may have been the pre- rifting thermal swelling that resulted from migration of eastern North America over hot spots or mantle plumes. This was an epeirogenic process independent of plate marginal processes, although it coincidentally caused the break up of the continents along the old suture. The continued uplift of New York State up to the Miocene time, and to the present day in the Adirondacks, also can not be explained by plate-marginal processes. Although many mechanisms of epeirogenic crustal movement have been proposed, the cause of epeirogenic uplifts in New York, especially since the Triassic, are not clear.

APPENDIX - A: SAMPLE LOCATIONS

The sample locations are listed separately for the studied rock units starting from the oldest. Location numbers listed below are to be found in the location maps of individual chapters of the text.

BEEKMANTOWN GROUP: (CHAPTER 5)

Location # 66: Core sample from Hooker Chemical Company drillsite in Niagara County at lat. 43°-05-00 N and long. 79°-00-00 W.

Rock units: Theresa Fm. (865.3m - 885.4m)
Potsdam Fm. (885.4m - 928.4m)
Paragneissic arkose (below 928.4m)
Samples: H-1 (910m), H-2 (911.6m) and H-3 (918.8m)

Location # 68: Core sample from Robert Olin Company drillsite in Steuben County at lat. 42°-05-00 N and long. 77°-25-00 W.

Rock units: Theresa Fm. (3474.7m - 4022.1m)
Potsdam Fm. (4022.1m - 4054.4m)
Samples: Ro-1 (3799m) and Ro-2 (3821.2m)

Location #73: Roadcut on both sides of Rte 9N about 5 miles north of intersection with Rte 9 in Saratoga Springs, under railway pass.
Samples: TH-1A, TH-1B, TH-1C from Theresa Formation.

Location #74: Small roadcut on Rte 29, approximately 5miles west of Saratoga Springs.
Samples: TH-2A, TH-2B, TH-2C from Hoyt Limestones.

Location # 75: Roadcut on both sides of Rte 29 east of intersection with Rte 147 near Mosherville.
Samples: TH-3A, TH-3B, TH-3C, TH-3D from Theresa Formation.

Location# 76: Roadcut on Rte 67, approximately 2 miles west of intersection with Rte 147.
Samples: Z-1A, Z-1B, Z-1C from uppermost Tribes Hills Formation.

Location #77: Roadcut on Rte 67 few hundred meters west of location #76.
Samples: Z-2A, Z-2B, Z-2C from Gaylord Member of the Tribes Hills Formation.

Location #81: Cliff on the south side of Rte 5S along the Mohawk Water Gap.
Samples: LF-1, LF-2, LF-3, LF-4 from Little Falls Dolostones.

Location # 63: Streamcut along Canajahorie Creek in the town of Canajahorie. From Rte 5S in Canajoharie turn left on Montgomery Street, right on Moyer Street and right again on Floral Avenue. The creek is in front of the dead end on Floral Avenue.

Rock units: Utica Shale
Tribes Hill Fm.
Samples: CJ-1A, CJ-1B, CJ-1C from Tribes Hill Formation.

Location #90: Roadcut on northbound NY 81 about 6 miles north of exit to Theresa.

Rock units: Theresa Formation
Potsdam Formation
Samples: TH-4 (Theresa), PS-1 and PS-2 (Potsdam)

Location #91: Roadcut on northbound Rte 12 near Chippewa Bay 0.2 miles northeast of intersection with Pleasant Valley Road.
Samples: TH-5, TH-5A, TH-5B

Location #92: McConville Quarry in the town of Ogdensburg. From Rte 37N in Ogdensburg turn right on Ogden Street, and right again on Madison Avenue. Quarry on the right side of the bend on Madison Avenue. Samples collected from small roadcut on the left side of the bend.
Samples: OD-1A and OD-1B and OD-1C from Ogdensburg Dolostones.

BLACK RIVER AND TRENTON GROUPS: (CHAPTER 6)

Location #60: Northwest Newport Quarry. From Rte 28 in the town of Newport turn left onto Bridge street (=Old State Road), cross the bridge, turn right at the intersection with West Street. After 0.75 miles turn right onto gravel road leading to the quarry.
Samples: ORD-1, ORD-1A from Trenton Group.

Location # 61: Roadcut on the eastern side of Rte 28N, 0.6 miles north of the northern edge of Middleville.
Samples: ORD-2X, Z-3A and Z-3B from Trenton Group.

Location #64: Core samples from J. Matejka #1 drillsite in Chemung County at lat. 42°-12-30 N and long. 76°-37-30 W.

Rock units: Martinsburg Fm. (2613.3m - 2804.2m)
Utica Shale (2804.2m - 2843.5m)
Trenton Group (2843.5m - 2990m)
Black River Gp. (2990m - 3102.5m)
Samples: JM-2 (2957m), JM-5 (2980m), JM-3 (2986.6m), JM-4 (2997.4m)

Location # 65: DOT core from Encon Black River Dam, Hawkinnsville site in Oneida County at lat. 43°-30-17 N and long. 75°-17-19 W.

Rock units: Watertown Fm. (Trenton Gp.) : 6.4m - 7.9m
Lowville Fm. (Black River Gp.): 7.9m - 24.4m
Pamelia Fm. (Black River Gp.): 24.4m - 31.6m
Samples: BR-1 (9.1m), BR-2 (10.7m) and BR-3 (34.7m)

Location #78: Inactive quarry on the south side of Rte 67, 1/3 mile east of the village of Manny Corners (east of the city of Amsterdam).
Samples: TR-1, TR-1A from Trenton Group.

Location #83: Streamcut and small quarry face along waterfall just north of the town of Middleville. On Old City Road about 1/2 mile east of Rte 28N.
Samples: BL-1A and BL-1B from Black River Group.

Location #84: Roadcut on Rte 12N just south of Boonville.
Samples: TR-2A, TR-2B, TR-2C from Trenton Group.

Location #85: Roadcut on Rte 12N, 13 miles south of Lowville.
Sample: BL-2A, BL-2B, BL-2C from Black River Group.

Location #87: Roadcut on NY 81 few miles north of Watertown. Several exposures.
Samples: BL-3A, BL-3B, BL-3C from Black River Group.

Location #88: Roadcut on the west side of NY 81, 3-4 miles north of location #87.
Samples: BL-4A, BL-4B, BL-4C from Black River Group.

LOCATION #89: Roadcut on NY 81, 1.4 miles north of exit sign to Theresa.
Samples: Z-4A, Z-4B from Black River Group.

UTICA SHALE: (CHAPTER 7)

Location #64: See Location #64 under Black River-Trenton groups.
Samples: JM-1 (2825.8m)

Location #79: Roadcut on north side of Rte 5 few miles west of Fort Johnson.
Samples: UT-1A, UT-1B, UT-1C.

Location #80: Roadcut on Rte 5S, 1-2 miles west of Fultonville.
Samples: UT-2A, UT-2B, UT-2C.

Location #63: See location #63 under Beekmantown Group above.
Samples: UT-3A, UT-3B, UT-3C.

Location #82: Roadcut on Rte 80S between Fort Plain and Hallsville.
Samples: UT-4A, UT-4B, UT-4C

Location #93: Roadcut along NY Thruway (I-90) just west of intersection with Rte 169.
Samples: UT-6A, UT-6B, UT-6C, UT-6B.

Location #86: Small cliff in the Whetstone Gulf State Park along Rte 26 between Martinsburg and Houseville.
Samples: UT-5A, UT-5B, UT-5C.

THE CLINTON GROUP: (CHAPTER 9)

Location #50: Core sample from BHP87-2 site in Wayne County, Sodus Township at lat. 43°-11-46 N and long. 77°-04-04 W.

Rock units: Rochester Shale (2.1m - 55.5m)
Irondequit Limestone (55.5m -)
Samples: HL-2A (8.5m), HL-2B (12.5m), HL-2C (24.2m) from Rochester Shale.

Location #55: Core sample from BHP87-10 site in Wayne county, Ontario Township at lat. 43°-14-14 N and long. 77°-22-11 W.

Rock units: Williams Shale (3.3m - 5.3m)
Lower Sodus Shale (5.3m - 10.9m)
Reynales Limestones (10.9m - 14.6m)
Maplewood Sandstones (14.6m - 26.5m)
Grimsby Formation (26.5m - 49m)
Queenston Formation (49m -)
Samples: HL-10A (11.4m), HL-10B (13.5m) from Reynales Limestones.

LOCPORT GROUP: (CHAPTER 10)

Location #45: Frontier Stone Product Quarry, Lockport Town. Lat. 43°-09-08N and long. 78°-43-22 W.
Samples: LP-1, LP-7 and LP-8

Location #46: Roadcut at Lockport Junction. From northbound Rte 270, proceed across Upper Mountain Road onto Lockport Junction Road (Rte 93). Exposure 0.4 miles from intersection with Upper Mountain Road.

Samples: LP-2, LP-2B, LP-2C.

Location #47: Roadcut near Pekin beneath the overpass on Rte 429.
Samples: LP-3, LP-3A, LP-3B.

Location #48: Quarry of Clarendon Stone Company west of Rte 237 at southern end of the town of Clarendon.
Samples: LP-4, LP-4A, LP-4B

Location #49: DOT core from Hole 2C-73, well (5-4R) at lat. 43°-12-40 N and long. 78°-52-36 W.

Rock units: Eramus and Goat Island members (? - 36.6m)
Gasport Member (~36.6m - 40.7m)
Decew Member (40-7m -)
Samples: LP-5A, LP-5B, LP-6 from Gasport Member.

Location #54: Core sample from BHP87-9 site in Monroe County, Perinton Township at lat. 43°-09-10 N and long. 77°-24-55 W.

Rock units: Lockport Fm. (7.1m - 44.3m)
Rochester Shale (44.3m - 77.7+m)
Samples: HL-9A (19.5m) and HL-9B (25.3m)

THE SALINA GROUP: (CHAPTER 11)

Location #51: Core sample from BHP87-3 site in Wayne County, Lyons Township at lat. 43°-07-58 N and long. 77°-00-56 W.

Rock units: Vernon Shale (9.3m - 29.7m)
Lockport Fm. (29.7m - 59.4m)
Samples: HL-3A (23.8m) from Vernon Shale.

Location # 52: Core sample from BHP87-5 site in Wayne County, Arcadia Township at lat. 43°-05-53 N and long. 77°-03-45 W.

Rock units: Vernon Shale (8.5m - 58.2m)
Lockport Fm. (58.2m - 62.7+m)
Samples: HL-5A (30.8m) from Vernon Shale

Location #53: Core samples from BHP87-7 site in Wayne County, Macedon Township at lat. 43°-03-05 N and long. 77°-19-31 W.

Rock units: Camillus Shale (16.7m - 52.7m)
Vernon Shale (52.7m - 77.7+m)
Samples: HL-7A (64.6m) from Vernon Shale.

Location #56: DOT core taken by Church and Dwight Co in Onondaga County at 43°-03-44 N and 76°-11-52W.
Samples: X-17A, X-17B from Vernon Shale.

Location #57: DOT Core I-481 (DNX-1) from Onondaga County at lat. 43°-?-? N and long. 76°-07-32 W.
Samples: X-7A (12.3 m), X-7B (12.6m) from Bertie Dolomite.

Location #58: Roadcut on Rte 174, 3.4 miles south of Camillus near Marcellus Falls.
Samples: SAL-1, SAL-1A from Syracuse Formation.

Location #59: Roadside exposure near the town of Jordanville. From Jordanville Road, 0.1 miles east of intersection with NY 51, turn right (N) onto Elizabethtown Road. Turn right (E) on Brewer Road after 3.1 miles. Turn right on Spohn Road after 1.1 miles. Exposure 0.3 miles from there.
Samples: SAL-2, SAL-2A, SAL-2B, from Camillus Formation.

HELDERBERG GROUP: (CHAPTER 12)

Location #8: DOT core, Olney Thacher hole #1, well #2-94, Oneida County, Marshal Township at lat. 42°-56-49 N and long. 75°-27-30 W.

Rock units: Onondaga Fm. (0m -8.2m)
Oriskany Fm. (8.2m - 10.7m)
Kalkberg Fm. (Helderberg Gp.) : (10.7m - 16m)
Coeymans Fm. (---) : (16m - 27.7m)
Manlius Fm. (---) : (27.7m - 51m)
Rondout Fm. (Upper Silurian) : (51m -)
Samples: OTK-1, OTK-1 (from Kalkberg)

Location #9: Jamestown Penitentiary Quarry. From Rte 173 in the town of Jamesville, turn south on Rte 91. The large two-level quarry is on the left side of the road after 0.5 miles. The Manlius Formation is exposed in the lower quarry, Onondaga in the upper quarry.
Samples: HLB-3, HLB-4

Location #22: Core sample from Cayuga Mine of Cargill, Inc., Lansing Hole #17 in Tompkins County, Lansing Township at lat. 42°-35-00 N and long. 76°-30-00 W.

Rock units: Sherburne and Geneseo Shale (0m - 76.65m)
Tully Limestone (76.6m - 85.5m)
Hamilton Group (83.5m - 436.3m)
Moscow Shale
Portland Point Lst.
Ludlowville Fm.
Centerfield Lst.
Skaneateles Fm.
Mottville Lst.
Marcellus Fm.
Onondaga Fm. (436.3m - 460.2m)
Oriskany Sandstone (460.2m - 462.5m)
Manlius Fm. (462.5m - 477m)
Rondout-Cobbleskill fms. (477m - 502.9m)
Salina Gp. (503m - 848.6m+)

Samples: CGH-1 (476.4m) and CGH-1A (468m) from Manlius Fm.

Location #26: Exposure in Catskill Creek, below and just south of the Rte 23 bridge over the creek, approximately 0.35 miles northwest of Rte 23 bridge over I-87.

Rock units: Port Ewen Fm. (2m)
Alsen Fm. (11m)
Becraft Fm. (5m)
Samples: B-5, B-5A, B-6, B-6A from the Becraft Fm.

Location #27: Becraft Mountain. Inactive quarry of the Independent Cement Corporation located just east of Rte. 9, approximately 1 mile south of the town of Hudson.

Rock units: Alsen Fm. (2.5m)
Becraft Fm. (14.5m)
New Scotland Fm. (1.8m)
Samples: B-3A, B-3B, B-4 from the Becraft Fm.

Location #28: Near the Town of Munsville, off Rte. 46.
Samples: HLB-1, HLB-2.

Location #29: Dot core, Hole #5 (2-9R), Oneida County, at lat. 42°-56-49 N and 75°-37-30 W.
Rock units: Oriskany Fm. (19.9m - 22.9m)
Kalkberg Fm. (22.9m - 28m)
Coeymans Fm. (28m - 33.5m)
Manlius Fm. (33.5m - 62.6m)
Rondout Fm. (62.6m -)

Samples: OC-1 (28.1m), OC-1A (30.3m), OM-1 (53.3m)

ONONDAGA FORMATION : (CHAPTER 13)

Location #1: Exposure off Rte 209 next to warehouse east of Allenville.
Samples: OAL-1, OAL-1A

Location #2A: Roadcut on east side of Rte 209, 14 miles north of the town of Wawarsing.
Samples: OX-1, OX-1A

Location #2B: Roadcut on west side of Rte 209, 2.6 miles north of location #2.
Samples: OX-2, OX-2A

Location #3: Streamcut on Kaaterskill Creek under the bridge on Rte 23A.
Samples: OX-3 and OX-3A

Location #4: Exposure of "Albright Reef". Taking exit 21B from N.Y. State Thruway, turn right on Rte 9W north, turn left onto Greene County Rte 51 and proceed 2.8 miles. Turn left onto Robert's Hill Road and proceed 0.4 miles. Exposures on both sides of the road.
Samples: OG-22, AB-58, and OA-5

Location #5: Exposure of "Robert's Hill Reef". From location #4, proceed another 0.2 miles down Robert's Hill Road, turn right onto County Rte 54, turn left onto Reservoir Road after 1.0 mile and proceed 0.7 miles to Lime Kiln Road. Turn right and proceed 0.4 miles. Exposure forms a prominent, wooded topographic high on the left side of the road.
Samples: OG-20, OG-21, OG-21A and R-74

Location #6: Exposure of "Mount Tom Reef". Broad, low hill 0.5 miles west-southwest of Mount Tom in East Springfield.
Samples: OG-16 and OG-17

Location #7: Several roadcuts at Cherry Valley along intersections of Rte 20, 166 and 32.
Samples: OG-1X, OG-1XA, OG-1XB

Location #8: See Location #8 under Helderberg Group above.
Samples: OTO-1, OTO-1A

Location #9: See Location #9 under Helderberg Group above.
Samples: OG-1, OG-2 and OG-3

Location #10: Roadcut along Rte 11 near Nedrow, immediately north of intersection with Kennedy Road.
Samples: OG-4, OG-5, OG-6, and OG-7

Location #11: Roadcut on Rte 175 at the edge of the city of Marcellus.
Sample: OG-8

Location #13: Small roadside quarry on Rte 326 just east of intersection with Rte 90.
Samples: OG-9 and OG-9A

Location #14: Small roadcut on Rte 326, 21/2 miles northeast of location #13.
Samples: OG-10A and OG-10B.

Location #15: Roadcut on NY 96 about 1/4 miles west of traffic light in the village of Phelps. lat. 42°-55-00 N, long. 77°-00-00 W.
Samples: OG-11 and OG-11A

Location #16: Roadcut on NY 88, 0.6 miles north of intersection with NY 96, just before the railroad overpass.
Samples: OG-12, OG-12A, OG-12C

Location #17: Sewage Treatment Plant Quarry in the Village of Honeoye Falls. On southbound Rte 65, cross bridge over Honeoye Creek in Honeoye Falls and turn right onto Maplewood Avenue, then turn right on Ulrich Lane. Exposure starts from outside the entrance to the plant. Lat. 42°-55-00 N, long. 77°-31-30 W.
Samples: OG-13, OG-13A, OG-13B

Location #18: Quarry in "Leroy Bioherm" of General Crushing Stone Company 1.5 miles east of Leroy.
Samples: OG-14, OG-18, OG-19 and L-11A

Location #20: Roadcut on I-290 due east of Buffalo.
Samples: OG-15 and OG-15A

Location #21: DOT core, Hole #2 (2-61), well 9-5R in Schoharie County, Cobbleskill Township at 42°-41-20 N and 74°-28-9 W.
Samples: OG-23A and OG-23B.

Location #22: See Location #22 under Helderberg Group above.
Samples: CGO-1 and CGO-2

Location #23: Core sample from Ruth A. Place Company's drillsite in Tompkins County, Enfield Township at lat. 42°-25-00 N and long. 76°-40-00 W.
Samples: RP-1 (930.5m) and RP-1A (933.8m)

Location #24: Core samples from Sylvania Company's drillsite in Steuben County, Bath Township at lat. 42°-17-30 N and long. 77°-25-00 W.
Samples: SYO-3 (1126.2m) and SYO-4 (1085m)

Location #25: Core sample from EGSP's Valley Vista View, Inc #1 site in Steuben County, Rathbone Township at lat. 42°-09-50 N and long. 77°-23-42 W.
Samples: VVO-1 (1170m) and VVO-2 (1172.9m)

Location #38: Core sample from Klossner Company's drillsite in Tioga County at lat. 42°-10-00 N and long. 76°-10-00 W.
Sample: K-1 (1430.8m) and K-2 (1345.1m).

Location #70: Port Colborne Quarry in Niagara Falls, Ontario, Canada.
Samples: OGC-3, OGC-4 and OGC-5.

Location #71: Ridgemont Quarry in Niagra Peninsula, Ontario, Canada.
Samples: OGC-1 and OGC-2.

THE MARCELLUS FORMATION: (CHAPTER 14)

Location #3: See Location #3 under Onondaga Formation above.
Samples: BK-1, BK-1A from Bakoven Member.

Location #11: Roadcut on Rte 175 at the edge of the city of Marcellus.
Samples: MC-5/6

Location #22: See Location #22 under Helderberg Group above.
Samples: CGU-2 (430.7m), CGU-2A (420.6m), MR-4 (361.8m).

Location #25: See Location #25 under Onondaga Formation above.
Samples: MR-4A and MR-4(B).

Location #32: DOT core from Glenheim Gilboa site in Schoharie County.
Lat. 42°-26-38 N, long. 74°-26-57 W.
Samples: MR-1 (59.4m) and MR-1A (56.7m)

Location #33: Roadcut on Rte 20 few miles west of the town of Richfield Springs. Lat. 42°-50-00 N, long. 75°-00-00 W.
Samples: MC-1, MC-1A and MR-2

Location #34: Quarry near Jamesville, south of Syracuse. From Rte 173, turn south on Gates Road. Quarry is 0.1 mile to the left.
Samples: MR-3, CHT-1

Location #36: Core sample from EGSP's F.E. Donnel drillsite in Sullivan County at lat. 41°-45-00 N and long. 74°-40-00 w.
Samples: FO-1 (2208.3m) and FO-1A (2220m)

Location #94: Exposure along Skaneateles Creek, approximately 2 miles north of the town of Skaneateles.
Samples: MR-5 and MR-5A

Location #95: Stream-exposure in the town of Leroy.
Samples: MR-6A, MR-6B.

THE UPPER DEVONIAN BLACK SHALES

Location #22: See Location #22 under Helderberg Group above.
Samples: GN-1 (79.9m) from Geneseo Shale

Location #42: EGSP core, well #3, Steuben County, at lat. 42°-11-56 N and long. 77°-04-59 W.
Samples: RH-4 (376.8m) from Rhinestreet Formation.

APPENDIX B: BEEKMANTOWN GROUP

LOCATION: 73

SAMPLE NUMBERS: TH-1A, TH-1B, TH-1C.

FLUID-INCLUSION DATA: Measured in vug-filling saddle dolomite and quartz.

*Inclusion shape	**Inclusion size (µm)	Bubble diameter (µm)	Th (°C)	Tm (°C)
In saddle dolomite:				
Elliptical	5,3	1.0	140	
---	7,3	1.5	136.7	
---	6,4	0.8	124.5	
---	6,4	1.0	126.4	
---	7,4	1.8	146	
---	v. small	v. small	145	
---	v. small	v. small	147	
---	9,6	1.2	205	
---	8,5.5	1.5	217.3	
---	5,2.5	1.0	145.3	
---	6,4	1.0	135.5	
---	6.5,4	1.2	219	
Semi-circular	v. small	v. small	145	
---	4,3	0.8	135.2	
---	5,4	0.8	215	
---	6,4	1.0	144	
---	5,4	1.2	133	
Circular	3.0	1.0	130.3	
Rectangular	7,6	1.7	130	
---	7,4	1.0	208	
---	8,3	1.5	223.3	
---	9,6	2.0	160.5	
Square	4.0	1.0	145	
---	4.0	1.0	165	
---	4.0	1.0	145.6	
Irregular	18,9	2.7	175.4	
---	17,6	2.5	152	
---	9,6	2.0	157.2	
---	---	1.5	162	
---	---	1.5	160.6	
---	---	1.0	150	
---	---	---	224	
In quartz:				
Elliptical	15,6	1.6	189	
---	11,6	1.5	170	
---	9,6	1.2	150.5	
---	21,7	3.0	138	
---	5,3	0.5	140	
---	7,3	1.5	171	
---	13,7	2.2	125	-24
---	7,3	1.5	149.5	
---	6,4	1.0	126.5	
Semi-circular	5,4.5	0.5	140.6	
---	9,8	2.0	170	
---	6,4	1.0	167	
---	4,3	0.7	144	
Irregular	---	---	169	
---	---	---	123.5	
---	7,4	1.3	144	-30
---	7,4	1.0	150	
---	15,5	2.5	160.5	
---	9,9	1.3	132	

*(s) = secondary inclusions; (ps) = pseudo-secondary inclusions; all others are primary.
**(Longest, shortest axes) for elliptical/semi-circular/irregular inclusions. (Diameter) for circular inclusions. (Length of a side) for square inclusions. (Length of two sides) for rectangular/rhombic inclusions. (Length of sides) for triangular inclusions.

(Location #73 continued)

Rectangular	5,4	1.5	159
---	7,5	0.8	130
---	7,6	1.0	133
---	8,6	1.0	161
---	6,4.5	1.5	146.5
Triangular	6,6,6	1.2	162
Circular	3.5	1.0	141

LOCATION: 74

SAMPLE NUMBERS: TH-2A, TH-2B, TH-2C

FLUID-INCLUSION DATA: Measured in vug-filling calcite.

Inclusion shape	Inclusion size (µm)	Bubble diameter (µm)	Th (°C)	Tm (°C)
Elliptical	7,4	1.2	157	
---	5,3	0.8	143.4	
---	10,3	1.2	165	
---	8,5	1.5	206.5	
Irregular	21,8	3.5	170	
---	30,6	2.0	165	+0.7
---	---	---	108	
---	15,7	2.0	220	
---	---	---	172	
---	30,15	3.5	156	
---	30,26	9.0	235	
---	---	---	123	
---	15,9	4.0	152	
---	15,10	2.0	149.8	
---	---	---	160	
Circular	6.0	1.7	195.6	
Semi-circular	13,12	4.0	161.5	
---	9,6	2.0	221.7	
---	7.5,4	1.0	212.4	
---	5,3	0.8	133	
Rectangular	15,9	3.0	206	0
---	12,8	3.0	185.5	+1.2
---	10,3	1.7	239	
---	18,8	4.0	235.2	
---	6,5	1.0	115.4	
---	12,9	1.5	172	
---	10,6	1.5	207	
---	14,10	4.0	154	
---	27,7	3.0	148	
---	10,9	3.0	180	
Square	4.0	1.0	117.5	

LOCATION: 75

SAMPLE NUMBERS: TH-3A, TH-3B, TH-3C, TH-3D.

FLUID-INCLUSION DATA: Measured in vug-filling saddle dolomite.

Inclusion shape	Inclusion size (µm)	Bubble diameter (µm)	Th (°C)	Tm (°C)
Elliptical	10,3	1.5	196.4	
---	10,4	2.5	206	-20
---	6,3	1.0	220	
---	7,3	1.0	224.3	
---	10,5	1.8	215.4	
---	9,5	1.8	220.5	
---	8,5	1.5	232.7	
Square	9,6	2.5	179.3	

---	9,8	3.0	227
Semi-circular	9,8	2.7	234
---	6,5	1.0	212.7
---	7,4.5	1.5	214
---	8,6	2.0	236.6
Irregular	---	---	154.5
---	---	---	232.8
---	---	---	230.4

LOCATION: 76

SAMPLE NUMBERS: Z-1A, Z-1B, Z-1C

FLUID-INCLUSION DATA: Measured in fracture-filling calcite.

Inclusion shape	Inclusion size (µm)	Bubble diameter (µm)	Th (°C)	Tm (°C)
Elliptical	12,9	2.0	145	
---	6,3	1.5	194.4	
---	6,4	1.0	128.8	
---	15,6	2.0	185	
---	6,4	1.0	120	-15
---	6,2.5	1.0	179	
---(s)	4,3	1.0	137.7	
---	5,3.5	1.2	133.3	
---	8,6	1.5	126	
---	8,4	1.0	215.5	
Semi-circular	4,3	1.0	164.6	
---	6,4	0.8	124	
---	6,5	1.5	147.2	
---	9.5,7	2.8	219.7	
---	5,4	0.8	127	
---	7,6	1.8	192	
---	10,8	2.2	125.7	
---	8,6.5	1.5	128.5	
---	5,4	0.8	131.3	
Rectangular	12,10	3.0	225	
---	21,12	2.5	120.7	
---	12,3.5	1.5	130.6	-10
---	4,3	2.0	129	
Square	3.0	0.5	155.4	
---	10.0	1.8	139.9	
---	4.0	1.0	132	
Irregular	7,5	1.8	139	-10.4
---	---	---	178.6	
---	6,6	1.5	178	
---	---	---	175	
---	---	---	140.3	
---	6,5	1.0	137	
---	14,14	2.5	154	
---	6,5	1.2	149.6	

LOCATION: 77

SAMPLE NUMBERS: Z-2A, Z-2B, Z-2C

FLUID-INCLUSION DATA: Measured in vug-filling calcite.

Inclusion shape	Inclusion size (µm)	Bubble diameter (µm)	Th (°C)	Tm (°C)
Elliptical	12,5	1.5	92	
---	8,6	2.8	213.5	
---	12,5	2.5	212	
---	12,9	4.0	228.3	-22
---	9,5	1.5	163	
---	15,10	3.5	166	
---	22,5	2.2	179.2	

---	27,6	3.0	175	
Circular	7.0	2.5	230.6	
Semi-circular	8,6	1.5	222.3	
---	7,5	1.0	230	
Rectangular	14,6	2.5	145	-12
---	9,6	2.8	245	
Triangular	12,9,6	1.5	210.6	
---	7,7,5	1.0	158	
Irregular	9,5	1.2	88	
---	30,15	5.0	149	
---	9,9	1.0	126.3	
---	24,12	4.0	241	
---	12,5	1.2	218	-2.9
---	30,15	3.0	173.1	
---	30,6	1.8	189	
---	9,2	1.0	155	

LOCATION: 81

SAMPLE NUMBERS: LF-1, LF-2, LF-3. LF-4.

FLUID-INCLUSION DATA: Measured in vug-filling calcite.

Inclusion shape	Inclusion size (µm)	Bubble diameter (µm)	Th (° C)	Tm (° C)
Elliptical	6,4	1.2	145	
---	7,5	1.6	171.5	
---	12,6	2.6	197.2	
---	7,4	1.5	164	
---	7,5	1.0	98.6	
Rectangular	9,3	1.0	177	
---	8,4	1.5	165.2	
---(s)	6,5	1.0	165	
---	7,5	2.0	169	
---	7,3	1.2	191	
Circular	4.0	1.0	156.6	
Square	4.0	1.0	170	
---	4.0	0.8	80	
---	5.0	2.0	219.7	
---	6.0	2.0	200.5	
Rhombic	6,6	1.0	84.3	
---	30,22	1.5	139	
Triangular	5,5,4	1.2	179	
Irregular	45,15	3.5	125	+1.1
---	13,6	2.2	205.3	
---	3,3	0.6	162	
---	7,6	1.3	167.5	
---	15,6	2.0	155	
---	---	---	78.5	

LOCATION: 63

SAMPLES: CJ-1A, CJ-1B, CJ-1C

FLUID-INCLUSION DATA: Measured in vug-filling saddle dolomite, calcite and quartz.

Inclusion shape	Inclusion size (µm)	Bubble diameter (µm)	Th (°C)	Tm (°C)
In saddle dolomite:				
Elliptical	15,9	1.6	93	
---	10,5	2.2	158.8	
---	8,3	0.8	158	
---	6,3	1.0	95	
---	6,3	1.0	95.6	

---	9,5	1.5	138	
---	10,6.5	2.0	89	
Semi-circular	5,4	0.8	111.5	
---	6,5	1.0	108.8	
---	7.5,5	1.6	159	
---	5,3	0.6	97	
---	5,4	1.5	158.7	
Square	4.0	0.8	148	
Rectangular	8,6	1.0	96	
---	7,5	1.5	127.5	
---	7.5,4	1.0	149	
---	8,6	1.2	95	
Triangular	4,3,3	0.7	112	
Irregular	15,5	1.2	110.4	
---	7,3	1.0	143.1	
---	25,7	2.0	109	
---	12,4	1.2	162	
---	18,7	1.3	107.4	
In Calcite:				
Elliptical	12,6	1.2	108.6	
---	8.5,4	1.5	104.4	
---	7,4	1.0	106	
Semi-circular	5,4	1.2	89	
Rectangular	9,6	2.0	101	
Triangular	15,15,6	1.5	99	
Irregular	43,13	2.6	83	
---	---	---	110.2	
---	12,6	1.5	84	
---	---	---	94.8	
In quartz:				
Elliptical	5,3	0.8	112.3	
---	9,6	1.4	117.8	
---	7,4	1.0	95.8	
---	7,4.5	1.2	121	
---	4,3	0.7	78.7	
Circular	3.5	0.5	88	
---	3.0	1.0	85.7	
---	4.0	1.0	78.1	
---	3.5	0.5	89	
Semi-circular	4,3	0.5	115	
---	4,3	0.6	119.6	
---	7,6	1.2	113.4	-18
---	4,3	0.7	102	
Rectangular	10,8	1.2	101	
---	8,6	1.0	128	
---	15,12	3.0	100.6	+1.0
---	6,3	1.2	132	
---	4,3	0.8	112	
Triangular	15,12,12	3.0	113.8	
Irregular	30,15	1.8	82.5	
---	12,9	1.5	117	

LOCATION: 90

SAMPLE NUMBERS: TH-4, PS-1, PS-2

FLUID-INCLUSION DATA: Measured in authigenic quartz overgrowth on quartz sand grains.

Inclusion shape	Inclusion size (µm)	Bubble diameter (µm)	Th (°C)	Tm (°C)
Elliptical	6,4.5	1.0	162	
---	5,3	0.8	170.5	
---	7,5	1.2	139.3	
Triangular	6,5,2	0.5	156	

Semi-circular	4,3	0.5	165.3	
---	5,4	1.0	167	
---	5,4	0.8	170.5	
---	5,3	0.6	149	

LOCATION: 92

SAMPLE NUMBERS: OD-1, OD-1B, OD-1C.

FLUID-INCLUSION DATA: Measured in fracture-filling calcite.

Inclusion shape	Inclusion size (µm)	Bubble diameter (µm)	Th (°C)	Tm (°C)
Elliptical	30,4	3.0	222	
---	9,7	1.5	160	
---	6,4	1.0	141.7	
---	11,6	1.2	183	
---	13,6	1.0	79	
---	10,6	1.2	89	
---	10,4	1.5	119.5	
---	9,7	1.6	116.2	
---	9,6	1.2	205.4	
---	6,4	1.2	148	
--- (ps)	9,6	2.7	94	
--- (ps)	5,3	1.7	89.3	
--- (ps)	5,3	1.5	91	
Circular (ps)	10.0	2.6	92	
--- (ps)	6.0	1.5	91.6	
--- (ps)	6.0	1.7	90.9	
---	6.0	1.8	211	
Semi-circular	7,6	1.5	85	
---	10,8	1.8	165	
---	5,4	1.0	157	
---	9,7.5	2.0	152.2	
---	8,6	1.2	126	
---	9,7	1.5	175.8	
Triangular	11,11.5	1.5	157	
Rectangular	30,12	3.0	85	
---	10,6	1.4	149	
---	15,6	3.0	190	+2.5
---	45,12	6.0	217.6	+2.5
---	24,18	4.0	148	
---	12,9	1.2	125	
---	13,12	3.0	225.1	
---	8,3.5	1.0	127.7	
---	18,5	2.5	215	
---	12,10	1.7	109	
---	12,6	2.0	130	-15
Triangular	21,21,15	3.0	128.8	
---	4,4,3	1.0	105	
Square	10.0	1.5	109	
Irregular	---	---	88.9	
---	10,6	1.5	129	
---	21,15	2.0	166	
---	---	---	125.5	
---	13,6	1.5	165.6	
---	---	---	163	
---	15,11	2.5	185.5	

LOCATION: 66

SAMPLE NUMBERS: H-1, H-2, H-3

FLUID-INCLUSION DATA: Measured in vug-filling calcite.

Inclusion shape	Inclusion size (µm)	Bubble diameter (µm)	Th (°C)	Tm (°C)
Elliptical	8,3	1.0	135	
---	7,5	1.2	135	-26
---	9,6	1.3	118.2	
---	8,3	1.3	134	
---	7,3	0.8	136.3	
---	15,5	1.0	139	
---	12,4	1.0	149	
---	7,3.5	1.0	109.5	
---	6,4	1.2	147	
---	6,3	1.0	115	
---	6,3	1.0	117.1	
---	8,6	1.0	125	
---	15,9	3.0	148	-22
---	6,4	0.8	125	
---	7,3	1.0	139	
---	17,9	1.3	135.7	
---	9,3	1.0	127.9	
---	6,4	1.0	127	
---	6,4	0.8	125.5	
---	7,4	1.0	151	
Circular	6.0	1.0	148	
---	9.0	2.0	141.4	
---	4.0	1.2	138	
Semi-circular	9,7	1.5	135	
---	12,9	2.3	166.4	
---	8,7	1.5	121.9	
---	6,5	1.5	125.7	
---	7,6	1.5	131.8	
Square	5.0	1.0	139	
---	9.0	2.0	127.6	
---	5.0	1.0	125	
---	4.0	0.9	137	
---	6.0	1.0	132.4	
Rectangular	9,6	1.3	141	
---	10,6	2.0	147	
---	7,6	1.0	119	
---	5,2.5	0.5	152.6	
---	24,15	4.0	135	
---	7,5	1.0	123	
---	9,7	1.0	123	
Rhombic	40,20	6.0	153	-21.7
---	9,8	1.7	151	
Triangular	9,9,8	2.0	132	
---	24,24,20	4.0	140	
---	6,6,3	0.8	143.5	
---	6,6,4	0.9	136.8	
Irregular	7,5	1.0	135.2	
---	15,12	1.8	124	
---	15,12	2.0	124.7	-21
---	8,5	1.5	128.3	
---	15,4	1.2	139	
---	9,6	1.5	126.6	
---	18,12	2.2	111	
---	12,6	2.6	124	-20.6
---	6,6	1.2	162	
---	12,9	2.5	151.3	
---	7,6	2.5	128.6	

LOCATION: 68

SAMPLE NUMBERS: RO-1, RO-2.

FLUID-INCLUSION DATA: Measured in vug-filling dolomite.

Inclusion shape	Inclusion size (μm)	Bubble diameter (μm)	Th (°C)	Tm (°C)
Elliptical	3,2	0.5	159	
---	4,2.5	0.5	155.4	
---	5,3	1.0	171	
---	4.5,3	0.8	185	
---	3.5,2	0.5	194	
---	5,2.5	0.4	172.5	
---	5,3	0.6	175	
Circular	3.0	0.5	185.5	-22
Semi-circular	4,3	0.5	199.9	
---	4,3	0.6	177	
---	5,3.5	1.0	166.7	
Rectangular	5,3.5	0.8	190.5	
---	5,3	1.0	156	
---	4,2	0.7	162	
---	4,3	0.8	177.3	
---	4,2	0.5	185.3	
---	5,4	1.2	182	
Triangular	3,3,2	0.5	185	
Irregular	4,4	0.8	180.6	
---	5,4	0.8	182	
---	4,4	0.6	189.5	
---	---	---	149.7	
---	4,3	0.5	168	
---	---	---	187.5	

APPENDIX C: THE BLACK RIVER AND TRENTON GROUPS

LOCATION: 61

SAMPLE NUMBERS: ORD-2X, Z-3A, Z-3B

FLUID-INCLUSION DATA: Measured in vug- and fracture-filling calcite.

*Inclusion shape	+Inclusion size (µm)	Bubble diameter (µm)	Th (°C)	Tm (°C)
Elliptical	7,4	1.5	130	-22.7
---	6,3	1.5	155.4	
---	6,3	1.0	142	
---	9,6	1.3	155	
---	9,5	1.2	153.8	
---	7,2	1.0	165.4	
---	6,3	1.5	205	
---	5,2	1.6	130	
---	9,3	1.5	174	
---	7,5	1.0	112.2	
---	7,4	1.0	153	
---	5,3	0.8	133.6	
---	8,2	1.0	150	
---	6,3	0.5	109	
Rectangular	9,6	2.0	140.4	-24.7
---	6,5	1.5	152	
---	6,4.5	1.5	147	
---	3,2	0.5	164.5	
---	3,2	0.5	164	
---	3,2.5	0.5	165.2	
---	6,3.5	1.0	194.5	
---	7,6	1.0	175	
---	4,3	0.7	165.3	
---	6,3	1.0	145	
---	7,2	1.2	135	
---	8,4	1.0	180.6	
---	7,2.5	1.5	160	
---	4,3	1.0	153.4	
---	9,6	1.0	139.8	
---	9,3	1.0	148	
---	6,4	1.3	172	
---	6,4.5	1.5	212	
Square	3.0	0.5	210	
---	4.0	0.8	171.7	
Triangular	9,8,6	1.5	150.4	
---	9,7,3	1.2	125	
---	6,6,5	1.5	148	
---	5,4,4	2.0	195.1	
---	6,3,3	1.0	179	
Circular	5.0	0.6	166	
Semi-circular	12,8	1.5	194.8	
---	7,6	1.8	176.2	
---	8,6.5	2.0	155	
---	6,4.5	1.5	176.5	
---	5,4	0.8	140	
--- (s)	6,4	1.2	170.6	
Irregular	9,6	2.0	132	-23.5
---	6,5	2.0	166	-23.3
---	22,6	3.0	147.5	
---	7.5,5	1.0	180.6	

* (s) = secondary inclusions; (ps) = pseudo-secondary inclusions; all others are primary.

+ (Longest, shortest axes) for elliptical/semi-circular/irregular inclusions. (Diameter) for circular inclusions. (Length of a side) for square inclusions. (Length of two sides) for rectangular/rhombic inclusions. (Length

of sides) for triangular inclusions.

(Location #61 continued)

---	---	---	207
---	9,9	2.0	173
---	7,4	1.5	195
---	7,5	1.6	215.7
---	12,6	2.0	174.4
---	---	---	147
---	6,4	0.5	128
---	---	---	137
---	---	---	193.6
---	12,4	1.3	152
---	8,4	1.0	169

LOCATION: 64

SAMPLE NUMBERS: JM-2, JM-3, JM-4, JM-5

FLUID-INCLUSION DATA: Measured in fracture-filling calcite and dolomite.

Inclusion shape	Inclusion size (µm)	Bubble diameter (µm)	Th (°C)	Tm (°C)
In calcite:				
Rectangular	6,3	1.0	94	
---	6,4	1.0	121.7	
---	5,4	1.0	110.8	
---	12,8	2.0	140	
Semi-circular	4,3	0.6	126	
Square	4,4	1.0	110	
Irregular	4,4	0.8	92.4	
---	8,5.5	0.5	105	
---	7.5,3	0.8	127	
---	---	---	160.5	
---	6,2.8	0.6	175	
---	---	---	270.6	
In dolomite				
Elliptical (s)	3,2	1.2	275	
---	4,2	0.5	154	
---	---	---	140	
Circular	3.0	1.0	260.7	
---	2.5	0.4	276	
---	2.5	0.4	279	
Rectangular	5,3	1.0	180.5	
---	10,5	1.5	180	-11
---	4,3	0.5	209	
---	10,6	2.0	265	-15
Irregular	9,6	1.3	135	
---	9,6	1.5	182	
---	5,3	1.2	260	
---	7,6	1.5	155.8	

LOCATION: 65

SAMPLE NUMBERS: BR-1, BR-2, BR-3

FLUID-INCLUSION DATA: Measured in vug-filling calcite.

Inclusion shape	Inclusion size (µm)	Bubble diameter (µm)	Th (°C)	Tm (°C)
Elliptical	6,3	1.0	133	
---	5,3	0.6	150	

---	9,6	1.4	174.6	
---	8,4	1.0	184	
---	6,3	1.0	157.2	
---	5,3	0.7	203.6	
---	7,3	0.8	198	
---	8,4	0.8	143.4	
---	7,4	1.0	173	
---	6,4	1.2	172.5	
---	5,3	0.8	137	
---	7,4	1.2	145.1	
---	12,6	2.0	166.2	
---	6,3	1.0	125	
Rhombic	15,15	2.0	115.2	
Square	6.0	1.5	107	
---	3.0	0.5	138.6	
---	3.0	0.5	145.4	
---	3.0	1.0	133	
Triangular	9,6,6	1.5	131	
---	7,6,5	1.5	178	
Circular	3.0	0.7	137	
---	4.5	1.0	138.6	
---	5.0	1.2	171.8	
Semi-circular	15,9	1.5	124	
---	6,5	1.0	130.5	
---	5,4	0.9	204.2	
---	6,5	1.0	141	
---	6,4.5	0.8	205	
---	5,4	0.8	150.4	
---	12,9	2.0	178.5	
---	4,3	0.5	207.2	
Rectangular	4,3	0.7	149	
---	6,2.5	1.2	151	
---	6,3	1.0	148.5	
---	3,2	0.4	139	
---	10,4	1.2	166.7	
---	7.5,6	1.2	165	
---	8,6	1.0	150	-5.8
---	7,3	1.2	145	
---	4,2	0.5	120.7	
---	9,6	1.0	150	
---	6,4	1.0	144.7	
---	5,2	0.3	149	
---	6,3.5	1.0	168.1	
---	3,2	0.5	140.7	
Irregular	24,15	3.0	148	+1.5
---	9,7	1.0	110.9	
---	4,3	0.8	134	
---	---	---	185	
---	8,7	1.2	145	-2.5
---	---	---	102.9	
---	6,5	1.0	137.4	
---	6,6	1.3	124.6	
---	9,6	1.2	174.6	
---	---	---	148.4	
---	---	---	107.8	
---	9,6	1.5	152	
---	6,3	1.0	143	
---	9,5	1.5	147	-2.4
---	9,5	1.0	147.3	
---	12,5	1.0	151	
---	10,5	1.8	177.2	
---	---	---	134.3	

LOCATION: 84

SAMPLE NUMBERS: TR-2A, TR-2B, TR-2C

FLUID-INCLUSION DATA: Measured in vug- and vein-filling calcite.

Inclusion shape	Inclusion size (μm)	Bubble diameter (μm)	Th (°C)	Tm (°C)
Elliptical	4,3	0.5	142.3	
---	5,3	0.8	89.7	
---	6,4	0.8	93	
---	13,6	2.5	197	
---	8,5.5	1.2	188.8	
Semi-circular	6,5	1.0	199.8	
---	5,4	0.7	87.2	
Square	3.0	0.8	136	
---	5.5	1.2	168.1	
Triangular	3,2,2	0.5	145.5	
Rectangular	3,2	0.5	128.3	
---	5,4	0.7	99.4	
---	9,6	0.4	155	
---	10,4	1.0	113.3	
---	6,5	1.0	85	
Irregular	4,4	1.0	125	
---	21,6	2.7	130	-11.8
---	9,5	1.0	120	
---	---	---	85	
---	12,12	1.7	125.6	
---	33,18	3.0	129.6	
---	---	---	119	

LOCATION: 85

SAMPLE NUMBERS: BL-2A, BL-2B, BL-2C

FLUID-INCLUSION DATA: Measured in inter-particle sparry calcite.

Inclusion shape	Inclusion size (μm)	Bubble diameter (μm)	Th (°C)	Tm (°C)
Elliptical	10,2.5	1.0	127	
---	15,3	1.6	155	
---	8,6	1.2	219	
Circular	3.0	0.8	150.2	
Semi-circular	8,6	1.4	208.5	
Triangular	6,2.8	1.0	120	
---	3,3,2	0.7	115	
Rectangular	5,3	1.0	140	
---	9,4	1.2	116.1	
--- (ps)	3,2	0.6	134	
---	3,2	0.5	174.5	
---	5,3	1.0	193.8	
---	3.5,3	0.6	176	
Irregular	9,9	2.5	120.6	+1.6
---	7,6	1.7	160.6	
---	6,4	1.7	214	
---	---	---	123.7	
---	8,4	1.0	126	

LOCATION: 87

SAMPLE NUMBERS: BL-3A, BL-3B, BL-3C

FLUID-INCLUSION DATA: Measured in inter-particle sparry calcite.

Inclusion shape	Inclusion size (µm)	Bubble diameter (µm)	Th (°C)	Tm (°C)
Elliptical	4,3	0.5	142.2	
---	7,6	1.0	164	
---	7,5	1.5	145.2	
---	10,5	1.5	193.3	
---	10,7	1.3	155	
---	12,10	3.0	169	
---	9,5	2.0	160	-18
---	9,6	1.7	215	
---	12,6	1.6	144.4	
Rectangular	9,6	1.5	150.3	
---	8,6	1.8	207.6	
---	4,3	0.8	119	
---	5,3	1.0	196.4	
---	8,3	0.8	133.8	
Rhombic	5,4	1.0	131	
---	8,6	2.0	137	
Triangular	14,14,3	1.3	104	
Circular	4.0	0.8	149	
---	5.0	1.0	133.8	
Irregular	---	---	145	
---	9,9	1.0	131	
---	---	---	119	
---	9,5	1.5	132	
---	12,8	1.6	155	
---	12,12	2.0	125	
---	9,6	2.0	139.1	
---	---	---	139.5	
---	12,10	1.6	132	
---	30,12	2.8	173	

LOCATION: 88

SAMPLE NUMBERS: BL-4A, BL-4B, BL-4C

FLUID-INCLUSION DATA: Measured in inter-particle sparry calcite.

Inclusion shape	Inclusion size (µm)	Bubble diameter (µm)	Th (°C)	Tm (°C)
Elliptical	6,3	1.0	59	
--- (s)	4,2.5	0.8	129	
---	3,1.5	0.5	116	
---	3,2	0.7	118	
---	4,3	1.0	135	
---	5,3	0.8	117.7	
---	4,3	0.9	107	
---	5,3	1.0	190.5	
---	5,3	1.0	107	
Rectangular	3,2	0.4	120.6	
---	5,3	1.0	100.6	
---	6,3	1.0	228	
---	7,3	1.2	114.7	
---	8,4	0.9	143.3	
---	6,3	1.0	118	
---	6,4	0.8	98	
---	5,3	1.0	114	-20
Circular	3.0	0.8	88.8	

---	3.0	0.8	89.5
--- (s)	3.0	1.0	132
--- (s)	3.0	1.0	127.5
--- (s)	4.0	1.0	125
---	4.0	0.8	111.1
---	3.5	0.9	108.7
*Semi-circular	4,3	1.0	100-120
---	6,5	1.2	219.6
Square	3.0	0.6	121
---	3.0	0.7	105
--- (s)	3.0	0.8	117
---	3.0	0.9	112.8
---	2.5	0.8	112
---	3.0	0.8	117.2
Irregular	6,6	1.0	121
---	12,6	1.2	120
---	---	---	96.3
---	11,10	1.8	183
---	8,7	1.5	117.8

* 12 readings from a cluster of small inclusions.

LOCATION: 89

SAMPLE NUMBERS: Z-4A, Z-4B

FLUID-INCLUSION DATA: Measured in vug-filling calcite.

Inclusion shape	Inclusion size (μm)	Bubble diameter (μm)	Th (°C)	Tm (°C)
Elliptical	6,3	1.0	129	
Rectangular	6,2	0.8	110.5	
---	4,3	0.8	153.8	
Square	3.0	1.0	110.4	
Irregular	3.5,3	0.8	139	
---	---	---	98.7	
---	7,7	1.5	97	

APPENDIX: D: THE UTICA SHALE

X-RAY ANALYSIS: Scanning range = 4 - 30° 2θ
Goniometer speed = 1° 2θ/minute
CuK radiation source set at 40KV and 20MA

Parameters used in the "Peak finding program":

Threshold values = 1.0, 1.0
Relative cutoff intensity = 2.0
Typical full width-half maximum = 0.20 °2θ
Minimum full width-half maximum = 0.10 °2θ

LOCATION: 79 SAMPLE: UT-1A (GLYCOLATED)

Peak	Peak position (°2θ)	D-space (Å)	Relative Intensity	*FWHM (°2θ)
1	8.84	9.99	16.67	0.459
2**	17.75	----	-----	----
3	19.80	4.48	16.38	0.599
4	20.90	4.24	27.67	0.135
5	23.10	3.84	17.92	0.278
6	26.68	3.33	100.00	0.215
7	29.46	3.02	92.91	0.275

TAI: UT-1A = 3.5

LOCATION: 80 SAMPLE: UT-2A (GLYCOLATED)

Peak	Peak position (°2θ)	D-space (Å)	Relative Intensity	*FWHM (°2θ)
1	8.84	9.99	33.11	0.399
2**	17.76	----	-----	-----
3**	19.78	----	-----	-----
4	20.90	4.24	23.28	0.117
5**	23.00	----	-----	-----
6	26.68	3.33	100.00	0.237
7	29.46	3.02	77.13	0.275

TAI: UT-2A = 3.0

LOCATION: 63 SAMPLE: UT-3A (GLYCOLATED)

Peak	Peak position (°2θ)	D-space (Å)	Relative Intensity	*FWHM (°2θ)
1	8.86	9.97	9.92	0.859
2**	17.76	----	----	-----
3**	19.80	----	----	-----
4	20.86	4.25	26.36	0.133
5**	23.12	3.84	15.03	0.197
6	26.66	3.34	52.58	0.236
7	29.48	3.02	100.00	0.236

TAI: UT-3A = 2.8

* FWHM (Full Width Half Maximum)= Width of the peak at half its height.

**These peaks were not detected by the "Peak Finding" program, because compared to the background "noise" their intensities were less than 2, the "relative cutoff intensity" (see above). Their positions have been calculated manually from the diffractograms.

LOCATION: 82 SAMPLE: UT-4A (GLYCOLATED)

Peak	Peak position (°2θ)	D-space (Å)	Relative Intensity	*FWHM (°2θ)
1	8.86	9.97	14.68	0.499
2	12.56	7.04	3.92	0.538
3**	17.76	----	----	-----
4**	19.80	----	----	-----
5	20.88	4.25	22.60	0.177
6	26.68	3.33	100.00	0.217
7	27.96	3.18	8.40	0.439
8	29.46	3.02	20.74	0.238

TAI: UT-4A = 2.6

LOCATION: 93 SAMPLE: UT-5B (GLYCOLATED)

Peak	Peak position (°2θ)	D-space (Å)	Relative Intensity	*FWHM (°2θ)
1	6.28	14.06	4.56	0.252
2	8.88	9.95	17.89	0.418
3	12.52	7.06	10.54	0.254
4**	17.76	----	----	----
5**	18.68	----	----	----
6	19.84	4.47	8.35	0.758
7	20.88	3.33	100.00	0.195
8	28.00	3.18	8.47	0.138

TAI: UT-5A = 2.4; UT-5B = 2.4

LOCATION: 86 SAMPLE: UT-6A (GLYCOLATED)

Peak	Peak position (°2θ)	D-space (Å)	Relative Intensity	*FWHM (°2θ)
1	8.84	9.99	12.19	0.498
2	17.76	4.99	7.56	0.418
3**	19.80	----	----	----
4	20.88	4.25	22.41	0.171
5	26.66	3.34	100.00	0.233
6	27.98	3.18	9.26	0.176

TAI: UT-6A = 2.7

LOCATION: 64 SAMPLE: JM-1 (UNTREATED)

Peak	Peak position (°2θ)	D-space (Å)	Relative Intensity	*FWHM (°2θ)
1	6.26	14.10	5.55	0.256
2	8.88	9.95	15.23	0.359
3	12.54	7.05	30.64	0.214
4**	17.76	----	----	----
5**	18.68	----	----	----
6**	19.80	----	----	----
7	20.90	4.24	22.23	0.214
8	25.20	3.53	21.38	0.278
9	26.68	3.33	100.00	0.213

TAI: JM-1 = 3.8

*,** = see page 414

APPENDIX E: THE CLINTON GROUP

LOCATION: 50

SAMPLE NUMBERS: HL-2A, HL-2B, HL-2C

FLUID-INCLUSION DATA: Measured in inter-particle calcite cement, in calcite of recrystallized bivalve shells, and in mega-quartz cement in coral cavities.

Inclusion shape	*Inclusion size (µm)	Bubble diameter (µm)	Th (°C)	Tm (°C)
In Calcite				
Elliptical	9,4	1.5	208	
---	5,3	1.3	160.8	
---	8,5	1.0	196.1	
---	5,3	1.2	227	
---	5,4	0.8	136.7	
---	6,3	1.3	220.5	
---	7,3	1.0	211	
---	---	---	90.5	
---	8,6	1.0	141	
Square	4.0	0.8	153.3	
Triangular	6,6,6	1.5	145	
---	3,3,2	0.5	108	
Rectangular	9,5	1.5	154	
---	5,4	1.0	140.8	
---	9,4	1.5	196.9	
---	8,5	1.2	133	
---	8,6	1.1	120	
---	---	---	80.4	
Irregular	10,6	2.0	200	
---	6,3	1.0	188	
---	18,5	1.0	150.5	
---	7,6	1.0	171	
---	---	---	144.4	
---	8,8	1.8	213.5	
---	18,4	1.2	85	
---	12,6	1.5	197.4	
---	8,7	1.0	195	
---	---	---	80	
In Quartz:				
Elliptical	6,3	1.2	95	
---	6,3	0.8	91	
---	12,4	1.5	107.2	
Square	4.0	1.0	93.4	
---	3.0	0.8	100	
---	4,3	0.6	96	
---	8,3	0.7	106.4	
Rectangular	6,4	0.7	95	
Circular	5.0	0.8	90	
---	3.0	1.0	110.2	
Semi-circular	3,2.5	0.8	105.6	
---	4,3	0.6	98	
---	5,4	1.2	97.7	
Triangular	5,4,3	1.0	117	
Irregular	5,3	0.8	100	
---	14,6	1.5	90	
---	---	---	115	
---	3,3	0.9	104.3	
---	---	---	105	

TAI DATA: HL-2C = 2.5

*(Longest, shortest axes) for elliptical/semi-circular/irregular inclusions. (Diameter) for circular inclusions. (Length of a side) for square inclusions. (Length of two sides) for rhombic/ rectangular inclusions. (Length of sides) for triangular inclusions.

LOCATION: 55

SAMPLE NUMBERS: HL-10A, HL-10B

FLUID-INCLUSION DATA: Measured in megaquartz in partially replaced bivalve shells.

Inclusion shape	Inclusion size (μm)	Bubble diameter (μm)	Th (°C)	Tm (°C)
Elliptical	10,5	1.2	105.2	
---	6,3	1.0	90	
---	6,4	1.3	77.7	
---	7,4	0.8	100	
---	6,4	1.0	114.5	
---	16,5	2.0	102.3	
---	8,6	1.2	105	
---	6,4	1.1	109	
---	8,7	1.0	197	-17.4
Semi-circular	5,4	1.0	98	
Square	4,0	0.8	94	
Triangular	4,4,3	1.0	126	
---	6,5,4	1.2	135	
Rectangular	10,5	2.0	162	
---	8,4	1.6	185.5	
Irregular	5,5	1.2	129	
---	7,4	1.5	130.7	
---	---	---	171	
---	9,7	1.6	181.5	
---	16.5	2.0	115	
---	---	---	106	
---	6,5	1.0	135	
---	11,5	1.0	70.2	
---	7,4	1.0	146	
---	10,6	1.0	80.7	

APPENDIX F: LOCKPORT GROUP

LOCATION: 45

SAMPLE NUMBERS: LP-1, LP-7, LP-8

FLUID-INCLUSION DATA: Measured in vug- and fracture-filling saddle dolomite.

*Inclusion shape	+Inclusion size (µm)	Bubble diameter (µm)	Th (°C)	Tm (°C)
Elliptical	6,3	1.2	128	
---	6,4	1.5	135	
---	6,3.5	1.0	115.2	
---	12,3	1.8	143	
---	5,3	0.6	118	
---	5,2	0.6	126	
---	4,2	0.5	115	
---	6.5,3.5	1.5	129.4	
---	13,6	2.0	125	
---	12,6	1.5	153	
---	6,3.5	1.7	129	
---	5,3	1.7	91	
---	4,3	0.7	107	
Circular	2.0	0.5	115.5	
Semi-circular	16,14	2.7	121	26.5
---	10,8	1.2	133	
---	6,6	1.2	140.2	
---	5,4.5	1.0	97.5	
---	5,4	1.2	106	
Triangular	4,4,3	0.8	100	
---	6.5,4,3	1.0	120	
Rectangular	6,5	1.2	125.4	
---	5,2	0.8	116	
---	10,6	1.2	128.9	
---	12,6	1.5	130	-32
---	6,4	1.5	126	
---	6,4	1.2	138.1	
---	6,4	1.2	129.6	
---	6,5	1.0	137	
---	6,5	1.0	83	-33
---	5,2.5	1.0	123	
Irregular	6,5	1.0	129	
---	18,4	1.3	112.6	
---	7,4.5	1.1	115	
---	19,6	1.5	141.8	
---	12,3	1.2	141	
---	6,5	1.0	137	
---	10,6	1.5	107	
---	5.5,5	1.5	139.5	
---	5,3	0.7	117.3	
---	---	---	119	

STABLE ISOTOPE DATA: LP-1: $\delta^{18}O$= -7.3‰ PDB; $\delta^{13}C$= +4.3‰ PDB

*(s) = secondary inclusions; (ps) = pseudo-secondary inclusions; all others are primary.

+(Longest, shortest axes) for elliptical/semi-circular/irregular inclusions. (Diameter) for circular inclusions. (Length of a side) for square inclusions. (Length of two sides) for rhombic/rectangular inclusions. (Length of sides) for triangular inclusions.

LOCATION: 46

SAMPLE NUMBER: LP-2A, LP-2B, LP-2C

FLUID-INCLUSION DATA: Measured in inter-particle sparry calcite cement.

Inclusion shape	Inclusion size (µm)	Bubble diameter (µm)	Th (°C)	Tm (°C)
Elliptical	12,6	1.2	100	
---	7,5	1.0	136.8	
Irregular	15,6	1.2	104	
---	9,5	1.0	109.3	
---	18,12	2,2	127	
---	22,7	1.3	117	-5.4
---	10,6	1.2	85	
---	15,10	1.5	124.5	
---	9,9	2.0	134.9	
---	10,5	1.0	94	-20.6

LOCATION: 47

SAMPLE NUMBERS: LP-3, LP-3B

FLUID-INCLUSION DATA: Measured in vug-filling saddle dolomite.

Inclusion shape	Inclusion size (µm)	Bubble diameter (µm)	Th (°C)	Tm (°C)
Elliptical	7,5	1.4	123	
---	6,3	1.2	125.5	
Circular (ps)	3.0	0.5	119.3	
---	5.0	1.5	118.2	
Triangular	5,5,3	1.2	115	
Rectangular	7,3.5	1.0	131	
---	6,4	1.2	129	
---	9,4	1.0	128.6	
Irregular	---	---	112	
---	9,5	1.5	122.5	
---	10,5	1.5	135	
---	---	---	116.3	

STABLE ISOTOPE DATA: LP-3A: $\delta^{18}O$ = -7.92‰ PDB
$\delta^{13}C$ = +4.5‰ PDB

LOCATION: 48

SAMPLE NUMBER: LP-4, LP-4A, LP-4B

FLUID-INCLUSION DATA: Measured in vug-filling saddle dolomite.

Inclusion shape	Inclusion size (µm)	Bubble diameter (µm)	Th (°C)	Tm (° C)
Elliptical	7,4	1.0	114	
---	10,5	1.5	116.3	
---	5,3	0.8	121	
---	8,4	0.8	119.3	
---	7,3.5	1.0	132	
Circular	4.0	1.2	105.4	
Semi-circular	7,5.5	1.6	120.5	
---	6,5	1.2	124.6	
Rectangular	8,4	1.0	102	
---	5,3	0.6	120.3	
Irregular	10,5	1.2	131.6	
---	9,5	1.0	116	
---	---	---	106	

STABLE ISOTOPE DATA: LP-4A: $\delta^{18}O$ = -6.85‰ PDB
$\delta^{13}C$ = +4.2‰ PDB

LOCATION: 49

SAMPLE NUMBERS: LP-5A, LP-5B, LP-6

FLUID-INCLUSION DATA: Measured in vug-filling saddle dolomite.

Inclusion shape	Inclusion size (µm)	Bubble diameter (µm)	Th (°C)	Tm (°C)
Elliptical	5,3	1.0	127	
---	5,3	1.0	135	
Semi-circular	8,7	1.8	128	
---	7,6	1.2	138.5	
Irregular	10,10	2.5	116.8	
---	7,6	2.0	143.2	-32
---	7,6	1.6	145	
---	8,6	2.0	125	
---	6,5	1.0	139.8	

APPENDIX G: THE SALINA GROUP

LOCATION: 57

SAMPLE NUMBERS: X-7A, X-7B, X-7C

FLUID-INCLUSION DATA: Measured in vug-filling quartz cement.

Inclusion shape	*Inclusion size (µm)	Bubble diameter (µm)	Th (°C)	Tm (°C)
Elliptical	5,2	0.5	110.4	
---	6,3	0.8	118	
---	14,7	2.0	146.3	
---	8,6	1.1	186.5	
---	16,6	2.5	162	
---	9,7	1.0	130.5	
Square	6.0	2.2	165	
Rectangular	10,4	1.2	150.5	
---	6,4	1.2	145	
---	9,6	1.5	189.3	
---	6,4	1.0	144.8	
Semi-circular	4,3	0.8	118	
---	4,3	0.8	120.6	
---	4,2.5	0.5	122	
---	5,4	1.3	160	
---	6,4	1.1	142	
---	21,9	3.0	150.6	
---	9,8	1.3	140	-20
Irregular	12,6	1.7	172	
---	19,7	2.3	149.1	
---	7,5	1.8	151	
---	13,7	1.8	145.7	
---	19,9	2.2	166	
---	8,6	1.3	147	-15
---	27,5	2.0	148.4	
---	30,9	3.3	154	-19.8

* (Longest, shortest axes) for elliptical/semi-circular/irregular inclusions. (Diameter) for circular inclusions. (Length of a side) for square inclusions. (length of two sides) for rhombic/ rectangular inclusions. (Length of sides) for triangular inclusions.

LOCATION: 58

SAMPLE NUMBERS: SAL-1, SAL-1A, SAL-1B

FLUID-INCLUSION DATA: Measured in vug-filling dolomite cement.

Inclusion shape	Inclusion size (µm)	Bubble diameter (µm)	Th (°C)	Tm (°C)
Elliptical	4,3	1.0	136	
---	3,2	0.6	123	
---	30,6	4.0	149	
---	9,4	1.0	133.2	
---	2.5,1.5	0.4	131	
---	3,2	0.5	132.7	
---	8,6	1.4	161.4	
---	3,2	0.4	134.6	
---	15,3	1.0	139	
---	4,2.5	0.5	167	
Rectangular	9,3	1.5	125.3	
---	4,2	0.5	138.7	
---	7,3.5	0.8	124	
---	5,3	0.8	129	

---	8,4	1.2	122.6	
Square	5.0	1.1	141	
Circular	5.0	0.6	135	
Semi-circular	4,3	0.9	131.2	
---	4,3.5	1.0	142	
---	6,5	1.2	142.8	
---	7,6	1.0	135.5	
---	7,6	1.2	172	
Triangular	8,7,7	1.3	149.2	-21
---	12,12,4	1.5	125	
Irregular	12,8	2.0	152	
---	6,4	1.5	140	
---	10,4	0.4	102	
---	12,8	2.0	145.5	-23
---	12,8	2.0	142	
---	16,3	1.3	135.9	

TAI: SAL-1 = 2.8

STABLE ISOTOPE DATA: SAL-1:$\delta^{18}O$ = -8.02‰ PDB; $\delta^{13}C$ = -25.9‰ PDB

X-RAY DATA: See Appendix-D for x-ray parameters used.

LOCATION: 51

SAMPLE NUMBER: VR-1

Peak	Peak position (°2θ)	D-space (Å)	Relative Intensity	*FWHM (°2θ)
1	8.92	9.90	19.25	0.439
2	12.46	7.09	4.94	0.256
3	17.80	4.97	11.21	0.499
4	19.84	4.47	11.75	0.333
5	20.94	4.23	18.85	0.172
6	26.72	3.33	100.00	0.275

LOCATION: 52

SAMPLE NUMBER: VR-2

Peak	Peak position (°2θ)	D-space (Å)	Relative Intensity	*FWHM (°2θ)
1	8.90	9.92	16.22	0.458
2	12.54	7.05	5.89	0.175
3**	17.70	----	----	-----
4**	19.80	----	----	-----
5	20.90	----	----	-----
6	26.70	3.33	100.00	0.234

* FWHM (Full Width Half Maximum) = width of the peak at half it's height.

** These peaks were not detected by the "Peak Finding" program, because compared to the "background" noise, their intensities were less than 2, the "relative cut-off intensity" (see Appendix- D). Their positions have been calculated manually from the diffractograms.

APPENDIX H: THE HELDERBERG GROUP

LOCATION: 8

SAMPLE NUMBERS: OTK-1, OTK-1A

FLUID-INCLUSION DATA: Measured in sparry calcite of recrystallized bivalve shells.

*Inclusion shape	+Inclusion size (µm)	Bubble diameter (µm)	Th (°C)	Tm (°C)
Circular	6.0	1.0	122	
Semi-circular	3,2	0.3	128.2	
Rectangular	6,4	1.2	132	
Square	4.0	0.8	107	
Irregular	—	—	126.5	

LOCATION: 26

SAMPLES: B-5, B-5A, B-6, B-6A

FLUID-INCLUSION DATA: Measured in fracture-filling sparry calcite cement.

Inclusion shape	Inclusion size (µm)	Bubble diameter (µm)	Th (°C)	Tm (°C)
Elliptical	5.5,4	0.9	115	
---	4,3	0.8	125	
---	6,4	1.0	186.3	
---	4,3	0.8	185.4	
---	5,3	0.9	186	
---	12,5.5	1.4	138	+3.2
---	7,3.5	0.8	170.6	
---	6,3	1.0	174	
---	4,2.5	0.6	172	
---	4,2.5	0.7	164.8	
---	7,4	1.3	176	
Semi-circular	10,9	1.2	155.3	
---	4,3.5	0.5	164.2	
Circular	3.0	0.5	163	
---	4.5	1.0	186	
Rectangular	4,3	1.0	145	
---	10,7	1.5	159.5	
---	8,4	1.5	145	
Irregular	—	—	170.4	+0.2
---	—	—	160.8	
---	—	—	180.6	
Square	6.0	1.2	161	

ISOTOPE DATA: B-5: $\delta^{18}O$ = -6.18‰ PDB, $\delta^{13}C$ =+0.1‰ PDB
B-6: $\delta^{18}O$ = -8.4‰ PDB, $\delta^{13}C$= +0.5‰PDB

* (s) = secondary inclusions; (ps) = pseudo-secondary inclusions; all others are primary inclusions.

+ (Longest, shortest axes) for elliptical/semi-circularirregular inclusions. (Diameter) for circular inclusions. (Length of a side) for square inclusions. (Length of two sides) for rhombic/rectangular inclusions. (Length of sides) for triangular inclusions.

LOCATION: 27

SAMPLES: B-3A, B-3B, B-4

FLUID-INCLUSION DATA: Measured in sparry calcite of healed fractures.

Inclusion shape	Inclusion size (μm)	Bubble diameter (μm)	Th (°C)	Tm (°C)
Elliptical	8,4.5	1.5	170.4	
---			165	
---	10,5.5	1.8	187	-4.6
--- (s)	4,3	0.5	122	
--- (s)	4,3	0.6	123.6	
---	4,3	1.0	172	
---	6,3	1.2	168	
---	6,3	1.0	175	
---	9,3	0.9	169	
---	4,3	0.7	179	
---	3,2	0.5	113	
---	4,2.5	0.5	183	
Rectangular	5,4	1.0	156	
---	6,4	1.2	160.3	
---	7,3	0.8	167	
---	5,3	1.0	166	
---	5.5,3	0.8	141	
---	3,1.5	0.5	140	
---	7,3.5	1.0	170.3	
---	3,1.5	0.8	167	
---	5,3	1.0	149	
Circular	3.5	0.8	163.2	
--- (s)	3,1.5	0.5	124	
---	5.0	1.3	156	
---	3.0	1.0	167.3	
---	2.5		146	
Semi-circular	6,5	1.4	150.2	
Rhombic	6,3	1.5	164	
---	6,5	1.0	151	
Irregular	—	—	145	
---	—	—	140.6	
---	—	—	158.5	

ISOTOPE DATA: B-3A: $\delta^{18}O$ = -6.37‰ PDB, $\delta^{13}C$ = -0.9‰ PDB

LOCATION: 28

SAMPLES: HLB-1, HLB-2

FLUID-INCLUSION DATA: Measured in skeletal mold and vug-filling sparry calcite cement.

Inclusion shape	Inclusion size (μm)	Bubble diameter (μm)	Th (°C)	Tm (°C)
Elliptical	8,4	1.0	129	
---	6,3	0.9	133	
---	5,3	0.8	113	
---	7,4.5	1.0	127.2	
---	7,4.5	1.2	137	
Rectangular	6,4	1.5	116	
Semi-circular	6.5,5.5	1.2	122	
Irregular	—	—	135.5	

ISOTOPE DATA: HLB-1: $\delta^{18}O$ = -9.18‰ PDB, $\delta^{13}C$ = +2.2‰ PDB

LOCATION: 29

SAMPLES: OC-1, OC-1A, OM-1, OM-1A

FLUID-INCLUSION DATA: Measured in interparticle sparry calcite cement.

Inclusion shape	Inclusion size (μm)	Bubble diameter (μm)	Th (°C)	Tm (°C)
Elliptical	4,3	0.8	126	
---	11,3.5	0.6	101	
---	6,3	1.0	122	
--- (s)	5,3	0.8	102	
--- (s)	5,3.5	1.0	105	
---	4,3	0.8	113	
---	4,3	0.7	117	
---	6,2.5	0.6	128	
---	10,6	2.0	149.9	-13.7
---	6,4	1.0	137.5	-7.4
Rectangular	4,2	0.7	124	
---	3,2	0.6	124	
---	6,5	0.8	102	
---	6,3	1.0	136.6	
--- (s)	6,3	1.0	129.5	
---	7,3	0.9	121	
Semi-circular	9,8	1.0	95.5	
---	9,7	1.5	115	
---	3,2	0.8	120.7	
---	8,7	2.5	163	
---	15,10	2.8	133.7	
---	6,5	1.0	140.5	
---	5,4	1.0	130.4	
---	9,6	1.2	160.5	-9.7
Rhombic	6,5	1.2	140.6	
---	4,3	0.8	107	
--- (s)	4,3	0.7	102.2	
---	5,5	1.0	134	
Circular	3.0	0.7	145.5	
Square	3.0	0.6	130.7	
Irregular	___	___	130	
---	---	---	115	
---	---	---	122	
---	---	---	165.2	
---	9,6	1.5	120	-7.9
---	---	---	110.6	
ISOTOPE DATA:	OC-1: $\delta^{18}O$ = -3.07‰ PDB, $\delta^{13}C$ = +3.1‰ PDB, OM-1: $\delta^{18}O$ = -4.3‰ PDB, $\delta^{13}C$ = +2.0‰ PDB, OM-1A: $\delta^{18}O$ = -6.18‰ PDB, $\delta^{13}C$ = +3.0‰ PDB.			

LOCATION: 9

SAMPLE NUMBERS: HLB-4A, HLB-4B, H:B-4C

FLUID-INCLUSION DATA: Measured in vug-filling fluorite and saddle dolomite.

Inclusion shape	Inclusion size (μm)	Bubble diameter (μm)	Th (°C)	Tm (°C)
In Fluorite:				
Elliptical	8,4	1.2	138	
---	7,4	1.2	138.2	
---	10,5	2.0	144.7	
---	9,5	2.0	139	
---	4,2.5	0.5	96	
--- (s)	5,3	1.0	109	
--- (s)	5,3	1.0	112.6	
--- (s)	4.5,3	0.8	106.5	

---	5,3.5	1.0	135.4	
---	8,5	1.5	152.7	-24
---	7,4	1.2	146	
---	6.5,4	1.2	146	
---	8,5	1.5	139.1	
Circular (ps)	4.0	1.0	137	
---	4.0	0.8	139	
--- (s)	3.0	0.8	93.2	
--- (s)	3.5	0.8	95	
Circular-to-elliptical (s)	smaller than 5,5	smaller than 1.0	122-128 (#30)	
--- (s)	smaller than 4,4	smaller than 1.0	115-120 (#11)	
--- (s)	smaller than 4,4	smaller than 1.0	83-87 (#11)	
--- (s)	---	---	90-100 (#15)	
--- (s)	---	---	100-110 (#15)	
--- (s)	smaller than 5,5	smaller than 1.2	100-115 (#25)	
Semi-circular	6,5	1.0	138	
---	5,4	1.0	133.5	
---	8,6	1.4	139	
---	5,4	1.0	137.8	
---	6,4.5	1.5	160.7	
Semi-circular-to-elliptical (s)	smaller than 6,5	smaller than 1.5	100-106 (#22)	
--- (s)	---	1.0	102-109 (#8)	
Rectangular	5,3	1.0	126.7	
---	5,4	1.0	158.6	
Irregular	8,7	2.0	136.5	
---	7,6	1.8	154	
---	---	---	116.6	
---	10,7	2.2	122	
---	8,6	1.5	162	
<u>In saddle dolomite:</u>				
Elliptical	5,3	0.8	115.6	
--- (s)	smaller than 7,5	smaller than 1.5	112-118.5 (#6)	
---	6,4	1.5	126	
---	6,4	1.0	133.7	
---	6,3	1.2	136	
Circular	3.0	0.8	128.8	
Semi-circular	5,4	1.2	125	
---	6,4	1.5	143.8	
---	3,2	---	138	
---	4,2.5	0.5	98	
Rectangular	8,3	1.0	108.1	
---	7,4	1.0	97.5	
---	5,4	0.8	105	
Irregular	10,7	1.8	116.6	
---	9,6	1.5	145	
---	8,8	1.5	122.9	
---	7,6	1.0	136.6	
			137	

(#) number of inclusions.

TAI: HLB-4A: 2.7

STABLE ISOTOPE DATA: HLB-4A: $\delta^{18}O$ = -5.2‰ PDB; $\delta^{13}C$ = +2.9‰ PDB.

LOCATION: 22

SAMPLE NUMBERS: CGH-1, CGH-1A, CGH-1B

FLUID-INCLUSION DATA: Measured in sparry calcite cement in coral cavities.

Inclusion shape	Inclusion size (μm)	Bubble diameter (μm)	Th (°C)	Tm (°C)
Elliptical	6,4	0.5	72.5	
---	6,3	0.6	70	
---	---	---	83.8	
---	12,6	1.0	151	-24
---	7,4	0.8	75	
--- (ps)	5,3	0.8	83	
--- (ps)	5,3	0.8	81.3	
---	12,4	1.0	142	
---	7,3	1.0	176	
---	2.5,1.5	0.2	118	
--- (s)	6,3	1.0	149	
--- (s)	5,3	0.8	152	
Rectangular	3,2	0.4	163.6	
---	5,4	1.2	165	
---	12,4	0.5	119	
Circular (s)	2.5	0.4	79	
---	2.0	0.4	120	
Semi-circular	4,3	0.8	138	
---	7,6	1.2	169.2	
---	6,4.5	1.0	154.4	
Irregular	---	---	150.6	
---	---	---	170	
---	10,4	1.5	129.4	
---	12,9	1.0	81.7	

STABLE ISOTOPE DATA: CGH-1: $\delta^{18}O$ = -6.66‰ PDB; $\delta^{13}C$ = +1.7‰ PDB.

APPENDIX I: THE ONONDAGA FORMATION

LOCATION: 1

SAMPLE NUMBERS: OAL-1, OAL-1A

FLUID INCLUSION DATA: Measured in vein-filling sparry calcite.

*Inclusion shape	+Inclusion size (μm)	Bubble diameter (μm)	Th (°C)	Tm (°C)
Elliptical	7,6	1.0	165	
---	8,5	2.0	187	
---	8,4	1.5	165	
---	5,3	1.5	175.6	
---	7,4	1.0	196	
---	6,5	0.7	199.5	
---	10,6	1.0	190	-16.3
Irregular	---	---	102	

ISOTOPE DATA: OAL-1: $\delta^{18}O$ = - 6.08‰ PDB, $\delta^{13}C$ = +1.1‰ PDB

LOCATION: 2

SAMPLES: OX-1, OX-1A, OX-2

FLUID-INCLUSION DATA: Measured in vein-filling calcite and dolomite.

Inclusion shape	Inclusion size (μm)	Bubble diameter (μm)	Th (°C)	Tm (°C)
Elliptical	5,3	1.5	140	
---	---	---	185.6	
---	---	---	179.5	
---	4,2	1.0	150	
---	5,3	1.0	140.3	
---	---	---	184	
---	5,3	1.8	199.4	
Semi-circular	6,5	1.5	171	
---	6,5	1.2	168.5	
---	9,8	2.2	178.8	-15
*Elliptical	smaller than	smaller than	165-180	
-circular	4,3	0.5		
Circular(s)	3.0	1.0	185	
Rectangular	5,3	1.2	180.7	

* 8 very small two-phase cloudy inclusions in a cluster. Difficult to measure individual Th, but all bubbles disappear between 165 - 180°C.

COMMENTS: Two-phase inclusions are rare and/or too small to measure. Numerous, small, one-phase primary and two rows of similar secondary inclusions are observed. The one-phase inclusions exhibit dark rims, probably indicating a gas phase.

TAI DATA: OX-2 = 2.3

ISOTOPE DATA: OX-2: ^{18}O = -4.72%. PDB, ^{13}C = +0.7%. PDB

* (s)= secondary inclusions; (ps) = pseudo-secondary inclusions; all others are primary inclusions.

+ (Longest, shortest axes) for elliptical/semi-circular/irregular inclusions. (Diameter) for circular inclusions. (Length of a side) for square inclusions. (Length of two sides) for rectangular/rhombic inclusions. (length of sides) for triangular inclusions).

LOCATION: 3

SAMPLE NUMBERS: OX-3, OX-3A

FLUID-INCLUSION DATA: Measured in vein-filling calcite. The dolomite is cloudy and contains no inclusion large enough to measure.

Inclusion shape	Inclusion size (µm)	Bubble diameter (µm)	Th (°C)	Tm (°C)
Elliptical	---	---	186	
---	7,3	1.2	188	
---	---	---	180.8	
---	---	---	174	
---	---	---	172.2	
---	12,7	2.0	170	
---	12,3	1.3	133	
---	9,4	1.5	155.3	- 4.2
---	13,4	1.6	152	
---	7,3,5	1.7	123.9	- 3.2
---	10,5	v.small	140	
---	---	v.small	160	
---	24,8	5	182.5	- 0.3
---	---	---	199	- 1.2
---	12,6	1.8	123	
---	7,5	1.0	112.7	
Circular	4.0	1.0	62	
---	---	---	187.2	
---	3.0	0.8	105	
---	4.5	1.5	197.4	
Irregular	---	---	165	
---	---	---	105	
---	---	---	120	

TAI DATA: OX-3 = 3.2

ISOTOPE DATA: OX-3: $\delta^{18}O$ = -8.9‰ PDB, $\delta^{13}C$ = -0.7‰ PDB

LOCATION-4

SAMPLES: OG-22, AB-58, OA-5

FLUID-INCLUSION DATA: Measured in sparry calcite in coral chambers and vugs.

Inclusion Shape	Inclusion Size (µm)	Bubble diameter (µm)	Th (°C)	Tm (°C)
Elliptical	v. small	v. small	90.5	
---	5,2	0.5	94	
---	3,1.5	0.3	85	
---	---	---	108.4	
---	6,2	0.5	95	
---	5,2	1.0	98.3	
---	---	---	94	
---	7,4	1.0	96	
---	6,4	1.0	119.4	
---	6,3.5	1.2	104	
---	6,4	0.8	99	
---	7,4	1.0	104	
---	7,6	1.2	107.7	
Circular	3,3	0.7	56	
---	v. small	v. small	92	
---	---	---	97	
---	3.0	0.6	85.6	
---(s)	3.0	0.4	80.7	
---	4.5	0.8	87	
---	5.0	1.0	86.5	

COMMENTS: Inclusion sizes are generally very small. Small 1-phase inclusions are locally abundant.
TAI DATA: AB-58 = 3.0

LOCATION: 5

SAMPLE NUMBERS: OG-20, OG-21, OG-21A and R-74

FLUID-INCLUSION DATA: Measured in sparry calcite in coral chambers and vugs.

Inclusion shape	Inclusion size (μm)	Bubble diameter (μm)	Th (°C)	Tm (°C)
*Circular and	smaller than	smaller than		
elliptical (s)	3,3	1.0	50-65	
Elliptical	6,3	1.0	65	
---	4.5,3	1.0	83	
---	4,2.5	0.5	91	
---	4,3	0.5	83	
---	6,4	1.0	108.5	
---	9,5	1.2	97.3	
---	6,4	1.0	101	
---	12,3	1.0	115	
---	6,4	1.0	110	
---	6,3	0.5	95.3	
---	9,6	1.1	129.9	
---	12,3	1.5	118	-4.6
---	10,3	1.0	101	
---	6,5	0.9	90	
---	6,3	1.0	105	
---	10,4	1.0	105	
Circular	v.small	v.small	70	
Semi-circular	4,3	0.8	80	
---	4.3,3.3	1.0	104	
---	7,6	1.3	95	
---	4,3	0.8	99	
---	4,3	0.8	105	
---	4,3	0.5	75	
Square	3.5	1.0	116	
Irregular	---	---	80.8	
---	---	1.2	122	
---	---	---	119	

* 12 very small secondary inclusions.

TAI DATA: R-74 = 2.7

ISOTOPE DATA: OG-20: $\delta^{18}O$ = -5.98‰ PDB, $\delta^{13}C$ = +2.8‰ PDB
OG-21A: $\delta^{18}O$ = -4.0 ‰ PDB , $\delta^{13}C$ = +3.4‰ PDB

LOCATION:6

SAMPLES: OG-16, OG-17:

FLUID-INCLUSION DATA: Measured in calcite cement in coral chambers.

Inclusion shape	Inclusion size (μm)	Bubble diameter (μm)	Th (°C)	Tm (° C)
Elliptical	3,2	0.5	90	
---	12,6	1.5	104.9	
---	---	---	100.3	
---	9,6	1.0	95.8	
---	9,3	1.2	101	-14
Circular	5,5	0.7	107	
Semi-circular	4,3	0.7	106	
---	6,5	1.0	106	
---	6,4	0.7	101	
Irregular	---	---	95	

ISOTOPE DATA: OG-17: $\delta^{18}O$ = -3.75‰ PDB, $\delta^{13}C$ = 3.0‰ PDB

LOCATION: 7:

SAMPLES: OG-1X, OG-1Xa

FLUID-INCLUSION DATA: From quartz and calcite in coral chambers.

Inclusion shape	Inclusion size (μm)	Bubble diameter (μm)	Th (°C)	Tm (°C)
In quartz:				
Elliptical	4,2	0.8	90	
---	4,2	0.9	93	
---	5,3	0.7	95	
---	6,3.5	1.0	93.5	
---	---	---	85	
---	5,3	0.8	94	
---	---	---	96	
---	---	---	95	-9.8
---	6,3	1.0	95.6	
Circular	4	1.2	90.6	
Semi-circular	---	---	88	
---	5,4	1.3	91.3	
---	6,5	1.3	99	
---	7,5	1.5	94.6	
In calcite:				
Elliptical	6,3.5	0.8	83.4	
---	5,3	1.0	77	
---	7,4	1.0	108	
---	6,3	0.9	109	
---	5,2.5	0.7	110.2	
---	7,3	1.2	115.2	
---	6.5,3	1.0	116	
---	5,3	1.0	119	
---	6,3	0.8	109	
---	7,4.5	1.5	109.6	
Irregular	---	---	95.5	
Circular	5	1.3	97	

LOCATION: 8

SAMPLES: OT-1, OT-1A

FLUID-INCLUSION DATA: Measured in vein-calcite. No measurable inclusion observed in either dolomite of quartz.

Inclusion shape	Inclusion size (μm)	Bubble diameter (μm)	Th (°C)	Tm (°C)
Elliptical	6,3	1.2	107.4	
---	6,3	0.9	110.5	
---	---	---	117	
---	4,2	0.5	133.2	
---	5,3	1.0	133.4	-13.0
Circular	5.0	2.0	95	
---	---	---	75.4	
Semi-circular	3,2	0.5	130.6	

TAI DATA: OTO-1 = 2.5

ISOTOPE DATA: OTO-1: $\delta^{18}O$ = -7.3‰ PDB, $\delta^{13}C$ =1.2‰ PDB

LOCATION: 9

SAMPLES: OG-1, OG-2, OG-3

FLUID-INCLUSION DATA: Measured in inter-particle calcite cement.

Inclusion shape	Inclusion size (μm)	Bubble diameter (μm)	Th (°C)	Tm (°C)
Elliptical	6,4	0.8	172	
---	5,2	0.5	151	
---	6,3	1.0	150.5	
---	v.small	v.small	168	
---	---	---	155	
---	15,7	2.0	145.2	
---	8,5	1.2	137	
---	6,4	1.0	116	
---	---	---	103	
Circular	v.small	v.small	129	
---	---	---	110.3	
---	5.0	12	160.3	
Semi-circular	---	---	106	

ISOTOPE DATA: OG-1: $\delta^{18}O$ = -2.78‰ PDB, $\delta^{13}C$ = 2.1‰ PDB

LOCATION: 10

SAMPLES: OG-4, OG-5, OG-6, OG-7

FLUID-INCLUSION DATA: Measured in calcite and dolomite. Two-phase inclusions are not observed in microquartz.

Inclusion shape	Inclusion size (μm)	Bubble diameter (μm)	Th (°C)	Tm (°C)
In calcite:				
Elliptical	5,3	1.0	113	
---	7,4	1.2	123.8	
---	---	---	120.4	
Rectangular	6,5	1.5	136	
Irregular	---	---	115.6	
In dolomite:				
Elliptical	8,4	1.5	125	
---	7,4	1.0	127	
---	5,3	0.9	128.7	
---	---	---	126.5	
---	4,2	0.5	123	
---	6,4	1.0	141	
---	6,3	1.0	139	
---	6,4	1.2	115.6	
---	7,4.5	1.3	141.5	
---	7,5	1.7	151.8	
---	6,3	1.0	162	
---	8,4	1.3	177.6	-15.6
---	8,5	1.3	178	-14.7
Semi-circular	6,5	1.6	131	
Rectangular	7,6	1.5	119	
Irregular	---	---	132	
---	---	---	91	

TAI DATA: OG-7 = 2.8

ISOTOPE DATA: OG-7 (dol.): $\delta^{18}O$ = -2.78‰ PDB, $\delta^{13}C$ = +2.4‰ PDB

LOCATION: 11

SAMPLES: OG-8

FLUID-INCLUSION DATA: No inclusions found in dark micrite.

TAI DATA: OG-8 = 2.9

LOCATION: 13

SAMPLES: OG-9, OG-9A

FLUID-INCLUSION DATA: Measured in calcite and saddle dolomite veins.

Inclusion shape	Inclusion size (µm)	Bubble diameter (µm)	Th (°C)	Tm (°C)
In calcite:				
Elliptical	8,4	1.5	147	
---	6,3	1.0	157	
---	6,3	0.8	132.5	
---	5,3	1.0	136	
Rectangular	6,3	1.5	150.2	
In dolomite:				
Rhombic	5,4	1.0	155	
Elliptical	7,3.5	1.2	163	-15.9

LOCATION: 14

SAMPLES: OG-10

FLUID-INCLUSION DATA: No inclusion found in micrite.

TAI DATA: OG-10 = 2.3

LOCATION: 16

SAMPLES: OG-12, OG-12A, OG-12B

FLUID-INCLUSION DATA: No inclusion found in sandy micrite.

TAI DATA: OG-12 = 2.2, OG-12A = 2.3

LOCATION: 17

SAMPLES: OG-13, OG-13A

FLUID-INCLUSION DATA: Measured in intergranular sparry calcite.

Inclusion shape	Inclusion size (µm)	Bubble diameter (µm)	Th (°C)	Tm (°C)
Elliptical (s)	5.5,3	1.0	93.2	
--- (s)	5,3	1.0	91	
---	6,3	1.2	86	
---	6.5,3	0.9	102	
---	5,2.5	0.7	103	
---	4,2.5	0.5	113	
---	5,3	0.8	134.6	
---	3,2	0.5	92.4	
---	5.5,3	1.0	105.4	
--- (s)	---	---	103.8	
--- (s)	3,2	0.5	90	

--- (s)	3,2	0.5	88.6	
--- (s)	4,2.5	0.7	87	
---	3.5,2	0.5	101.3	
---	---	---	84	
---	8,5	1.0	96	
---	5,2.5	0.8	114	
---	6,2.5	1.0	116.3	
---	---	---	114.7	
---	6.5,4	1.4	119.5	
---	8,4.5	1.5	143	
Semi-circular	4,3	0.8	103	
---	6,5	1.3	114	
---	5,4	1.0	102.5	
Rectangular	6,4	1.4	106.8	
---	6,5	2.0	133	-9
Square (s)	4.0	1.2	80.6	
Circular (s)	4.0	1.0	92	
Irregular (s)	---	---	103	
---	---	---	107	
---	---	---	111.5	
In quartz				
Elliptical	6,3.5	1.0	85.2	
---	5,2.5	0.5	90.7	
---	5,3	0.5	123	
---	6,3.5	1.0	93	
---	5,3	0.8	116.2	
Semi-circular	6,5	1.5	112	
---	5,4	1.0	113	
Irregular	---	---	100.8	
---	---	---	108	

TAI DATA: OG-13 = 2.8

ISOTOPE DATA: OG-13: $\delta^{18}O$ = -10.25‰ PDB, $\delta^{13}C$ = 0.6‰ PDB

LOCATION: 18

SAMPLES: OG-14, OG-14A, OG-18, OG-19, L-11A

FLUID-INCLUSION DATA: Measured in sparry calcite and mega-quartz. Very few inclusions occur in quartz.

Inclusion shape	Inclusion size (μm)	Bubble diameter (μm)	Th (°C)	Tm (°C)
In Calcite:				
Elliptical	3,2	0.6	110	
--- (s)	4,2	0.5	76	
--- (s)	4,2	0.6	89	
---	5,3	0.5	114.6	
---	5,2.5	0.7	92	
---	6,4	1.4	121.6	
---	7,4	1.5	123.4	
---	6.5,4.5	1.2	105.6	
---	5,3	0.7	113	
---	7,4	1.0	138	-10.3
---	7,3.5	1.0	132	
Square	4.0	1.0	63	
*Rectangular-semi-circular	smaller than 6,5	smaller than 1.0	80-90	
Irregular	---	---	119	
---	---	---	95	
---	---	---	121	
In quartz:				
Square	3.0	0.8	109	
Circular	3.0	0.7	96	

Elliptical	5,3	0.7	103.9
Semi-circular	4,3.5	0.8	119.7

* Thirteen very small inclusions.

TAI DATA: L-11A = 3.3

ISOTOPE DATA: OG-14 = $\delta^{18}O$ = -7.92‰ PDB, $\delta^{13}C$ =1.1‰ PDB
OG-19 = $\delta^{18}O$ = -6.18‰ PDB, $\delta^{13}C$ =2.1‰ PDB

LOCATION: 20

SAMPLES: OG-15, OG-15A, OG-15B

FLUID-INCLUSION DATA: Measured in sparry calcite in coral chambers.

Inclusion shape	Inclusion size (μm)	Bubble diameter (μm)	Th (°C)	Tm (°C)
Elliptical	6,3.5	1.0	108	
---	6,3	0.8	109	
---	7,3	1.0	106.6	
---	7,4.5	1.5	98.6	
---	5,3	0.8	95	
---	6,3	1.0	100.6	
---	5,3	0.6	96	
---	5,2.5	0.5	75	
Circular	5.0	1.2	99.2	
---	3.0	0.5	50.8	
Irregular	---	---	94.8	
---	---	---	50.5	
Triangular	3,3,3	0.7	97	

TAI DATA: OG-15 = 2.3

ISOTOPE DATA: OG-15: $\delta^{18}O$ =-7.44‰ PDB, $\delta^{13}C$ = 1.1‰ PDB

LOCATION: 22

SAMPLES: CGO-1, CGO-2

FLUID-INCLUSION DATA: Measured in sparry calcite veins.

Inclusion shape	Inclusion size (μm)	Bubble diameter (μm)	Th (°C)	Tm (°C)
Elliptical	6,3	1.5	46	
---	8,6	1.6	35	
---	6,4	1.3	46	
---	9,3	1.8	79.3	
---	4.5,3	0.8	51	
---	7,3	0.6	41	
*Elliptical-semi-circular	smaller than 9,6	smaller than 1.5	30-38	+0.6-+2.5
Circular (s)	3.0	0.8	50.7	
Semi-circular	3.5,2.5	1.0	65	
---	9,8	1.5	28.5	
---	6,4.5	1.5	25.5	
Irregular	---	---	49	
---	---	---	66.6	
---	---	---	68	

* 10 inclusions.

COMMENTS: The measured two-phase inclusions are associated with numerous one-phase inclusions. Primary inclusions are few.

TAI DATA: CGO-2 = 2.3

ISOTOPE DATA: CGO-1: $\delta^{18}O$ = -8.5‰ PDB, $\delta^{13}C$ = 1.6‰ PDB
CGO-2: $\delta^{18}O$ = -7.8‰ PDB, $\delta^{13}C$ = 3.4‰ PDB

LOCATION: 23

SAMPLES: RP-1, RP-2

FLUID-INCLUSION DATA: Two-phase inclusions are not found. Some one-phase inclusions are present.

ISOTOPE DATA: RP-1: $\delta^{18}O$ = -8.9‰ PDB, $\delta^{13}C$ = -3.3‰ PDB

LOCATION: 24

SAMPLES: SYO-3, SYO-4

FLUID-INCLUSION DATA: Measured in inter-particle and syntaxial calcite.

Inclusion shape	Inclusion size (μm)	Bubble diameter (μm)	Th (°C)	Tm (°C)
Elliptical	4,2	0.8	113	
---	7,4	0.6	119	
---	7,4	1.0	126	-17.7
---	7,2	1.0	128	
---	12,6	1.8	177	
---	12,5	1.6	169	
---	5,3	0.8	93.4	
---	6,2	0.8	124.4	
---	6,2	0.6	125	
---	11,4	2.5	99.5	
---	9,6	1.2	147.5	
---	6,4	1.0	96	
---	11,6	1.7	119.7	
---	7,3.5	2.0	126	
---	10,7	2.0	173	
---	8,5	1.5	167.2	
Circular	7.0	1.2	96	
---	4.0	1.0	96.3	
---	4.0	1.0	123.6	
Semi-circular	4,3	0.8	127	
---	4,3	0.7	109	
Square	5.0	1.4	95	
---	4.0	1.2	120	
Rhombic	4,3.5	1.0	105	
---	4,4	1.0	113	
Rectangular	5,4	1.0	96	
---	10,6	2.5	100.5	
---	7,6	1.3	97	
---	14,3	1.2	120.4	
Irregular	—	—	137	
—	—	—	105	
—	—	—	114	
—	—	—	80.7	
—	—	—	113	

TAI DATA: SYO-3 = 2.7

ISOTOPE DATA: SYO-3: $\delta^{18}O$ = -2.97‰ PDB, $\delta^{13}C$ = 1.17‰ PDB

LOCATION: 25

SAMPLES: VVO-1, VVO-2

FLUID-INCLUSION DATA: Two-phase inclusions are not observed. Few one-phase inclusions present.

LOCATION: 70

SAMPLES: OGC-3, OGC-4, OGC-5.

FLUID-INCLUSION DATA: Measured in quartz and calcite cement in coral chambers.

Inclusion shape	Inclusion size (µm)	Bubble diameter (µm)	Th (°C)	Tm (°C)
In quartz:				
Elliptical	9,6	1.0	90.5	
---	10,6	1.5	100.5	
---	10,4	1.5	118	
---	7,4	1.3	112	
Rectangular	65,8	4.0	100.5	
---	16,13	1.5	93.5	-14
---	13,10	0.9	89	-17
---	7,4	1.0	88	
Irregular	9,4	1.0	95.6	
---	15,9	1.5	89	
In calcite:				
Elliptical	8,4	0.8	111	
---	6,5	1.0	97.8	
---	5,3	1.0	93.6	
---	6,4	0.8	98	
---	7,5.5	1.7	113.7	
Square	6.0	1.2	123.8	
Semi-circular	7,6	1.5	118	
---	6,4.5	1.5	98.2	
---	7,5.5	2.0	106.7	
---	5,4	0.6	73	
Irregular	---	---	85	
---	---	---	72.5	
---	---	---	105	
---	---	---	86.6	

LOCATION: 71

SAMPLES: OG-1, OG-1A, OG-2

FLUID-INCLUSION DATA: Measured in sparry calcite in coral chambers. No measurable inclusion found in microquartz.

Inclusion shape	Inclusion size (µm)	Bubble diameter (µm)	Th (°C)	Tm (° C)
Elliptical	18,9	2.0	125	
---	12,6	1.0	75.7	
---	8,4.5	1.2	115.3	
---	7,4	1.0	100.9	
---	6,4	1.0	108.3	
Rectangular	9,6	1.0	110.7	
Square	3.0	0.7	125	
Semi-circular	6,5	1.2	123	
---	6,5	1.0	93.5	
Irregular	---	---	95	

LOCATION: 72

SAMPLES: OGC-6, OGC-6A, OGC-6B

FLUID-INCLUSION DATA: Measured in vug-filling calcite crystals.

Inclusion shape	Inclusion size (µm)	Bubble diameter (µm)	Th (°C)	Tm (°C)
Elliptical	18,3.5	1.7	149	-3.5
---	8,3	1.1	152	
---	16,10	2.0	152.7	
---	10,3	1.3	135	
---	24,6	1.6	120.5	
---	13,6	1.3	150.9	
---	10,6	1.3	130	
---	9,3.5	1.4	121.5	
---	19,6	2.0	132	
---	22,5.5	2.2	190	
---	10,6	2.1	199	
---	16,9	2.5	155	-15
---	6,4	1.0	105	
---	10,6	1.2	185	
---	8,5.4	1.0	198.3	
---	14,9	1.0	82.8	
---	25,7	1.5	132.1	
---	7,3	2.0	100	
Semi-circular	7,6	1.0	85	
Circular	10.0	1.7	130	-17.9
Rectangular	10,7	1.0	85	
---	6,5	1.0	106	
---	20,6	1.5	136	
---	4,1.5	0.8	75	
Square	6.0	1.0	91	
---	6.0	1.0	121	
Irregular	---	---	169	
---	---	---	72.5	
---	---	---	73	
---	---	---	80	
---	---	---	107	

APPENDIX J: MARCELLUS FORMATION

X-RAY DATA: See Appendix-D for x-ray conditions and parameters used.

LOCATION: 36 SAMPLE: FO-1 (Glycolated)

Peak	Peak position (°2θ)	D-space (Å)	Relative Intensity	FWHM* (°2θ)
1**	6.20	----	----	----
2	8.86	9.97	69.76	0.317
3	12.54	7.05	34.84	0.195
4**	17.30	----	----	----
5**	25.00	----	----	----
6	25.32	3.51	38.66	1.28
7	26.66	3.34	100.00	0.338

* FWHM (Full Width-Half Maximum) = width of the peak at half its height.

** These peaks are not picked up by the "Peak Finding" computer program probably because compared to the background 'noise', their intensity is less than 2 which is the 'relative cutoff intensity' (see above). Their peak positions have been calculated manually from the diffractogram.

LOCATION:3 SAMPLE: BK-1 (Glycolated)

Peak	Peak position (°2θ)	D-space (Å)	Relative Intensity	FWHM (°2θ)
1	8.74	10.10	14.39	0.320
2	12.54	7.05	9.26	0.298
3	17.76	4.99	9.39	0.396
4**	19.80	----	----	----
5	20.92	4.24	19.62	0.151
6**	25.00	----	----	----
7	26.70	3.33	100.00	0.233
8**	27.60	----	----	----

** See location: 36

LOCATION: 32 SAMPLE: MR-1 (Glycolated)

Peak	Peak position (°2θ)	D-space (Å)	Relative Intensity	FWHM (°2θ)
1	6.26	14.10	4.59	0.356
2	8.86	9.97	32.82	0.358
3	12.54	7.05	26.29	0.257
4	17.78	4.98	16.88	0.378
5	18.76	4.72	5.80	0.317
6	19.76	4.48	7.17	0.398
7	20.90	4.24	17.94	0.154
8	25.20	3.53	14.88	0.274
9	26.66	3.34	100.00	0.256

** See location 36

LOCATION: 33 SAMPLE: MR-2 (Glycolated)

Peak	Peak position (°2θ)	D-space (Å)	Relative Intensity	FWHM (°2θ)
1	6.24	14.15	9.91	0.299
2	8.86	9.97	80.10	0.399
3	12.52	7.06	42.07	0.297
4	17.74	4.99	33.01	0.398
5	18.82	4.71	10.66	0.560
6**	19.65	----	----	----
7	20.88	4.25	11.94	0.134
8	25.20	3.53	27.71	0.339
9	26.66	3.34	100.00	0.339
10	27.44	3.24	7.89	0.540

** See location: 36

LOCATION: 11 SAMPLE: MC-5/6 (Glycolated)

Peak	Peak position (°2θ)	D-space (Å)	Relative intensity	FWHM (°2θ)
1	8.78	10.06	100.00	0.438
2	12.48	7.08	11.86	0.356
3	17.78	4.98	32.58	0.520
4	26.70	3.33	58.81	0.438

LOCATION: 22 SAMPLE: MR-4(22) (Glycolated)

Peak	Peak position (°2θ)	D-space (Å)	Relative intensity	FWHM (°2θ)
1	6.18	14.29	8.68	0.120
2	8.70	10.15	56.24	0.399
3	12.40	7.13	38.75	0.317
4	17.66	5.01	29.65	0.379
5	18.66	4.75	10.26	0.396
6**	19.60	----	----	----
7	20.78	4.27	13.08	0.377
8	25.14	3.53	26.63	0.358
9	26.56	3.35	100.00	0.357

** See location: 36

LOCATION: 22 SAMPLE: CGU-2 (Glycolated)

Peak	Peak position (°2θ)	D-space (Å)	Relative intensity	FWHM (°2θ)
1	8.86	9.97	79.19	0.398
2	17.78	4.98	24.84	0.200
3	20.88	4.25	28.51	0.192
4	26.66	3.34	100.00	0.313

LOCATION: 25 SAMPLE: MR-4(25) (Glycolated)

Peak	Peak position (°2θ)	D-space (Å)	Relative intensity	FWHM (°2θ)
1	6.26	14.10	10.79	0.197
2	8.84	9.99	81.09	0.398
3	12.48	7.08	35.35	0.297
4	17.78	4.98	29.78	0.376
5	18.84	4.70	11.46	0.298
6**	19.60	----	----	----
7	20.90	4.24	16.08	0.133
8	25.20	3.50	22.84	0.260
9	26.68	3.33	100.00	0.316

** see location: 36

VITRINITE REFLECTANCE DATA:

LOCATION: 36 SAMPLE: FO-1

(NO. OF READINGS = 10) 0.47 0.81 0.84 0.85 0.86 0.90 1.30 1.34 2.00 2.10

POPULATION	NO. OF READINGS	MIN. Ro (%)	MAX. Ro (%)	MEAN Ro (%)	STD. DEV. (%)	REMARKS
(1)	1	0.47	0.47	0.47	-	MODERATELY IMMATURE
(2)	5	0.81	0.90	0.85	0.033	MATURE
(3)	2	1.30	1.34	1.32	-	MATURE
(4)	2	2.00	2.10	2.05	-	VERY MATURE

TOTAL MEAN Ro (%) = 1.27

LOCATION: 3 SAMPLE: BK-1

(NO. OF READINGS = 50) 1.08 1.09 1.11 1.13 1.39 1.41 1.47 1.48 1.48 1.48 1.49 1.60 1.80 1.80
1.80 1.81 1.86 1.88 2.10 2.20 2.20 2.20 2.20 2.20 2.30 2.30 2.30 2.30 2.30 2.30 2.30 2.40
2.40 2.40 2.40 2.40 2.40 2.40 2.50 2.50 2.50 2.50 2.50 2.50 2.50 2.60 2.60 2.60 2.60 2.70

POPULATION	NO. OF READINGS	MIN. Ro (%)	MAX. Ro (%)	MEAN Ro (%)	STD. DEV. (%)	REMARKS
(1)	4	1.08	1.13	1.10	0.022	MATURE
(2)	8	1.39	1.60	1.48	0.063	MATURE
(3)	6	1.80	1.88	1.83	0.036	VERY MATURE
(4)	32	2.10	2.70	2.39	0.148	VERY MATURE

TOTAL MEAN Ro (%) = 2.07

LOCATION: 32 SAMPLE: MR-1

(NO. OF READINGS = 49)			0.35	0.36	0.40	0.40	0.45	0.53	1.02	1.02	1.23	1.23	1.24	1.25	1.25	1.26	
1.39	1.42	1.44	1.44	1.45	1.45	1.47	1.48	1.53	1.53	1.55	1.55	1.55	1.56	1.57	1.99	2.00	2.00
2.00	2.00	2.00	2.10	2.10	2.10	2.10	2.10	2.10	2.10	2.20	2.20	2.20	2.20	2.30	2.40	2.50	

POPULATION	NO. OF READINGS	MIN. Ro (%)	MAX. Ro (%)	MEAN Ro (%)	STD. DEV. (%)	REMARKS
(1)	4	0.35	0.40	0.38	0.026	IMMATURE
(2)	2	0.45	0.53	0.49	-	MOD. IMMATURE
(3)	8	1.02	1.26	1.19	0.104	MATURE
(4)	15	1.39	1.57	1.49	0.059	MATURE
(5)	20	1.99	2.50	2.13	0.139	VERY MATURE

TOTAL MEAN Ro (%) = 1.56

LOCATION: 33 SAMPLE: MC-1

(NO. OF READINGS = 82)			1.20	1.28	1.28	1.31	1.31	1.32	1.34	1.34	1.36	1.41	1.42	1.42	1.42	1.50	
1.53	1.54	1.54	1.54	1.54	1.55	1.55	1.55	1.55	1.56	1.57	1.58	1.58	1.59	1.68	1.74	1.75	1.75
1.76	1.78	1.79	1.79	1.79	1.80	1.80	1.80	1.80	1.80	1.80	1.80	1.81	1.81	1.81	1.81	1.82	1.82
1.83	1.84	1.84	1.84	1.85	1.85	1.85	1.85	1.85	1.85	1.86	1.86	1.92	1.93	2.00	2.00	2.70	2.80
2.90	2.90	2.90	2.90	3.00	3.10	3.10	3.10	3.10	3.20	3.20	3.20	3.30	3.30				

POPULATION	NO. OF READINGS	MIN. Ro (%)	MAX. Ro (%)	MEAN Ro (%)	STD. DEV. (%)	REMARKS
(1)	28	1.20	1.59	1.45	0.118	MATURE
(2)	38	1.68	2.00	1.82	0.062	VERY MATURE
(3)	16	2.70	3.30	3.04	0.179	SEVERELY ALTERED

TOTAL MEAN Ro (%) = 1.93

LOCATION: 34 SAMPLE: MR-3

(NO. OF READINGS = 59)			0.84	1.12	1.13	1.13	1.13	1.13	1.13	1.14	1.14	1.15	1.16	1.21	1.21	1.24	
1.25	1.30	1.31	1.33	1.33	1.33	1.35	1.35	1.41	1.42	1.43	1.43	1.43	1.43	1.43	1.44	1.44	1.47
1.49	2.10	2.20	2.20	2.20	2.20	2.30	2.30	2.30	2.30	2.30	2.30	2.40	2.40	2.40	2.40	2.40	2.40
2.50	2.50	2.50	2.60	2.60	3.00	3.10	3.10	3.20									

POPULATION	NO. OF READINGS	MIN. Ro (%)	MAX. Ro (%)	MEAN Ro (%)	STD. DEV. (%)	REMARKS
(1)	1	0.84	0.84	0.84	-	MATURE
(2)	14	1.12	1.25	1.16	0.045	MATURE
(3)	18	1.30	1.49	1.40	0.059	MATURE
(4)	26	2.10	3.20	2.47	0.302	VERY MATURE

TOTAL MEAN Ro (%) = 1.80

LOCATION: 22 SAMPLE: CGU-2

(NO. OF READINGS = 46) 0.23 0.57 0.57 0.60 0.75 1.01 1.02 1.02 1.02 1.04 1.08 1.09 1.09 1.09
1.10 1.11 1.11 1.11 1.11 1.12 1.12 1.12 1.12 1.12 1.12 1.12 1.12 1.12 1.13 1.13 1.13 1.13
1.14 1.15 1.15 1.15 1.16 1.18 1.20 1.31 1.46 1.49 1.49 1.64 2.10 2.10

POPULATION	NO. OF READINGS	MIN. Ro (%)	MAX. Ro (%)	MEAN Ro (%)	STD. DEV. (%)	REMARKS
(1)	1	0.23	0.23	0.23	-	IMMATURE
(2)	4	0.57	0.75	0.62	0.086	MOD. IMMATURE
(3)	34	1.01	1.20	1.11	0.044	MATURE
(4)	4	1.31	1.49	1.44	0.086	MATURE
(5)	3	1.64	2.10	1.95	0.266	VERY MATURE

TOTAL MEAN Ro (%) = 1.13

LOCATION: 25 SAMPLE: MR-4(25)

(NO. OF READINGS = 29) 0.50 0.53 0.58 0.59 0.61 0.61 0.61 0.63 0.73 0.74 0.74 0.74 0.76 0.80
0.81 0.90 0.91 0.91 0.91 0.91 0.92 1.09 1.23 1.23 1.24 1.65 1.65 1.76 1.97

POPULATION	NO. OF READINGS	MIN. Ro (%)	MAX. Ro (%)	MEAN Ro (%)	STD. DEV. (%)	REMARKS
(1)	2	0.50	0.53	0.52	-	MOD. IMMATURE
(2)	12	0.58	0.80	0.68	0.079	MOD. MATURE
(3)	7	0.81	0.92	0.90	0.038	MATURE
(4)	5	1.09	1.65	1.29	0.212	MATURE
(5)	3	1.65	1.97	1.79	0.163	VERY MATURE

TOTAL MEAN Ro (%) = 0.94

FLUID-INCLUSION DATA:

LOCATION: 22

SAMPLE NUMBER.: CGU-1, CGU-2, CGU-2A. Measured in the vein-calcite.

Inclusion shape	*Inclusion size (μm)	Bubble diameter (μm)	Th (°C)	Tm (°C)
Rectangular	3,2.5	0.7	135.6	
Irregular	----	---	112	
Rectangular	5,1.5	1.0	142	
Irregular	----	----	136	
Elliptical	6,3	1.0	118.5	
Square	3.5	0.8	146	
Elliptical	6,3.5	1.0	168	
Elliptical	6.5,4	1.2	118	
Rectangular	6,2	0.7	177	
Circular	3.0	0.8	171	
Elliptical	3.5,2.5	0.7	180.6	
Elliptical	8,4	1.5	184	

* (Longest, shortest axes) for elliptical inclusions. (Length of two sides) for rectangular inclusions. (Length of a side) for square inclusions. (Diameter) for circular inclusions.

ISOTOPE DATA: CGU-2: $\delta^{18}O$ = -7.8‰ PDB, $\delta^{13}C$ = +3.4‰ PDB

REFERENCES

Allen, M.B., Windley, B.F., Chi, Z., Zhong-Yan, Z., and Guang- Rei, W., 1991, Basin evolution within and adjacent to the Tien Shan Range, NW China: J.Geol. Soc. Lond., v. 148, p.369-378.

Anderson, G.M., 1975, Precipitation of Mississippi Valley-type ores: Econ. Geol., v.70, p.937-942.

_____ and Macqueen, R.W., 1982, Ore deposit model - 6. Mississippi Valley-type lead zinc deposits: Geoscience Canada, v.9, p.108-117.

Anderson, T.F. and Arthur, M.A., 1983, Stable isotopes of oxygen and carbon and their application to sedimentologic and paleoenvironmental problems, p.1-11 --1-151, in Arthur. M.A., Anderson, T. F., Kaplan, I. R, Veizer, J. and Land, L. S. (eds.) Stable Isotopes in Sedimentary Geology: Soc. Econ. Paleon. Mineralogists Short Course no. 10, 436p.

Ando, C.J., Cook, F.A., Oliver, J.E., Brown, L.D. and Kaufman, S., 1983, Crustal geometry of the Appalachian orogen from seismic reflection studies, p.83-102, in Hatcher, R.D.Jr., Williams, H. and Zietz, I. (eds.) Contribution to the Tectonics and Geophysics of Mountain Chains: Geol. Soc. Amer. Memoir 158, 223p.

Arthur, M.A., Anderson, T.F., Kaplan, I.R., Veizer, J. and Land, L.S., 1983, Stable Isotopes in Sedimentary Geology: Soc. Econ. Paleon. Mineralogists Short Course no. 13, 436p.

Aulstead, K.L. and Spencer, R.J., 1985, Diagenesis of the Keg River Formation, northwestern Alberta: Fluid inclusion evidence: Bull. Can. Petrol. Geol., V. 33(2), p.167-183.

Barker, Ch.E., 1983, Influence of time on metamorphism of sedimentary organic matter in liquid-dominated geothermal systems, western North America: Geology, v.11, p.384-388.

_____, 1988, Temperature and time i n thermal maturation of sedimentary organic matter, in Naeser, N.D. and McCulloh, T.H. (eds.), Thermal History of Sedimentary Basins, p.73-98. Springer-Verlag, New York.

---------- and Goldstein, R.H., 1990, Fluid-inclusion technique for determining maximum temperature in calcite and its comparison to the vitrinite reflectance geothermometer: Geology, v.18, p.1103-1106.

---------- and Halley, R.B., 1986, Fluid inclusion, stable isotope, and vitrinite reflectance evidence for the thermal history of the Bone Spring Limestone, southern Guadalupe Mountains, Texas: in Gautier, D.L. (ed.), Roles of Organic Matter in Sediment Diagenesis: Soc. Econ. Paleon. Mineral. Spec. Pub. 38, p.189-203.

_____ and Pawlewicz, M.J., 1986, The correlation of vitrinite reflectance with maximum temperature in organic matter, in Buntebarth, G. and Stegena, L. (eds.) Paleogeothermics, lecture notes in earth sciences, V.5, Springer-Verlag, Berlin, p.79-93.

Basu, R.A., Rubury, E., Mehnert, H. and Tatsumoto, M., 1984, Sm-Nd, K-Ar, and petrologic study of some kimberlites from the eastern United States and their implications for mantle evolution: Contr. Mineral. Petrology, v.86, p.35-44.

Beales, F.W., 1975, Precipitation mechanism for Mississippi Valley-type ore deposits: Econ. Geol., v.70, p.943-948.

Beaumont, C., Quinlan, G.M. and Hamilton, J., 1987, The Alleghenian Orogeny and its relationship to the evolution of the Eastern Interior, North America: Can. Soc. Pet. Geol. Mem. 12, p.425-445.

Bedard, J.H., 1985, The opening of the Atlantic, the Mesozoic New England Province, and mechanism of continental breakup: Tectonophysics, v.113, p.209-232.

Bethke, C.M., 1986, Hydrologic constraints on the genesis of the Upper Mississippi Valley district from Illinois Basin brines: Econ. Geol., v.81, p.33-249.

Bird, J.M., 1969, Middle Ordovician gravity sliding, Taconic region, in, Kay, G.M. (ed.), North Atlantic Geology and Continental Drift: Amer. Assoc. Petrol. Geol. Mem. 12, p.670-686.

_____ and Dewey, J.F., 1970, Lithosphere plate-continental margin tectonics and evolution of the Appalachian orogen: Geol. Soc. Amer. Bull., v.81, p.1031-1060.

Bodnar, R.J., 1983, A method of calculating fluid inclusion volumes based on vapor bubble diameters and P-V-T-X properties of inclusion fluids: Econ. Geol., v.78, p.535- 542.

_____ and Bethke, P.M., 1984, Systematics of stretching of fluid inclusions I: fluorite and sphalerite at 1 atmosphere confining pressure: Econ. Geol. v.79, p.141-161.

Boles, J.R. and Franks, S.G., 1979, Clay diagenesis in Wilcox Sandstones of southwest Texas: J. Sed. Pet., v.49, p.55- 70.

Borak, B. and Friedman, G.M., 1981, Textures of sandstones and carbonate rocks in the world's deepest wells: Anadarko Basin, Oklahoma: Sed. Geol., v.29, p.133-151.

Bosworth, W., Rowley, D.B., Kidd, W.S.F. and Steinhardt, C., 1988, Geometry and style of post-obduction thrusting in a Paleozoic orogen: the Taconic frontal thrust system: J. Geology, v.96, p.163-180.

Bottinga, Y., 1968, Calculation of fractionation factors for carbon and oxygen exchange in a system calcite-carbon dioxide-water: J. Chem. Phys., v.72, p.800-808.

Brett, C.E., 1982, Stratigraphy and facies variation of the Rochester Shale (Silurian: Clinton

Group) along Niagara Gorge, p.217-246, in Buehler, E.J. and Calkin, P.E. (eds.) Geology of the Northern Appalachian Basin, Western New York: Field trip guidebook, NY State Geol. Assoc. 54th annl. meetg., 385p.

Briggs, N.D., Naeser, C.W. and MacCulloch, T.H., 1981, Thermal history of sedimentary basins by fission track dating: Nuclear Tracks, v.5, p.235-237.

Brockerhoff, F.G. and Friedman, G.M., 1987, Paleo-depths of burial of Middle Ordovician carbonates in New York state and Vermont: Northeastern Geol., v.9, p.51-58.

Brookfield, M., 1982, Glacio-eustatic sedimentary cycles in Trenton Limestone (Middle Ordovician) of southern Ontario: Amer. Assoc. Petrol. Geol. Bull., v. 66, p.1165.

Broughton, J.G., Fisher, D.W. Isachsen, Y.W. and Rickard, L.V., 1966, Geology of New York, a short account: Educational Leaflet, NY State Museum and Sci. Serv., 20, 45p.

Buchan, K.L. and Schwarz, E.J., 1987, Determination of maximum temperature profile across dyke contacts using remanent magnetization, and its applications, p.221-220, in Halls, H.C. and Fahrig, W.F. (eds.) Mafic Dyke Swarms, Geol. Assoc. Can. Spec. pap. 34, 503p.

Burke, K., Kidd, W.S., and Wilson, J.T., 1973; Relative and latitudinal motion of Atlantic hotspots: Nature, v. 245, p.133-137.

Burrus, R.C., 1981, Hydrocarbon fluid inclusions in studies of sedimentary diagenesis, in Hollister,L.S. and Crawford,M.L. (eds.) Short Course in Fluid Inclusions, application to petrology: Toronto, Mineral. Assoc. Canada, p.138-156.

_____ , 1987, Diagenetic paleotemperatures from aqueous fluid inclusions: Re-equilibration of inclusions in carbonate cements by burial heating: Mineral. Magazine, v.51, p.477-481.

_____ , 1988, Paleotemperatures from fluid inclusions: advances in theory and technique, in Naeser, N.D. and McCulloh, T.H. (eds.), Thermal History of Sedimentary Basins, Methods and Case Histories, p.119-131. Springer-Verlag, New York.

Burst, J.F., 1969, Diagenesis of Gulf Coast clay sediments and its possible relation to petroleum migration: Amer. Assoc. Petrol. Geol. Bull., v.53, p.73-93.

Cardott, B.J. and Lambert, M.W., 1985, Thermal maturation by vitrinite reflectance of Woodford Shale , Anadarko Basin, Oklahoma: Amer. Assoc. Petrol. Geol. Bull., v.69, p.1982- 1998.

Castano. J.D. and Sparks, D.M., 1974, Interpretation of vitrinite reflectance measurements in sedimentary rocks and determination of burial history using vitrinite reflectance and authigenic minerals: Geol. Soc. Amer. Spec. Pap. 153, p.31-52.

Cathles, L.M. and Smith, A.T., 1983, Thermal constraints on the formation of Mississippi Valley-type lead-zinc deposits and their implications for episodic basin dewatering and

deposit genesis: Econ. Geol., v.78, p.983-1002.

Challapalli, R. S., 1990, Depositional environments and diagenetic imprints of the Lockport Group of New York: Unpub. M.S. thesis, Brooklyn College, 60p.

Ciurca, S.J.Jr., 1982, Eurypterids, stratigraphy, Late Silurian -Early Devonian of western New York and Ontario, Canada, p.99-120, in Buehler, E.J. and Calkin, P.E. (eds.) Geology of the Northern Appalachian Basin, Western New York: Field trip guidebook, NY State Geol. Assoc., 54th annl. meetg., 385p.

Clayton, G., 1989, Vitrinite reflectance data from the Kinsale Harbour - Old Head of Kinsale area, southern Ireland, and its bearing on the interpretation of the Munster Basin: Jour. Geol. Soc. Lond., v.146, p.611-616.

Clayton, R.N., Friedman, I., Graf, D.L., Mayeda, T.K. and Shimp, N.F., 1966, The origin of saline formation waters, I. Isotopic composition: J. Geophys. Res., v. 71, p.3869-3882.

Clynne, M.A. and Potter, R.W. II, 1977, Freezing point depression of synthetic brines: Geol. Soc. Amer. Abst. with Programs, 9, p.930.

Colten-Bradley, V.A., 1987, Role of pressure in smectite dehydration-effects on geopressure and smectite-to-illite transformation: Amer. Assoc. Petrol. Geol. Bull., v.72, p.1414-1427.

Connolly, C.A., 1989, Thermal history and diagenesis of the Wilrich Member shale, Spirit River Formation, northwest Alberta: Bull. Can. Petrol. Geol., v.37(2), p.182-197.

Cook, F.A., 1984, Geophysical anomalies along strike of the southern Appalachian piedmont: Tectonics, v.3, p.45-61.

_____, Albough, D.S., Brown, L.D., Kaufman, S., Oliver, J.E., and Hatcher, R.D., 1979, Thin-skinned tectonics in the crystalline southern Appalachian; COCORP seismic reflection profiling of the Blue Ridge and Piedmont: Geology, v.7, p.563-567.

_____, Brown, L.D., Kaufman, S., Oliver, J.E. and Petersen, T.A., 1981, COCORP Seismic profiling of the Appalachian orogen beneath the coastal plains of Georgia: Geol. Soc. Amer. Bull., v.92, p.738-748.

_____, Brown, L.D., Kaufman, S., Oliver, J.E. and Petersen, T.A., 1981, COCORP seismic profiling of the Appalachian orogen beneath the coastal plain of Georgia: Geol. Soc. Amer. Bull., v.92, p.738-748.

COSUNA (Correlation of Stratigraphic Units of North America) Chart Series, 1985, Appalachian Region Set, Catalog no. 692, Amer. Assoc. Petrol. Geol.

Craig, H., 1865, The measurements of oxygen isotope paleotemperatures, in Tongioni,E. (ed.) Stable Isotopes in Oceanographic Studies and Paleotemperatures: Consiglio Nazionale delle Richerche, laboratorio de Geologia Nucleare, Pisa,161-182.

Crawford, M.L., 1981, Phase equilibrium in aqueous fluid inclusions, in Hollister,L.S. and Crawford,M.L. (eds.) Short Course in Fluid Inclusions, application to petrology: Toronto, Mineral. Assoc. Canada, p.75-99.

Crelling, J.C. and Dutcher, R.R., 1980, Principles and Applications of Coal Petrology, Great Lake Sect. Soc. Econ. Paleon. Mineralogists Short Course, no. 8, 127p.

Crough, S.T., 1981, Mesozoic hotspot epeirogeny in eastern North America: Geology, v.9, p.2-6.

Crowley, K.D., Ahern, J.L. and Naeser, C.W., 1985, Origin and epeirogenic history of the Williston Basin: evidence from fission track analysis of apatite: Geology, v.13, p.620-623.

DeBoer, J. and Snider, F.G., 1979, Magnetic and chemical variations of Mesozoic diabase dikes from eastern north America: evidence for a hotspot in the Carolinas? Geol. Soc. Amer. Bull., v.90, p.185-198.

_____, McHone, J.G., Puffer, J.H., Ragland, P.C. and Whittington, D., 1988, Mesozoic and Cenozoic magmatism, p.217-241, in Sheriden, R.E. and Grow, J.A. (eds.) The Geology of North America, Vol. 1-2, The Atlantic Continental Margin, U.S., Geol. Soc. Amer.

Delaney, P.T., 1987, Heat transfer during emplacement and cooling of mafic dykes, p.31-46, in Halls, H.C. and Fahrig, W.F. (eds.) Mafic Dyke Swarms, Geol. Assoc. Can. Spec. Pap. 34, 503p.

Dennison, J.M., 1983, Comment on 'Tectonic model for kimberlite emplacement in the Appalachian Plateau of Pennsylvania': Geology, v.11, p.252-253.

Dickson, J.A.D. and Coleman, M.L., 1980, Changes in carbon and oxygen composition during limestone diagenesis: Sedimentology, v.27, p.1-12.

Dickinson, S.L. and Seely, D.R., 1979, Structure and stratigraphy of forearc regions: Amer. Assoc. Petrol. Geol. Bull., v.63, p.2-31.

Doborck, S.L., 1987, Petrography, geochemistry and origin of burial diagenetic facies, Siluro-Devonian Helderberg Group (carbonate rocks), Central Appalachians: Amer. Assoc. Petrol Geol. Bull., v.71, p.492-514.

Dodd, J.R. and Stanton, R.J.Jr., 1981, Paleoecology, Concepts and Applications: Wiley Interscience, NY, 559p.

Doherty, J.T. and Lyons, J.B., 1980, Mesozoic erosion rates in northern New England: Geol. Soc. Amer. Bull., v.91, p.16-20.

Donaldson, A.C. and Schumaker, R.C., 1981, Late Paleozoic molasse of central Appalachian, in Miall, A.D. (ed.), Sedimentation and Tectonics in Alluvial Basins: Geol. Assoc. Can. Spec. Pap. 23, p.99-124.

Dow, W.G. and O'Connor, D.I., 1982, Kerogen maturity and type by reflected light microscopy applied to petroleum exploration: How to Asses Maturation and Paleotemperatures, Soc. Econ. Paleon. Mineralogists Short Course, No. 7, p.133- 158.

Duba, D. and William-Jones, A.E., 1983, The application of illite crystallinity, organic matter reflectance and isotopic techniques to mineral exploration: a case study in southwestern Gaspe, Quebec: Econ. Geol., v.78, p.1350-1363.

Duddy, I.R., Gleadow, A.J.W., Green, P.F., Hegarty, K.A., Marshallsea, S.A., Tingate, P.R., and Lovering, J.F., 1987, Quantitative estimates of thermal history and maturation using AFTA (Apatite Fission Track Analysis) in extensional and foreland basins - selected case studies: Amer. Assoc. Petrol. Geol. Bull., v.71, p.550-551.

Dunoyyer de Segonzac, G., 1970, The transformation of clay minerals during diagenesis and low grade metamorphism: A review: Sedimentology, v.15, p.281-346.

Eberl, D., 1978, The reaction of montmorillonite to mixed-layer clay: the effect of interlayer alkali and alkaline earth cations: Geochim. Cosmochim. Acta, v.42, p.1-7

Edmunds, W.E., Berg, T.M., Sevon, W.D., Piotrowski, R.C., Heyman, L. and Rickard, L.V., 1979, The Mississippian and Pennsylvanian systems in the United States - Pennsylvania and New York: U.S. Geol. Surv. Prof. Paper 1110-B, 33p.

England, P. and Molnar, P., 1990, Surface uplift, uplift of rocks, and exhumation of rocks: Geology, v.18, p.1173-1177.

Engelder, T., 1985, Loading paths to joint propagation during a tectonic cycle: an example from the Appalachian Plateau, U.S.A.: J. Struc. Geol., v.7, p.459-476.

_____ and Engelder, R., 1977, Fossil distortion and decollement tectonics on the Appalachian Plateau: Geology, v.5, p.457-460.

_____ and Geiser, P.A., 1979, The relationship between pencil cleavage and lateral shortening within the Devonian section of the Appalachian plateau, New York: Geology, v.5, p.460-464.

_____ and _____, 1980, On the use of regional joint sets as trajectories of paleostress fields during the development of the Appalachian Plateau, New York: J. Geophys. Res., v.85, p.6319-6341.

_____ and Oertel, G., 1985, Correlation between abnormal pore pressure and tectonic jointing in the Devonian Catskill Delta: Geology, v.13, p.863-866.

Epstein, A.G., Epstein, J.B. and Harris, L.D., 1977, Conodont color alteration - an index to organic metamorphism: US Geol. Surv. Prof. Pap. 995, 27p.

Epstein, J.B. and Lyttle, P.T., 1987, Structure and stratigraphy above, below and within the

Taconic unconformity, southeastern New York: Field trip guidebook, NY State Geol. Assoc., 59th ann. meetg., p.C1-C78.

Epstein, S., Lowenstam, H.A. and Urey, H.C., 1953, Revised carbonate water isotopic scale: Geol. Soc. Amer. Bull., v.2, p.417-425.

Eslinger, E. and Pevear, D., 1988, Clay Mineralogy for Petroleum Geologists and Engineers: Soc. Econ. Paleon. Mineralogists Short Course Notes, no. 22, 415p.

Ettensohn, F.R., 1985a, The Catskill delta complex and the Acadian Orogeny: a model, p.39-50, in Woodrow, D.L. and Sevon, W.D. (eds.), The Catskill Delta, Geol. Soc. Amer. Spec. Pap. 201, 246p.

_____, 1985b, Controls on development of Catskill delta complex basin-facies, p.65-78, in Woodrow, D.L. and Sevon, W.D. (eds.), The Catskill Delta, Geol. Soc. Amer. Spec. Pap. 201. 246p.

Faill, R.T., 1973, Tectonic development of the Triassic Newark- Gettysburg basin in Pennsylvania: Geol. Soc. Amer. Bull., v.84, p.725-740.

_____, 1985, The Acadian orogeny and the Catskill delta, p.15-38, in Woodrow, D.L. and Sevon, W.D., (eds.) The Catskill Delta, Geol. Soc. Amer. Spec. Pap. 201, 246p.

Fakundiny, R.H., Myers, J.T., Pomeroy, P.W., Pferd, J.W. and Nowak, T.A.Jr., 1978, Structural instability features in the vicinity of the Clarendon-Linden fault system, western New York and Lake Ontario: Advances in Analysis of Geotechnical Instabilities, Univ. Waterloo Press, SM Study No.13, Pap.4, p.121-178.

_____, Cadwell, D.H. and Fleisher,P.J., 1989, Geology of Wine Country of New York: field trip guidebook, Int. Geol. Congress 28th meetg., 64p.

Faure, G., 1977, Principles of Isotope Geology: Wiley, New York, 464p.

Fisher, D.W., 1977, Correlation of the Hadrynian, Cambrian and Ordovician Rocks in New York State: New York State Museum Map and Chart Series No. 25.

_____, Isachsen, Y.W. and Whitney, P.R., 1979, New Mountains from Old Rock: the Adirondacks: NY State Geol. Surv. Educational Leaflet 23, 8p.

Frey, M., Teichmuller, M., Teichmuller, R., Mullins, J., Kunzi, B., Breitschmid, A., Gruner, U., and Schwizer, B., 1980, Very low-grade metamorphism in external parts of the Central Alps: illite crystallinity, coal rank and fluid-inclusion data: Eclogae Geol. Helv., v.73, p.173-203.

Friedman, G.M., 1959, Identification of carbonate minerals by staining methods: J. Sed. Pet., v.29, p.87-97.

_____, 1985, Devonian reefs of New York: Northeastern Geol., v.7 (2), p.65-73.

_____, 1987a, Deep-burial diagenesis: its implication for vertical movements of the crust, uplift of the lithosphere and isostatic unroofing - a review: Sedimen. Geol., v.50, p.67-94.

_____, 1987b, Vertical movement of the crust; case histories from the northern Appalachian Basin: Geology, v.15, p.1130-1133.

----------, 1988a, Comment on "On Orogeny and Epeirogeny in the Study of Phanerozoic and Archean Rocks": Geoscience Canada, v. 15, p.230-231.

----------, 1988b, Episodes of crustal epeirogeny: Appalachian Basin: Abst. with Programs, Geol. Soc. Amer. northeastern sect. ann. meetg., p.

----------, 1989, Case history of deep-burial sulfide mineralization in the northern Appalachian basin: Carbonates and Evaporites, v.4, p.231-241.

---------- and Braun, M., 1975, Shoaling and tidal deposits that accumulated marginal to proto-Atlantic Ocean: The Tribes Hill Formation (Lower Ordovician) of the Mohawk Valley, New York, p.307-314, in Ginsburg, R.N. (ed.) Tidal Deposits, a Casebook of Recent Examples and Fossil Counterpart: Springer-Verlag, New York-Amsterdam-Berlin, 428p.

_____ and Sanders, J.E., 1978, Principles of Sedimentology: John Wiley and Sons, N.Y., 792p.

_____ and _____, 1982, Time-temperature-burial significance of Devonian anthracite implies former great (6.5km) depth of burial of Catskills Mountains, New York: Geology, v.10, p.93-96.

_____ and _____, 1983, Reply on "Time - temperature-burial significance of Devonian anthracite implies former great (~6.5km) depth of burial of Catskill Mountains, New York": Geology, v.11, p.123-124.

_____, _____ and Martini, P., 1982, Excursion 17A: Sedimentary Facies: Products of Sedimentary Environments in a Cross-section of the Classic Appalachian Mountains and Adjoining Appalachian Basin in New York and Ontario: Int. Assoc. Sedimentologists 11th Int. Conf., field excursion guidebook, 274p.

_____ and Shukla, V., 1980, Significance of authigenic quartz cuhedra after sulfates: examples from the Lockport Formation (Middle Silurian) of New York: J. Sed. Pet., v.50, p.1299-1304.

_____ and Sternbach, C.A., 1985, Dolomites formed under deep-burial conditions: Hunton Group carbonate rocks (Upper Ordovician to Lower Devonian) in deep Anadarko Basin of Oklahoma and Texas: Amer. Assoc. Petrol. Geol. Bull., v.69, p.1317 (abst.).

_____, Cataffe, J. and Borak,B., 1984, Deep-burial diagenesis of the Hunton (Late Ordovician to Early Devonian) carbonates in the Anadarko Basin, in Hinds, N.J. (ed.) Limestones of the Mid-continent: Tulsa Geol. Soc. Spec. Pub., p.183-199.

Friedman, I. and O'neil, J.R., 1977, Compilation of stable isotope fractionation factors of geochemical interest, in Fleischer, M. (ed.) Data of Geochemistry, 6th ed., U.S. Geol. Surv. Prof. Paper, 440 KK.

Fritz, P. and Smith, D.G.W., 1970, The isotopic composition of secondary dolomite: Geochim. Cosmochim. Acta, v.34, p.1161- 1173.

Gale, P.E. and Siever, R., 1986, Diagenesis of Middle to Upper Devonian Catskill facies sandstones in southeastern New York: Amer. Assoc. Petrol. Geol. Bull., v.70, p.592-593 (abst.).

Geiser, P. and Engelder, T., 1983, The distribution of layer parallel shortening fabrics in the Appalachian foreland of New York and Pennsylvania: evidence for two non-coaxial phases of the Alleghanian orogeny, p.161- 177, in Hatcher, R.D.Jr., Harold, W. and Zietz, I. (eds.) Contribution to the Tectonics and Geophysics of Mountain Chains: Geol. Soc. Amer. Memoir 158, 223p.

Gerlach, J.B., 1987, Post-Devonian burial history of the New York state Appalachian Basin based on Lopatin modeling of regional vitrinite reflectance trends: Unpub. M.S. thesis, SUNY at Stony Brook, 135p.

Goldstein, R.H., 1986, Reequilibrium of fluid inclusions in low-temperature calcium-carbonate cement: Geology, v.14, p.792-795.

_____, 1988, Cement stratigraphy of Pennsylvanian Holder Formation, Sacramento Mountains, New Mexico: Amer. Assoc. Petrol. Geol., v.72, p.425-438.

Graven, G. and Freeze, A.R., 1984, Theoretical analysis of role of groundwater flow in the genesis of stratabound ore deposits I. Mathematical and numerical model. 2. Quantitative results: Amer. J. Sci., v.284, p.1085-1174.

Gregg, J.M. and Sibley, D.F., 1984, Epigenetic dolomitization and the origin of xenotopic dolomite texture: J. Sed. Pet., v.54, p.908-931.

_____ and Shelton, K.L., 1989, Minor and trace element distributions in the Bonneterre Dolomite (Cambrian), southeast Missouri - evidence for possible multiple basin fluid sources and pathways during lead-zinc mineralization: Geol. Soc. Amer. Bull., v.101, p.221-230.

Gromet, L.P., 1989, Avalonian terranes and Paleozoic tectonism in southeastern New England; constraints and problems, p.193-212, in Dallmeyer, R.D. (ed.) Terranes in the Circum-Pacific Paleozoic Orogens: Geol. Soc. Amer. Spec. pap. 230, 277p.

Gross, M.R. and Engelder, T., 1989, Natural fractures in the Lockport dolomite of western New York state and southern Ontario: a case for Acadian fluid circulation: Abst. with Programs, Geol. Soc. Amer. northeastern sect. ann. meetg., v.21, p.19.

Grossman, E.T. and Ke, T.L., 1981, Aragonite-water isotopic paleotemperature scale based on the benthic foraminifera Hoeglundia elegans: Abst. with Programs, Geol. Soc. Amer. Ann. Meetg, p.464.

Gurney, G.G. and Friedman, G.M., 1987, Burial history of the Devonian Cherry Valley carbonate sequence, Cherry valley, New York: Northeastern Geol., v.9, p.1-11.

Gurrieri, J.T. and Musiker, L.B., 1990, Late Wisconsinan ice margins and recessional events in the north-central Adirondack Mountains, New York: Northeastern Geol., 12, p.185-197

Guthrie, J.M., Houseknecht, D.W. and Johns, W.D., 1986, Relationships among vitrinite reflectance, illite crystallinity, and organic geochemistry of Carboniferous strata, Ouachita Mountains, Oklahoma and Arkansas: Amer. Assoc. Petrol. Geol. Bull., v.70, p.26-33.

Gwinn, V.E., 1964, Thin-skinned tectonics in the Plateau and northwestern Valley and Ridge Provinces of the central Appalachians: Geol. Soc. Amer. Bull., v.75, p.863-900.

Haas, J.L.Jr., 1976, Physical properties of the co-existing phases and the thermo-chemical properties of the H_2O component in boiling NaCl solutions: U.S. Geol. Surv. Bull. 1421-A, 73p.

Hacquebard, P.A., 1977, Rank of coal as an index of metamorphism for oil and gas in Alberta, in The Origin and Migration of Petroleum in the Western Canadian Sedimentary Basin, Alberta: Geol. Surv. Can. Bull., v.262, p.11-22.

Hammel, R.D. and Ciurca, S.J.Jr., 1986, Paleoenvironmental analysis of the Fiddlers Green Formation (Late Silurian) in New York state, p.199-218 : Field trip guidebook, NY State Geol. Assoc., 58th ann. meetg.,

Hanor, J.S., 1987, Origin and Migration of Subsurface Sedimentary Brines: Soc. Econ. Paleon. Mineral. Short Course no. 21, 247p.

Harris, A.,1979, Conodont color alteration: an organo- metamorphic index and its application to Appalachian Basin Geology,in Scholle, P.A. and Schluger, P.R. (eds.) Aspects of Diagenesis: Soc. Econ. Paleont. Mineralogists Spec. Pub.,26, p.3-16.

_____, Harris, L.D. and Epstein,J .B., 1978, Oil and gas data from Paleozoic rocks in the Appalachian Basin: maps for assessing hydrocarbon potential and thermal maturity (conodont color alteration isograds and overburden isopachs): U.S. Geol. Surv. Misc. Invest. Map I-917-E.

Harrison, T.M. and Spear, F.S., 1987, P-T-t paths in central New England; the evolution of a

paired metamorphic belt as revealed by petrologic and isotopic data: Geol. Assoc. Can. - Mineral. Assoc. Can. Abst. with Programs, v.12, p.53.

Harrison, W.E, Luza, K.V., Prater, M.L. and Cheung, P.K., 1983, Geothermal resource assessment in Oklahoma: Oklahoma Geol. Surv. Spec. pub., 83-1, 44p.

Hatcher, R.D.Jr., 1978, Tectonics of the western Piedmont and Blue Ridge, southern Appalachians: review and speculation: Amer. J. Sci., v.278, p.276-304.

_____ and Zietz, I., 1980, Tectonic implications of regional aeromagnetic and gravity data from the southern ones, D.R. (ed.), The Caledonides of the U.S.A.: Blacksburg Appalachians, in, Wones, D.R. (ed.), The Caledonides of the U.S.A., Blacksburg, Virg. Polytech. Inst. and State Univ., Mem. no. 2, p.235-244.

Hearns, P.P. and Sutter, J.F., 1985, Authigenic potassium feldspar in Cambrian carbonates: evidence of Alleghanian brine migration: Science, v.228, p.1529-1531.

Heckel, P.H., 1973, Nature, origin and significance of the Tully Limestone, an anomalous unit in the Catskill Delta, Devonian of New York: Geol. Soc. Amer. Spec. Pap. 138, 244p.

Heroux, Y., Chagnon, A. and Bertrand, R., 1979, Compilation and correlation of major thermal maturation indicators: Amer. Assoc. Petrol. Geol. Bull., v.63, p.2128-2144.

Hinze, W.J., Braile, L.W., Keller, G.R. and Lidiak, E.G., 1980, Models for midcontinent tectonism in (eds.) Studies in Geophysics: Continental Tectonics, Nat. Acad. Science, Washington D.C.

Hiscott, R.N., Pickering, K.T. and Beeden, D.R., 1986, Progressive filling of a confined Middle Ordovician foreland basin associated with Taconic Orogeny, Quebec, Canada in Allen, P.A. and Homewood, P. (eds.) Foreland Basins: Int. Assoc. Sedimentologists Spec. Pub. no. 8, p.309-325.

Hitchon, B., 1984, Geothermal gradients, hydrodynamics, and hydrocarbon occurrences, Alberta, Canada: Amer. Assoc. Petrol. Geol. Bull., v.68, p.713- 743.

_____ and Friedman, I, 1969, Geochemistry and origin of formation waters in the western Canada sedimentary basin I: Stable isotopes of hydrogen and oxygen: Geochim. Cosmochim. Acta, v.33, p.1321-1349.

Hodge, D.S., 1984, Heat flow and subsurface temperature distributions in central and western New York: N.Y. State Energy Research and Development Authority Rep. 84-8.

_____, 1990, Heat flow in New York and implication of epeirogenic uplift: Abst. with Programs, Geol Soc. Amer. northeastern sect., 25th annl. meetg., p.24.

_____, Eckert, R., and Raveta, F., 1982, Geophysical signatures of central and western New York state: NY State Geol. Assoc. 54th Ann. Field Trip Guidebook, p.3-18.

_____, Hifiker, K, Morgan, P. and Swanberg, C.A., 1979, Preliminary geothermal investigations in New York State: Geotherm. Res. Coun. Ann. Meeting.

Hoffman, J. and Hower, J., 1979, Clay mineral assemblages as low grade metamorphic geothermometers - application to the thrust-faulted disturbed belt of Montana, USA, in Scholle, P.A. and Schluger, P.R. (eds.), Aspects of Diagenesis: Soc. Econ. Paleon. Mineral. Spec. Pub. no. 26, p.55-79.

Hollister, L.S., 1981, Techniques for analyzing fluid inclusions in Hollister, L.S. and Crawford, M.L. (eds.) Short Course in Fluid Inclusions: application to petrology: Toronto, Mineral. Assoc. Canada, p.272-277.

_____, L.S. and Crawford, M.L. (eds.), 1981, Short Course in Fluid Inclusions: application to petrology: Toronto, Mineral. Assoc. Can.,75-99.

Hood, A., Gutjahr, C.C.M. and Heacock, R.L., 1975, Organic metamorphism and the generation of petroleum: Amer. Assoc. Petrol. Geol. Bull., v.59, p.986-996.

Houseknecht, D.W. and Matthews, S.M., 1985, Thermal maturity of Carboniferous strata, Ouachita Mountains: Amer. Assoc. Petrol. Geol. Bull., v.69, p.335-345.

Hower, J., Eslinger, E., Hower, M.E., Perry, E.A., 1976, Mechanism of burial metamorphism of argillaceous sediments: I. Mineralogical and chemical evidence: Geol. Soc. Amer. Bull., v.87, p.725-737.

Hower, J.C. and Davis, A., 1981, Application of vitrinite reflectance anisotropy in the evaluation of coal metamorphism: Geol. Soc. Amer. Bull., v.92, p.350-366.

Inoue, A., Kohyama, N., Kitagawa, R., and Watanabe, T., 1987, Chemical and morphological evidence for the conversion of smectite to illite: Clays and Clay Minerals., v.35, p.111-120.

Irwin, M.L., 1965, General theory of epeiric clear water sedimentation: Amer. Assoc. Petrol. Geol. Bull., v.49, p.445-459.

Isachsen, Y.W., 1985, Structural and tectonic studies in New York State: N.Y. State Geol. Surv., prepared for Div. of Radiation Programs and Earth Sciences, Office of Nuclear Regulatory Research, Washington, 74p.

_____, Landing, E., Lauber, J.M., Rickard, L.V., and Rogers, W.B., (eds.), Geology of New York: A Simplified Account: New York State Museum Educational Leaflet 28, 284p.

Issler, D.R., 1984, Calculation of organic maturation levels for offshore Canada - implications for general application of Lopatin's method: Can. J. E. Sci.,v.21, p.477-488.

Jackson, M., McCabe, C., Ballard, M.M. and Van der Voo, R., 1988, Magnetite authigenesis and diagenetic paleotemperatures across the northern Appalachian basin: Geology, v.16,

p.592-595.

Jackson, M.L., 1979, Soil Chemical Analysis -- Advanced Course, 2nd. ed., published by author, Madison, Wisconsisn, 580p.

Jackson, S.A. and Beales, F.W., 1967, An aspect of sedimentary basin evolution: the concentration of Mississippi Valley- type ores during late stages of diagenesis: Bull. Can. Petrol. Geol., v.15, p.383-433.

Jacobi, C.H. and Dellwig, L.F., 1974, Appalachian foreland thrusting in Salina salt, Watkins Glen, New York, in Coogen, A.H. (ed.), Fourth Symposium on Salt, Northern Ohio Geol. Soc., Cleavland, p.227-233.

Jacobi, R.D., 1981, Peripheral bulge - a causal mechanism for the Lower/Middle Ordovician unconformity along the western margin of the Northern Appalachians: Earth and Planet. Sci. Letters, v.56, p.245-251.

Johnson, K.G. and Friedman, G.M., 1969, The Tully clastic correlatives (Upper Devonian) of New York State: A model for recognition of alluvial, dune(?), tidal, nearshore (bar and lagoon), and offshore environments in a tectonic delta complex: J. Sed. Pet., v.39, p.451-485.

Johnsson, M., 1985, Late Paleozoic - middle Mesozoic uplift rate, cooling rate and geothermal gradient for south-central New York state: Nuclear Tracks, v.10, p.295-301.

_____, 1986, Distribution of maximum burial temperatures across the northern Appalachian Basin and implication for Carboniferous sedimentation patterns: Geology, v.14, p.383- 387.

_____, 1987, Reply on "Distribution of maximum burial temperatures across the northern Appalachian Basin and implication for Carboniferous sedimentation patterns": Geology, v.15, p.279-280.

Jones, R.W. and Edison, T.A., 1978, Microscopic observations of kerogen related to geochemical parameters with emphasis on thermal maturation, in Oltz, D.F. (ed.) Symposium on Geochemistry: Low-temperature Metamorphism of Kerogen and Clay Minerals, Pacific Sect., Soc. Econ. Paleon. Mineralogists, p.1-12.

Jones, P.H. and Wallace Jr., R.H., 1974, Hydrogeologic aspects of structural deformation in the northern Gulf of Mexico Basin: J. Res., U.S. Geol. Surv., v.2, p.511-517.

Kalkreuth, W. and McMechan, M.E., 1984, Regional pattern of thermal maturation as determined from coal-rank studies, Rocky Mountain foothills and front ranges north of Grande Cache, Alberta - implications for petroleum exploration: Bull. Can. Petrol. Geol., v.32, p.249-271.

Karig, D.E., 1987, Comments on "Distribution of maximum burial temperatures across northern Appalachian Basin and its implications for Carboniferous sedimentation patterns": Geology, v.15, p.278-279.

Kaufman, J., Meyers, W.J., and Hanson, G.N., 1990, Burial cementation in the Swan Hills Formation (Devonian), Rosevear Field, Alberta, Canada: J. Sed. Pet., v.60, p.918-939.

Kay, S.M., 1990, Central New York kimberlites - evidence for an early Cretaceous thermal disturbance in the Appalachian basin: Abst. with Programs, Geol. Soc. Amer. northeastern sect. 25th ann. meetg., p.28.

_____ and Foster, B.P., 1986, Kimberlites of the Finger Lakes region: NY State Geol. Assoc. 58th Annl. Meetg. Field Trip Guidebook, p.219-238.

_____, Snedden, W.T., Foster, B.P., and Kay, R.W., 1983, Upper mantle and crustal fragments in the Ithaca kimberlites: J. Geology, v.91, p.277-290.

Kean, B.F. and Strong, D.F., 1975, Geochemical evolution of an Ordovician island arc of the central Newfoundland Appalachians: Amer. Jour. Sci., v.275, p.97-118.

Keith, B. D., 1988, Regional facies of Upper Ordovician series of eastern North America, in Keith, B.D. (ed.) The Trenton Group (Upper Ordovician Series) of Eastern North America - Deposition, Diagenesis, and Petroleum: Amer. Assoc. Petrol. Geol. Studies in Geol. no. 29, p.1-16.

Kent, D.V., 1985, Paleocontinental setting for the Catskill Delta, in Woodrow, D.L and Sevon, W.D. (eds.), The Catskill Delta, Geol. Soc. Amer. Spec. Pap. 201, p. 9-13.

King, G. and Ellis, M., 1990, The origin of large local uplift in extensional region: Nature, v. 348, p.689-692.

Kisch, H.J., 1980, Incipient metamorphism of Cambro-Silurian clastic rocks from the Jamtland Supergroup, central Scandinavia Caledonides, western Sweden: Illite crystallinity and 'vitrinite' reflectance: J. Geol. Soc. London, v.137, p.271-288.

Kissling, D.L. and Coughlin, R.M., 1979, Succession of faunas and frameworks in Middle Devonian pinnacle reefs of south- central New York: Geol. Soc. Amer., N.E. Section, Abst. with Programs, 11, p.19.

Kreidler, W.L., Van Tyne, A.M. and Jorgensen, K.M., 1972, Deep Wells in New York State: N.Y. State Museum and Sci. Serv. Bull. no. 418A, 335p.

Kubler, B., 1967, La cristallinitie de l'illite et les zones tout a fait superieures du metamorphisme: Etage tectoniques, A la Baconniere, Neuchatel (Suisse), p.105-121.

_____, 1968, Evaluation quantitative du metamorphisme par la cristallinite de l'illite; etat des progres realises annees: Bull. Centre due Recherches de Pau, v.2, p.385-397.

Lakatos, S. and Miller, D.S., 1983, Fission-track analysis of apatite and zircon defines a burial depth of 4 to 7km for lowermost Upper Devonian Catskill Mountains, New York: Geology, v.11, p.103-104.

Land, L.S., 1980, The isotopic and trace element geochemistry of dolomite: the state of the art, in Zenger, D.H., Dunham, J.B., and Ethington, R.L. (eds.) Concepts and Models 6
Dolomitization: Soc. Econ. Paleon. Mineral. Spec. Pub. 28, p.87-110.

_____, 1983, The application of stable isotopes to studies of the origin of dolomite and to problems of diagenesis of clastic sediments, p.4-1--4-22, in Arthur, M.A., Anderson, T.F., Kaplan, I., Veizer, J., and Land, L.S. (eds.) Stable Isotopes in Sedimentary Geology: Soc. Econ. Paleon. Mineral. Short Course no.10, 436p.

Laporte, L.F., 1967, Carbonate deposition near mean sea-level and resultant facies mosaic, Manlius Formation (Lower Devonian) of New York state: Amer. Assoc. Petrol. Geol. Bull., v.51, p.73-101.

_____, 1969, Recognition of transgressive carbonate sequence within an epeiric sea: Helderberg Group (Lower Devonian) of New York state, p.98-119, in Friedman, G.M. (ed.) Depositional Environments in Carbonate Rocks - A Symposium: Soc. Econ. Paleon. Mineral. Spec. Pub. no. 14, 209p.

Leach, D.L., Nelson, R.C. and Williams, D., 1975, Fluid inclusion studies in the northern Arkansas Zinc District: Econ. Geol., V. 70, p.1084-1091.

Lee, Y. Il, and Friedman, G,M., 1987, Deep burial dolomitization in the Ordovician Ellenburger Group carbonates, western Texas and south-eastern New Mexico: J. Sed. Pet., v.57, p.544-557.

Levine, J.R., 1983, Comment on "Time-temperature-burial significance of Devonian anthracite implies former great (~6.5km) depth of burial of Catskill Mountains, New York": Geology, v.11, p.122-123.

_____, 1986, Deep burial of coal bearing strata, Anthracite region, Pennsylvania: sedimentation or tectonics: Geology, v.14, p.577-580.

Lindeman, R.H., 1979, Stratigraphy and depositional history of the Onondaga Limestone in eastern New York, in Friedman, G.M. (ed.) N.Y. State Geol. Assoc. Guidebook, 51st Ann. Mtg., Troy, p.351-387.

Lopatin, N.V., 1971, Temperature and geologic time as factors in coalification: Akademiya Nauk SSSR Izvestiya, Seriya Geologicheskaya, no. 3, p.95-106.

Machel, H., 1987, Saddle dolomite as a by-product of chemical compaction and thermochemical sulfate reduction: Geology, v.15, p.939-940.

_____ and Mountjoy, E.W., 1986, Chemistry and environments of dolomitization - A reappraisal: E. Sci. Review, v.23, p.175-222.

Majorowicz, J.A., Rahman, M., Jones, F.W. and McMilan, N.J., 1985, The paleogeothermal and

present thermal regimes of the Alberta Basin and their significance for petroleum occurrence: Bull. Can. Petrol. Geol., v.33, p.12-21.

Maliva, R.G. and Siever, R., 1988, Mechanism and controls of silicification of fossils in limestones: J. Geology, v. 96, p.387-398.

Mangas, J. and Arribas, A., 1988, Hydrothermal fluid evolution of the Sn - W mineralization in the Parrilla ore deposit (Caceres, Spain): J. Geol. Soc. Lond., v. 145, p.147-155.

Manspeizer, W., 1985, Early Mesozoic history of the Atlantic passive margin, in Poag. C.W. (ed.) Geologic Evolution of the United States Atlantic Margin, Van Nostrand Reinhold Co. Inc., p.1-23.

_____ and Cousminer, H.L., 1988, Late Triassic - Early Jurassic synrift basins of the U.S. Atlantic margin, in Sheridan, R.E. and Grow, J.A. (eds.) The Geology of North America, Vol. 1-2, The Atlantic Continental Margin, U.S.: Geol. Soc. Amer., p.197-216.

Marshak, S., 1986, Structure and tectonics of the Hudson Valley fold-thrust belt, eastern New York State: Geol. Soc. Amer. Bull., v.97, p.354-368.

Mathews, W.H., 1975, Cenozoic erosion and erosion surfaces of eastern North America: Amer. J. Sci., v.275, p.818-824.

Mattes, B.W. and Mountjoy, E.W., 1980, Burial dolomitization of the Upper Devonian Miette buildup, Jasper National Park, Alberta, in Zenger et al (eds.) Concepts and Models of Dolomitization: Soc. Econ. Paleont. Mineralogists Spec. Pub., v.28, p.259-297.

McClelland-Brown, E., 1981, Paleomagnetic estimates of temperatures reached in contact metamorphism: Geology, v.9, p.112-116.

McGetchin, T.R., Burke, K.G., Thompson, G.A., and Young, R.A., 1980 , Mode and Mechanisms of plateau uplift, in Baly, A.W., Bender, P.L., McGetchin, T.R., and Walcott, R.I. (eds.) Dynamics of Plate Interiors: Amer. Geophys. Union, Geol. Soc. Amer. Geodynamic Series, v.1, p.99-110.

McKenzie, D., 1981, The variation of temperature with time and hydrocarbon maturation in sedimentary basins formed by extension: E. Planet. Sci. Letters, v.55, p.87-98.

McLimans, R. K. and Videtich, P.E., 1989, Diagenesis and burial history of Great Oolite Limestonee, southern England: Amer. Assoc. Petrol. Geol. Bull., v.73(10). p.1195-1205

Meckel, L.D., 1970, Paleozoic alluvial deposition in central Appalachians: a summary in Fisher et al. (eds.) Studies of Appalachian Geology, Central and Southern: New York Interscience, p.49-67.

Mehrtens, C.J., 1988, Bioclastic turbidites in the Trenton Limestones: significance and criteria for recognition, in Keith, B.D. (ed.) The Trenton Group (Upper Ordovician Series) of Eastern

North America - Deposition, Diagenesis and Petroleum: Amer. Assoc. Petrol. Geol. Studies in Geol. no.29, p.139-158.

Mesolella, K.J., 1978, Paleogeography of some Silurian and Devonian reef trends, central Appalachian Basin: Amer. Assoc. Petrol. Geol. Bull., v.53, p.1035-1042.

Meyers, W.J. and Lohman, K.C., 1985, Isotopic geochemistry of regionally extensive calcite cement zones and marine components in Mississippian limestones, New Mexico, in Schneiderman, N. and Harris, P. (eds.) Carbonate Cements: Soc. Econ. Paleont. Mineralogists Spec. Pub., 36, p.223-239.

Miller, D.S., 1990, Geothermometry of NY Upper Devonian sediments based on fission track analysis of apatite and zircon: Abst. with Programs, Geol. Soc. Amer. northeastern sect., 25th annl. meetg., p.57.

_____ and Duddy, I.R., 1986, Burial and uplift history of northern Appalachian basin: Apatite and zircon fission- track chronology: Abst. with Programs, Geol. Soc. Amer. northeastern sect. annl. meetg., p.55.

_____ and _____, 1989, Early Cretaceous uplift and erosion of the northern Appalachian Basin, New York, based on apatite fission track analysis: E. Planet. Sci. Letters, v.93, p.35-49.

_____ and Lakatos, S., 1983, Uplift rate of Adirondack anorthosite measured by fission-track analysis of apatite: Geology, v.11, p.284-286.

Miller, J.D. and Kent, D.V., 1988, Regional trends in the timing of Alleghanian remagnetization in the Appalachians: Geology, v.16, p.588-591.

_____ and _____, 1989, Paleomagnetism of selected Devonian age plutons from Maine, Vermont, and New York: Northeastern Geol., v.11, p.66-76.

Morgan, W.J., 1981, Hotspot tracks and the opening of the Atlantic and Indian oceans, in Emilian, C. (ed.), The Sea, Vol. 7, The Oceanic Lithosphere, John Wiley, NY, p.443- 487.

Moore, C.H., 1985, Upper Jurassic subsurface cements: a case history, p. 291-308, in Schneidermann, H. and Harris, P.M. (eds.) Carbonate Cements: Soc. Econ. Paleon. Mineral. Spec. Pub. 36, 379p.

_____ and Druckman, Y., 1981, Burial diagenesis and porosity evaluation, Upper Jurassic Smackover, Arkansas and Louisiana: Amer. Assoc. Petrol. Geol. Bull., v.65, p.597- 628.

Moore, D.M. and Reynolds, R.C.Jr., 1989, X-ray Diffraction and the Identification and Analysis of Clay Minerals: Oxford Univ. Press, Oxford, New York, 332p.

Morgan, W.J., 1980, Hotspot tracks and opening of the Atlantic and Indian Oceans, in Emiliani. C. (ed.) The Oceanic Lithosphere; The Sea: John Wiley and Sons, N.Y., v.7, p.443- 487.

Mose, D.G., Ratcliffe, N.M., Odom, A.L., and Hayes, J., 1976, Rb-Sr geochronology and tectonic setting of the Peekskill pluton, southeastern New York: Geol. Soc. Amer. Bull., v.87, p.361-365.

Murray, R,C., 1964, Origin and diagenesis of gypsum and anhydrite: J. Sed. Pet., v.34, p.512-523.

Nadeau, P.H., Wilson, M.J., McHardy, W.J., and Tait, J.M., 1984, Interparticle diffraction: a new concept for interstratified clays: Clays and Clay Minerals, v. 19, p.757-769.

Nahnybida, C., Hutcheon, I. and Kirker, J., 1982, Diagenesis of Nisku Formation and the origin of late-stage cements: Can. Mineralogist, V. 20, p.129-140.

Neugebauer, H.J., 1987, Models of lithospheric thinning: Ann. Rev. E. Planet. Sci., v.15, p.421-443.

Northrop, D.H. and Clayton, R.N., 1966, Oxygen isotope fractionation in systems containing dolomite: J. Geology, v.74, p.174-196.

Nurkowski, J.R., 1984, Coal quality, coal rank variation and its relation to reconstructed overburden, Upper Cretaceous and Tertiary Plains coals, Alberta, Canada: Amer. Assoc. Petrol. Geol. Bull., v.68, p.285-295.

Oliver, J., 1986, Fluids expelled tectonically from orogenic belts: their role in hydrocarbon migration and other geologic phenomena: Geology, v.14, p.99-102.

Oliver, W.A., 1954, Stratigraphy of the Onondaga Limestone (Devonian) in central New York: Geol. Soc. Amer. Bull., v.65, p.621-652.

_____, 1956, Biostromes and bioherms of the Onondaga Limestone in eastern New York: N.Y. State Mus. and Sci. Serv., Circular 45, 23p.

_____,1976, Noncystimorph colonial rugose corals of the Onesquethaw and Lower Cazenovia Stages (Lower and Middle Devonian) in New York and adjacent areas: U.S. Geol. Survey Prof. Pap. No. 869, 156p.

Olsen, P.E., McCune, A.R., and Thompson, K.S., 1982, Correlation of early Mesozoic Newark Supergroup (eastern North America) by vertebrates, especially fishes: Amer. J. Sci., v. 282, p.1-44.

O'neil , J.R. and Epstein, S., 1966, Oxygen isotope fractionation in system dolomite-calcite-carbon dioxide: Science, v.152, p.198-201.

Osberg, P.H., 1988, Silurian to Lower Carboniferous tectonism in the Appalachians of the USA, in Harris, A.L. and Fettes, D.J. (eds.), The Caledonian - Appalachian Orogen: Geol. Soc. Spec. Pub., no.38, p.449-452.

Owen, R.W. and Friedman, G.M., 1984, Late Cambrian algal deposition in the Hoyt Limestone,

eastern New York state: Northeastern Geol., v.6, p.222-237.

Pelletier, B.R., 1958, Pocono paleocurrents in Pennsylvania and Maryland: Geol. Soc. Amer. Bull., v.69, p.1033-1064.

Perry, E.A. and Hower, J., 1970, Burial diagenesis in Gulf Coast pelitic sediments: Clays and Clay Min., v. 18, p.165- 177.

Perry, W.J.,Jr., 1978, Sequential deformation in the central Appalachians: Amer. J. sci., v.278, p.518-542.

Pevear, D.R., Williams, V.E., and Mustoe, G.E., 1980, Kaolinite, smectite, and K-rectorite in bentonites: relation to coal rank at Tulameen, British Columbia: Clays and Clay Minerals, v. 28, p.241-254.

Phillips, T.L. and Peppers, R.A., 1984, Changing patterns of Pennsylvania coal-swamp vegetation and implication of climatic control on coal occurrence: Internat. J. Coal Geol., v.3, p.205-255.

Pollastro, R.M. and Barker, Ch. E., 1986, Application of clay- mineral, vitrinite reflectance, and fluid inclusion studies to the thermal burial history of the Pinedale Anticline, Green River Basin, Wyoming, in Gautier, D.L. (ed.) Roles of Organic Matter in Sediment Diagenesis, Soc. Econ. Paleon. Mineralogists Spec. Pub. no. 38, p.73-84.

Potter, R.W.II, 1977, Pressure corrections for fluid inclusion homogenization temperatures based on volumetric properties of system NaCl-H_2O: Jour. Res., U.S. Geol. Surv., 5, p.603- 607.

_____ and Brown, D.L., 1975, The volumetric properties of aqueous sodium chloride solutions from 0 to 500 C at pressures up to 200 bars based on regression of the available literature data: U.S. Geol. Surv. Open-file Rept. 75-636, 31p.

---------- and ----------, 1976, The volumetric properties of vapor saturated aqueous potassium chloride solutions from 0 to 400 based on a regression of the available literature data: U.S. Geol. Surv. Open-file Rept. 76-243, 6p.

_____ and Clynne, M.A., 1978, Pressure corrections for fluid inclusion homogenization temperatures: Abst. with Programs, Int. Assoc., Genesis Ore Deposits Symp., Alta, Utah, p.146.

_____, Clynne, M.A. and Brown, D.L., 1978, Freezing point depression of aqueous sodium chloride solutions: Econ. Geol., v.73, p.284-285.

Poty, B. and Pagel, M., 1988, Fluid inclusions related to uranium deposits: a review: J. Geol. Soc. Lond., V. 145, p.157-162.

Prezbindowski, D.R., 1985, Burial cementation - is it important? A case study, Stuart city Trend, south central Texas, p.241-264, in Schneidermann, N. and Harris, P.M. (eds.) Carbonate

Cements: Soc. Econ. Paleon. Mineral. Spec. Pub. 36, 379p.

---------- and Larese, R.E., 1987, Experimental stretching of fluid inclusions in calcite - implication for diagenetic studies: Geology, v.15, p.333-336.

Price, L.C., 1983, Geologic time as a parameter in organic metamorphism and vitrinite reflectance as an absolute paleogeothermometer: J. Petrol. Geol., v.6, p.5-38.

Price, R.A. and Hatcher, R.D.Jr., 1983, Tectonic significance of similarities in the evolution of the Alabama - Pennsylvania Appalachians and the Alberta - British Columbia Canadian Cordillera in Hatcher, R.D.Jr., Williams, H. and Zietz, I. (eds.) Contributions to the Tectonics and Geophysics of Mountain Chains: Geol. Soc. Amer. Memoir, 158. p.149-160.

Quinlan, G.M. and Beaumont, C., 1984, Appalachian thrusting, lithospheric flexure, and the Paleozoic stratigraphy of the eastern interior of North America: Can. J. Earth. Sci., v.21, p.973-996.

Radke, B.M. and Mathis, R.L., 1980, On the formation and occurrence of saddle dolomite: J. Sed. Pet., v.50, p.1149- 1168.

Ramsayer, K. and Boles, J.R., 1986, Mixed-layer illite/smectite minerals in Tertiary sandstones and shales, San Joaquin Basin, California: Clays and Clay Minerals, v.34, p.115-124.

Reitan, P.H., Szekely, J. and Foster, B.P., 1970, Material emplacement models for dikes extending to the mantle: Trans. Amer. Geophys. Union (EOS), v.51, p.447.

Rickard, L.V., 1973, Stratigraphy and structure of the subsurface Cambrian and Ordovician carbonates of New York: New York State Museum Map and Chart Series no. 18.

----------, 1975, Correlation of Silurian and Devonian rocks in New York State: New York State Museum Map and Chart Series no. 24.

_____, 1981, The Devonian System of New York state, in Oliver, W.A. and Klapper, G. (eds.), Devonian Biostratigraphy of New York: Washington D.C., Meeting of Subcommission on Devonian Stratigraphy, p.5-22.

_____ and Fisher, D.W., 1970, Geologic Map of New York, Niagara Sheet, NY State Museum and Sci. Serv. no. 15.

Roberson, H.E. and Lahann, R.W., 1981, Smectite to illite conversion rates, effects of solution chemistry: Clays and Clay Minerals, v.29, p.129-135.

Robinson, S., 1825, A catalogue of American minerals with their localities: Boston (private pub.), 316p.

Roden, M.K., 1991, Apatite fission-track thermochronology of the southern Appalachian basin: Maryland, West Virginia, and Virginia: J. Geology, v.99, p.41-53.

_____, Parrish, R.R., and Miller, D.S., 1990, The absolute age of the Eifelian Tioga Ash Bed, Pennsylvania: J. Geology, v.98, p.282-285.

Rodgers, J., 1967, Chronology of tectonic movements in the Appalachian region of eastern North America: Amer. Jour. Sci., v.265, p.408-427.

_____, 1970, The Tectonics of the Appalachians: Wiley- Interscience, New York, 271p.

_____, 1971, The Taconic orogeny: Geol. Soc. Amer. Bull., v.82, p.1141-1178.

Roedder, E., 1962, Studies of fluid inclusions I: low temperature application of dual-purpose freezing and heating stage: Econ. Geol., v. 57, p.1045-1061.

----------, 1971, Fluid-inclusion evidence on the environment of formation of mineral deposits of the southern Appalachian Valley: Econ. Geol., V.66, p.777-791.

_____, 1972, Composition of fluid inclusions: U.S. Geol. Surv. Prof. Pap. 440JJ, 164p.

_____, 1976, Fluid-inclusion evidence on the genesis of ores in sedimentary and volcanic rocks. in Wolf, K.H. (ed.) Handbook of Stratabound and Stratiform Ore Deposits, Elsevier, Amsterdam, p.67-110.

_____, 1979a, Origin and significance of magmatic inclusions: Mineral. Bull., v.102, p.487-510.

_____, 1979b, Fluid inclusions as samples of ore fluid. in Barnes, H.L. (ed.) Geochemistry of Hydrothermal Ore Deposits, John Wiley, New York, p.684-737.

_____, 1984, Fluid Inclusions. in Ribbe, P.H. (ed.) Reviews in Mineralogy: Mineral. Soc. Am., 12, 644p.

_____ and Bodnar, R.J., 1980, Geologic pressure determinations from fluid inclusion studies: Ann. Rev. Earth Planet. Sci., v.8, p.263-301.

_____ and Coombs, D.S., 1967, Immiscibility in granitic melts, indicated by fluid inclusions in ejected granitic blocks from Ascension Island: J. Petrol., v.8, p.417- 451.

_____ and Howard, K.W., 1988, Taolin Zn-Pb-fluorite deposit, People's Republic of China: an example of some problems in fluid inclusion research on mineral deposits: Jour. Geol. Soc. Lond., v. 145, p.163-174.

_____ and Skinner, B.J., 1968, Experimental evidence that fluid inclusions do not leak: Econ. Geol., v.63, p.715-730.

Rowley, D.B. and Kidd, W.S.F., 1981, Stratigraphic relationships and detrital composition of the medial Ordovician flysch of western New England: implications for the tectonic evolution

of the Taconic Orogeny: J. Geology, v.89, p.199-218.

Ruedemann, R., 1925, The Utica and Lorraine Formations of New York, Part-I: Stratigraphy: N.Y. State Museum Bull., v. 253, 175p.

_____, 1935, The ecology of black mud shales of New York: J. Paleon., v.9, p.79-91.

Saigol, G.C. and Bjorlykke, K., 1987, Carbonate cements in clastic reservoir rocks from offshore Norway - relationships between isotopic composition, textural development and burial depth: in Marshall, J.D. (ed.), Diagenesis of Sedimentary Sequences: Geol. Soc. Spec. Pub. no.36, p.313- 324.

Sanders, J.E., 1963, Late Triassic tectonic history of north- eastern United States: Amer. J. Sci., v.261, p.501-524.

_____, 1974, Guidebook to field trip in Rockland County, New York: Petrol. Explor. Soc., N.Y., 87p.

Schneidermann, N. and Harris, P.M. (eds.), 1985, Carbonate cements: Soc. Econ. Paleon. Mineral. Spec. Pub. 36, 379p.

Scholle, P.A. and Halley, R.B., 1985, Burial diagenesis: out of sight, out of mind!, p.309-334, in Schneiderman, N. and Harris, P.M. (eds.) Carbonate Cements: Soc. Econ. Paleon. Mineral. Spec. Pub., 36, 379p.

Scoffin, T.P., 1987, An Introduction to Carbonate Sediments and Rocks: Blackie, Glasgow, New York, 274p.

Shepherd, T.J., Rankin, A.H., and Alderton, D.H.M., 1985, A Practical Guide to Fluid Inclusion Studies: Blackie, Glasgow and London, 239p.

Shukla, V. and Friedman, G.M., 1983, Dolomitization and diagenesis in a shallowing-upward sequence: the Lockport Formation (Middle Silurian) of New York state: J. Sed. Pet., v.53, p.703-717.

---------- and Baker, P.A. (eds.), 1988, Sedimentology and geochemistry of dolostones: Soc. Econ. Paleon. Mineral. Spec. Pub. 43, 266p.

Simonsen, J. and Friedman, G.M., 1991, Deep-burial diagenesis of the Lower Devonian Becraft Formation (Helderberg Group) of the Hudson Valley area: Northeastern Geol., v.13, p.39-63.

Sloss, L.L., 1963, Sequences in the cratonic interior of North America: Geol. Soc. Amer. Bull., v.74, p.93-113.

_____, 1972, Synchrony of Phanerozoic sedimentary- tectonic events of North American craton and Russian platform: 24th Int. Geol. Cong., Montreal, Sect. 6, p.24- 32.

_____, 1978, Global sea level changes; a view from the craton, in Watkins, J.S., Montadert, L., and Dickerson, P.W. (eds.) Geological and geophysical investigations of continental margins: Amer. Assoc. Petrol. Geol. Mem. 39, p.461-468.

Smart, G. and Clayton, T., 1985, The progressive illitization of interstratified illite-smectite from Carboniferous sediments of northern England and its relationship to organic maturity indicators: Clay Minerals, v.20, p.455-466.

Sorby, H.C., 1858, On the microscopic structure of crystals, indicating the origin of minerals and rocks: Quart. J. Geol. Soc. Lond., v.14, p.453-500.

Stach, E., Mackowski, M.Th., Teichmuller, M., Taylor, G.H., Chandra, D., and Teichmuller, R., 1982, Coal Petrology, 3rd Ed., Berlin-Stuttgart, Gebruder Borntraeger, 535p.

Stalder, P.J., 1979, Organic and inorganic metamorphism in the Taveyannaz Sandstone of the Swiss Alps and equivalent sandstones in France and Italy: J. Sed. Pet., v.49, p.463- 482.

Stanley, R.S. and Ratcliffe, N.M., 1985, Tectonic synthesis of the Taconic orogeny in western New England: Geol. Soc. Amer. Bull., v.96, p.1227-1250.

Staplin, F.L., 1969, Sedimentary organic matter, organic metamorphism, and oil and gas occurrences: Can. Petrol. Geol. Bull., v.17, p.47-66.

_____, 1977, Interpretation of thermal history from color of particulate organic matter - a review: Palynology, v.1, p.9-18.

Steam, R.G. and Reesman, A.L., 1986, Cambrian to Holocene burial history of Nashville Dome: Amer. Assoc. Petrol. Geol. Bull., v.70, p. 143-154.

Stevens, R.K., 1970, Cambro-Ordovician flysch sedimentation and tectonics in west Newfoundland and their possible bearing on a proto-Atlantic ocean, in Lajoie, J. (ed.) Flysch Sedimentology in North America: Geol. Assoc. Can. Spec. Pap. 7, p.165-

Stockmal, G.S., Beaumont, C. and Boutilier, R., 1986, Geodynamic models of convergent margin tectonics: transition from rifted to overthrust belt and consequence for foreland- basin development: Amer. Assoc. Petrol. Geol. Bull., v.70, p. 181-190.

Stockwell, C.H., 1961, Structural provinces, orogenies, and time classification of the Canadian Precambrian Shield: Can. Geol. Surv. Pap. 61-17, p.108-118.

Swanenberg, H.E.C., 1980, Fluid inclusions in high-grade metamorphic rocks from southwest Norway: Geologica Ultraiectina, Univ. Utrecht, no. 25, 147p.

Tankard, A.J., 1986, On the depositional response of thrusting and lithospheric flexure: examples from the Appalachian and Rocky Mountain basins. in Allen, P.A. and Homewood, P. (eds.) Foreland Basins, Int. Assoc. Sedimentologists Spec. Pub. no. 8, p.369-392.

Tarutani, T., Clayton, R.N. and Mayeda, T.K., 1969, The effect of polymorphism and magnesium substitution of oxygen isotope fractionation between calcium carbonate and water: Geochim. Cosmochim. Acta, v.33, p.987-996.

Teichmuller, M., 1952, Die Anwendung des polierten Dunnschliffes bei der Mikroskopic von Kohlen and versteinerten Torfen, in Freund, H. (ed.), Handbuch der Mikroskopic in der Technik, Bd. 2, Teil I, p.235-310. Umschau Verlag. Frankfurt am Main.

Thomas, W.A. and Schenk, P.E., 1988, Late Paleozoic sedimentation along the Appalachian orogen, in Harris, A.L. and Fettes, D.J. (eds.) The Caledonian-Appalachian Orogen, Geol. Soc. Spec. Pub. 38, p.515-530.

Tilley, B.J., Nesbitt, B.E. and Longstaffe, F.J., 1989, Thermal history of Alberta Deep Basin: comparative study of fluid inclusions and vitrinite reflectance data: Amer. Assoc. Petrol. Geol. Bull., v.73(10), p.1206-1222.

Tillman, J.E. and Barnes, H.L., 1983, Deciphering fracturing and fluid migration histories in the northern Appalachian Basin: Amer. Assoc. Petrol. Geol. Bull., v. 67, p.692-705.

Tissot, B.P. and Welte, D.H., 1978, Petroleum formation and occurrence, A New Approach to Oil and Gas Exploration: Springer-Verlag, Berlin, 538p.

----------, Pelet, R. and Ungerer, Ph., 1987, Thermal history of sedimentary basins, maturation indices and kinetics of oil and gas generation: Amer. Assoc. Petrol. Geol. Bull., v. 71, p.1445-1466.

Titus, R., 1988, Facies of the Trenton Group of New York, p.55- 76, in Keith, B.D. (ed.) The Trenton Group (upper Ordovician Series) of Eastern North America - Deposition, Diagenesis and Petroleum: Amer. Assoc. Petrol. Geol. Studies in Geol. no. 29, 317p.

---------- and Cameroon, B., 1976, Fossil communities of the lower Trenton Group (Middle Ordovician) of central and northwestern New York state: J. Paleont., v.50, p.1209-1225.

Thomas, W.A., 1985, The Appalachian - Ouachita connection: Paleozoic orogenic belt at the southern margin of North America: Ann. Rev. Earth Planet. Sci., v. 13, p.175-199.

Touret, J., 1977, The significance of fluid inclusions in metamorphic rocks. in Fraser, D.G. (ed.) Thermodynamics in Geology, D. Reidel Publishing Co., Dordrecht, Holland, p.203-227.

Treesh, M.I. and Friedman, G.M., 1974, Sabkha deposition of the Salina Group (Upper Silurian) of New York state, p.35-46, in Coogan, A.H. (ed.) Northern Ohio Geol. Soc. Symp. on Salt, 4th Proc., v.1, 530p.

Turner, D.A., 1977, Diagenetic patterns of surface and subsurface samples from the bioherm facies of the Edgecliff member of the Onondaga Formation (Middle Devonian) of New York State: Unpublished M.S. Thesis, Rensselaer Polytechnic Institute, Troy, NY, 188p.

Urschel, S.F. and Friedman, G.M., 1984, Paleodepth of burial of Lower Ordovician Beekmantown carbonates in New York State: Compass, Sigma Gamma Epsilon, v.61, p.205-215.

Van Houten, F.B., 1977, Triassic-Liassic deposits, Morocco and eastern North America: Amer. Assoc. Petrol. Geol. Bull., v.61, p.79-99.

Van der Voo, R., 1979, Age of Alleghenian folding in the central Appalachians: Geology, v.7, p.297-298.

Van Gijzel, P., 1982, Characterization and identification of kerogen and bitumen and determination of thermal maturation by means of qualitative and quantitative techniques: How to Assess Maturation and Paleotemperatures, Soc. Econ. Paleon. Mineralogists Short Course, no. 7, p.159-216.

Videtich, P.A., McLimans, R.K., Watson, H.K.S. and Nagy R.M., 1988, Depositional, diagenetic, thermal, and maturation histories of Cretaceous Mishrif Formation, Fatch Field, Dubai: Amer. Assoc. Petrol. Geol. Bull., v.72(10), p.1143- 1159.

Waples, D., 1980, Time and temperature in petroleum formation: application of Lopatin's method to petroleum exploration: Amer. Assoc. Petrol. Geol. Bull., v.64, p.916-926.

Walker, K.R., 1973, Stratigraphy and environmental sedimentology of Middle Ordovician Black River Group in the type area - New York state: NY State Mus. Sci. Serv. Bull. 419, 43p.

Weaver, C.E., 1960, Possible use of clay minerals in search for oil: Amer. Assoc. Petrol. Geol. Bull., v.44, p.1505-1518.

_____, 1978, Geothermal alteration of clay minerals and shales: diagenesis: Tech. Rept. ONW1-21, 176p.

_____ and Beck, K.C., 1971, Clay water diagenesis during burial: How mud becomes gneiss: Geol. Soc. Amer. Spec. Pap. no.134, 96p.

_____ and Brockstra, B.R., 1984, Illite-mica, p.67-98, in Weaver, C.E. and associates (eds.) Shale-Slate Metamorphism in Southern Appalachians, Development in Petrology 10, Elsivier, 239p.

_____ and Wampler, J.M., 1970, K, Ar, illite burial: Geol. Soc. Amer. Bull., v.81, p.3423-3430.

_____, Eslinger, E.V. and Yeh, H.-W., 1984, Oxygen isotopes, p.141-152, in Weaver, C.E. and associates (eds.) Shale-Slate Metamorphism in Southern Appalachians, Developments in Petrology 10, Elsivier, 239p.

Weiner, R.W., McLelland, J.M., Isachsen, Y.W. and Hall, L.M., 1984, Stratigraphy and structural geology of the Adirondack Mountains, New York: review and synthesis: Geol. Soc. Amer. Spec. Pap. 194, p.1-55.

Weisbrod, A. and Poty, B., 1975, Thermodynamics and geochemistry of the hydrothermal evolution of Myres Pegmatite, Southeastern Massif Central (France), part I and II: Petrologic, v.1, p.1-16 and 89-102.

White, W.A., 1972, Deep erosion by continental ice sheets: Geol. Soc. Amer. Bull., v.83, p.1037-1056.

Whitney, P.R. and Davin, M.T.,1 987, Taconic deformation and metasomatism in Proterozoic rocks of the easternmost Adirondacks: Geology, v.15, p.500-503.

Williams, H., 1979, Appalachian orogen of Canada: Can. J. Earth Sci., v.16, p.792-807.

_____ and Hatcher, R.D.Jr., 1982, Suspect terranes and accretionary history of the Appalachian orogen: Geology, v.10, p.530-536.

Williams, L.A., 1980, Community succession in a Devonian patch reef (Onondaga Formation, New York) - physical and biotic controls: J. Sed. Pet., v.50, 1p.169-1186.

Wolosz, T., 1989, Water-turbulence- the controlling factor in colonial rugose succession within Edgecliff reefs: Geol. Soc. Amer., N.E. Section Ann. Mtg., Abst. with Programs, p.77.

_____ and Paquette, D.E., 1989, Middle Devonian reefs of the Edgecliff of the Onondaga Formation of New York, in McMillan, N.J., Embry, A.F. and Glass, D.J. (eds.), Devonian of the Word Vol. II Sedimentation: CSPG Mem. 14, p.

Wood, G.H.Jr., Trexler, J.P., and Kehn, T.M., 1969, Geology of west-central part of the southern Anthracite field and adjoining areas, Pennsylvania: U.S. Geol. Surv. Prof. Pap. 602, 150p.

Woronick, R.E. and Land, L.S., 1985, Late burial diagenesis, Lower Cretaceous Pearsall and lower Glen Rose formations, south Texas, p.265-276, in Schneidermann, N. and Harris, P.M. (eds.) Carbonate Cements: Soc. Econ. Paleon. Mineral. 36, 379p.

Zadins, Z.Z., 1984, Thrusting, folding and cleavage development in the Silurian-Devonian section of eastern New York: Abst. with Programs, Geol. Soc. Amer. northeastern sect. ann. meetg., p.73.

Zen, E-an, 1967, Time and space relationships of the Taconic allochthon and autochthon: Geol. Soc. Amer. Spec. Pap. 97, 107p.

_____, 1972, The Taconide zone and the Taconic orogeny in the western part of the northern Appalachian orogen: Geol. Soc. Amer. Spec. Pap. 135, 72p.

_____, 1983, Exotic terranes in the New England Appalachians - limits, candidates, and ages: a speculative essay. in Hatcher, R.D., Williams, H. and Zietz. I. (eds.) Contribution to the Tectonics and Geophysics of Mountain Chains: Geol. Soc. Amer. Memoir 158, p.55-82.

Zenger, D.H., 1965, Stratigraphy of the Lockport Formation (Middle Silurian) in New York State:

NY State Mus. Sci. Serv. Bull. no.404, 210p.

_____, 1971, Uppermost Clinton (Middle Silurian) Stratigraphy and Petrography, East-central New York: NY State Mus. Sci. Serv. Bull.417, 58p.

_____, 1983, Burial dolomitization in the Lost Burro Formation (Devonian), east-central California, and the significance of late diagenetic dolomitization: Geology, v.11, p.519-522.

---------- and Dunham J.B., 1988, Dolomitization of Siluro- Devonian limestones in a deep core (5, 350m), southeastern New Mexico, p.161-174, in Shukla, V. and Baker, P.A. (eds.) Sedimentology and Geochemistry of Dolostones: Soc. Econ. Paleon. Mineralogists Spec. Pub. no. 43, 266p.

_____, _____, and Ethington, R.L. (eds.), 1980, Concepts and Models of Dolomitization: Soc. Econ. Plaeon. Mineral. Spec. Pub. 28, 379p.